N70-32031

NASA CONTRACTOR REPORT

NASA CR-1509

NASA CR-1509

CASE FILE COPY

Cb-1Zr RANKINE SYSTEM CORROSION TEST LOOP

by E. E. Hoffman and J. Holowach

Prepared by
GENERAL ELECTRIC COMPANY
Cincinnati, Ohio
for Lewis Research Center

NATIONAL AERONAUTICS AND SPACE ADMINISTRATION • WASHINGTON, D. C. • JUNE 1970

1. Report No. NASA CR-1509	2. Government Accession No.	3. Recipient's Catalog No.
4. Title and Subtitle Cb-1Zr RANKINE SYSTEM CORROSION TEST LOOP		5. Report Date June 1970 6. Performing Organization Code
7. Author(s) E. E. Hoffman and J. Holowach		8. Performing Organization Report No. GESP-246
9. Performing Organization Name and Address General Electric Company Cincinnati, Ohio		10. Work Unit No. 11. Contract or Grant No. NAS 3-2547
12. Sponsoring Agency Name and Address National Aeronautics and Space Administration Washington, D. C. 20546		13. Type of Report and Period Covered Contractor Report 14. Sponsoring Agency Code
15. Supplementary Notes		

16. Abstract

A 5000-hour test was conducted on a two-loop Cb-1Zr system, in which sodium was circulated in the heater circuit and potassium was boiled and circulated in a two-phase secondary loop, which contained turbine simulator test sections of Mo-TZM alloy. Maximum and minimum temperatures in the sodium circuit were 2150° F and 1960° F, respectively, while temperatures in the two-phase potassium circuit ranged from 2000° F (superheated vapor) at the boiler outlet to a minimum of 600° F in the coolest portion of the loop. Operation of the test system was completely satisfactory and extremely stable at the endurance test operating conditions with no significant temperature or pressure fluctuations in the two-phase boiling potassium circuit. Extensive chemical and metallurgical evaluations indicated that the containment alloy, Cb-1Zr, and the candidate turbine simulator alloy, Mo-TZM, have excellent compatibility with the alkali metal environments. No significant corrosion was detected in the system, and the substantial oxygen migration from the hotter to cooler regions of the sodium circuit, which was observed, had no detectable effect on either the strength or the ductility of the Cb-1Zr alloy.

17. Key Words (Suggested by Author(s))	18. Distribution Statement
Refractory alloys Potassium corrosion Rankine system	Unclassified - unlimited

19. Security Classif. (of this report)	20. Security Classif. (of this page)	21. No. of Pages	22. Price*
Unclassified	Unclassified	465	$3.00

*For sale by the Clearinghouse for Federal Scientific and Technical Information
Springfield, Virginia 22151

FOREWORD

The work described herein was performed by the General Electric Company under National Aeronautics and Space Administration Contract NAS 3-2547. The primary purpose of the potassium corrosion test loop development program was to develop a Cb-1Zr Rankine system corrosion test loop for the evaluation of refractory alloys in boiling and condensing potassium environments which simulate projected space electric power systems. This report describes the Cb-1Zr Rankine system corrosion test loop experiment and is the last in a series of seven topical reports covering the program. The report was originally issued as General Electric report GESP-246.

This program was administered for the General Electric Company by Dr. J. W. Semmel, Jr., Manager, Materials and Processes. Mr. E. E. Hoffman, Manager, Corrosion Technology, acted as the Program Manager of the potassium corrosion test loop development program, of which the loop test covered in this report is a part. Mr. R. L. Davies, of the Space Power Systems Division, Lewis Research Center, was the Project Manager for the National Aeronautics and Space Administration.

TABLE OF CONTENTS

SECTION		PAGE
I	INTRODUCTION	1
II	LOOP DESIGN	4
	A. Helical Induction Electromagnetic Pumps	6
	B. Metering Valve	14
	C. Potassium Preheater	21
	D. Vapor Bubble Nucleator	21
	E. Potassium Boiler	24
	F. Turbine Simulator	29
	G. Condenser and Subcooler	33
	H. Flowmeters	37
III	MATERIAL PROCUREMENT	44
IV	LOOP FABRICATION	45
	A. General Welding Procedures	45
	B. Slack Diaphragm Transducers	47
	C. Valves	50
	D. Electromagnetic Pump Ducts	50
	E. Stressed Diaphragm Pressure Transducer	52
	F. Vapor Nucleator	55
	G. Potassium and Sodium Surge Tanks	55
	H. Potassium Preheater and Sodium Heater	55
	I. Boiler	60
	J. Turbine Simulator	69
	K. Boiler Subassembly	73
	L. Condenser Subassembly	77
	M. Postweld Annealing	80
	N. Condenser Fin Coating Application	82
	O. Final Assembly of Loop	83

TABLE OF CONTENTS (Cont'd)

SECTION		PAGE
V	TEST EQUIPMENT	93
	A. Vacuum Systems	93
	B. Chamber Pressure Measurement	103
	C. Partial Pressure Gas Analyzer	105
	D. Heater Power Supply	105
	E. Air-Cooled Metal Vapor Collector	108
VI	ALKALI METAL PURIFICATION, TRANSFER, AND SAMPLING SYSTEMS	110
	A. Sodium Purification	110
	B. Potassium Purification	114
	C. Sodium and Potassium Transfer and Sampling System	119
VII	LOOP INSTALLATION AND INSTRUMENTATION	121
	A. Installation and Instrumentation Enclosure	121
	B. Installation of Loop in the Spool Section of the Vacuum Chamber	121
	C. Thermal Insulation	123
	D. Instrumentation	125
	E. Chamber Installation	136
VIII	PRETEST OPERATION	144
	A. Pumpdown and Bakeout of the Vacuum System	144
	B. Filling, Flushing, and Sampling of Alkali Metal in the Cb-1Zr Corrosion Loop System	146
	C. Checkout of Loop Equipment and Controls	146
	D. Calibration of Loop Instrumentation	148
IX	TEST LOOP STARTUP	158
	A. Potassium Inventory Control	158
	B. Start of Boiling Operation	159
	C. Stability of Loop Operation During Test Startup	160
X	TEST LOOP OPERATION	166
	A. Loop Operation During the 5000-Hour Test	175
	B. Termination of the Test	188
	C. Total Pressure and Partial Pressures in the Chamber During the 5000-Hour Test	189

TABLE OF CONTENTS (Cont'd)

SECTION		PAGE
XI	DISTILLATION, DRAINING, AND DISASSEMBLY OF THE LOOP.	209
	A. Distillation of Sodium and Potassium From the Loop Circuits	209
	B. Draining and Sampling of Alkali Metals From the Loop	215
	C. Analysis of Sodium and Potassium Samples From the Loop.	216
	D. Disassembly and Examination of Loop Components .	218
XII	CHEMICAL AND METALLURGICAL EVALUATION OF THE LOOP COMPONENTS	238
	A. Results of Chemical Analysis of Loop Components.	238
	B. Metallographic Evaluation of Loop Components . .	247
	C. Electron Beam Microprobe Analyses.	278
	D. Tensile Test Results on Cb-1Zr Tubing.	286
	E. Bend Test Results on Cb-1Zr Tubing	286
	F. Microhardness Evaluation of Cb-1Zr and Mo-TZM Components	289
XIII	EVALUATION OF LOOP PERFORMANCE	294
	A. Metering and Isolation Valves.	294
	B. Vapor Bubble Nucleator	295
	C. Helical Induction Electromagnetic Pump	295
	D. Permanent Magnet Flowmeter	296
	E. Sodium Heater and Potassium Preheater	296
	F. Boiler	299
	G. Turbine Simulator	306
	H. Condenser/Subcooler.	308
	I. Slack Diaphragm Pressure Transducer.	311
	J. Stressed Diaphragm Pressure Transducer	313
	K. Temperature Measurement.	315
XIV	SUMMARY AND CONCLUSIONS.	316
XV	PUBLISHED REPORTS.	318
XVI	APPENDICES	319
	A. List of Drawings of the Cb-1Zr Rankine System Corrosion Test Loop.	320

TABLE OF CONTENTS (Cont'd)

SECTION		PAGE
XVI	APPENDICES (Continued)	
	B. Major Drawings of the Cb-1Zr Rankine System Corrosion Test Loop.	326
	C. Nomenclature Used in Design Calculations	348
	D. Boiler Plug Design	351
	E. Refluxing Potassium Tests to Evaluate Mo-TZM Inserts in Cb-1Zr Capsules.	355
	F. Test to Evaluate a High-Emittance Iron Titanate Coating for the Cb-1Zr Condenser Fin. .	375
	G. Calibration of the Partial Pressure Gas Analyzer	384
	H. Calibration of W-3Re/W-25Re Thermocouple Wire. .	390
	I. Test Startup Procedure	402
	J. Stress-Corrosion Cracking of the Vacuum Chamber Cooling Channel.	410
	K. Draining, Sampling, and Filtering of the Potassium and Sodium Circuits of the Loop	429
XVII	REFERENCES	435

LIST OF ILLUSTRATIONS

FIGURE NO.		PAGE
1	Isometric Drawing of the Cb-1Zr Rankine System Corrosion Test Loop	5
2	Schematic Diagram of the Cb-1Zr Rankine System Corrosion Test Loop	7
3	Helical Induction Electromagnetic Pump	8
4	Calculated Pump Performance of General Electric Helical Induction EM Pump Model 5KY414PFI	12
5	Calculated Pump Performance of General Electric Helical Induction EM Pump Model 5KY414PB2	13
6	Modified Hoke Valve and Associated Drive Components for the Cb-1Zr Rankine System Corrosion Test Loop	15
7	Detail of Metering Valve Plug Body Bore and Port for the Cb-1Zr Rankine System Corrosion Test Loop	16
8	Flow Rate for the Cb-1Zr Corrosion Test Loop Metering Valve as a Function of Stem Rotation for 1, 2 and 4 psi Pressure Drop Across the Valve	18
9	Cb-1Zr Corrosion Test Loop Metering Valve Pressure Loss as a Function of Stem Rotation	19
10	Outline Drawing and Schematic Drawing of Magnetic Rotary Feedthrough. Varian Associates Model No. 954-5039	20
11	Schematic Drawing of the Vapor Nucleator	23
12	Turbine Simulator Expansion on Potassium Mollier Diagram for the Ten Stages of the Cb-1Zr Corrosion Test Loop	34
13	Condenser Length as a Function of Fin Width for Single-Tube Finned Cb-1Zr Condenser	36
14	Magnetic Flowmeter Principle	39
15	Permanent Magnet Flowmeter Located Between the Boiler Outlet and the EM Pump Inlet in the Sodium Circuit of the Cb-1Zr Corrosion Test Loop	41
16	Calculated Output Voltage Versus Flow Rate for the Cb-1Zr Corrosion Loop Permanent Magnet Flowmeter	43

LIST OF ILLUSTRATIONS (Cont'd)

FIGURE NO.		PAGE
17	Fabrication Sequence for the Cb-1Zr Rankine System Corrosion Test Loop	46
18	Vacuum-Purge Inert Gas Welding Chamber with Helium Supply and Purity Control System	48
19	Vacuum-Purge Inert Gas Welding Chamber and Helium Purity Control System with Welding Chamber Extension Tank Attached	49
20	Modified Hoke Valve and Associated Drive Components for the Cb-1Zr Corrosion Test Loop	51
21	Potassium Duct (Top) and Sodium Duct (Bottom) of the Helical Induction Electromagnetic Pumps for the Cb-1Zr Corrosion Test Loop	53
22	Stressed Diaphragm Pressure Transducer for the Cb-1Zr Corrosion Test Loop at Various Stages During Fabrication	54
23	Vapor Nucleator (Cb-1Zr) for the Cb-1Zr Corrosion Test Loop (a) Before and (b) After Welding	56
24	Potassium Surge Tank (6" OD) for the Cb-1Zr Corrosion Test Loop Partially Assembled	57
25	Bimetallic Joint Between Cb-1Zr Alloy and Type 316 Stainless Steel	58
26	Potassium Preheater Coil-Vapor Nucleator Subassembly for the Cb-1Zr Corrosion Test Loop	59
27	Cb-1Zr Alloy Preheater Coil Electrodes for the Cb-1Zr Corrosion Test Loop	61
28	Radiograph of a Copper Mockup of the Cb-1Zr Corrosion Test Loop Boiler	62
29	Cb-1Zr Boiler Tube Spacer Before and Following Attachment to the 0.375-Inch Cb-1Zr Potassium Containment Tube by Welding	64
30	Radiographs of Portions of the Cb-1Zr Corrosion Test Loop Boiler Coil	65
31	Radiograph of Cb-1Zr Corrosion Test Loop Boiler Coils	66
32	Cb-1Zr Corrosion Test Loop Tube-in-Tube Helical Boiler	67

LIST OF ILLUSTRATIONS (Cont'd)

FIGURE NO.		PAGE
33	Two Radiographs of the Boiler Inlet Region of the Cb-1Zr Corrosion Test Loop Showing the Plug Configuration.....	68
34	Mo-TZM Alloy Turbine Simulator Nozzle and Blade Assembly.....	70
35	Machining Sequence Required to Produce the Mo-TZM Alloy Nozzle for the Cb-1Zr Corrosion Test Loop - Turbine Simulator.....	71
36	Overall and Enlarged View of the First-Stage Turbine Simulator and the Potassium Vapor Carryover Pipe.....	74
37	Turbine Simulator (Stages 2-10) of the Cb-1Zr Corrosion Test Loop Prior to Assembly.....	75
38	Preheater Boiler First-Stage Turbine Simulator Assembly Wrapped with Cb-1Zr Alloy Foil Prior to Annealing.....	76
39	Cb-1Zr Corrosion Test Loop Condenser and Fixture During Welding of Fin to Condenser Pipe.....	78
40	Turbine Simulator, Condenser/Subcooler and Subcooler Reservoir of the Cb-1Zr Corrosion Test Loop.....	79
41	Type 304 Stainless Steel Support Structure for the Cb-1Zr Corrosion Test Loop.....	84
42	Cb-1Zr Corrosion Test Loop Mounted on Welding Fixture.....	85
43	Cb-1Zr Corrosion Test Loop Positioned in the Welding Chamber During Final Assembly.....	86
44	Cb-1Zr Corrosion Test Loop and the Welding Fixture Positioned in the Welding Chamber in Preparation or Final Welding Operation.	87
45	Refractory Metal Furnace for Vacuum Annealing of Cb-1Zr Loop Weldments in the Welding Chamber.....	88
46	Cb-1Zr Corrosion Test Loop Prior to Installation in the Vacuum Chamber Spool Section.....	90
47	Cb-1Zr Corrosion Test Loop Following Installation in the Test Chamber Spool Piece.....	91
48	Lower Portion of the Cb-1Zr Corrosion Test Loop Following Installation in the Vacuum Chamber Spool Piece.....	92
49	High-Vacuum System (10^{-10} Torr Range) for the Cb-1Zr Corrosion Test Loop During Checkout Test at the Vendor's Plant.....	94

LIST OF ILLUSTRATIONS (Cont'd)

FIGURE NO.		PAGE
50	Sorption Pumping System Used to Evacuate the Vacuum Chamber for the Cb-1Zr Corrosion Loop Test Prior to the Initiation of Getter-Ion Pumping	95
51	High-Vacuum Chamber and Auxiliary Equipment of the Cb-1Zr Rankine System Corrosion Test Loop	97
52	Pumping Speed Curve and Illustrations of the Turbo-Molecular Pump	98
53	Water Cooled, 1000-Ampere Electrical Power Feedthrough	102
54	Ion Gauge, Partial Pressure Analyzer Tube and Variable Leak Valve Mounted on Chamber Sump	106
55	Electronic Control Unit and X-Y Recorder for the Partial Pressure Analyzer	107
56	Simplified Schematic of Sodium and Potassium Purification and Transfer System for the Cb-1Zr Corrosion Test Loop	111
57	Sodium Purification System Showing Hot Trap and Charge Tank After Installation in Oven	112
58	Potassium Hot Trap for the Cb-1Zr Corrosion Test Loop Prior to Assembly	116
59	Potassium Purification and Loop Filling System	117
60	Potassium Distillation Unit for Purifying Potassium. Components of System Shown Prior to Assembly	118
61	Sodium and Potassium Transfer Systems After Installation in Oven Enclosure	120
62	Reinforced Polyethylene Air Shelter Used During Instrumentation of the Cb-1Zr Corrosion Test Loop	122
63	Cb-1Zr Corrosion Test Loop Showing the Number of Layers of Reflective Foil Thermal Insulation Used on the Various Loop Components	124
64	Cb-1Zr Corrosion Test Loop Thermocouple Instrumentation Layout.	129
65	Method Used to Mount W-3Re W-25Re Thermocouple Wires on Cb-1Zr Alloy Tubing for the Cb-1Zr Corrosion Test Loop	130

LIST OF ILLUSTRATIONS (Cont'd)

FIGURE NO.		PAGE
66	Photograph of Tube-in-Tube Helical Boiler Showing the Method Used to Mount Boiler Thermocouples	131
67	Thermocouple Wire Terminals (192 Total) Located in the Sump of the Test Chamber	133
68	Typical Thermocouple Lead Wire Feedthrough Flange	134
69	Six Thermocouple Lead Wire Feedthrough Flanges with 32 Wires in Each Flange	135
70	Schematic of the Thermocouple Circuit of the Cb-1Zr Corrosion Test Loop	137
71	Sodium Pump Stator and Pump Duct Vacuum Can Prior to Assembly.	140
72	Lower Section (a) of Cb-1Zr Corrosion Test Loop and Enlarged View (b) of the Metering Valve Drive and Sighting Wire Used to Monitor Valve Adjustments	141
73	Corrosion Test Loop and Lower Portion of the Vacuum Chamber Prior to Lowering Chamber Bell Jar Onto Spool Piece	143
74	Plan View Showing Spatial Arrangement and Interconnecting Lines Between Purification Systems, Transfer Systems, and Loop	147
75	Calibration of Slack Diaphragm Pressure Transducer (No. 1) Located at the Potassium Pump Outlet	149
76	Calibration of Fast Response Stressed Diaphragm Pressure Transducer Located at the Metering Valve Outlet	151
77	Results Obtained During Calibration of W-3Re/W-25Re Thermocouples Located in the Boiler Section of the Loop	152
78	Theoretical Sodium Flow vs. Flow Determined by Energy Balance Across Sodium Heater	154
79	Theoretical Potassium Flow vs. Flow Determined by Energy Balance Across Potassium Preheater	155
80	Control Console of the Cb-1Zr Corrosion Test Loop	157
81	Total Pressure and Partial Pressures of Various Gases During Startup and Early Operation of the Cb-1Zr Corrosion Test Loop.	161
82	Sodium Temperature at Various Locations in the Boiler Illustrating Movement of the Potassium Boiling Region During Test Startup	163

FIGURE NO.		PAGE
83	Boiler Temperature Changes and Boiler Outlet Pressure Fluctuation Associated with Movement of the Potassium Boiling Region.	164
84	Cb-1Zr Corrosion Test Loop Operating Conditions.....	167
85	Temperature Fluctuations in Potassium Circuit During Period When Flow Was Lost Due to Vapor Locking in the Pump.....	170
86	Fluctuations in Boiler Outlet Pressure Following Vapor Lock in Potassium Pump.....	171
87	Effect of Metering Valve on the Potassium Flow Rate and Boiler Outlet Pressure.....	174
88	Temperature Fluctuations in the Sodium and Potassium Circuits of the Loop Following Failure of the Potassium Preheater Power.	176
89	Temperature Fluctuations in the Sodium and Potassium Circuits During the Period When the Loop Was Being Returned to Design Conditions Following Failure of Potassium Preheater Power.....	177
90	Fluctuations in Potassium Pressure and Flow in the Loop During the Time Period When the Potassium Preheater Power Was Lost and Then Restored.....	179
91	Fluctuations in Potassium Boiler Inlet Pressure Recorded by the Fast Response Stressed Diaphragm Pressure Transducer Following Failure of Preheater Power.....	180
92	Change in Pressure Drop Ratio in the Potassium Circuit of the Loop as a Function of Time.....	182
93	Cb-1Zr Corrosion Test Loop After Removal of the Vacuum Chamber Bell Jar Following Completion of the 5000-Hour Test.....	190
94	Lower Portion of the Loop Following Removal of the Vacuum Chamber Bell Jar.....	191
95	Vacuum Chamber Pressures During the 5000-Hour Cb-1Zr Corrosion Loop Test.....	196
96	Vacuum Chamber Pressures During Startup and Operation Following Shutdown at 3809 Hours.....	198
97	Pressure Rise Rate Tests on Vacuum Chamber with Cb-1Zr Corrosion Test Loop at Temperature and Following Cooling to Room Temperature.....	200

LIST OF ILLUSTRATIONS (Cont'd)

FIGURE NO.		PAGE
98	Typical Pressure Surge in the Test Chamber Resulting From an Argon Instability in the Getter-Ion Pump.....	204
99	Cb-1Zr Corrosion Test Loop After Removal of the Vacuum Chamber Bell Jar Following Completion of the 5000-Hour Test.....	210
100	Lower Portion of the Loop Following Removal of the Vacuum Chamber Bell Jar.....	211
101	Cb-1Zr Corrosion Test Loop Following Installation of Quartz Lamp Heaters for Distillation.....	213
102	Loop Following Installation of Two Layers of Stainless Steel Foil Reflective Insulation in Preparation for Distillation of Alkali Metals From the Loop Circuits to the Surge Tanks....	214
103	Manual and Hydraulic Cold Weld Pinch-Off Devices Used to Seal Cb-1Zr Alloy Tubing During Sectioning of Corrosion Test Loops.	219
104	Lower Portion of the Loop Following Removal of Insulation and Condenser Shield Assembly.....	220
105	Potassium and Sodium Pump Ducts Following Separation From the Loop Circuits and Removal of the Vacuum Enclosure Cans and Cb-1Zr Insulating Foil.....	222
106	Potassium Pump Duct After Removal of Half of the Pump Duct Can Following Completion of the 5000-Hour Test.....	223
107	Prints of Radiographs of the Plug Section and Coils of the Boiler of the Loop Following Test.....	224
108	Potassium Containment Tube (3/8-Inch OD) and Sodium Containment Tube (1-Inch OD) From the Tube-in-Tube Helical Boiler....	225
109	Condenser Pipe and Fin Following Completion of 5000-Hour Test.	227
110	Metering Valve Following Completion of the 5000-Hour Test.....	228
111	Bellows and Plug Assembly of the Metering Valve After Disassembly Following the 5000-Hour Test.....	229
112	Nine-Stage Turbine Simulator Prior to Assembly Showing the Alignment Wire Which Was Cut Into During Component Disassembly.	230
113	Cb-1Zr Casing of Nine-Stage Mo-TZM Alloy Turbine Simulator Showing Milled Groove and Cb-1Zr Allignment Wire.....	232

LIST OF ILLUSTRATIONS (Cont'd)

FIGURE NO.		PAGE
114	Mo-TZM Alloy Turbine Simulator Nozzles, Blade Specimens, and Specimen Holding Pads Following 5000-Hour Exposure to Potassium.	233
115	Outlet Side of Nozzles of Turbine Simulator Stages No. 1 Thru No. 10.....	234
116	Photographs of Concave(a) and Convex(b) Sides of Mo-TZM Alloy Blade Specimens and Blade Pads Following Loop Disassembly.....	236
117	Location of Chemical Analysis Specimens Taken From the Potassium and Sodium Circuits of the Cb-1Zr Corrosion Test Loop....	242
118	Oxygen Concentration of Various Regions of the Boiler of the Cb-1Zr Loop Following 5000 Hours Operation.....	248
119	Photomicrographs Illustrating Before Test Appearance of Cb-1Zr Tubing Used in Fabrication of the Cb-1Zr Corrosion Test Loop..	250
120	Location of Metallographic Specimens Taken From the Potassium and Sodium Circuits of the Cb-1Zr Corrosion Test Loop.....	251
121	Cb-1Zr Tubing From Potassium Circuit. Specimen Locations Given in Figure 120.....	253
122	Cb-1Zr Tubing From Potassium Circuit. Specimen Locations Given in Figure 120.....	254
123	Photomicrographs of Condenser/Subcooler Cb-1Zr Pipe Following 5000 Hours Exposure to Potassium.....	255
124	Photomicrograph of the Potassium Side of the Cb-1Zr Pump Wrapper Following Disassembly After the 5000-Hour Test.....	256
125	Cb-1Zr Tubing From Sodium Circuit. Specimen Locations Given in Figure 120.....	258
126	Cb-1Zr Tubing From Sodium Circuit Near Boiler Inlet. Specimen Locations Given in Figure 120.....	259
127	Cb-1Zr Tubing Located in Sodium Return Line Between the Boiler and the EM Pump. Specimen Locations Given in Figure 120.....	260
128	Boiler Diagram Showing the Location of Metallographic Specimens From Various Regions of the Boiler Shown in the Figures Which Follow.....	262

FIGURE NO.		PAGE
129	Cb-1Zr Tubing From Boiler. Location of Metallographic Specimens Given in Figure 128.....	263
130	Cb-1Zr Tubing From Boiler. Location of Metallographic Specimens Given in Figure 128.....	264
131	Cb-1Zr Tubing From Boiler. Location of Metallographic Specimens Given in Figure 128.....	265
132	Surface of Cb-1Zr Butt Weld in 1-Inch-OD Sodium Containment Tube From Boiler (Location D) Following Test.....	266
133	Sodium Containment Tube (1-Inch-OD) From Location E (2130°F) in Boiler Showing Effect of Boiler Forming on Abnormal Grain Growth.	268
134	Potassium Containment Tube (3/8-Inch-OD) From Location E (Na, 2130°F; K, 2000°F) Showing Effect of Boiler Forming on Abnormal Grain Growth.....	269
135	Cb-1Zr Components Taken From the Plug Region of the Boiler Showing the Location of Metallographic Specimens Shown in the Figures Which Follow.....	270
136	Cb-1Zr Tube (3/8-Inch-OD) From Sodium Exit - Potassium Entrance Region of Boiler.....	271
137	Cb-1Zr Tube (3/8-Inch-OD) From Boiler Plug Region, Five Inches From Potassium Boiler Entrance/Sodium Exit.....	272
138	Cb-1Zr Potassium Containment Tube (3/8-Inch-OD) Six Inches From Potassium Boiler Entrance/Sodium Exit.....	273
139	Cross Section Views and Photomicrographs of Turbine Simulator Nozzles Following Exposure to Potassium for 5000 Hours.....	275
140	Mo-TZM Turbine Simulator Blade Specimens Showing Microstructure of Impingement Area Following 5000-Hour Test.....	276
141	Metallographic Appearance of Metering Valve Components Following 5000-Hour Test.....	277
142	Metallographic Appearance of Iron Titanate Coating on Top Fin of Cb-1Zr Loop Condenser Following 5000-Hour Test.....	279
143	Surface of Cb-1Zr Tube Specimen Taken From the Potassium Containment Tube in the Plug Section of the Boiler Showing Deposit.	281

FIGURE NO.		PAGE
144	Electron Beam Microprobe X-Ray Scan for Zirconium Across the Deposit Found on the Sodium Side of the Potassium Containment Tube in the Plug Region of the Boiler.....	282
145	Zirconium X-Ray Image and a Series of Electron Back Scatter (EBS) Images with Increasing Beam Current on the Deposit Region.	283
146	Appearance of Fractures of Reduced Gauge Length Tube Tensile Specimens Prepared From 3/8-Inch-OD Cb-1Zr Tubing.....	288
147	Cb-1Zr Specimen Which Was Taken From the High Oxygen Concentration (1240 ppm) Region of the Plug Section of the Boiler.....	290
148	Surfaces of Flattened Specimens of the 1-Inch-OD Cb-1Zr Sodium Containment Tube Illustrating the Ductility of the Tubing.....	291
149	Flux Density vs. Temperature of Sodium Flowmeter Magnet Before and After 5000-Hour Loop Test.....	297
150	Temperature Distribution in Sodium Heater Electrodes After 259 Hours and 5000 Hours of Test Operation.....	298
151	Sodium Temperature Distribution in the Boiler for Two Off-Design Conditions During Test Startup.....	301
152	Cb-1Zr Corrosion Test Loop Thermocouple Instrumentation Layout.	303
153	Cb-1Zr Corrosion Test Loop Boiler Operating Conditions After 5000 Hours Operation.....	304
154	Test Condition at 5000 Hours Just Prior to Test Shutdown.....	305
155	Temperature Distribution in the Condenser/Subcooler of the Loop.	309
156	Temperature Distribution in the Condenser Fin at Steady State Conditions.....	310
157	Calibration of the Slack Diaphragm Pressure Transducer That Was Used to Measure the Potassium Boiler Outlet Pressure.....	312
158	Comparison of the Pretest and Posttest Calibration of the Slack Diaphragm Pressure Transducer Used to Measure Boiler Outlet Pressure.....	314
159	Cb-1Zr Rankine System Corrosion Test Loop Assembly.....	328

FIGURE NO.		PAGE
160	Loop Support Structure Assembly	330
161	Sodium Heater Coil Assembly	331
162	Turbine Simulator Assembly	332
163	Turbine Simulator Nozzle Assembly	333
164	Turbine Simulator Nozzle	334
165	Turbine Simulator Blade Assembly	335
166	Boiler Assembly	336
167	Gas Pressure Tube Assembly for Potassium Circuit	337
168	Bimetallic Joint Assembly	338
169	Gas Pressure Tube Assembly for Sodium Circuit	339
170	Potassium Pumo Outlet Assembly	340
171	Stressed Diaphragm Pressure Transducer and Mounting Tube Assembly	341
172	High Temperature Valve Assembly	342
173	Ball Bearing Stem Assembly of the High Temperature Valve	343
174	Potassium Preheater Coil Assembly	344
175	Vapor Bubble Nucleator	345
176	Potassium Condenser and Subcooler	346
177	Condenser Shield Drive Assembly	347
178	Boiler Tube Inserts Used in Pressure Drop Tests	352
179	Cb-1Zr Refluxing Potassium Corrosion Capsule Containing TZM Alloy Inserts in Condensing Region	356
180	Components of the Refluxing Potassium Capsule Test Systems, Cb-1Zr Capsules with Mo-TZM Alloy Inserts	358

FIGURE NO.		PAGE
181	High Vacuum Test Chamber (10^{-10} Torr Range) in Which Cb-1Zr/Mo-TZM Refluxing Potassium Chamber Tests Were Performed.....	360
182	Reflux Corrosion Capsule Test Facility with Bell Jar Removed..	361
183	Water-Cooled, Dowtherm-Filled Heat Exchanger for the Cb-1Zr/Mo-TZM Refluxing Potassium Test Facility.....	362
184	Potassium Reflux Capsule Components Following 2500-Hour Test at 2000°F.....	366
185	Potassium Reflux Capsule Components Following 5000-Hour Test at 2000°F.....	372
186	Test Configuration Used in the Evaluation of the High Emittance, Fe_2TiO_5 Coating on the Cb-1Zr Alloy Specimens.....	376
187	Steady State Temperature Profile of Fe_2TiO_5 Coated Cb-1Zr Alloy Specimens During Coating Evaluation Test.....	379
188	Steady State Temperature Profile of Coated and Uncoated Cb-1Zr Alloy Fin Specimens During Coating Evaluation Test.....	380
189	End Temperature of a 2-Inch x 2-Inch x 0.25-Inch-Thick Cb-1Zr Fin with a Base Temperature of 1500°F as a Function of Surface Emittance.....	382
190	Cb-1Zr Alloy Fin Specimen Coated with Iron Titanate.....	383
191	Sensitivity of Partial Pressure Analyzer, Initial Calibration (3-3-65).....	386
192	Vacuum Furnace for Calibrating W-3Re/W-25Re Thermocouple Wire.....	391
193	Components of Thermocouple Calibration Vacuum Furnace Before Assembly.....	392
194	Inside of Thermocouple Calibration Furnace Prior to Insertion of Mo-TZM Alloy Isothermal Block.....	394
195	Thermocouple Calibration Furnace Attached to the 24-Inch-Diameter Getter-Ion Pumped Vacuum Chamber.....	395
196	Thermocouple Bundle Used in Calibration of W-3Re/W-25Re Thermocouple Wire for the Prototype Corrosion Loop.....	396

FIGURE NO.		PAGE
197	Difference Curve Vs. Temperature Obtained in Calibration of Two W-3Re/W-25Re Thermocouples Made from Wire Used to Instrument the Cb-1Zr Rankine System Corrosion Test Loop.....	399
198	Schematic Diagram of the Cb-1Zr Rankine System Corrosion Test Loop.....	403
199	Cb-1Zr Rankine System Corrosion Test Loop Thermocouple Instrumentation Layout.....	404
200	Cb-1Zr Corrosion Loop Test Chamber and Associated Equipment. Water Channel in Which Stress-Corrosion Cracking Occurred Is Indicated by Arrows.....	411
201	Cb-1Zr Corrosion Loop Vacuum Chamber Pressure During Period When the Test Was Shut Down Because of a Water-to-Vacuum Leak in the Top Cooling Channel of the Spool Piece.....	412
202	Spool Section of Vacuum Chamber Showing Locations, A, B, and C, Where Portions of the Cooling Channel Were Removed.....	413
203	Upper Portion of the Spool Piece of the Chamber Corresponding to Area (A) in Figure 2 Showing Where First Section of Cracked Water Channel Was Removed. Lower Channel Was Found To Be Ductile and Free of Cracks.....	414
204	Upper Portion of the Spool Piece of the Chamber Corresponding to Area (B) in Figure 2 Showing Where Section of Cracked Water Channel Was Removed.....	416
205	Water Side of the Top Portion of the Upper Cooling Channel of the Chamber Spool Piece.....	417
206	Appearance of Water Side of a Specimen Cut From the Region of the Top Cooling Channel Near the Water-Line Deposit.....	418
207	Metallographic Sections of the Top Portion (a) and Lower Portion (b) of the Upper Water Cooling Channel of the Chamber Spool Piece.....	419
208	Photomicrographs of the Water Cooling Channel Wall at Two Magnifications.....	420
209	Cadmium-Plated Steel Fitting Used to Connect Water Inlet and Outlet Lines to Spool Piece Cooling Channel.....	425

FIGURE NO.		PAGE
210	Spool Piece and Sump Section of the Prototype Corrosion Loop Test Chamber Showing the Evacuation Line and the Turbomolecular Pumping System Used to Pump Cracked Cooling Channel to a Pressure of 10^{-8} Torr.....	427
211	Schematic Diagram of the Cb-1Zr Corrosion Test Loop Draining, Sampling, and Filtering System.....	431

LIST OF TABLES

TABLE	TITLE	PAGE
I	General Information on Helical Induction Electromagnetic Pump, General Electric Model No. 5KY414PF1	10
II	General Information on Helical Induction Electromagnetic Pump, General Electric Model No. SKY414PB2	11
III	Calculated Boiler Length Required for Various Sodium Flow Rates and Inlet Temperatures for Cb-1Zr Rankine System Corrosion Test Loop	28
IV	Turbine Simulator Design	32
V	Finned Tube Condenser/Subcooler	38
VI	Magnetic Flux vs Temperature of the Alnico V Flowmeter Magnet After Thermal Stabilization and Prior to the Loop Test	42
VII	Orifice Diameters for the Mo-TZM Alloy Nozzles for the Cb-1Zr Corrosion Test Loop Turbine Simulator as Determined by Air-Gauge Inspection	72
VIII	Results of Chemical Analyses of Cb-1Zr Alloy Welds After Heat Treatment	81
IX	Performance Test of the 4-Foot-Diameter by 11-Foot-High Getter-ion Pumped Vacuum Chamber at Varian Associates	101
X	Ionization Gauge Calibration Data	104
XI	Analyses of Alkali Metals for the Cb-1Zr Corrosion Test Loop System	113
XII	Thermocouple Reference Table for the W-3Re/W-25Re Wire Used to Instrument the Cb-1Zr Corrosion Test Loop	127
XIII	Loss of Potassium Flow Resulting from Potassium Temperature Rise in the Pump and Resultant Vapor Locking of the EM Pump	169
XIV	Test Chamber Pressure and the Temperature of the Hottest Loop Components During the Test Shutdown Period on January 8, 1966	185
XV	Cb-1Zr Corrosion Test Loop Operation History August 2, 1965 - March 9, 1966	192

LIST OF TABLES (Cont'd)

TABLE	TITLE	PAGE
XVI	Typical Mass Spectrum Obtained During Loop Operation	194
XVII	Residual Gas Analyses Before and After Pressure Rise Rate Measurement with Loop at Ambient Temperature	201
XVIII	List of a Few of the Typical Rapid Pressure Rises ("Argon Instabilities") Noted in the Test Chamber Pressure During the Loop Test	205
XIX	Argon and Hydrogen Pressure Surges During "Argon Instabilities" in the Test Chamber	207
XX	Results of Analyses of Sodium, Potassium and Filter Residues After the 5000-Hour Endurance Test of the Prototype Loop	217
XXI	Summary of Dimensional Measurement Changes on the Mo-TZM Nozzles and the Weight Change Data on Both Nozzle and Blade Specimens	235
XXII	Results of Chemical Analysis of Cb-1Zr Foil Taken From the Single Layer of Insulation that Surrounded the Nine-Stage Turbine Simulator During the 5000-Hour Prototype Corrosion Loop Test	239
XXIII	Results of Chemical Analysis of Mo-TZM Alloy Turbine Simulator Blade Specimens Following the 5000-Hour Test	241
XXIV	Results of Chemical Analysis of Cb-1Zr Specimens from the Potassium Circuit of the Cb-1Zr Corrosion Test Loop Following the 5000-Hour Test	243
XXV	Results of Chemical Analysis of Cb-1Zr Specimens from the Sodium Circuit of the Cb-1Zr Corrosion Test Loop Following the 5000-Hour Test	245
XXVI	Results of Tensile Tests Performed on Reduced Gauge Length Cb-1Zr Tube Tensile Specimens Taken from the Sodium Circuit of the Corrosion Test Loop	287
XXVII	Results of Microhardness Surveys of the Cb-1Zr Tubing from Various Regions of the Cb-1Zr Corrosion Loop Following the 5000 Hour Test	293

LIST OF TABLES (Cont'd)

TABLE	TITLE	PAGE
XXVIII	Summary of the Loop Boiler Performance for Two Runs During Loop Startup	300
XXIX	Performance of Cb-1Zr Rankine System Corrosion Test Loop Boiler Compared to 300 KW Heat Transfer Test Data	307
XXX	Summary of Cb-1Zr Corrosion Test Loop Design Conditions and Pressure Drop Test of a Boiler Insert	353
XXXI	Test Results of 1 2", 1", and 2" Pitch Insert in a 0.25" ID Tube	354
XXXII	Frictional Pressure Drop Characteristics of the Cb-1Zr Corrosion Test Loop Boiler Insert in Air at Re = 40,000	354
XXXIII	Test Chamber Pressure During 2500-Hour and 5000-Hour, 2000°F Refluxing Potassium Capsule Tests	364
XXXIV	Weight Change Data Obtained on Specimens Following Cb-1Zr/ Mo-TZM Refluxing Potassium Capsule Test	367
XXXV	Weight Change and Chemistry Data Obtained on Mo-TZM Alloy Insert Specimens from the Condenser Region of a Cb-1Zr Capsule Following Exposure to Potassium for 5000 Hours at 2000°F	369
XXXVI	Results of Chemical Analysis of Cb-1Zr Capsule Following Completion of 5000-Hour, 2000°F Refluxing Potassium Test	370
XXXVII	Residual Gas Analysis Calibration Factors for the Cb-1Zr Rankine System Corrosion Test Loop	389
XXXVIII	Characteristic Curve for W-3Re/W-25Re Based on Vacuum Calibration Data	400
XXXIX	Comparison of Reference Thermocouples and Optical Pyrometer Readings During Thermocouple Wire Calibration in Vacuum	401
XXXX	Cb-1Zr Rankine System Corrosion Test Loop Operation	408
XXXXI	Analysis* of Water Sample Taken from Cooling Channel Exit Line	422
XXXXII	Chemical Analyses of Samples of Type 304L Stainless Steel* from the Top Cooling Channel of the Vacuum Chamber Spool Piece	422

Cb-1Zr RANKINE SYSTEM CORROSION TEST LOOP

by E. E. Hoffman and J. Holowach

I. INTRODUCTION

This report describes the design, fabrication, instrumentation, operation, and evaluation of a Cb-1Zr Rankine System Corrosion Test Loop which was operated for 5000 hours. The purpose of this program was to develop a prototype corrosion test loop system for use in the evaluation of refractory alloys in boiling and condensing potassium environments which simulate projected Rankine systems. The prototype test system consisted of a two-loop Cb-1Zr facility; sodium being heated by direct resistance in the primary loop and used in a heat exchanger (boiler) to boil potassium in the secondary test loop. The method chosen to heat the boiler of the Cb-1Zr Rankine System Corrosion Test Loop was the use of a primary or heater loop in which I^2R[(a)] heated sodium was to be pumped through the outer annulus of a tube-in-tube counterflow boiler where the required heat was to be transferred to the potassium in the secondary, two-phase circuit. One of the principal goals of this test program was to incorporate as many components in tne Cb-1Zr Corrosion Test Loop as required to assure an accurate determination of the test conditions and, thereby, minimize the possibility of undetected test variations; e.g., high-frequency boiling instabilities, which might compromise loop operation or the posttest compatibility evaluation.

In order to assure the optimum performance and reliability of the individual components of the Cb-1Zr Corrosion Test Loop, a plan was established to evaluate as many of the critical loop components as was practical in two preliminary loop tests, the Cb-1Zr Sodium Thermal

(a) I^2R will be used to designate the self-resistance heater in this report.

Convection Loop[1] and the Cb-1Zr Pumped Sodium Loop.[2] These loop tests were designed and operated in a manner to evaluate primarily the critical components associated with the all-liquid heater circuit.

The Cb-1Zr Sodium Thermal Convection Loop was operated for 1000 hours at a maximum temperature of 2380°F with a calculated mass flow of 11 pounds per hour which is equivalent to a flow velocity of 1.3 feet per minute. This earlier test was conducted to obtain a preliminary evaluation of the electrical resistivity characteristics of the heater segment, the method of attaching the heater electrodes, the electrical power vacuum feedthroughs, thermocouple materials and procedures, and the performance of selected thermal and electrical insulation materials.

The Cb-1Zr Pumped Sodium Loop was operated for 2650 hours at a heater outlet temperature of 2050°F with a calculated mass flow of 415 pounds per hour which is equivalent to a maximum flow velocity of 8 feet per second. This loop was considerably more complex than the thermal convection loop described above and was designed to operate at a pump temperature of approximately 2000°F. In addition to evaluating the helical induction EM pump at this relatively high temperature to simulate the requirements of the heater circuit of the Cb-1Zr Rankine System Corrosion Test Loop, this loop was also required to evaluate both slack diaphragm and stressed diaphragm pressure transducers and refractory alloy metering and isolation valves. Of the major components required for the Cb-1Zr Corrosion Test Loop, only the boiler, turbine simulator, and the condenser which operate in either the two-phase or all-vapor phase were not evaluated in the two preliminary loop tests.

The Cb-1Zr alloy was chosen by NASA as the primary containment material for the entire Potassium Corrosion Test Loop Development Program based on its advanced state of commercial development and the indicated

---

(1) Hoffman, E. E. and Holowach, J., Cb-1Zr Thermal Convection Loop, Potassium Corrosion Test Loop Development Topical Report No. 5, R67SD3014, General Electric Company, Cincinnati, Ohio, June 15, 1967.

(2) Hoffman, E. E. and Holowach, J., Cb-1Zr Pumped Sodium Loop, Potassium Corrosion Test Loop Development Topical Report No. 6, R67SD3015, General Electric Company, Cincinnati, Ohio.

corrosion resistance of this alloy to high-purity alkali metal environments. It was anticipated that subsequent to this program, advanced refractory metal alloys having considerably greater high-temperature strengths than Cb-1Zr could be evaluated at significantly higher temperatures in test systems which utilized the proven design and the components evaluated in the Cb-1Zr Rankine System Corrosion Test Loop.

The quarterly progress reports issued during the course of the program and the topical reports describing the various support activities of the program are listed in Section XV of this report.

II. LOOP DESIGN

The primary objective of the Cb-1Zr Rankine System Corrosion Test Loop was to evaluate refractory alloys in boiling and condensing potassium environments which would simulate space electric power systems. This loop would serve as the prototype or reference design for future test loops in evaluating advanced refractory alloys. The design test conditions in the potassium circuit of the Cb-1Zr Test Loop are given below:

Boiling Temperature	1900°F
Superheat Temperature	2000°F
Condensing Temperature	1350°F
Subcooling Temperature	800°F
Potassium, Mass Flow Rate	20 to 40 lb/hr
Vapor Velocity	100 to 150 ft/sec
Average Heat Flux in Potassium Boiler	50,000 to 100,000 Btu/hr ft^2
Test Duration	5000 hours

An isometric drawing of the loop showing the relative position and orientation of the principal loop components is given in Figure 1. The complete list of engineering drawings for Cb-1Zr Rankine System Corrosion Test Loop are included in Appendix A of this report. Reproductions of a number of the principal drawings of the test system are included in Appendix B. The two-loop system consists of a primary sodium heater loop and a secondary potassium boiling and condensing loop.

In the primary circuit, the sodium is discharged from the helical induction electromagnetic pump and flows through an electrical resistance (I^2R) heater to a tube-in-tube counterflow boiler where heat is transferred to the potassium in the secondary circuit. The sodium heater circuit simulates the reactor coolant circuit of a nuclear-powered Rankine system.

In the boiling and condensing secondary loop, the potassium is discharged from the EM pump through a metering valve to an electrical resistance preheater where the temperature of the potassium is increased to near the

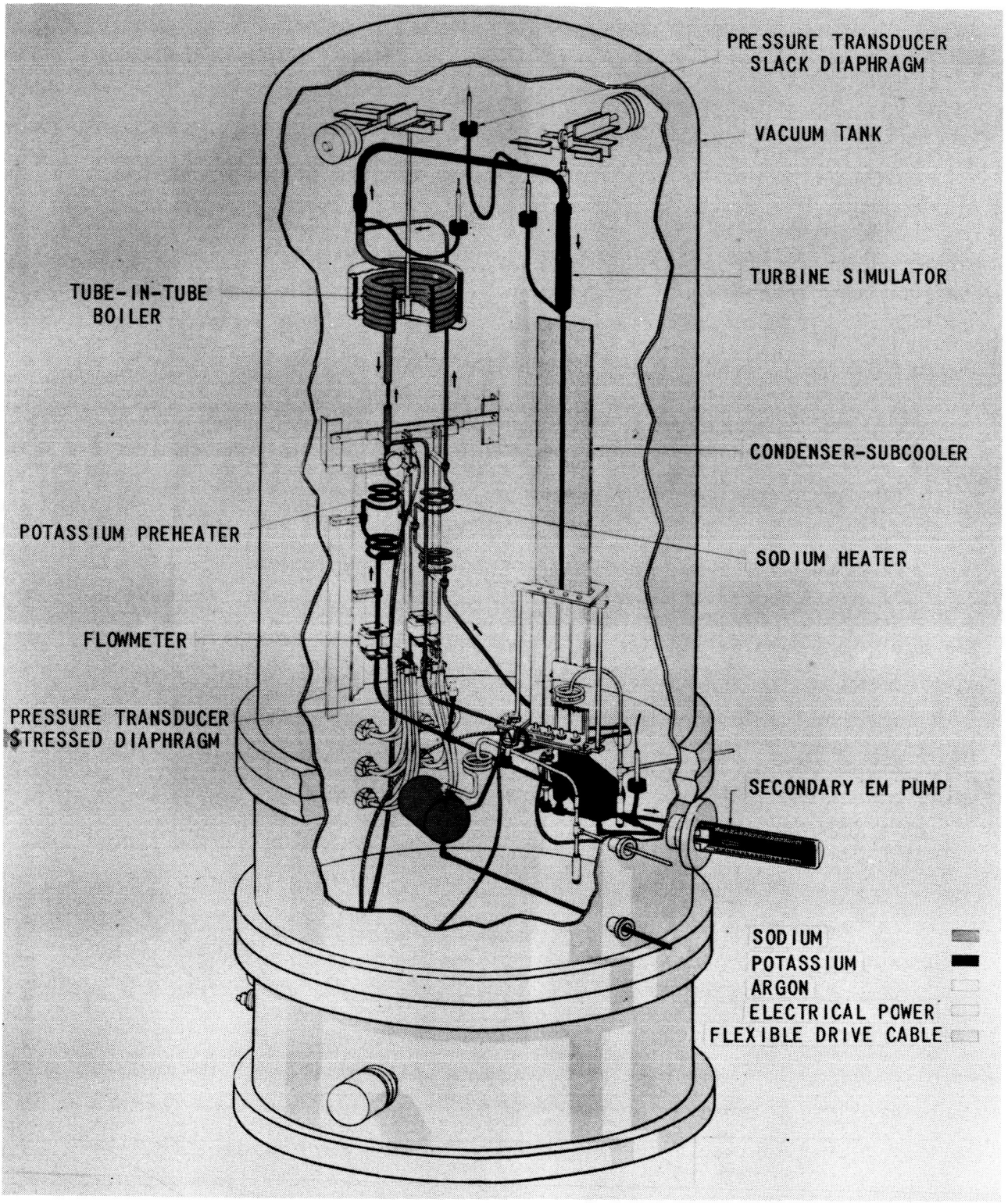

Figure 1. Isometric Drawing of the Cb-1Zr Rankine System Corrosion Test Loop. (Orig. C66011899)

saturation temperature before entering the tube-in-tube counterflow boiler. The potassium is converted from liquid to superheated vapor and passes through the first nozzle and impinges upon the test blade specimen. The superheated vapor passes through a radiation-type heat rejector where the vapor quality is reduced to 88 percent. The wet vapor then passes through stages 2 to 10 of the turbine simulator to a finned-tube radiation-type condenser coated with iron titanate to increase its emittance to >0.86. The condensed vapor returns through the subcooler reservoir to the EM pump. The design test condtions and test loop configuration are illustrated schematically in Figure 2. A description of the various loop components follows.

A. HELICAL INDUCTION ELECTROMAGNETIC PUMPS

The helical induction electromagnetic pumps used in both the sodium and potassium circuits were designed by the Atomic Products Section of the Large Generator and Motor Department of the General Electric Company. The sodium pump was successfully tested in the Cb-1Zr Pumped Sodium Loop[3] for 2650 hours at an inlet temperature of 1985°F. The potassium pump is similar in design and operation to the sodium pump except in the detail design of the helical flow passages of the pump duct and the size of power rating of the stator which were specifically designed for the low-flow, high-head requirements of the potassium circuit.

The pump shown in Figure 3 operates on the principle of the induction motor where three-phase, 60-cycle power in the stator windings produce a two-pole magnetic field revolving at 60 revolutions per second. A pressure head is developed by the interaction of the magnetic field and current which flows as a result of the voltage induced in the liquid metal contained in the pump. The pump duct consists of an outer can and an inner tube with machined helical passages so that the fluid passing through the pump is constrained to flow in a spiral path. The tangential force on the fluid is thus converted into a developed head. The pump will operate in either

(3) Hoffman, E. E. and Holowach, J., Cb-1Zr Pumped Sodium Loop, Potassium Corrosion Test Loop Development Topical Report No. 6, R67SD3015, General Electric Company, Cincinnati, Ohio.

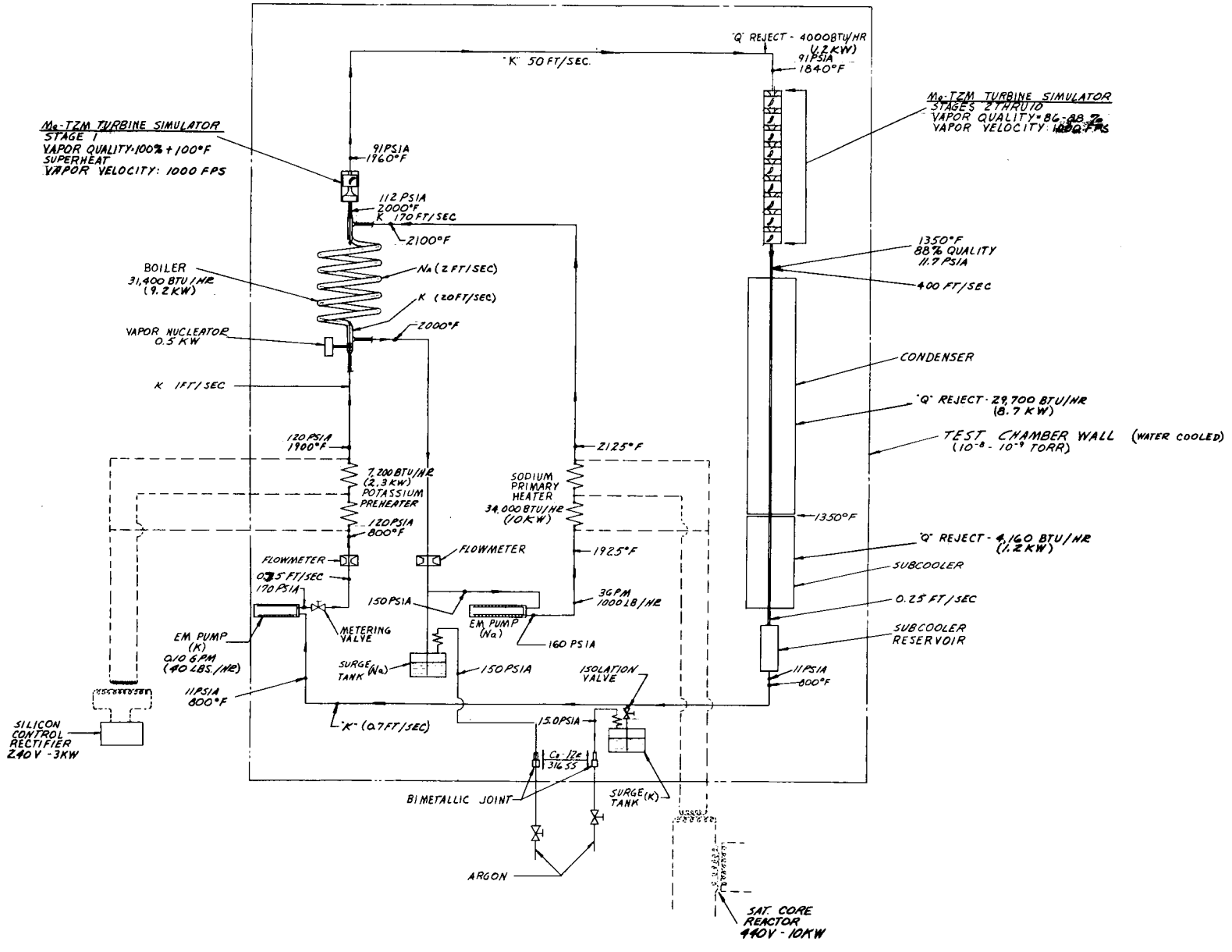

Figure 2. Schematic Diagram of the Cb-1Zr Rankine System Corrosion Test Loop.

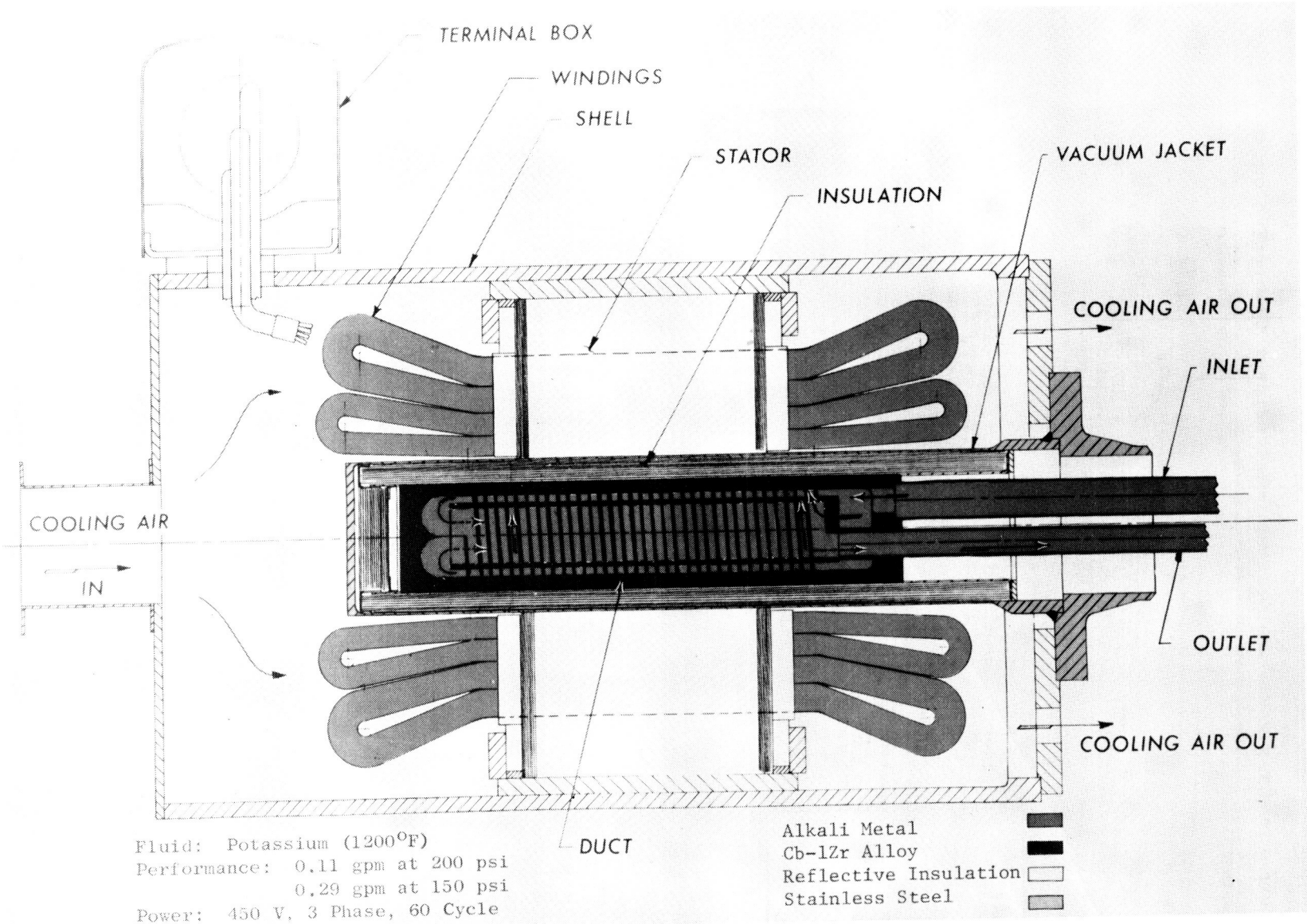

Figure 3. Helical Induction Electromagnetic Pump. (Orig. C65041501)

direction, but it is designed for the fluid to enter the helical annulus and return through the central passage of the inner tube. The outer can is shrink-fitted on the helical fins of the inner tube to prevent leakage between flow passages. Since the inlet and discharge tubes are on the same end of the duct, the pump duct can freely expand into the thermal insulation assembly. The stainless steel can containing the Cb-1Zr alloy reflective foil that thermally insulates the pump duct from the stator windings also serves as the vacuum envelope and is sealed to the main vacuum chamber by welding. The flow rate and pressure head are controlled by varying the applied voltage to the pump winding. The power input and developed pressure at a particular flow vary approximately as the square of the applied voltage.

Cooling air is supplied to the center of the stator bore and around the stainless steel pump can. Each stator tooth has ventilating passages which permit axial flow of cooling air from the center duct through the stator core and into the end turn region. The cooling air passes through the end turns and out the pump to ventilating ports located at each end of the pump. Two copper-constantan thermocouples are located in the end windings to provide a means of monitoring the pump winding temperature during operation. The winding insulation system is Class H which is suitable for operation in temperature to 200°C.

The general information of the potassium and sodium pumps including the pump rating, coolant requirements, and the design characteristics are shown in Tables I and II. The calculated performance of the potassium and sodium pumps is shown graphically in Figures 4 and 5.

TABLE I

GENERAL INFORMATION ON HELICAL INDUCTION ELECTROMAGNETIC PUMP, GENERAL ELECTRIC MODEL NO. 5KY414PF1

Pump Rating		
Fluid	Potassium	1200°F Max
Flow		.116/.29 gpm
Developed Pressure		200/150 psi
Power Supply		480 volts, 3 phase, 60 cycle
Power Input		2.96/2.54 kw
Efficiency		0.3/0.7%
Power Factor	Pump	11.3/11.5%
	System	74.3/75.1%
Coolant Requirements		
Coolant		Air
Coolant Flow		400 cfm
Coolant Inlet Temperature		104°F, Max
Design Characteristics		
Pressure		250 psig
Number of Poles		2
Duty Rating		Continuous
Hot Spot Temperature (Insulation)		400°F
Weight, Less Duct		530 lb

TABLE II

GENERAL INFORMATION ON HELICAL INDUCTION ELECTROMAGNETIC PUMP, GENERAL ELECTRIC MODEL NO. SKY414PB2

Pump Rating		
Fluid	Sodium	2200°F Max
Flow		1.29/5 gpm
Developed Pressure		100/20 psi
Power Supply	480 volts, 3 phase,	60 cycle
Power Input		8.2/9.5 kw
Efficiency		.68/.46%
Power Factor	Pump	10.7/10.4%
	System	95%
Coolant Requirements		
Coolant		Air
Coolant Flow	0.5 pounds per second (400 CFM)	
Coolant Inlet Temperature		104°F, Max
Design Characteristics		
Pressure		335 psig
Number of Poles		2
Duty Rating		Continuous
Hot Spot Temperature (Insulation)		400°F
Weight, Less Duct		530 lb

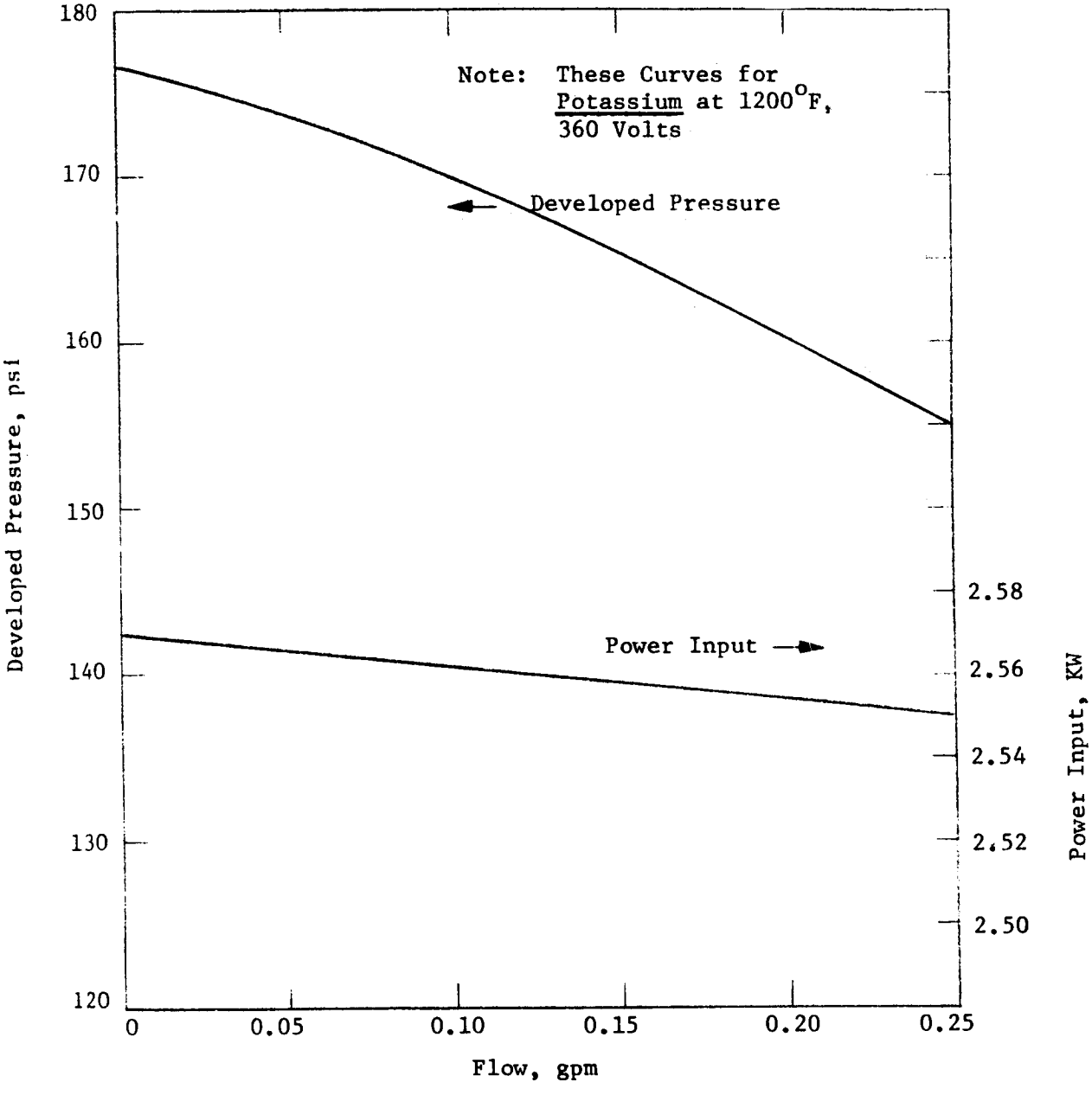

Figure 4. Calculated Pump Performance of General Electric Helical Induction EM Pump Model 5KY414PFI.

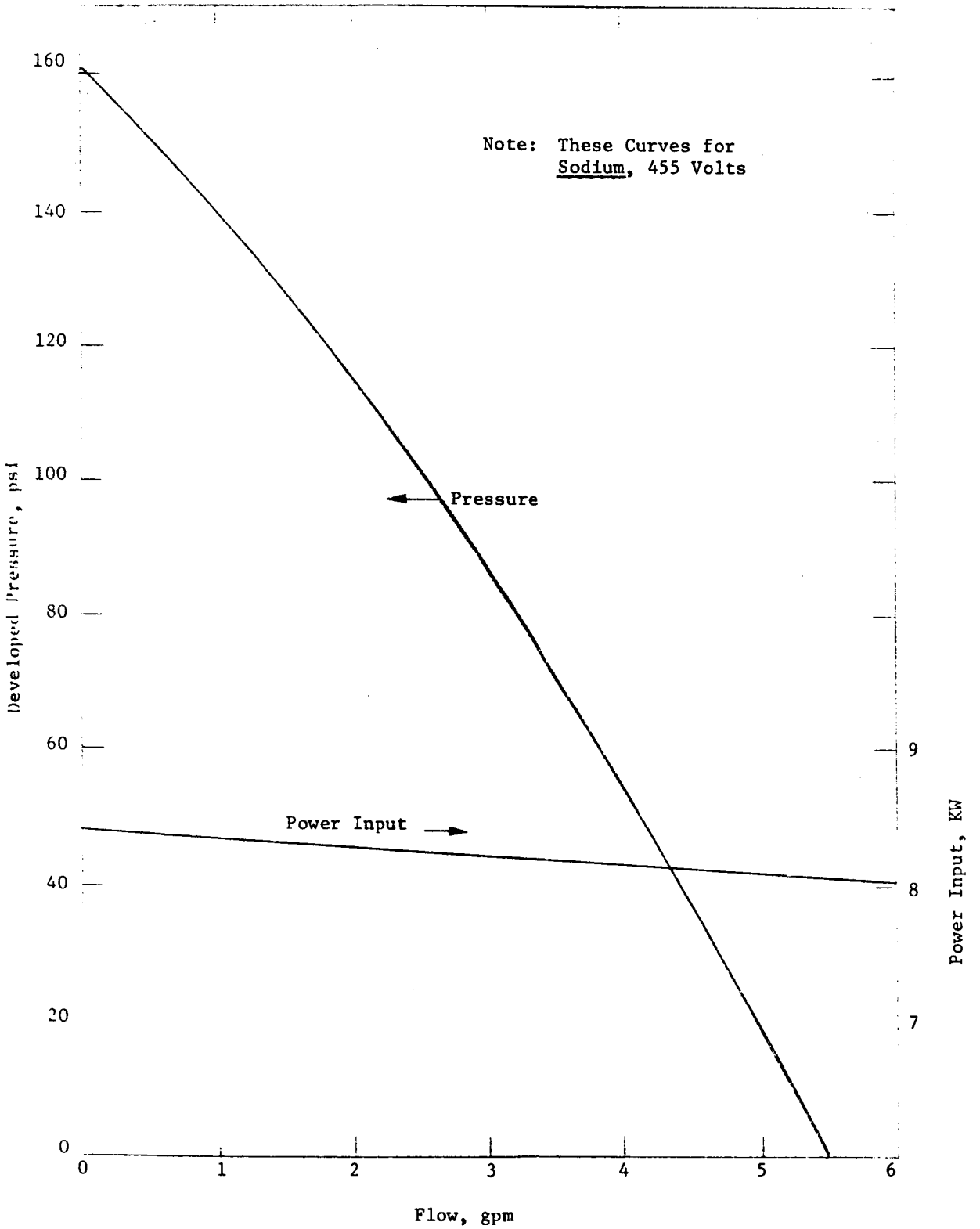

Figure 5. Calculated Pump Performance of General Electric Helical Induction EM Pump Model 5KY414PB2.

B. METERING VALVE

The metering valve selected for the loop was the Hoke, Inc. Model CB-442 valve shown in Figure 6. A similar valve had been successfully tested in sodium for 2650 hours at 800°F in the Cb-1Zr Pumped Sodium Loop. The general design specifications for this valve are as follows:

Type: Bellows seal, manually operated;

Maximum Body Temperature: 1800°F;

Maximum Pressure: 200 psia;

Flow Rate: 0.25 gpm;

Fluid: Potassium or Sodium;

Materials: All parts in contact with process fluid are Cb-1Zr except a molybdenum-TZM alloy plug and plug pin;

Connections: 0.375-inch-OD x 0.065-inch-wall Cb-1Zr tube;

Environment: 1×10^{-8} torr vacuum.

An outline drawing of the valve giving the rating, manufacturing, and quality control specifications is included in Appendix B. G.E.-SPPS's main effort in the design of the valve was in the specification and procurement of materials and the detail design of the welded joints, especially the bellows assembly. The modifications of the valve design to eliminate the galling difficulties in the stem drive system by the substitution of a ball bearing screw nut in place of a threaded bushing were described in detail in Topical Report No. 6.[4]

The operating characteristics of the metering valve with the valve plug shown in Figure 7 were experimentally determined in room temperature flow tests using high-purity nitrogen gas. The manually operated valve has a maximum plug lift-off of 0.125 inch and is operated by a threaded stem in a ball bearing screw nut having a pitch of 0.125 inch. The lift-off is equal to 0.001 inch for each three degrees of rotation of the valve stem. Therefore, the first 30-40° of rotation, equivalent to 0.010-0.015-inch lift-off, is required to lift the plug sufficiently to raise the cylindrical section above the taper from the orifice. The 75° included angle tapered section is essentially the control surface. The remaining 95° of rotation

(4) Hoffman, E. E. and Holowach, J., Cb-1Zr Pumped Sodium Loop, Potassium Corrosion Test Loop Development Topical Report No. 6, R67SD3015, General Electric Company, Cincinnati, Ohio.

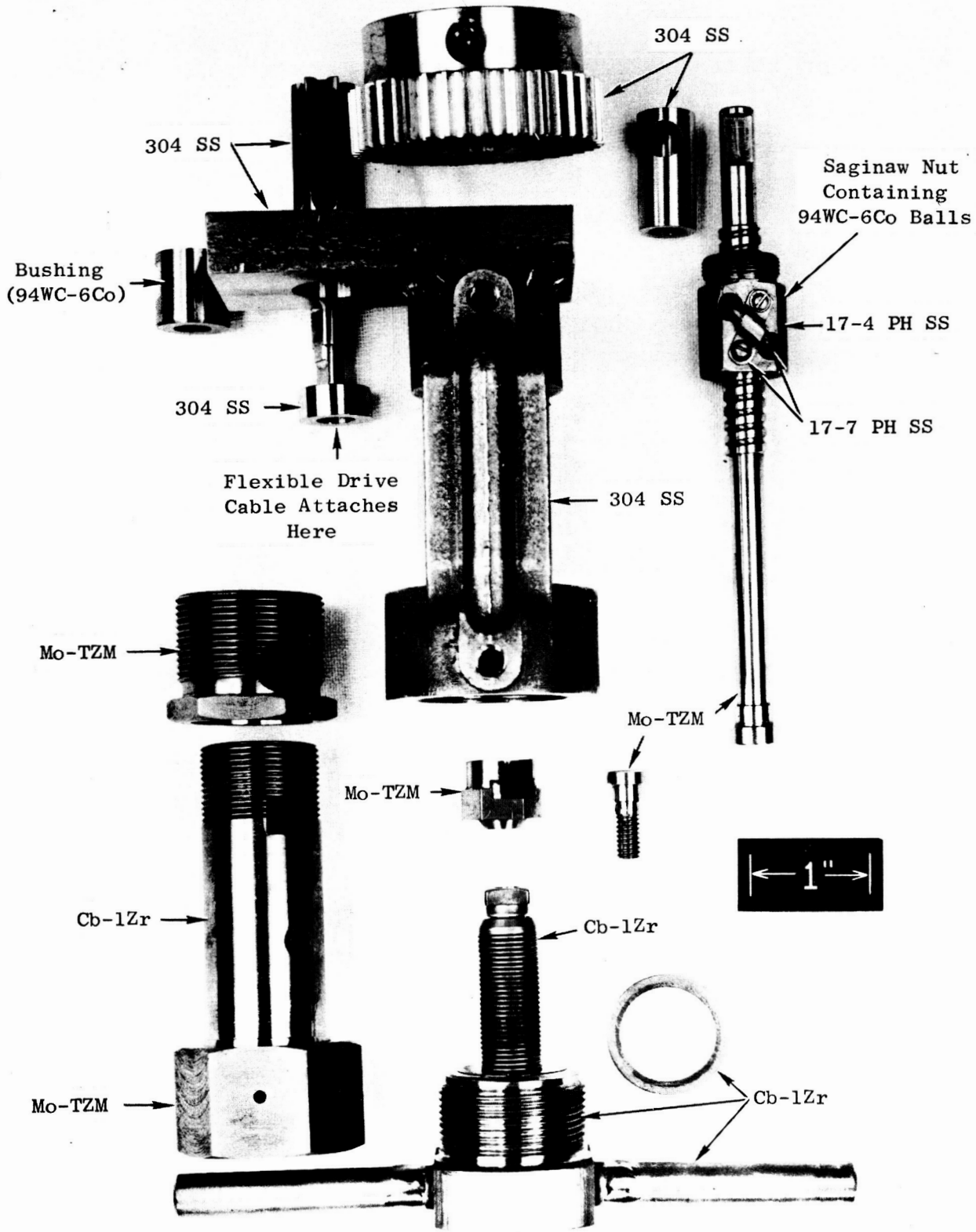

Figure 6. Modified Hoke Valve and Associated Drive Components for the Cb-1Zr Rankine System Corrosion Test Loop. (Orig. C65032923)

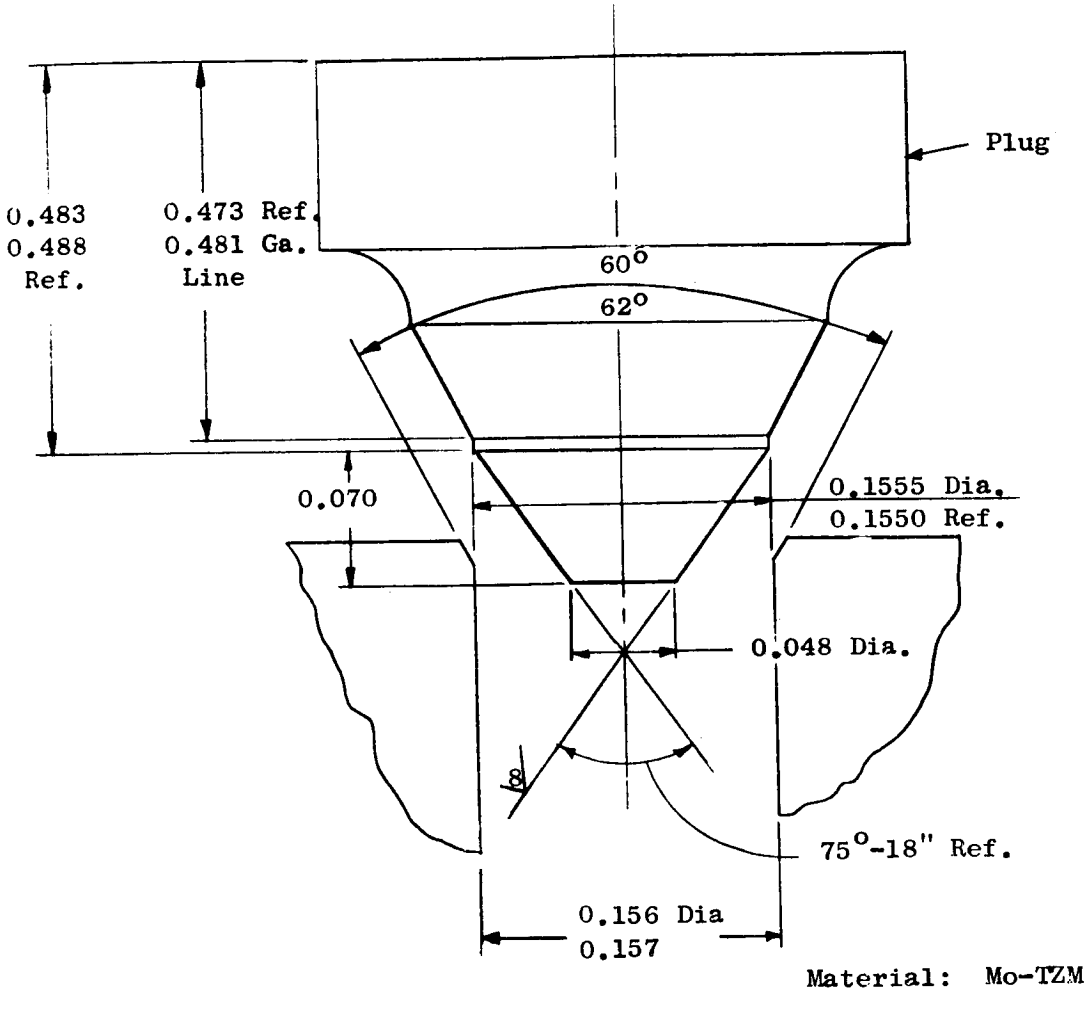

Figure 7. Detail of Metering Valve Plug Body Bore and Port for the Cb-1Zr Rankine System Corrosion Test Loop.

equivalent to 0.033-inch lift-off, increases the gap between the base of the plug and the seat until the flow area of the gap is approximately equal to the area of the 5/32-inch orifice.

The results of the flow test on the metering valve are shown in Figure 8 for nitrogen gas with pressure losses of 1, 2, and 4 psi utilizing an atmospheric discharge. The metering zone can be seen to extend from approximately 30° to 230° of rotation.

Flow coefficients based on the flow test were computed for the full range of valve plug lift-off as a function of rotation. The flow coefficient computed for gases is essentially equivalent to liquid having viscosities equal to or less than water. The pressure drop as a function of rotation was then computed for potassium at the loop test condition of 40 lb/hr at 800°F and is shown in Figure 9.

These results indicate that control of potassium flow in the secondary circuit can be achieved in the pressure loss range of 1 to 50 psi; however, the control in the 10 to 50 psi range is very sensitive to small changes in the plug position.

The valve design was modified by G.E.-SPPS so that the valve could be manually operated from outside the vacuum chamber. The actuation system consisted of an ultrahigh vacuum, rotary, magnetic feedthrough connected by a flexible, stainless steel shaft to a 3 to 1 right angle gear drive mounted on the valve yoke. The right angle gear drive is required to eliminate a compound bend in the flexible shaft since the rotary feedthrough is located below the valve. The magnetic rotary feedthrough for the metering valve is shown in Figure 10. This feedthrough transmits torque into a vacuum chamber by magnetic coupling between an external multipole magnet and an internal rotor having the same number of poles. The thin-walled rotor housing of nonmagnetic stainless steel constitutes an all-metal, leak-tight vacuum wall. Both the rotor and the external magnet are mounted on ball bearings for low friction operation.

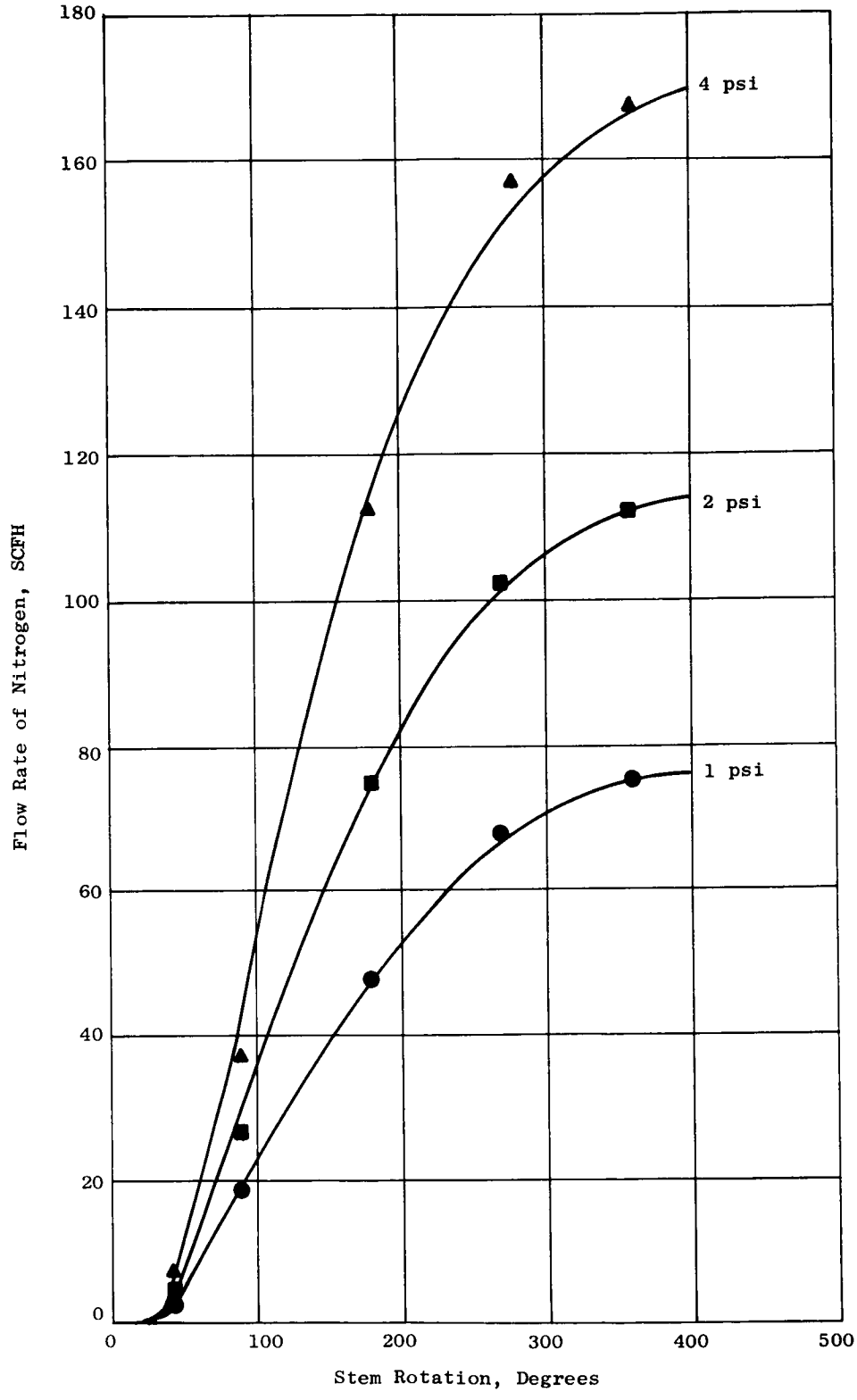

Figure 8. Flow Rate for the Cb-1Zr Corrosion Test Loop Metering Valve as a Function of Stem Rotation for 1, 2 and 4 psi Pressure Drop Across the Valve.

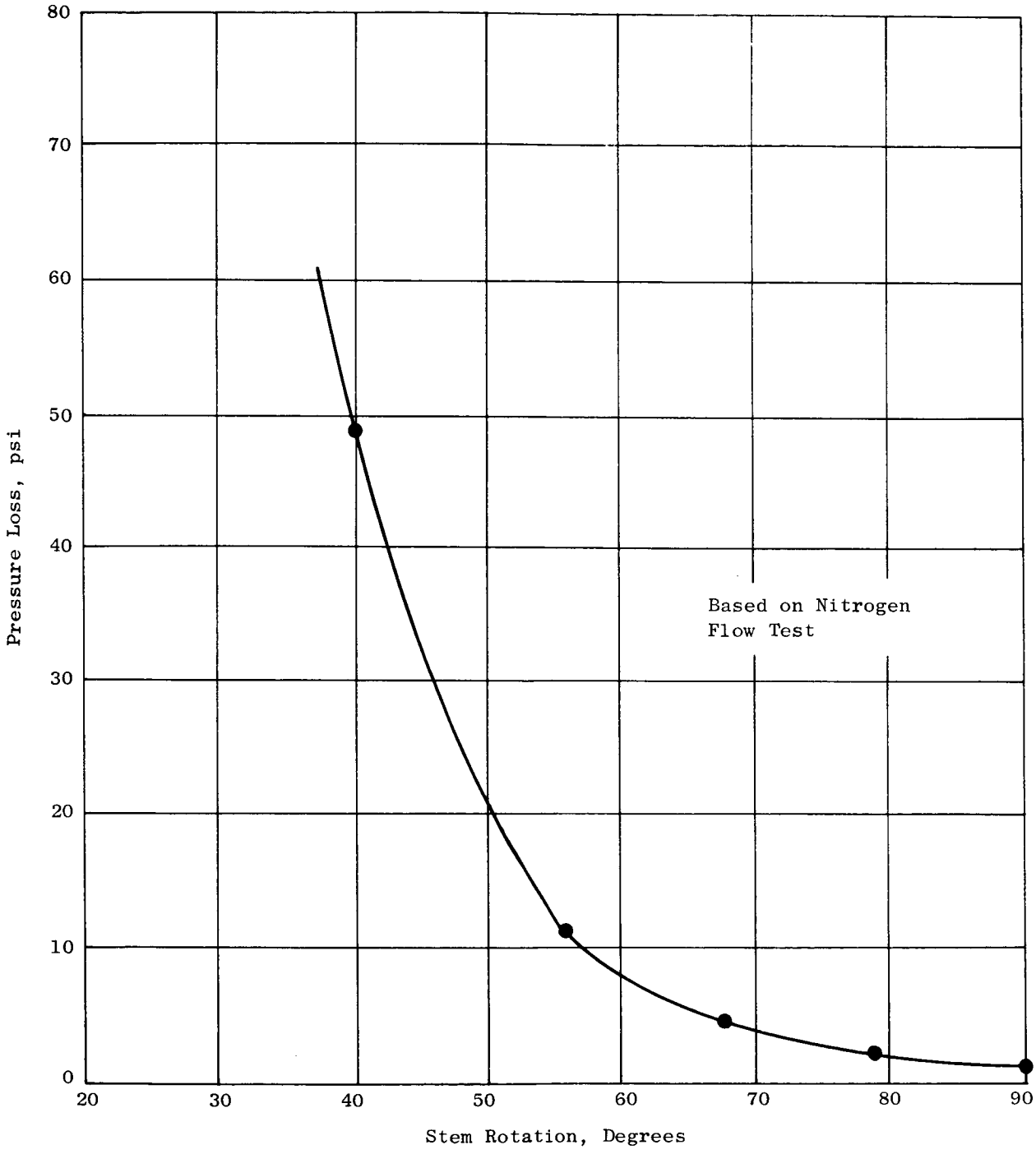

Figure 9. Cb-1Zr Corrosion Test Loop Metering Valve Pressure Loss as a Function of Stem Rotation for a Potassium Flow Rate of 40 Pounds Per Hour at 800°F.

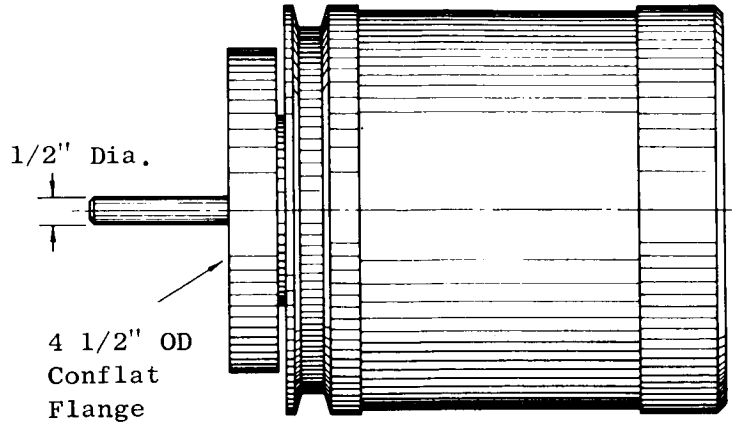

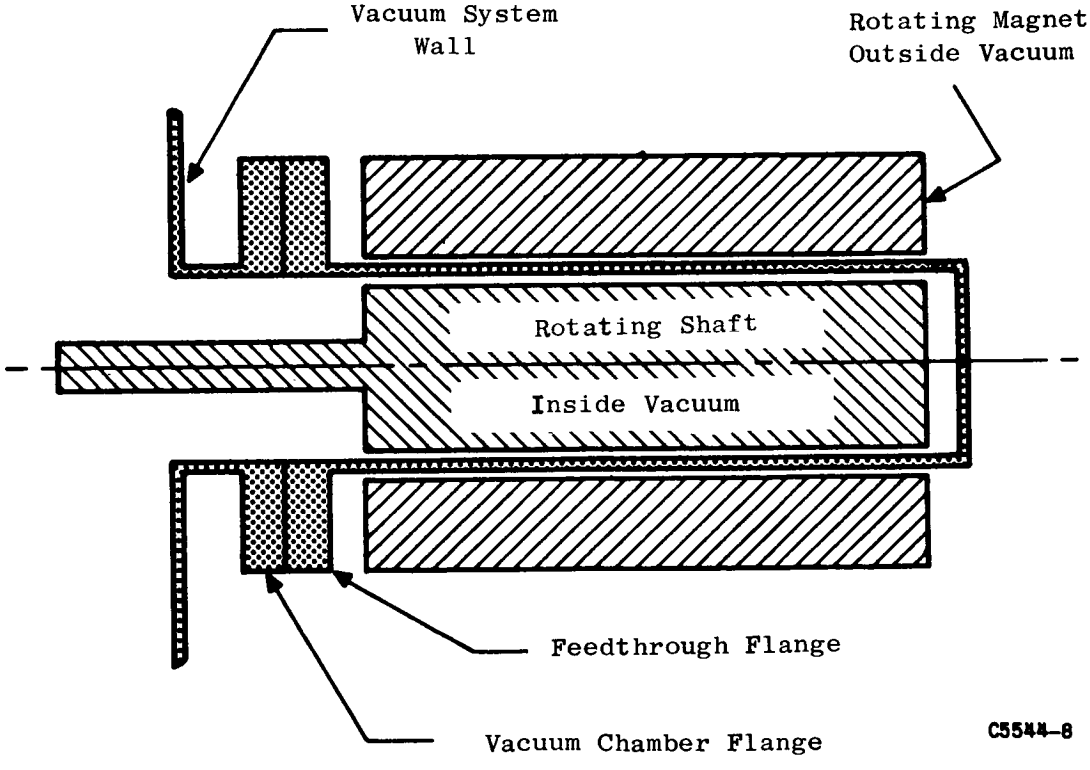

Figure 10. Outline Drawing and Schematic Drawing of Magnetic Rotary Feedthrough. Varian Associates Model No. 954-5039

C. POTASSIUM PREHEATER

The potassium preheater is similar in design to the sodium heater successfully tested in the Cb-1Zr Pumped Sodium Loop. The preheater is used to heat the liquid potassium to near its saturation temperature before it enters the bubble nucleator and the boiler. The preheater is also used to calibrate the potassium flowmeter by the calorimetric method. Since the flow rate is more critical to the operation of the potassium circuit than in the sodium circuit, a greater emphasis is made to minimize heat losses to improve the accuracy of the calorimetric calibration. The electrodes were lengthened from 3.5 inches to 5.75 inches. Two 0.5-inch-diameter holes were specified for each of the preheater electrodes. The holes were to act as thermal dams and reduce conductive heat losses along the electrodes.

The power required to preheat the 40-lb/hr of potassium from 800°F to 1900°F is 2.57 kw which is considerably less than the 6.75 kw used in the sodium heater of the Cb-1Zr Pumped Sodium Loop. The power leads to the preheater electrodes were connected so that the power input to the upper or lower coil could be measured independently. Thermocouple wells were added at the end of each coil so that the temperature rise and the power input to each coil could be obtained from the thermal balance.

D. VAPOR BUBBLE NUCLEATOR

Numerous investigations of corrosion phenomenon in boiling alkali metal test systems have reported operational difficulties resulting from unstable or discontinuous boiling. A discussion of these difficulties, which in many cases have resulted in system failures due to thermal fatigue, has been published together with a discussion of a vapor nucleation device which had eliminated these instabilities.[5] Subsequent investigators

---

(5) Hoffman, E. E., "Boiling Potassium Stability Studies," Metal and Ceramic Division Annual Progress Report for Period Ending May 31, 1963, ORNL-3470, November 11, 1963, p. 114-118.

have provided additional confirmation of the effectiveness of various nucleation devices which produce local hot spots on the boiler walls. These hot spots generate vapor bubbles which in turn prevent the accumulation of large amounts of superheat in the bulk liquid. The flashing of large volumes of superheated liquid into vapor results in unstable or discontinuous boiling. Boiling potassium systems at the Oak Ridge National Laboratory[6] and boiling mercury systems at Brookhaven National Laboratory[7] have been stabilized by means of hot-spot vapor bubble nucleators.

A vapor bubble nucleator of this type was added to the loop in the event that the loop was unstable and could not be stabilized by normal loop operations such as throttling the potassium flow rate with the metering valve or adjusting the power input to the sodium heater or potassium preheater. The reliability and the ease of installation of the vapor nucleator warranted its addition during the initial assembly of the loop even though its need could not be determined until the loop was operated. The nucleator was designed with its own power supply and temperature control so that it could be operated independently of the other loop components.

The vapor nucleator is shown in Figure 11. It consists of a radiantly heated heat lens welded to the boiler inlet. A small-diameter cavity in the base of the nucleator is the vapor bubble generator; the diameter of the cavity regulates the size of the bubble generated, and the power input to the nucleator controls the frequency of bubble injection into the liquid potassium. The nucleator must operate several hundred degrees higher than the saturation temperature of the potassium to generate a steady stream of small-diameter bubbles. The entire heater assembly is well insulated with multiple layers of Cb-1Zr foil to minimize heat losses

(6) Private Communication, R. E. MacPherson, Oak Ridge National Laboratory.

(7) Private Communication, C. J Klamut, Brookhaven National Laboratory.

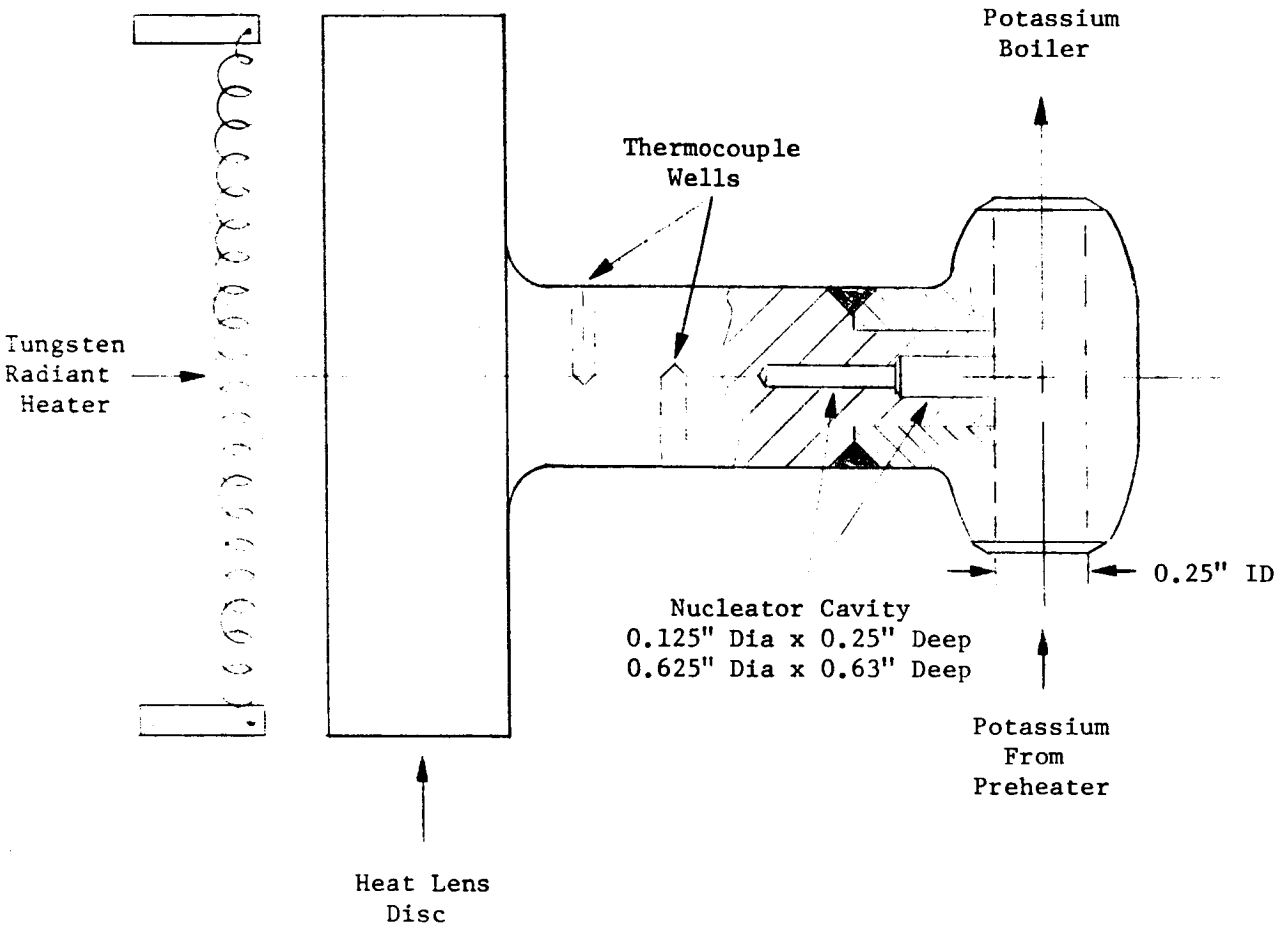

Figure 11. Schematic Drawing of the Vapor Nucleator.

from the heater during its operation and to prevent the formation of a cold spot at the boiler inlet if the nucleator is inactive.

E. POTASSIUM BOILER

A coiled tube-in-tube, counterflow boiler design was selected for the Cb-1Zr Corrosion Test Loop since it closely simulates one type of an advanced Rankine cycle space power system boiler, and the coiled configuration accommodated the desired boiler length within the 4-foot-diameter x 11-foot-high vacuum chamber. Also, the tube-in-tube boiler approach is desirable in material evaluation tests where both the primary and secondary circuit materials can be tested and evaluated simultaneously.

The purpose of the boiler is to convert 40 pounds per hour of liquid potassium at 1900°F to 2000°F vapor having 100°F superheat. The tube-in-tube boiler consists of a 0.375-inch-OD x 0.065-inch-wall center tube for containing the potassium and a 1.00-inch-OD x 0.100-inch-wall outer tube with sodium flowing in the 0.21-inch annulus. The length of the boiler was determined by simultaneously solving the heat transfer and pressure loss equations for the sodium and potassium circuits.[8]

1. Heat Transfer. The expression for differential heat transfer rate may be written in terms of quality as:

$$\frac{dL}{dX} = \frac{\pi D_i H_{fg} G_K}{4U_i (T_{Na} - T_K)} \quad (1)$$

where U_i = overall heat transfer coefficient for the length dL.

For a counterflow boiler, the sodium temperature distribution may be represented as a function of quality by:

$$T_{Na} = T_{Na_{in}} - \frac{(X_{out} - X)\pi D_i G_K H_{fg}}{4W_{Na} C_{PNa}} \quad (2)$$

(8) Tippets, F. E., Alkali Metal Boiling and Condensing Investigations, Report No. 5, NASA Contract NAS 3-2528, General Electric Company, Cincinnati, Ohio, April 20, 1964, p. 12.

* Nomenclature used in the design calculations are listed in Appendix C.

For conservative lengths calculations, the potassium temperature may be assumed constant and equal to the inlet saturation temperature. This assumption yields the lowest thermal driving force, and hence, the most conservative estimate of surface area requirements. If it is postulated that the overall heat transfer coefficient is essentially constant over a given quality interval, Equation (1) may be integrated, after substitution for the sodium temperature distribution. The result for a quality interval X, to X_2 is then:

$$L_{\Delta X} = \frac{(WC_P)_{Na}}{\pi D_i U_i} \ln \left[\frac{4(WC_P)_{Na}(T_{Na_{in}} - T_{K_{in}}) - \pi D_i^2 G_K H_{fg}(X_{out} - X_2)}{4(WC_P)_{Na}(T_{Na_{in}} - T_{K_{in}}) - \pi D_i^2 G_K H_{fg}(X_{out} - X_1)} \right] \quad (3)$$

The total length of the boiler may then be expressed in terms of the inlet saturation temperature as:

$$L_{(X_{in} \text{ to } X_{out})} = \frac{(WC_P)_{Na}}{\pi D_i} \int_{X = X_{in}}^{X = X_{out}} \frac{1}{U_i} \ln \left[\frac{4(WC_P)_{Na}(T_{Na_{in}} - T_{K_{in}}) - \pi D_i^2 G_K H_{fg}(X_{out} - X_2)}{4(WC_P)_{Na}(T_{Na_{in}} - T_{K_{in}}) - \pi D_i^2 G_K H_{fg}(X_{out} - X_1)} \right] \quad (4)$$

2. Pressure Drop. The boiler length may also be expressed in terms of the inlet saturation temperature by means of the pressure drop relationship. The total pressure drop is composed of the friction pressure drop and the momentum pressure drop. Two options are available for estimating the two-phase friction pressure drop.

1. The pressure drop may be computed assuming the flow of 100% vapor.
2. The pressure drop may be computed using an "integrated average" Martinelli multiplier on the all-liquid pressure drop.

The former method is expected to give a more conservative answer in cases in which the quality goes from zero to 1.0. The momentum pressure drop is based on the so-called "homogeneous model," where the ratio between

liquid and vapor phase velocities is 1. This assumption yields a maximum value for the momentum pressure drop. The defining equations then are:

$$L_{\Delta P} = \frac{\bar{\rho}_g g_o D_i}{2fG_K^2} \left\{ (P_{K_{in}} - P_{K_{out}}) - \frac{G_K^2}{g_o \rho_L} \left[(1-X_{out}) + X_{out} \left(\frac{\rho_L}{\rho_g} \right) - 1 \right] \right\} \quad \text{(5)}$$

Gas Phase ΔP Friction

$$L_{\Delta P} = \frac{\bar{\rho}_L g_o D_i}{2fG_K^2 \phi} \left\{ (P_{K_{in}} - P_{K_{out}}) - \frac{G_K^2}{g_o \rho_L} \left[(1-X_{out}) + X_{out} \left(\frac{\rho_L}{\rho_g} \right) - 1 \right] \right\} \quad \text{(6)}$$

Two-Phase ΔP Friction

where ϕ = Integrated Average Martinelli Multiplier

$$\phi = \frac{1}{(X_{out} - X_{in})} \int_{X_{in}}^{X_{out}} \frac{\left(\frac{dP}{dL} \right)_{TPF} dX}{\left(\frac{dP}{dL} \right)_L}$$

$$\& \quad P_{K_{in}} = P_{K_{in}} (T_{K_{in}})$$

The required tube length and inlet saturation temperature may now be determined by simultaneous solution of Equations (4) and (5) or Equations (4) and (6), depending on the option chosen for computing the friction pressure drop. As indicated by the equations, the calculation is necessarily of an "iterative" nature; vis, inlet saturation temperatures are assumed until the lengths computed by the heat transfer and the pressure drop equations are equal.

The following assumptions were made in determining the boiler length.

a. In the region from zero to 70 percent quality, the overall resistance to heat transfer was taken as 115 percent of the sodium resistance and the wall resistance. These assumptions yield overall heat transfer of the same magnitude as those obtained in the 300 KW Heat Transfer Facility.[9, 10]

(9) Alkali Metals Boiling and Condensing Investigation, Quarterly Progress Report No. 4, NASA Contract NAS 3-2583, SPPS, MSD, General Electric Company, July 1963.

(10) Alkali Metals Boiling and Condensing Investigations, Quarterly Progress Report No. 6, NASA Contract NAS 3-2583, SPPS, MSD, General Electric Company, May 1964.

b. Limited experimental data are available in the region from 70 to 100 percent quality. In order to obtain a conservative estimate of the required length, the heat transfer coefficient for the potassium vapor region was assumed to be that given by the conventional gas phase forced convection expression; vis. $Nu = 0.021\ Re^{0.8}Pr$. The sodium and wall resistances were negligible compared to the potassium vapor resistance.

c. The differential rate expression for the heat transfer was based on a constant temperature level in the secondary fluid. The temperature level was assumed to be the inlet saturation temperature, thus yielding the lowest driving force.

d. The friction component of the pressure drop was based on the flow of 100 percent quality vapor along the entire tube where the friction factor, $f, = 0.079\ Re^{0.25}$

3. Calculated Performance. The results of the calculations are shown in Table III for sodium inlet temperature of 2100°F, 2150°F, and 2200°F. As indicated in the table, the shortest boiler length was obtained with a sodium inlet temperature of 2200°F and a sodium flow rate of 0.1098 lb/sec. In this case, two values of sodium heat transfer coefficient were used (5000 Btu/ft^{2}hr°F and 3000 Btu/ft^{2}hr°F). The latter value is felt to be more representative based on liquid sodium heat transfer data from the 50 and 100 KW Heat Transfer Facility. These data indicate that the Nusselt number continues to drop as the Peclet number becomes less than 100. The sodium heat transfer coefficient of 3000 Btu/ft^{2}hr°F corresponds to a Nusselt number of 3.5.

The maximum heat flux occurs in the region of zero to 70 percent quality. The average heat flux in this section is tabulated in Table III and ranges from 406,000 Btu/ft^{2}hr at 2100°F sodium inlet temperature to 187,000 Btu/ft^{2}hr at a 2200°F sodium inlet temperature. It is desirable to keep the heat flux as low as is practical to avoid film boiling. The relative advantages of a high sodium inlet temperature and a low sodium flow rate are apparent in this respect. The maximum heat flux of 475,000

TABLE III

CALCULATED BOILER LENGTH REQUIRED FOR VARIOUS SODIUM FLOW RATES AND INLET TEMPERATURES FOR Cb-1Zr RANKINE SYSTEM CORROSION TEST LOOP

$T_{Na_{in}}$, °F	$T_{K_{in}}$, °F	w_{Na}, lb_m/sec	Pe_{Na}	L_{total}	Lengths, in. $L_{0-70\%}$	$L_{70-100\%}$	$L_{superheat}$	L_{insert}	q/A (average) $Btu/ft^2 hr \times 10^{-5}$
*2100	1938	0.485	244	221	10	193	18	2.52	4.06
*2150	1929	0.29	146	171	8	149	14	2.04	5.13
*2150	1930	0.1945	97.8	178	11	153	14	3.08	3.96
*2150	1933	0.15	75.5	195	16	165	14	6.17	2.60
**2150	1934	0.15	75.5	203	22	167	14	8.44	1.91
*2200	1927	0.1098	55.2	159	17	131	11	7.81	2.50
**2200	1928	0.1098	55.2	166	22.5	132	11	9.75	1.87

*h_{Na} = 5000 $Btu/ft^2 hr°F$

**h_{Na} = 3000 $Btu/ft^2 hr°F$

Btu/ft^2-hr occurs at a length of 22.5 inches from the boiler inlet. This is the location at which film boiling was assumed to start.

The required lengths for 100°F superheat are also shown in Table III. They vary from 11 inches at sodium inlet temperature of 2200°F to 18 inches at a sodium inlet temperature of 2100°F.

4. Flow Swirling Insert. A flow swirling insert was added to the boiler inlet to increase the heat transfer rate in the low-quality region of the boiler and to improve the stability of the loop by adding a fixed resistance at the boiler inlet. The insert length given in Table III for various sodium inlet temperatures is the calculated distance from the boiler inlet to the point where the vapor quality has increased to 15 percent. The effect of adding an insert on the performance of the boiler was not included in the calculations. Therefore, if the insert did increase the heat transfer rate, the exit quality from the insert section would be greater than 15 percent.

The insert configuration selected consisted of a 1/16-inch-diameter wire wrapped around a 1/8-inch center rod with a one-inch pitch. The one-inch pitch was selected after room temperature air pressure loss tests. The results of the air flow test for 1/2-inch, 1-inch, and 2-inch pitch inserts are given in Appendix D.

The length of the boiler was selected as 244 inches including the swirl section. This length could be compactly formed into an eight-turn, ten-inch-diameter helical coil. The potassium center tube was held concentric to the outer tube by triform spacers located at ten-inch intervals along the boiler length and by an elaborate forming sequence described in detail in Section IV, Fabrication, of this report.

F. TURBINE SIMULATOR

In a Rankine cycle space power system, operating on potassium vapor, it is expected that some or all of the turbine stages will operate in the wet vapor region for 10,000 hours or more. Materials specified for turbine components must be corrosion resistant to the vapor and resistant to droplet impact erosion if the design life of the power conversion system is to be achieved.

The high strength-to-density ratio of Mo-TZM alloy and the indicated corrosion resistance of the alloy to alkali metals dictated the selection of this material for evaluation as nozzle and blade specimens in the Cb-1Zr Corrosion Test Loop. Only limited corrosion testing of molybdenum and its alloys in liquid potassium had been conducted, and even less data existed on the results of exposure to refluxing potassium. Tests of Mo-TZM alloy in refluxing potassium at Battelle Memorial Institute[11] revealed mass transfer of molybdenum under certain test conditions. As a result of the lack of definitive information regarding the corrosion resistance of molybdenum to potassium under conditions similar to those anticipated in the Cb-1Zr Loop, two capsule tests were conducted. The results of these tests, which were conducted for time periods of 2500 and 5000 hours, are described in detail in Appendix E and indicated that Mo-TZM alloy has excellent resistance to refluxing potassium at 2000°F. The results obtained on the Mo-TZM alloy nozzle and blade specimens in the Cb-1Zr Corrosion Test Loop were anticipated to supplement those which would be obtained in the two-stage potassium turbine test.[12]

The design objective of a turbine simulator is to simulate rotating turbine buckets operating in a wet vapor with a stationary blade test where high velocity vapor impinges on the surface of the stationary blade. The turbine simulator was designed to operate at test conditions even more severe than those given above to accelerate the erosion damage. These test conditions are listed below:

1. Turbine inlet: 2000°F potassium vapor with 100°F superheat
2. Vapor quality: Stage 1, 100°F superheat; Stages 2-10, 86-88%
3. Vapor velocity: 1000 fps for all stages
4. Turbine outlet temperature: 1350°F

The basic assumption in the design of the turbine simulator is that wet potassium expands through the nozzle in a supersaturated condition and then reaches equilibrium conditions in the expansion zone and downstream of the nozzle. The nozzle exit or equilibrium pressure is calculated for a design exit velocity of 1000 fps for a known inlet pressure. The equation[13] relating the vapor velocity in a nozzle for either superheated

(11) AEC-NASA Liquid Metals Information Meeting, CONF-650411, 1965, p. 237.

(12) Rossbach, R. J., Space-Vehicle Rankine Cycle Power Plant Potassium-Turbine Development, ASME 63-WA-326, November 1963.

(13) Faires, V., Applied Thermodynamics, The MacMillan Co., New York, 1947, p. 351.

or supersaturated vapor to the inlet and exit pressure (for negligible inlet velocity) is:

$$V_s = \left\{ \frac{e_n 2gnP_1V_1}{1-n} \left[\left(\frac{P_2}{P_1} \right)^{\frac{n-1}{n}} - 1 \right] \right\}^{1/2}$$

The equilibrium properties of the potassium vapor can be found in the vapor property tables.[14] These properties are then used in calculating the next stage. The process is repeated until the exit vapor temperature is equal to the specified turbine exit temperature. In the present design, ten stages are required to reduce the vapor temperature to 1350°F from an inlet temperature of 2000°F with 100°F superheat.

The throat area of each nozzle can be calculated from the continuity of mass equation,

$$A_t = \frac{W V_t}{V_s}$$

where, V_t, the volume of the superheated or supersaturated vapor at the nozzle throat can be estimated from

$$V_t = V_1 \left(\frac{P_1}{P_2} \right)^{1/n}$$

The calculated vapor temperature and pressure for each stage of the turbine simulator are given in Table IV. The throat diameters given in Table IV are the room temperature diameters adjusted for the thermal expansion from the turbine operating conditions and then decreased in size by an additional 5 percent to account for uncertainties in the calculation and vapor properties. The reduction was made since no adjustments can be made in the performance of the turbine simulator after fabrication and the operation of the boiler, condenser, and heater are sized to the design flow rate and a higher than design flow rate could exceed their operating capabilities.

(14) Ewing, C. T., Stone, J. P., Spann, J. R., Steinkuller, E. W., Williams, D. D., and Miller, R. R., High-Temperature Properties of Potassium, NRL Report 6233, September 24, 1965.

TABLE IV

TURBINE SIMULATOR DESIGN

Stage Number	Inlet Temperature °F	Inlet Pressure psia	Quality Percent	Nozzle Throat Diameter, Inches
1	2000	113.7	100°F Superheat	0.100
2	1837	91.7	86-88	0.101
3	1770	73.2	86-88	0.116
4	1708	58.4	86-88	0.129
5	1656	46.9	86-88	0.142
6	1600	37.3	86-88	0.159
7	1549	29.8	86-88	0.176
8	1494	23.5	86-88	0.206
9	1447	18.5	86-88	0.222
10	1399	14.5	86-88	0.250

In the turbine simulator, the vapor in each stage undergoes a throttling process which is an irreversible adiabatic process with no work being done. In a throttling process high-quality vapor becomes superheated or for the case of low-quality vapor, the quality will increase. In the present design, if no heat is removed during the throttling process, the vapor quality would increase from 88 percent to 92 percent. To maintain the inlet quality to each stage at 88 percent, heat must be rejected between each stage. An interstage cooler would be expensive and difficult to design for the space available in the vacuum chamber. A compromise solution with heat rejected along the entire length of the turbine simulator was used. The total heat rejection required to maintain the vapor at 88 percent quality is equal to the enthalpy change from 88 to 92 percent quality or 30 Btu/lb or 1200 Btu/hr for 40 lb/hr of potassium. This quantity of heat can be rejected from the turbine simulator by radiation if only one thermal shield of Cb-1Zr foil is used, and an emittance of 0.2 is assumed.[15]

The modified thermodynamic process is shown on a Mollier diagram for potassium in Figure 12. A supersaturated expansion process can not be properly shown on a Mollier diagram since it represents equilibrium state points, therefore dashed lines are used to connect the equilibrium points at the inlet and exit of each stage.

G. CONDENSER AND SUBCOOLER

Several condenser and subcooler design configurations were considered before a radiating finned tube condenser was selected. Although both condensing and subcooling occur in this unit, it will be referred to as the condenser to facilitate the discussion. The primary requirement of the design was to condense 40 lb/hr of 88 percent quality potassium vapor at 1350°F. It was also desirable to have a high vapor velocity and condensing rates approximating the operating conditions of an advanced space power alkali metal condenser.

---

(15) Dotson, L. E., Emittance Coating Studies on Cb-1Zr Alloy, General Electric Company Report, R61FPD571, March 15, 1962.

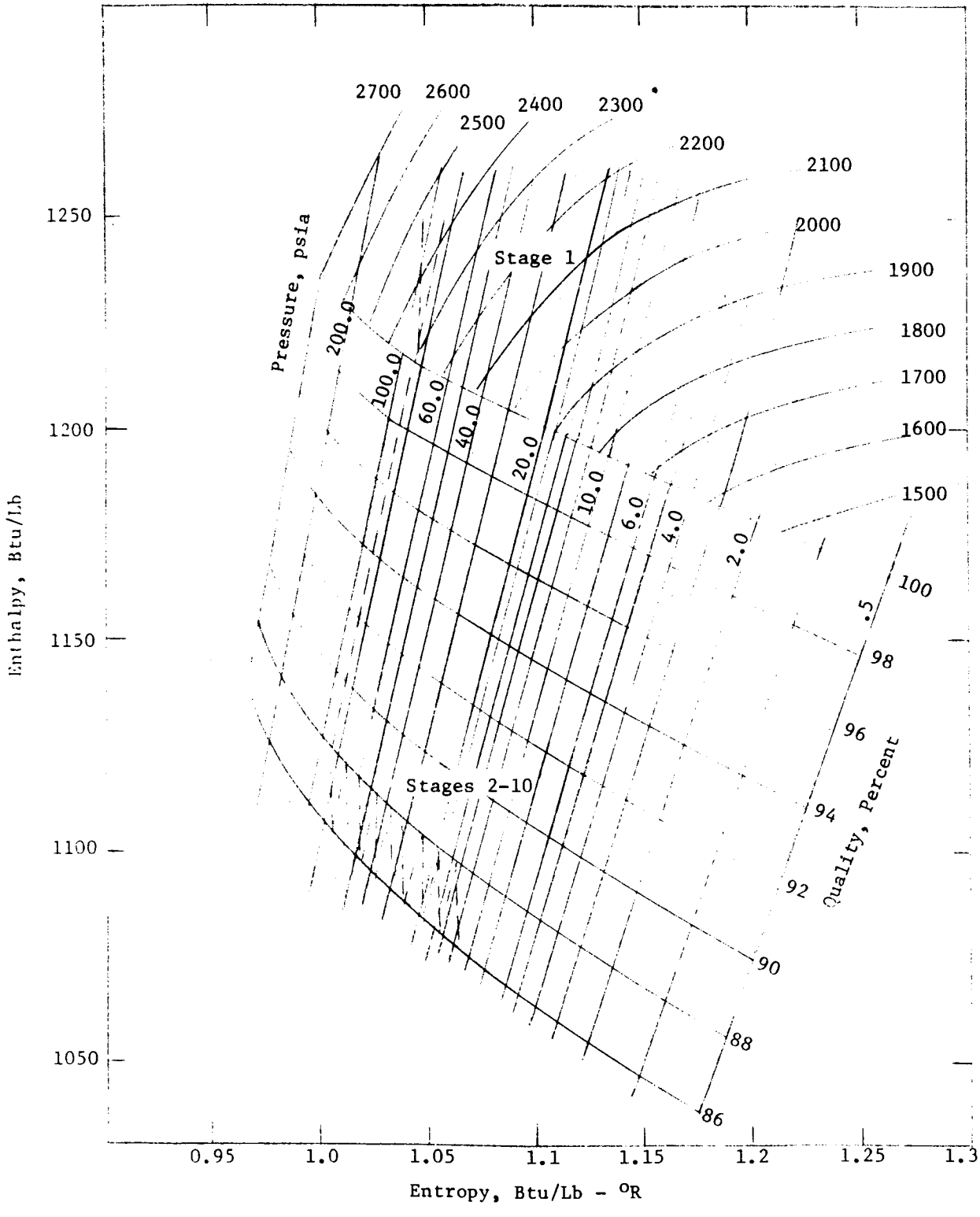

Figure 12. Turbine Simulator Expansion on Potassium Mollier Diagram for the Ten Stages of the Cb-1Zr Corrosion Test Loop.

A single-tube, helical coil condenser was initially favored because of its inherent simplicity in both the design and fabrication. It was rejected, however, because of the low condensing rate which is limited by the radiating capability of the outer surface of the tube and the excessive pressure drop which would result in selecting a tube diameter (0.423 inch) to have an entrance velocity of 400 fps. By adding radiating fins to the tube, the condensing rate could be significantly increased and a shorter condenser with a low pressure loss could be achieved. A multitube radiating fin condenser using the standard 0.375-inch-OD by 0.25-inch-ID tube from which most of the connecting piping in the loop is fabricated was considered but rejected primarily because of the possibility of either initiating or contributing to the instability of the loop.

A finned tube condenser design is limited in its ability to reject heat by the effectiveness of the radiating fins since the condensing coefficient for potassium vapor is extremely high, and the temperature drop of the condensing film can be neglected in computing the performance of the condenser. The fin effectiveness is a function of the thermal conductivity of the fin, the emittance of the fin surface, the thickness and width of the fin, the base temperature and the sink temperature. Iron titanate (Fe_2TiO_5) with an emittance of 0.86 was selected as a condenser fin coating.[16] In order to assure that the iron titanate would be suitable for use in coating the Cb-1Zr condenser fin, a 1000-hour test was conducted by SPPS on 0.25-inch-thick x 2-inch-wide x 2.5-inch-long coated specimens. During the 1000-hour test the specimens were cycled 26 times between 1500°F and 150°F. The selected design was judged satisfactory as a result of this evaluation. A description of this test and the results of the evaluation are included in Appendix F, Tests to Evaluate Iron Titanate on Cb-1Zr Condenser Fin, of this report.

The length of a 0.25-inch-thick fin Cb-1Zr condenser required to condense 40 lb per hour of potassium vapor at 1350°F is shown in Figure 13.

(16) Emanuelson, R. C., Determination of the Emissivity of Materials, Semiannual Progress Report for Period May 14, 1964 to November 15, 1964, Pratt and Whitney Aircraft, NASA CR-54268.

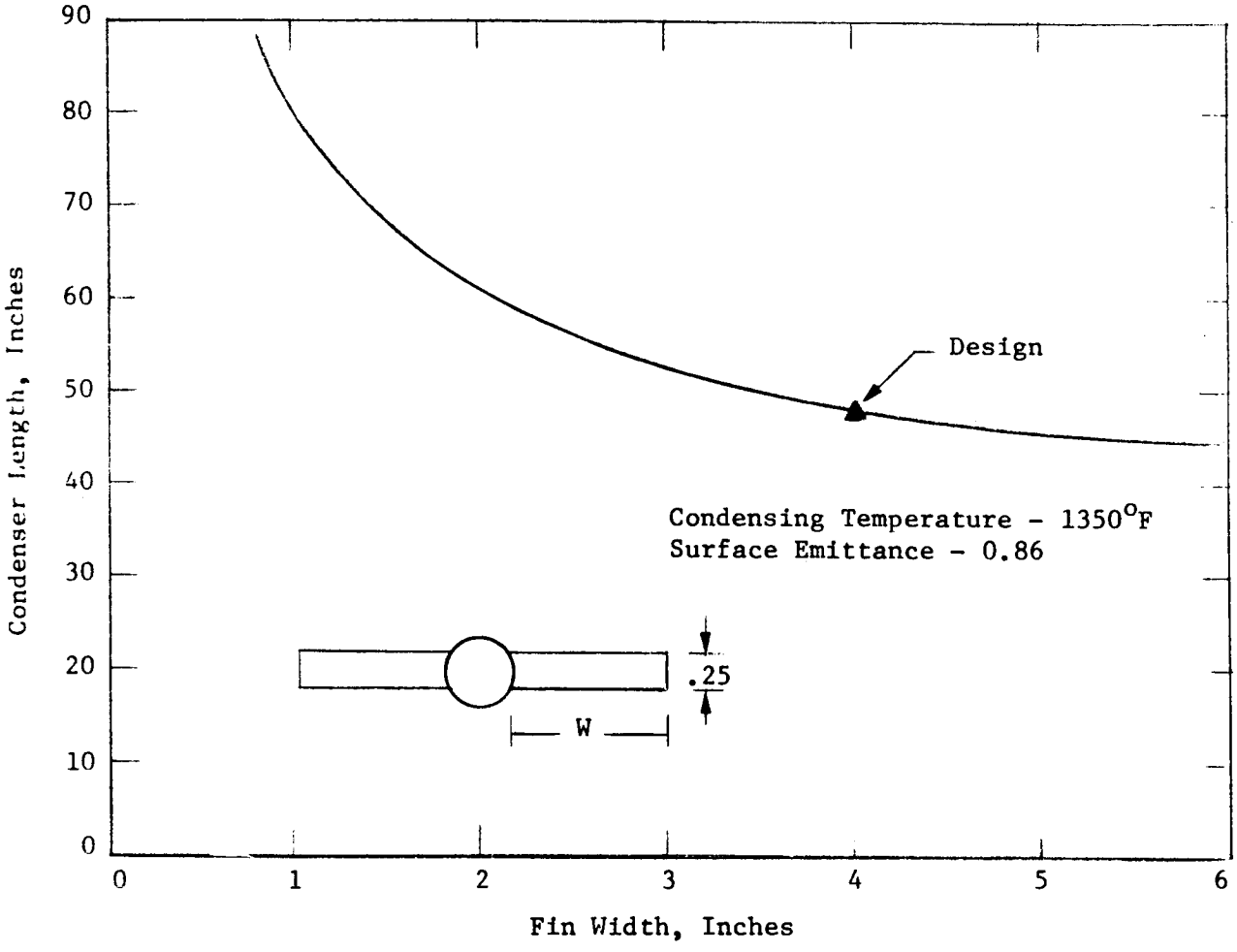

Figure 13. Condenser Length as a Function of Fin Width for Single Tube Finned Cb-1Zr Condenser. (40 Lb/Hr Potassium Vapor - 88% Quality)

A 4-inch width which will require a condensing length of 48 inches was selected since the vacuum chamber size limited the condenser length to 60 inches, and approximately 12 inches of condenser length would be required to subcool the potassium condensate to 800°F.

A 3/8-inch Schedule 80 pipe was selected as the condenser tube size. The 0.426-inch ID with a flow area of 0.140-inch^2 has a vapor velocity of 400 fps at the condenser entrance. The 0.126-inch wall is of sufficient thickness to allow the fins to be welded to the tube with a minimum of distortion in the tube. Specifications for the finned tube condenser/subcooler are summarized in Table V.

H. FLOWMETERS

A permanent magnet flowmeter was selected for measuring the sodium and potassium flow rates in the Cb-1Zr Corrosion Test Loop because of its simplicity, reliability, and accuracy. A schematic diagram of a typical permanent magnet flowmeter is shown in Figure 14. Its operation is similar in principle to that of a d-c generator. A d-c output voltage is generated across the flow tube by the conducting fluid moving through the pipe at right angle to the magnetic field established across the pipe by the permanent magnet.

The output voltage is expressed by Faraday's law for induced voltage, i.e.,

$$E = BlV \times 10^{-8}$$

where

E = Output voltage;

B = Flux density, gauss;

l = Length of conductor, cm;

V = Velocity of conductor, cm/sec.

Certain practical effects result in differences from the ideal case given above, and they must be accounted for if accurate measurements are to be obtained. These effects and their contributions have been presented previously by R. Affel and coworkers.[17]

(17) Affel, R. G., Burger, G. H., and Pearce, C. L., Calibration and Testing of 2- and 3 1/2-in. Magnetic Flowmeters for High-Temperature NaK Service, ORNL-2793.

TABLE V

FINNED TUBE CONDENSER/SUBCOOLER

Material	Cb-1Zr
Condensing Temperature	1350°F
Heat Rejection Capacity	30,000 Btu/hr
Length	5.5 feet
Tube OD	0.625-inch
Tube Wall Thickness	0.125-inch
Number of Fins	2
Fin Geometry	0.25-inch thick by 4-inch wide
Inlet Vapor Velocity	400 fps
Potassium Flow Rate	40 lbs/hr

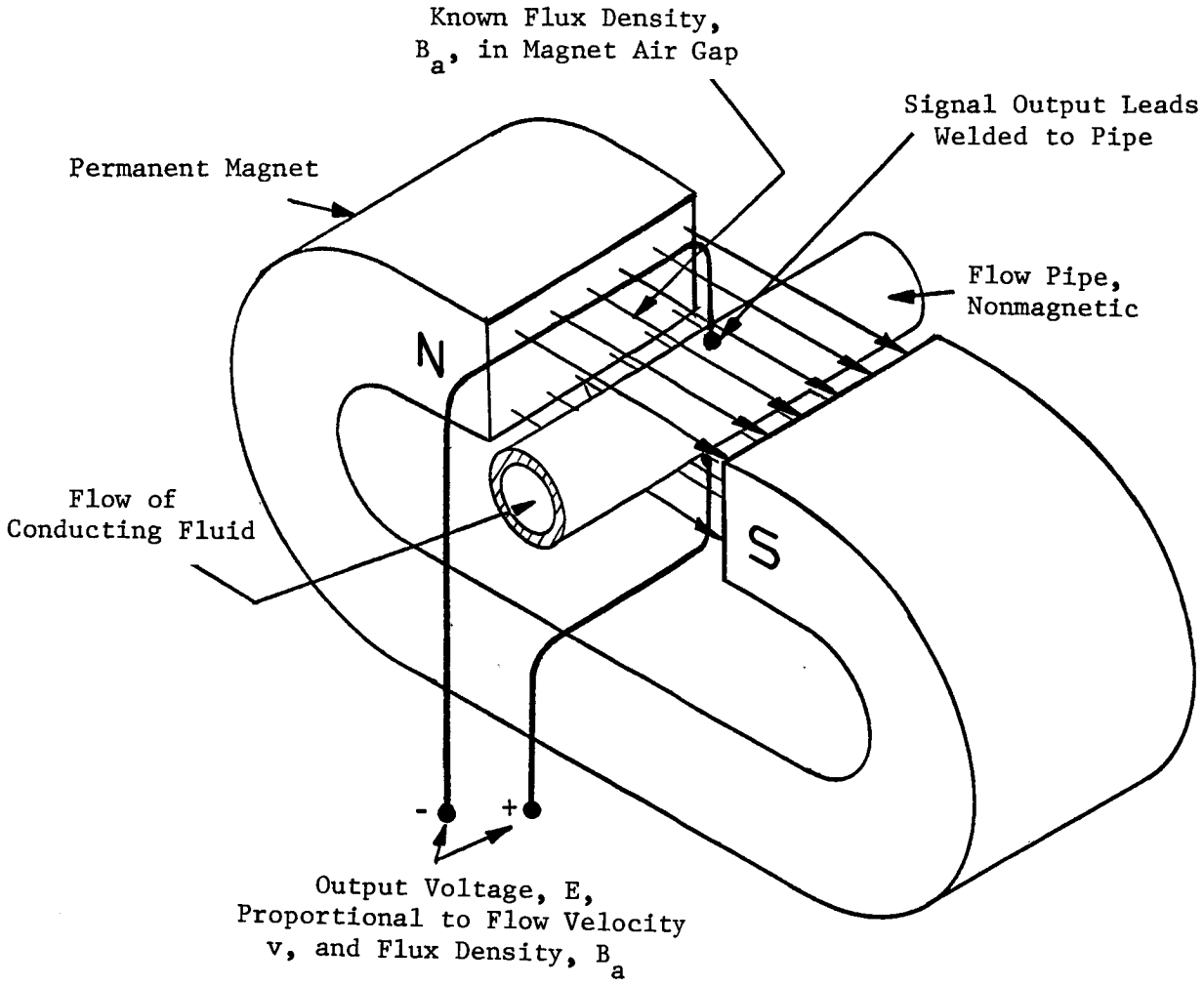

Figure 14. Magnetic Flowmeter Principle.

The actual design of the flowmeter shown in Figure 15 was limited to the selection of a commercially available Alnico V magnet with a gap between pole faces having adequate clearance for a 0.375-inch-OD Cb-1Zr tube and a magnetic flux density high enough to produce a millivolt output that could be easily recorded by a standard recording potentiometer. The magnet selected was a cast Alnico V magnet assembly Type MA39* with a nominal 3000 gauss magnetic flux in a 3/4-inch gap with a specified maximum variation of the flux density less than 10 percent between the 1 1/2-inch-diameter pole faces.

The magnet was stabilized by repeated thermal cycling between room temperature and 900°F which is approximately 200°F higher than the anticipated magnet temperature during loop operation. The magnetic flux as a function of temperature is shown in Table VI in the room temperature to 900°F range for a typical Alnico V flowmeter magnet. These values are used in calculating the flow rate at the operating temperature.

The flow tube is fabricated from a 0.375-inch-OD Cb-1Zr tube with 0.065-inch wall. The electrodes are 0.062-inch-diameter Cb-1Zr wire which was purchased to the same chemistry specifications as the tube to minimize the spurious thermal emf which could result from dissimilar materials at operating temperatures. A calculated output voltage as a function of flow rate for the sodium loop flowmeter is shown in Figure 16.

* Magnetic Materials Section, General Electric Company, Edmore, Michigan.

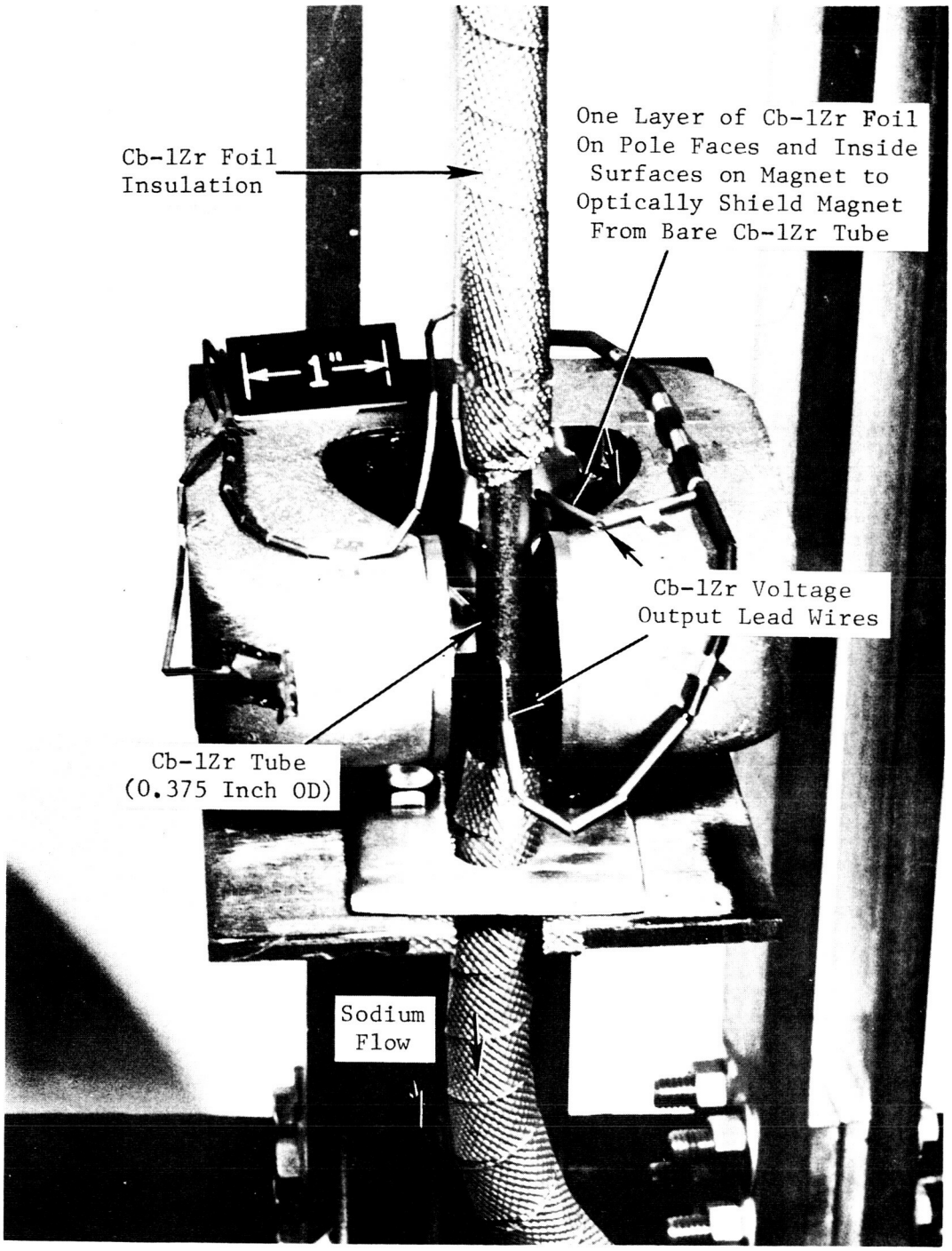

Figure 15. Permanent Magnet Flowmeter Located Between the Boiler Outlet and the EM Pump Inlet in the Sodium Circuit of the Cb-1Zr Corrosion Test Loop. (Orig. C66031434)

TABLE VI

MAGNETIC FLUX VS TEMPERATURE OF THE ALNICO V FLOWMETER MAGNET AFTER THERMAL STABILIZATION AND PRIOR TO THE LOOP TEST

Magnet Temp., °F	Magnetic Flux, Gauss		
	Run #1	Run #2	Run #3
70	2675	2675	2675
200	2675	2675	2675
400	2675	2675	2675
500	2675	2675	2675
600	2675	2610	2675
700	2675	2610	2675
800	2610	2610	2675
900	2610	2610	2610

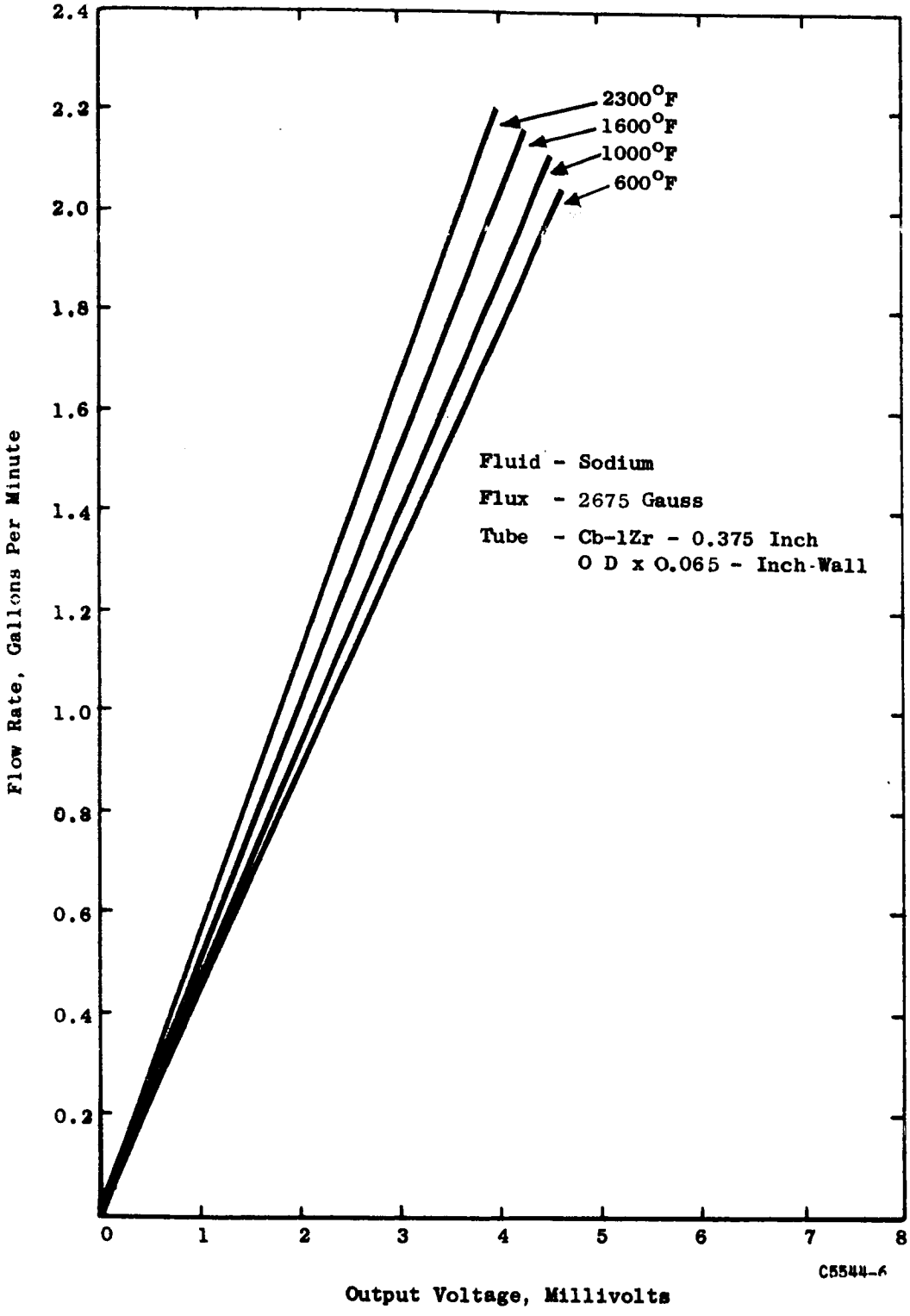

Figure 16. Calculated Output Voltage Versus Flow Rate for the Cb-1Zr Corrosion Loop Permanent Magnet Flowmeter.

III. MATERIAL PROCUREMENT

The procedures and specifications utilized on this program to obtain the highest quality refractory alloy materials commensurate with the existing technology were described in detail in an earlier topical report[18] in this series. General Electric-SPPS specifications cited in this report may be found in the referenced report.[18]

A quality assurance program was established to provide adequate identification and documentation of the quality of the refractory alloys used in the construction of the test loops. In addition, the information acquired in the quality assurance program fulfilled the material documentation required for the test history of the loop components.

The majority of the quality assurance measures utilized to evaluate incoming material were performed by the materials producers, and check tests performed by the General Electric Company generally were limited to chemical analyses to determine the concentration of the interstitial elements, metallographic examination, hardness measurements, and visual inspection.

Upon receipt of material from the materials producers, a Material Control Number (MCN) was assigned to each homogeneous lot of material. A homogeneous lot included all material of the same size, shape, condition, and finish from one heat of material and which had received the same processing, had been annealed in the same vacuum annealing charge, and had been processed in the same manner in all operations in which the processing temperatures exceeded 500°F.

A listing of the refractory alloy mill products procured for the program, the specifications to which they were procured, and the results of the quality assurance tests were presented in the earlier report.[18]

---

(18) Frank, R. G., et al., Material and Process Specifications for Refractory Alloy and Alkali Metals - Potassium Corrosion Test Loop Development Topical Report No. 2, R66SD3007, December 13, 1965, General Electric Company, Cincinnati, Ohio.

IV. LOOP FABRICATION

The overall fabrication sequence for the Cb-1Zr Rankine System Corrosion Test Loop is illustrated in Figure 17. During loop fabrication, four major subassemblies, the boiler, condenser, sodium heater, and potassium surge tank were constructed. The condenser and boiler subassemblies were postweld annealed at 2200°F for one hour in a vacuum furnace. In the other subassemblies, components were individually postweld annealed prior to assembly welding. These assembly welds were postweld annealed locally using a small refractory metal annealing furnace positioned over the weld joint.

The final loop assembly consisted of first joining the boiler and potassium surge tank major subassemblies. This unit together with the condenser and sodium heater was then positioned in the loop support structure. The welding fixture was then placed in position and attached to the various support positions on the loop. This fixture provided rotation of the loop within the welding chamber to facilitate welding of seven joints required during the final assembly. These welds were postweld annealed locally at 2200°F for one hour using the small refractory metal annealing furnace positioned over the weld joint.

The Cb-1Zr Rankine System Corrosion Test Loop components as delineated in Figure 17 were the boiler, condenser, sodium heater, turbine simulators, potassium preheater, two electromagnetic (EM) pump ducts, two surge tanks, a stressed diaphragm pressure transducer, four slack diaphragm pressure transducers, vapor nucleator, and two bellows sealed valves. Each component and the welding procedures employed will be discussed individually below.

A. GENERAL WELDING PROCEDURES

Prior to the welding of the Cb-1Zr Rankine System Corrosion Test Loop, a preliminary qualification test of the welding equipment was conducted according to requirements defined in SPPS Specification No. 03-0005-00-A (3c). This specification requires that the inert gas be

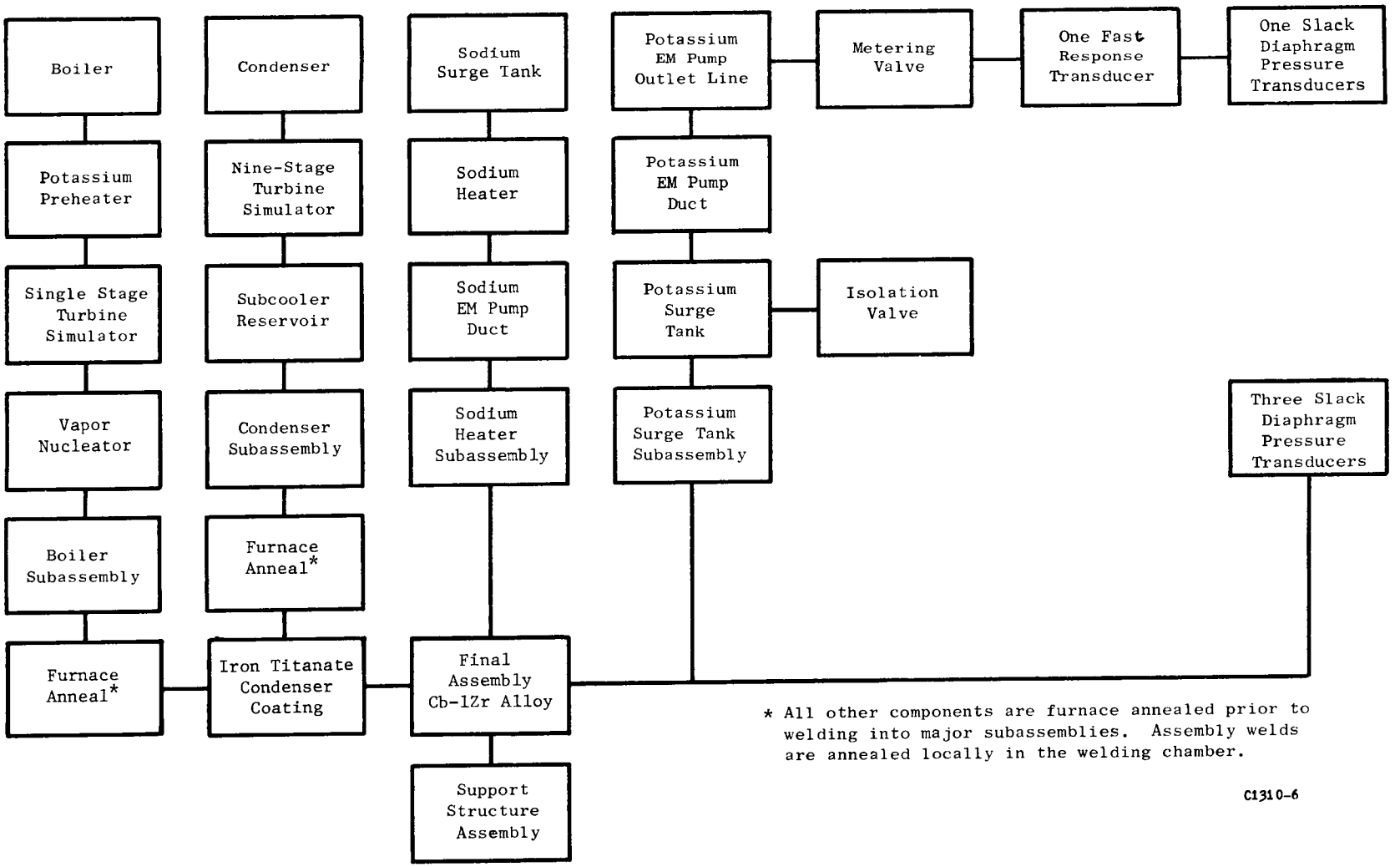

Figure 17. Fabrication Sequence for the Cb-1Zr Rankine System Corrosion Test Loop.

purified to contain less than 1 ppm active impurities by volume and that contamination of the weld metal be held to less than 50 ppm oxygen, 50 ppm nitrogen, 10 ppm carbon, and 5 ppm hydrogen.

The mass spectrometer helium analysis system described in an earlier report[19] was used to monitor the welding chamber helium for oxygen and nitrogen. An electrolytic hygrometer was used to monitor the helium for moisture concentration. This analysis system was introduced after the slack diaphragm transducers and bellows sealed valve bodies had been welded using procedures described in an earlier report[20] on the Cb-1Zr Pumped Sodium Loop. The welding chamber shown in Figures 18 and 19 was used for all tungsten inert gas welding performed on the loop. To accommodate long, straight tubing sections such as the boiler, an extension tube shown in Figure 18 was attached to the basic chamber. During final loop assembly, the 8-foot-diameter extension tank illustrated in Figure 19 was used.

The general welding procedure consisted of an overnight vacuum pump-down with hot water bakeout (140°F) on the chamber. After cooling the chamber, a pressure of less than 1×10^{-5} torr was attained. The pressure rise rate on the chamber was then taken prior to backfilling with purified helium gas. Welding operations were continued until completed or until gaseous contaminants reached the upper limits of SPPS Specification No. 03-0005-00-A (3c).

B. SLACK DIAPHRAGM TRANSDUCERS

Six Taylor Instrument Companies slack diaphragm transducers were fabricated for the Cb-1Zr Corrosion Test Loop during the construction of

---

(19) Lyon, T. F., Purification and Analysis of Helium for the Welding Chamber, Potassium Corrosion Test Loop Development Topical Report No. 1, NASA CR-54168, General Electric Company, Cincinnati, Ohio, July 1, 1965, p. 35

(20) Hoffman, E. E. and Holowach, J., Cb-1Zr Pumped Sodium Loop, Potassium Corrosion Test Loop Development Topical Report No. 6, R67SD3015, General Electric Company, Cincinnati, Ohio, December 20, 1967, p. 35.

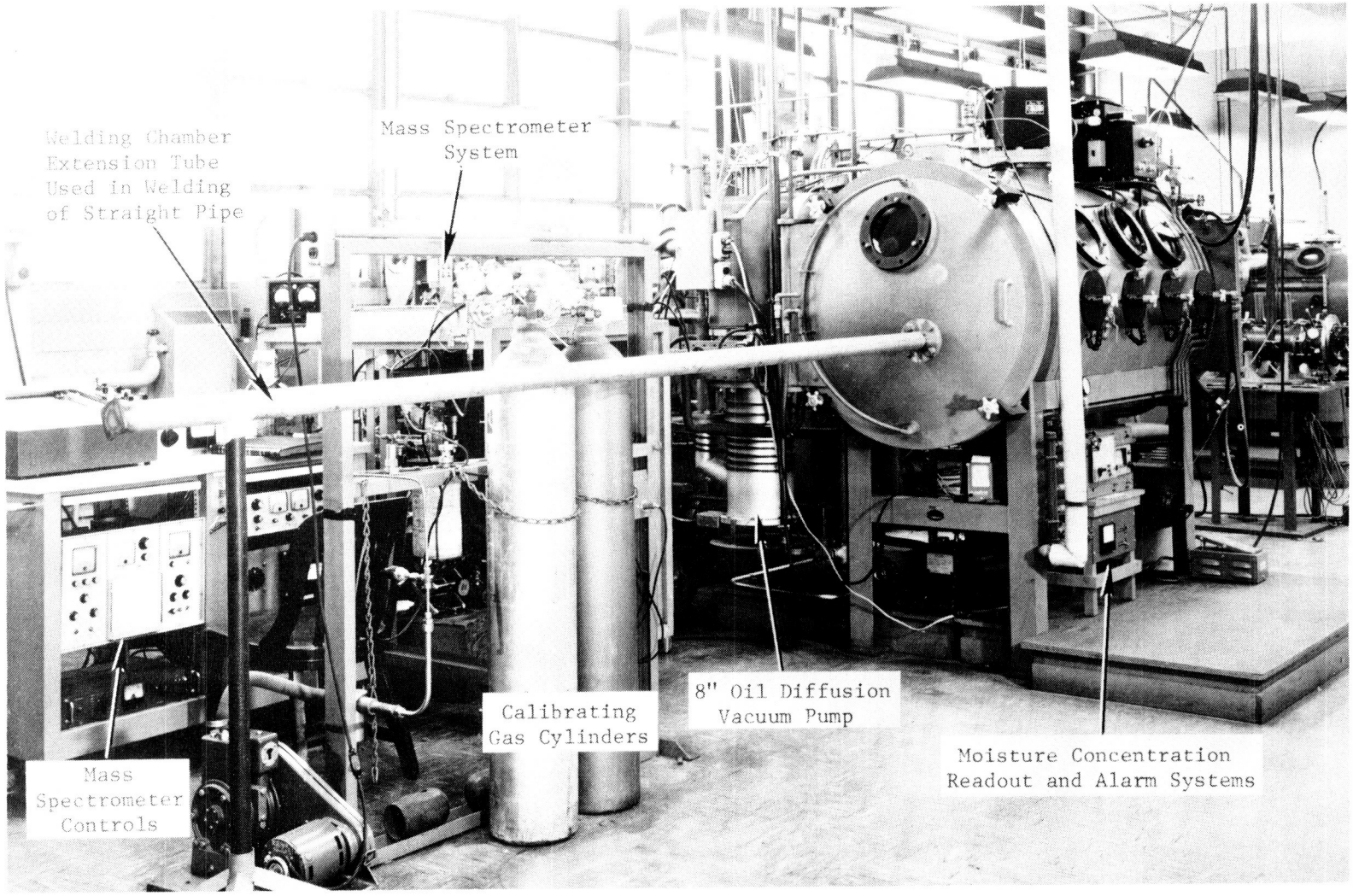

Figure 18. Vacuum-Purge Inert Gas Welding Chamber (3 Foot Diameter x 6 Foot Long) with Helium Supply and Purity Control System Showing the Pipe Welding Extension Tube Attached to the Chamber Door. (Orig. C67112001)

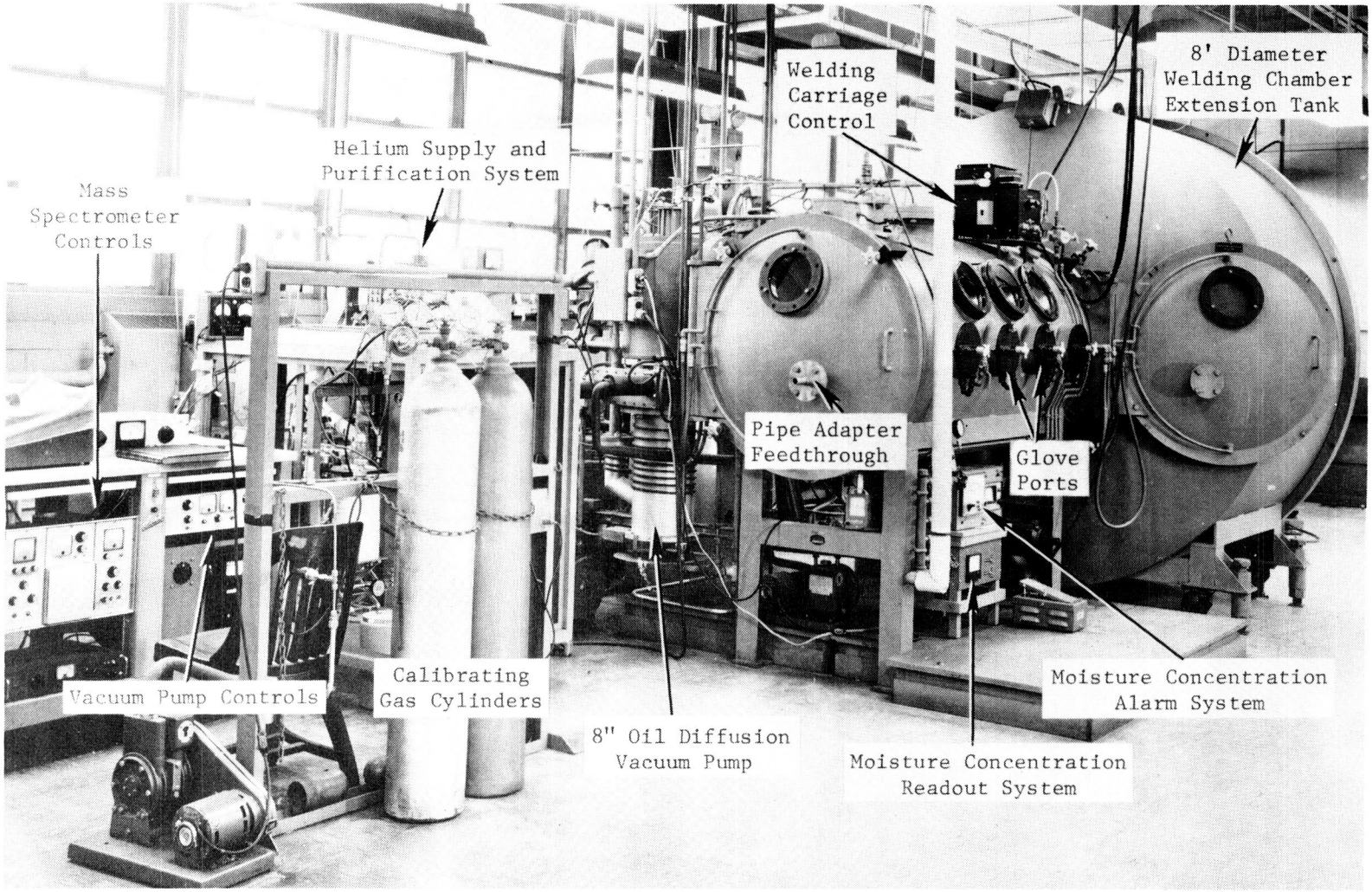

Figure 19. Vacuum-Purge Inert Gas Welding Chamber and Helium Purity Control System with Welding Chamber Extension Tank Attached to 3 Foot Diameter x 6 Foot Long Welding Chamber. (Orig. C6711228)

the Cb-1Zr Pumped Sodium Loop described in an earlier report.[21] The manufacturing sequence was identical with the procedure described in the referenced report and will not be duplicated here.

The NaK filling operation by Taylor Instrument Companies was modified from that used previously to assure that the NaK used to fill the transducer was high-purity material. A sample of NaK taken by Taylor during the filling was analyzed by SPPS. An average of 3.8 ppm oxygen was determined based on 3.3 ppm oxygen in a 3.3-gram sample and 4.3 ppm oxygen in a 3.5-gram sample. Additional analyses on the NaK used to fill the transducers gave the following results: less than 1 ppm-Mn, Mg, Cu, Be, Ag, Sr, Cu; less than 2 ppm-Ba; less than 5 ppm-Fe, B, Co, Al, Sn, Pb, Cr, Ti, Ni, Mo, V; less than 10 ppm-Si, Zr. These results indicated that the purity of the NaK was maintained during the filling operation.

C. VALVES

The fabrication sequence for both the Cb-1Zr Pumped Sodium Loop and the Cb-1Zr Corrosion Test Loop was reported previously.[22] During the pumped sodium loop operation, the valve actuation system was further modified by inclusion of a Saginaw ball bearing screw to eliminate galling tendencies in the stem drive system. For this loop, additional design and material modifications were made, and these were incorporated in the valve shown in Figure 20. All components which may operate above the 500-600°F ambient temperature of the vacuum chamber during test were made from Mo-TZM or Cb-1Zr alloy. Also, a tungsten carbide bushing was added to minimize galling of the stainless steel pinion gear shaft.

D. ELECTROMAGNETIC PUMP DUCTS

The electromagnetic (EM) pump duct principal component is a helical finned duct which is interference fit into an outer wrapper to provide the liquid metal flow channel. After machining and careful dimensional

---

(21) Hoffman, E. E. and Holowach, J., Cb-1Zr Pumped Sodium Loop, Potassium Corrosion Test Loop Development Topical Report No. 6, R67SD3015, General Electric Company, Cincinnati, Ohio, December 20, 1967, p. 42.

(22) Ibid, p. 37.

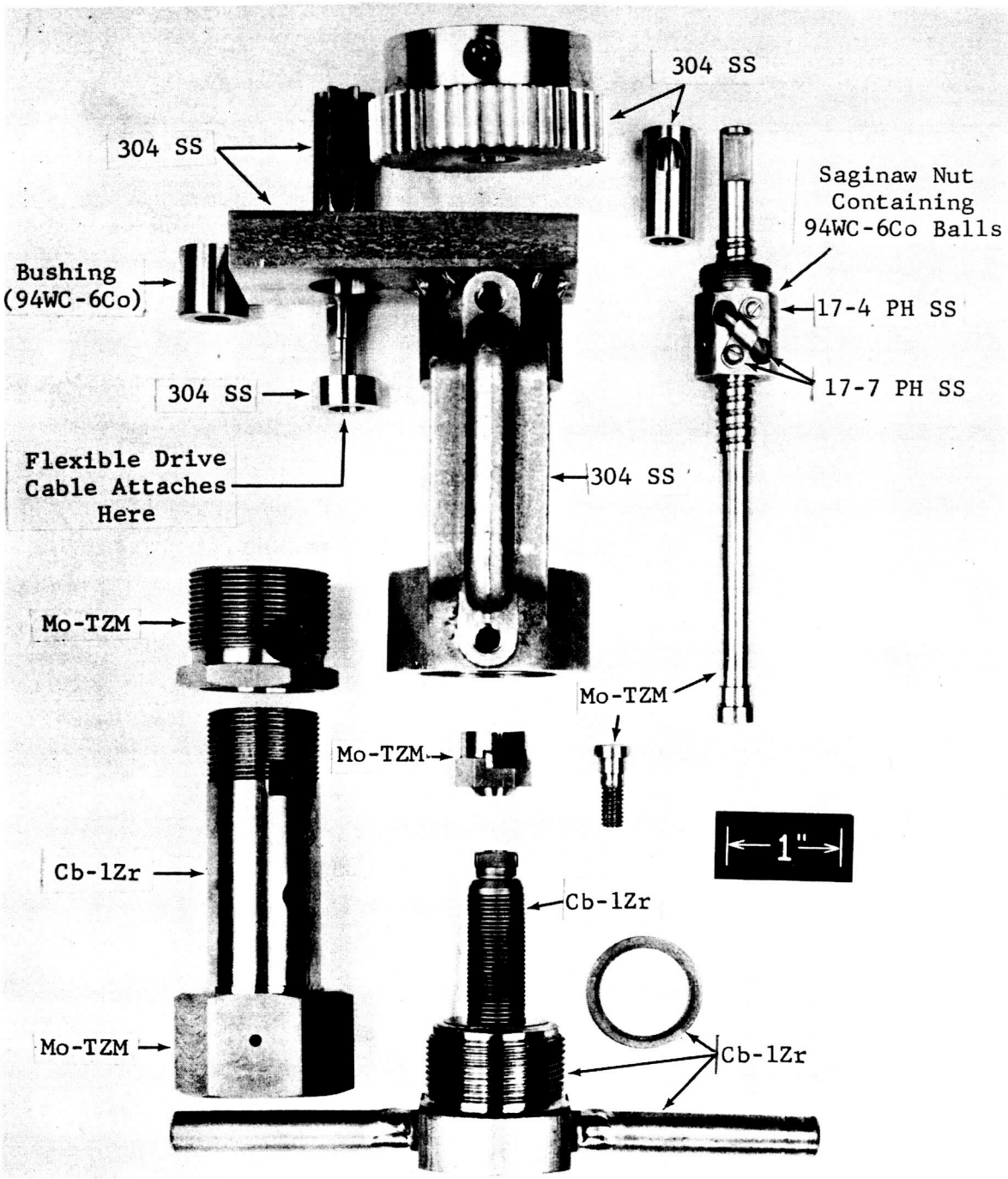

Figure 20. Modified Hoke Valve and Associated Drive Components for the Cb-1Zr Corrosion Test Loop. (Orig. C65032923)

inspection, these interference fits were produced by heating the outer wrapper to 500°F in air and immersing the finned duct in liquid nitrogen just prior to inserting the duct into the wrapper. The closure welds on the end caps and connectors were made, and each pump duct was final machined on the outside diameters. The complete EM pump ducts are shown in Figure 21.

E. STRESSED DIAPHRAGM PRESSURE TRANSDUCER

The design of stressed diaphragm pressure transducer was modified from that used in the Cb-1Zr Pumped Sodium Loop[23] by the inclusion of a corrugated 0.006-inch-thick T-222 tantalum alloy diaphragm. The transducer is shown in Figure 22 at various stages during the fabrication sequence. Since the flat diaphragm used in the earlier design and the new corrugated diaphragm had different diameters, the transducer housing and housing cap were remachined as shown in Figure 22 (a).

The T-111 tantalum alloy housing was first welded to the Cb-1Zr retainer body which was then welded to the reducer and process tube. This subassembly was then annealed at 2200°F for one hour per SPPS Specification No. 03-0005-00-A (3c)

The diaphragm assembly shown in Figure 22 (b) was produced by first electron beam welding the 0.020-inch-diameter W-25Re wire to the T-111 alloy probe mount. A second electron beam weld attached the probe mount to the T-222 alloy diaphragm. The diaphragm was then positioned between the T-111 housing and housing cap and electron beam welded. As an added precaution, an electron beam weld was made between the T-111 alloy housing and the Cb-1Zr retainer body on the outside diameter, which, in combination with the internal tungsten inert gas weld, effected a double seal between these components.

---

(23) Hoffman, E. E. and Holowach, J., Cb-1Zr Pumped Sodium Loop Potassium Corrosion Test Loop Development Topical Report No. 6, R67SD3015, General Electric Company, Cincinnati, Ohio, December 20, 1967, p. 51.

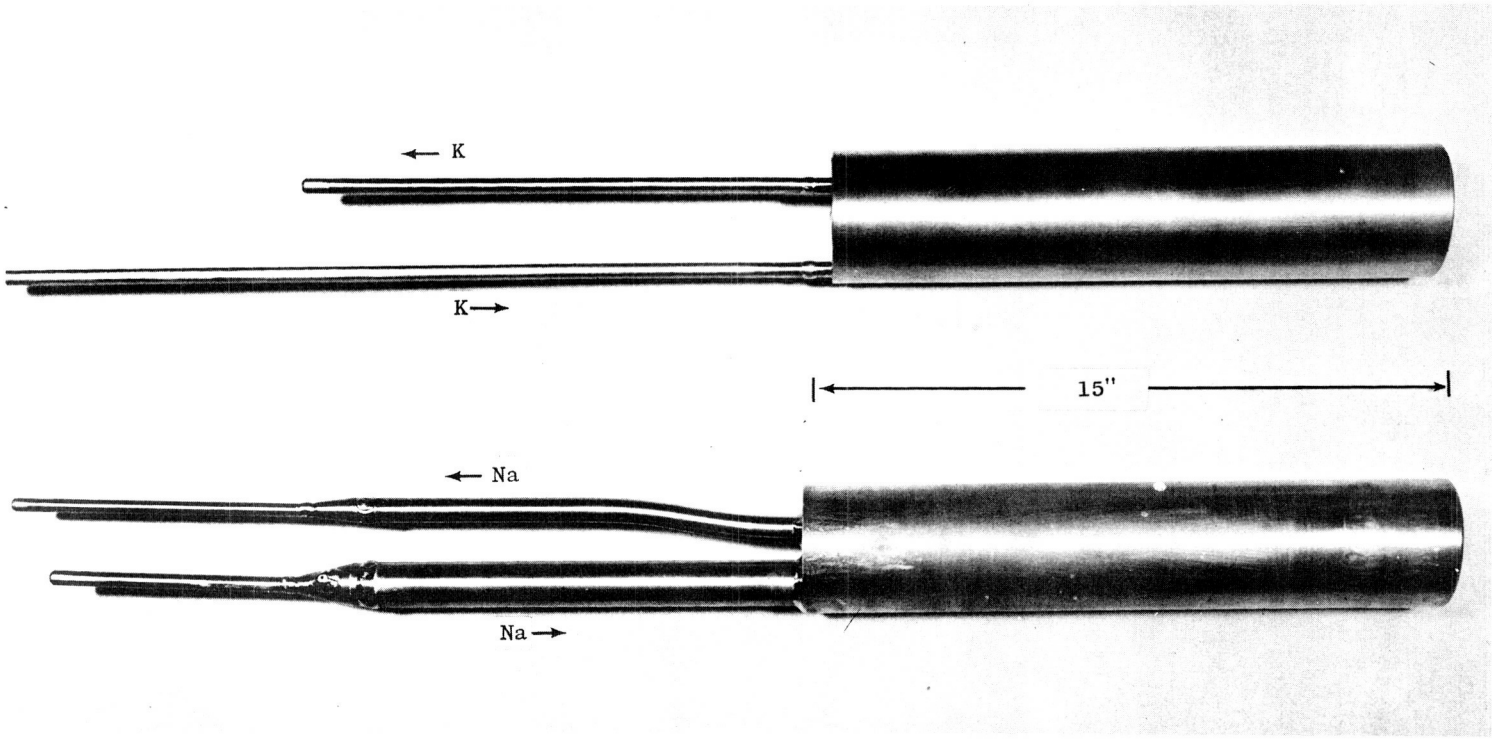

Figure 21. Potassium Duct (Top) and Sodium Duct (Bottom) of the Helical Induction Electromagnetic Pumps for the Cb-1Zr Corrosion Test Loop. All Parts Made of Cb-1Zr Alloy. (Orig. C65012829)

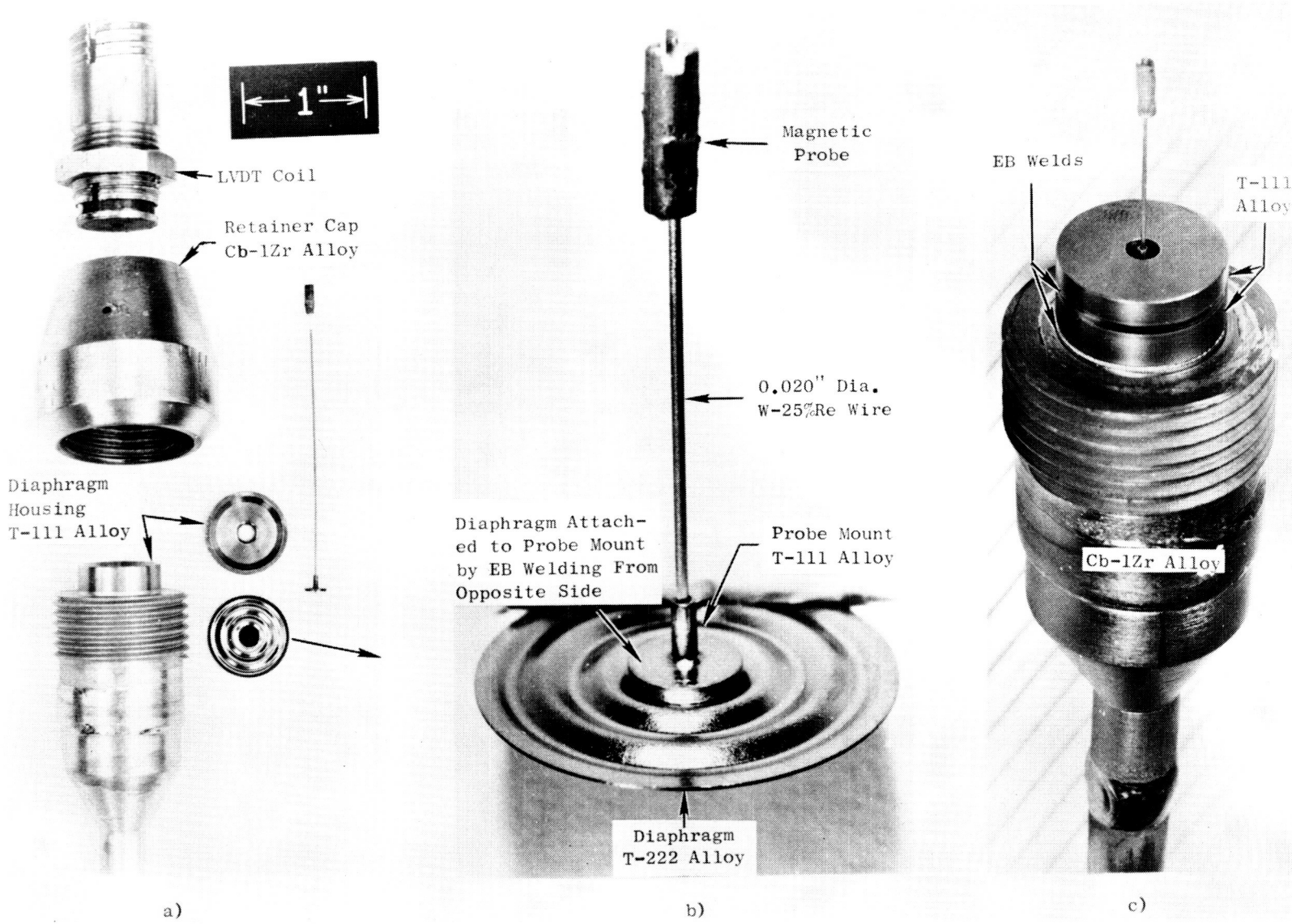

Figure 22. Stressed Diaphragm Pressure Transducer for the Cb-1Zr Corrosion Test Loop at Various Stages During Fabrication. (Orig. C65062193)

The final fabrication step was the brazing of the magnetic probe to the 0.020-inch-diameter W-25Re wire. Brazing was accomplished using localized heating with a graphite-tipped heater probe under high-purity argon in the welding chamber shown previously in Figure 19. The brazing alloy (72Ag-28Cu) was applied to the joint manually in wire form. The completed assembly, shown in Figure 22 (c), was mass spectrometer leak tested successfully and submitted to instrumentation for room temperature calibration prior to installation in the loop.

F. VAPOR NUCLEATOR

The vapor nucleator components are shown in Figure 23 before and after welding. The nucleator cavity is located in the "heat lens," which is heated by a tungsten coil, and consists of a stepped hole with the larger entrance cavity leading to a smaller nucleator cavity.

G. POTASSIUM AND SODIUM SURGE TANKS

These Cb-1Zr components include an argon gas pressure line, fill and dump line, tank outlet line, and surge tank as illustrated by the potassium surge tank shown in Figure 24. After completion of the welding, the surge tanks were postweld annealed as described in Section M

Four bimetallic joints between the Cb-1Zr and Type 316 stainless steel process tubes were required to provide alkali metal fill and gas pressure line connections. The machined components of these joints are illustrated in Figure 25. Process tubes were welded to the Cb-1Zr joint component, and the welds were heat treated prior to brazing of the joints. The brazing was performed in accordance with SPPS Specification No. 03-0008-00-B.[24]

H. POTASSIUM PREHEATER AND SODIUM HEATER

The general heater configuration is illustrated by the potassium preheater shown in Figure 26 with the vapor nucleator welded in place.

---

(24) Frank, R. G., et al., Material and Process Specifications for Refractory Alloy and Alkali Metals - Potassium Corrosion Test Loop Development Topical Report No. 2, R66SD3007, December 13, 1965, General Electric Company, Cincinnati, Ohio, p. 269.

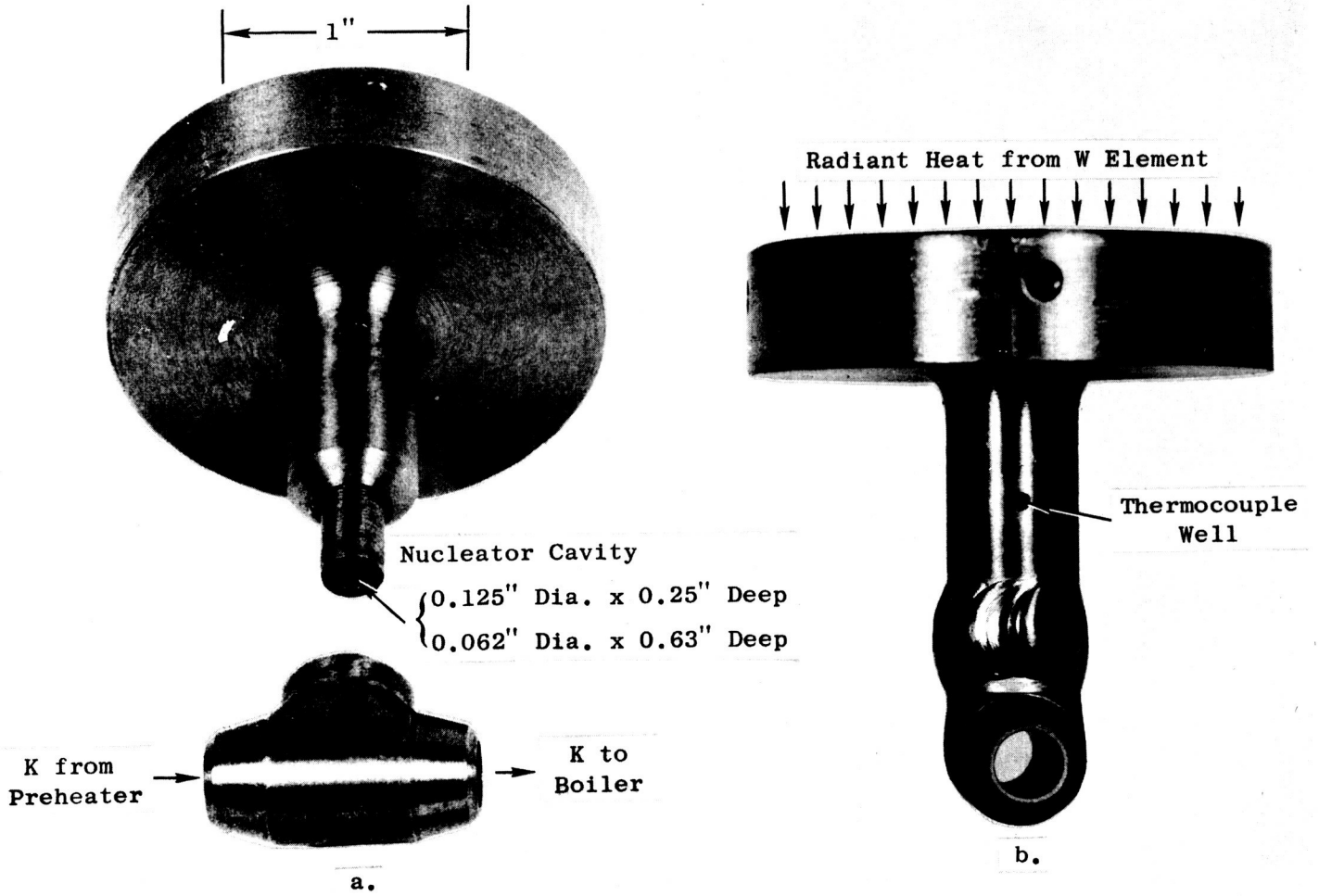

Figure 23. Vapor Nucleator (Cb-1Zr) for the Cb-1Zr Corrosion Test Loop (a) Before and (b) After Welding. (a) (Orig. C64122904) (b) (Orig. C64123003)

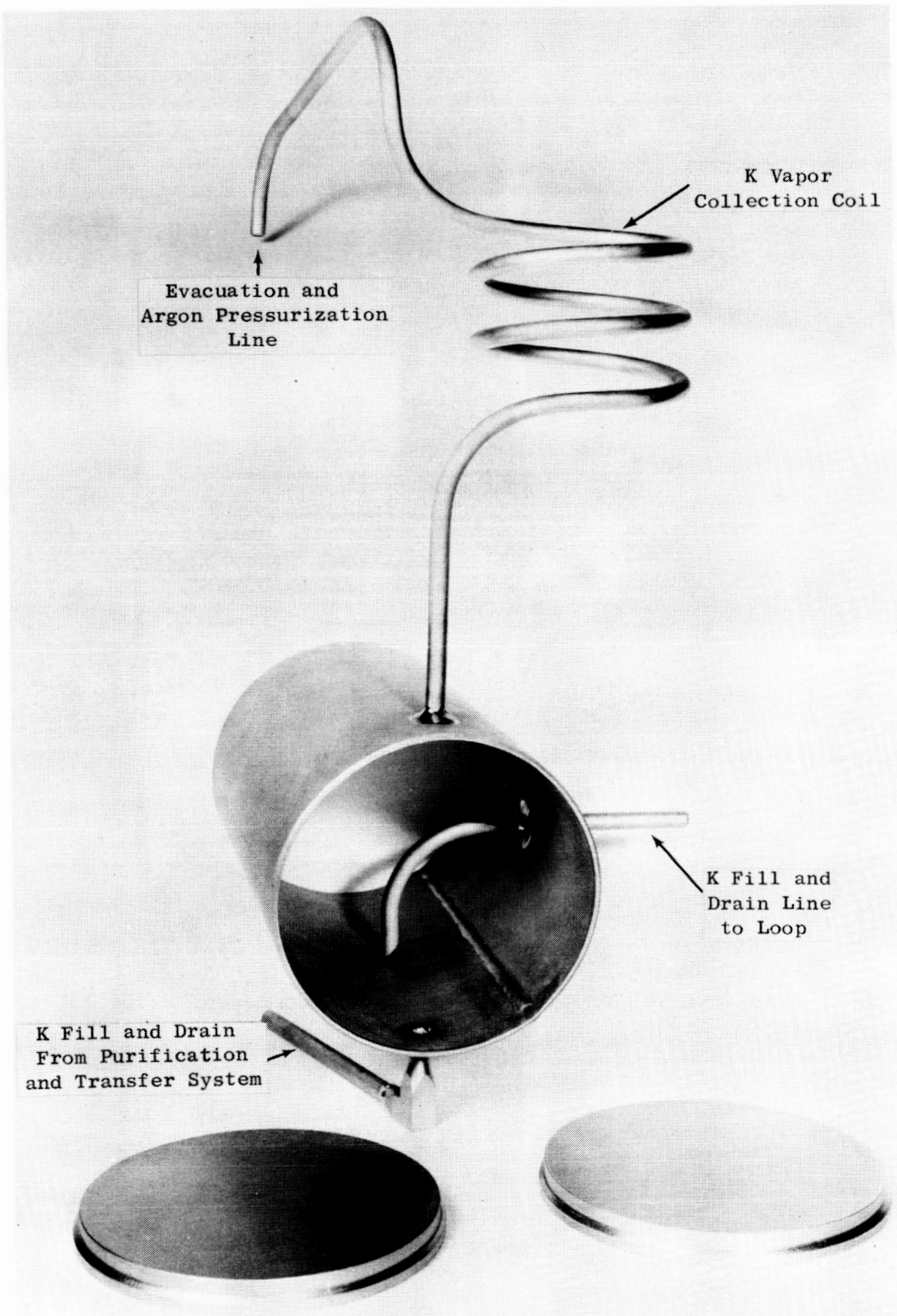

Figure 24. Potassium Surge Tank (6" OD) for the Cb-1Zr Corrosion Test Loop Partially Assembled. (Orig. C65021044)

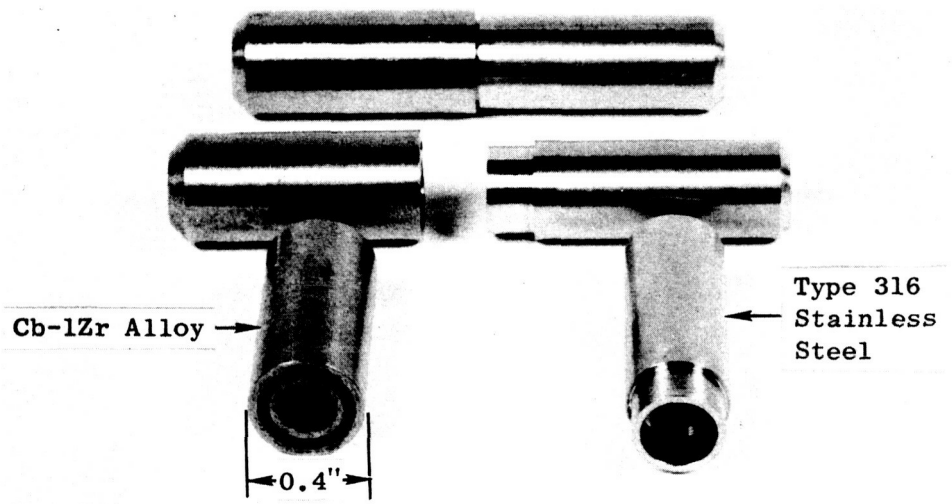

Figure 25. Bimetallic Joint Between Cb-1Zr Alloy and Type 316 Stainless Steel. Process Tubes, 0.375-Inch OD by 0.065-Inch Wall Thickness, are Welded to the Cb-1Zr Alloy Component Prior to Brazing. (Orig. C64122908)

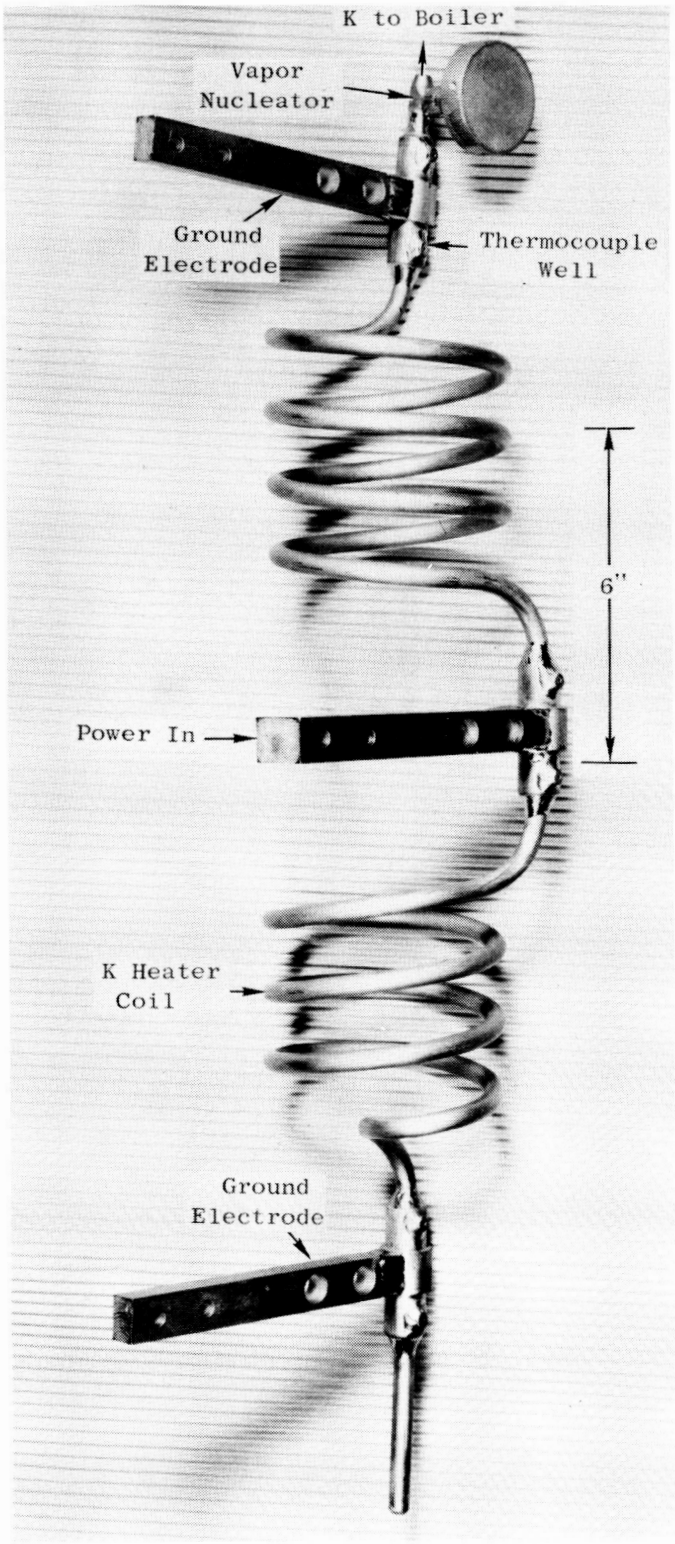

Figure 26. Potassium Preheater Coil-Vapor Nucleator Subassembly for the Cb-1Zr Corrosion Test Loop. (Orig. C65010631)

The electrodes as shown in Figure 27 illustrate the welding of the thermocouple wells and the joint between the electrode and electrode bar. Full penetration butt welds were then used to join the electrodes to the heater coil tubing.

I. BOILER

To establish the tube-in-tube boiler coiling procedures, a boiler prototype was formed from half-hard copper tubing. A radiograph of one of the copper coils is shown in Figure 28. A dimensional inspection indicated a maximum outer tube eccentricity of plus 0.050 inch and minus 0.080 inch from the nominal 1.002-inch outside diameter. This condition occurred at the ends of the coil section. The coil itself was a uniform plus 0.030 inch, minus 0.037 inch from nominal. These dimensional variations were considered acceptable for the design of the Cb-1Zr Corrosion Test Loop boiler.

The degree of concentricity maintained between the inner (potassium containment) and the outer (sodium containment) tubes was determined radiographically. The annular spacing, nominally 0.208 inch, varied from a minimum 0.15 inch to a maximum 0.22 inch in the coil proper, which was considered acceptable. This condition occurred at the midpoint between spacers which were located at 10-inch intervals along the boiler. The bends at the end of the coil produced slightly greater eccentricity. No accurate measurements could be obtained, however, since no spacers were located on the free ends of the bends.

This boiler prototype was formed with sugar packed into the annular spacing and the inner tube. After the above inspection, the sugar was dissolved by rinsing with water. The Molisch Test[25] was used to permit detection of sucrose in the wash water. No residual sugar was detected during the destructive inspection of the copper boiler prototype thus confirming the effectiveness of the cleaning procedures employed.

---

(25) Cheronis, N. D., Techniques of Organic Chemistry, Interscience Publishers, Inc., New York, N. Y., 1954, p. 466-467.

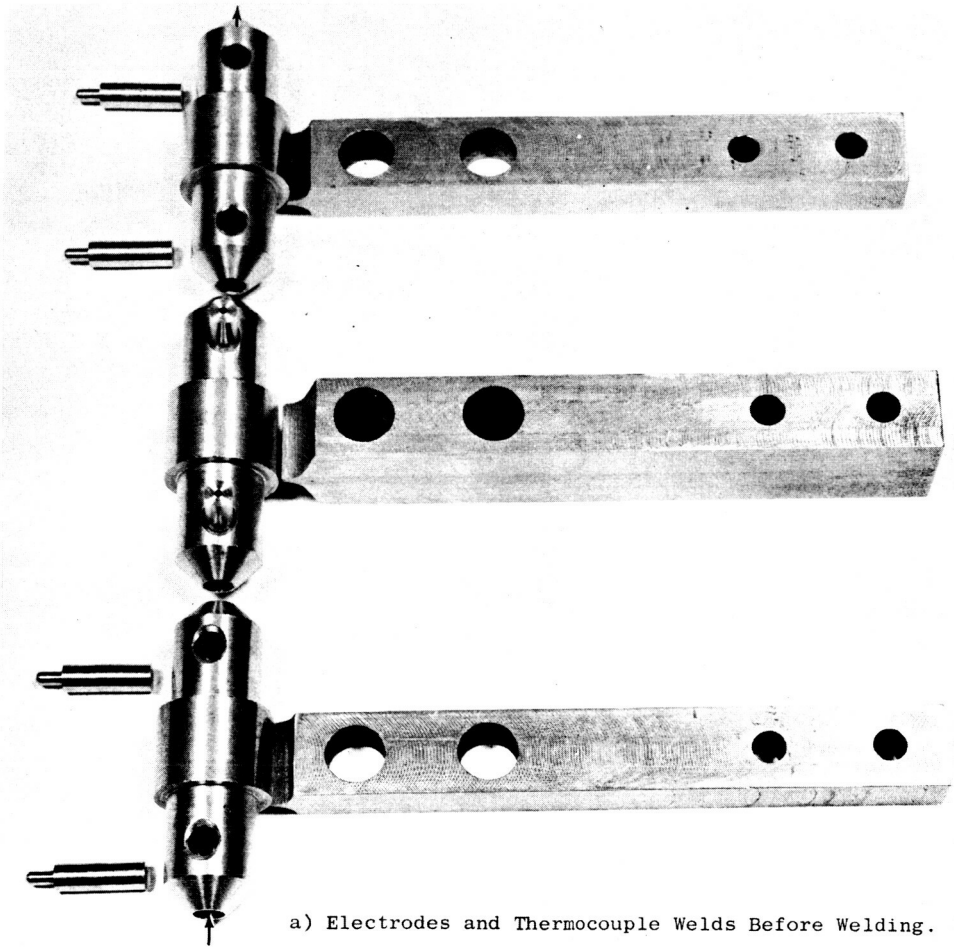

a) Electrodes and Thermocouple Welds Before Welding.

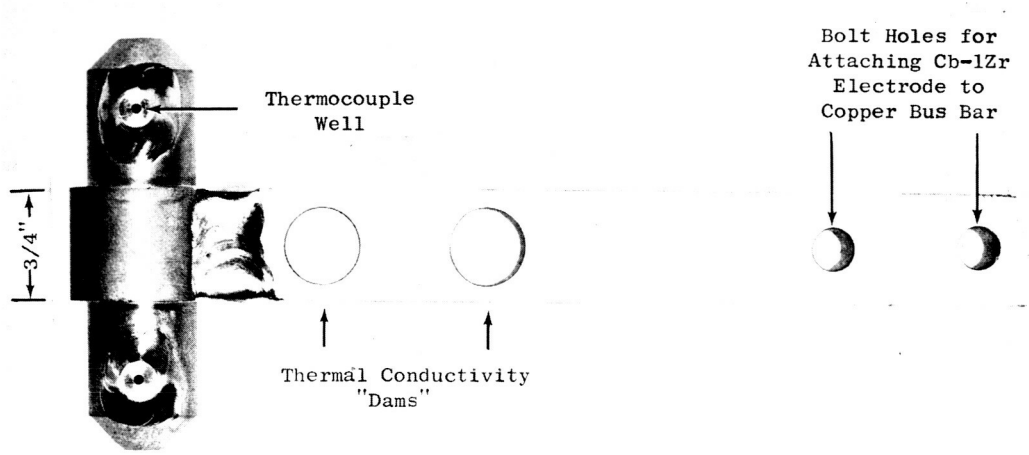

b) Electrode After Welding.

Figure 27. Cb-1Zr Alloy Preheater Coil Electrodes for the Cb-1Zr Corrosion Test Loop.

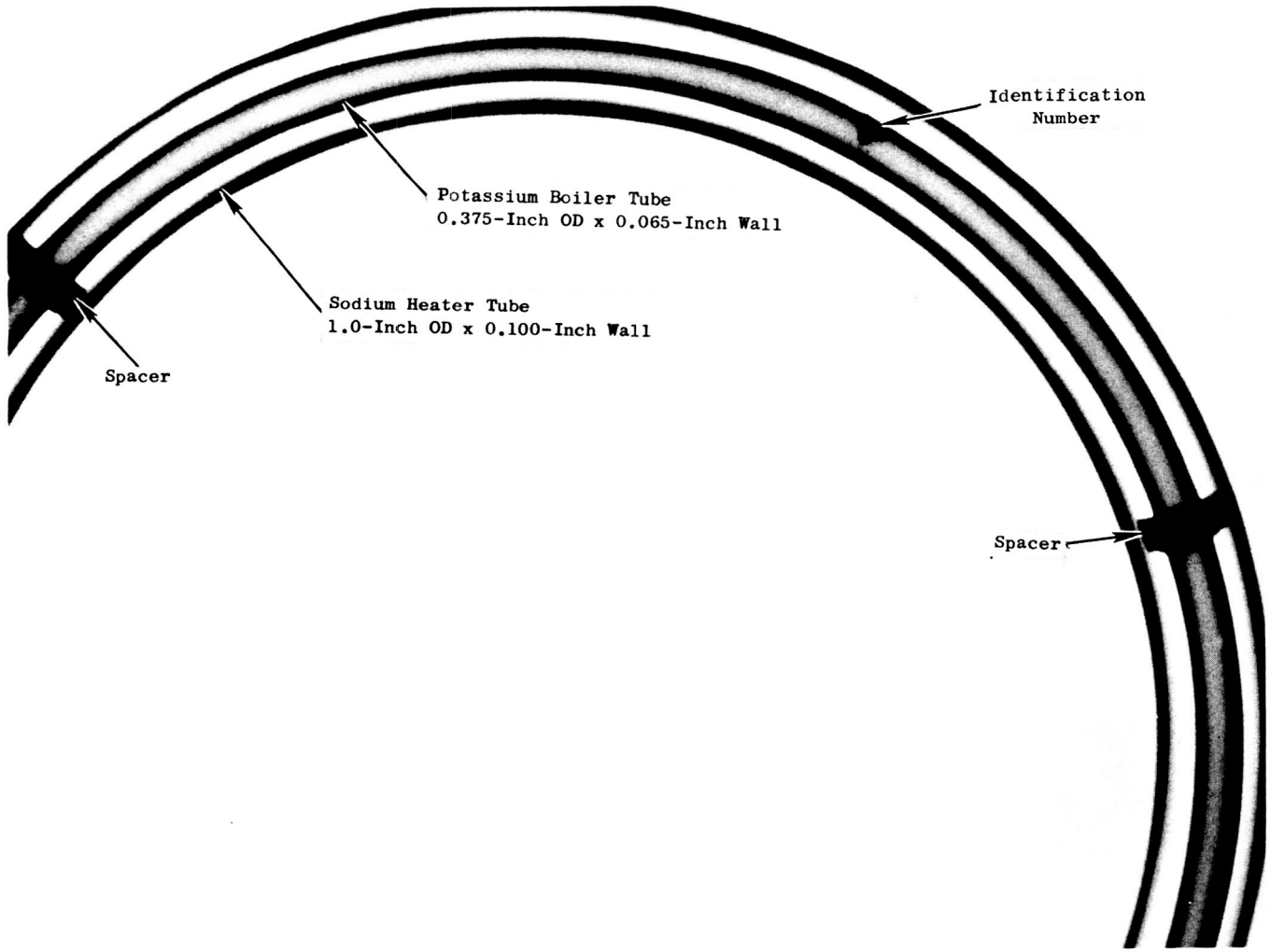

Figure 28. Radiograph of a Copper Mockup of the Cb-1Zr Corrosion Test Loop Boiler. Packed Sugar was Used to Maintain Concentricity of Tubes During Forming.

Fabrication of the Cb-1Zr boiler was initiated by butt welding straight lengths of the inner tube using the welding chamber tube extension, Figure 18, to provide sufficient lateral travel. Triform spacers, illustrated in Figure 29, were tungsten inert gas welded at 10-inch intervals along the boiler. This assembly was formed by the Philadelphia Pipe Bending Company. Prior to forming, the inner tube and the annulus were packed with sugar to aid in maintaining concentricity.

Upon receipt of the formed boiler from the vendor, the sugar was removed by dissolving and rinsing in filtered hot water. Approximately 12 hours of rinsing were employed, four hours on the inner tube and four hours in each direction on the annular spacing. Distilled water was used for a final rinsing operation. Application of the Molisch Test cited above to samples of the final rinse water indicated no detectable sugar content.

The cleaned boiler assembly was then radiographed to determine the concentricity of the inner and outer tubes. Examination of these radiographs indicated that good concentricity was maintained. Radiographs of the potassium boiler inlet tube and the boiler coils are shown in Figures 30 and 31.

Welding of the boiler components shown in Figure 32 was then initiated. The inner and outer tubes were cut to the proper length, and the tube plug was welded to the inner tube. After inspection of this weld, the end connectors for the outer tube were positioned and welded along with the thermocouple wells and inlet plug. Radiographs of the potassium inlet section shown in Figure 33 illustrate the inlet plug configuration. A 0.060-inch-diameter Cb-1Zr wire was formed into a 1.0-inch-pitch helix on the 0.125-inch-diameter Cb-1Zr center rod. One TIG weld tack per revolution of the plug wire was made to hold the wire in place. The plug was then positioned within the straight section of the boiler inlet pipe and welded to the inlet fitting. The welded assembly was radiographed and leak tested prior to its inclusion in the boiler subassembly.

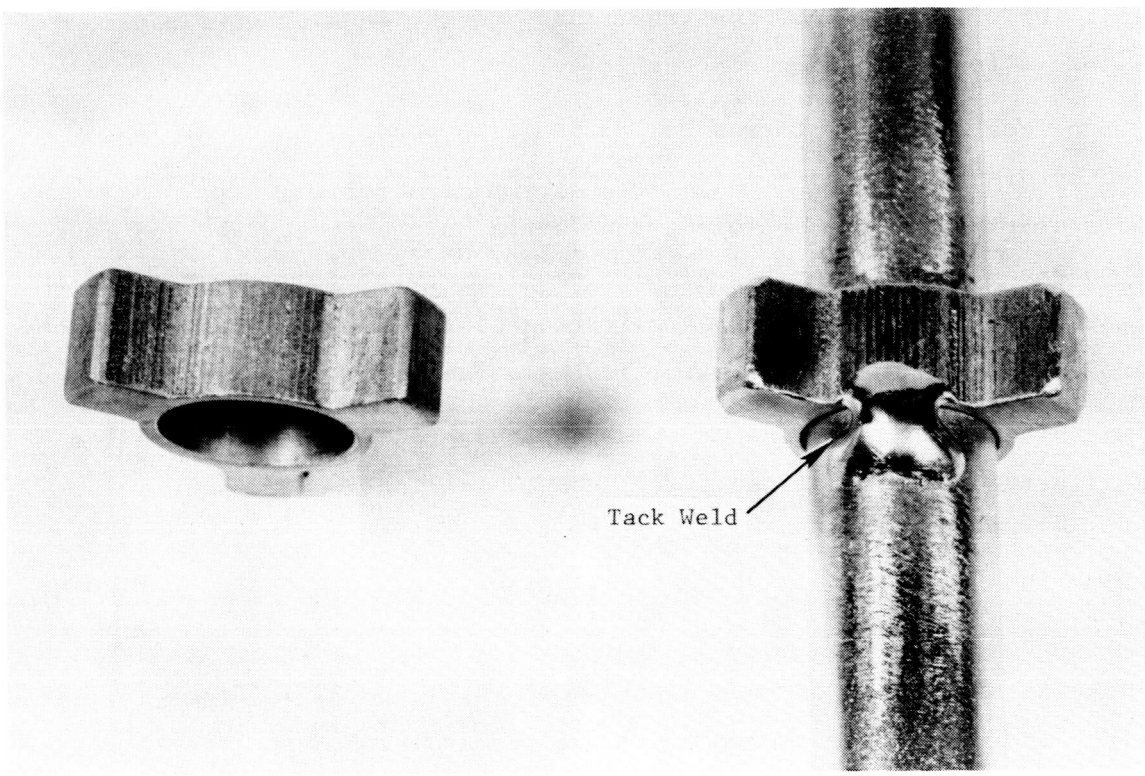

Figure 29. Cb-1Zr Boiler Tube Spacer Before and Following Attachment to the 0.375 Inch Cb-1Zr Potassium Containment Tube by Welding. (Orig. C65012828)

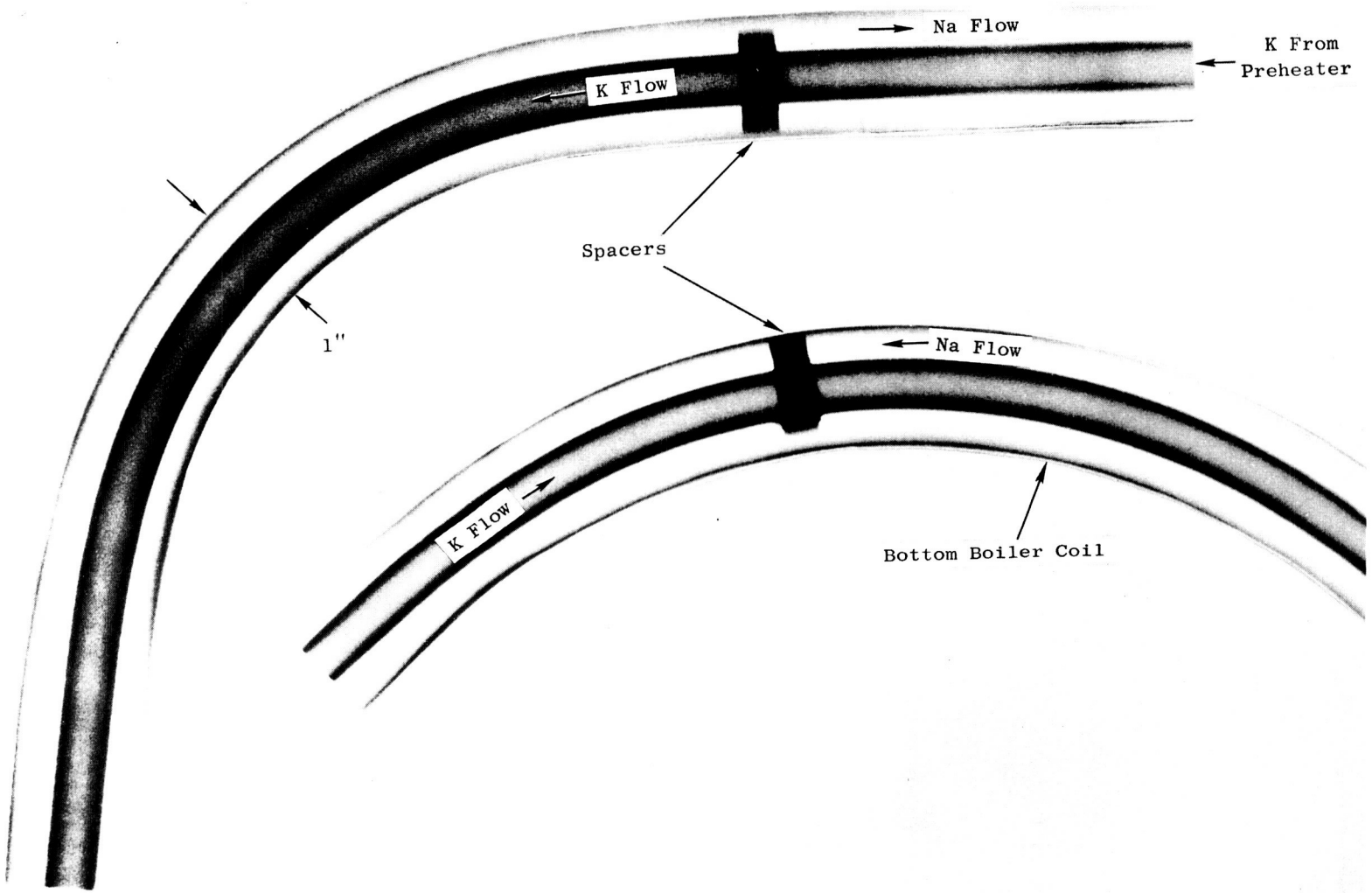

Figure 30. Radiographs of Portions of the Cb-1Zr Corrosion Test Loop Boiler Coil. Packed Sugar was Used to Maintain Concentricity of Tube During Forming.

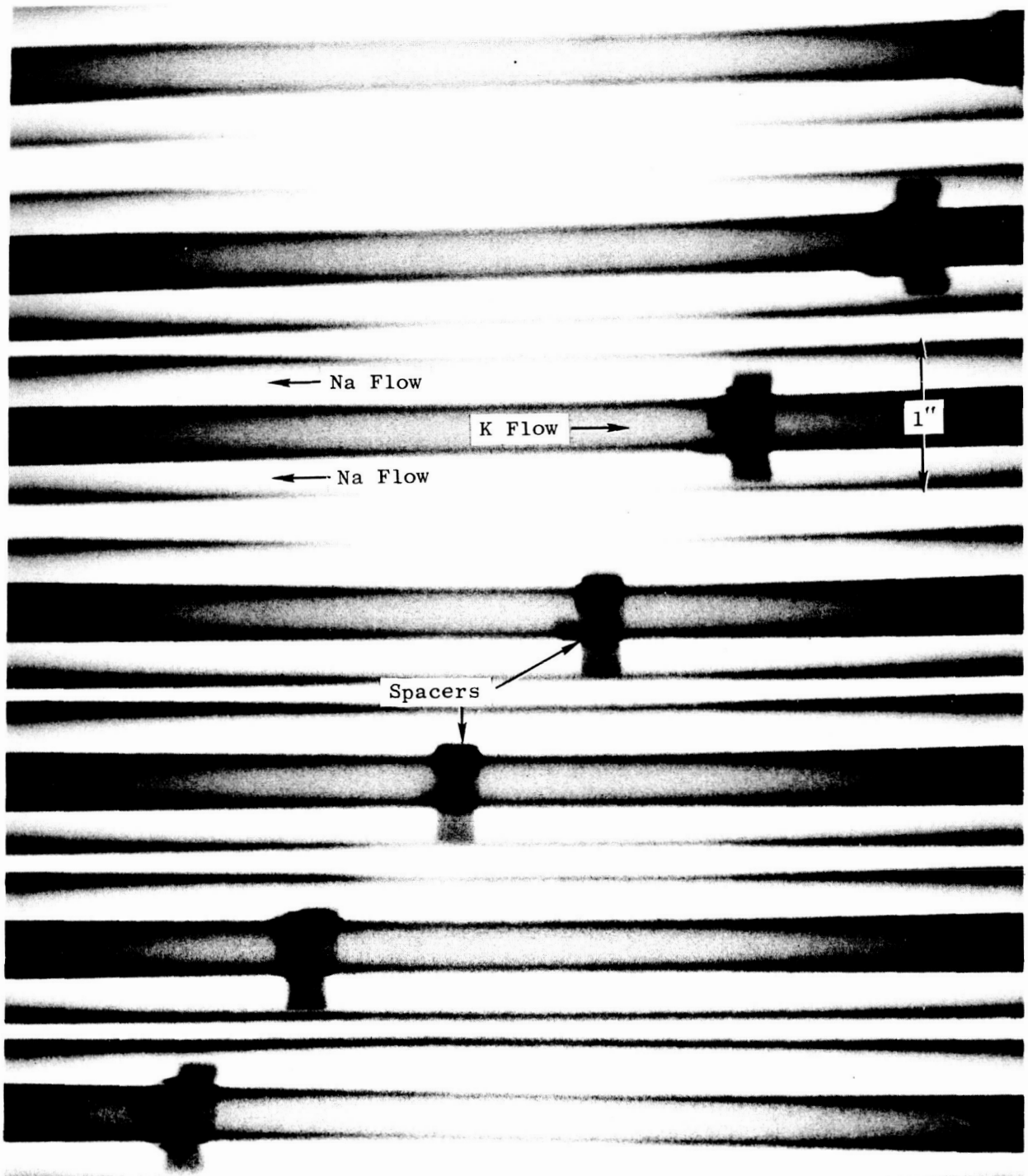

Figure 31. Radiograph of Cb-1Zr Corrosion Test Loop Boiler Coils. Packed Sugar was Used to Maintain Concentricity of Tubes During Forming.

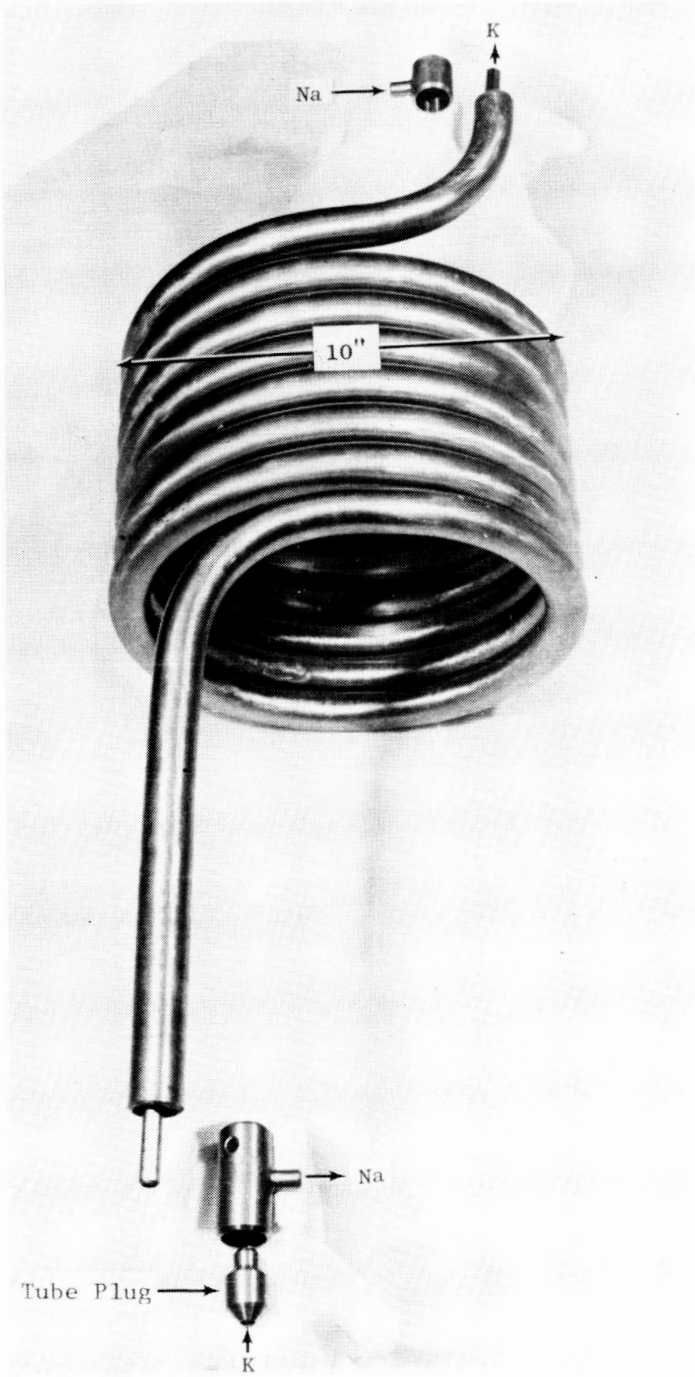

Figure 32. Cb-1Zr Corrosion Test Loop Tube-in-Tube Helical Boiler. (Orig. C650621101)

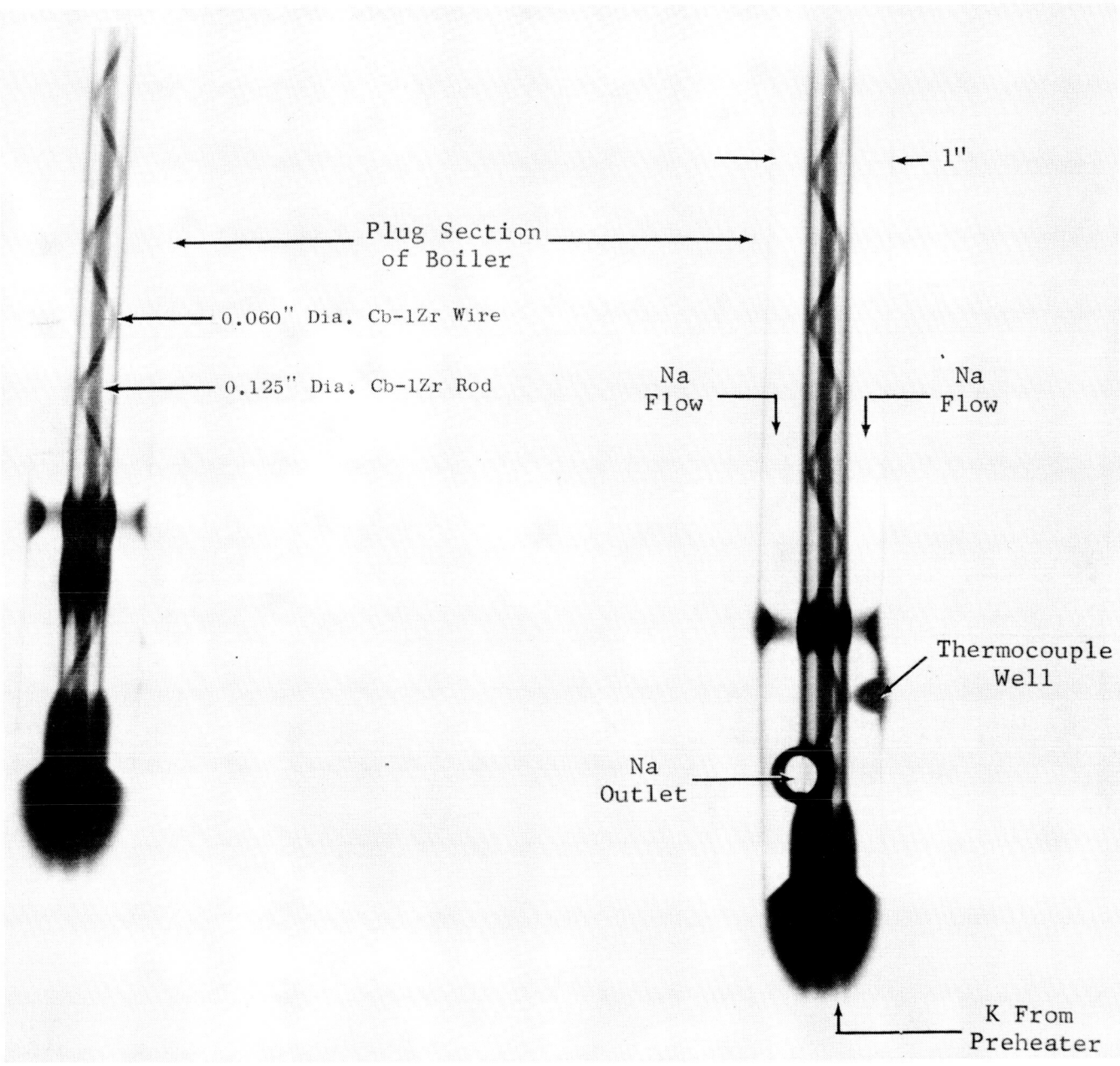

Figure 33. Two Radiographs of the Boiler Inlet Region of the Cb-1Zr Corrosion Test Loop Showing The Plug Configuration. (Orig. C65121737)

J. TURBINE SIMULATOR

Each turbine simulator stage consisted of a nozzle, turbine blade, and two specimen support pads as shown in Figure 34 for the tenth stage. The fabrication and assembly procedures used to construct the turbine simulators were dictated by the requirement to obtain very precise weight change data on these components following the 5000-hour test. The Mo-TZM alloy blades were polished to a 16-rms surface finish by the vendor utilizing a 240-grit alumina cloth followed by a final polish with 5-micron alumina before final cleaning and assembly. The Mo-TZM alloy nozzles were Elopolished, a refinement of electric spark discharge machining, to produce a 32-rms surface finish in the nozzle throat. The machining sequence is shown in Figure 35. This surface was further polished with 400-grit alumina paper to remove approximately 0.001 inch from the surface. A final polish with 5-micron alumina produced an 8-rms finish. Zyglo inspection of the finished parts indicated that the surfaces were free of cracks. It hould be noted that numerous surface cracks were detected in the blade pads (see Figure 34) after electric spark discharge machining of the airfoil shape. The majority of the cracks were located in the sharp radii at each end of the airfoil snape and were easily removed by filing and hand polishing with 5-micron alumina powder as required.

Prior to the assembly of the turbine simulator, the throat diameters of the Mo-TZM alloy nozzle specimens were measured in order to determine if minute enlargement or restriction of the nozzle throats occurred. The measurements were performed by the Sheffield Corporation, Dayton, Ohio, by means of an electronic comparator using a frictionless electronic transducer directly compared to master gauge blocks. Results of these measurements are given in Table VII. Nozzle number 9 was 0.0008-inch oversize, number 2 was 0.0001-inch oversize, and number 4 was 0.00003-inch oversize in one location. These minor discrepancies were accepted as they would not have a significant effect on loop performance.

The nozzle/blade assemblies were then disassembled, cleaned with ethyl alcohol, and the weights of each component were recorded and filed for subsequent use during posttest evaluation.

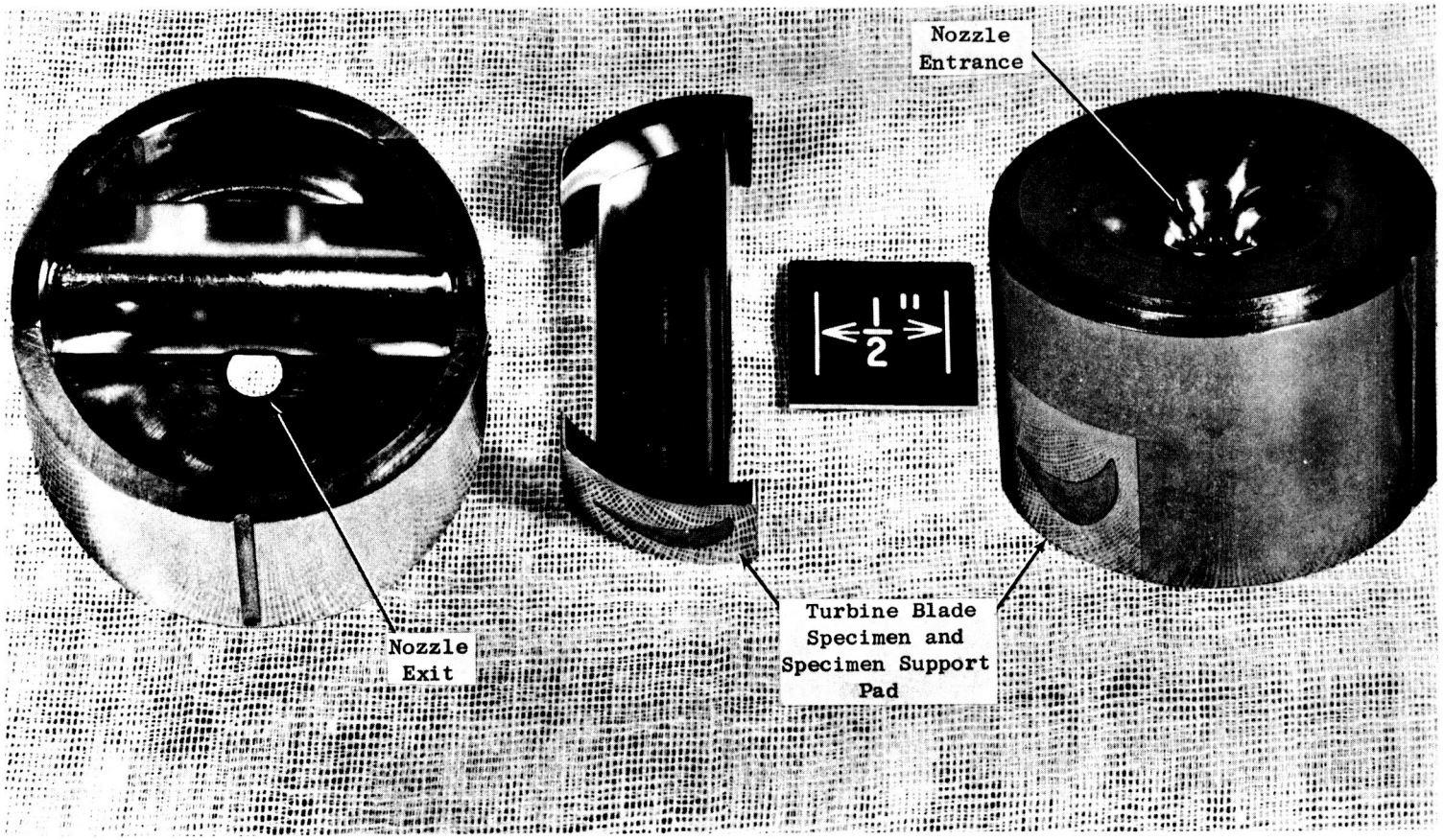

Figure 34. Mo-TZM Alloy Turbine Simulator Nozzle and Blade Assembly. (Orig. C65031228, C65031227, C65031230)

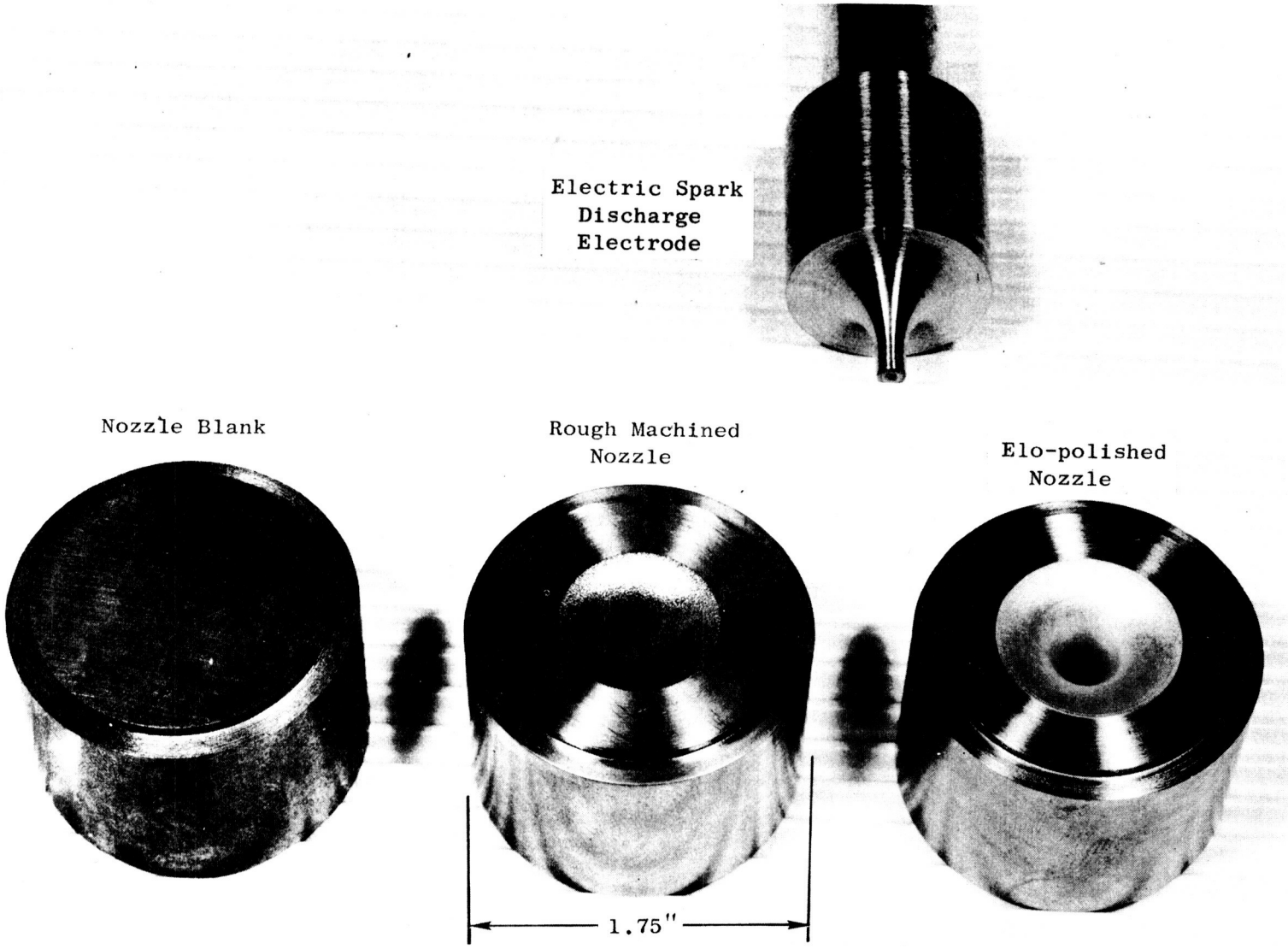

Figure 35. Machining Sequence Required to Produce the Mo-TZM Alloy Nozzle for the Cb-1Zr Corrosion Test Loop - Turbine Simulator. Two Additional Polishing Operations are Required to Produce an 8-rms Surface Finish. (Orig. C6412207)

TABLE VII

ORIFICE DIAMETERS FOR THE Mo-TZM ALLOY NOZZLES FOR THE Cb-1Zr CORROSION TEST LOOP TURBINE SIMULATOR AS DETERMINED BY AIR-GAUGE INSPECTION

Stage No.	Identification	Specified Diameter, Inches	Actual Diameter, Inches	
			0 Degrees[a]	90 Degrees
1	Dwg. 119C2853 P1	0.099 - 0.100	0.09940	0.09945
2	Dwg. 119C2853 P2	0.100 - 0.101	0.101080	0.101100
3	Dwg. 119C2853 P3	0.115 - 0.116	0.115300	0.115270
4	Dwg. 119C2853 P4	0.128 - 0.129	0.129030	0.128960
5	Dwg. 119C2853 P5	0.141 - 0.142	0.141170	0.141205
6	Dwg. 119C2853 P6	0.158 - 0.159	0.158050	0.158025
7	Dwg. 119C2853 P7	0.175 - 0.176	0.175720	0.175660
8	Dwg. 119C2853 P8	0.205 - 0.206	0.205080	0.205075
9	Dwg. 119C2853 P9	0.221 - 0.222	0.222790	0.222785
10	Dwg. 119C2853 P10	0.249 - 0.250	0.249225	0.249215

[a] In line with OD slot on Stages No. 2 through 10.

The number one nozzle/blade assembly was positioned in its Cb-1Zr outer casing as shown in Figure 36. The end caps, thermocouple wells, and one-inch-diameter potassium flow tube were then welded to complete the single-stage turbine simulator. Postweld annealing of this subassembly was conducted after it was joined to the boiler to form a major subassembly.

The remaining nine nozzle/blade assemblies were positioned as shown in Figure 37. These assemblies are rabbeted together and aligned in their Cb-1Zr casing with a 0.062-inch-diameter wire which extends through a keyway in the nozzles and casing. This wire insert prevents rotation of the individual nozzle in the casing during test operation, but its primary purpose is to facilitate disassembly of the turbine simulator without damaging the individual nozzles and blade as this would make it impossible to obtain accurate weight change data on these components. The assembly of the nozzle/blade stack in the casing was somewhat complex since both unit straightness and axial alighment had to be maintained. During assembly it was found that additional diametrical clearance between the nozzles and casing was required. This additional clearance was obtained by heating the Cb-1Zr casing to approximately 325°F in air. Using this procedure, the delicate fitting operation was accomplished. The assembly was at the temperature specified for approximately 15 minutes. The Cb-1Zr end caps and thermocouple wells were then welded to the casing to complete the assembly.

K. BOILER SUBASSEMBLY

This major subassembly which constitutes about one-half of the potassium loop is illustrated in Figure 38. Four welds were required to join the components which included the preheater coil, vapor nucleator, boiler, pressure transducer connector, single-stage turbine simulator, and 1.0-inch-diameter tube. This major subassembly was then wrapped with 0.002-inch Cb-1Zr foil in preparation for the postweld annealing treatment described in Part M of this section.

This subassembly is also representative of the procedure utilized for

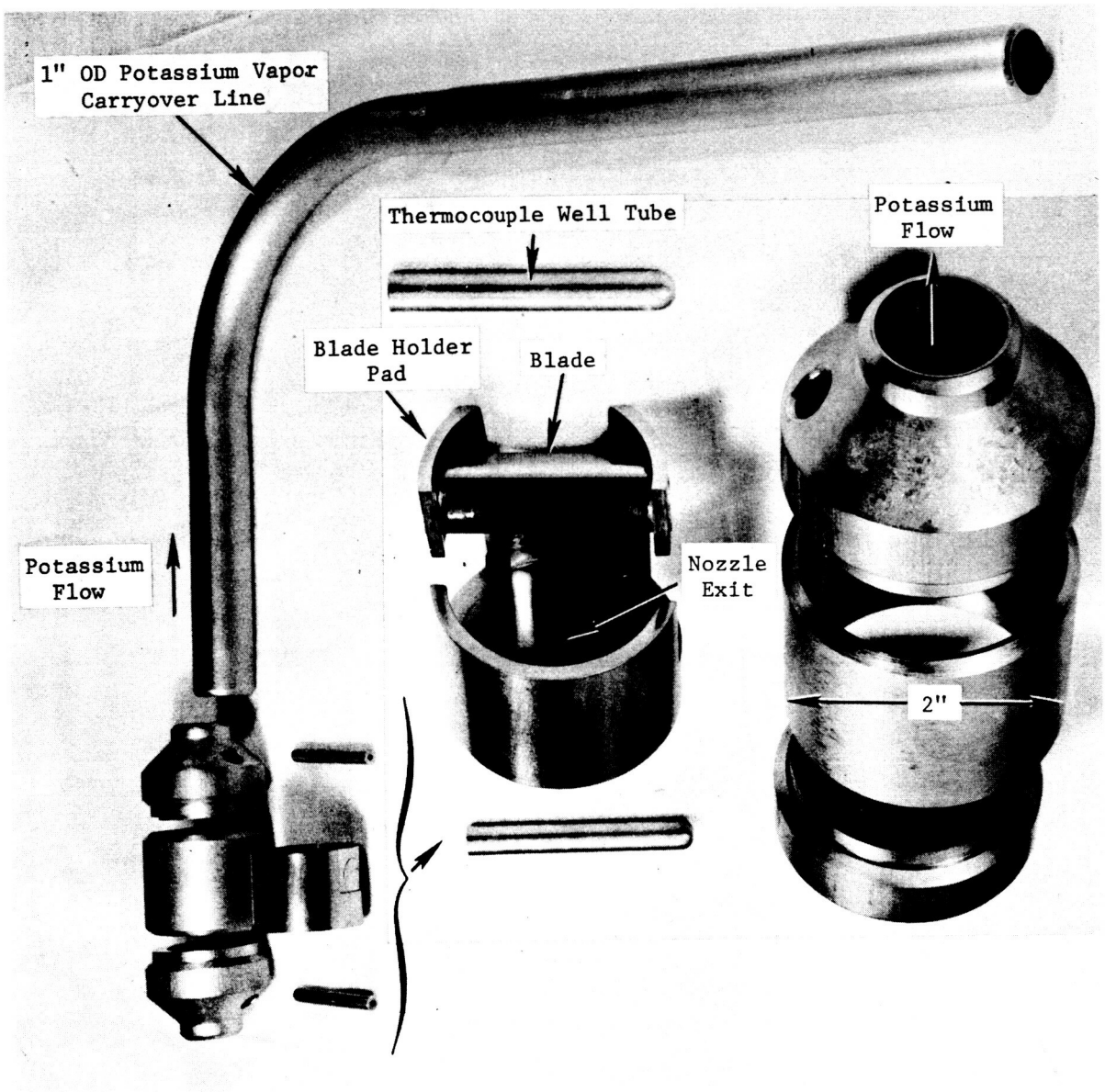

Figure 36. Overall and Enlarged View of the First Stage Turbine Simulator and the Potassium Vapor Carryover Pipe. (Overall View, C65030136) (Enlarged View, C65030135)

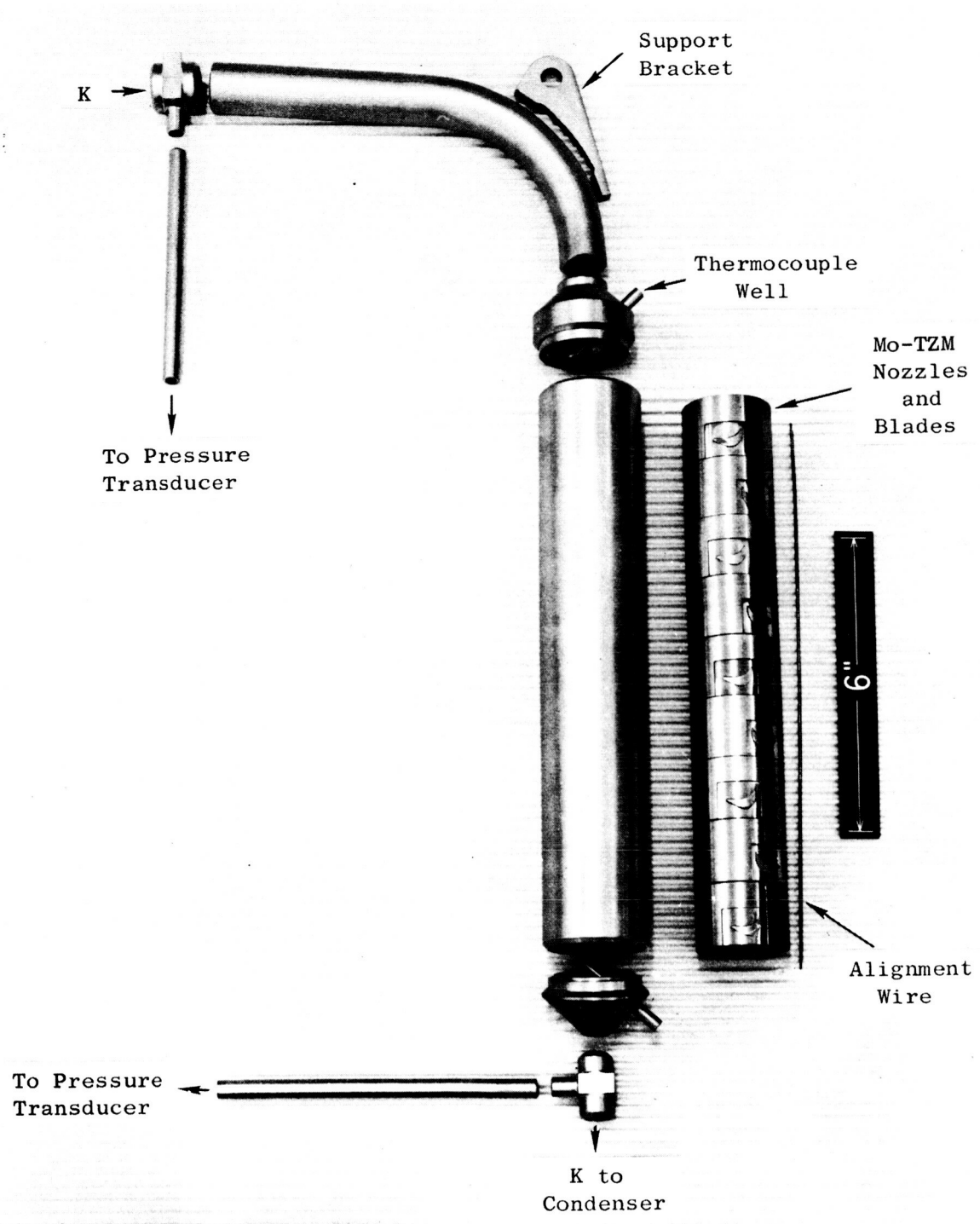

Figure 37. Turbine Simulator (Stages 2-10) of the Cb-1Zr Corrosion Test Loop Prior to Assembly. Nozzles and Blades: Mo-TZM. Tubing, Reducers, Casing and Miscellaneous Fittings: Cb-1Zr. (Orig. C65062198)

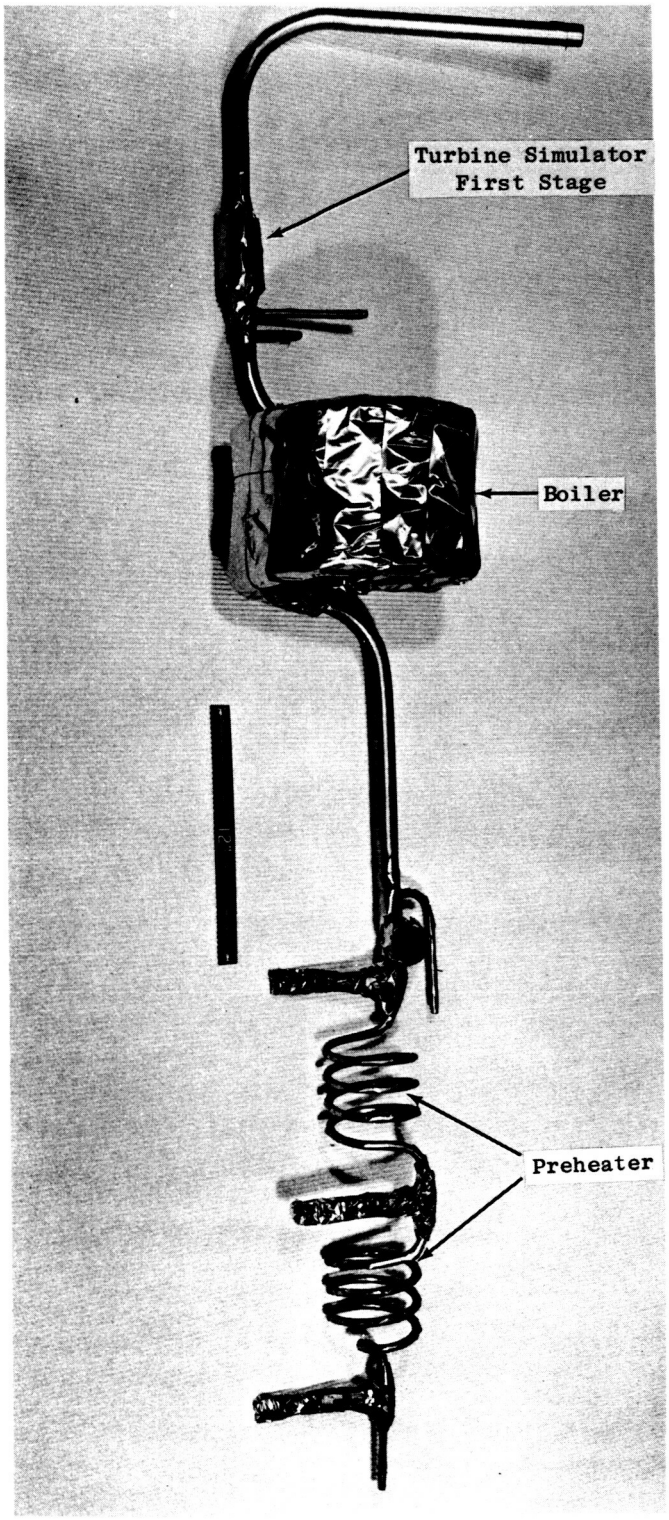

Figure 38. Preheater/Boiler/First Stage Turbine Simulator Assembly Wrapped with Cb-1Zr Alloy Foil Prior to Annealing. (Orig. C65031235)

joining the 0.375-inch-diameter process tubes to the larger diameter piping sections. As shown in Figure 38, short lengths of the 0.375-inch tubing were welded to the pressure transducer connectors, boiler inlet and outlet, and preheater electrode prior to postweld annealing treatment This procedure permitted final assembly welds and local postweld annealing treatments to be performed on the 0.375-inch tubing at readily accessible locations. Only one weld in the 1.0-inch-diameter potassium carryover tube at the top of the loop was required during the final assembly phase.

L. CONDENSER SUBASSEMBLY

The weld between the condenser pipe and the 0.25-inch thick Cb-1Zr radiator fins represented the largest continuous weldment required for loop fabrication. Approximately 1.5 pounds of 0.125-inch-diameter filler wire was consumed. Alignment of the fins and condenser pipe was maintained by a welding fixture shown in Figure 39. This photograph was taken through one of the welding chamber viewports opposite the welding station. All the welding fixture parts which contacted the Cb-1Zr were made from unalloyed molybdenum.

As expected from earlier welding trials, the 0.375-inch-OD Schedule 80 condenser pipe was distorted by the welding operation. Radiographic inspection of the condenser assembly revealed a decrease in inside diameter in a direction parallel to the fins. The nominal 0.421-inch inside diameter in this direction decreased to 0.295-0.315 inch. At each of the 0.050-inch gaps between the fins, weld shrinkage was less pronounced with the inside diameter decreasing to a minimum of 0.370-0.380 inch. On an axis perpendicular to the fins, the inside diameter increased to 0.425-0.440 inch.

Following attachment of the fins, the condenser was welded to the subcooler and the nine-stage turbine simulator which completed this major subassembly as shown in Figure 40 (a). This subassembly was then wrapped with 0.002-inch Cb-1Zr foil in preparation for postweld annealing treatment.

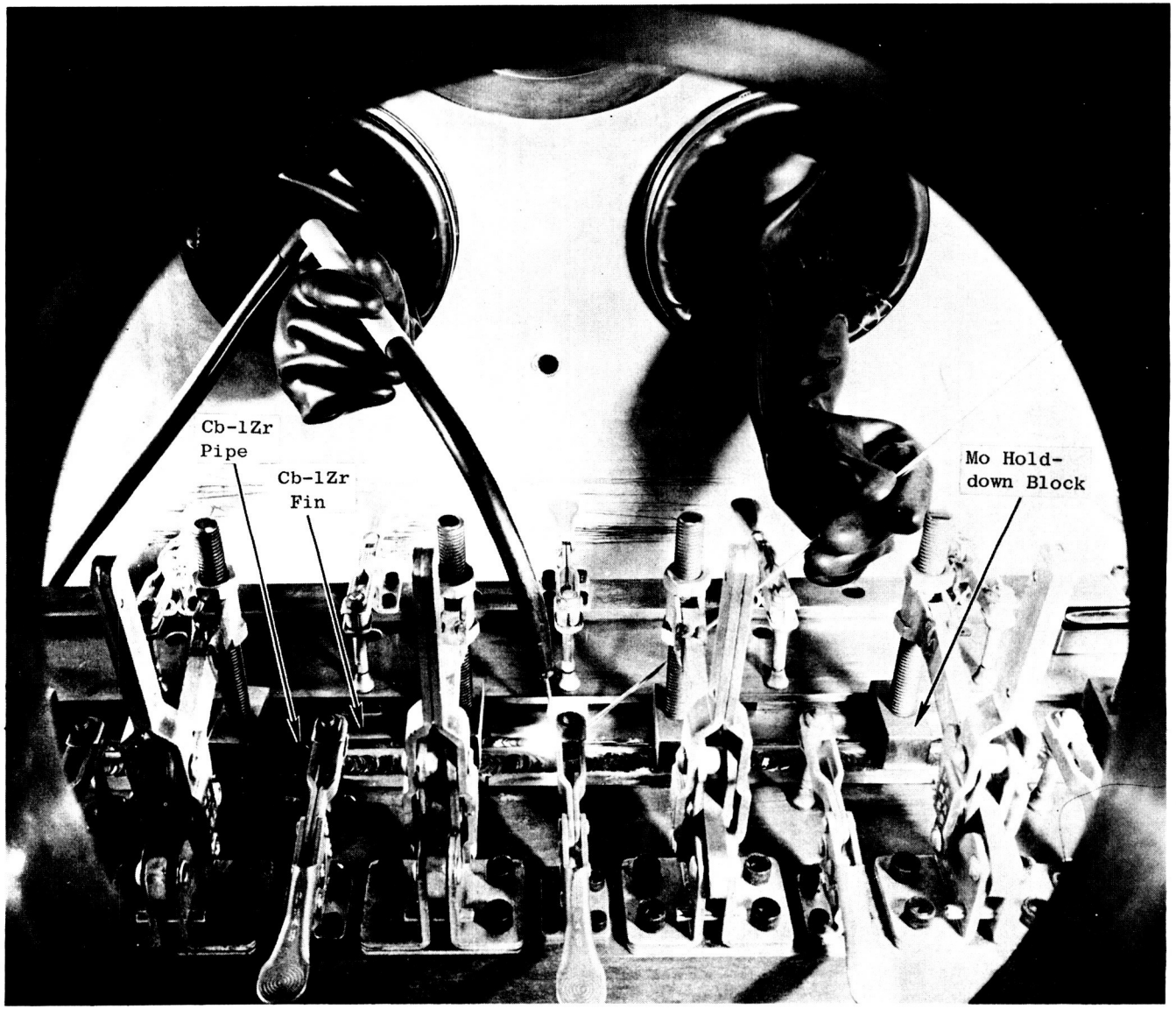

Figure 39. Cb-1Zr Corrosion Test Loop Condenser and Fixture During Welding of Fin to Condenser Pipe. (Orig. C65022602)

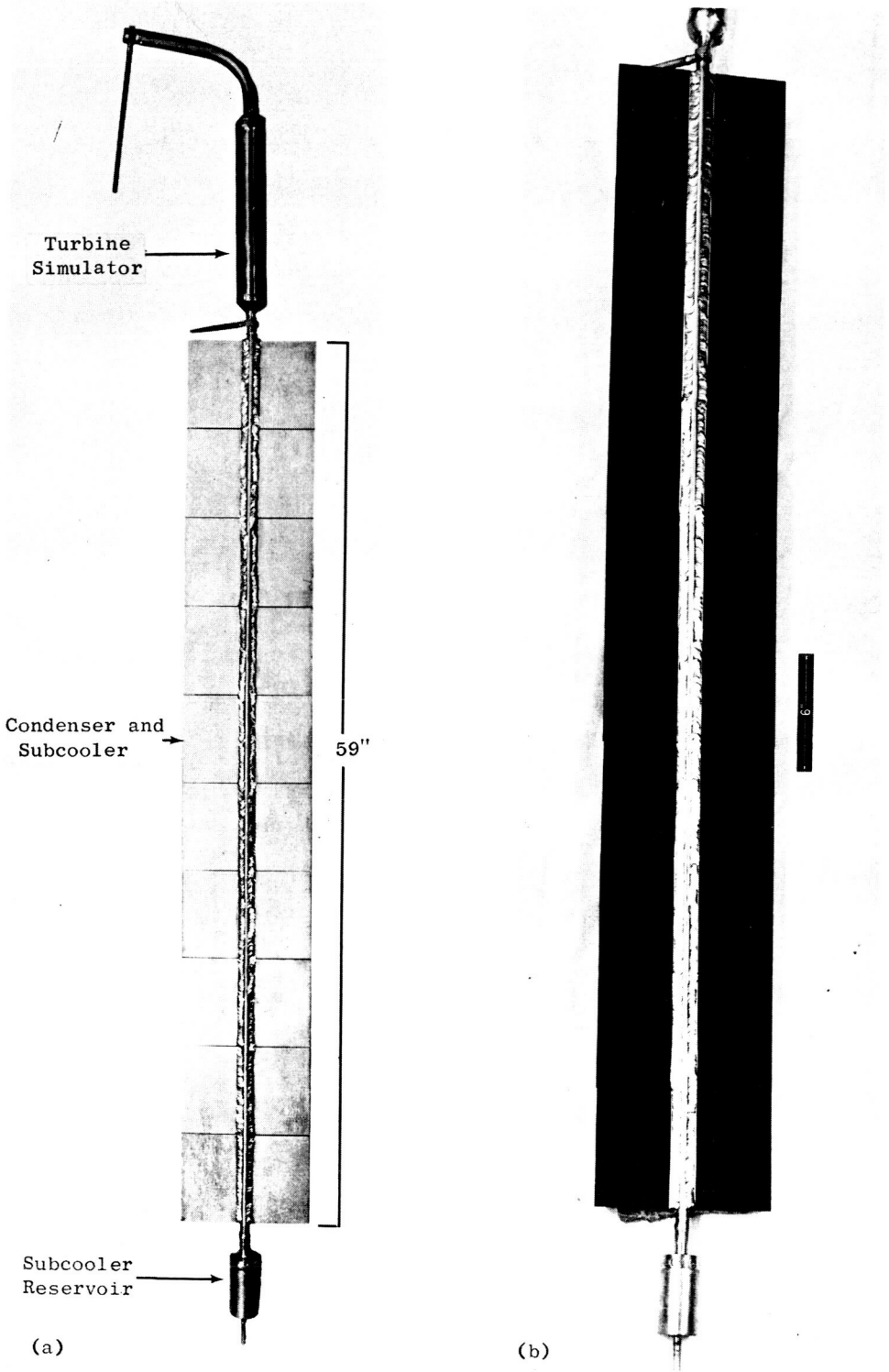

Figure 40. Turbine Simulator, Condenser/Subcooler and Subcooler Reservoir of the Cb-1Zr Corrosion Test Loop Before (a) and Following (b) Application of the Iron Titanate Coating. (a) (Orig. C65031734) (b) (Orig. C65032921)

M. POSTWELD ANNEALING

The postweld annealing of components was performed in vacuum furnaces which were previously qualified by analysis of Cb-1Zr control samples for oxygen, nitrogen, hydrogen, and carbon concentration. In all instances, it was found necessary to deviate from SPPS Specification No. 03-0005-00-A (3C) by setting the upper limit of pressure near 5×10^{-5} torr rather than the 1×10^{-5} torr specified. Pressure levels maintained during qualification furnace runs were duplicated or improved during the annealing of actual components. As an added precaution one overlapping layer of 0.002-inch-thick Cb-1Zr foil was used to wrap each assembly.

Using these procedures, no significant contamination of control samples which accompanied the loop components during the 2200°F for one-hour anneal was evident, as shown in Table VIII.

A postweld anneal which was typical of the procedures employed was that of the boiler, Figure 38, and condenser, Figure 40 (a), subassemblies, and the sodium heater coil which were annealed in one furnace run. The application of the high emittance coating to the condenser, which is described in the next part of this section of the report, was done following annealing of this component. Quality assurance specimens included with the furnace run were 1.0-inch- and 0.375-inch-diameter tubes, and two specimens of 0.040-inch-thick Cb-1Zr sheet.

After positioning of the three subassemblies described above, the vacuum heat treating furnace was evacuated overnight with hot water circulating through the cooling channels to promote outgassing. After turning on the cold water, the pressure in the furnace was 1×10^{-6} torr. At this point, furnace power was turned on and the components were heated to 600°F for two hours. During the first one-half hour, the furnace pressure increased to 2.5×10^{-4} torr, then decreased to 8×10^{-6} torr at the end of two hours at 600°F. A gradual temperature increase to 2200°F was accomplished in one and one-half hours. During this time, furnace pressure increased to 8×10^{-5} torr at 1200°F, then decreased to 2.5×10^{-5} torr at 2200°F. During the one-hour annealing run at 2200°F, the pressure decreased to 8×10^{-6} torr.

TABLE VIII

RESULTS OF CHEMICAL ANALYSES OF Cb-1Zr ALLOY WELDS[1] AFTER HEAT TREATMENT

Specimen Description	Pressure, Torr: Start of Run	Pressure, Torr: End of Run	Element, ppm: O	N	H	C
Base Metal Analysis by Vendor[2]			90	42	5	35
Base Metal Analysis by GE[2]			56	14	6	10
Weld Metal-As Welded			69	10	1	10
Weld Metal After 2200°F/One-Hour Heat Treatment in the C.I. Hayes, Inc. Furnace (Model PS-107, 20-Inch Diameter x 36-Inch) at Stellite Division, UCC (Wrapped)[3] - Sample Which Accompanied EM Pump Ducts	6.8×10^{-5}	6.5×10^{-5}	65	23	1	10, 50
Weld Metal After 2200°F/One-Hour Heat Treatment in the C.I. Hayes, Inc. Furnace (Model PS-107, 20-Inch Diameter x 36-Inch) at Stellite Division, UCC (Wrapped)[3] - Sample Which Accompanied Surge Tank Assemblies	7.5×10^{-5}	7.5×10^{-5}	79	21	2	35
Weld Metal After 2200°F/Two-Hour Heat Treatment in the Brew Company Furnace (42-Inch x 12-Inch x 104-Inch) at DuPont Company - Qualification Sample	7.0×10^{-5}	5.5×10^{-5}	99	16	1	10

[1] Only weld metal portion of weldments analyzed.

[2] 0.040-inch thick sheet, Materials Control Number (MCN) 454.

[3] Specimens and components wrapped with one overlapped layer of 0.002-inch Cb-1Zr foil.

Approximately three minutes from the end of the furnace run, a series of small pressure pulses indicated an intermittent electrical short between a component and the furnace elements. The run was immediately terminated. After overnight cooling, the subassemblies were removed from the furnace, and the point of electrical contact was found at the end of the process tube on the sodium heater coil. No harm was done since this tube had excess length which was removed before final assembly.

During the postweld annealing operation, the area between the nine-stage turbine simulator and the condenser bent slightly causing a misalignment of these components. This condition was corrected by manual straightening in the welding chamber using a tungsten inert arc torch to heat the bent region.

N. CONDENSER FIN COATING APPLICATION

The evaluation of the high-emittance iron titanate coating for the condenser is described in Appendix F. After successful conclusion of this preliminary test, a stainless steel mock-up of the condenser was fabricated and shipped to Pratt & Whitney Aircraft for use in establishing techniques for coating of the condenser fins.

Prior to application of the iron titanate coating to the Cb-1Zr fin, the surface of the Cb-1Zr fin was grit blasted with 50-micron alumina. Each fin side was grit blasted just prior to application of the coating. Previous coating tests indicated that poor adherence of the coating to the metal surface has resulted when there is a considerable time delay (in excess of a few hours) between the grit blasting and coating operations. During grit blasting and coating, aluminum tape was used to mask off other regions of the condenser. The coating was applied by means of a plasma-arc device (Plasmatron) utilizing argon to form the plasma. Conditioning the surface by going over it completely with the argon plasma only (no iron titanate feed into the plasma) had been found to promote adherence, and this approach was used. Each pass gave an iron titanate deposit 1/2-inch to 3/4-inch wide, and after each pass of the gun back and forth over the length of the fin, the gun was manually indexed about 1/4 inch. Each pass

laid down a deposit about 1/2 mil in thickness. A total coating thickness of approximately 3 mils was obtained. The temperature of the back side of the condenser fin was monitored during application of the coating and did not exceed 300°F. The coated condenser subassembly is shown in Figure 40 (b).

O. FINAL ASSEMBLY OF LOOP

The final assembly phase of loop construction was initiated by the joining of two major subassemblies, the boiler and potassium surge tank, as depicted in Figure 17. This step involved making one weld between the potassium preheater and the potassium pump outlet line. The stainless steel loop support structure shown in Figure 41 was then mounted on the vacuum chamber spool piece, and the major Cb-1Zr subassemblies were placed in position. The loop welding fixture was then positioned inside the support frame, and the attachments were made to the loop. This step permitted the loop to be supported in the exact location required for loop operation. The loop support structure was then disassembled and the loop, supported by its welding fixture, was removed from the vacuum chamber spool section as shown in Figure 42. The position of the loop within the welding chamber is shown in Figure 43. The loop position within the 36-inch-diameter section of the welding chamber is shown in Figure 44, which also illustrates the function of the welding fixture support ring.

A total of seven welds and local postweld annealing heat treatments were done to complete the Cb-1Zr welding. During welding, the loop welding fixture was rotated to provide the necessary welding positions. The local postweld anneals were done using radiant tungsten coil furnaces, Figure 45, positioned on the individual joints. Temperatures were monitored by two Pt/Pt-10Rh thermocouples attached to the joint area. A Cb-1Zr control specimen and overlapping 0.002-inch-thick Cb-1Zr foil for additional protection from contamination were included in the heated section. Two postweld anneals were done in sequence during each welding chamber evacuation. The vacua maintained during these seven local postweld anneals ranged between 1.3×10^{-5} and 7.4×10^{-6} torr.

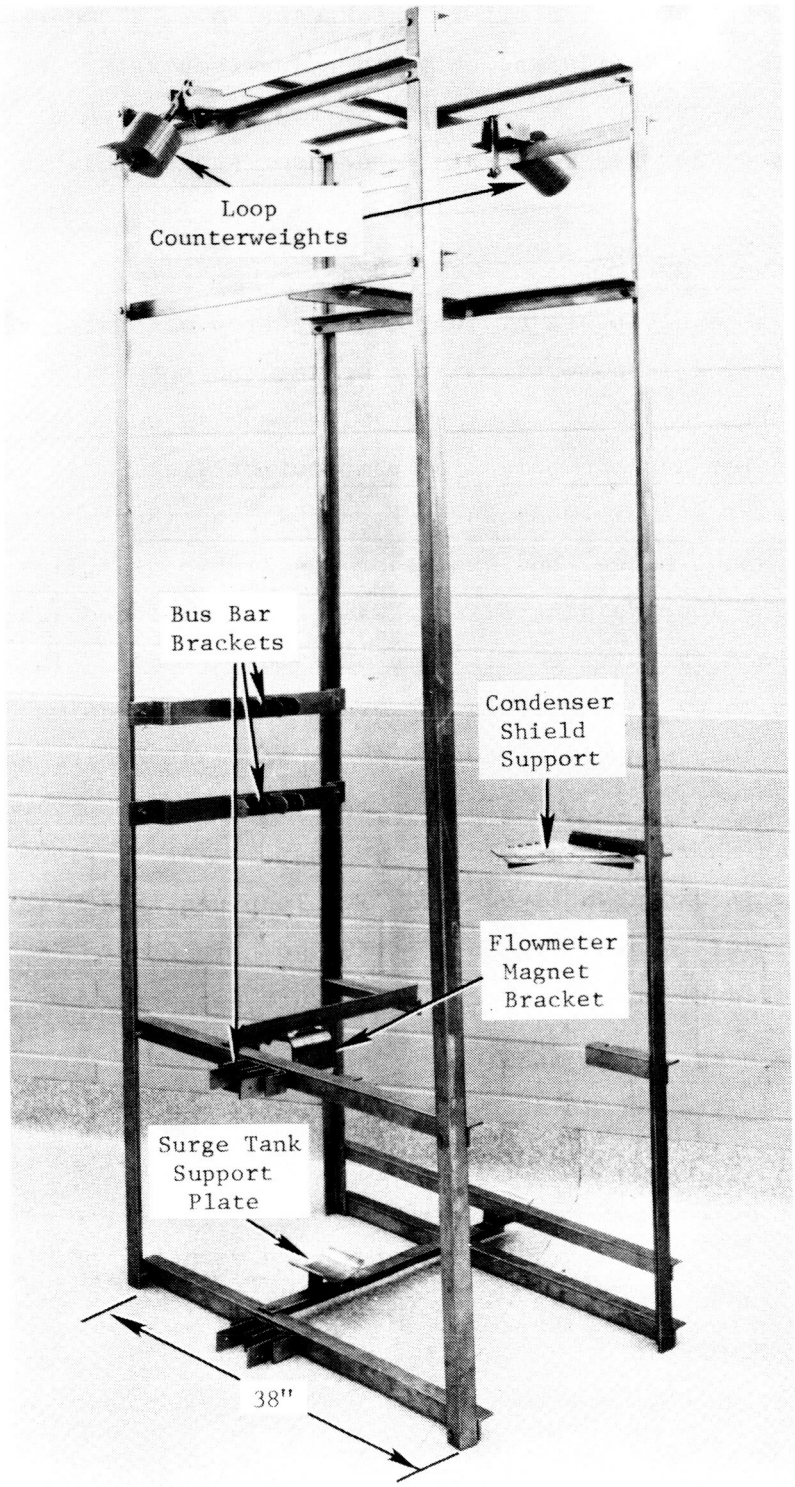

Figure 41. Type 304 Stainless Steel Support Structure for the Cb-1Zr Corrosion Test Loop. (Orig. C65031232)

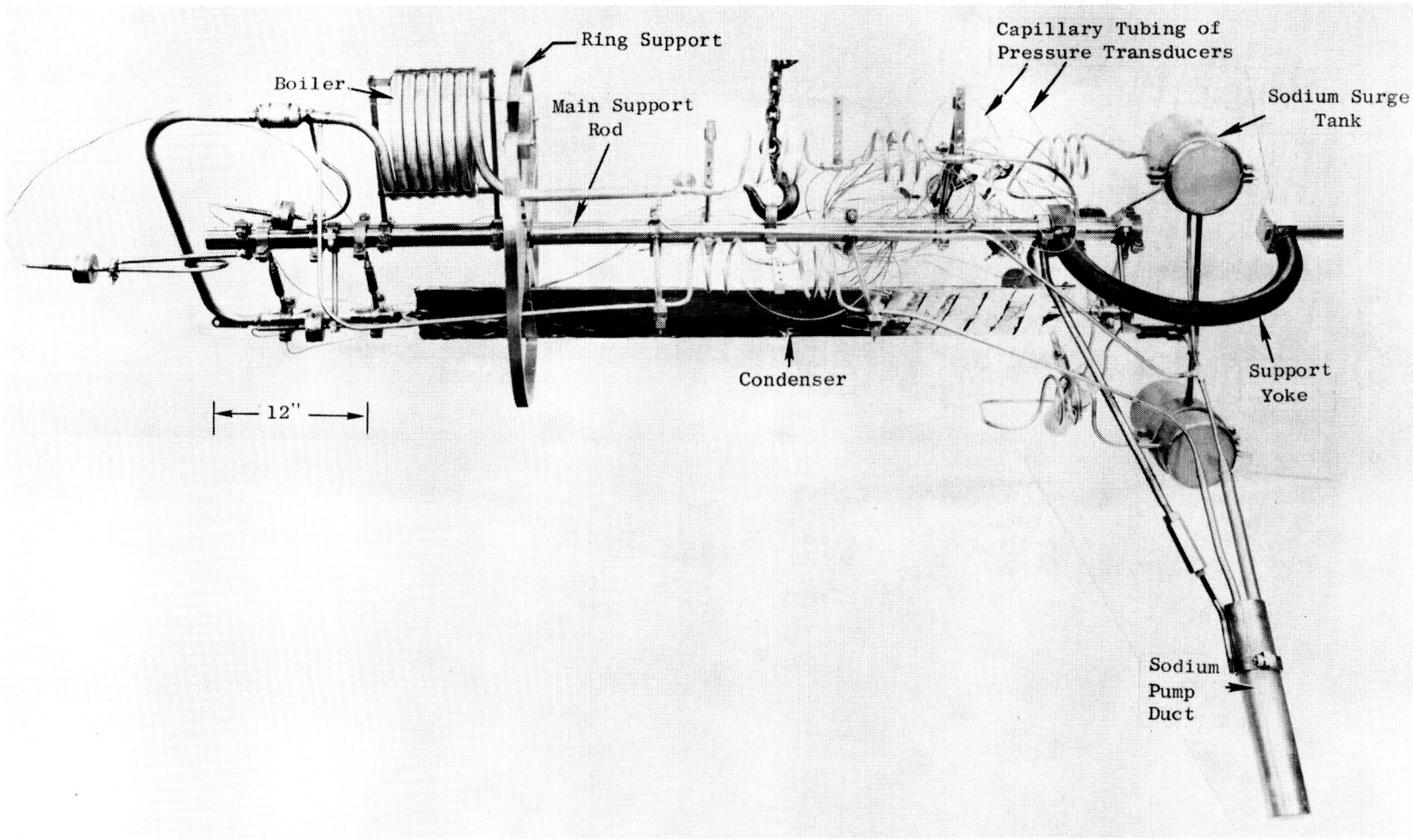

Figure 42. Cb-1Zr Corrosion Test Loop Mounted on Welding Fixture.
(Orig. C65051297)

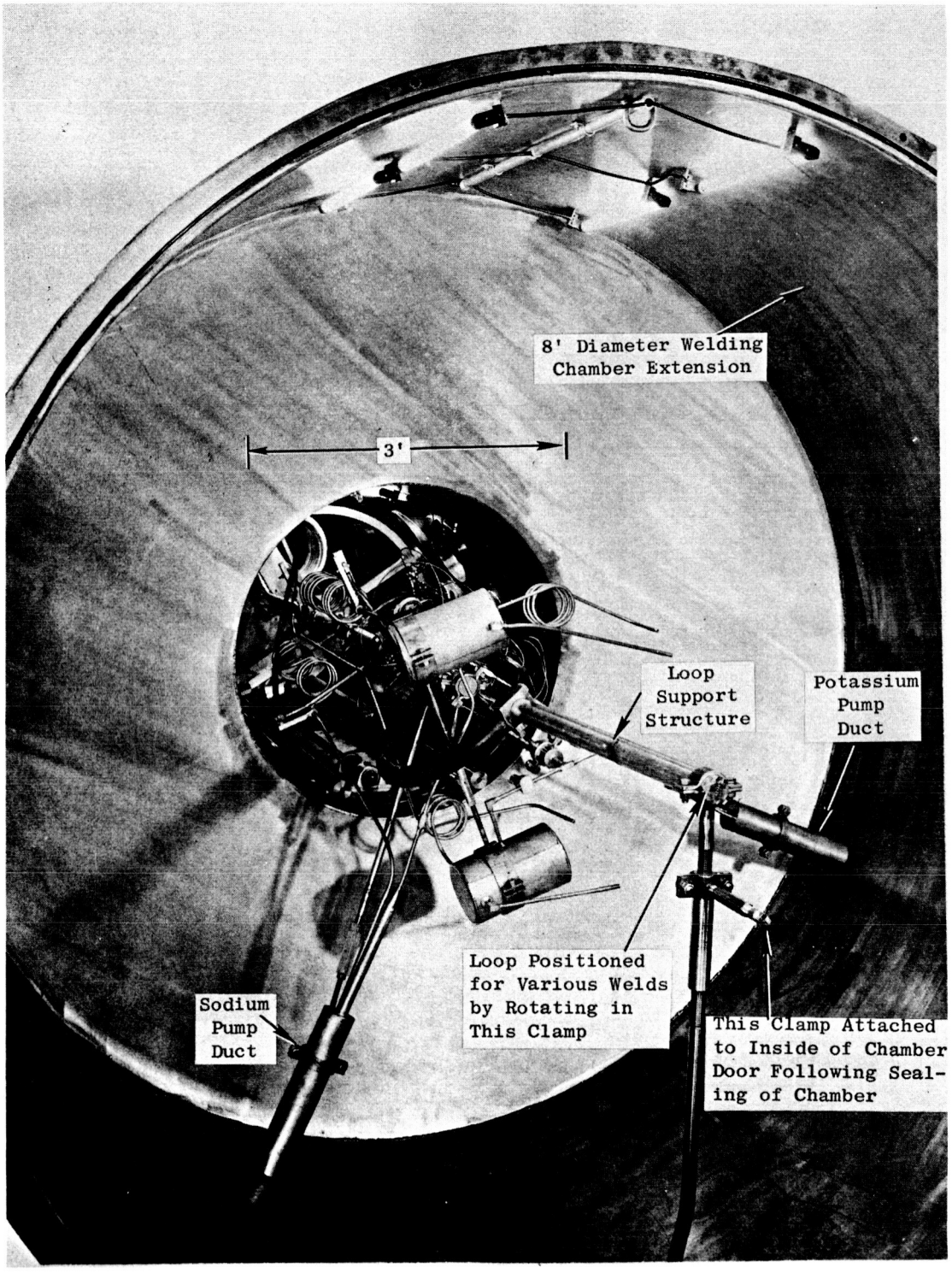

Figure 43. Cb-1Zr Corrosion Test Loop Positioned in the Welding Chamber During Final Assembly. (Orig. C65051295)

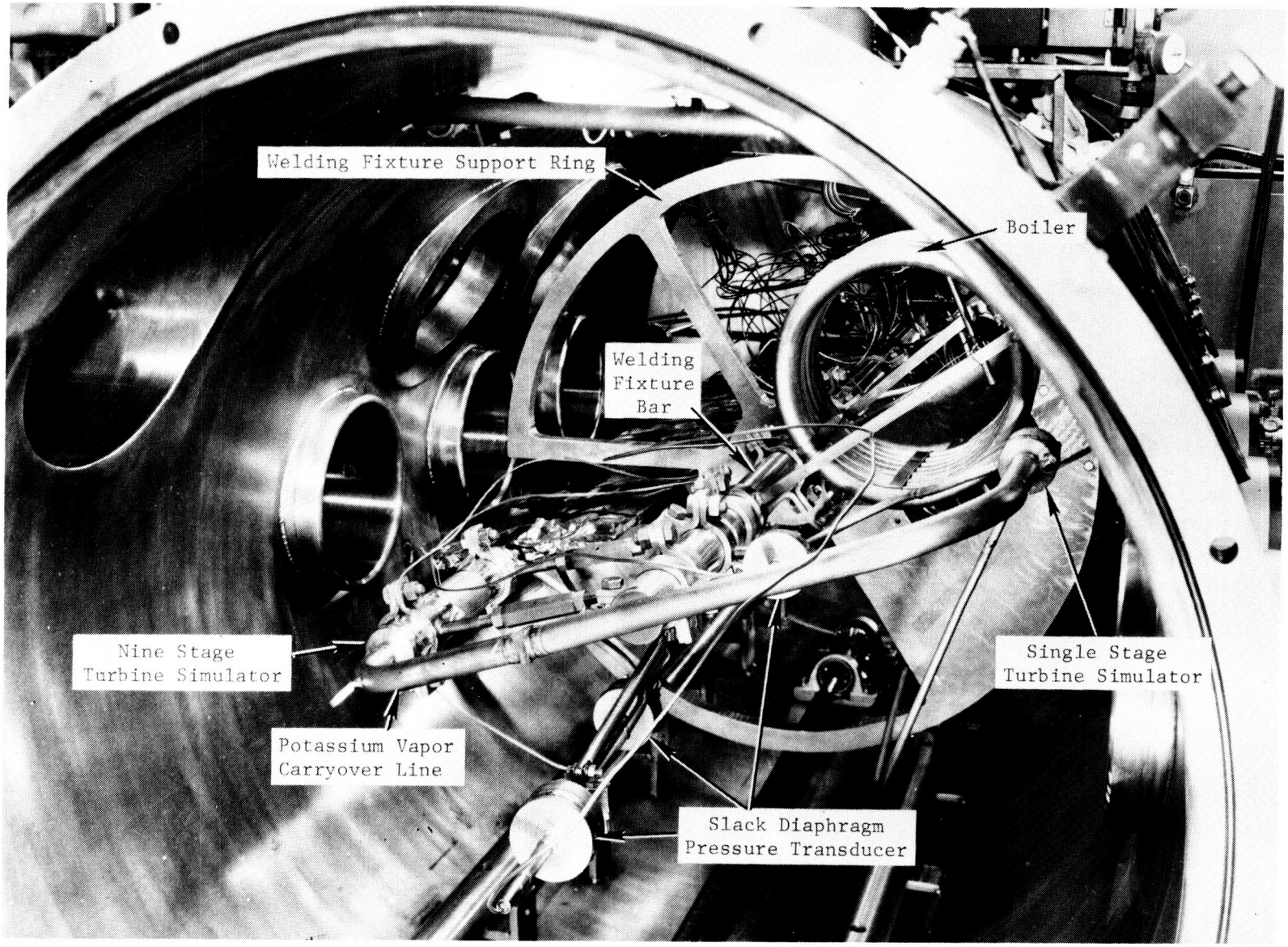

Figure 44. Cb-1Zr Corrosion Test Loop and the Welding Fixture Positioned in the Welding Chamber in Preparation or Final Welding Operations. (Orig. C65051294)

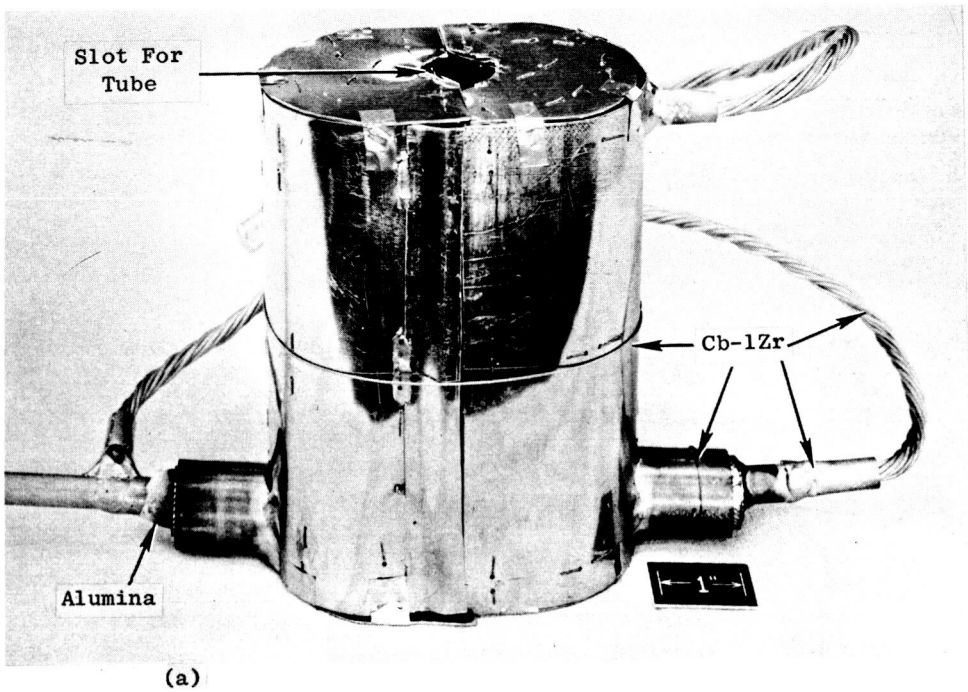

(a)

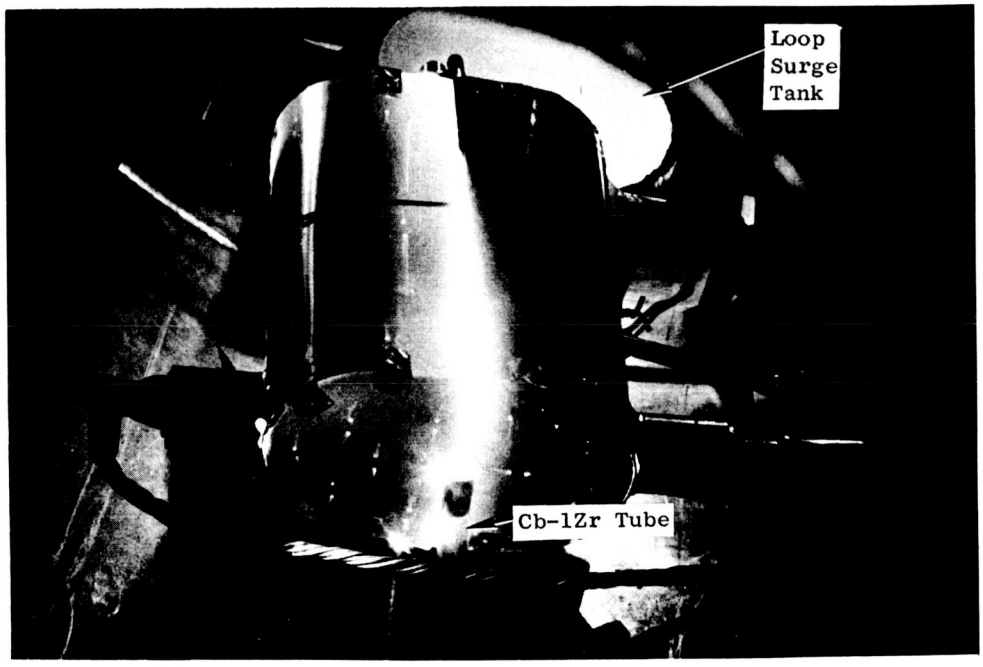

(b)

Figure 45. Refractory Metal Furnace for Vacuum Annealing of Cb-1Zr Loop Weldments in the Welding Chamber. Helical Heater Elements of Tungsten Wire and Eight Layers of Tantalum Reflective Foil Insulation Used to Achieve 2200°F Annealing Temperature. View (a) Shows Furnace Prior to Mounting on Loop Tube Weldments and (b) Shows Furnace in Operation. (a) (Orig. C65032922) (b) (Orig. C65032301)

Following the annealing of the welds, the loop, supported on the welding fixture, was removed from the welding chamber and repositioned in the vacuum tank spool section. The loop is shown in Figure 46 just prior to positioning in the spool section. The loop support structure was then assembled to provide permanent support for the loop. After removal of the welding fixture, the Type 316 stainless steel fill and dump lines and gas pressure lines were welded to the vacuum chamber ports. Also, stainless steel components of the EM pumps and vacuum feedthroughs for the slack diaphragm transducer were welded in position. Several minor adjustments in the stainless steel support structure were also made to accommodate the position of the potassium flowmeter, heater electrodes, and condenser shield drive assembly. The assembly of the loop in the support structure and vacuum chamber spool section is illustrated in Figure 47. A more detailed view of the spool section, Figure 48, shows the loop arrangement in that area.

The final leak checks of the system and the transfer of the spool piece and loop to the test area are described in Section VII of this report.

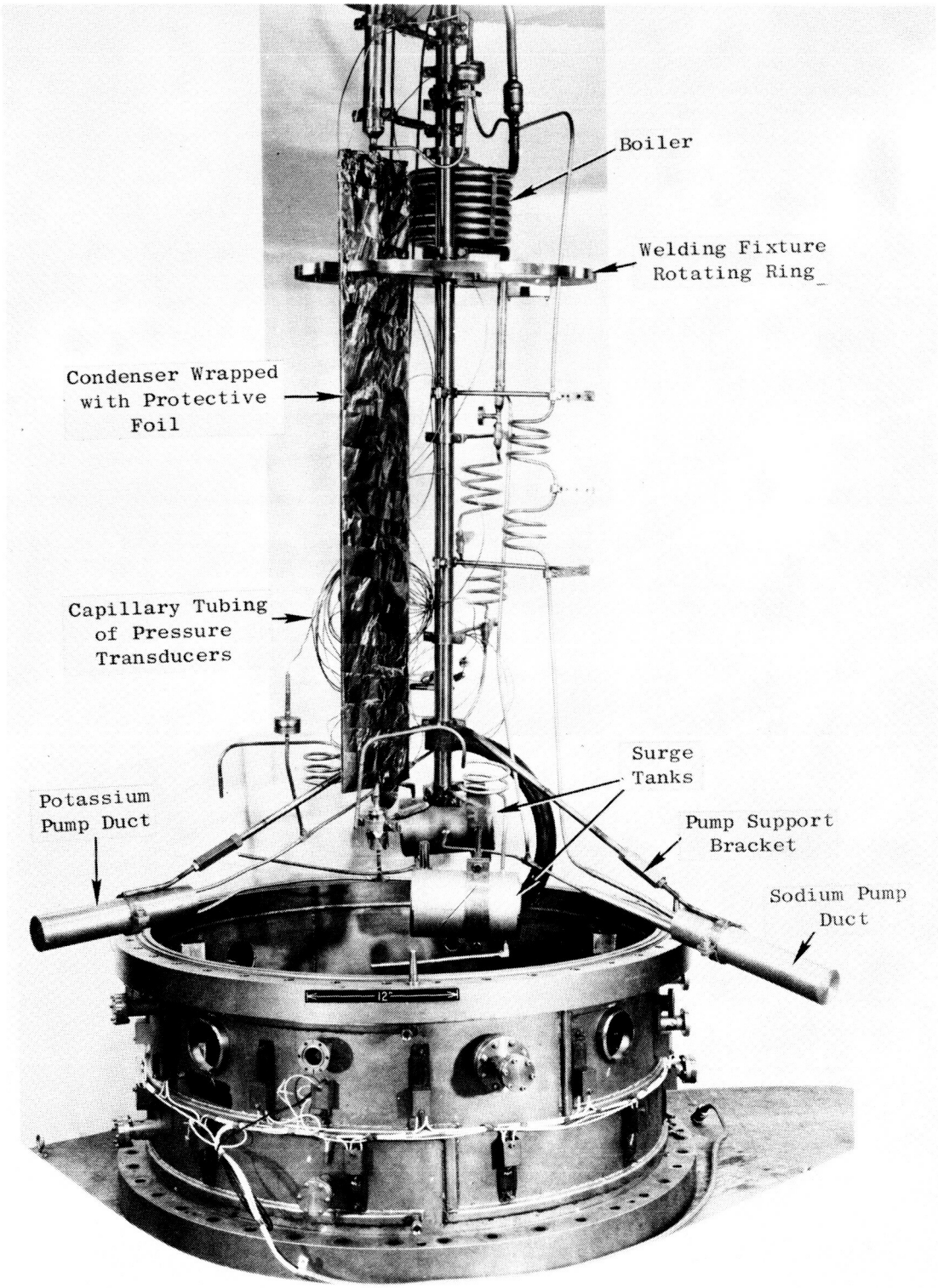

Figure 46. Cb-1Zr Corrosion Test Loop Prior to Installation in the Vacuum Chamber Spool Section. (Orig. C65051298)

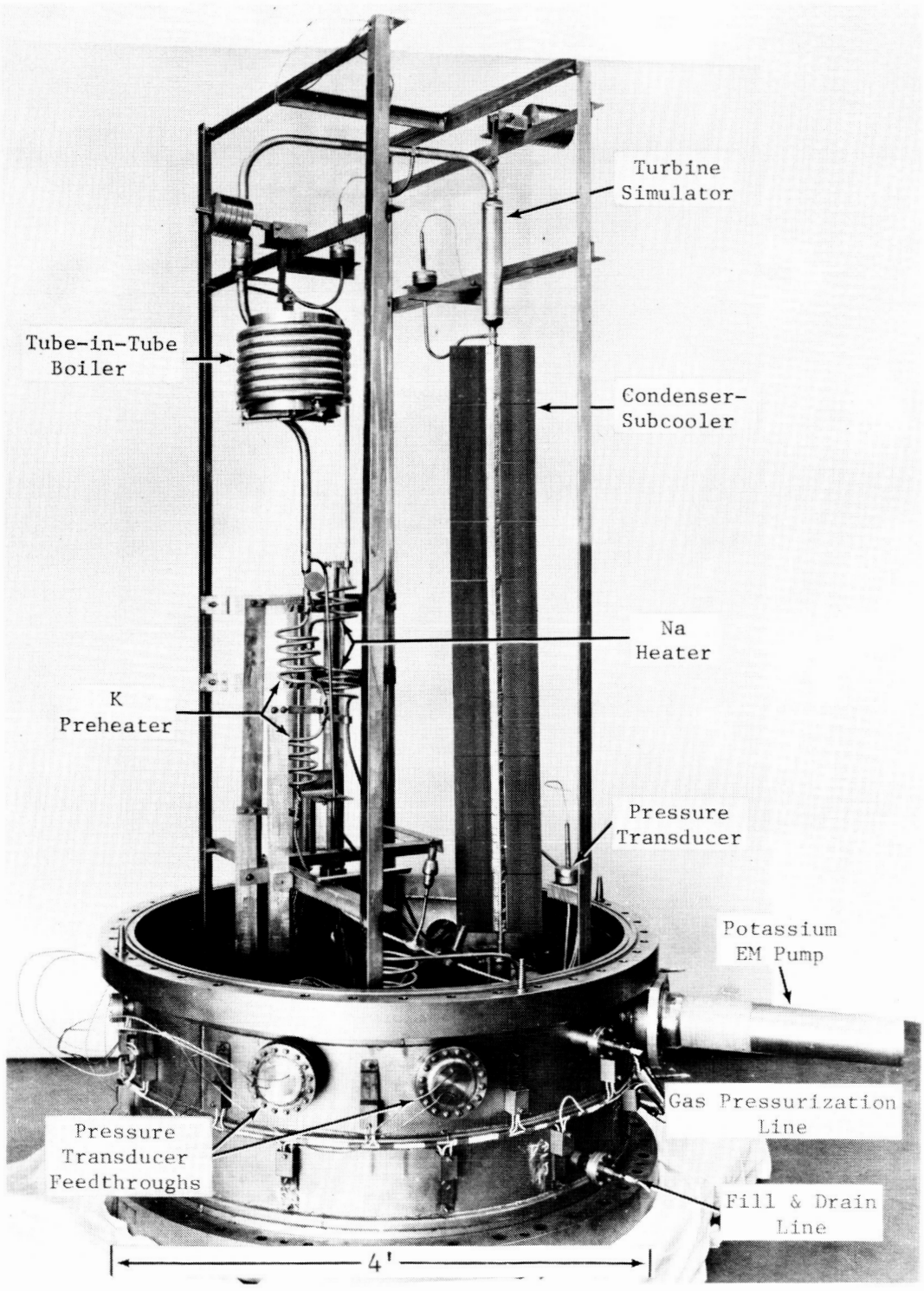

Figure 47. Cb-1Zr Corrosion Test Loop Following Installation in the Test Chamber Spool Piece. (Orig. C65051802)

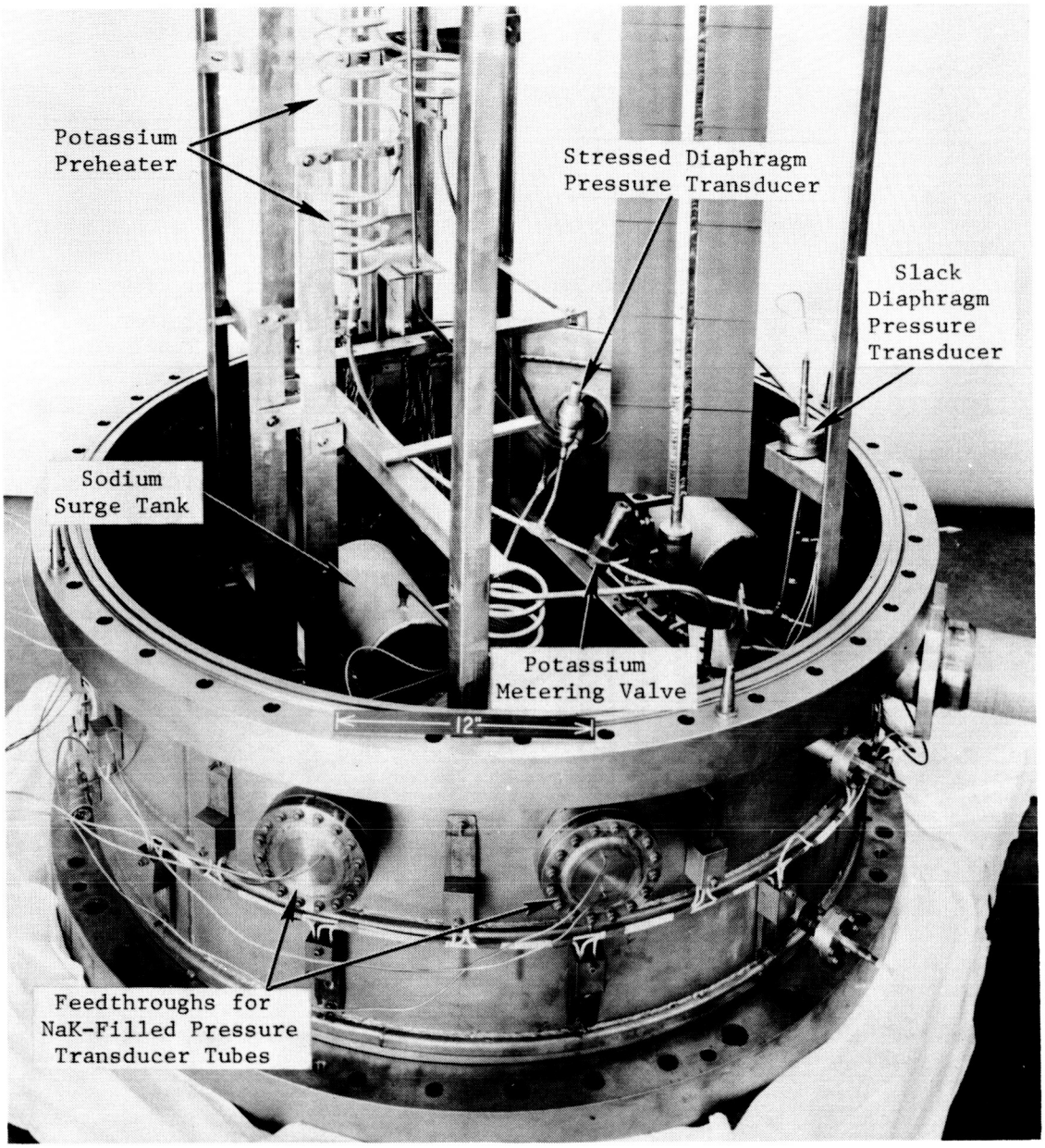

Figure 48. Lower Portion of the Cb-1Zr Corrosion Test Loop Following Installation in the Vacuum Chamber Spool Piece. (Orig. C65051805)

V. TEST EQUIPMENT

A. VACUUM SYSTEMS

The 4-foot-diameter by 11-foot-high vacuum chamber, shown in Figure 49, consists of a stainless steel bell jar, a spool piece, and a sump fabricated by Varian Associates, Palo Alto, California. The three sections are joined together with Wheeler[(a)] flanges which use a 0.125-inch-diameter copper wire gasket. Electrical resistance strip heaters are attached to the chamber wall to permit continuous bakeout of the chamber to 500°F. The chamber is covered with an aluminum shroud which thermally insulates the chamber, results in more uniform heating. and provides maximum safety to operating personnel. The chamber has water cooling channels welded to the wall which are capable of removing approximately 100 kw of heat during test operation.

The rough pumping system for the vacuum chamber shown in Figure 50 was a special Vac Sorb[(a)] sorption pumping system[(b)] which consisted of three sorption pump assemblies mounted on a roughing pump cart and connected to a common pumping manifold. Each sorption pumping unit was filled with highly porous, Type 5A, molecular sieve, a synthetic zeolite material, with sieve pores 5 angstroms in diameter. The sorption pumps are equipped with an integral liquid nitrogen center sump which is used to prechill the pumps before use. Prior to chilling, the sorption pumps are baked out to reactivate them. Heating of the sorption pumps to 450°F after use accelerates the release of previously pumped gases from the molecular sieve to the atmosphere and readies them for the next pumpdown cycle. A thermocouple gauge located on the sorption pump manifold is used to indicate the chamber pressure during sorption pumping. Systems of this type have the capability of reaching a base pressure of 1×10^{-3} torr. After rough pumping the system to less than 10 microns, the

(a) Trademark, Varian Associates.

(b) Varian Associates Drawing No. 610609.

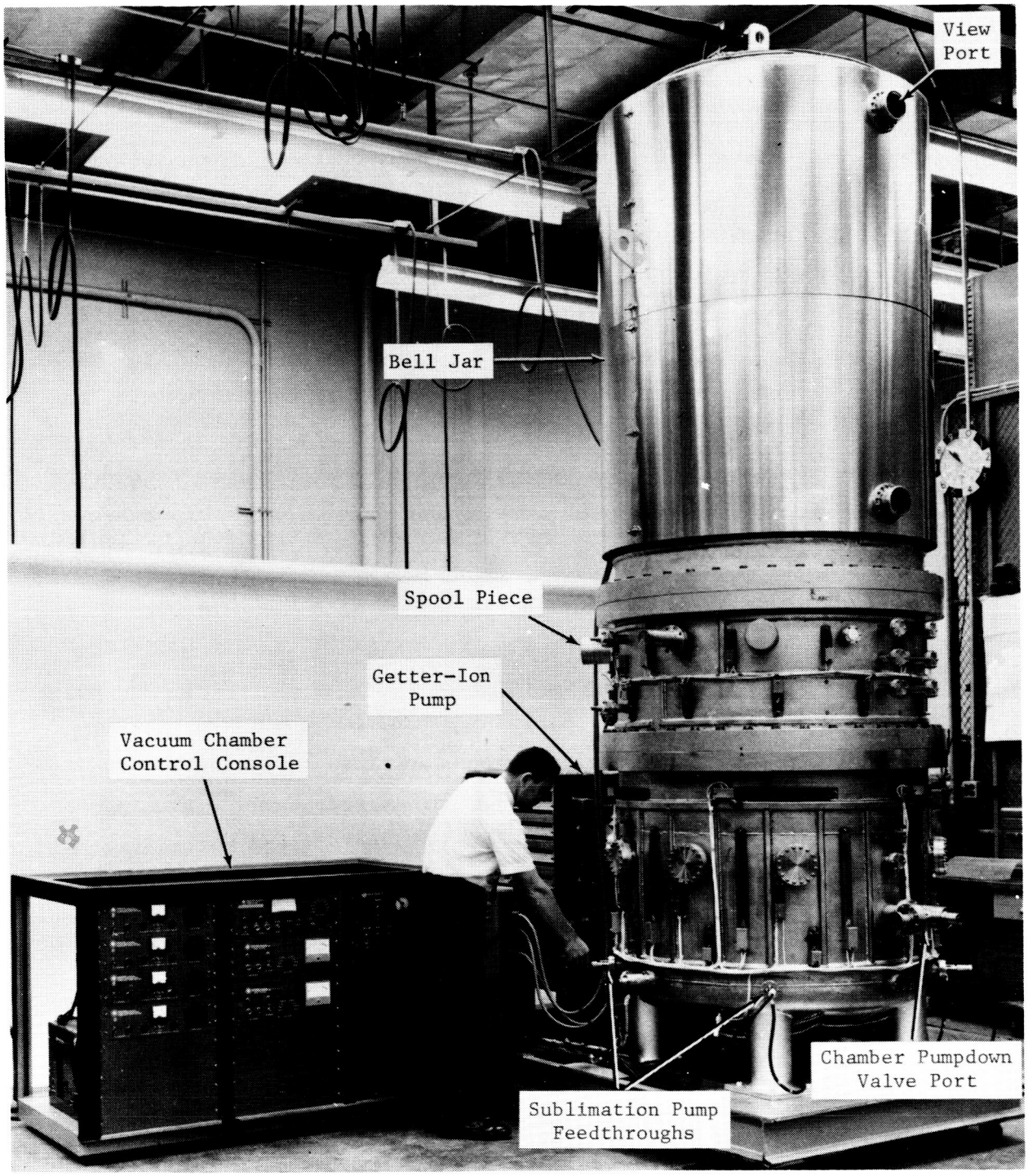

Figure 49. High Vacuum System (10^{-10} Torr Range) for the Cu-1Zr Corrosion Test Loop During Checkout Test at the Vendor's Plant. Chamber is 4 Feet in Diameter by 11 Feet High and is Pumped by a 2400 Liter/Sec Getter-Ion Pump, Titanium Sublimation Pumps and Liquid Nitrogen Sorption Pumps. (Orig. Varian Neg. No. 15609)

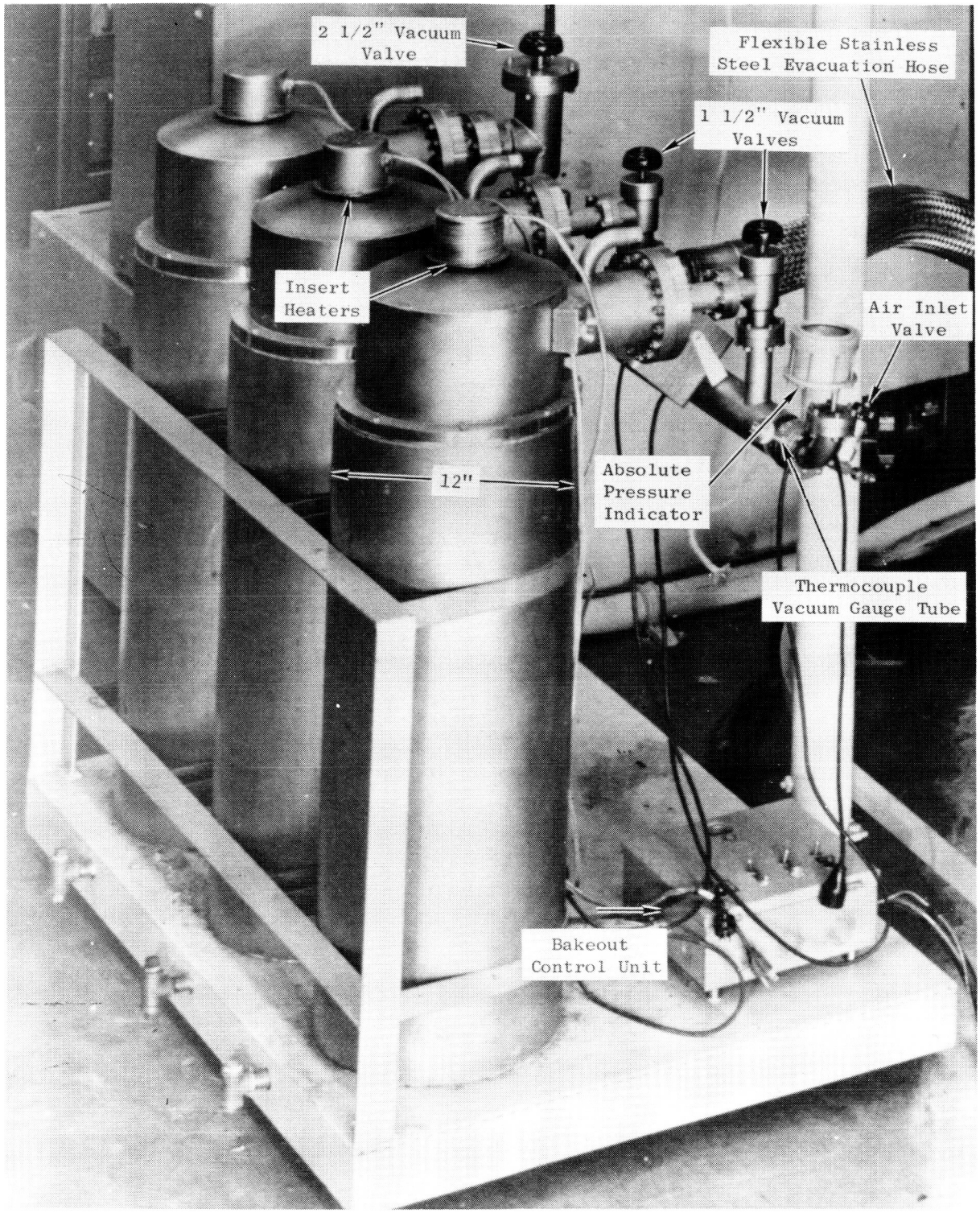

Figure 50. Sorption Pumping System Used to Evacuate the Vacuum Chamber for the Cb-1Zr Corrosion Loop Test Prior to the Initiation of Getter-Ion Pumping. (Orig. C67112716)

bakeable stainless steel valve which isolates the sorption pumps from the chamber proper is closed. The sorption pump station was only used in the initial checkout of the vacuum system and was replaced for the loop operation by the turbo-molecular pumping system described below.

The turbo-molecular pumping unit is shown in Figure 51, which is an overall view of the vacuum chamber and the auxiliary test equipment. This unit[(a)] consists of a 260-liter-per-second pump with a two-stage, vane-type, 15CFM mechanical fore pump. It also includes a closed-cycle, mechanical refrigerator to cool the oil lubricated bearings located at the ends of the turbo-molecular pump rotor. Particular advantages of the turbo-molecular pump over the sorption pumping system described earlier for this particular application include: (a) no limit to the amount of gas pumped, (b) all vapors or gases including helium are pumped, and (c) an ultimate blank-off pressure of 1×10^{-9} torr can be achieved. The 260-liter-per-second pumping speed is constant over the 1×10^{-2} to 1×10^{-8} torr pressure range as shown in Figure 52(a). Molecular pumps obtain their pumping action by frictional contact of the gas molecules with a surface moving at high velocity inside a hermetically sealed case, imparting directional motion to the molecules. Thus, the gas is literally dragged from the inlet to the exhaust port along a slot in the case, creating a pressure difference. The pump rotor shown in Figure 52(b) runs at 16,000 rpm, supported by precision bearings at each end. Figure 52(c) is a schematic of the pump illustrating the gas flow path.

The high-vacuum pumping system previously shown in Figure 49 utilizes a getter-ion pump[(b)] with a rated pumping speed of 2400 liters per second of air. The pump operated on the principal of ion sputtering and requires a high DC voltage and a strong magnetic field. A magnetic field of more than 1800 gauss is provided by permanent magnets attached externally to

---

(a) Welch Scientific Company, Skokie, Illinois, Model 3102A.

(b) Varian Associates, Model 912-5002 (Modified).

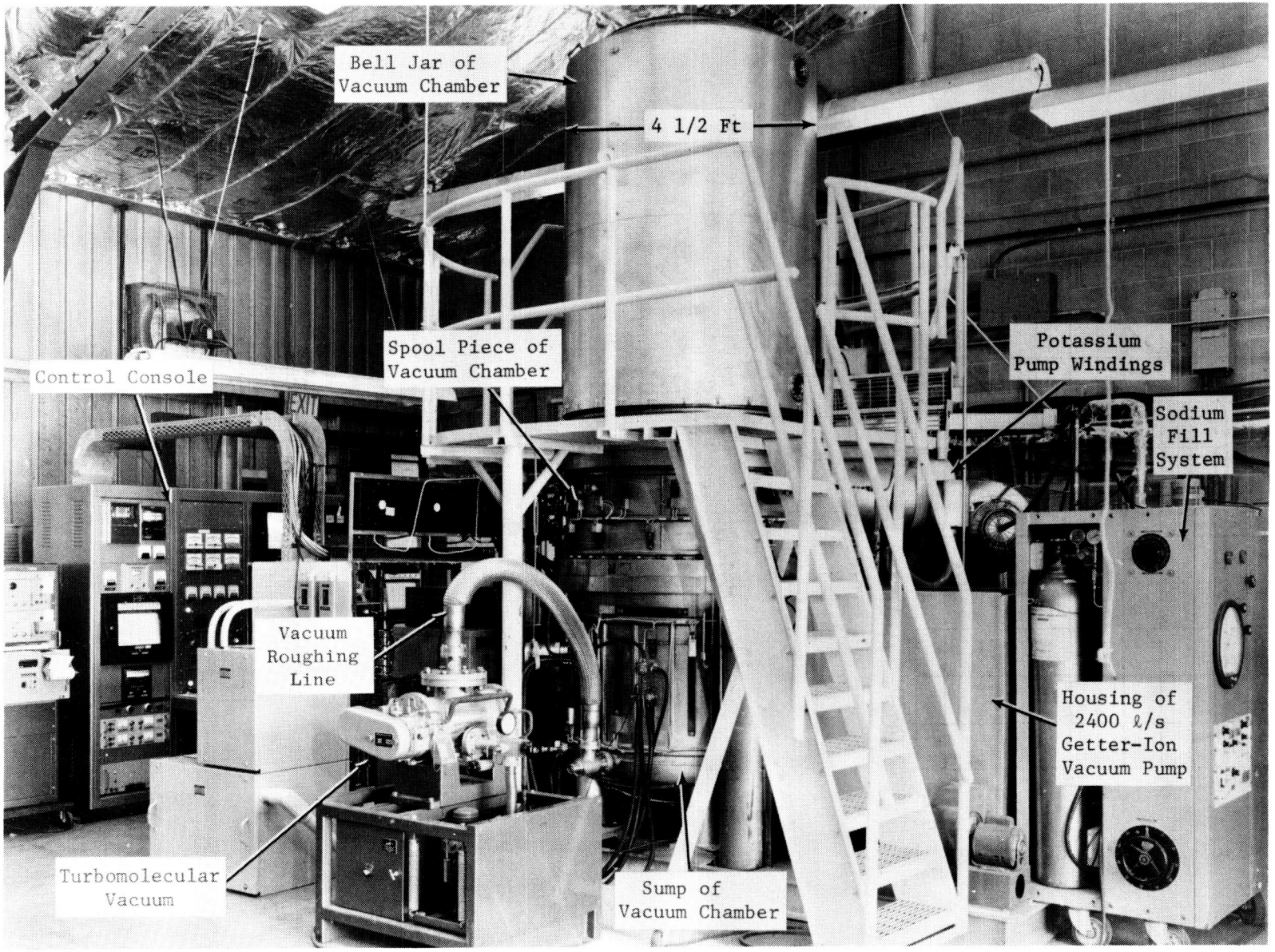

Figure 51. High Vacuum Chamber and Auxiliary Equipment of the Cb-1Zr Rankine System Corrosion Test Loop. (Orig. C65080602)

(a)

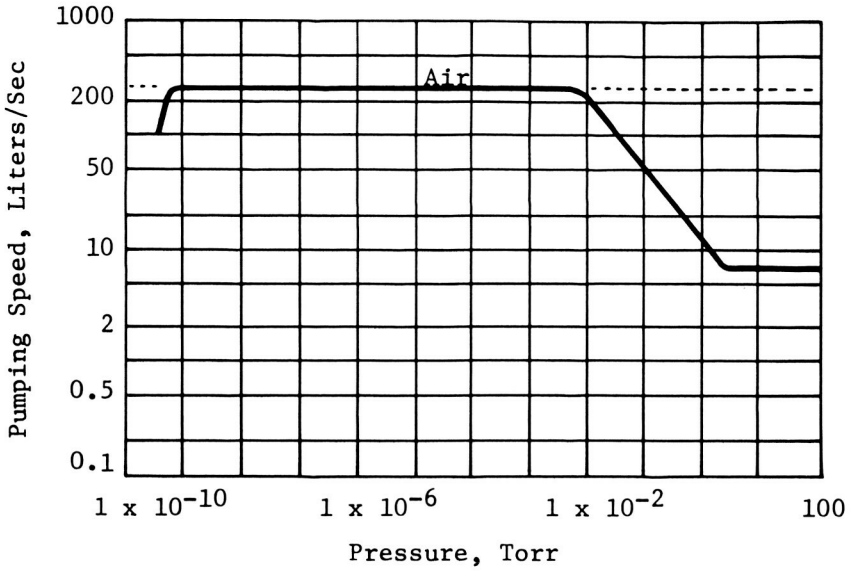

(b)

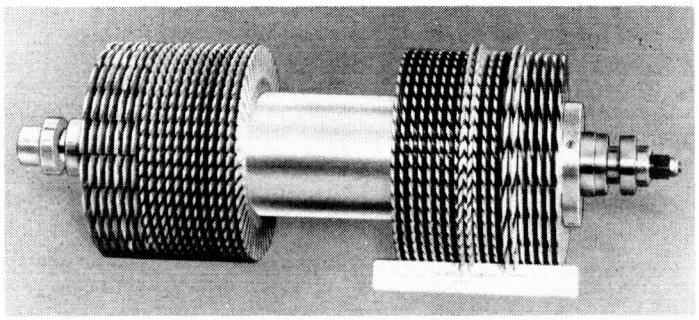

The High-Precision, High-Speed Rotor

(c)

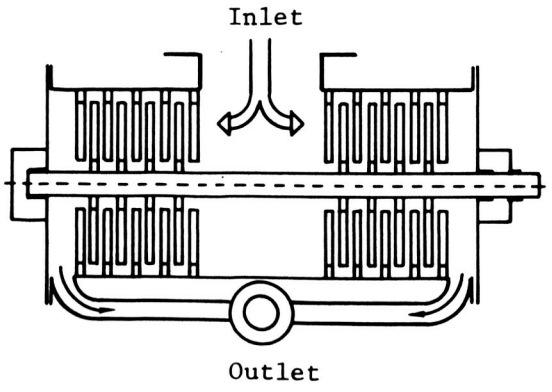

Figure 52. Pumping Speed Curve and Illustrations of the Turbo-Molecular Pump.

the pump. Barrington[26] has described the operating characteristics of this type of pump and the pumping mechanism for the various gases in detail. The getter-ion pump includes an internal bakeout heater and an external centrifugal air blower to cool the ion pump after bakeout is completed.

The pumping speed characteristics of the Varian getter-ion pump are given below. The pumping speeds for various gases are relative to nitrogen taken as unit.

	Pumping Speed
Nitrogen	1.00
Oxygen	0.57
Argon, Krypton, Xenon	0.01
Hydrogen	2.70
Deuterium	1.90
Helium	0.10
Neon	0.05
Carbon Dioxide, Water Vapor, Carbon Monoxide	1.00
Light Hydrocarbons	0.90-1.60

In addition to the getter-ion pump, four titanium sublimation pumps[a] are available for use during periods of high outgassing. The location of two of the four sublimation pump feedthroughs is indicated in Figure 49. The high-speed pumping of these units is accomplished by titanium filament sublimation and deposition on the chamber surfaces. The pumping action depends on forming titanium compounds with active gases. This method can be used during the entire pressure range of 15 microns to the 10^{-11} torr. The recommended duty cycle (on time) for the sublimation pumps decreases from 100 percent down to a pressure of 10^{-6} torr to 25 percent in the 10^{-7} to 10^{-8} torr pressure range. The variable duty cycle is aimed at conserving the titanium filament life while maintaining a fresh "gettering" surface to obtain optimum pumping speeds.

---

(26) Barrington, Alfred A., High-Vacuum Engineering, Prentice-Hall, Inc., Englewood Cliffs, N. J., 1963, p. 91.

(a) Varian Associates: Power Supply Model No. 922-0006; Filament Cartridge, Model No. 956-0030; and Titanium Filament, Model No. 956-0010.

Two to four hours of continuous operation are possible with each of the three filaments per pump when operated at the highest recommended deposition rate. Four duplicate sets of sublimation pump controls are included, as shown in Figure 49, which permits independent operation of these units, if desired.

The bell jar section of the chamber is raised and lowered by a 2-ton chain hoist. Four 4-inch-diameter bakeable Pyrex glass viewing ports are mounted in the wall of the bell jar. These view ports permit observation and photography of loop components during test operation.

The spool section of the vacuum chamber has the following wall penetrations:

a) Two - 4-inch-diameter flanges for the EM pump ducts,

b) One - 4-inch-diameter flanges for rotary motion magnetic drive feedthrough,

c) Six - 2 3/4-inch-diameter flanges with 1000-ampere power feedthroughs,

d) Six - 2 3/4-inch-diameter flanges for thermocouple, ion gauge, and auxiliary power feedthroughs,

e) Two - 4-inch-diameter flanges for slack diaphragm pressure transducer capillary tubes.

In addition to the feedthroughs on the spool section, six 4-inch-diameter flanges are available on the sump for additional instrumentation and feedthrough requirements as well as seven 2 3/4-inch diameter flanges for the titanium sublimation pumps and additional instrumentation requirments, and a 2 1/2-inch-ID vacuum roughing port. An exploded and an assembled view of one of the six water-cooled, electrical power feedthroughs is shown in Figure 53. All flanges are sealed with flat OFHC copper gaskets and are capable of withstanding prolonged bakeout at temperatures as high as 800°F.

A qualification test on the 48-inch-diameter vacuum chamber was performed at Varian Associates prior to shipment to General Electric. The results of this test which included a 24-hour bakeout are given in Table IX. An ionization gauge pressure of 7.5×10^{-11} torr was

TABLE IX

PERFORMANCE TEST OF THE 4-FOOT-DIAMETER BY 11-FOOT-HIGH GETTER-ION PUMPED VACUUM CHAMBER AT VARIAN ASSOCIATES

Elapsed Time Minutes	Remarks	Pressure Torr
0	Sorption Pumping Started	Atmospheric
90	Getter-Ion Pump Started	16×10^{-3}
160	Getter-Ion Pump Confined; On Continuously for Remainder of Test	--------
170	Start of 24-Hour Bakeout	4×10^{-6}
1510	Bakeout Off	--------
1525		1.8×10^{-8}
1645		7.7×10^{-10}
1653	Titanium Sublimation Pumps On	--------
1661	Titanium Sublimation Pumps Off	6×10^{-9}
1672		4.2×10^{-10}
1720	Titanium Sublimation Pumps On 1 Minute	1.8×10^{-10}
1805	Titanium Sublimation Pumps On 2 Minutes	1×10^{-10}
1915	Final Pressure	7.5×10^{-11}

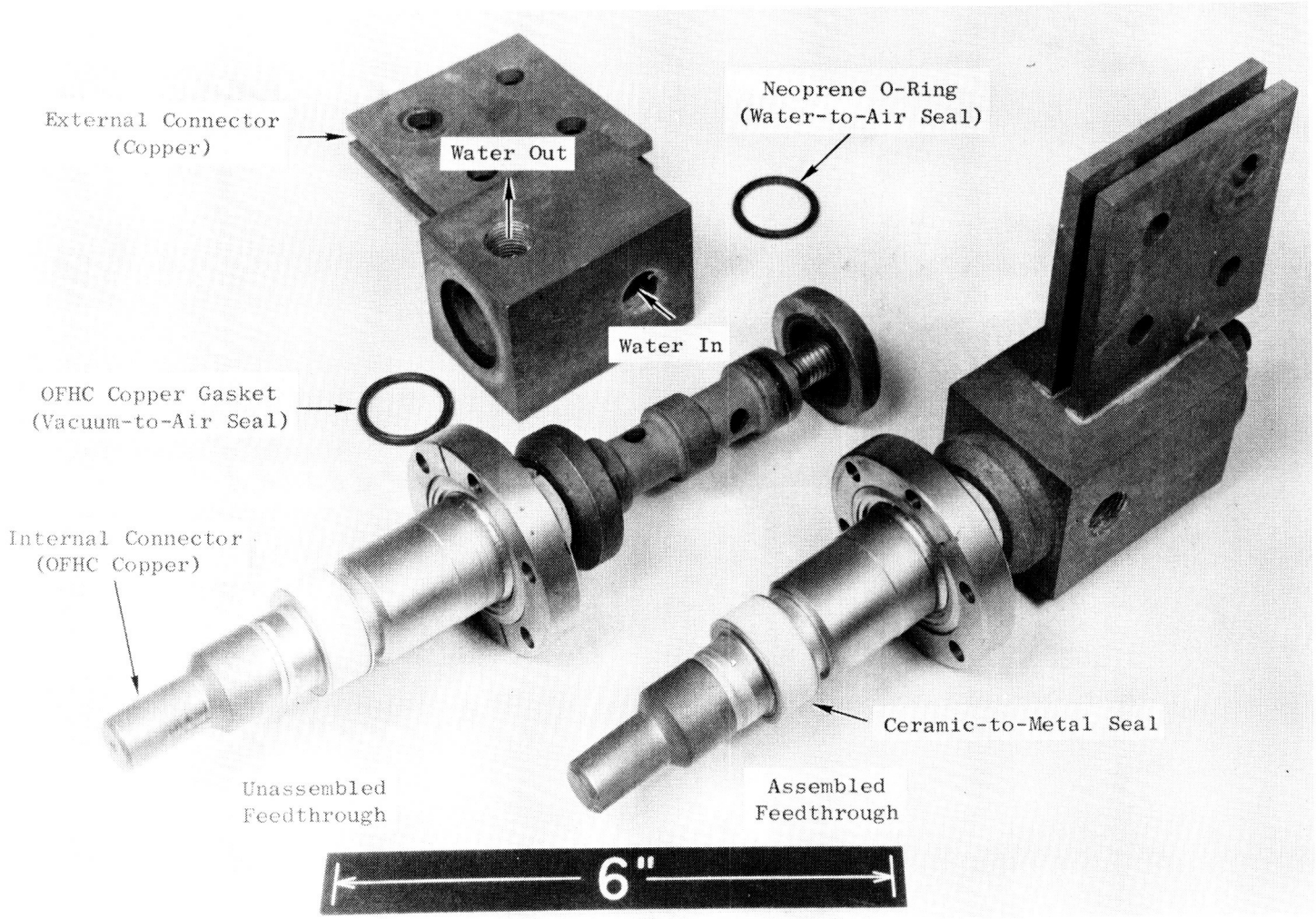

Figure 53. Water Cooled, 1000-Ampere Electrical Power Feedthrough. (Orig. C67041801)

reached on cooldown following bakeout. This pressure was achieved 32 hours after the sorption pumps were opened to initiate evacuation of the system.

Following installation of the vacuum chamber at General Electric, an acceptance test was performed. A pressure of 4×10^{-10} torr was obtained in less than 60 hours including a 24-hour bakeout, without the use of the titanium sublimation pumps, thereby meeting the specification requirement of 1×10^{-9} torr in 100 hours or less.

B. CHAMBER PRESSURE MEASUREMENT

The pressure inside the vacuum chamber is measured and recorded during the entire cycle. In the sorption rough pumping system, a thermocouple gauge is used to measure the pressure in the range from atmospheric to 1×10^{-3} torr.

Vacuum chamber pressures in the range 10^{-4} to 10^{-10} torr were measured using a calibrated hot cathode ionization gauge.[(a)] The gauge was calibrated with its control unit at Varian Associates, using an accurately known pumping speed(s) with a measurement of flow rate (q) to establish a calibrated pressure, $P = q/s$. The maximum error of this technique with the equipment is ±6 percent. The calibration data for the ionization gauge used to measure chamber pressure during the Cb-1Zr Corrosion Loop Test are given in Table X. A detailed description of calibration procedure used has been described in a paper by Hayward and Jepsen.[27]

The getter-ion pump current is a function of the chamber pressure and, therefore, it can be used as an approximate check of the ionization gauge pressure reading at any time during test operation. The pump control unit also has a logarithmic pressure scale as shown in the top

---

(a) Varian Associates, Model UHV-12.

(27) Hayward, W. H. and Jepsen, R. L., "A Simple High Vacuum Gauge Calibration System," Transactions of the American Vacuum Society, 1962.

TABLE X

IONIZATION GAUGE CALIBRATION DATA

Calibration Date	22 January 1964
Gauge Type and Number	Varian UHV-12, No. G-26
Ionization Gauge Control Unit Type and Number	Varian Model No. 971-0003, Unit No. 757
Test Gas	Nitrogen
Emission Current	4 ma
Degas Method and Power	Electron Bombardment - 40 Watts

Pg, Gauge Pressure Indicated on the Ionization Gauge Control, torr	Pa, Absolute Calibration Pressure, torr	Pa/Pg, Correction Factor, torr
5.34×10^{-7}	6.24×10^{-7}	1.17
9.80×10^{-7}	1.12×10^{-6}	1.14
0.97×10^{-6}	1.12×10^{-6}	1.15
3.80×10^{-6}	4.70×10^{-6}	1.24
9.93×10^{-6}	1.27×10^{-5}	1.28
1.00×10^{-5}	1.27×10^{-5}	1.27
2.17×10^{-5}	2.75×10^{-5}	1.27
5.20×10^{-5}	7.74×10^{-5}	1.48
7.00×10^{-5}	1.21×10^{-4}	1.73
9.60×10^{-5}	2.03×10^{-4}	2.11
1.75×10^{-4}	2.03×10^{-4}	1.16

panel illustrated in Figure 49, which indicates the pressure directly over the 10^{-4} to 10^{-8} torr range.

C. PARTIAL PRESSURE GAS ANALYZER

A partial pressure gas analyzer[(a)] was used to monitor the concentration of the residual gases in the test chamber. The analyzer tube,[(b)] which is shown in Figure 54, consists of a Nier-type, electron bombardment ion source, a 90-degree sector magnetic analyzer with a 5-cm radius of curvature, and a 10-stage electron multiplier ion detector entirely enclosed in a Type 304 stainless steel envelope with metal-ceramic sealed electrical lead-ins. The metal tube permits bakeout temperatures to 800°F. The electron multiplier ion detector allows the use of a conventional low-current amplifier to read the output signal. The analyzer tube is magnetically focused with a 3-kilogauss bakeable permanent magnet mounted on the analyzer tube to achieve ion beam peak separation over the 2 to 50 AMU (atomic mass units) range. The metal tube is designed to operate at total pressures up to 10^{-5} torr and to detect partial pressures of 10^{-14} torr. The electronic control unit and the X-Y recorder for the analyzer are shown in Figure 55. A discussion of the calibrations performed on the analyzer are given in Appendix G, Calibration of the Partial Pressure Analyzer.

D. HEATER POWER SUPPLY

The heater power supply consisted of a combined temperature controller and stepless power regulator system with a stepdown current transformer. The system had a continuous power rating of 20 kw with an input power of single-phase 440 volt AC. The combined temperature controller and power regulator include:

1) A manual power adjustment,
2) Automatic set point control,
3) Current limiter control.

(a) General Electric Partial Pressure Analyzer, Model 22PC110.

(b) General Electric Partial Pressure Analyzer Tube, Model 22PT110.

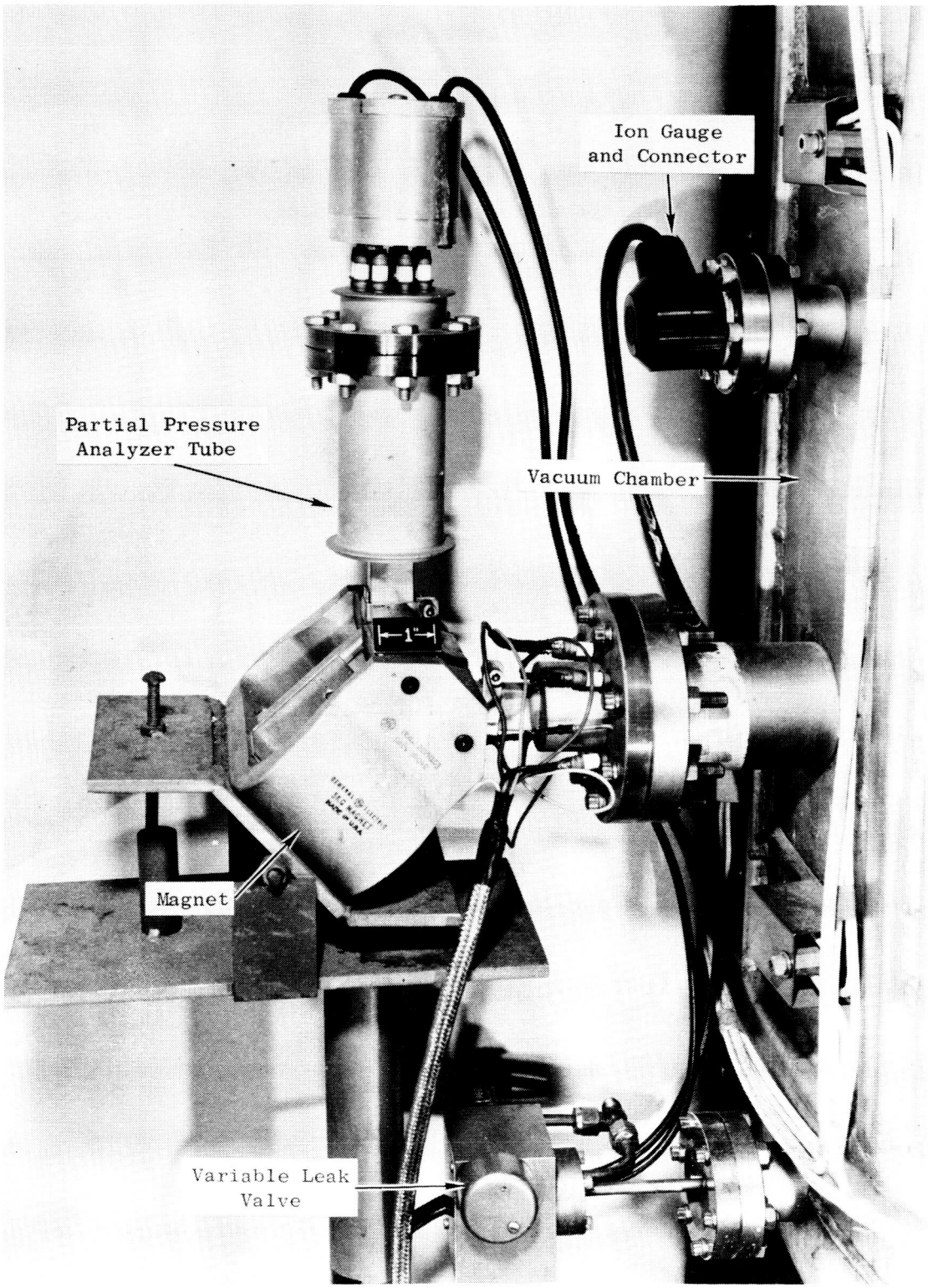

Figure 54. Ion Gauge, Partial Pressure Analyzer Tube and Variable Leak Valve Mounted on Chamber Sump. (Orig. C66050427)

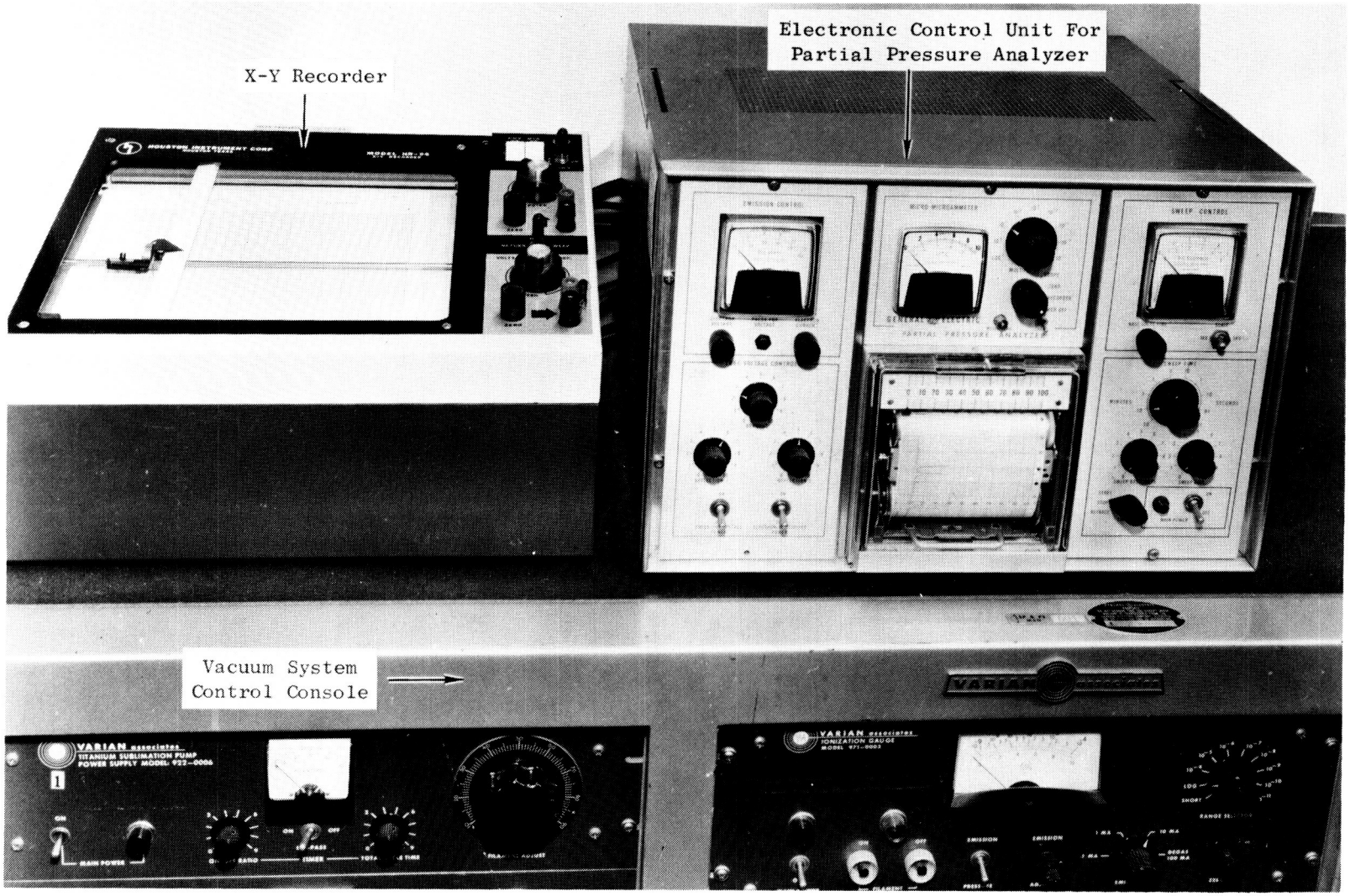

Figure 55. Electronic Control Unit and X-Y Recorder for the Partial Pressure Analyzer. (Orig. C66050426)

The system included a single-pen, 1/4 percent, null-balance, servo-operated recording potentiometer with a General Electric Model 524 controller (3-mode proportional control with rate action and automatic reset) and an amplistat plus a saturable core reactor and current transformer. The system functioned as follows:

An input signal to the recorder is obtained from the control thermocouple and is measured by the recorder. This input signal is compared to a known voltage developed across the measurement slidewire. The slidewire is part of a bridge circuit, the other part of which is located in the 3-mode controller. The output of the controller is directly proportional to the unbalance of the bridge circuit and provides a DC control signal to an amplistat. The control signal is amplified by the amplistat to a sufficient level to operate a saturable reactor. The output of the saturable reactor is connected to a stepdown transformer rated at 5000 amperes continuous duty. The high current is fed through the vacuum chamber to the loop heaters by water-cooled, 1000-ampere feedthroughs of the type shown earlier in Figure 53.

E. AIR COOLED METAL VAPOR COLLECTOR

During the operation of alkali metal test loops in vacuum chambers, it is desirable to be able to collect and concentrate metal vapors which may be present in the system. These metal vapors might arise either from the inadvertent use of materials such as commercial copper containing small but volatile concentrations of zinc and lead[28] or from alkali metal in the event of an alkali metal leak in the system. If a leak in the loop should occur it would be possible by use of the collector coil to decontaminate the loop and chamber components before exposing the system to the atmosphere. The collector tube assembly, which was

(28) Hoffman, E. E. and Holowach, J., Cb-1Zr Thermal Convection Loop, Potassium Corrosion Test Loop Development Topical Report No. 5, R67SD3014, June 15, 1967, General Electric Company, Cincinnati, Ohio, p. 63.

shown previously in Topical Report No. 6,[29] consists of a 16-inch long coil of 1/4-inch stainless steel tubing mounted on a 2 3/4-inch flange. When in use the inlet air to the coil is cooled to approximately -20°F by passing it through a Ranque-Hilsch Vortex tube.[a]

---

(29) Hoffman, E. E. and Holowach, J., Cb-1ZR Pumped Sodium Loop, Potassium Corrosion Test Loop Development Topical Report No. 6, R67SD3015, December 20, 1967, General Electric Company, Cincinnati, Ohio, p. 83.

(a) Fulton Cryogenics, Cincinnati, Ohio.

VI. ALKALI METAL PURIFICATION, TRANSFER, AND SAMPLING SYSTEMS

A detailed description of the procedures and equipment used to purchase, purify, transfer, sample, and analyze the sodium and potassium for the Cb-1Zr Corrosion Test Loop was presented in an earlier topical report in this series.[30] Only an abbreviated review of this portion of the test program will be included in this report. The approach which was used in the preparation of the sodium and potassium for the Cb-1Zr Corrosion Test Loop was to procure the highest quality alkali metals, subject them to purification techniques designed to further reduce the impurity concentrations, transfer them to the loop using equipment and techniques designed to reduce the possibility of recontamination to a minimum, and finally to reanalyze the alkali metal after it had been flushed through the loop to insure its purity. A simplified schematic of the purification and transfer systems for the sodium and potassium is given in Figure 56. The sequential steps in purifying and transferring the alkali metals are listed below:

Sodium	Potassium
a. Filtration	a. Filtration
b. Hot Trapping	b. Hot Trapping
c. Filtration	c. Filtration
d. Transfer to Charge Tank	d. Distillation
e. Transfer to Surge Tank of Loop	e. Filtration
	f. Transfer to Charge Tank
	g. Transfer to Surge Tank of Loop

A. SODIUM PURIFICATION

Reactor grade sodium was purchased from U. S. Industrial Chemical (USI). A 15-pound-capacity sodium hot trap was designed and fabricated for use in purifying sodium for the loop. The principal components of the sodium purification system are illustrated in Figure 57. All parts of the system designed to

(30) Dotson, L. E. and Hand, R. B., Purification, Analysis, and Handling of Sodium and Potassium - Potassium Corrosion Test Loop Development Topical Report No. 4, R66SD3012, General Electric Company, Cincinnati, Ohio, June 13, 1966, p. 15.

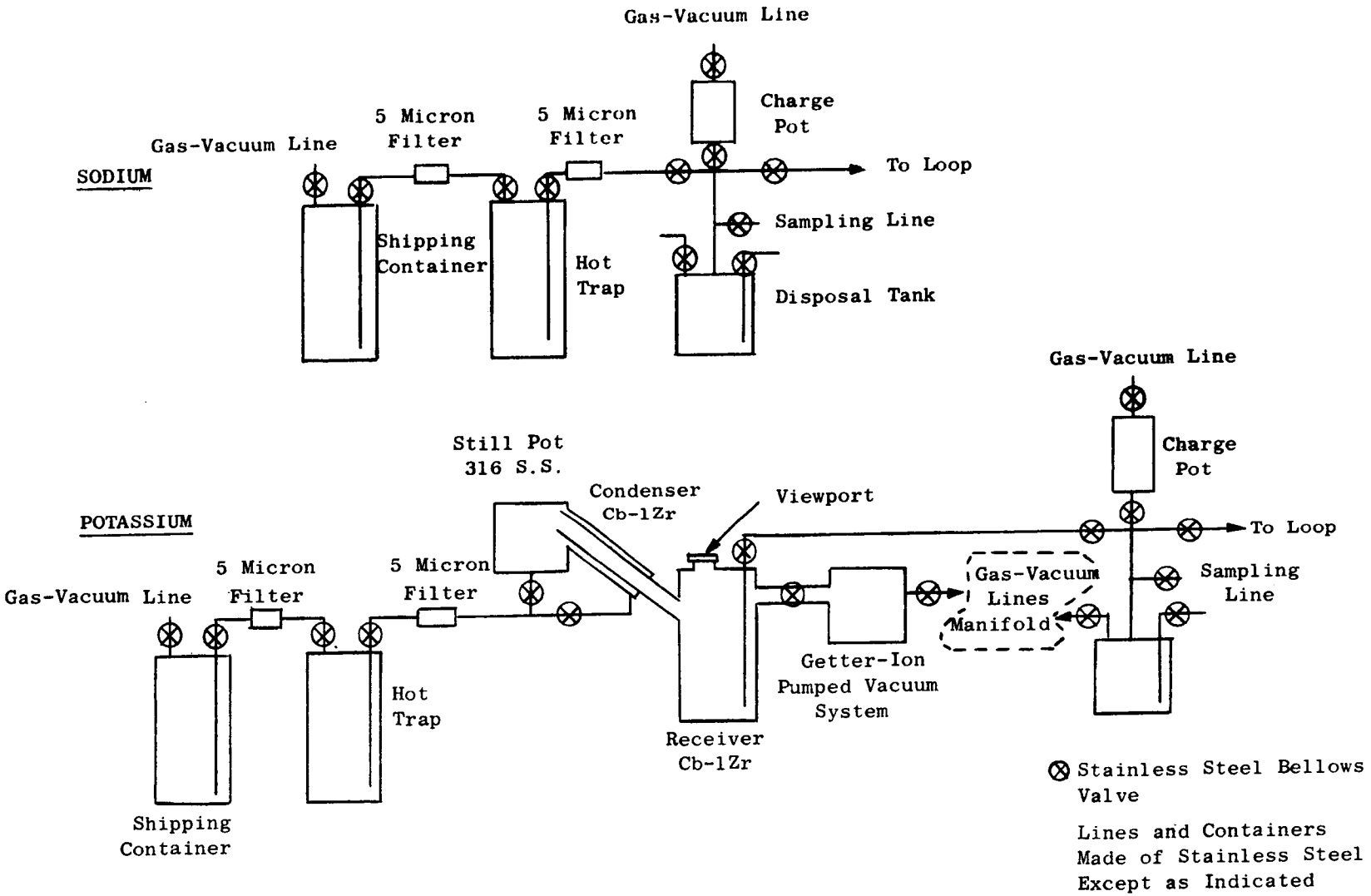

Figure 56. Simplified Schematic of Sodium and Potassium Purification and Transfer System for the Cb-1Zr Corrosion Test Loop.

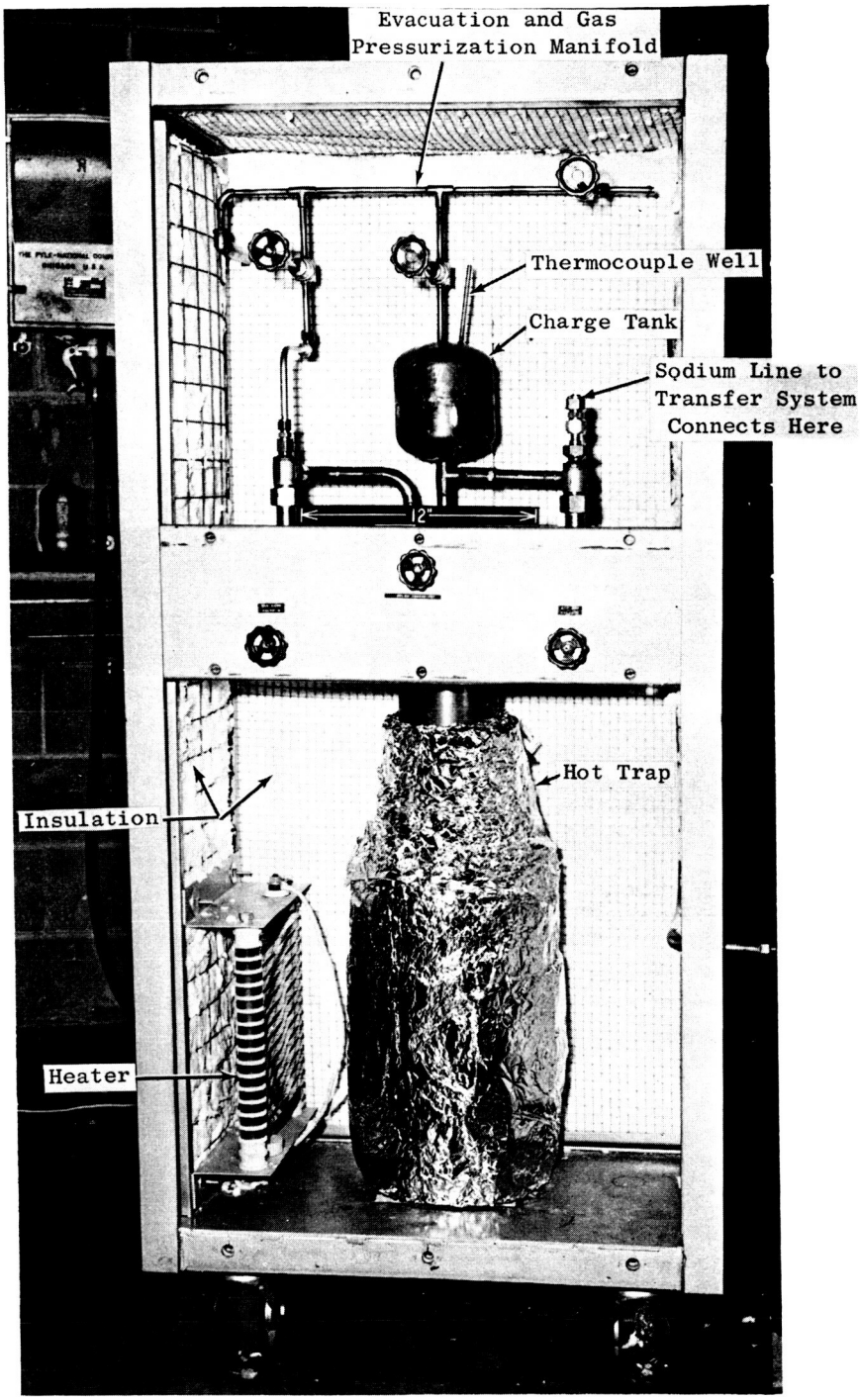

Figure 57. Sodium Purification System Showing Hot Trap and Charge Tank After Installation in Oven. Cover Panels Removed to Take Picture. (Orig. C65041402)

TABLE XI. ANALYSES OF ALKALI METALS FOR THE Cb-1Zr CORROSION TEST LOOP SYSTEM

Sample Identity	Sample Weight gms.	Oxygen,[3] ppm	Oxygen, Avg[1] ppm	ppm in Alkali Metal																						
				Fe	B	Co	Mn	Al	Mg	Sn	Cu	Pb	Cr	Si	Ti	Ni	Mo	V	Be	Ag	Zr	Sr	Ba	Ca	K	Na	Cb
Sodium hot trap before primary fill, No. 204	4.306 2.146	4.1 8.9	6.5	<3	--	<3	<3	<3	<3	<13	<3	<3	<3	<3	<3	<3	3	-	--	<3	<13	--	--	<25	-	-	3
Sodium after transfer system flush, No. 232	4.174 4.016	11.5 17.0	14.3																							
Sodium after primary loop flush, No. 234	4.552 3.726	5.4 7.4	6.4	<3	--	<3	<3	<3	<3	<13	<3	<3	<3	<13	<3	3	<3	<25	<3	<3	<13	--	--	3	-	-	<3
Potassium before hot trapping, No. 213	1.916 3.961	4.2 6.2	5.2	2	--	<2	<2	2	<2	--	<2	<2	<2	10	<2	<2	<2	<2	--	<2	<10	--	--	10	-	<50	<2
Potassium after hot trapping, No. 216	3.777	7.1	7.1																							
Potassium after distillation, No. 229	4.090 2.463	3.9 4.1	4.0	2	--	<2	<2	<2	<2	<2	<2	<2	<2	<2	<2	<2	<2	-	<2	<2	<10	--	--	2	-	>50	<2
Potassium after transfer system flush, No. 233	4.321 4.696	5.7 6.7	6.2																							
Potassium after secondary loop flush, No. 235	3.980 3.496	5.6 8.7	7.2	<2	--	<2	<2	<2	<2	<10	<2	<10	<2	<10	<2	<2	--	<10	<2	<2	<10	--	--	2	-	50	<2
NaK(78) used in pressure transducers, No. 173	3.268 3.353	3.3 4.3	3.8	<10[2]	<10	<10	<2	<10	<2	<10	<2	<10	<10	<20	<10	<10	<10	<10	<2	<2	<20	<2	<4	<2	-	--	--
Sodium, potassium and NaK purity requirements			20	25	65	25	25	25	25	25	25	25	25	65	25	25	25	40	25	25	25	25	25	25	500	500	25

(1) Oxygen calculated as monoxide by titration - avg. ppm = total μgms divided by total sample weights

(2) Analyzed by Nuclear Materials and Equipment Corporation, Apollo, Pa.

(3) Analytical blank, 5-10 μgms oxygen per sample, not subtracted.

run hot during the purification treatment were made of Types 304 or 316 stainless steel except the titanium liner and the zirconium getter bundle. The in-line filter located in the dip leg line near the dip leg valve was sintered, Type 316 stainless steel with an average pore size of 5 microns. Transfer and filtration operations were carried out at 250°-300°F. The 15-pound hot trap was equipped with a charge pot of known volume for adding the desired amount of sodium to the loop surge tank. The ratio of the quantity of sodium to the zirconium surface area was 2.7 grams/inch^2. The hot trap was outgassed in the temperature range 400° to 600°F for about 100 hours to achieve a system pressure of less than 10^{-6} torr. A quantity of sodium weighing 12.8 pounds was added to the hot trap and gettered for 120 hours at 1275° to 1375°F. The analyses of the sodium before and after the various hot trapping and flushing operations are listed in Table XI.

B. POTASSIUM PURIFICATION

Two hundred pounds of high-purity potassium were purchased to G.E. - SPPS Specification No. 01-0039-00-B[31] from Mine Safety Appliances Research Corporation, Callery, Pennsylvania. Although this lot of potassium was very pure, according to both the vendor and G. E. - SPPS quantitative analyses, it was nevertheless processed by filtration, hot trapping, and vacuum distillation.

The sequential procedures used to purify the potassium were illustrated in Figure 56. In addition to obtaining high-purity potassium initially and subsequently purifying by low-temperature filtration and hot gettering, the potassium was further purified by vacuum distillation in order to supply ultrahigh-purity potassium to the two-phase secondary circuit of the loop.

All filtration operations were accomplished at 200°-250°F through in-line filters composed of sintered, Type 316 stainless steel with a 5-micron average pore size. Filtration was performed after hot trapping and again after distillation.

---

(31) Frank, R. G., et al., Material and Process Specifications for Refractory Alloy and Alkali Metals - Potassium Corrosion Test Loop Development Topical Report No. 2, R66SD3007, December 13, 1965, General Electric Company, Cincinnati, Ohio

Hot trapping of the potassium was done in the titanium-lined, zirconium-gettered system of 50 pounds capacity. The components of the hot trap prior to assembly are shown in Figure 58. The gettering operation was carried out on 46.5 pounds of potassium for a time period of 50 hours at a temperature of 1250°-1300°F. The analysis of the potassium following gettering is given in Table XI. Prior to the distillation operation, the hot trap, the vacuum-argon system, and the still were assembled together on a portable dolly. The overall arrangement of equipment is best shown by the schematic diagram in Figure 59.

The potassium still consisted of a stainless steel boiler, a Cb-1Zr condenser, and a Cb-1Zr condensate receiver. A photograph of the still components prior to assembly is shown in Figure 60. The condenser was a coaxial type, containing an inner Cb-1Zr tube such that all condensate which entered the receiver contacted only Cb-1Zr. The outer stainless steel tube of the condenser was attached to the Cb-1Zr tube by a brazed joint. Copper cooling coils were wound on and brazed to the stainless steel condenser pipe. During distillation, the annular space between the tubes was filled with potassium which acted as the heat transfer medium for rejecting the heat of condensation. The boiler section was heated circumferentially by band heaters to promote surface evaporation. The receiver was equipped with a viewport, thermocouple well, and dip leg. The dip leg in the receiver was attached to a stainless steel filter and a Hoke HY473A cleanable valve.

After assembling the potassium purification system on the portable dolly, the various components of the system were baked out at temperatures in the range 250°-800°F for up to two weeks until the pressure rise rate at room temperature was less than 1.0 micron-liter per hour.

The distillation was carried out at 500° to 600°F. The condenser tube temperature was maintained at 250° to 350°F by flowing air through the copper cooling coils. The receiver was held at or below the melting point of potassium. About 27.5 pounds of potassium were distilled at an average rate of one pound per hour. The resulting distillate was analyzed and the results are given in Table XI.

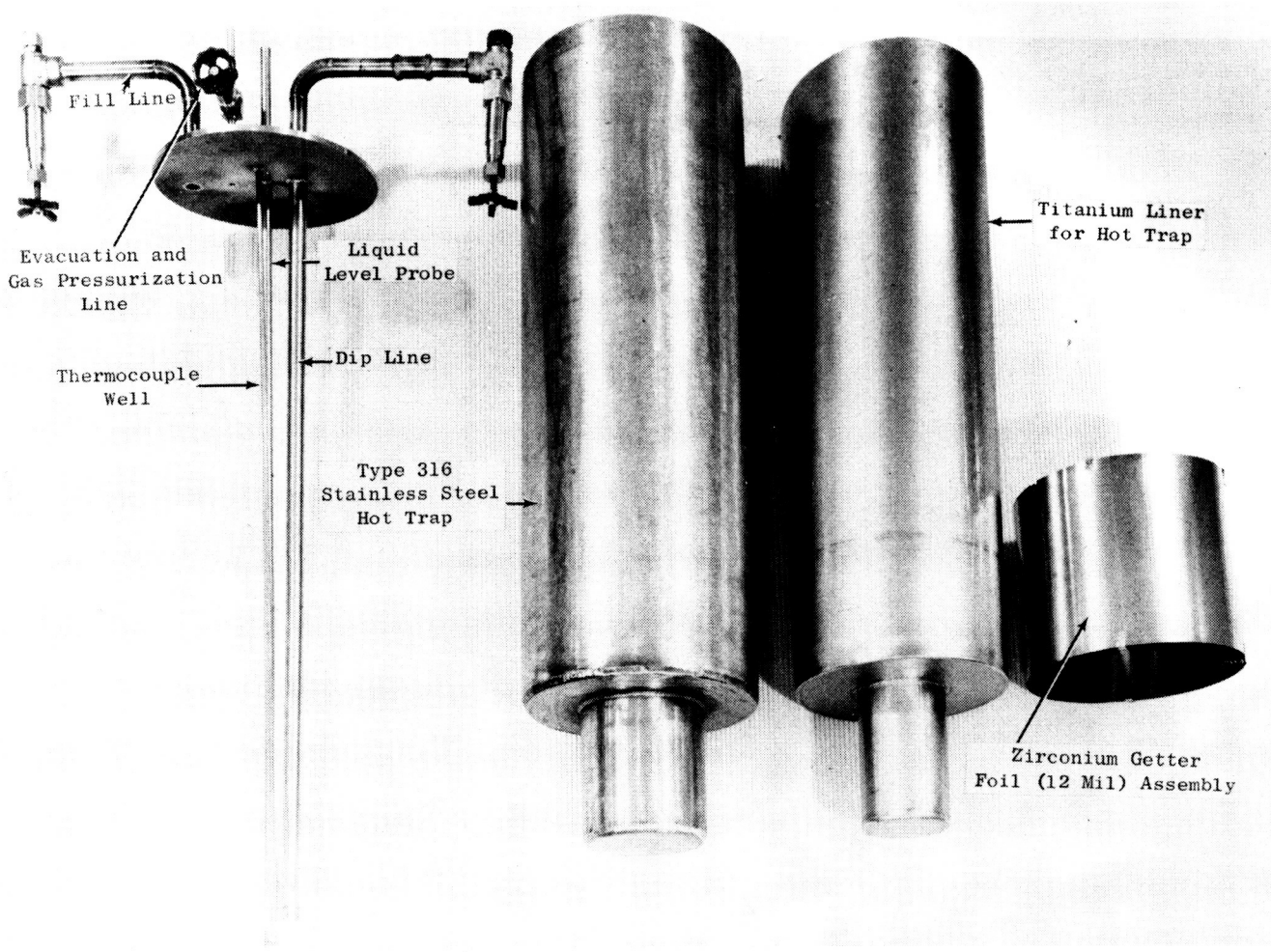

Figure 58. Potassium Hot Trap for the Cb-1Zr Corrosion Test Loop Prior to Assembly. Type 316 Stainless Steel Container (10" Schedule 40 Pipe), Titanium Liner (0.040" Thick), and Zirconium Foil (0.012" Thick) Are Shown.

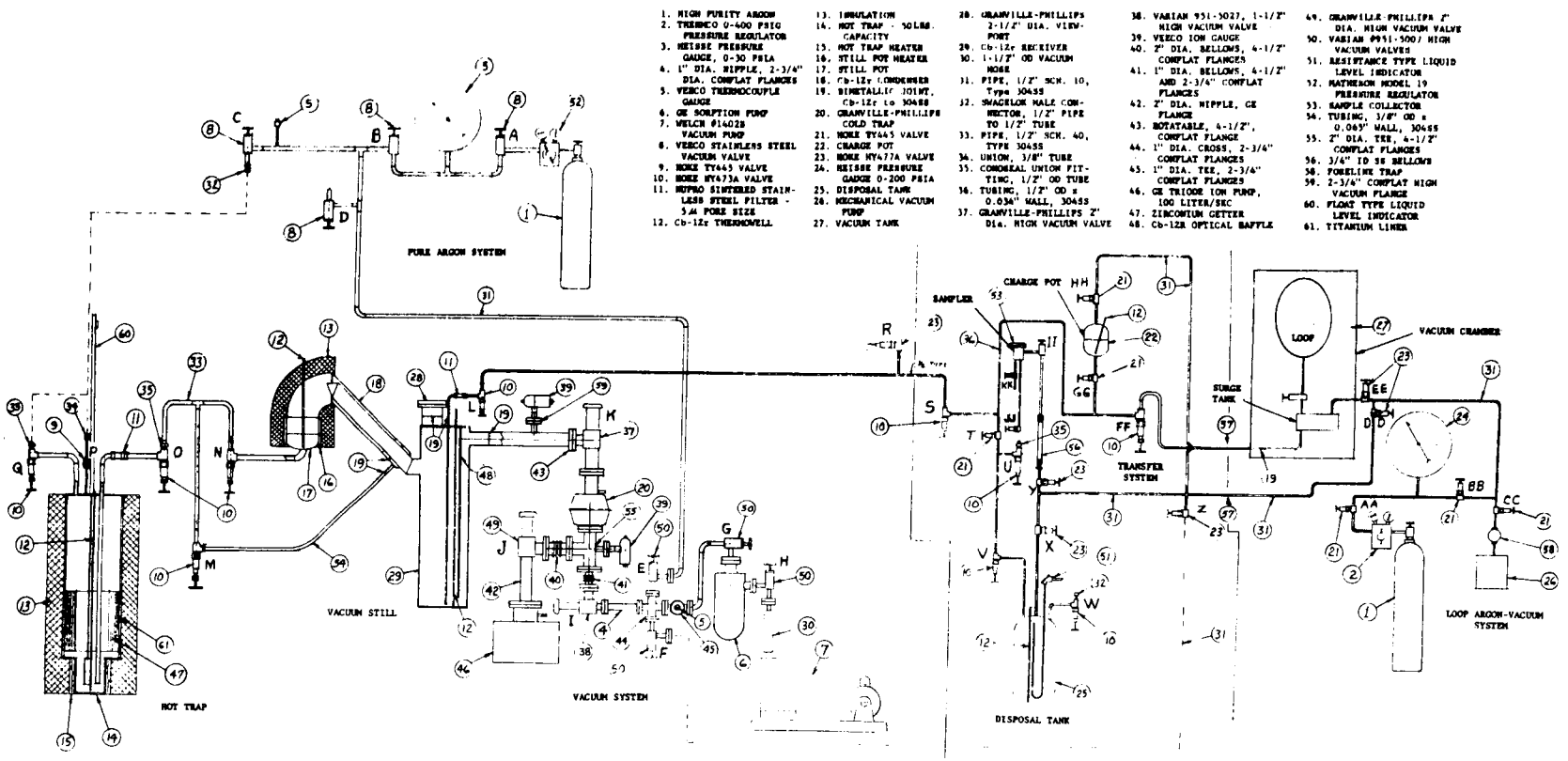

Figure 59. Potassium Purification and Loop Filling System.

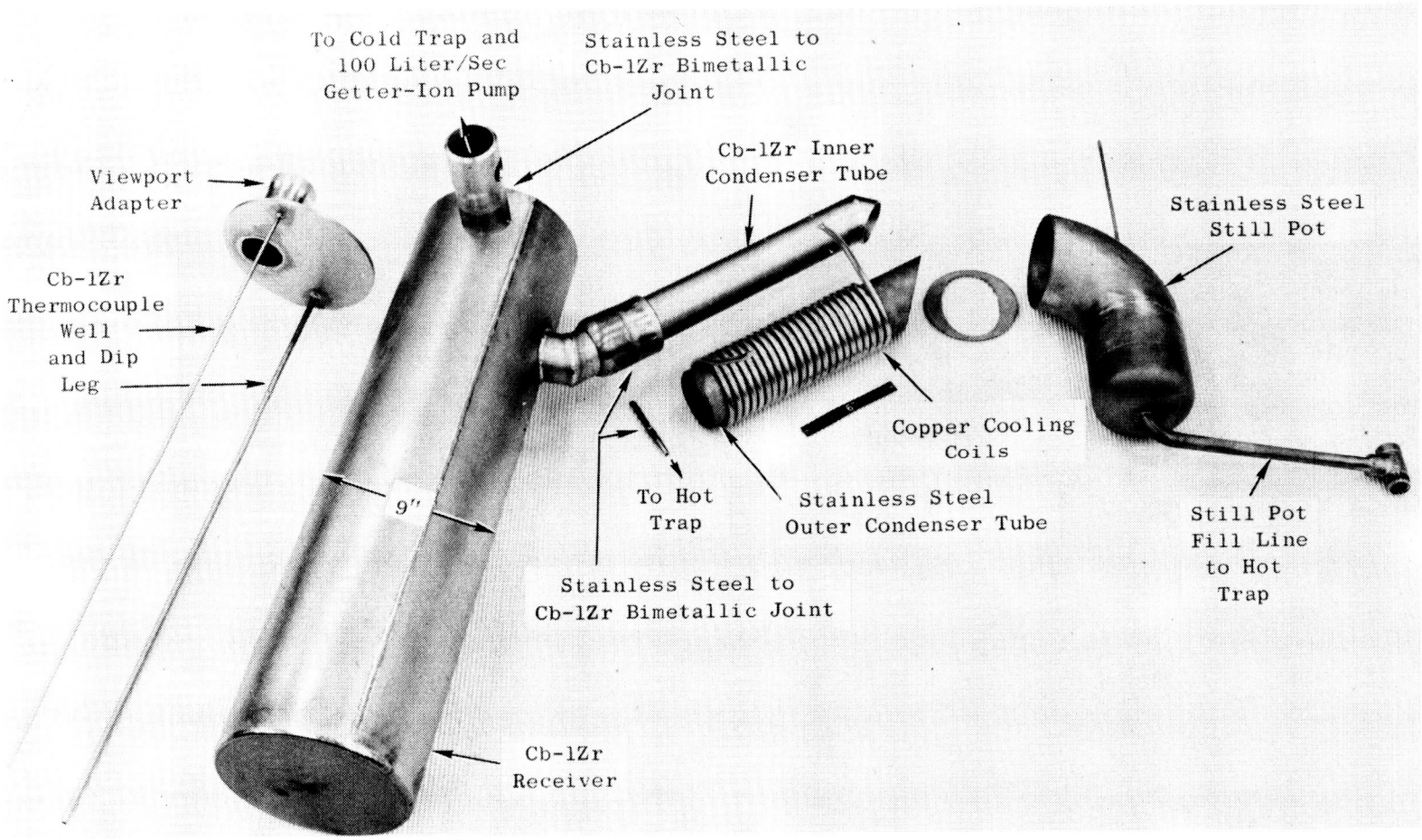

Figure 60. Potassium Distillation Unit for Purifying Potassium. Components of System Shown Prior to Assembly. (C65062186)

C. SODIUM AND POTASSIUM TRANSFER SYSTEM

The dual transfer system required for dispensing the sodium and potassium to the separate loop circuits from the purification systems is shown in Figure 61 with one of the side panels of the oven removed. The sodium and potassium transfer and sampling systems shown are mirror images of one another. Arrangement of the transfer system with relation to the other portions of the alkali metal supply system was indicated previously in Figures 56 and 59. Each transfer system contained a charge pot of known volume, a disposal tank, a sampling valve, and the necessary transfer and vacuum-argon lines.

The purification system, transfer system, and fill lines to the two loop circuits were interconnected by TIG welding the stainless steel tubes. After connection, the transfer system was leak checked and thoroughly baked out. The filling procedures for both loop circuits were identical, and the description of this operation is included in Section VIII, Pretest Operations, of this report.

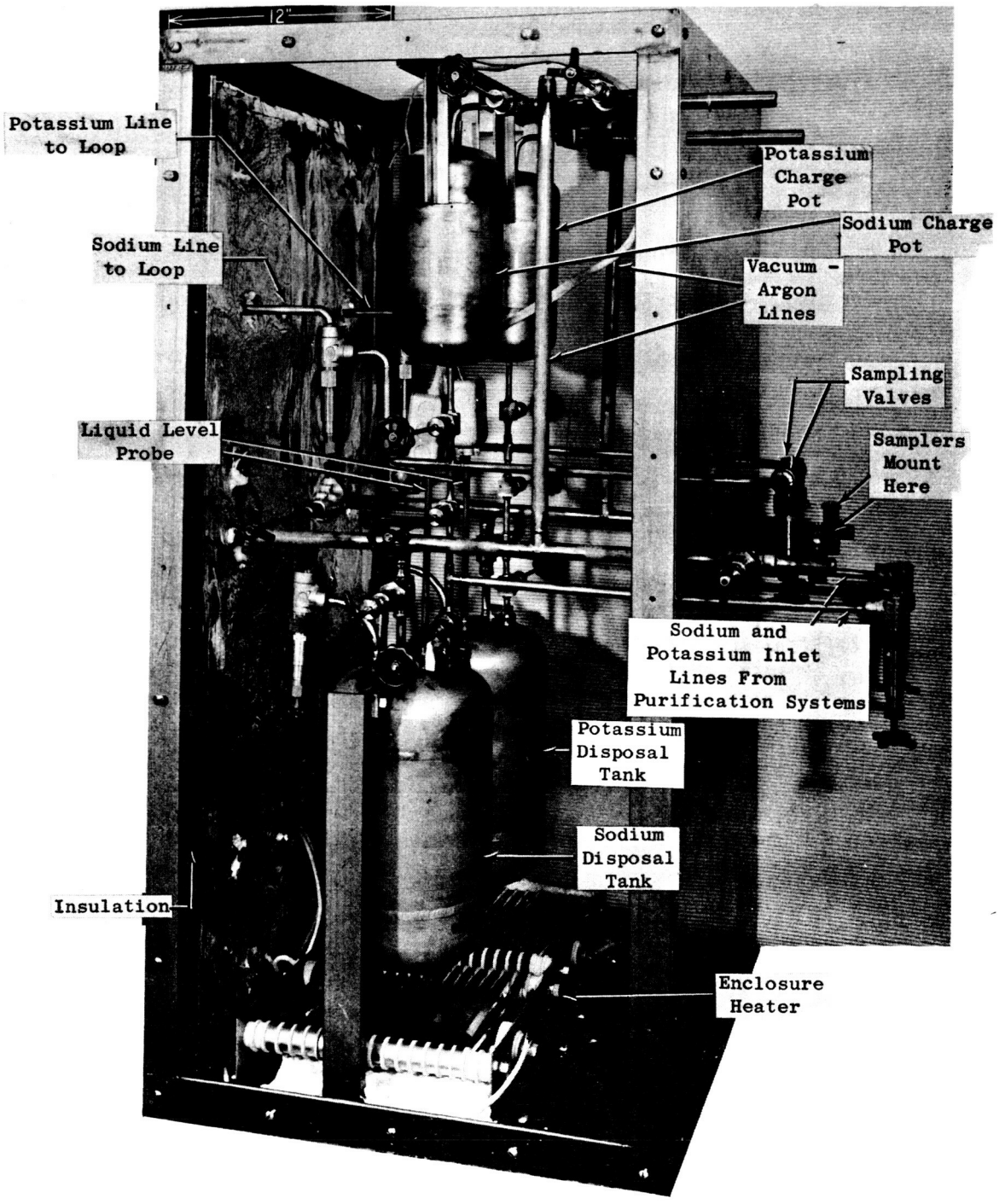

Figure 61. Sodium and Potassium Transfer Systems After Installation in Oven Enclosure. Cover Panels Removed to Take Picture. (Orig. C65040926)

VII. LOOP INSTALLATION AND INSTRUMENTATION

Upon completion of the final welding and heat treating operations on the Cb-1Zr Corrosion Test Loop, a final helium mass spectrometer leak check of the assembly was made. No leaks were detected using a helium mass spectrometer having a sensitivity of 5×10^{-10} standard cc of air per second. The loop, mounted in the test chamber spool piece, was then transferred from the fabrication area to a portable air shelter in the test area for the installation of components, the attachment of loop thermocouples, and the application of Cb-1Zr foil thermal insulation.

A. INSTALLATION AND INSTRUMENTATION ENCLOSURE

The 15-foot-diameter reinforced polyethylene air shelter used to house the loop and spool piece during installation and instrumentation is shown in Figure 62. A constant supply of filtered air was forced into the shelter by a blower which maintained an internal pressure of 0.2 psig to support the weight of the polyethylene enclosure. The walls of the air shelter were sealed to the concrete floor by sand bags. A semirigid steel-framed air lock attached to the main room permitted personnel movement into and out of the air shelter without release of the supporting air pressure. The interlock area was also used as a change room by the technicians entering the air shelter. All personnel engaged in instrumenting the loop were required to wear lint-free clothing which included white shoe covers, coveralls, and gloves. All loop components were vacuum cleaned, then washed with ethyl alcohol, and vacuum cleaned again to remove any dust or foreign material that could have accumulated during the fabrication or final shipment of the loop to the test area.

B. INSTALLATION OF THE LOOP IN THE SPOOL SECTION OF THE VACUUM CHAMBER

Following the placement of the loop and spool piece in the air shelter, the temporary supports used in fabrication and transfer of the loop to the test site were removed and permanent brackets and supports were installed. The loop was supported by two constant-load, lever-type counterweights attached to the vapor carryover line of the potassium circuit. The 25-pound boiler and the 2.5-pound first-stage nozzle assembly were supported by one counterweight, and the 22-pound turbine simulator and the 45-pound condenser

Figure 62. Reinforced Polyethylene Air Shelter Used During Instrumentation of the Cb-1Zr Corrosion Test Loop. (Orig. C68013197)

were balanced by the second counterweight system. The counterweights were 4-inch-diameter, 0.5-inch-thick, stainless steel discs mounted on a lever arm having a mechanical advantage of approximately 5 to 1.

The sodium heater and preheater coils were supported by their electrodes which were bolted to 2-inch-wide by 0.25-inch-thick OFHC copper bus bars which were in turn fastened to the support structure. The bus bars were electrically insulated from the support structure by 99.7 percent alumina insulators. Additional fixed supports were used for the slack diaphgram and stressed diaphragm pressure transducers, the permanent magnet flowmeter, and the surge tank.

C. THERMAL INSULATION

Dimpled foil made from 0.002-inch-thick by 0.5-inch-wide Cb-1Zr strip was selected as the reflective insulating material for all test loops in the Potassium Corrosion Test Loop Development Program. This approach was chosen for the following reasons:

1. The narrow, flexible strip could easily be wrapped around components of odd shapes and sizes, e.g., heater coils, to give any desired number of layers of insulation.
2. The dimpled foil with its self-spacing feature and minimum thermal conductive path (point contact between successive layers) yielded an insulation assembly of minimum mass and surface area which, in turn, reduced outgassing loads and radiation losses.

The dimpling of the foil was accomplished by passing the Cb-1Zr foil and a sheet of plasticized polyvinylchloride[(a)] through manually operated rolls together. The hardened steel, coarse-knurled roller embossed the foil with the indentations which spaced the successive layers of foil during subsequent application on the loop components. Dimpling the foil increased its effective thickness from 0.002 inch to approximately 0.010 inch. As the foil was removed from the rolls, it was thoroughly cleaned with absolute ethyl alcohol. The type and number of layers of foil used in insulating the loop are shown in Figure 63. The number of layers of foil selected was determined

(a) Kayflex L-10; Source: S&C Manufacturing Company, Cincinnati, Ohio.

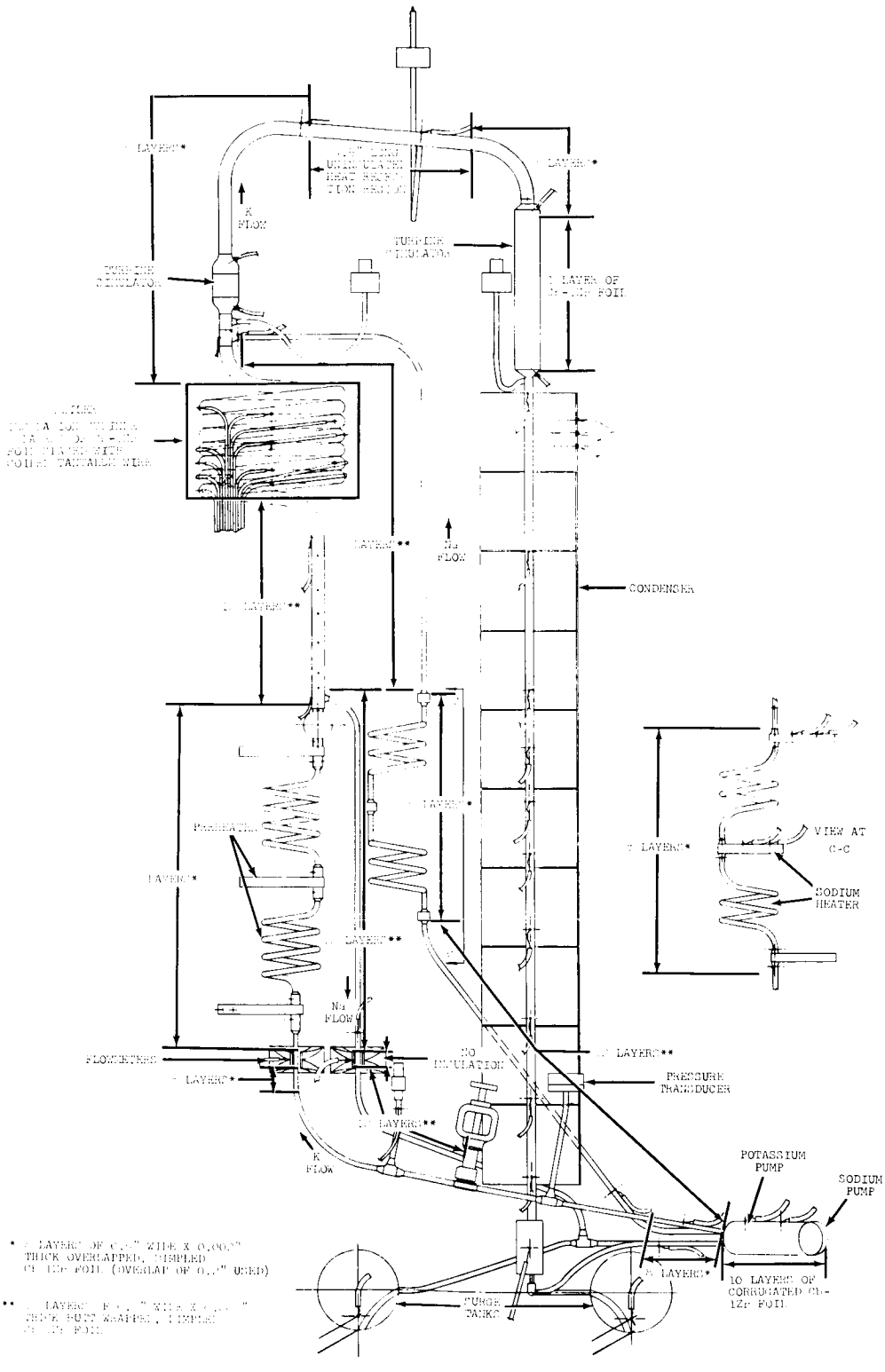

Figure 63. Cb-1Zr Corrosion Test Loop Showing the Number of Layers of Reflective Foil Thermal Insulation Used on the Various Loop Components.

by a consideration of the allowable heat loss in the various regions of the loop. For the heater coils, it was necessary to consider both the allowable heat loss and the allowable decrease in electrical resistivity. The eight layers of foil on the heater coils provide additional current flow paths, but this is not enough to significantly lower the resistance because of the relatively high resistance of the point contact path through the layers of foil.

The foil was applied to the tubing by continuously wrapping it in a spiral manner with approximately 10 percent (0.050-inch) overlap. The insulation was held in position by spot welding the foil to the tube and to itself as succeeding layers were applied. A minimum number of spot welds were used to minimize the conduction heat loss through the foil. A molybdenum electrode was used rather than the standard copper electrode to avoid contamination of the foil surfaces with copper. An argon cover gas was used to protect the spot weld areas from oxidation. Great care was taken in applying the foil over the thermocouples attached to the tube walls to minimize the possibility of foil-to-thermocouple wire contact during test which might result from the slight movement of either material. The approach used is further described below in the section covering the thermocouple installation procedures.

The insulation method described above was not used on the boiler because of its geometry and the large number of thermocouples attached to the boiler tube. The boiler insulation was preassembled into several self-supporting sections that could be easily installed around the boiler after the thermocouples were attached to the boiler tube. The assembly consisted of a center cylinder, two outer semicylindrical halves, and a top and bottom end shield. The layers of Cb-1Zr foil in the assemblies were spaced by means of wraps of coiled and partially stretched tantalum wire.

D. INSTRUMENTATION

The temperature of the various loop components was measured by 79 thermocouples made of 0.005-inch-diameter W-3Re and W-25Re wire. The basic thermocouple alloy combination selected for instrumenting the three alkali metal loops in the Potassium Corrosion Test Loop Program was the W-3Re/W-25Re combination. The selection was based on its compatibility with the test

loop alloy, Cb-1Zr; its high and fairly linear thermal emf; and its reported excellent stability over extended periods of time in vacuum at elevated temperatures.[32] The W-3Re alloy was selected for the one leg of the thermocouple in preference to pure tungsten because of its superior handling properties, i.e., less breakage during installation and operation.

Although various tungsten-rhenium alloy combinations have been used for a number of years, a national standard has not as yet been adopted. Matched tungsten-rhenium thermocouple wire of various alloy combinations, however, can be purchased with a specified accuracy to tentative calibration tables adopted by the thermocouple wire suppliers. The policy adopted for this program was to purchase wire to a chemical or material specification and conduct calibration tests at General Electric on the thermocouple wire in accordance with the overall quality control plan. The W-3Re wire was purchased from the Lamp Metals Components Department of the General Electric Company, Cleveland, Ohio, and the W-25Re wire was purchased from Hoskins Manufacturing Company, Detroit, Michigan. All thermocouple wire used in a specific loop test was taken from one matched lot with its own calibration.

The results of the calibration of the thermocouple wire used to instrument the loop are shown in Table XII. The calibration test was run in a high-vacuum thermocouple test facility using a certified Pt/Pt-10Rh thermocouple as the calibration standard. The calibration equipment and procedures used are described in Appendix A, Calibration of W-3Re/W-25Re Thermocouple Wire, of this report.

The thermocouple wires inside the chamber were electrically insulated with high-purity, two-hole 99.5 percent alumina insulators to the point of contact with the Cb-1Zr tubing. Beryllium oxide insulators (99.5 percent) were used in contact with the regions of the loop designed to operate at temperatures in excess of 2000°F, and alumina was used in the lower temperature regions. The insulators were supported at frequent intervals by small straps of Cb-1Zr foil spot welded to the support structure. A foil strap near the junction

(32) Hendricks, J.W. and McElroy, D.L., High Temperature High Vacuum Thermocouple Drift Tests, ORNL-TM-833, August 1964.

TABLE XII

THERMOCOUPLE REFERENCE TABLE FOR THE W-3Re/W-25Re WIRE USED TO INSTRUMENT THE Cb-1Zr CORROSION TEST LOOP

Temp.→ ↓	°F	0°	10°	20°	30°	40°	50°	60°	70°	80°	90°	100°
						emf, Millivolts*						
	0	0.	0.	0.	0.	0.048	0.109	0.170	0.231	0.291	0.352	0.413
	100	0.413	0.479	0.545	0.612	0.678	0.744	0.810	0.881	0.951	1.022	1.092
	200	1.092	1.168	1.244	1.320	1.396	1.472	1.552	1.633	1.713	1.794	1.874
	300	1.874	1.960	2.046	2.132	2.218	2.304	2.393	2.481	2.570	2.658	2.747
	400	2.747	2.838	2.929	3.020	3.111	3.202	3.296	3.391	3.485	3.582	3.679
	500	3.679	3.776	3.875	3.973	4.072	4.170	4.269	4.368	4.466	4.565	4.663
	600	4.663	4.762	4.862	4.962	5.062	5.161	5.261	5.361	5.462	5.564	5.666
	700	5.666	5.767	5.868	5.970	6.073	6.176	6.278	6.381	6.484	6.587	6.691
	800	6.691	6.796	6.900	7.004	7.110	7.217	7.323	7.430	7.536	7.643	7.749
	900	7.749	7.856	7.963	8.071	8.178	8.285	8.393	8.502	8.610	8.719	8.827
	1000	8.827	8.937	9.047	9.157	9.267	9.377	9.487	9.597	9.707	9.817	9.927
	1100	9.927	10.038	10.149	10.261	10.372	10.483	10.594	10.705	10.817	10.928	11.039
	1200	11.039	11.151	11.263	11.375	11.487	11.599	11.712	11.824	11.936	12.048	12.160
	1300	12.160	12.272	12.384	12.496	12.607	12.719	12.831	12.943	13.055	13.167	13.279
	1400	13.279	13.391	13.502	13.614	13.726	13.838	13.950	14.063	14.175	14.287	14.399
	1500	14.399	14.512	14.624	14.736	14.849	14.961	15.073	15.186	15.298	15.410	15.522
	1600	15.522	15.635	15.747	15.859	15.972	16.084	16.196	16.307	16.419	16.530	16.642
	1700	16.642	16.754	16.865	16.977	17.088	17.200	17.311	17.421	17.532	17.643	17.753
	1800	17.753	17.864	17.975	18.086	18.196	18.307	18.417	18.527	18.637	18.747	18.857
	1900	18.857	18.968	19.078	19.188	19.298	19.408	19.517	19.626	19.736	19.845	19.954
	2000	19.954	20.063	20.172	20.282	20.391	20.500	20.609	20.717	20.826	20.934	21.043
	2100	21.043	21.152	21.260	21.369	21.477	21.586	21.694	21.802	21.910	22.018	22.126
	2200	22.126	22.235	22.343	22.451	22.559	22.667	22.774	22.882	22.989	23.096	23.203
	2300	23.203	23.311	23.418	23.525	23.633	23.740	--	--	--	--	--

* Reference junction, 32°F

was used to minimize stress on the spot-welded junctions.

The locations and designations of the 79 thermocouples which were installed on the loop are shown in Figure 64. Sixty-six of the loop thermocouples are of the wall junction or surface type with each thermocouple wire spot welded directly to the loop component and held in position by the techniques illustrated in Figures 65 and 66. A typical split spot-welded thermocouple junction is made with each wire laid parallel to the other, approximately 0.10 inch apart. Two consecutive spot welds are applied to each wire so that in the event the first spot weld breaks away from the surface without breakage of the wire, the thermocouple will continue to function. A small thermal shield is fixed around the junction to reduce heat radiation losses from the junction and to prevent thermocouple wire shorts when foil insulation is wrapped on the tube. Thirteen of the thermocouples were of the well type with the thermocouple wires joined together prior to insertion into a well. The well-type thermocouples were specified for components where an accurate average temperature was required, and the geometry of the component permitted the insertions of a well tube or a drilled hole. These included the inlet and outlet pipes to the EM pumps, the turbine simulators, and the potassium preheater. Well-type thermocouples were also placed in three drilled holes of varying depth in the condenser fin near the top of the condenser.

The procedure used in installing the loop thermocouples was a departure from the method used in the Cb-1Zr Sodium Thermal Convection Loop[33] and the Cb-1Zr Pumped Sodium Loop.[34] For these earlier tests the tungsten-rhenium thermocouple wire was routed from the loop through thermocouple feedthroughs to a constant temperature reference junction located outside of the vacuum

(33) Hoffman, E. E. and Holowach, J., Cb-1Zr Sodium Thermal Convection Loop, Potassium Corrosion Test Loop Development Topical Report No. 5, R67SD 3014, General Electric Company, Cincinnati, Ohio, June 15, 1967, p. 31.

(34) Hoffman, E. E. and Holowach, J., Cb-1Zr Pumped Sodium Loop, Potassium Corrosion Test Loop Development Topical Report No. 6, R67SD3014, General Electric Company, Cincinnati, Ohio, December 20, 1967, p. 90.

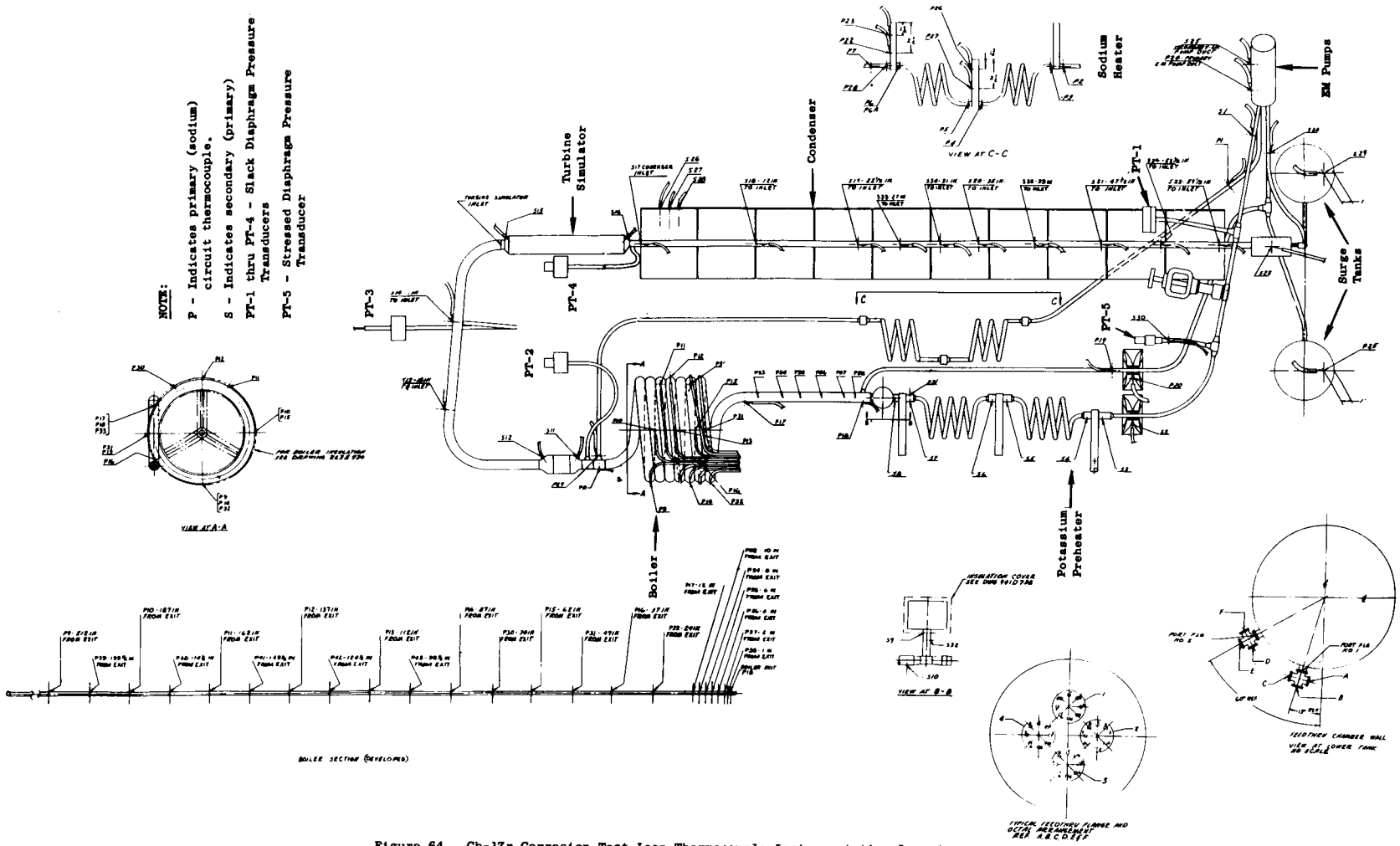

Figure 64. Cb-1Zr Corrosion Test Loop Thermocouple Instrumentation Layout.

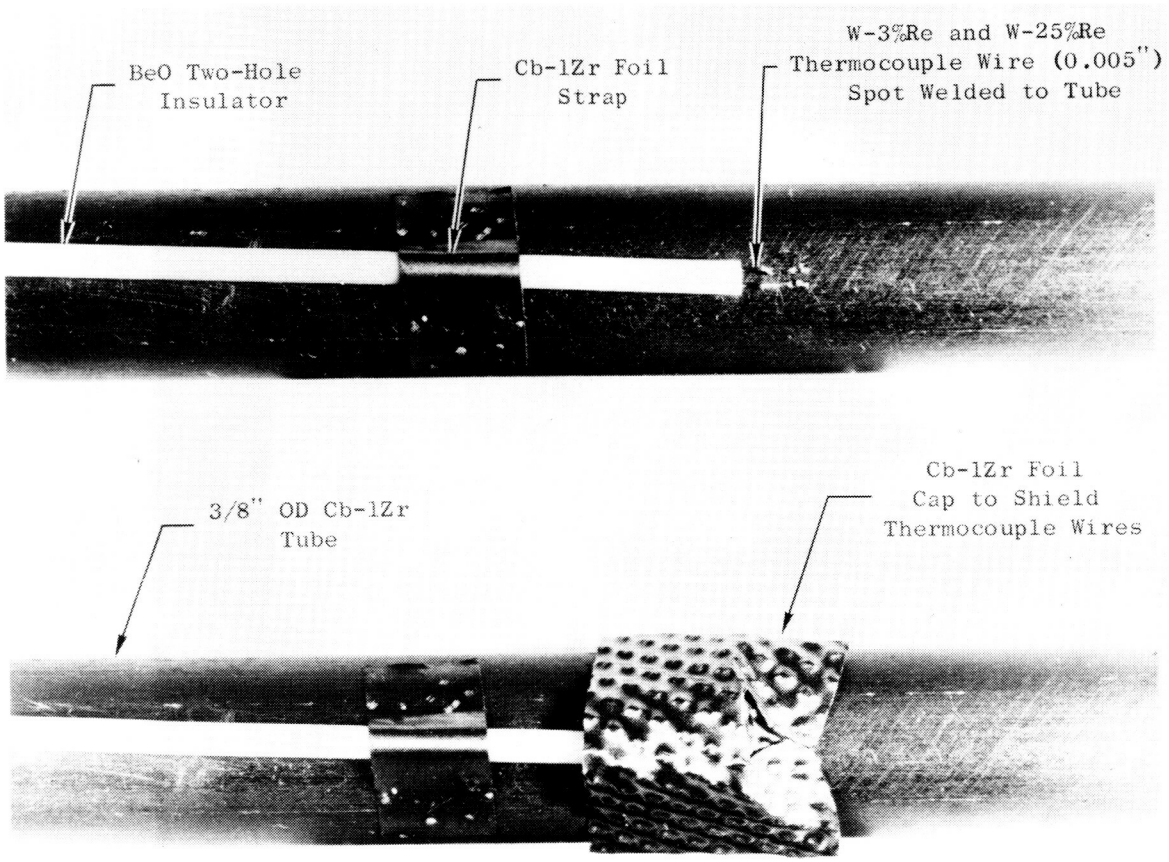

Figure 65. Method Used to Mount W-3Re/W-25Re Thermocouple Wires on Cb-1Zr Alloy Tubing for the Cb-1Zr Corrosion Test Loop. (Orig. C65020803) (Orig. C65020801)

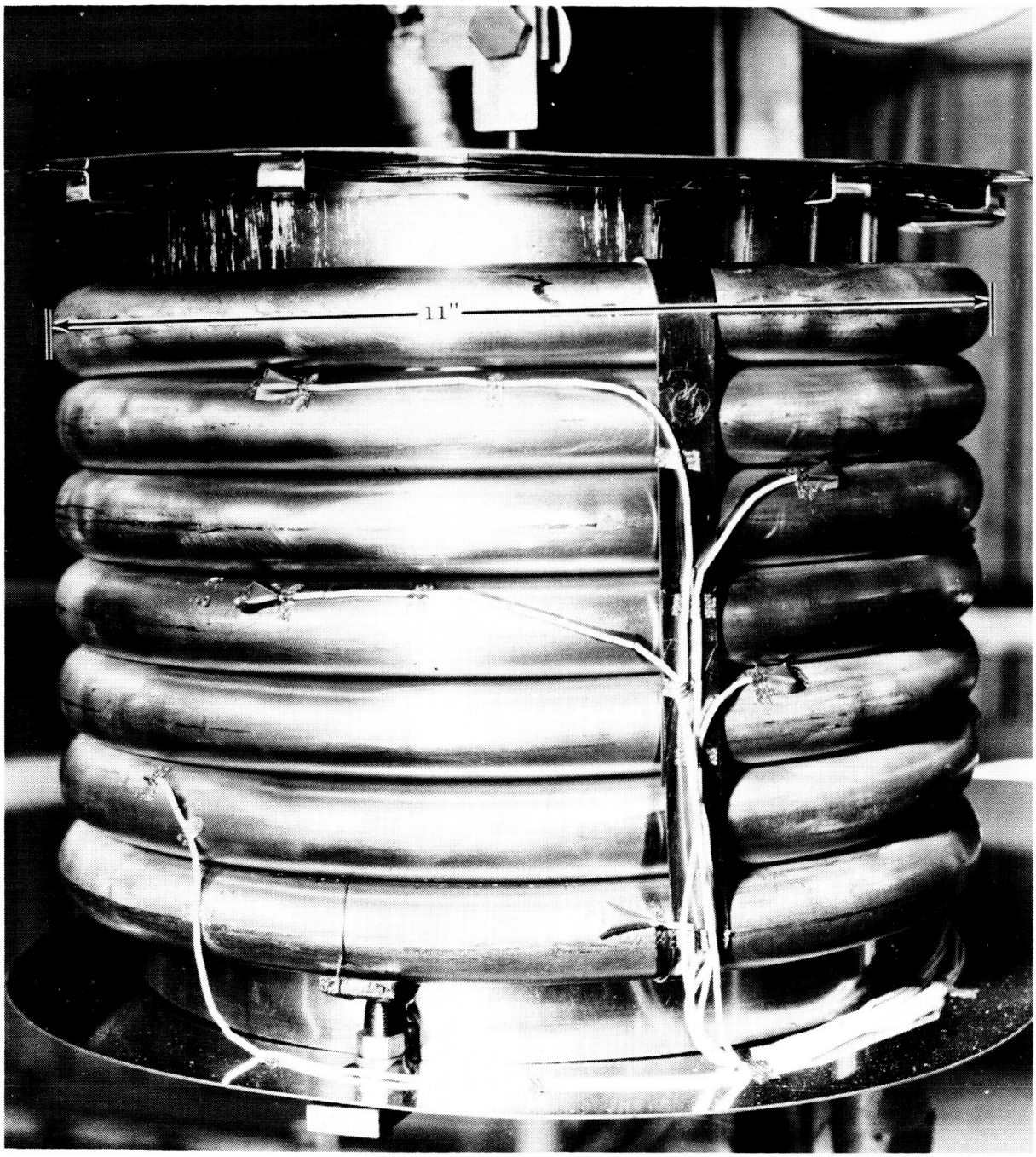

Figure 66. Photograph of Tube-in-Tube Helical Boiler Showing the Method Used to Mount Boiler Thermocouples. (Orig. C65061613)

tank. Copper lead wires were then used between the reference junction and the recorder. In both loops problems were encountered with the thermocouple vacuum feedthrough because of the difficulty of brazing tungsten-rhenium wire to the nickel tubulation of the vacuum feedthrough. Not only was the assembly difficult to seal effectively, but a number of failures occurred on the W-3Re wire near the brazed joint during installation and later during loop operation. To minimize these problems, a copper plate reference junction block was placed inside of the vacuum chamber as shown in Figure 67, and copper lead wire was routed from the junction block through the vacuum feedthrough to the recorder. This method is illustrated in Figure 68. The assembly shown in Figure 68(b) consists of four octal (8-tube) feedthroughs[(a)] welded into a 6-inch flange. The 10-mil-diameter copper wires were sealed to the 0.050-inch-OD x 0.040-inch-ID nickel feedthrough tubes by brazing with Premabraze 615 (62Ag-24Cu-14In) in an argon atmosphere using an electrical resistance heat clamp for local heating. Short lengths of single-hole alumina insulators were used to electrically insulate the thermocouple wire from the nickel feedthrough tube near the brazed seal. Teflon tubing was used to insulate the remaining length of thermocouple wire from the nickel feedthrough tube to eliminate spurious thermal emfs which would result from multiple electrical junctions if the wires touched the nickel tubes. By using a flanged cross,[(b)] it was possible to install forty-eight pairs of thermocouple wires though a single 6-inch flange in the chamber wall. The feedthrough assembly flanges shown in Figure 69 are sealed using flat copper gaskets and may be baked out at 500°F.

The reference junction block shown in Figure 67 consists of eight 99.7 percent Al_2O_3 tube terminal strips mounted on a 1/4-inch-thick copper plate which is bolted to the wall of the sump of the chamber. The entire assembly was shielded from the hot portions of the loop by means of a stainless steel sheet optical baffle to minimize temperature gradients in the junction block and to maintain a temperature which approached that of the water-cooled vacuum chamber wall.

(a) Varian Associates. Model No. 952-5041.

(b) Varian Associates, Vacuum Products Division, Model 954-5015.

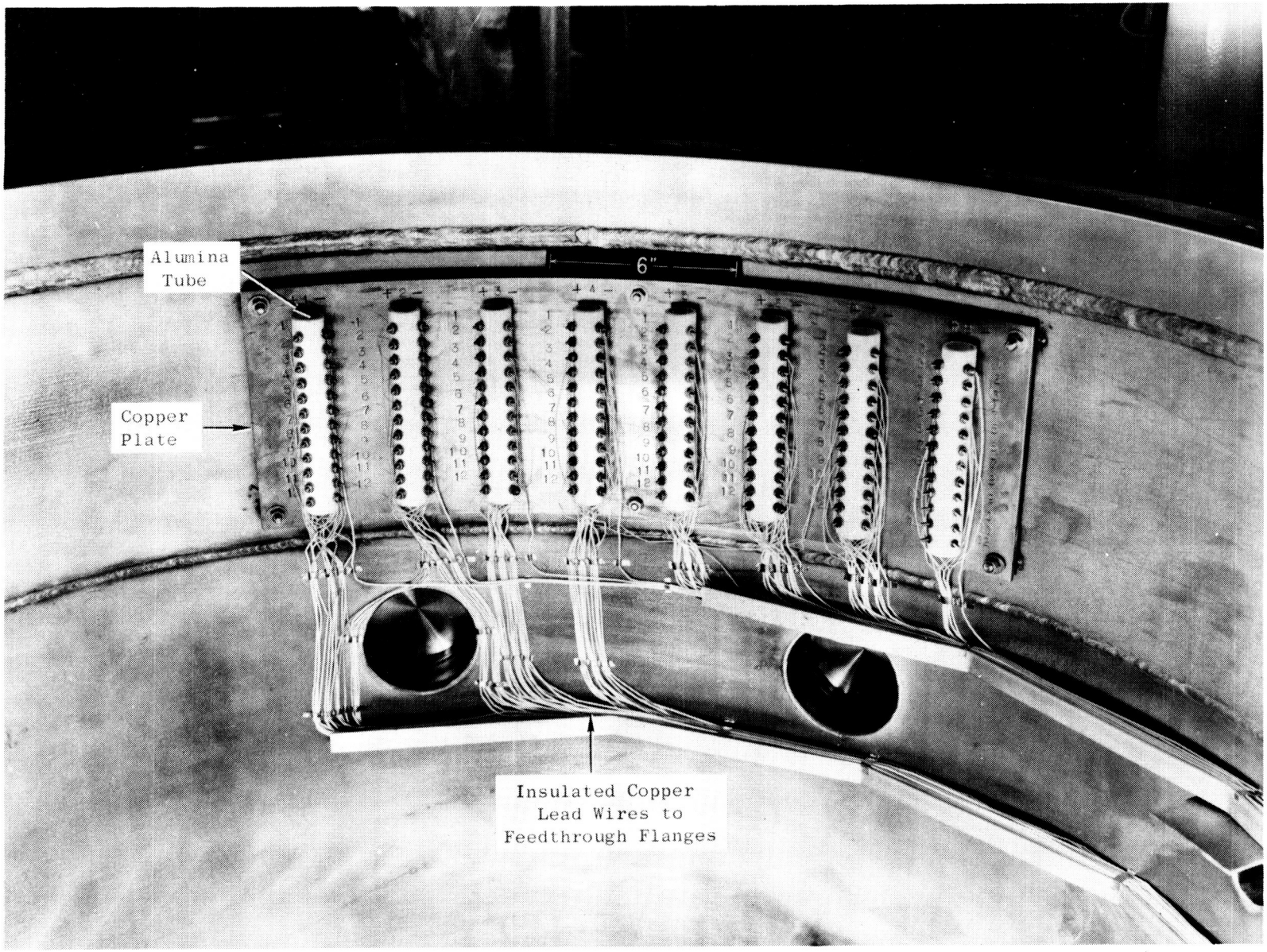

Figure 67. Thermocouple Wire Terminals (192 Total) Located in the Sump of the Test Chamber.

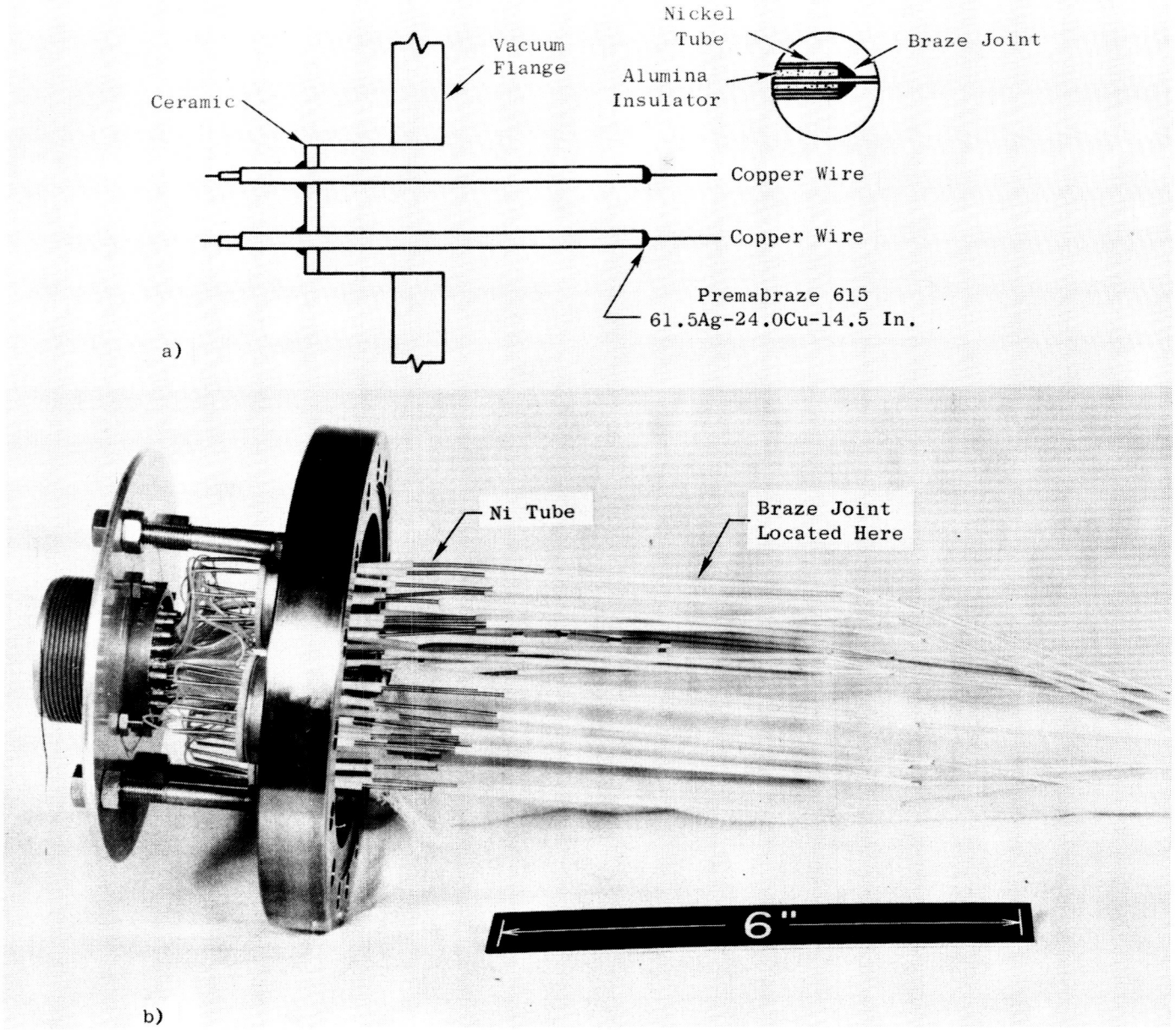

Figure 68. Typical Thermocouple Lead Wire Feedthrough Flange.
a) Sketch Illustrating Method Used to Seal Wire to Nickel Tube.
b) Feedthrough Containing 32 Lead Wires. (Orig. C650621103)

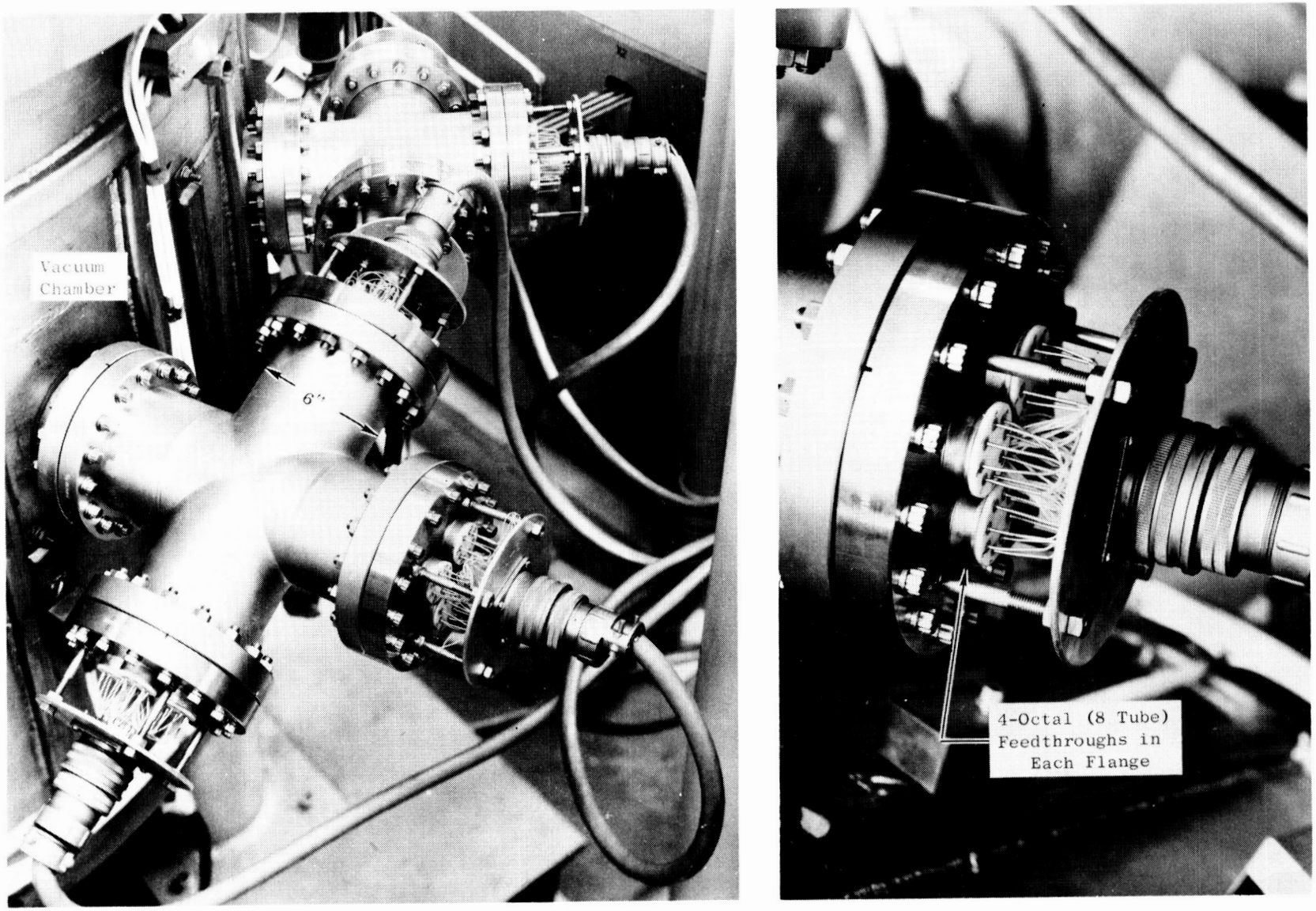

Figure 69. Six Thermocouple Lead Wire Feedthrough Flanges with 32 Wires in Each Flange. An Enlarged View of One of the Flanges is Shown on the Right.

An additional advantage of locating the reference junction block inside of the vacuum chamber is that it was possible to complete the routing of the thermocouple lead wires from the terminal strip to the recorder prior to mounting of the loop and spool piece on the chamber flange, which substantially reduced the time required for the final installation operations.

A schematic drawing of the thermocouple circuit used is shown in Figure 70. A typical thermocouple circuit starts at the hot junction of the thermocouple and terminates at the reference junction block attached to the inside of the wall of the sump section of the test chamber. At the reference junction block, a transition from the thermocouple wire to copper wire is made mechanically, and the copper wires are routed through a thermocouple vacuum feedthrough to a recording potentiometer. The temperature of each of the eight alumina tube reference junction blocks is measured by a copper/constantan thermocouple located on each block. The procedure used in determining the temperature of the loop is described below.

The temperature of the reference junction is determined by first measuring the millivolt output of a copper/constantan thermocouple with a 32°F reference junction. The indicated emf is converted to °F from a standard copper/constantan temperature conversion table. The reference junction temperature is converted back to a millivolt equivalent using the W-3Re/W-25Re conversion table. The reference junction voltage is then added to the measured loop thermocouple emf, and the corrected millivolt output is converted to the true loop temperature using the W-3Re/W-25Re conversion table.

An example of a typical temperature determination is given below:

Reference junction T/C (copper/constantan), emf: 6.33 mv

Reference junction temperature: 284°F

Loop T/C (W-3Re/W-25Re): 18.04 mv

Reference junction correction emf for 284°F: 1.75 mv

Corrected loop T/C emf: 18.04 + 1.75 = 19.79 mv

True loop temperature - 1985°F

E. CHAMBER INSTALLATION

After completion of the instrumentation and insulation of the loop, the loop was covered with a polyethylene bag, and the clean room was dismantled.

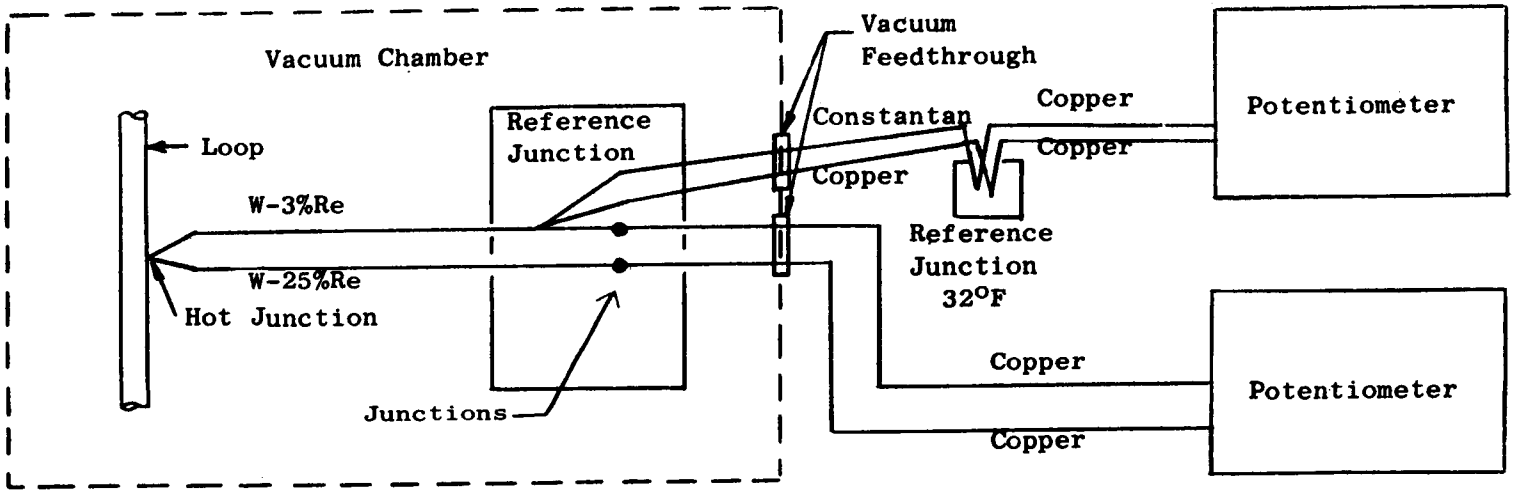

Figure 70. Schematic of the Thermocouple Circuit of the Cb-1Zr Corrosion Test Loop.

The loop and spool section on its plywood pallet was lifted by a fork truck above the vacuum sump, and the bell jar was lowered and then bolted to the spool flange. The bell jar and the attached spool section were raised together off the pallet and then lowered to the sump. The flanges were bolted together, and the vacuum chamber was evacuated and helium leak checked. This sequence was required to ensure a leak tight joint between the sump and lower spool flange because the spool becomes fixed in position when the EM pump windings for the two pumps are attached to their spool flanges, and the gas pressurization and liquid metal fill lines are welded to their spool piece ports.

Upon completion of the helium leak check, the vacuum system air release valve was opened, and the chamber was returned to atmospheric pressure. The bell jar was hoisted into the penthouse above the chamber, and the final instrumentation and the installation of loop components, which could only be completed with the loop in its final test position, were resumed.

The final connections joining the loop proper to the auxiliary test equipment and the control console were then made, and these are listed below.

1. The loop pressurization line was connected to an argon gas supply. The external argon gas supply system was of all-welded stainless steel construction with bellows-sealed valves and a metal diaphragm pressure regulator.[a] The argon system was used to pressurize the sodium in the surge tank of the loop and thereby prevent boiling in the heater coils during loop operation. It was also used to control the condensing temperature in the potassium circuit of the loop. The entire system was helium leak checked after assembly, and all components were baked out at 300°F under vacuum.

   The argon gas supply used for pressurization of the loop analyzed[b] as follows:

Ar	-	99.997%	CO	-	1 ppm
O_2	-	5 ppm	CO_2	-	1 ppm

(a) Thermco Company, LaPort, Indiana, 0-400 psig.

(b) Vendor Analysis - Matheson Company, Inc.

N_2	-	5 ppm	H_2	-	0.25 ppm
CH_4	-	0.2 ppm	H_2O	-	4.5 ppm

2. The sodium and potassium fill and drain lines were welded to their transfer system, helium leak checked, and baked out at 300°F under vacuum to remove adsorbed gases from the inner wall surface of the sodium fill tube.
3. The EM pump stators were slipped over the pump duct insulation cans and bolted to fixed flanges on the vacuum chamber. The sodium pump is shown in Figure 71 just prior to slipping the windings over the pump duct vacuum can.
4. The thermocouple leads were connected to the reference junction, and electrical resistance and continuity checks were repeated on all thermocouples from the loop to the recorder. The flowmeter and the pressure transducers connections to the recording potentiometer were completed at this time.

The actuating components of the metering and on-off isolation valves were then installed. These consisted of an ultrahigh vacuum rotary feedthrough with a torque rating of 6 ft-lbs[(a)] connected by a 0.31-inch-diameter flexible, stainless steel cable to a 5:1 right angle gear drive mounted on the valve yoke. The right angle gear drive was required to eliminate a compound bend in the flexible cable because the rotary feedthroughs are located below the valves. Two views of the metering valve and the valve drive assembly are shown in Figure 72. The enlarged view in Figure 72(b) shows the pinion drive gear and the spur gear which are mounted on the valve stem. By sighting on the wire shown and the 72 divisions laid out on the face of the gear, with the aid of a telescope located at one of the chamber viewports, precise measurements of valve adjustments could be made and observed. The flexible cables shown were cleaned ultrasonically and baked out at 500°F under a vacuum of less than 1×10^{-3} torr for 100 hours before installation. No lubrication of any type was used in the assembly.

The adjustable condenser shield assembly was the last component to be

(a) Varian Associates, Model No. 954-5039.

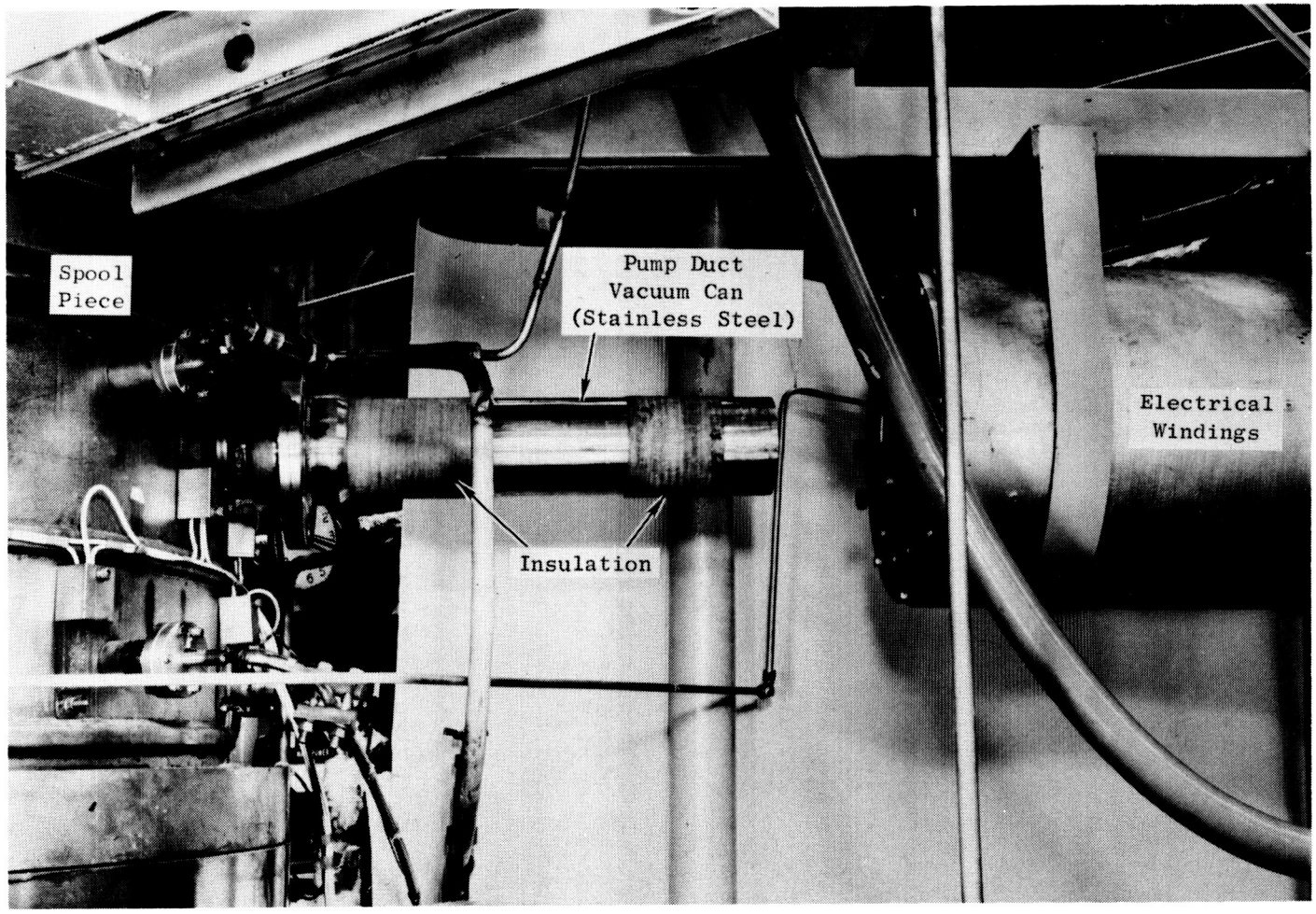

Figure 71. Sodium Pump Stator and Pump Duct Vacuum Can Prior to Assembly.

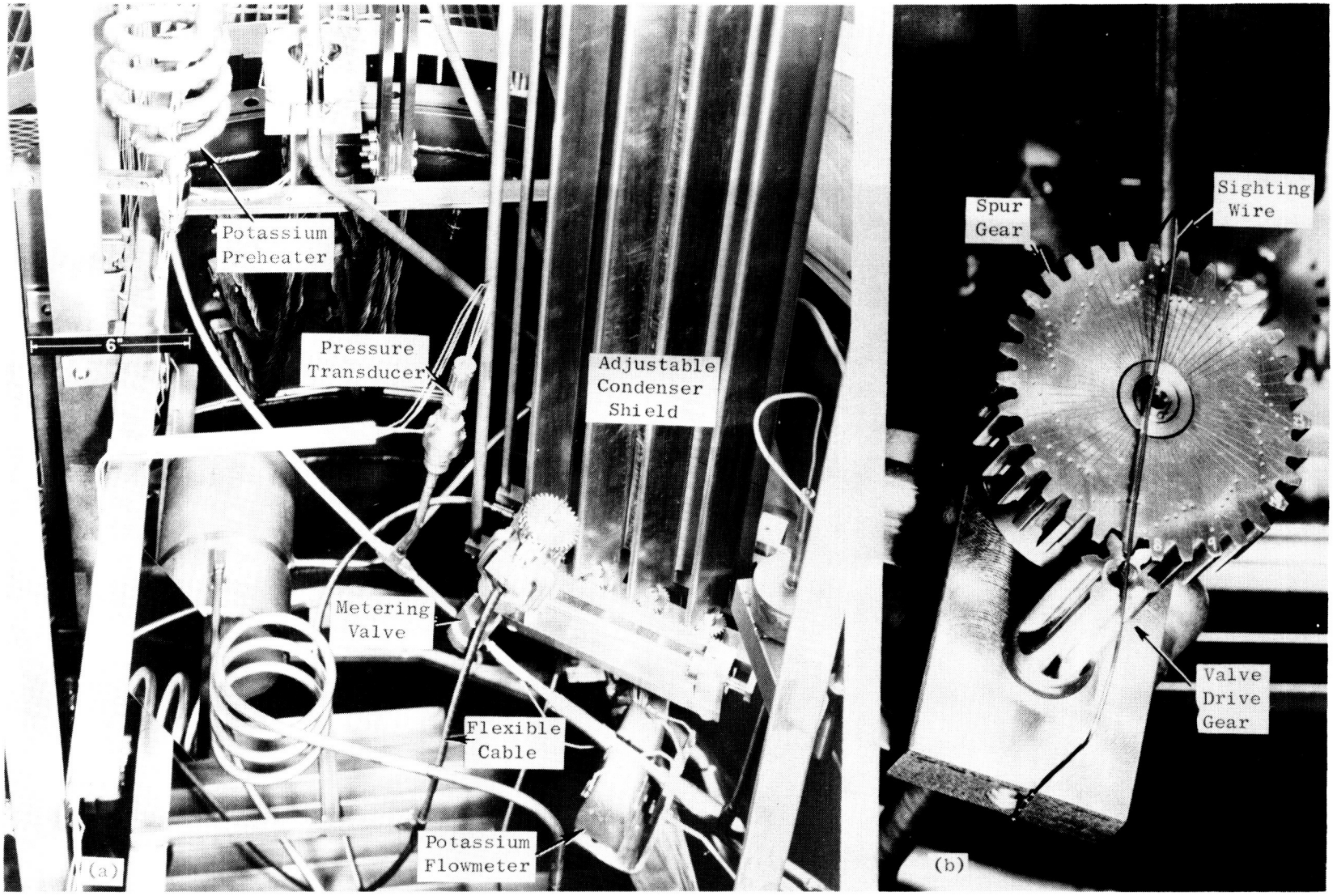

Figure 72. Lower Section (a) of Cb-1Zr Corrosion Test Loop and Enlarged View (b) of the Metering Valve Drive and Sighting Wire Used to Monitor Valve Adjustments. (a) (Orig. C65063018)
(b) (Orig. C65063016)

installed. A portion of the shield including the rack spur gear drive system and four of the eight movable shield fins constructed of Cb-1Zr are shown in Figure 72(a).

A final check on the loop instrumentation was then made, and the stainless steel mirrors which were attached to the support structure were adjusted to give full view of all components which were not directly visible through the viewports. The loop and auxiliary components are shown in Figure 73 following completion of the installation task.

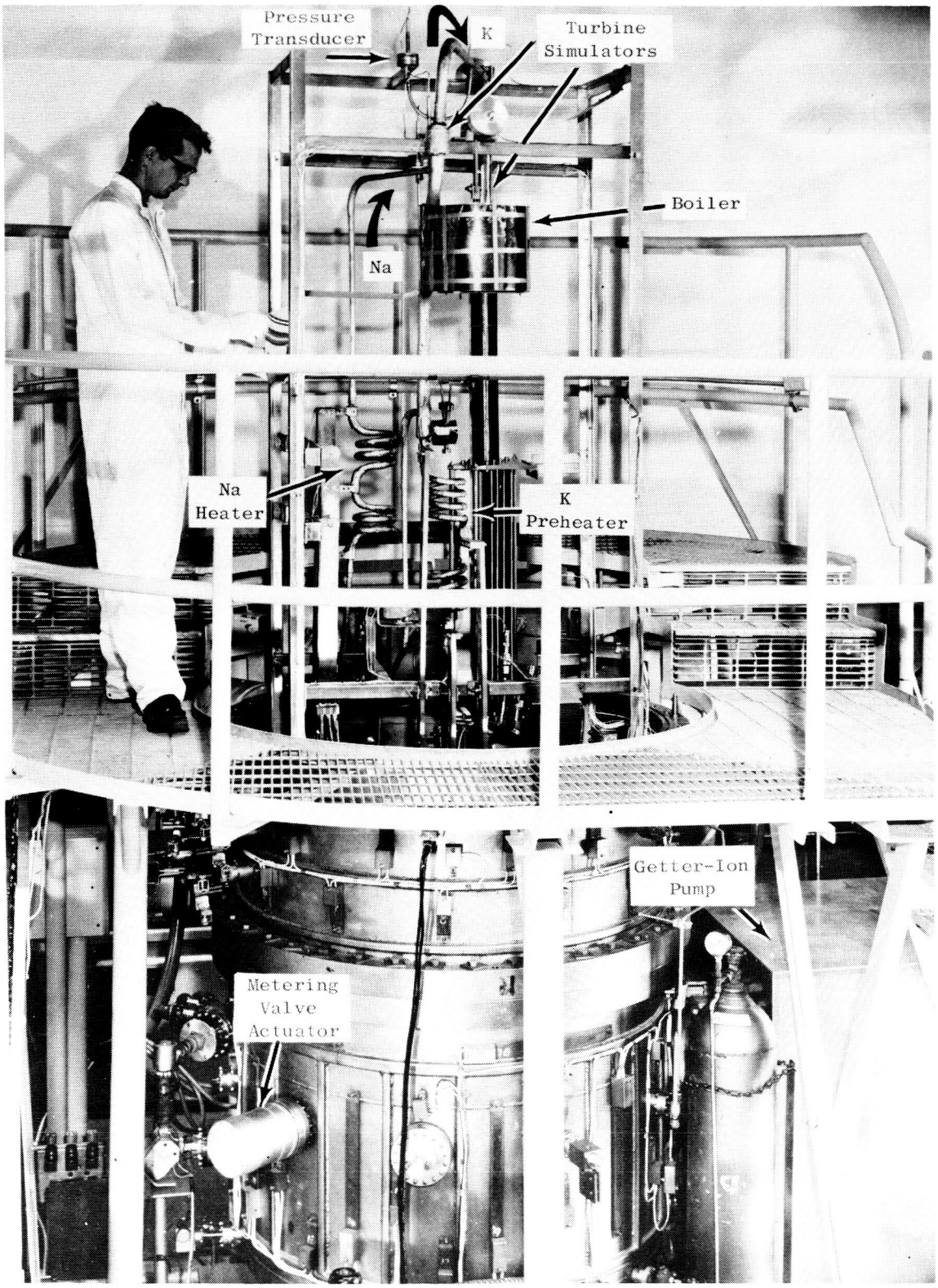

Figure 73. Corrosion Test Loop and Lower Portion of the Vacuum Chamber Prior to Lowering Chamber Bell Jar Onto Spool Piece. (Orig. C65083015)

VIII. PRETEST OPERATION

The portion of the test program of the Cb-1Zr Rankine System Corrosion Test Loop presented in this section describes the pretest activities from the initial sealing of the test chamber following the installation of the loop and spool section up to the start of boiling and condensing loop test operation.

A. PUMPDOWN AND BAKEOUT OF THE VACUUM CHAMBER

After completion of the installation of the loop in the 48-inch-diameter by 128-inch-high vacuum chamber, the bell jar was lowered and bolted to the spool piece flange. The vacuum system bakeout heaters were then turned on, and the chamber was evacuated to 10 microns and then backfilled with dry nitrogen gas. The system was again rough pumped with the liquid nitrogen-chilled sorption pumps. The sorption pumping system was then valved off, and the getter-ion pumps were turned on when the pressure at the roughing pump station was reduced to less than 5 microns.

Varian Associates, the manufacturer of the test chamber and pumping system, recommended that the titanium sublimation pumps be turned on when the chamber pressure was reduced to 15 microns by the sorption pumps. This procedure reduces the time required to lower the chamber pressure sufficiently to turn on the getter-ion pumps and confine the glow discharge. The "glow discharge" period is associated with high pressure conditions (5-20 microns) when the getter-ion pump voltage is low (approximately 200 volts), the current is high, and the pumping rate is low. In order to save the titanium sublimation pumps for use during the period of loop startup when high gas loads were anticipated, the sublimation pumps were not used during the initial startup of the getter-ion pumps. The "glow discharge" pumping condition persisted for three hours before the getter-ion pumps confined the discharge, and the high voltage, low current, high pumping rate condition was obtained.

After the vacuum chamber pressure had reached the 10^{-6} torr range, the titanium sublimation pumps were turned on maximum power to outgas the titanium filaments. Flexible heating tapes were used to bake out the partial pressure gas analyzer and the thermocouple feedthroughs.

The bakeout of the entire vacuum chamber and loop was then started. The bakeout heaters were regulated by an on-off controller actuated by a thermal switch mounted on the vacuum chamber wall. An overpressure relay, which is part of the ion pump control circuit, can override the heater control circuit if the pressure in the chamber exceeds 4×10^{-5} torr. This procedure is used to prevent the ion pump from being overloaded by the outgassing. However, during the start of the outgassing, the rate of rise in the pressure together with the large thermal capacity of the heating system can overshoot the overpressure set point and overload the ion pump. For this reason, an adjustable set point temperature controller would be a desirable feature for vacuum test chambers which have large outgassing rates. To circumvent the above outgassing problem, the bakeout was restricted initially to the bell jar of the chamber before the bakeout heaters for the spool and sump were turned on. The steady state temperatures of the loop and vacuum chamber varied from 250° to 525°F during the bakeout.

During the bakeout period numerous leak checks were made, and several leaks were detected in the main flange and one leak, in a gas pressurization feedthrough. The gas pressurization line leak was sealed by welding. The leaks in the main flange were sealed by retorquing all bolts to 225 ft-lbs; however, additional leaks were encountered in thermal cycling the vacuum chamber during the bakeout. The thermal cycling was the result of the on-off type of controller used in the bakeout system as described above. After considerable difficulty, all leaks in the main flanges were eliminated.

Although the loop system proper was helium leak checked following the final assembly, an additional leak check was performed in the test chamber during the bakeout period. This final leak check of the loop was performed by pressurizing the loop circuits with argon and scanning the residual gas in the vacuum chamber for an increase in argon with the partial pressure gas analyzer. The loop was found to be leak tight, and preparations for filling the loop with liquid metal were made.

The bakeout of the chamber continued during the preparation for filling the loop,and after 180 hours of getter-ion pumping the total pressure of

the system was 5 x 10^{-6} torr with the bakeout heaters on. Cooling the chamber to 250°F reduced the system pressure to 4.8 x 10^{-8} torr

B. FILLING, FLUSHING, AND SAMPLING OF ALKALI METALS IN THE Cb-1Zr CORROSION LOOP SYSTEM

The sodium and potassium purification systems and the transfer systems were interconnected and attached to the loops. A plan view of this arrangement is shown in Figure 74. All liquid metal transfer lines outside of the ovens were traced and insulated for heating. Thermocouples were attached to all valves and at numerous other locations in the system to monitor temperatures during the outgassing, liquid metal flushing, and loop filling operations.

The transfer systems and loops were outgassed at temperatures ranging from 250° to 500°F. The pressure rise rates for the combined loop and transfer systems were 0.3 micron-liters per minute for the sodium circuit and 0.9 micron-liters per minute for the potassium circuit while hot. Both systems were helium leak checked hot, and no leaks were found at a sensitivity of 5 x 10^{-11} std cc of air per second.

The transfer systems were flushed with liquid metal at 200° to 300°F, and specimens of the liquid metal used for flushing were obtained and analyzed. The loops were then filled at about 300°F, and additional specimens of the alkali metals were obtained after circulating in the loop for one hour at 500°F. The analytical results obtained on the samples of sodium and potassium taken during these operations are given in Table XI, Section VI. Results of all chemical analyses performed on the sodium and potassium indicated that all the purity requirements listed at the bottom of this table were achieved.

C. CHECKOUT OF THE LOOP EQUIPMENT AND CONTROLS

The low-temperature checkout of the loop operating equipment and controls was started immediately after the filling of the loop circuit with the operation charges of sodium and potassium. The loop safety circuits were first checked, and these are listed below:

1. An electro-mechanical switch on the inlet water supply to the vacuum systems turns off the heater and preheater power if the the water rate drops below 1.2 gpm;

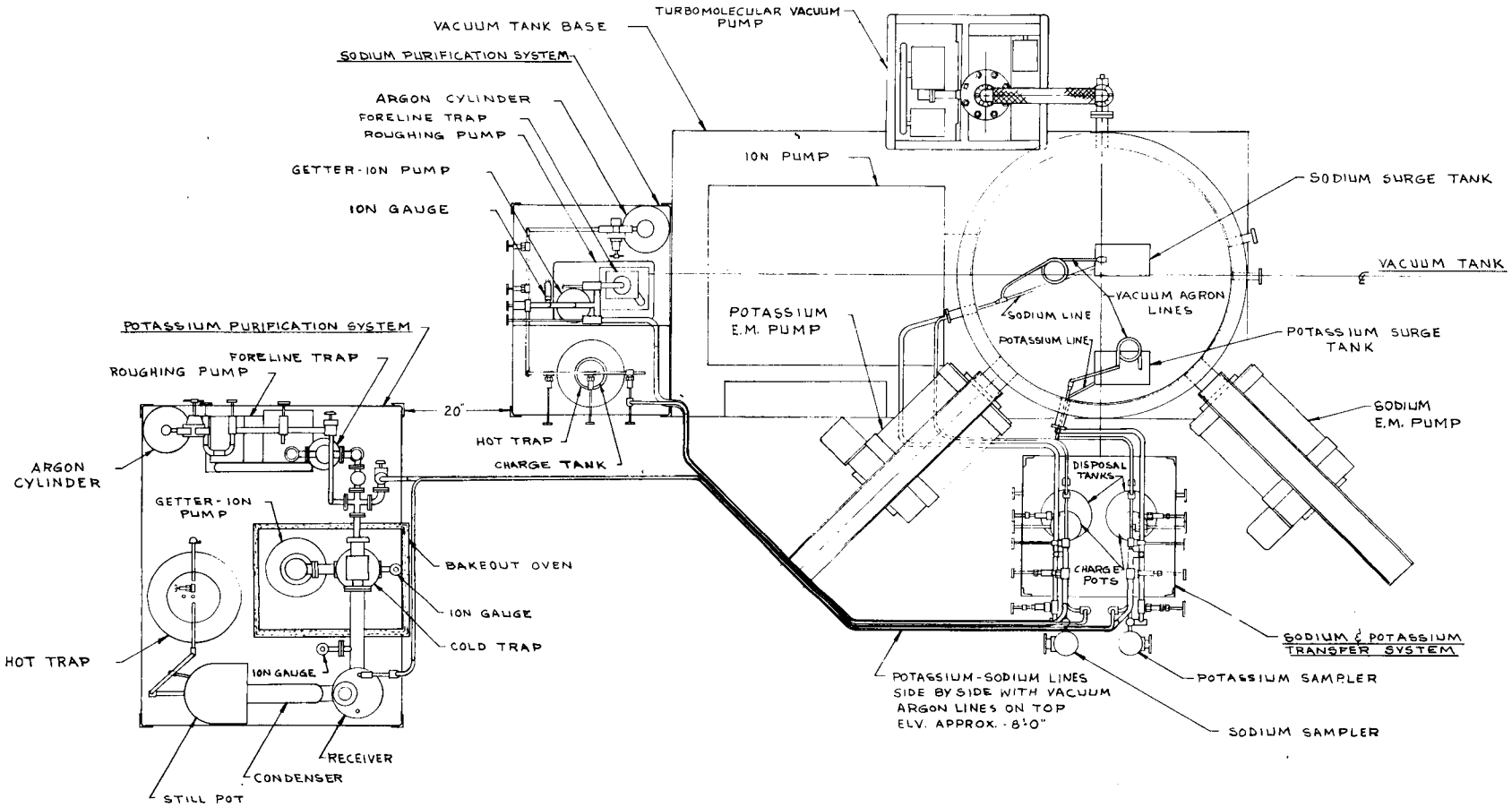

Figure 74. Plan View Showing Spatial Arrangement and Interconnecting Lines Between Purification Systems, Transfer Systems, and Loop.

2. An overtemperature thermocouple that turns off the heater power supply if the loop temperature exceeds the control temperature by 200°F;
3. An overtemperature thermocouple that turns off the EM pump, preheater, and heater power supply if the stator windings of the EM pump exceed 300°F;
4. An explosive valve argon flooding system which is activated by the getter-ion pump current if the pump current exceeds a valve equivalent to a pressure of 4×10^{-6} torr; and
5. A relay in the ionization gauge control which shuts off the loop heater power and EM pump if the pressure rises above 1.5×10^{-7} torr.

After the safety circuits were checked and reset to their proper set points, the EM pump, preheater, and heater power supplies were checked out. The only major problem encountered in the equipment checkout was in the failure of the electrical power supply for the potassium pump. A capacitor used to improve the power factor of the highly inductive load of the pump was defective and caused overheating and arcing in the motor-driven autotransformer used to control the electrical power to the pump. Replacement parts were installed and the checkout was resumed.

D. CALIBRATION OF LOOP INSTRUMENTATION

1. Calibration of the Pressure Transducers. Calibration of the potassium circuit pressure sensors, which had been originally calibrated before installation with inert gas, was repeated with the loop at 500°F and the chamber on bakeout using a calibrated pressure gauge[(a)] as the standard. Corrections for the liquid potassium heads were made for all pressure sensors according to their elevation above the surge tank. All pressure sensors showed good linearity and excellent repeatability.

The calibration results for slack diaphragm pressure transducer which measures the pump outlet pressure are shown in Figure 75 and are typical of the results obtained for the other three slack diaphragm transducers.

(a) Wallace and Tiernan, Model No. FW 145.

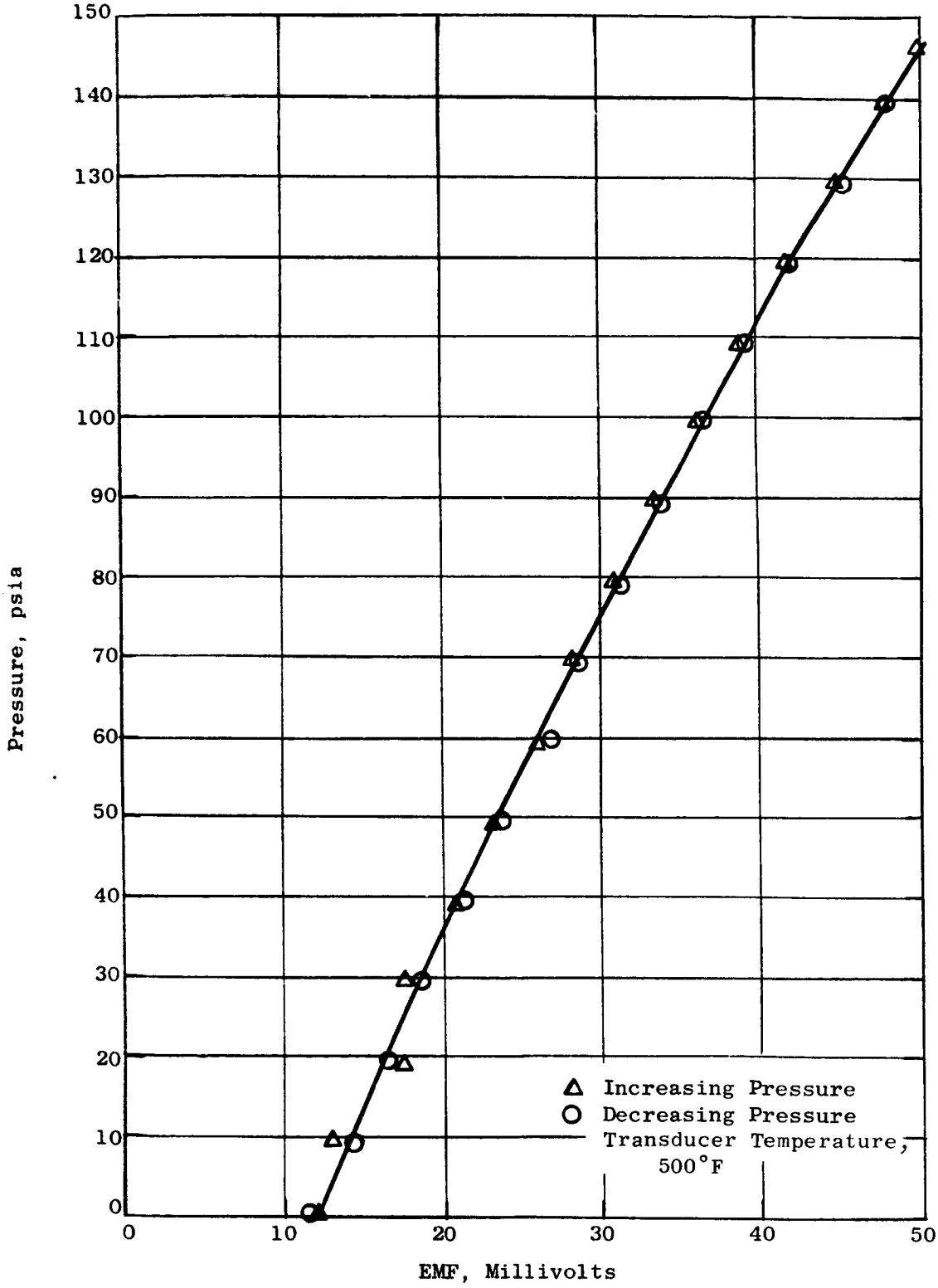

Figure 75. Calibration of Slack Diaphragm Pressure Transducer (No. 1) Located at the Potassium Pump Outlet.

The calibration of the stressed diaphragm pressure transducer with potassium prior to test startup is shown in Figure 76. This transducer showed a 20 percent increase in millivolt output in the 0-150 psia range compared to the preinstallation room temperature calibration with argon gas. The temperature of the transducer during the liquid metal calibration was 460°F which indicates that the transducer is temperature sensitive and should be thermally aged before calibration. Thermal treatment prior to calibration might reduce the temperature sensitivity observed in this transducer.

2. Thermocouple Calibration. The primary loop thermocouples were checked by operating the sodium circuit at near isothermal conditions and comparing the indicated temperature of each thermocouple with the temperatures of adjacent thermocouples. A near isothermal condition in the primary circuit was achieved by operating at a high sodium flow rate (2.5 gpm) with the potassium loop empty. The calibration was also useful in computing heat balances in subsequent loop operations because the temperature drop of the sodium during the calibration run can be equated to the heat loss of the boiler. The temperature distribution as a function of boiler length at the 1630°F calibration run is shown in Figure 77. A temperature drop of six degrees was noted from the sodium entrance to sodium exit region (220 inches of boiler length), and the temperature spread among seven thermocouples in the plug section of the boiler (12-inch length) was less than two degrees.

During this calibration of primary circuit thermocouples, the chamber pressure rose from 7.2×10^{-7} torr (sodium circuit temperature, 1200°F) to 1.2×10^{-6} torr (sodium circuit temperature, 1630°F) due to outgassing of the system. Thermocouple calibration runs at higher temperatures than those cited above were not deemed advisable at this time in order to avoid possible contamination of the loop components resulting from outgassing of the system.

3. Flowmeter Calibration. The primary and secondary loop flowmeters were calibrated by comparing the indicated flow based on the theoretical equation[35] with the flow rate obtained by an energy balance across the

(35) Affel, R. G., Burger, G. H., and Pearce, C. L., Calibration and Testing of 2- and 3 1/2-Inch Magnetic Flowmeters for High-Temperature NaK Service, Oak Ridge National Laboratory, ORNL-2793, p. 16.

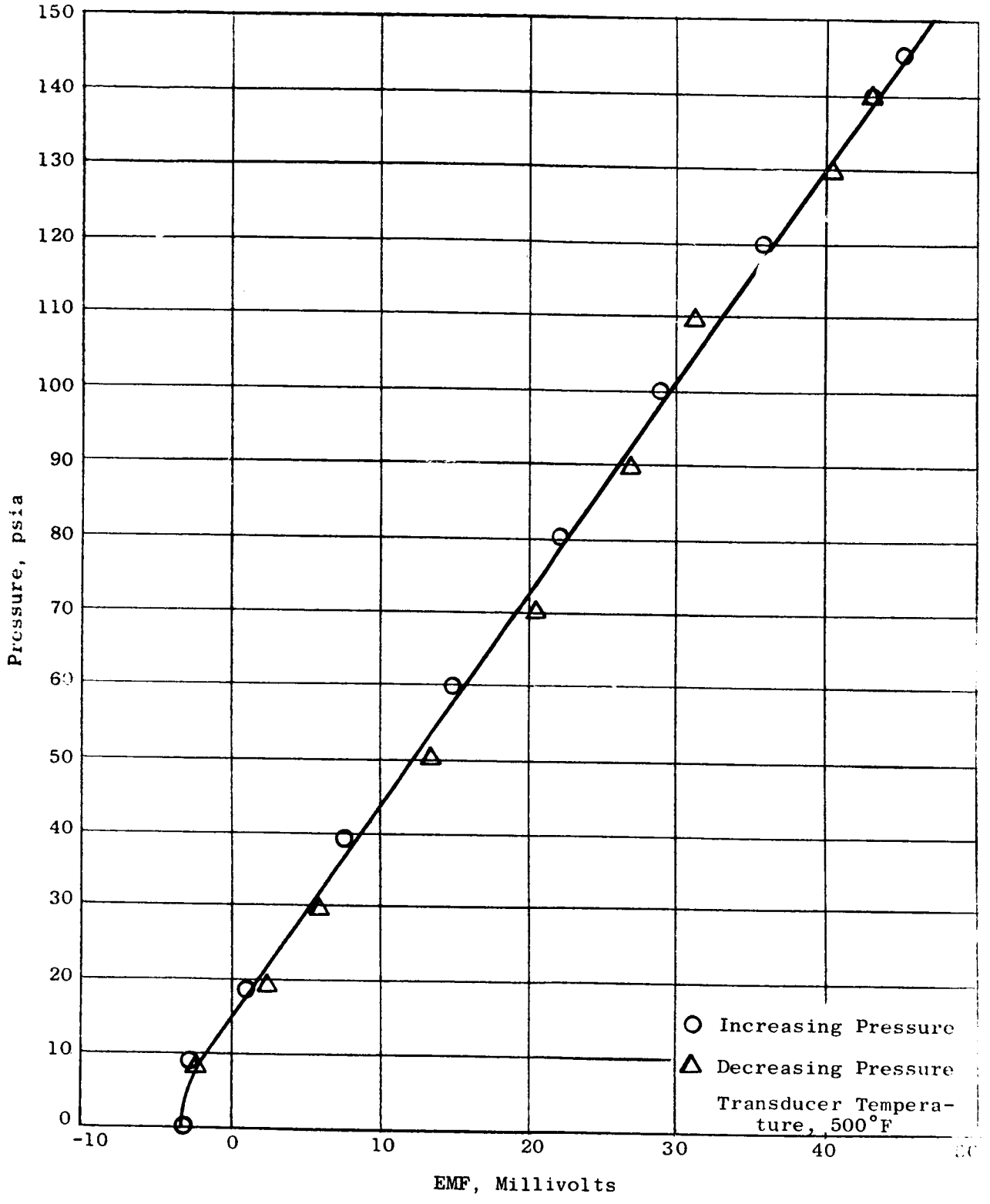

Figure 76. Calibration of Fast Response Stressed Diaphragm Pressure Transducer Located at the Metering Valve Outlet.

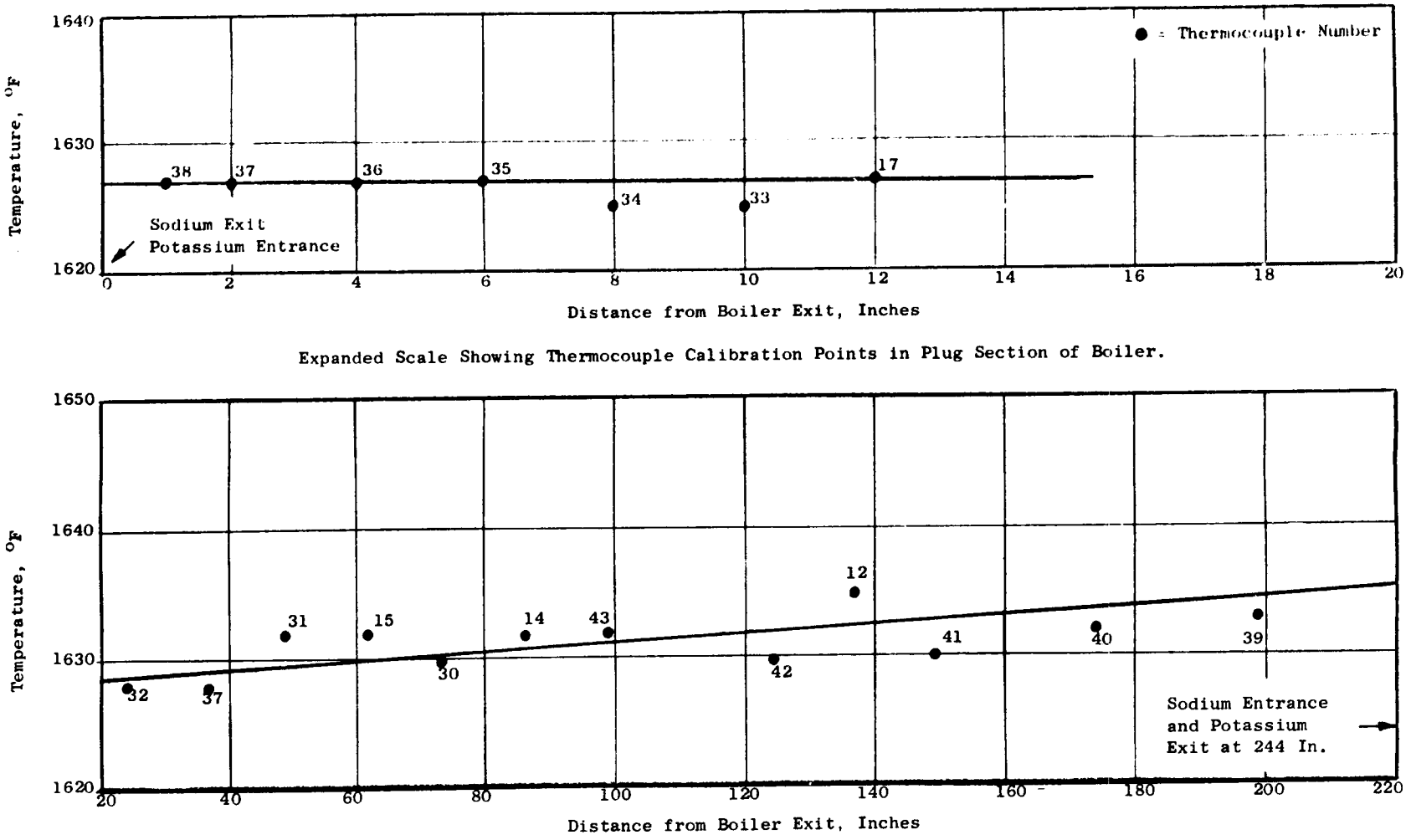

Figure 77. Results Obtained During Calibration of W-3Re/W-25Re Thermocouples Located in the Boiler Section of the Prototype Corrosion Loop. Calibration Test Conducted with a Sodium Flow of 2.5 gpm in the Primary Circuit and no Potassium in the Secondary Circuit.

preheater and heater during all liquid operation. The results of these tests are shown in Figures 78 and 79. The indicated primary flow rate is 37 percent lower than the flow rate calculated from the energy balance; the secondary flow rate is 32 percent lower. This discrepancy in flow rates has also been observed in heat transfer tests[36] where the indicated flow rate was as much as 33 percent lower. The discrepancy between the actual and indicated flow rate is not apparent at this time although it may be due to a larger shunting effect of the tube wall on the developed signal than has been assumed in development of the flowmeter equation.[35] The loop tubing is 0.25-inch ID with 0.065-inch walls with a ratio of outer diameter to inner diameter of 1.5:1, which is considerably larger than the diameter ratios previously used (1.12:1) by Affel, et al. in the referenced report.

4. Calibration of the Practical Pressure Gas Analyzer. The partial pressure gas analyzer, which was described earlier in Section V, Test Equipment, was initially calibrated before the loop was installed in the vacuum chamber. At this time base pressures in the 10^{-10} torr range could be obtained, and this low pressure facilitated the achievement of low background pressures of the various gases when the calibrating gases were admitted to the chamber. After the loop was installed in the chamber, there was no opportunity to perform an accurate calibration of the analyzer because of the relatively high pressure (10^{-7} torr range) within the chamber. Calibration factors, based on the assumption that the relative sensitivity from one gas to another was the same as for the initial calibration, were obtained during pretest operation and at various times during loop operation. The procedures and techniques used in calibrating the analyzer initially and in determining calibration factors during test operation are described in detail in Appendix G, Calibration of the Partial Pressure Analyzer, of this report.

5. Control Console Instrumentation Calibration. The control console, showing most of the instruments used to monitor loop test conditions, is

(36) Alkali Metals Boiling and Condensing Investigations, Quarterly Progress Report No. 11, NASA Contract NAS 3-2528, NASA-CR-54405, April 23, 1965, p. 41.

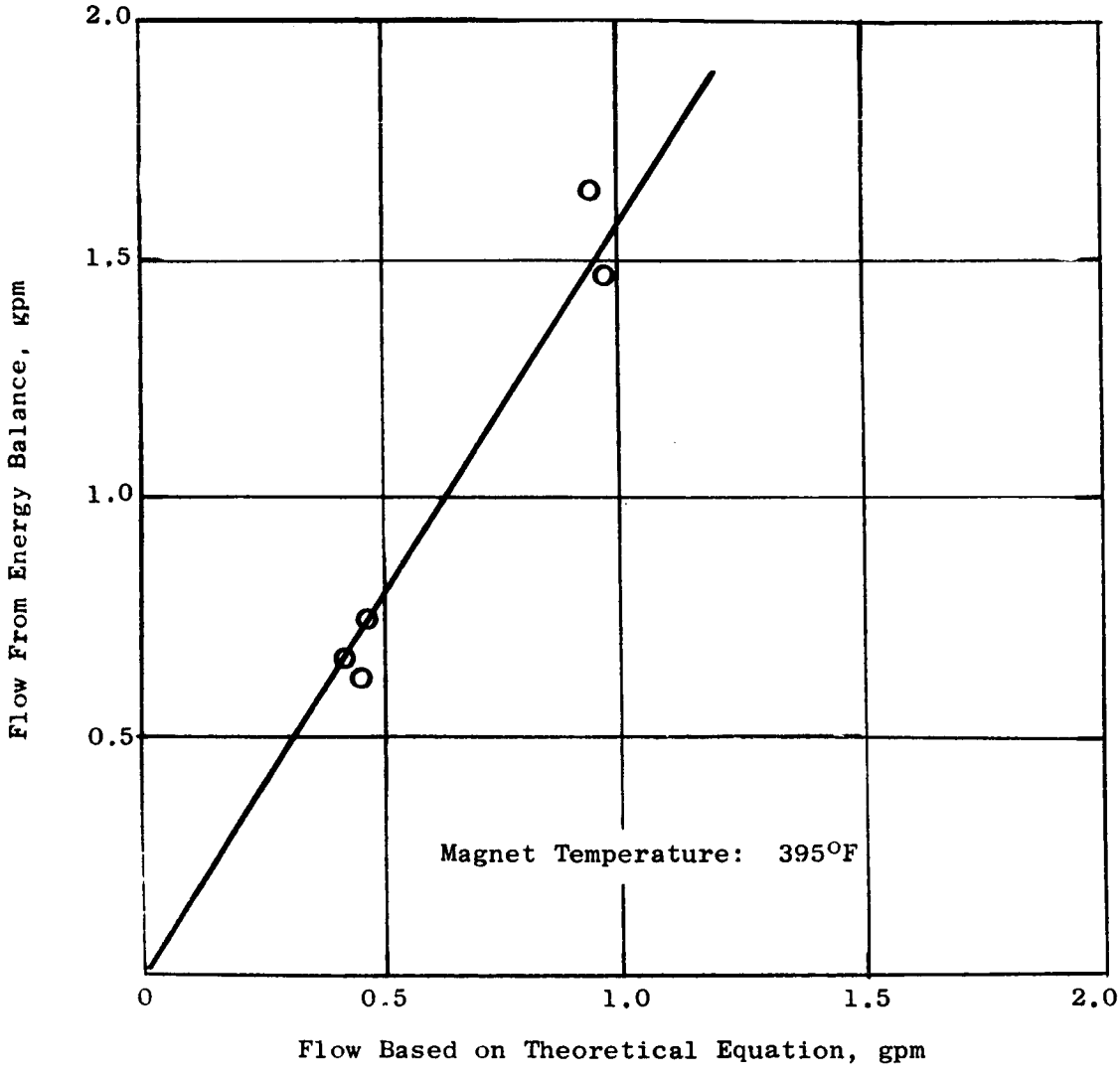

Figure 78. Theoretical Sodium Flow vs Flow Determined by Energy Balance Across Sodium Heater.

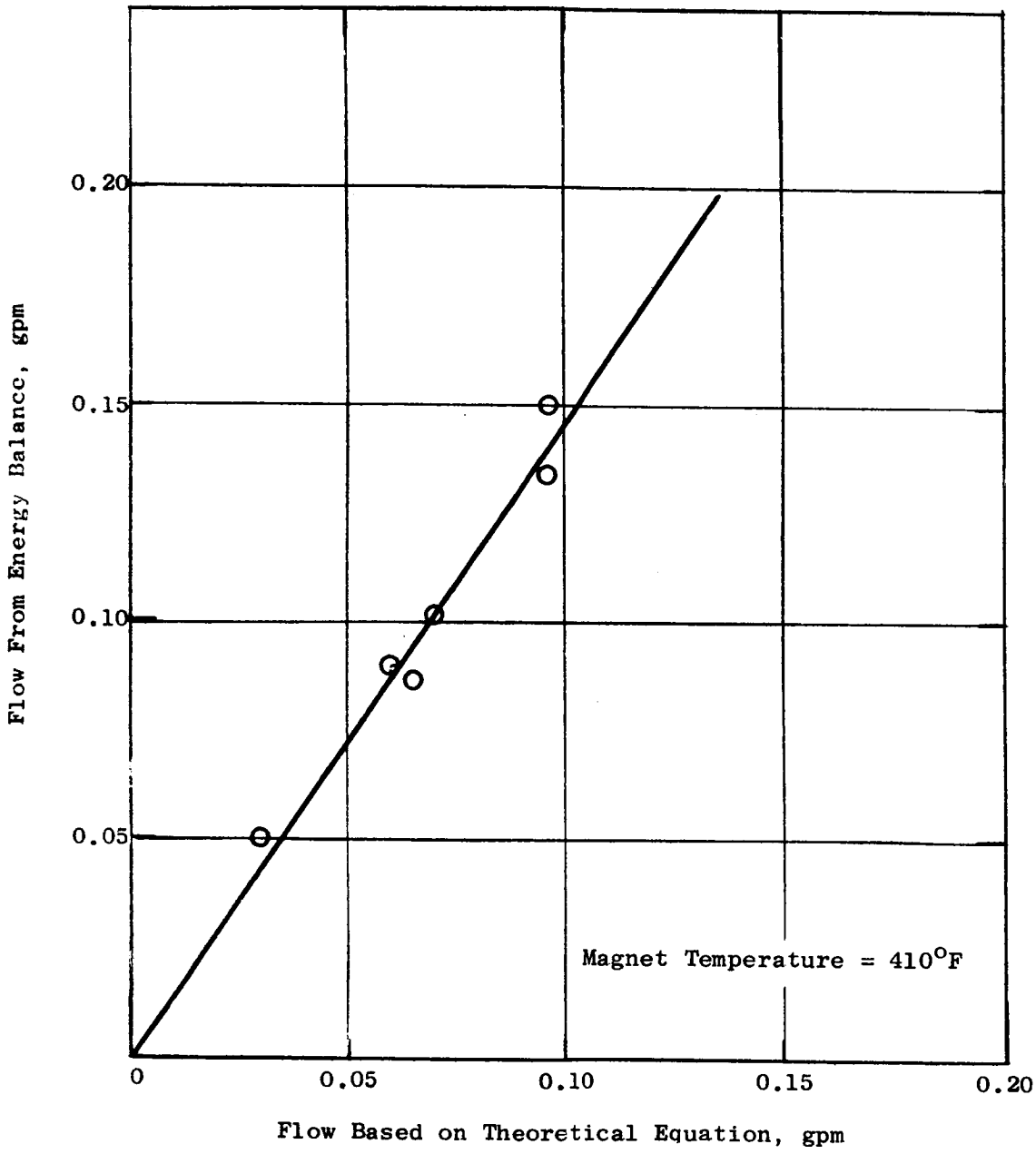

Figure 79. Theoretical Potassium Flow vs Flow Determined by Energy Balance Across Potassium Preheater.

shown in Figure 80. All instruments including pressure gauges, volt meters, watt meters, and recorders were calibrated prior to the start of the test as part of the overall quality control program of G. E. - SPPS.

(a) 2-Channel Sanborn Recorder
(b) K Preheater Control
(c) Na Pump Control and Flow Recorder
(d) Heater Overtemperature Control
(e) EM Pump Winding Temperatures
(f) Auxiliary Heater Controls
(g) Na Heater Control and Recorder
(h) K Pump Control and Flow Recorder
(i) Vacuum and Argon Pressure Gauges and Manifold
(j) K Pressures and Junction Block Temperatures
(k) Na Circuit Temperatures
(l) K Circuit Temperatures

Figure 80. Control Console of the Cb-1Zr Corrosion Test Loop. (Orig. C65080601)

IX. TEST LOOP STARTUP

The boiling and condensing operation of the Cb-1Zr Rankine System Corrosion Test Loop was started on July 29, 1965. The detailed startup procedure used is described in Appendix I, Test Startup Procedure. The test loop had completed several weeks of outgassing with all liquid operation and was at the following test conditions at the start of the boiling and condensing operation:

Vacuum Chamber Pressure	-	1.8×10^{-7} torr
Sodium Flow Rate	-	3 gpm
Potassium Flow Rate	-	0.3 gpm
Sodium Temperature	-	1000°-1050°F
Potassium Temperature	-	270°-1000°F

A. POTASSIUM INVENTORY CONTROL

The potassium loop was dumped by evacuating the surge tank and gravity draining the potassium into the surge tank. The metering valve was closed, and the surge tank was pressurized with argon to 2.0 psia, forcing the liquid potassium out of the surge tank into the loop to the top of the condenser. The rise of the potassium in the loop was easily followed by noting changes in the temperature of the condenser thermocouples.

The potassium fill procedure was designed to minimize the amount of liquid potassium carryover from the boiler to the test nozzles and specimens of the turbine simulator during the initial startup and associated periods of loop instability. The test startup plan called for a specific potassium inventory which would be pressurized into the secondary loop from the surge tank and then separated from the surplus potassium in the surge tank by means of the isolation valve. An alternate method of controlling the potassium inventory in the loop which was considered was adjustment of the argon pressure in the surge tank. The initial plan was to use the "isolation" approach because in some systems communication of a two-phase loop system with its associated surge tank has resulted in repetitive pressure, temperature, and liquid level oscillations in the system. It was demonstrated in

the Cb-1Zr High-Temperature Heat Transfer Facility[37] that oscillations of this type could be eliminated by closing the isolation valve and re-established by opening the isolation valve.

The potassium inventory selected for the loop was an amount sufficient to establish one liquid-vapor interface near the entrance to the boiler plug section and the other interface 12 to 18 inches from the condenser exit. During the filling operation, the potassium was pressurized into the portion of the loop between the metering valve and the top of the condenser, and the proper inventory was determined by observing temperature changes as the potassium level rose in the condenser. Pressure sensing tests conducted after closing the isolation valve indicated that there was some leakage across the seat. Rather than risk overtorquing the valve, the decision was made to control the potassium inventory by adjustment of the surge tank pressure. The valve was torqued to a maximum of approximately five ft-lbs to dampen any oscillations which might arise during loop operation. This method of controlling the loop inventory has proven to be a completely satisfactory method of operation as will be indicated in more detail later in this report.

B. START OF BOILING OPERATION

Boiling operation was started by first increasing the temperature of the sodium circulating in the primary loop to 1300°F. The secondary EM pump was then turned on, and a low flow of potassium was supplied to the boiler portion of the loop. The flow rate and sodium temperature were gradually increased and then allowed to stabilize at a potassium vapor temperature of 1300°F and a sodium boiler inlet temperature of 1550°F. The outgassing rate increased considerably at this stage, and the titanium sublimation pumps were used to assist the getter-ion vacuum pumps in maintaining a 10^{-7} torr pressure level in the vacuum chamber.

During the next 96 hours, the loop temperature and potassium flow

(37) Bond, J. A. and Converse, G. L., Vaporization of High Temperature Potassium in Forced Convection at Temperatures from 1800°F to 2100°F. NASA CR-843, July 1967, p. 113.

rate were gradually increased to the design operation condition. The rate of increase of the test conditions was limited by the outgassing of the loop components. The titanium sublimation pumps were operated continuously during this period to maintain the pressure in the 10^{-7} torr range. The total chamber pressure and the partial pressure of the principal residual gases during this period when the test conditions were being approached are shown for the -80 to 0 test-hour period in Figure 81. Nitrogen/carbon monoxide (m/e-28),[a] argon (m/e-40), and hydrogen (m/e-2) were the principal species present during this period. A total of approximately 600 hours of chamber bakeout preceded the initiation of test operation. Additional discussion of the total pressures of the individual species of the test chamber environment is covered in Section X, Test Loop Operation.

Since significant adjustments were required to reach the design operating conditions, the interdependence of the flow rate, power level, and pressure was evident during this period. The ability of the loop to return to a stable operating condition after each adjustment clearly demonstrated the intrinsic stability of the Cb-1Zr Corrosion Test Loop configuration.

C. STABILITY OF LOOP OPERATION DURING TEST STARTUP

Low frequency fluctuations of the order of 2 psi or less were encountered during certain portions of the startup period. Heating the vapor nucleator to a temperature 100° to 150°F above the boiler inlet temperature did not eliminate these minor fluctuations.

At the time, these small oscillations were thought to be characteristic of this particular loop system and not due to the common type of instability resulting from superheated liquid flashing into vapor due to a lack of nucleating sites, as in pool boiling or capsule testing where the vapor nucleator has proven to be extremely useful.[38]

(a) m e (mass/charge).

(38) Harrison, R. W., The Compatibility of Biaxially Stressed D-43 Alloy with Refluxing Potassium, NASA CR-807, June 1967, p. 7.

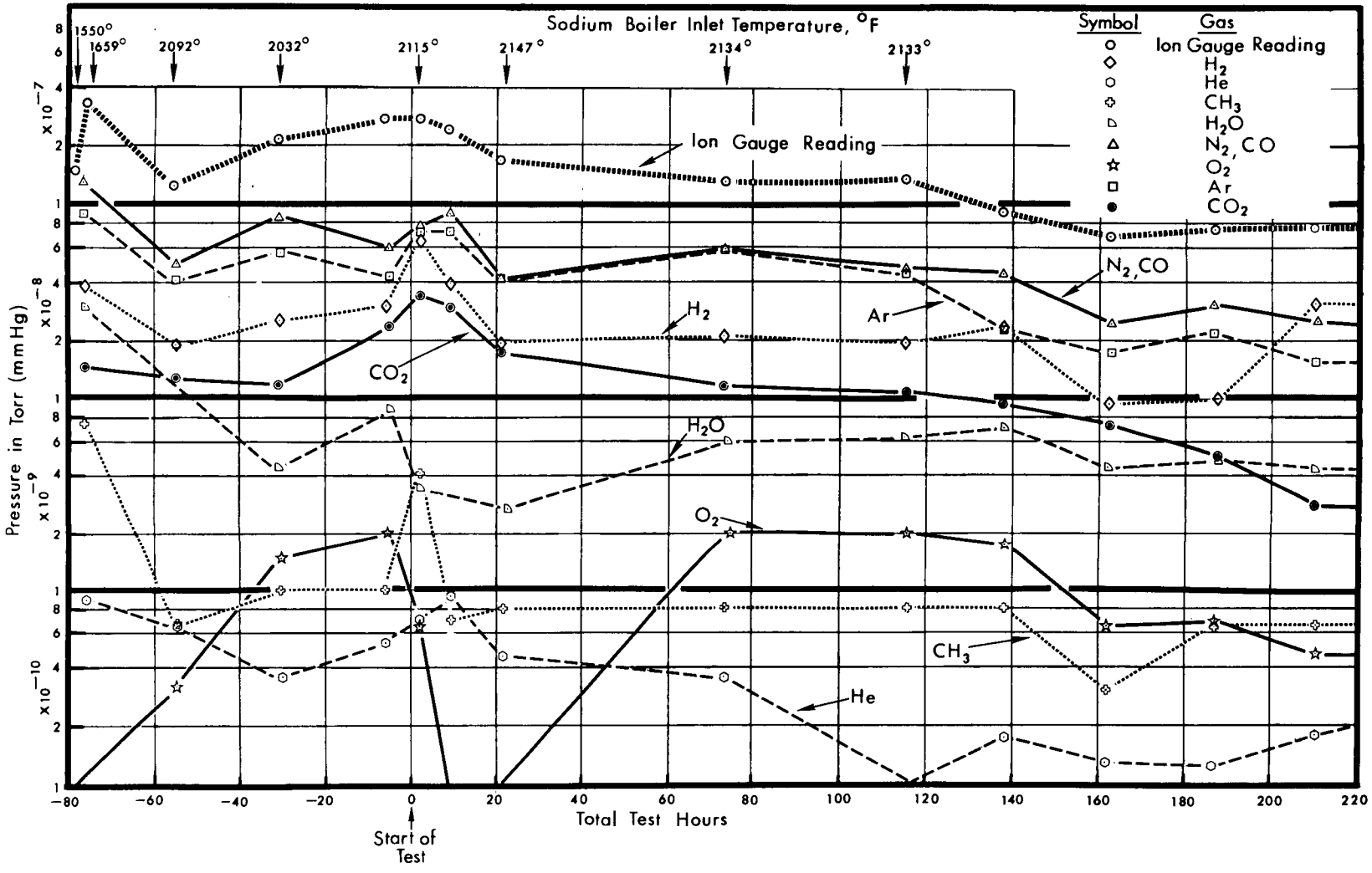

Figure 81. Total Pressure and Partial Pressures of Various Gases During Startup and Early Operation of the Cb-1Zr Corrosion Test Loop.

Large perturbations in the flow, pressure, and temperature which were recorded during certain periods of the startup, were found to be associated with shifting of the boiling zone. The shift in boiling zone was noted by observing the change in the sodium temperature profile in the boiler. Although stable loop operation was recorded with the boiling zone in the plug, the center portion and exit region of the 240-inch-long boiler, the 12-inch-long plug section located in the potassium entrance region, appeared to be the most stable boiling location. The boiling zone could be shifted by adjusting the potassium flow rate or the power input to the sodium heater circuit. Increasing the temperature of the sodium heater with constant sodium flow would drive the boiling zone towards the boiler plug; increasing the potassium flow shifted the boiling zone away from the plug toward the exit. Boiling at the center of the boiler, although stable, was difficult to maintain for long periods of time. Typical changes in the temperature of the sodium heater fluid in the boiler which indicate the shifting in the potassium boiling zone referred to above are illustrated in Figure 82. The temperature differences between the three thermocouples shown indicate the relative amount of boiling of the potassium between these thermocouple locations. The lower portion of the graph illustrates the transition from the condition of boiling beyond the plug section (40°F drop in plug) to boiling in the plug section (140°F drop in plug). This transition was triggered by a slight decrease in potassium flow. The top portion of the graph in Figure 82 illustrates the movement of the boiling zone partially out of the plug section of the boiler. This movement of the boiling zone was caused by slight increases in the potassium flow rate. Slight increases in the sodium boiler inlet temperature or in the sodium flow rate in all cases caused rapid movement of the boiling region back to the plug section.

As mentioned earlier, each movement of the potassium boiling zone in the boiler was accompanied by substantial oscillations in the pressures, temperatures, and flow in the potassium circuit. A typical example of the fluctuations in boiler outlet pressure which accompany movement of the boiling zone is given in Figure 83. At approximately 0040 hours, as

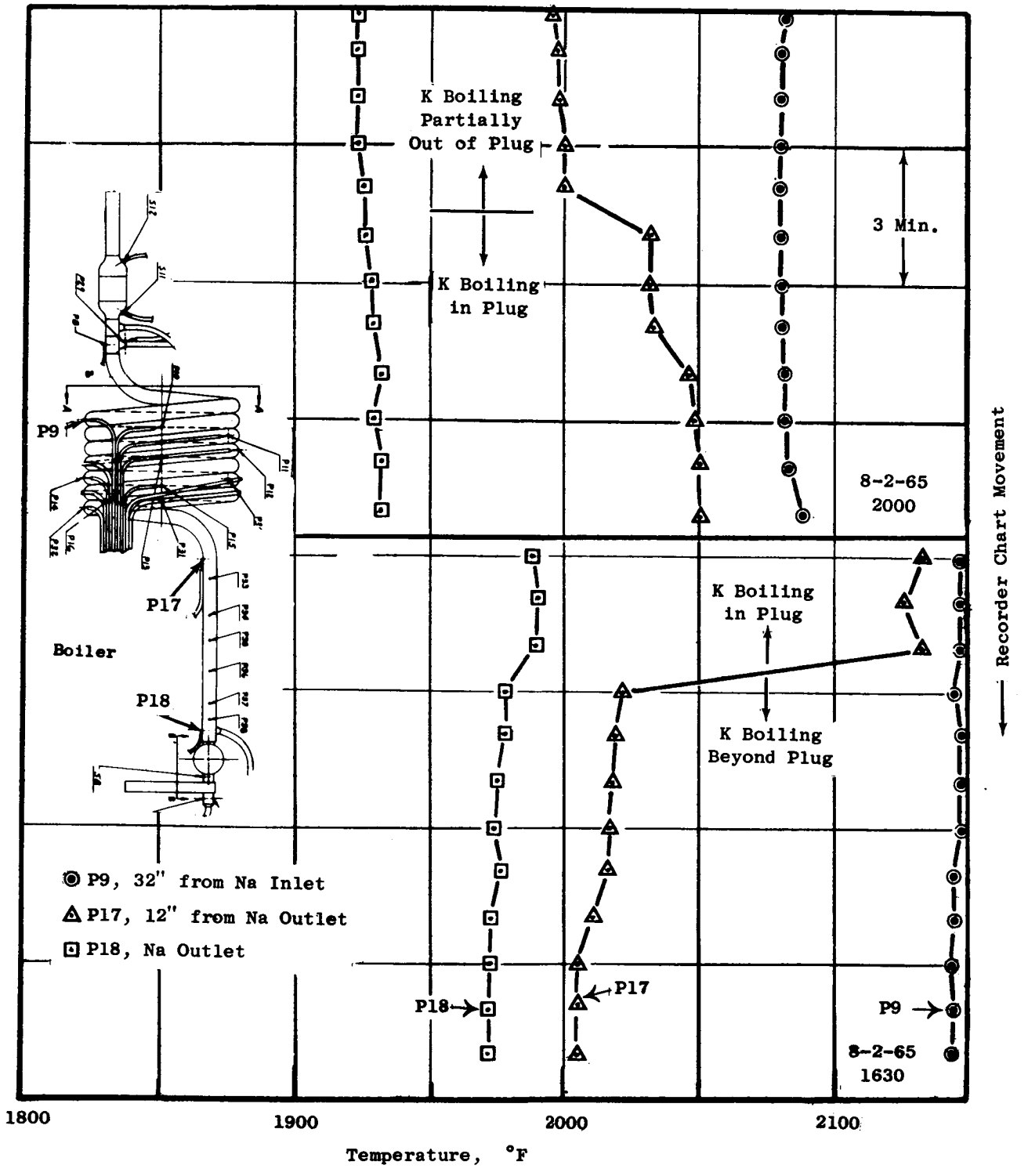

Figure 82. Sodium Temperature at Various Locations in the Boiler Illustrating Movement of the Potassium Boiling Region During Test Startup.

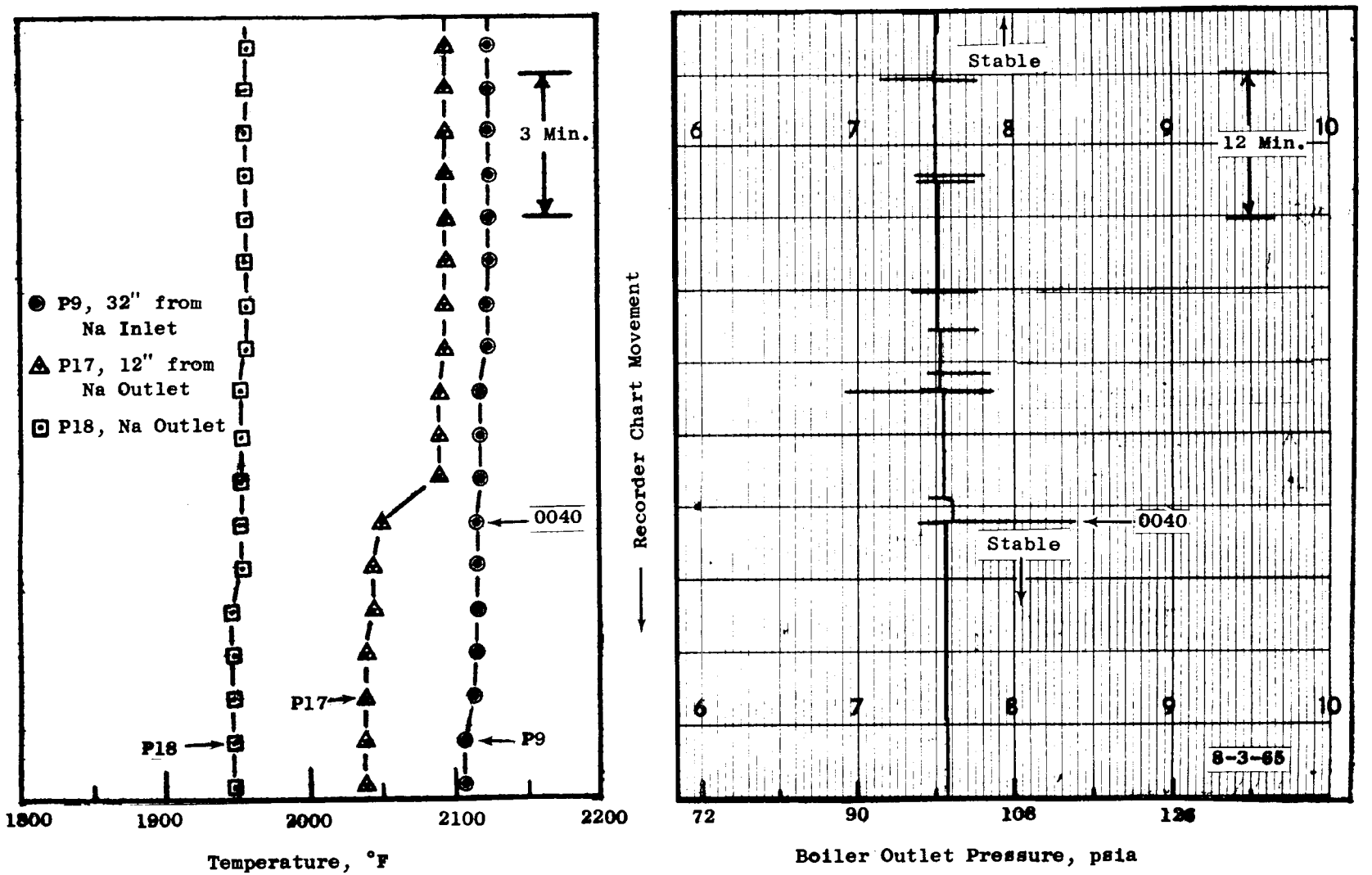

Figure 83. Boiler Temperature Changes and Boiler Outlet Pressure Fluctuation Associated with Movement of the Potassium Boiling Region.

indicated in the plots, a pressure fluctuation of approximately 20 psi was accompanied by an increase in the temperature difference between thermocouples P18 and P17 which signified movement of the boiling zone into the plug region. As may be noted in the pressure chart, fluctuations continued for approximately 35 minutes after the initial oscillation until the loop reached a steady state condition. Subsequent operation was completely stable with no pressure, temperature, or flow oscillations.

The design test conditions were reached at 1500 hours on August 2, 1965. As indicated in Figure 81, the temperature of the sodium at the boiler inlet was 2115°F and the vacuum chamber pressure was 3×10^{-7} torr.

X. TEST LOOP OPERATIONS

The pretest activities which preceded the attainment of the operating conditions required for the Cb-1Zr Corrosion Test Loop were described in the previous section. A detailed discussion of the total pressure and partial pressure measurements made during the 5000-hour endurance test will be presented in Part C of this section following the presentation of the other aspects of loop operation.

A. LOOP OPERATION DURING THE 5000-HOUR TEST

The logging of test time began at 1500 August 2, 1965, and the test conditions in the two-phase potassium circuit after steady state operation was reached are given below:

Boiling Temperature	-	1900°F
Superheat Temperature	-	2000°F
Condensing Temperature	-	1400°F
Subcooling Temperature	-	890°F
Mass Flow Rate	-	40 lbs/hr

During the entire test run, the loop was extremely stable with no significant fluctuations in pressure, temperature, or flow except during the test interruptions or incidents which will be described. The steady state operating conditions given in Figure 84 were obtained just before the termination of the 5000-hour test and are typical of the loop operating conditions observed during the entire 5000 hours of operation as no significant change or drift of any of the temperatures or flow rate in either the potassium or sodium circuit was detected except during the incidents described below.

A complete set of test data, of which that shown in Figure 84 was only a portion, was compiled daily during routine operation and more frequently during test startup or other periods when test conditions were changing.

1. Vapor Lock in the Potassium Pump. The first interruption in the steady state testing occurred after only 43 hours of operation when the potassium pump vapor locked, requiring that the loop be shut down. The

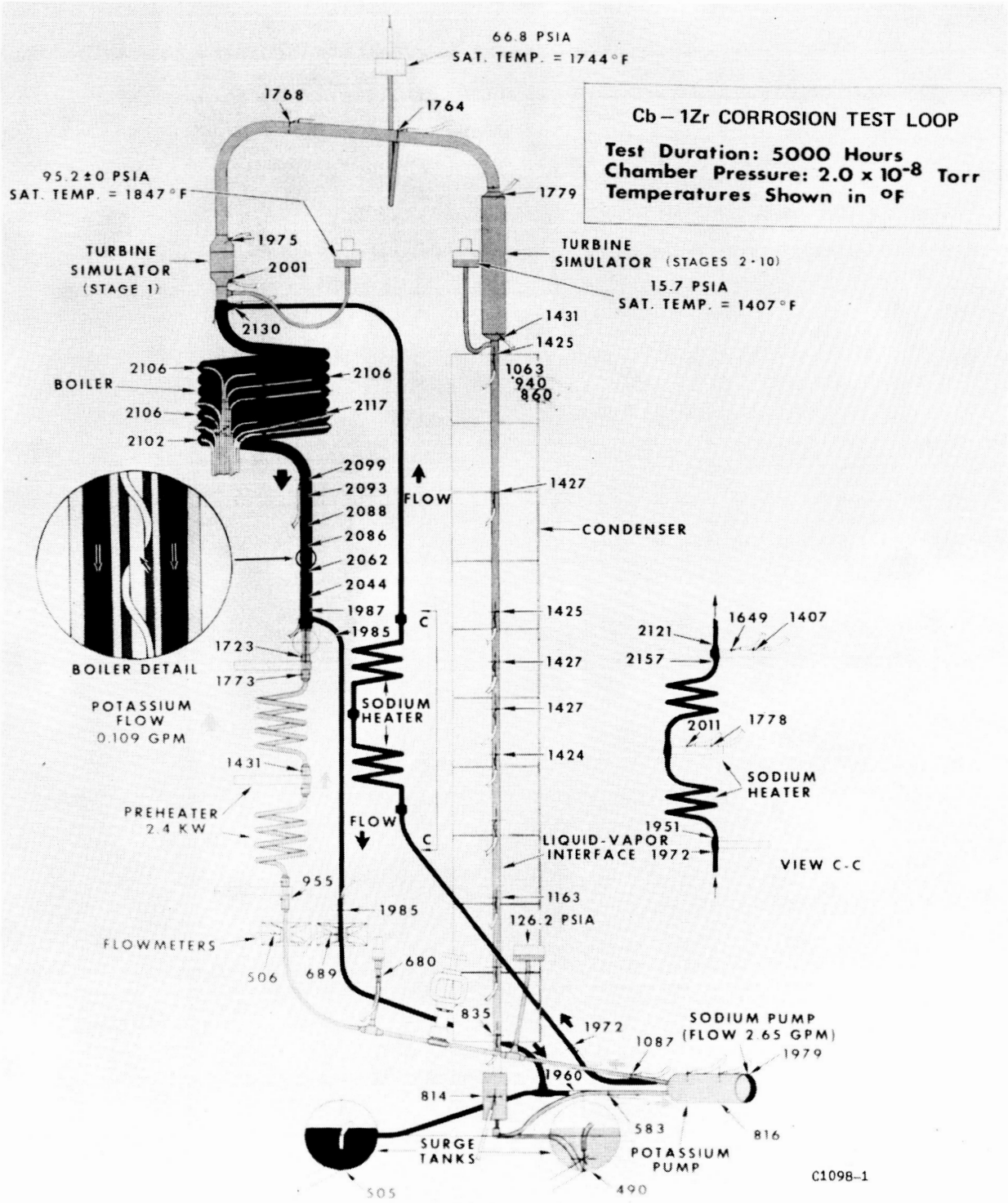

Figure 84. Cb-1Zr Corrosion Test Loop Operating Conditions. (C66061460)

vapor lock occurred following a series of small potassium pump power increases to boost the boiling temperature by increasing the boiler inlet pressure; the potassium flow dropped to zero within 30 seconds followed by severe flow oscillations which continued for eight minutes. All power to the loop was immediately turned off, and examination of the instrument records indicated that the potassium pump had vapor locked. The loop was restarted after the potassium temperature had dropped a few hundred degrees and the condenser pressure increased to 20 psia. The loop was back at the design operating conditions in less than one hour.

A description of the flow adjustments and their effect on the pump and boiler outlet temperature just prior to vapor locking the pump is given in Table XIII. The temperature fluctuations of the secondary loop during this period are shown in Figure 85. The fluctuations in the boiler outlet pressure in the potassium circuit when the vapor lock occurred and during the period when the loop was being restored to the test conditions are shown in Figure 86. Analysis of the loop performance following the vapor lock is summarized below.

Time Seconds	
0-60	a) Vapor lock in the pump; potassium flow dropped from 0.10 gpm to 0 gpm in 30 seconds.
	b) Temperature of the potassium vapor region thermocouples in the condenser dropped sharply (1410° to 1190°F in 60 seconds).
	c) Potassium pump outlet temperature dropped from 1410° to 1250°F in 60 seconds.
	d) Some of the potassium in the loop was forced into the surge tank.
60-120	a) Potassium temperature at the boiler inlet rose from 1795°, where it had held constant during the 0-60-second period, to 1930°F.
	b) Potassium pump outlet temperature rose from 1260° to 1320°F after falling rapidly during the 0-60-second period.
	c) Potassium temperature in subcooler reservoir rose rapidly from 740° to 850°F. Meanwhile, the temperatures in the condenser,

TABLE XIII

LOSS OF POTASSIUM FLOW RESULTING FROM POTASSIUM TEMPERATURE RISE IN THE PUMP AND RESULTANT VAPOR LOCKING OF THE EM PUMP

Time 8-4-65	Temperature, °F			Remarks[a]
	Condenser	K Pump Outlet	Boiler Outlet	
0300	1393	1260	1950	K flow 0.100 gpm - K pump power (8.7 a/255 V) - pump outlet pressure - 153 psia
0815	1400	1260	1975	K pump power increased - pump outlet pressure approximately 154 psia
0830	1400	1275	1975	K pump power increased - pump outlet pressure approximately 156 psia
0845	1405	1310	1980	K pump power increased - pump outlet pressure approximately 157 psia
0920	1410	1330	1985	K pump power increased - pump outlet pressure approximately 158 psia
1015	1410	1370	1985	K pump power increased - pump outlet pressure approximately 160 psia
1030	1408	1376	1983	K flow 0.100 gpm - K pump power (10 a/303 V)-160 psia
1115	1410	1405	1990	No change, pump outlet pressure - 160 psia
1130	K flow dropped from 0.10 gpm to 0 in 30 seconds and fluctuated between 0.05 and 0 gpm for approximately 8 minutes			

(a) No metering valve adjustments were made during this period.

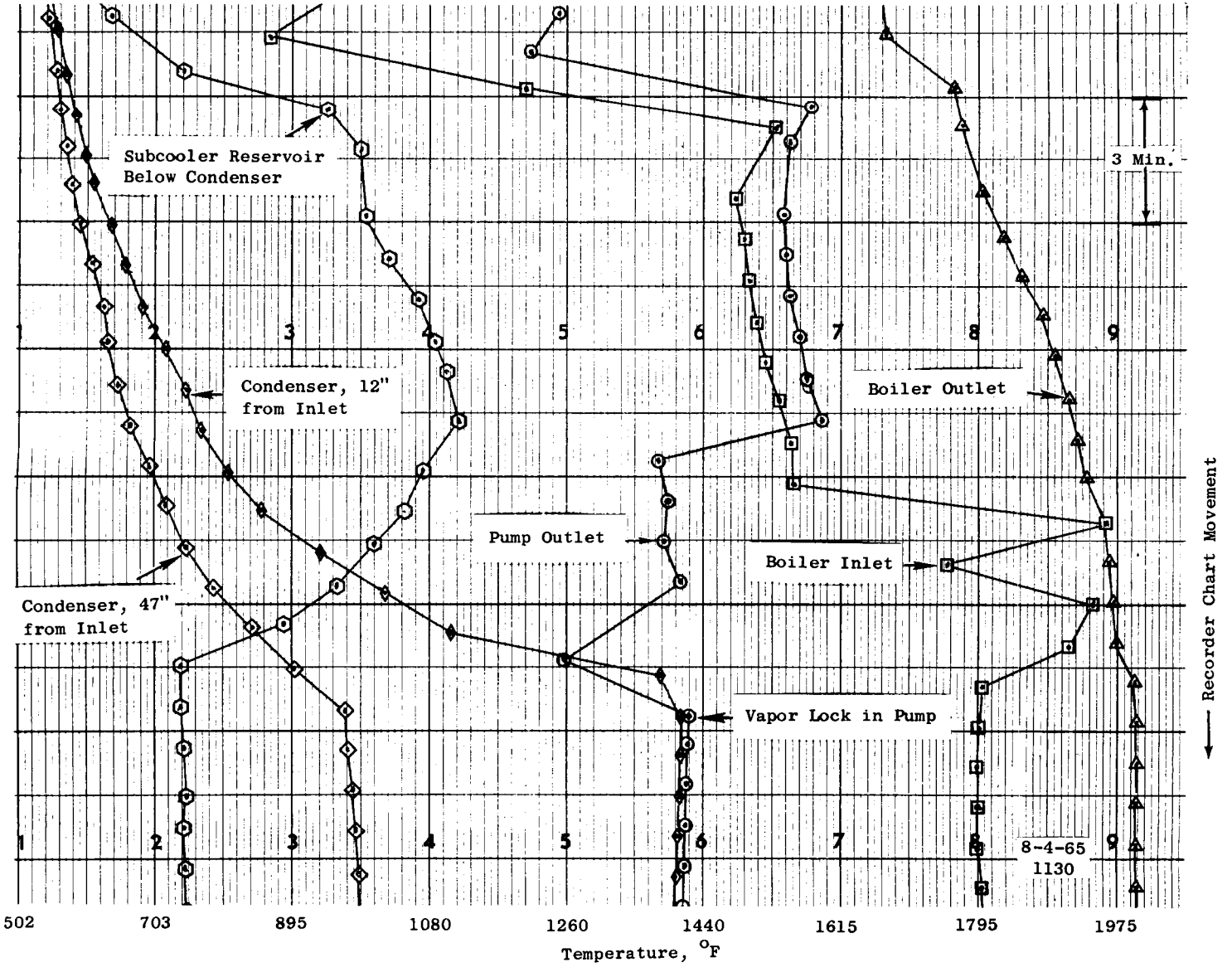

Figure 85. Temperature Fluctuations in Potassium Circuit During Period When Flow Was Lost Due to Vapor Locking in the Pump.

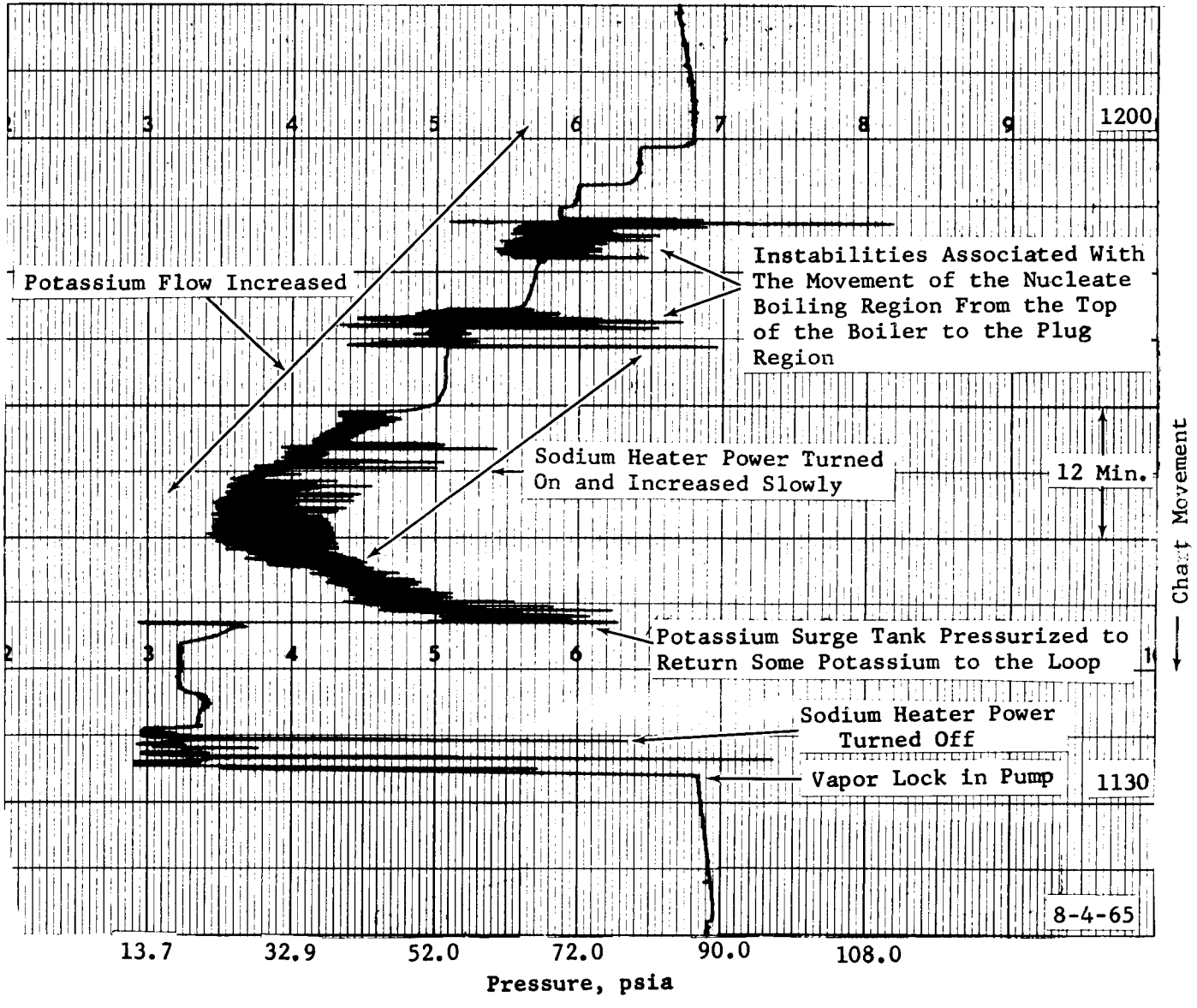

Figure 86. Fluctuations in Boiler Outlet Pressure Following Vapor Lock in Potassium Pump.

both in the liquid region and vapor region, showed rapid decreases.

d) Potassium surge temperature rose.

The observations described above indicate that the increase in the EM power resulted in sufficient increases in the potassium temperature to cause a vapor lock at the pump inlet. This loss of potassium flow caused the following things to occur:

1) Potassium was forced out of the pump by the increasing vapor pressure in the pump which caused subcooled liquid to flow back into the condenser to near the top of the condenser. This happened within 30 seconds of first indication of loss of potassium flow.
2) Potassium boiler inlet temperature rose rapidly starting 60 seconds after loss of flow resulting from reverse flow from boiler due both to the loss of pump head and the rapid rise in potassium temperature and pressure in the boiler associated with this low pump head condition.
3) Dumping of the potassium loop inventory into the surge tank.

It was not apparent at first during this incident that the loss of potassium flow was due to a vapor locked pump since the pump inlet temperature was only 565°F, or more than 800°F below the saturation temperature. However, the pump outlet temperature was 1405°F indicating a 840°F temperature rise in the potassium in passing through the pump. The pump outlet pressure was approximately 160 psia, and the pressure drop across the metering valve was approximately 60 psi at this time. The inlet and the outlet of the pump are separated by a thin-wall cyclinder within the pump; and due to the relatively low flow in the potassium circuit, sufficient heat was transferred to the inlet side of the pump to raise the temperature of the inlet potassium above the saturation temperature. (A redesign of the potassium pump duct will be made for future test loops to eliminate this potential problem.) Having established the source of the trouble, the problem was easily eliminated by opening the metering valve slightly to reduce the pressure drop across the valve from the 60 psi previously employed to approximately 9 psi. This reduced the required pump outlet pressure which permitted a reduction in power to the pump and a decrease

in the potassium temperature rise across the pump. By maintaining the pump outlet pressure below 150 psia, which is more than adequate for stable loop operation, the pump outlet temperature was easily maintained at 200°F less than the condenser temperature, thus avoiding the vapor lock problem.

2. Effect of the Metering Valve on Loop Stability. The effect of the pressure drop across the metering valve on the stability of the loop is best demonstrated by the potassium flow rate and boiler exit pressure recording shown in Figure 87. During the startup and up to the time of the vapor locking of the pump described above, the metering valve was set at 20° from the fully closed position with a pressure drop across the valve of approximately 50 psi.[(a)] (Each 3° of rotation of the metering valve stem was equivalent to 0.001 inch of axial movement of the valve plug.) The loop operation was extremely stable with the valve in this position. After the pump vapor lock incident described above, the metering valve was opened from the 20° position to 65° open to permit decreasing of the pump voltage and thereby reduce the temperature rise of potassium flowing through the pump. Opening of the metering valve decreased the pressure drop across the valve to less than 4 psi. The flow became extremely unstable with high-frequency flow oscillations of ± 40 percent of the desired 0.11 gpm potassium flow rate as indicated in Figure 87. The metering valve was then closed from 65° open to 50° open which increased the pressure drop across the metering valve to 7 psi with a decrease in the flow oscillations to less than ± 2 percent of the steady state flow rate. The test was continued at these conditions for the next 96 hours. At this time, the valve was closed from 50° to 40° in two 5° adjustments which increased the pressure drop across the valve to 9 psi. As shown in the upper portion of Figure 87, this final adjustment on 8-10-65 of the metering valve eliminated fluctuations in both the potassium flow and the boiler outlet pressure. The stressed diaphragm pressure transducer, which was located between the metering valve and the preheater inlet and

(a) The pressure drop across the valve is determined by subtracting the calculated pressure drop for the boiler (16 psi) from the total pressure drop across the metering valve and boiler as measured by slack diaphragm pressure transducers.

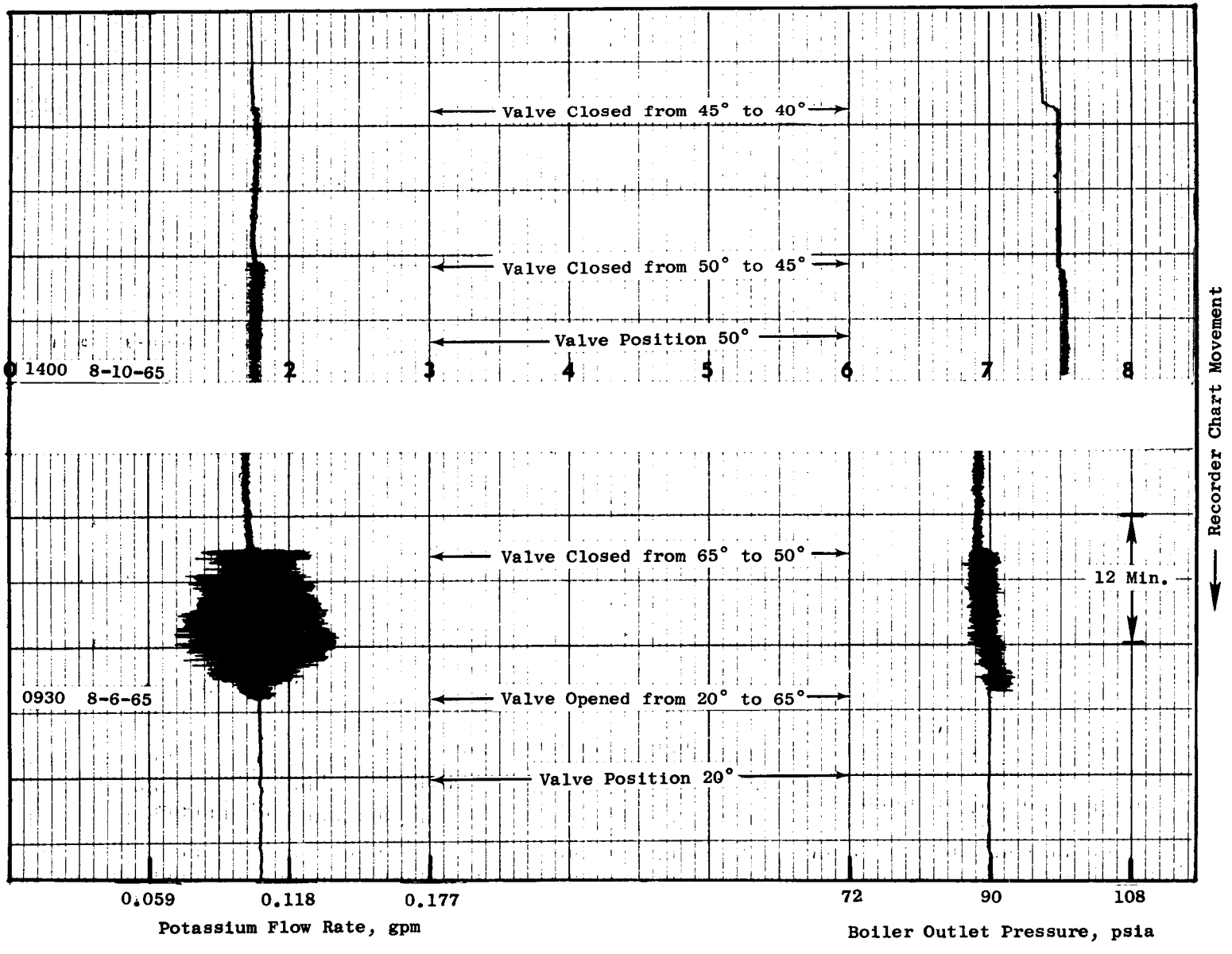

Figure 87. Effect of Metering Valve on the Potassium Flow Rate and Boiler Outlet Pressure.

was capable of sensing a 100 cps pressure oscillation, showed a pressure fluctuation of less than ± 0.3 psi with the 9 psi pressure drop across the metering valve. The metering valve adjustments[b] described above clearly indicated the marked effect of metering valve pressure drop in obtaining the remarkable stability of operation observed in the Cb-1Zr Corrosion Test Loop system.

3. Failure of Fuse in the Potassium Preheater Circuit. Loop operation continued in a stable and uneventful manner until 0500 hours on 8-19-65, when after 398 hours of test operation a fuse in the potassium preheater control circuit failed. This resulted in a complete loss of power to the preheater and a rapid drop in the temperature of the potassium at the boiler inlet. The circuit became operative with the replacement of the fuse, and no additional difficulty was encountered with this component.

The observations of loop performance during the period of unstable operation following the preheater power failure caused by the defective fuse will be presented in some detail to again illustrate the response of the loop to a major change in test conditions. In Figure 88, the temperatures of several key regions in both the sodium and the potassium circuits are shown during the period following the preheater power failure. The potassium boiler inlet temperature dropped rapidly following the preheater failure, and substantial oscillations of sodium boiler temperatures and potassium condenser temperatures were observed. The temperatures of these regions during the period following restoration of preheater power are given in Figure 89. The most substantial temperature fluctuations were those observed in the potassium circuit at the boiler inlet and in the lower portion of the condenser due to movement of the liquid-vapor interface in this component.

The fluctuation in the potassium boiler outlet pressure and potassium

(b) The plug of the metering valve will be redesigned for use in the tantalum alloy loop (T-111 Rankine System Corrosion Test Loop, NASA Contract NAS 3-6474) to obtain pressure drop characteristics which are less sensitive to minor changes in valve stem rotation than those of the Cb-1Zr Loop.

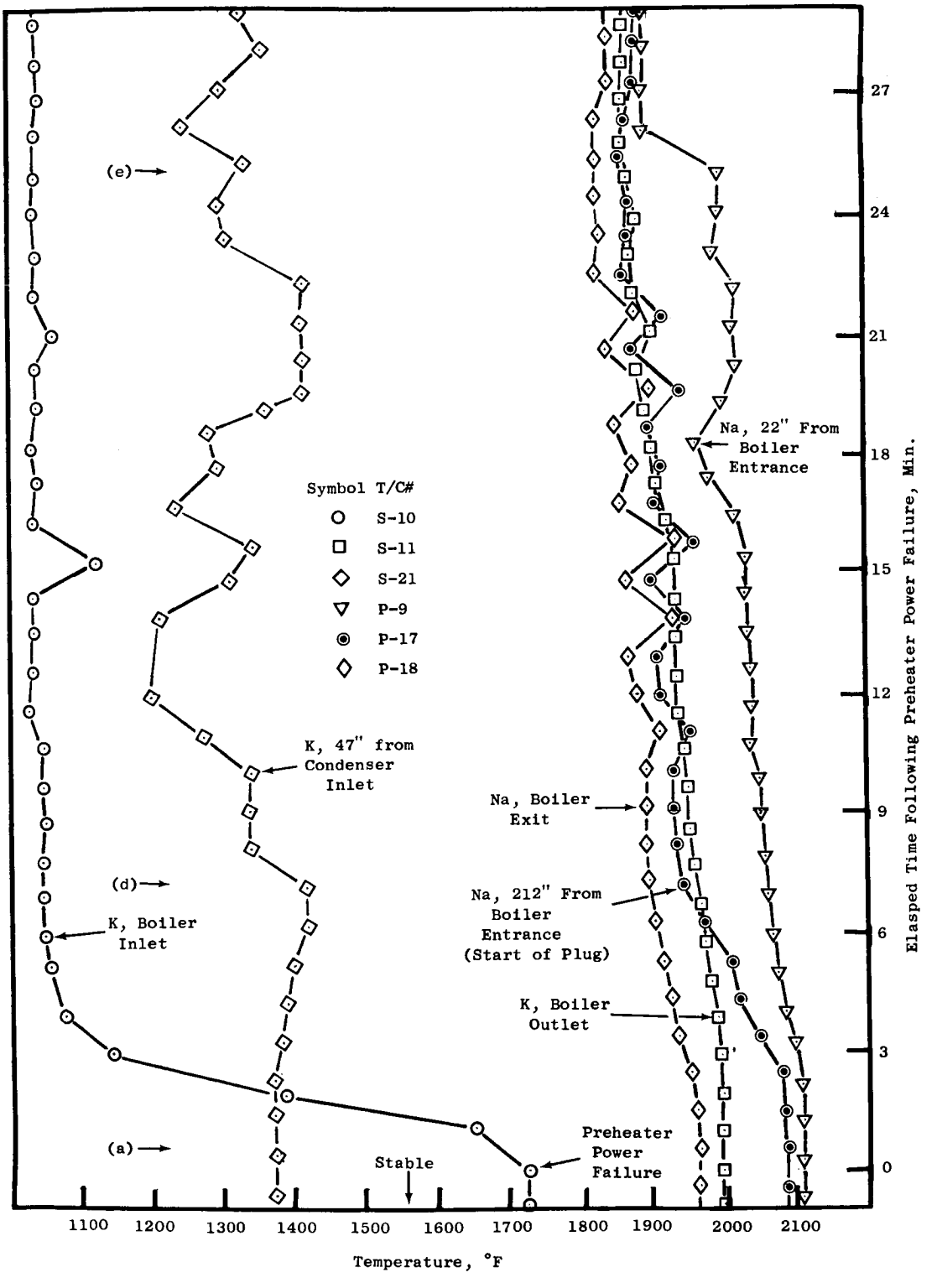

Figure 88. Temperature Fluctuations in the Sodium and Potassium Circuits of the Loop Following Failure of the Potassium Preheater Power (8-19-65, 0500).

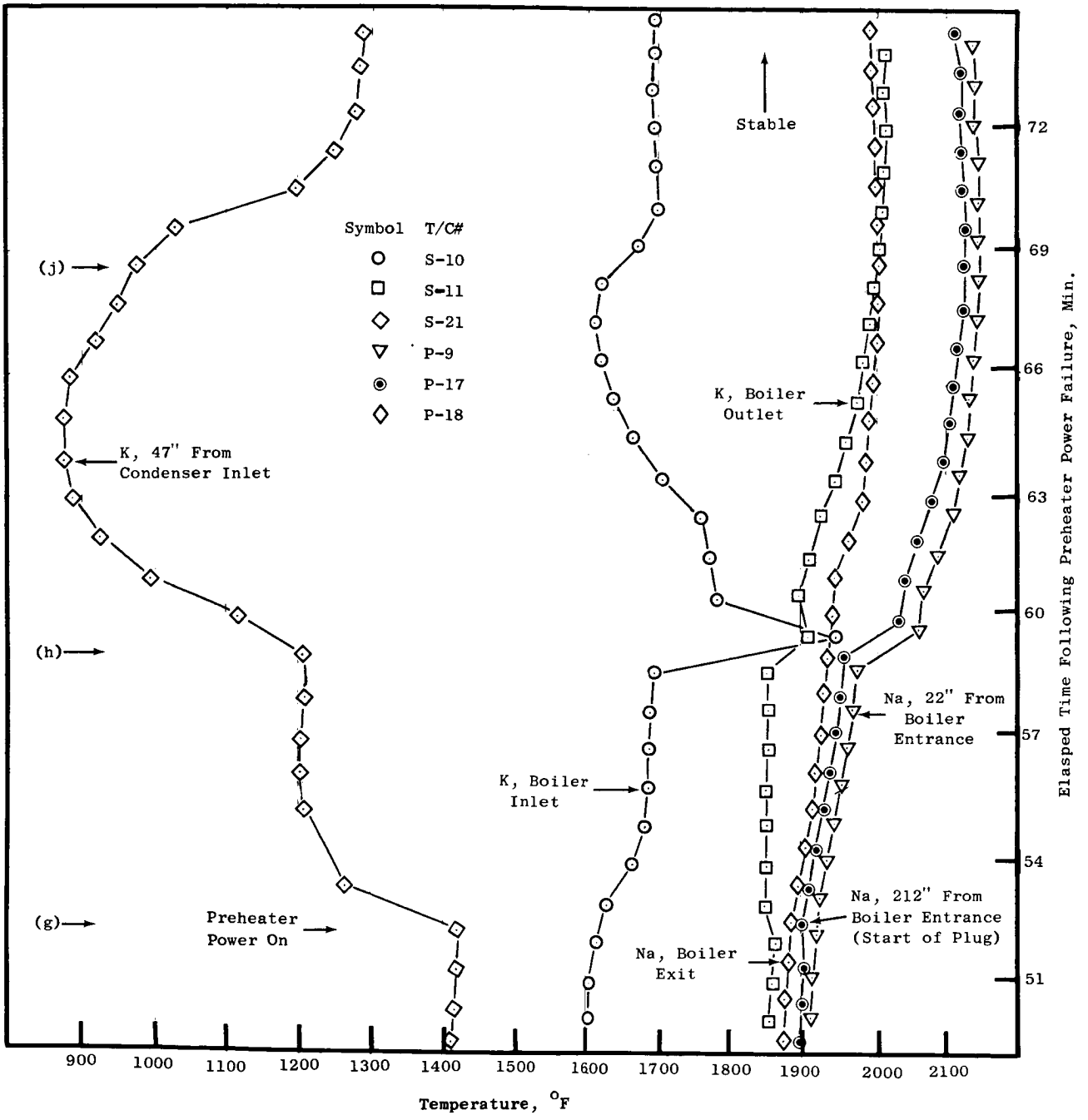

Figure 89. Temperature Fluctuations in the Sodium and Potassium Circuits During the Period When the Loop Was Being Returned to Design Conditions Following Failure of Potassium Preheater Power (8-19-65, 0600).

flow associated with the shifting of the nucleate boiling region out of the plug section of the boiler is illustrated in Figure 90. Three minutes after the loss of preheater power, the nucleate boiling region moved out of the plug, and the period of substantial oscillations of pressure and flow began. As may be noted in Figure 90 during the time period from (a) to (e), there were several brief periods of improved stability, and these are attributed to the temporary pauses in the movement of the nucleate boiling region along the boiler length from the plug region toward the boiler outlet. At the point designated (e), the nucleate boiling region had moved to near the potassium boiler exit, and a period of substantially improved stability began as indicated by both the pressure and flow charts. At point (g), the preheater power was restored, and at point (h), the nucleate boiling region moved rapidly from the boiler outlet region to the plug region at the boiler inlet. As may be noted in Figure 89 at point (h), the sodium temperature drop across the 12-inch plug increased from 20° to 100°F in approximately one minute when this occurred indicating that the vapor quality also increased to approximately 70 percent at the plug exit, which was the steady state condition.

During normal loop operation essentially no fluctuations of pressure, flow, or temperature were detected in the loop, and the period of unstable operation associated with the preheater power failure afforded an excellent opportunity to observe the response of the fast response stressed diaphragm pressure transducer. This transducer is located between the metering valve and the preheater in the potassium circuit as indicated in Figure 1 in Section II of this report. The Sanborn chart for the period following the preheater power failure is shown in Figure 91. Although zero drift of this transducer prevented its use in measuring absolute pressure, it performed its primary function, the detection of high-frequency pressure fluctuations, in a completely satisfactory manner. The shifts in the nucleate boiling region and the associated instabilities indicated in Figures 88, 89, and 90 are very evident in Figure 91. Based on the loop performance during the startup period, the stable boiling condition resulting from boiling primarily in the plug section could also be achieved by increasing the

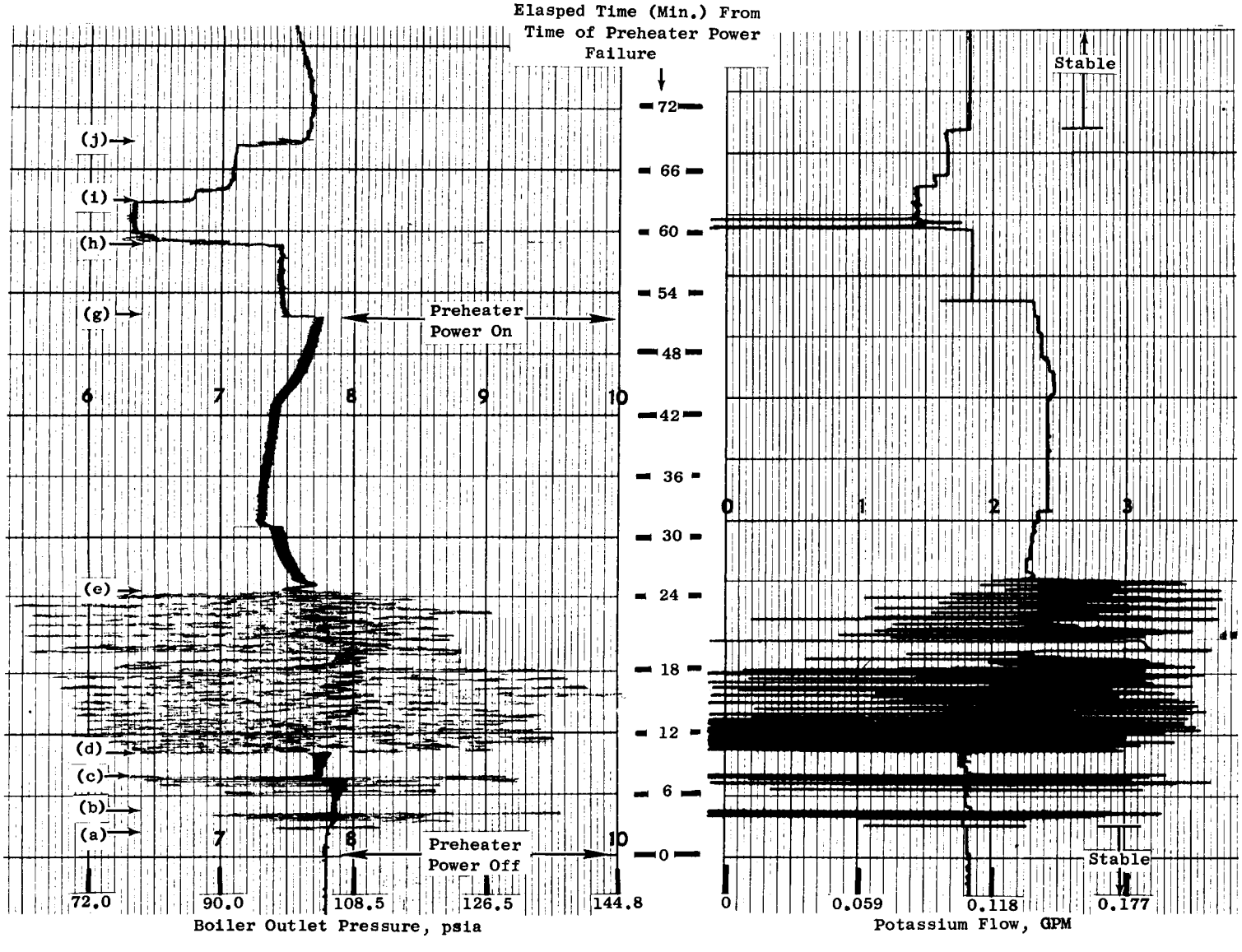

Figure 90. Fluctuations in Potassium Pressure and Flow in the Loop During the Time Period When the Potassium Preheater Power Was Lost and Then Restored (8-19-65, 0500 - 0600).

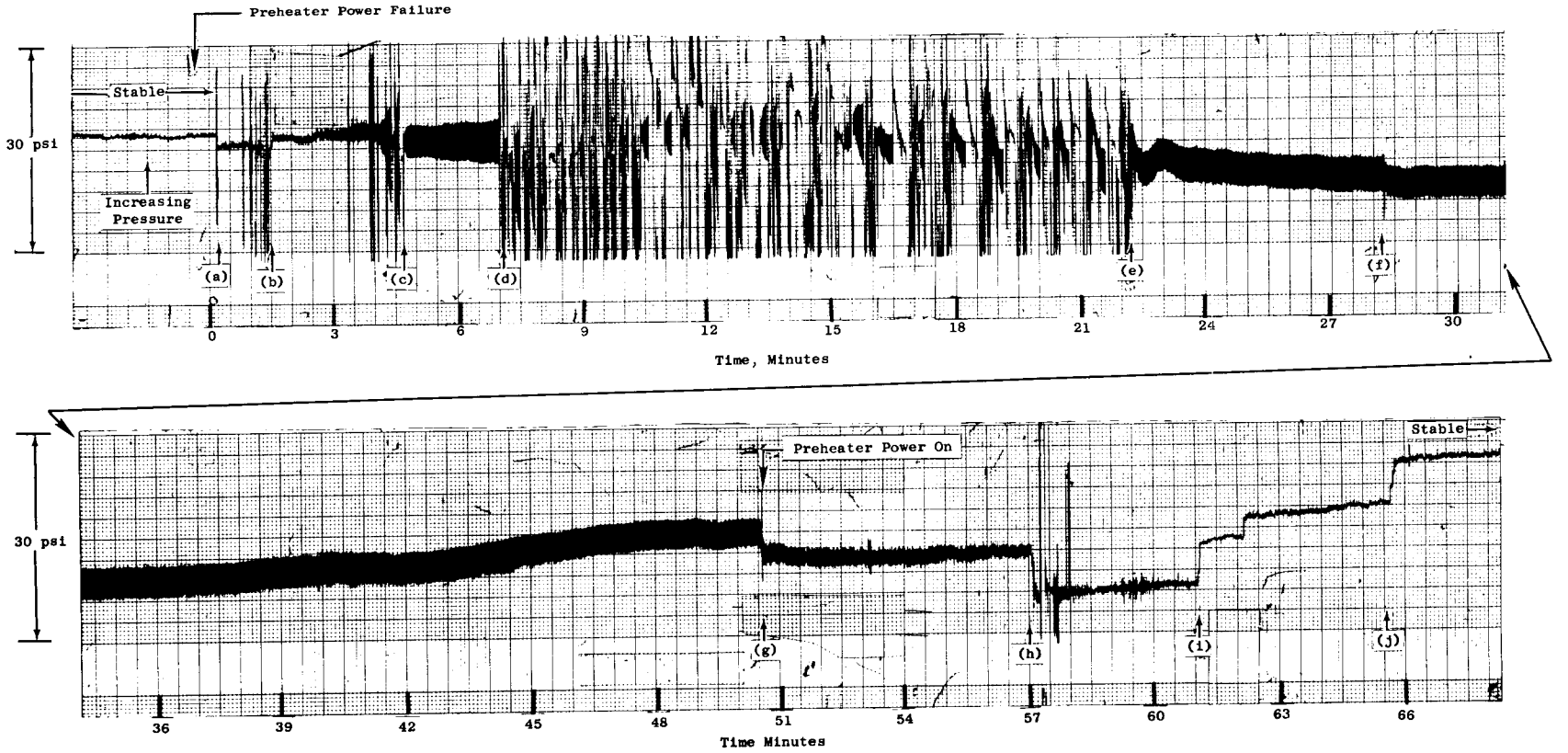

Figure 91. Fluctuations in Potassium Boiler Inlet Pressure Recorded by the Fast Response Stressed Diaphgram Pressure Transducer Following Failure of Preheater Power (8-19-75, 0500 - 0600).

sodium heater power input without the use of the preheater. However, this would have required the operation of the sodium heater at an outlet temperature in the 2150°-2200°F temperature range, rather than 2125°-2150°F as required when the preheater was used.

4. Changes in Pressure Drop in the Potassium Circuit. In general, the test conditions remained quite constant with no significant changes in the pressure drop across the turbine simulator stages which would indicate nozzle throat erosion, corrosion, or plugging. During the first 1785 hours of the test, small changes were detected in the pressure drop between the metering valve inlet and the boiler outlet as measured by the slack diaphragm pressure transducers at these locations. The ratio of this pressure drop to the metering valve inlet (pump outlet) pressure during 1785 hours of loop operation is plotted in Figure 92. Several observations can be made regarding this plot. The relatively large effect of rather small adjustments of the metering valve is apparent, especially the 30° opening adjustment (20° to 50°) after 90 hours of operation. The effect of several of these metering valve adjustments on system stability was illustrated earlier in Figure 87. It may also be noted that the pressure drop ratio increased slightly after approximately 400 hours of operation as a result of the brief period of unstable operation resulting from the failure of the preheater power described in the previous section of this report. During the period between 190 hours and 1386 hours, no adjustments of the metering valve were made. However, during this period, the pressure drop ratio showed a continuous increase. It was postulated at the time that minute amounts of solid particles, possible mass transfer particles, might be reducing the flow area between the Mo-TZM alloy valve plug and Cb-1Zr alloy valve seat. The flow area in the restricted region between the plug and seat, with the valve 40° open, is an annulus with an area of approximately 0.002 $in.^2$ and even quite small solid particles could have an appreciable effect on the potassium flow and pressure drop. For this reason the potassium circuit of the loop may be particularly responsive to extremely small amounts of particulate matter in the system. However, as described in the following paragraph, this trend did not continue during subsequent operation.

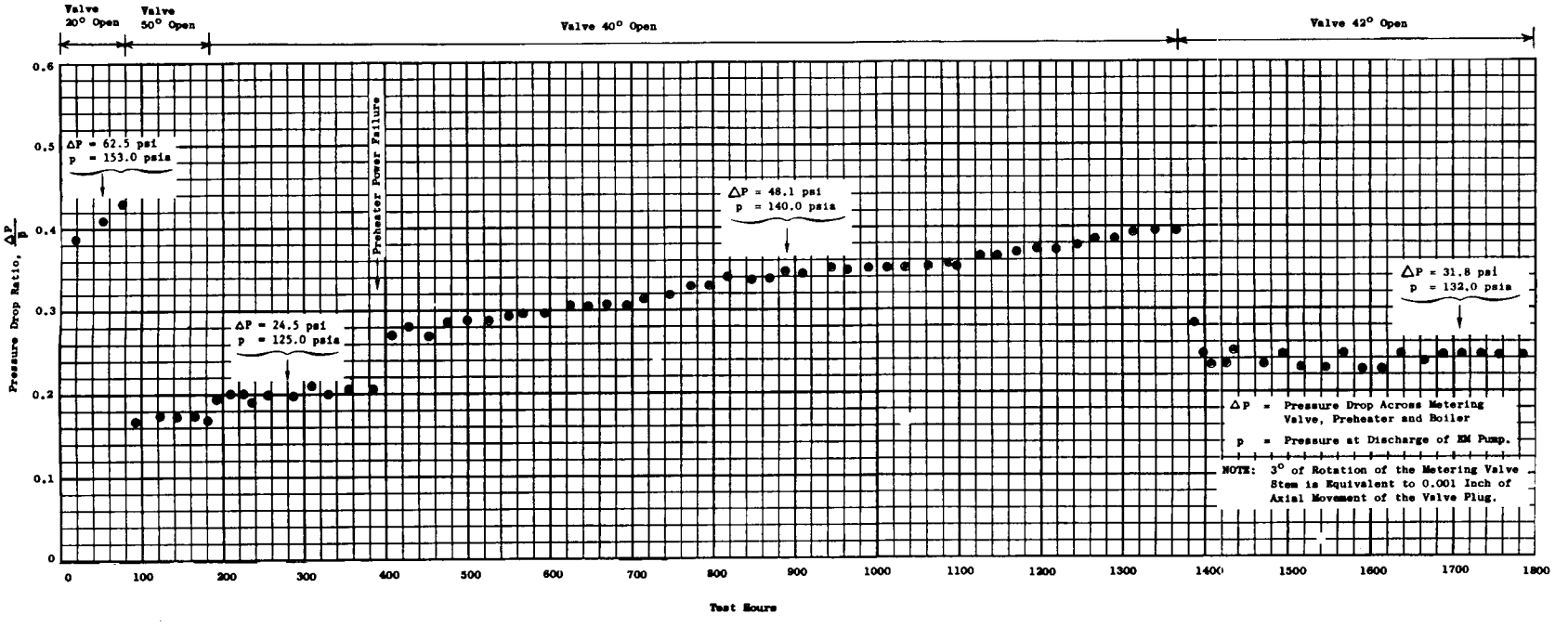

Figure 92. Change in Pressure Drop Ratio in the Potassium Circuit of the Loop as a Function of Time.

After 1386 hours of test operation, the metering valve was opened from 40° to 42° open, and the marked effect on the pressure drop ratio is readily apparent on the right side of Figure 92. It is assumed that particulate material was flushed out of the valve at this time since the pressure drop ratio conditions which resulted were very nearly the conditions that existed when the valve was first put in the 40° open position after 190 hours of operation. In the period between 1386 hours and 1785 hours, no significant changes in the pressure drop ratio were detected, and this would suggest that a temperature gradient mass transfer process was not responsible for the change in conditions noted during the period when the valve was 40° open.

It should be pointed out that although the pressure drop is measured between the metering valve inlet and the boiler inlet, the bulk of the pressure drop change is occurring in the metering valve. Although the absolute pressure at the metering valve outlet can not be determined because of the shift of the zero of the fast response transducer located in this area, the fact that the pump outlet pressure had to be increased to maintain a constant signal from the fast response transducer indicates that the pressure drop increase was due primarily to restriction of flow through the metering valve.

5. Fluctuations in the Electrical Power Supply to the Loop System. During test operation, minor fluctuations in the power supply to the test system necessitate minor adjustments in the heater power. The adjustments which were less than 0.5 percent of the total power were required approximately ten times per day to hold the sodium boiler inlet temperature variations to less than ± 5°F. Automatic temperature control equipment was incorporated into the power supply systems to the two circuits of the loop; however, during test startup it became quite apparent that manual adjustment of the heater and EM pump power yielded more satisfactory loop performance. On several occasions the 450-volt supply to the test system dropped approximately 5 percent when a large motor in an adjacent test facility was turned on. Immediate drops in the flow, pressure, and temperature in the potassium circuit and in the temperature of the sodium circuit occurred when the power drop

occurred but returned to the test design conditions in less than two minutes. Power drops of this type will be eliminated in future tests by modifications in the power supply system for the test area. These changes will be made following completion of the 5000-hour test.

On October 16, 1965, at 0800 the electrical power to the test area was interrupted momentarily as the result of a transformer changeover at the main power substation of the plant. The drop in line voltage was sufficient to activate the loop safety circuits which turn off power to the loop heaters and EM pumps. The power was turned back on immediately and the loop returned to its steady state test conditions within 30 minutes. Manual restart was found to be desirable in restoring power to loop circuits following activation of the safety circuits in order to avoid large current surges to the loop heaters and to restore stable loop operation in the minimum of time.

A momentary loss of electrical power to the test area on November 26, 1965, during an electrical storm, resulted in the activation of the safety circuits of the loop test system. Power to the loop heaters and EM pumps was restored by the operator on duty, and the loop was back to the steady state test conditions in less than five minutes. During the incident the potassium boiler outlet temperature dropped from the normal 2000°F to a minimum of 1980°F.

6. Water Leak in Cooling Channels. At 0800 on January 8, 1966, the Cb-1Zr Corrosion Test Loop was shut down after 3809 hours of continuous operation because of a pressure rise in the vacuum chamber. The pressure rose rapidly from the normal level of 2.1×10^{-8} torr to 1.0×10^{-6} torr in 17 minutes. Since the pressure trace gave no indication of being an argon instability,[(a)] as first suspected, the test engineer gave instructions to shut down the test. The test chamber pressure and the temperatures of several of the hottest loop components during the shutdown period are given in Table XIV. In view of the rapid drop in the temperature of the system, the protective wrapping of Cb-1Zr insulating foil on the loop components,

(a) Argon instabilities in the getter-ion pump are discussed in Part C of this section.

TABLE XIV

TEST CHAMBER PRESSURE AND THE TEMPERATURE OF THE HOTTEST LOOP COMPONENTS DURING THE TEST SHUTDOWN PERIOD ON JANUARY 8, 1966

Time	Pressure Torr	Na Loop- Max. Temp.(1) °F	K Loop- Max. Temp.(2) °F	K Loop- Next Highest Temp.(3) °F
0758	2.1×10^{-8}	2135	2000	1975
0800	7.0×10^{-8}	2135	2000	1975
0805	2.0×10^{-7}	2135	2000	1975
0810	5.0×10^{-7}	2135	2000	1975
0815(4)	1.0×10^{-6}	2135	2000	1975
0820	5.0×10^{-5}	1650	1655	1600
0825	4.0×10^{-5}	1600	1490	1375
0830	4.0×10^{-5}	1550	1350	1230
0845	4.5×10^{-5}	1330	1300	1100
0900	7.0×10^{-5}	1190	1100	850
0900 to 1400	Pressure held in 10^{-5} torr range until loop cooled to less than 300°F.			

(1) Heater exit.

(2) Boiler outlet.

(3) Turbine simulator (Stage No. 1) outlet.

(4) Loop heaters and EM pumps turned off.

and the chamber pressure levels during the shutdown period, it was concluded that no significant contamination of loop components occurred during this period.

Partial pressure scans taken after the test loop had been shut down indicated high concentrations of water vapor and subsequent leak checking established that leaks were present between the water channel in the vacuum chamber spool piece and the vacuum side in addition to numerous leaks from the water side of the cooling channel to the air side. A complete description of the test shutdown and the examinations which were performed to determine the nature and extent of the cracking of the test chamber water cooling channels is given in Appendix J, Stress-Corrosion Cracking of the Vacuum Chamber Cooling Channel.

The Cb-1Zr Corrosion Loop test was restarted on January 17, 1966, after repairs to the water cooling channel of the spool section were completed. The startup procedure is given here in detail as it departs from the procedure used in the initial startup which was described in Section IX. A change in the startup procedure was made so that it would not be necessary to move the metering valve plug from the set position. Although the valve could have been closed and subsequently returned to the approximate test position, it was felt that even a small change in the position of the plug could affect the operating conditions of the loop and obscure any small changes in the loop operating characteristics which could have occurred during the loop shutdown.

The 500°F chamber bakeout was limited to the bell jar since the epoxy resin used in sealing the water cooling channels on the spool section was limited to an operating temperature of 250°F. A bell jar temperature of 500°F was sufficient to heat the entire loop including the surge tank above the melting point of the liquid metal. The spool section reached a maximum temperature of 245°F during the bakeout, and a vacuum chamber pressure of 1.5×10^{-7} torr was obtained at the end of the 40-hour bakeout period. The sodium and potassium EM pumps were turned on and set at 10% of the rated power to heat the pump ducts to approximately 500°F and outgas the Cb-1Zr foil insulation which surrounded the duct.

Prior to filling the sodium circuit, the EM pump was turned off. The argon pressure in the sodium surge tank was then increased from 0 psia to 20 psia to fill the loop. The pump was restarted and when sodium circulation was established, the sodium heater was turned on and set at 1.5 kw. The secondary loop was then filled in the same manner by increasing the argon pressure in the potassium surge tank from 0 to 7 psia. The potassium pump was then set at 25 percent of the 0.11 gpm design flow rate, and all liquid operation at a maximum temperature of 1000°F was continued for the next 14 hours to outgas the loop. The vacuum chamber pressure decreased from 6×10^{-7} to 1.5×10^{-7} torr during this period.

Boiling in the potassium circuit was initiated by slowly increasing the power to the sodium heater. Boiling began when the potassium temperature exceeded the saturation temperature as set by the argon pressure in the surge tank. At 0853 hours on January 18, 1966, boiling started with a sodium inlet temperature of 1295°F and a potassium vapor (boiler outlet) temperature of 1290°F. Boiling was first detected by pressure oscillations of less than ± 1 psi at the boiler outlet. A decrease in the rate of temperature rise of the sodium circuit was also observed as more heat was transferred from the sodium circuit to the boiling potassium. During this rise in loop operating temperature, the vacuum chamber pressure increased to 2.6×10^{-6} torr.

During the next seven hours, the loop was slowly returned to the operating conditions which prevailed prior to the shutdown. The rate of the temperature rise was governed by the outgassing of the loop components as they increased in temperature.[(a)] Loop control during this period was smooth and normal. Small adjustments to the power and flow rate were made as the chamber pressure decreased into the 10^{-7} torr range. The procedure followed was to increase the heater power and then increase the secondary flow rate; using this technique, the boiling could be contained in the plug region. If the boiling moved out of the plug, a temporary

(a) Total pressure and partial pressures in the vacuum chamber during this period are discussed in Part C of this section.

instability occurred which could be corrected by either decreasing the potassium flow rate or increasing the sodium heater power, provided that the pressure in the test chamber was sufficiently low to permit an increase in loop temperature. During this stepwise procedure, the power to the preheater was also increased to raise the potassium inlet temperature.

A leak check of the vacuum system during the startup revealed a small leak in the main flange between the spool and the bell jar which was attributed to differential thermal expansion between the two flanges as the heat load varied in the chamber. The flange was resealed by retorquing the bolts to their prebakeout values.

The startup procedure described above was smoother and less complicated than the original startup and is recommended for future tests of this type. A comparison of the loop operating conditions before the 3809-hour shutdown and after resuming the test indicated no significant differences in operating conditions.

B. TERMINATION OF THE TEST

The loop test was terminated at 0700 on March 9, 1966, after completing 5000 hours of operation. The power to the heaters and pumps was gradually reduced over a one-hour period with no significant pressure or temperature instabilities occurring during the shutdown. While the loop was cooling down, tests were made to determine the ease of operation of the metering and isolation valves in the potassium circuit and the shutter assembly on the condenser-subcooler. Both valves were opened and closed approximately one-half the total valve stem travel (0.125 inch). Operation of the valves was very smooth for the first 20 to 30 mils of stem travel but became rough with additional opening. The roughness is attributed to galling between the stainless steel drive gears of the valves. (A material with less galling tendencies than stainless steel will be used in fabricating drive gears for valves in future tests.) The condenser shutter assembly was opened and closed three times and required very little torque on the magnetic rotary feedthrough. When the loop had

cooled to less than 800°F, the argon was pumped from the surge tanks and the two circuits drained to these tanks.

Pressure rise rates were obtained with the loop at operating temperature just before test shutdown and with the system at room temperature following shutdown. Following test shutdown and before opening the test chamber, the partial pressure gas analyzer was recalibrated using the gases. helium, hydrogen, nitrogen, and argon.

The test chamber was opened March 11, 1966, and the components examined visually by the NASA Technical Managers and program personnel. In general. the pretest and posttest appearance of the visible components was quite similar. Two views of the loop following removal of the bell jar are given in Figures 93 and 94.

The log summarizing the major activities during the 5000 hours of operation of the Cb-1Zr Rankine System Corrosion Test Loop are given in Table XV.

C. TOTAL PRESSURE AND PARTIAL PRESSURES IN THE CHAMBER DURING THE 5000-HOUR TEST

During operation of the loop test, residual gas analyses were performed using a G.E. magnetic deflection-type partial pressure analyzer system described in Section V, Part C, of this report.

1. Posttest Calibration of the Partial Pressure Analyzer. As indicated earlier in Section VIII, Part D(4), of this report, the partial pressure analyzer was calibrated initially with the test chamber empty; however, it was not possible to perform an additional calibration after placement of the loop in the chamber because of the relatively high chamber pressure (10^{-7} torr range) at that time. An additional calibration with the loop in the chamber was deferred until the completion of the 5000-hour test when, it was assumed, the pressure in the chamber would be considerably lower than before the test. This final calibration, which yielded calibration factors within 20 percent of those obtained in the initial calibration, is discussed in Appendix G, Calibration of the Partial Pressure Analyzer.

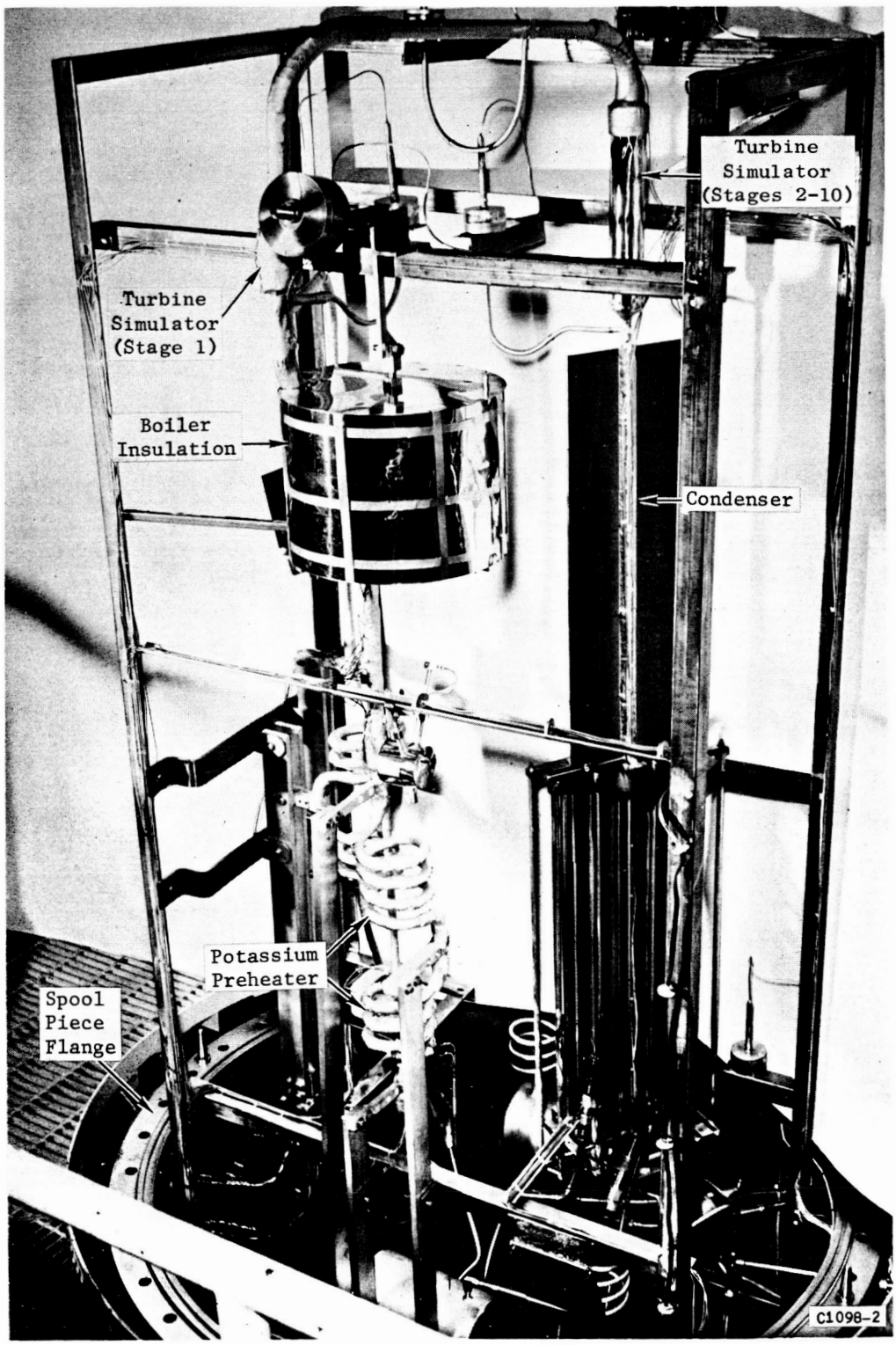

Figure 93. Cb-1Zr Corrosion Test Loop after Removal of the Vacuum Chamber Bell Jar Following Completion of the 5000-Hour Test. (Orig. C66031427)

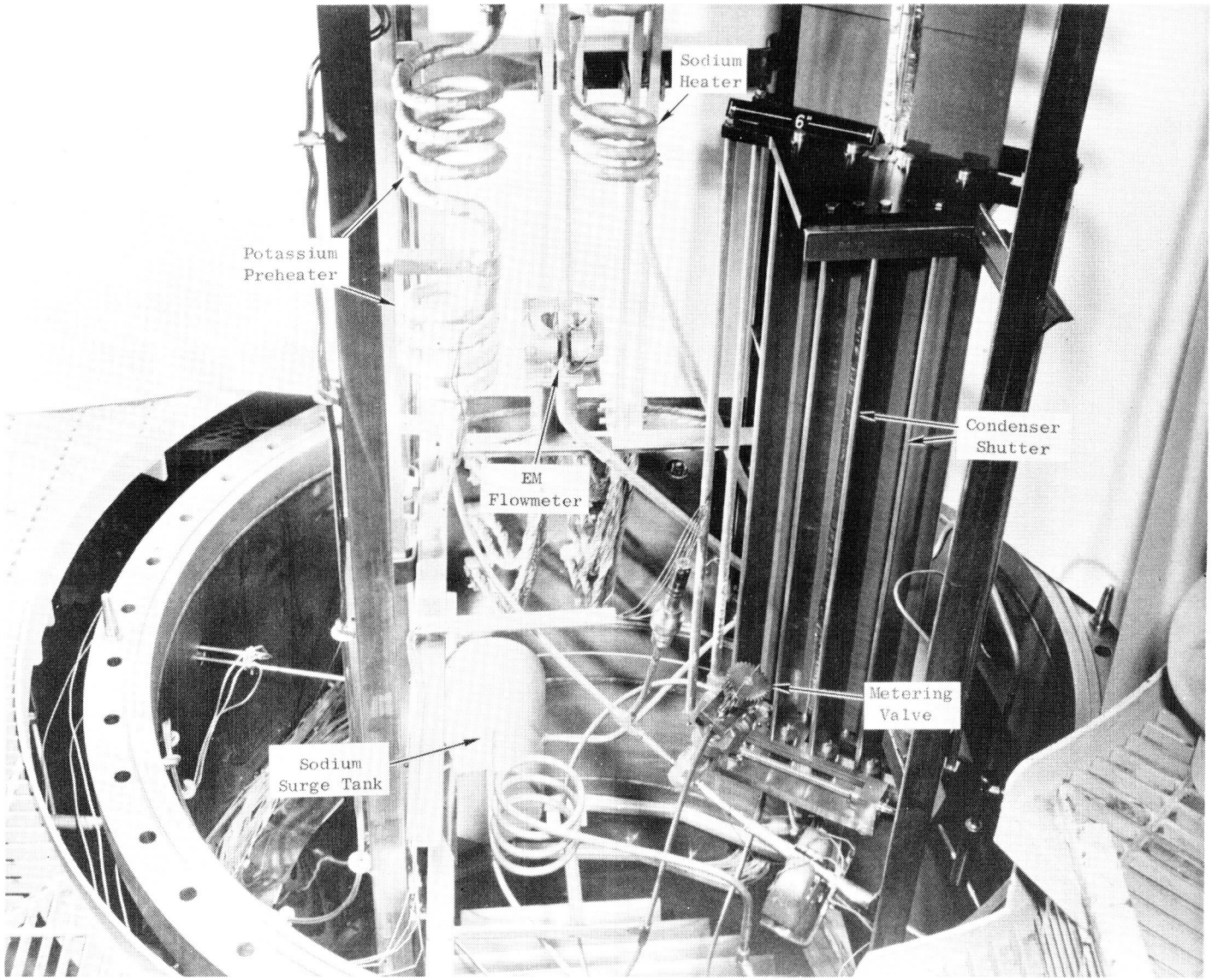

Figure 94. Lower Portion of the Loop Following Removal of the Vacuum Chamber Bell Jar. (Orig. C66031432)

TABLE XV

Cb-1Zr CORROSION TEST LOOP OPERATION HISTORY

August 2, 1965 - March 9, 1966

Time	Date	Test Hours	Remarks
1500	August 2	0	Loop startup.
1130	August 4	43	Unscheduled shutdown - vapor locked potassium pump.
0500	August 19	398	Unscheduled shutdown - fuse failure in preheater power circuit.
0800	October 16	1049	Unscheduled shutdown - commercial power outage due to transformer malfunction.
2330	November 26	2119	Unscheduled shutdown - commercial power outage due to electrical storm.
0800	January 8	3809	Unscheduled shutdown - water leak in vacuum chamber cooling channels.
0900	January 18		Test resumed.
0700	March 9	5000	Test completed.

2. Interpretation of Mass Spectra. Since complete cracking patterns were not obtained for all gaseous species, it was not possible to completely determine the contribution of each ion at every mass number. However, for most of the test duration, chamber pressures were in the low 10^{-8} torr range, and mass spectra were simple enough that there was little difficulty in calculating the partial pressures of the individual species.

A typical mass spectrum, obtained after 2494 hours of loop operation, is shown in Table XVI. The second column of Table XVI gives the ion with the greatest contribution at a particular mass number. The peak at m/e = 14 could possibly be due to CH_2^+, CO^{++}, or N^+. However, the magnitude of the 14 peak in comparison to the 12 and 15 peak indicates that the major contribution is from N^+. Similarly, the major contribution at m/e = 28 is from N_2^+. The magnitude of the 15 peak in comparison to the 32 peak indicates that the peak m/e = 16 contains contributions from both O^+ and CH_4^+. The ion current at m/e = 20 is attributed to Ar^{++} rather than Ne^+ since no appreciable ion current was detected for the m/e = 22 neon isotope.

The ion gauge partial pressures are shown in column 4 of Table XVI. Although the pressure calculated from the fragment CH_3^+ peak at m/e = 15 does not represent a real residual gas pressure within the chamber, it is a relative indication of the total hydrocarbon content. The sum of the ion gauge partial pressures is 13 percent lower than the actual ion gauge reading. This is considered to be quite good agreement, considering the approximations involved in the calibration of the analyzer. The fifth column of Table XVI gives the true partial pressures of the various species. It should be noted that the ion gauge partial pressures are obtained directly from the calibration of the partial pressure analyzer against the ion gauge. These values are sometimes referred to as "equivalent nitrogen pressures." The true partial pressures of the various gases are obtained from the ion gauge partial pressures and the relative ion gauge sensitivities which thus account for the differences in ionization efficiencies of the various gases. The main effect on the major species in the spectrum shown in Table XVI is that the true hydrogen partial pressure is considerably greater than the ion gauge partial pressure of hydrogen, while the

TABLE XVI

TYPICAL MASS SPECTRUM OBTAINED DURING LOOP OPERATION

Run #175 - 11-14-65 (1000)

Ion Gauge: 2.55×10^{-8} Torr - 2494 Test Hours

m e	Major Ion	Ion Current (Amp)	Ion Gauge Partial Pressure[a] (Torr)	True Partial Pressure[b] (Torr)
2	H_2^+	7.9×10^{-9}	2.2×10^{-9}	5.2×10^{-9}
4	He^+	1.0×10^{-11}	1.2×10^{-11}	6.3×10^{-11}
12	C^+	3.1×10^{-11}		
13	CH^+	0.5×10^{-11}		
14	N^+	6.0×10^{-10}		
15	CH_3^+	0.7×10^{-10}	0.7×10^{-10}	0.7×10^{-10}
16	O^+, CH_4^+	1.9×10^{-10}		
17	OH^+	1.9×10^{-10}		
18	H_2O^+	5.0×10^{-10}	5.4×10^{-10}	6.1×10^{-10}
20	Ar^{++}	5.0×10^{-10}		
28	N_2^+	5.1×10^{-9}	8.2×10^{-9}	8.2×10^{-9}
32	O_2^+	1.1×10^{-10}	2.2×10^{-10}	2.6×10^{-10}
40	Ar^+	2.9×10^{-9}	1.02×10^{-8}	6.5×10^{-9}
44	CO_2^+	1.2×10^{-10}	6.6×10^{-10}	4.8×10^{-10}
	TOTAL		2.21×10^{-8}	2.14×10^{-8}

(a) Ion Gauge Partial Pressure (Torr) is the product of the mass spectrometer ion current (amp) and the calibration factor (Torr/amp) obtained for the gas.

(b) True Partial Pressure (Torr) is obtained by dividing the Ion Gauge Partial Pressure (Torr) by the ion gauge sensitivity relative to nitrogen.

true argon partial pressure is lower than the ion gauge argon pressure. The true nitrogen partial pressure is, of course, the same as the ion gauge partial nitrogen pressure since the ion gauge is calibrated for nitrogen.

3. Partial Pressures of Various Species During Loop Operation. Analyses of the residual gases in the chamber were performed at least once each day during the 5000 hours of operation of the loop test. During the initial startup and the startup following the shutdown after 3809 hours of operation, analyses were performed more frequently in order to observe variations in partial pressures as the different components reached their operating temperatures. In Figure 95 are shown the ion gauge reading and the true partial pressures during the 5000 hours of loop operation. Data are plotted at approximately 50-hour intervals. The ion gauge reading remained below 1×10^{-7} torr after 130 hours of loop operation and was between 2×10^{-8} and 3×10^{-8} torr for most of the test. The major gaseous species in the system were N_2^+, Ar^+, and H_2^+. The peak at m/e = 28 contains contributions from both N_2^+ and CO^+, with the greater contribution from N_2^+, as discussed previously. In a typical mass spectrum such as shown earlier in Table XVI, N_2^+, H_2^+, and Ar^+ account for 92 percent of the total pressure in the chamber. (It is interesting to note that a general review of all the mass analyzer traces obtained during the operation of 10^{-8} torr creep systems on a recent NASA contract[39] indicated the following order of decreasing gas concentrations: CO^+, H_2O^+, CO_2^+, H_2^- with small quantities of CH_4^+, Ar^+, and He^+.)

The relatively high nitrogen pressure in the vacuum chamber during the loop test probably arose from very small air leaks in the system. The surprisingly high argon pressure throughout the duration of the test is also attributed to air leakage and to the relatively low pumping speed of the ion pumps for argon. The long-term "average" pumping speed for

(39) Generation of Long-Time Creep Data on Refractory Alloys at Elevated Temperatures, Twelfth Quarterly Report, NASA Contract NAS 3-2545, NASA-CR-72044.

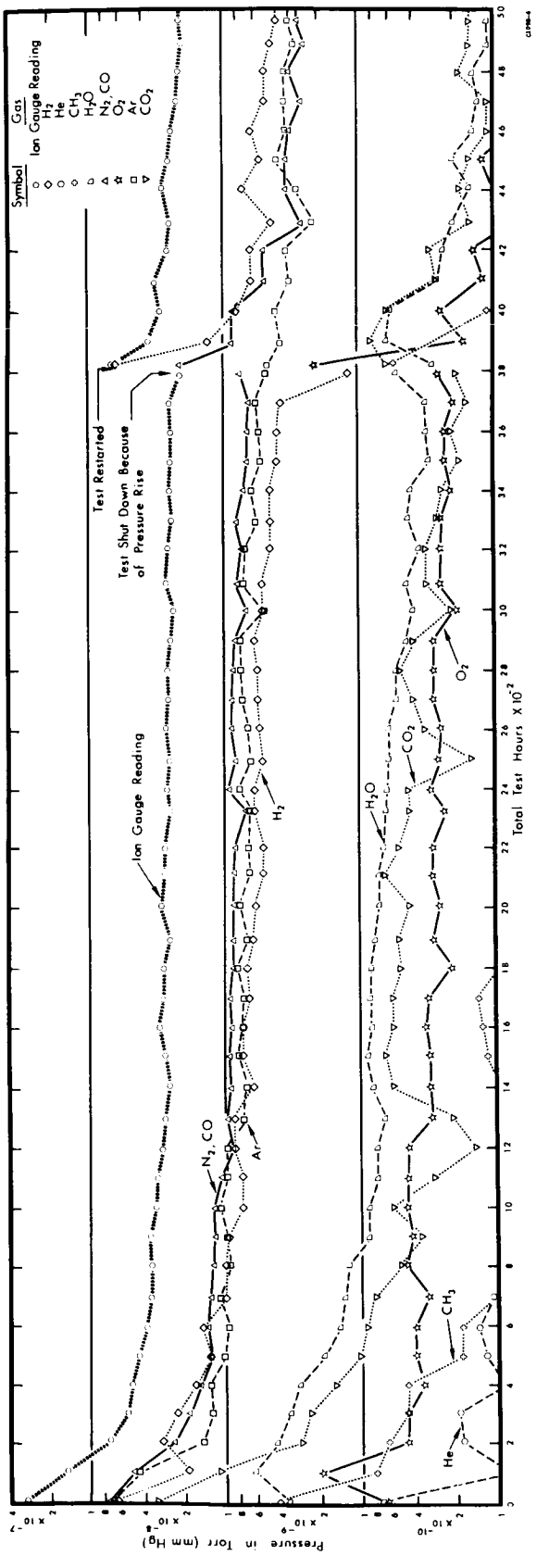

Figure 95. Vacuum Chamber Pressures During the 5000-Hour Cb-1Zr Corrosion Loop Test. (C66052351)

argon appears to be about 2 percent of the nitrogen pumping speed.[40] Since the pumping speed for argon is lower than for nitrogen, the argon concentration builds up until equilibrium is reached where the quantity of argon pumped is equal to the quantity being admitted with the air. The result is that, under the particular conditions of loop operation, the argon pressure is only slightly less than the nitrogen pressure, even though the nitrogen-to-argon ratio in air is about 80 to 1. Hydrogen is evolved from various components in the system and is invariably a major component of the residual pressure in a well-baked, ultrahigh vacuum system.

Of the minor constituents of the residual gases within the chamber, H_2O^+ and CO_2^+ are the most abundant. Since these substances are strongly adsorbed on internal surfaces, their presence can generally be detected even in a thoroughly baked ultrahigh vacuum system. Oxygen pressure was below 1×10^{-9} torr for most of test and was typically about 3×10^{-10} torr. The main source of oxygen appears to be air leakage. However, the nitrogen-to-oxygen ratio is about 30 compared to the value of about 4 for air even though oxygen pumping speed of the ion pumps is only about 60 percent of the pumping speed for nitrogen.[40] It thus appears that there are additional mechanisms active in removing oxygen from the system. An obvious additional mechanism for removal of oxygen is reaction with the Cb-1Zr components at elevated temperature. However, posttest chemical analyses of the Cb-1Zr components, as described in Section XII of this report, indicated an insignificant amount of oxygen contamination from the chamber environment.

Figure 96 shows the variation in ion gauge reading and true partial pressures observed as the loop was brought up to operating temperature following the shutdown after 3809 hours of loop operation. The main feature in this plot is the high hydrogen pressure observed during restarting

(40) Rutherford, S. L., et al., "On Pumping Mechanisms in Getter-Ion Pumps Employing Cold-Cathode Gas Discharges," American Vacuum Society Symposium Transaction, 1960, Pergamon Press, New York, 1961, p. 380.

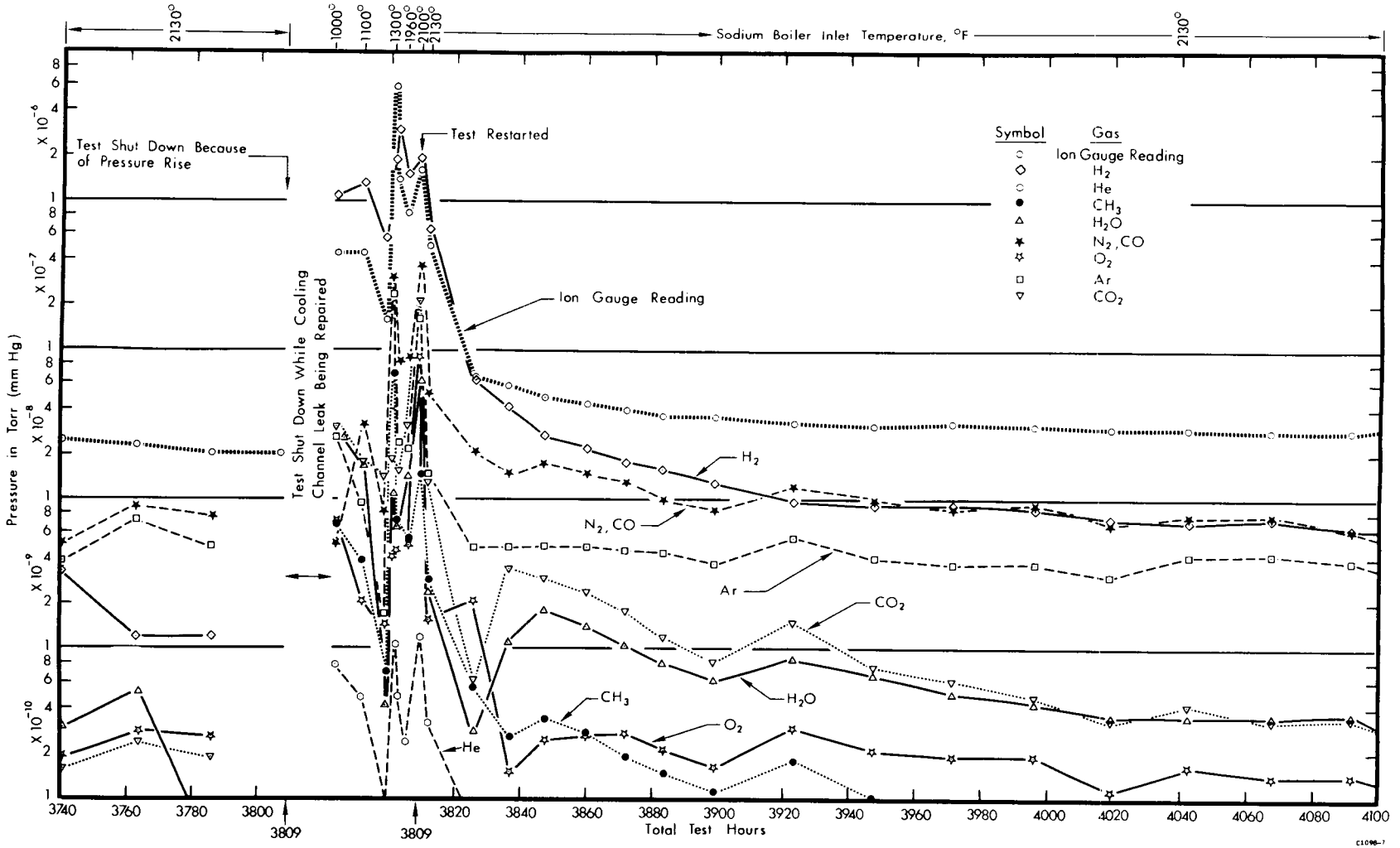

Figure 96. Vacuum Chamber Pressures During Startup and Operation Following Shutdown at 3809 Hours. (C66052352)

of the loop. It should be noted that such high hydrogen pressure was not observed during the initial startup of the loop as previously indicated in Figure 81. The fact that the hydrogen partial pressure calculated from the mass spectra actually exceeds the ion gauge reading for several points in Figure 96 does not necessarily represent an inconsistency since the reported true partial pressures have been corrected for ionization efficiency, and no such correction has been applied to the ion gauge reading. It might also be noted in Figure 96 that the rather large pressure excursions experienced during restarting of the loop were accompanied quite generally by an increase in each of the partial pressures.

4. Chamber Pressure Rise Rate with Ion Pumps Off. At the conclusion of 5000 hours of loop operation, the ion pumps were turned off, and the pressure rise rate within the chamber was noted over a period of one-half hour with the loop maintained at operating temperatures. A similar test was made after the loop was shut down and allowed to cool for about 20 hours. At the conclusion of this cool-down period, the loop components were essentially at ambient temperature. The results of these chamber pressure rise rate measurements with the ion pumps off are shown in Figure 97. With the loop at operating temperature, the pressure increased to 1.4×10^{-7} torr within 10 minutes followed by a more gradual rise to 2.5×10^{-7} torr at the end of a 30-minute period. With the loop at room temperature, an initial pressure rise to 9.2×10^{-8} torr in 5 minutes was followed by a more gradual increase to 2.5×10^{-7} torr after 35 minutes with the ion pumps off. After approximately 10 minutes, the pressure rise rate for the two conditions were essentially equal, 5.8×10^{-9} torr/minute.

Mass spectra of the residual gases in the chamber were obtained before and after the pressure rise measurements with the loop at room temperature. Partial pressures obtained from these spectra are shown in Table XVII. These data show that 82 percent of the pressure increase is accounted for by the increase in argon pressure accompanied by lesser increases in nitrogen and helium pressures. The increases in helium and argon are most probably due mainly to evolution of these gases from the pumps since the pressure rise rates are too high to be accounted for by air leakage, and there seems

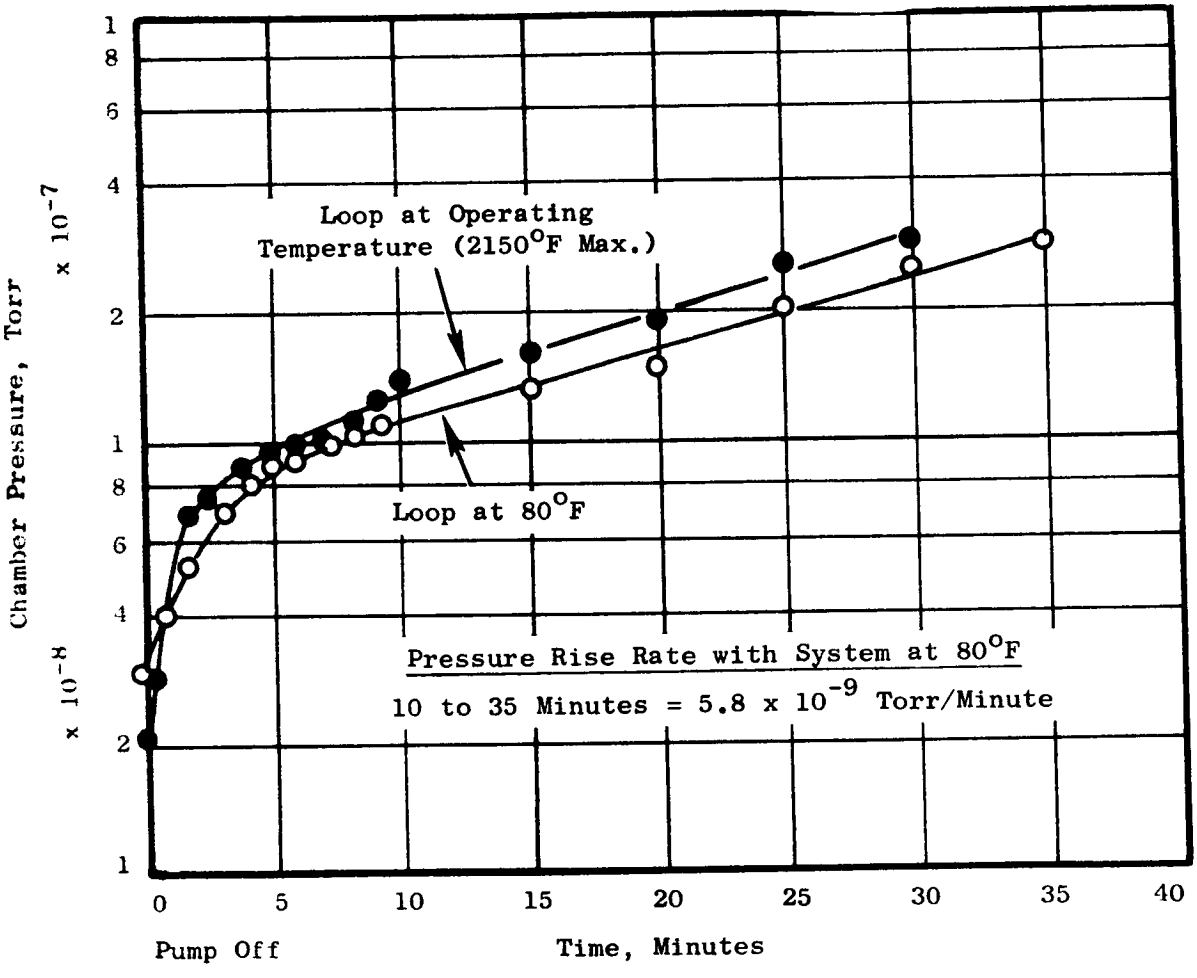

Figure 97. Pressure Rise Rate Tests on Vacuum Chamber with Cb-1Zr Corrosion Test Loop at Temperature and Following Cooling to Room Temperature.

TABLE XVII

RESIDUAL GAS ANALYSES BEFORE AND AFTER PRESSURE RISE RATE MEASUREMENT WITH LOOP AT AMBIENT TEMPERATURE

m e	Specie	Before Pressure Rise[a] Rate Measurement True Partial Pressure[c] Torr	After Pressure Rise[b] Rate Measurement True Partial Pressure[c] Torr
2	H_2^+	3.3×10^{-9}	3.8×10^{-9}
4	He^+	1.5×10^{-9}	2.9×10^{-8}
15	CH_3^+	---	5.6×10^{-9}
18	H_2O^+	---	---
28	N_2^+	5.5×10^{-9}	3.7×10^{-8}
32	O_2^+	4.6×10^{-10}	4.6×10^{-10}
40	Ar^+	2.8×10^{-9}	3.4×10^{-7}
44	CO_2^+	---	---
	T O T A L	1.4×10^{-8}	4.2×10^{-7}

(a) Ion pumps on Ion gauge reading - 1.35×10^{-8} torr.

(b) Ion pumps had been off for approximately 50 minutes. Ion gauge reading - 3.5 to 4.2×10^{-7} torr.

(c) True Partial Pressure (Torr) is obtained by dividing the Ion Gauge Partial Pressure by the ion gauge sensitivity relative to nitrogen.

to be no mechanism by which the pump could continue to remove the inert gases in the absence of an applied voltage. Concerning inert gas evolution from ion pumps, Rutherford, et al.[40] have stated that "argon re-evolution is thus of little concern during normal pump operation." On the basis of their argument, the statement should also apply when the pump is turned off. Roberts and Vanderslice,[41] on the other hand, state that "atoms which have been driven into the surface and are not buried by sputtered metal can diffuse back into the gas phase."

The data of Table XVII indicate that there is little increase in hydrogen pressure and no appreciable increase in oxygen pressure when the ion pumps are turned off for a 30-minute period with the loop at ambient temperature. Since there are certainly sources of these two gases, the small pressure increase indicates that there is some mechanism by which these gases are removed from the system even with no voltage applied to the ion pumps. It has, in fact, been reported[41] that when the discharge voltage is turned off, hydrogen pumping continues at a substantial rate for "some time."

One could assume also that a similar mechanism is effective in removing nitrogen from the system, and thus the rate of nitrogen pressure increase is the net result of air leakage into the system and some continued pumping by the ion pumps. The increase in CH_3^+ is apparently due to the buildup of methane pressure within the system. The origin of this methane is not apparent.

In summary, it appears that when the ion pumps are turned off, they evolve previously pumped inert gases while continuing to pump the active gases at a significant rate, at least for a period of 35 minutes. If similar pressure rise rate measurements were continued over a long period of time, presumably the rate of increase of argon and helium pressures would diminish and the pressures of these two gases would

(41) Roberts, R. W. and Vanderslice, T. A., Ultra-High Vacuum and Its Applications, Prentice-Hall, Inc., Englewood Cliffs, N. J. (1963), p. 19.

approach a nearly constant value, while the pressures of the more active gases would increase at an accelerated rate as the pumping surfaces become saturated. It is, therefore, recommended that pressure rise rates be determined for periods of at least several hours in future tests of this type to obtain more information regarding the gas sources and sinks in the systems of this type.

5. Argon Instabilities in the Getter-Ion Pump. During the 5000-hour loop test a large number of sudden pressure rises were noted in the vacuum chamber pressure. These momentary pressure rises occurred at time intervals which averaged 64 hours (minimum interval: 21 hours; maximum interval: 124 hours). A typical pressure surge of the type observed in the test chamber consists of a very rapid rise (less than 5 seconds) from a base pressure of 5.5×10^{-8} to 1.2×10^{-6} torr and a more sluggish (approximately 5 minutes) return to the presurge pressure level as illustrated in Figure 98. A list of a few of the recorded test chamber pressure surges which typify the extent of the pressure rises is given in Table XVIII. Pressure bursts of this type are frequently encountered in diode-type getter-ion pumps.[42] However, the referenced report states that it is typically necessary to pump air at 1×10^{-5} torr for several hundred hours or 1×10^{-6} torr for several thousand hours before argon instabilities are observed. During both the Cb-1Zr Pumped Sodium Loop test[43] and the Cb-1Zr Corrosion Loop test, "argon instabilities" were encountered after several hundred hours of operation at indicated ion gauge pressures in the 10^{-7} to 10^{-8} torr range. Although these instabilities have been studied for some time, Jepsen, et al.,[42] report that no completely satisfactory explanation for the unstable argon behavior has been proposed. In another study of the argon instability

(42) Jepsen, R. L., et al., "Stabilized Air Pumping with Diode-Type Getter-Ion Pumps," American Vacuum Society Vacuum Symposium Transactions, 1960, Pergamon Press, Inc., New York, 1961, pp. 45-50.

(43) Hoffman, E. E. and Holowach, J., Cb-1Zr Pumped Sodium Loop, Potassium Corrosion Test Loop Development Topical Report No. 6., R67SD3015, General Electric Company, Cincinnati, Ohio, December 20, 1967, p. 150.

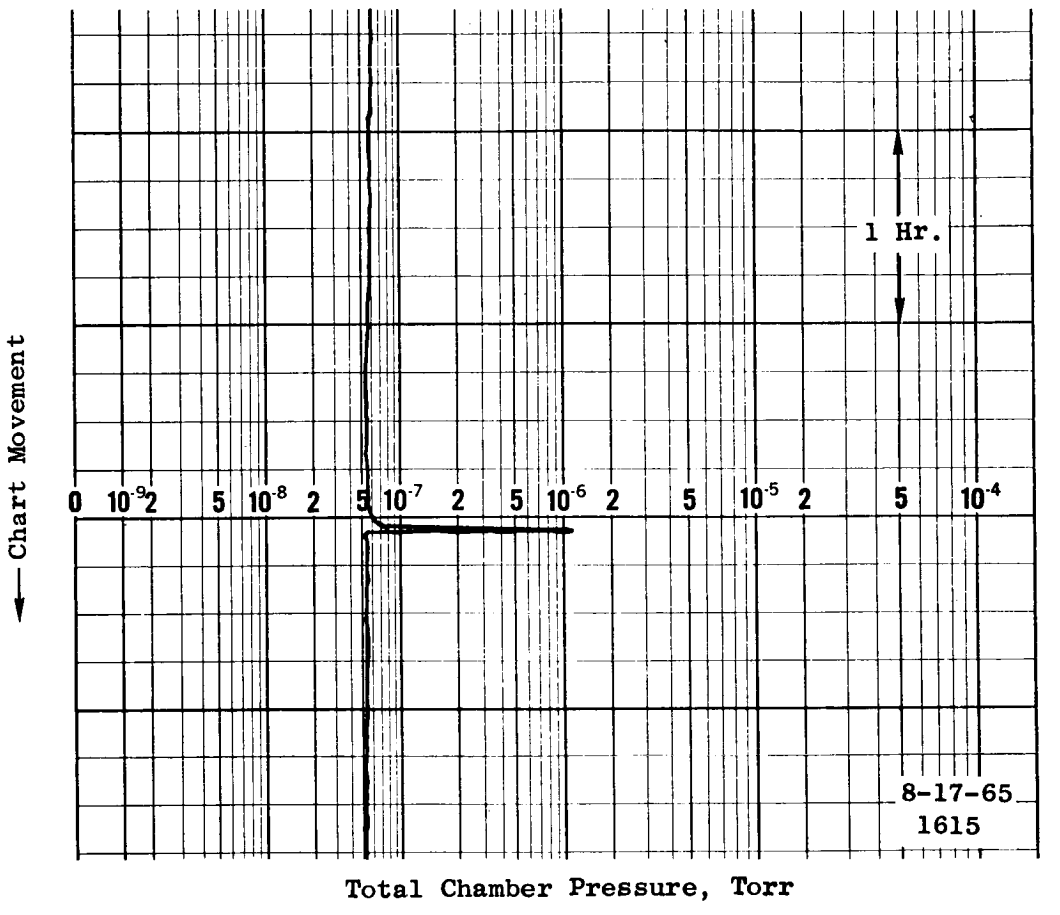

Figure 98. Typical Pressure Surge in the Test Chamber Resulting from an Argon Instability in the Getter-Ion Pump.

TABLE XVIII

LIST OF A FEW OF THE TYPICAL RAPID PRESSURE RISES ("ARGON INSTABILITIES") NOTED IN THE TEST CHAMBER PRESSURE DURING THE LOOP TEST

Hours of Loop Operation	Date	Time	Pressure, Torr[a]	
			Base Pressure	Peak Pressure
Start of Test	8-2-65	1500	3.0×10^{-7}	---
305	8-15-65	0800	5.4×10^{-8}	3.0×10^{-6}
617	8-28-65	0745	4.0×10^{-8}	7.0×10^{-7}
959	9-11-65	1400	3.0×10^{-8}	3.0×10^{-7}
1248	9-23-65	1445	2.9×10^{-8}	8.0×10^{-7}
1583	10-7-65	1415	2.9×10^{-8}	1.5×10^{-6}
1840	10-18-65	0705	3.0×10^{-8}	1.5×10^{-6}
2141	10-30-65	1930	2.7×10^{-8}	1.5×10^{-6}
2478	11-13-65	2105	2.6×10^{-8}	1.3×10^{-6}
2748	11-25-65	1315	2.5×10^{-8}	1.0×10^{-6}
3119	12-10-65	1530	2.4×10^{-8}	1.3×10^{-6}
3472	12-25-65	0645	2.5×10^{-8}	1.5×10^{-6}
3785	1-7-66	0825	2.2×10^{-8}	1.3×10^{-6}

(a) Pressure change indicated by getter-ion pump recorder. Base pressure corrected to value indicated by calibrated nude ion gauge on the chamber.

phenomena. Brubaker[44] has reported that none of the other gases present are found to partake in the violent pressure excursions experienced by the argon. In order to determine if the pressure surges observed in the test chambers at General Electric were due solely to argon, continuous scans for individual species were conducted. An argon peak height was measured during an instability which occurred on January 28, 1966, and the hydrogen peak height was measured during an instability which occurred on February 2, 1966. The relative changes in argon pressure and hydrogen pressure during these typical instabilities are given in Table XIX. It was somewhat of a surprise to note that the surge in hydrogen pressure during the instability was somewhat larger than the argon pressure surge. Since both argon and hydrogen, and possibly other gases, contribute to the observed pressure surges, these results do not agree with the results reported by Brubaker[43] above.

The instabilities observed during the 5000 hours of test operation occurred much less frequently than those usually cited in the literature and at a much lower argon pressure. For example, Brubaker[43] reports argon pressure instabilities at 1×10^{-5} torr argon pressure and at approximately 10-minute intervals while those found in the loop test chambers occurred at argon pressures near 5×10^{-9} torr and at 50- to 70-hour intervals. These observations substantiate the rather general rule that the frequency of the instabilities is roughly proportional to the argon pressure.

Although the pressure surges observed in the test chamber pressure described above are of no significance insofar as loop contamination is concerned, they did prevent the utilization of the emergency argon flooding system which was designed to provide protection for the hot refractory alloy loop components in the event of a serious leak in the vacuum system.

---

(44) Brubaker, W. M., "A Method of Greatly Enhancing the Pumping Action of a Penning Discharge," American Vacuum Society Vacuum Symposium Transactions, 1960, Pergamon Press, Inc., New York, 1961, p. 302.

TABLE XIX

ARGON AND HYDROGEN PRESSURE SURGES DURING "ARGON INSTABILITIES" IN THE TEST CHAMBER

	Continuous Argon Scan 1-28-66 (1520)	Continuous Hydrogen Scan 2-2-66 (1430)
Indicated Ion Gauge Pressure	3.0×10^{-8} torr	2.5×10^{-8} torr
True Base Pressure[(a)] of Gas Prior to Instability	4.3×10^{-9} torr	7.5×10^{-9} torr
True Peak Pressure of Gas During Instability	2.0×10^{-8} torr	$> 3.3 \times 10^{-8}$ torr[(b)]
True Pressure 10 Seconds Later	9.0×10^{-9} torr	1.4×10^{-8} torr

(a) True Pressure (Torr) is obtained by dividing the Ion Gauge Partial Pressure (Torr) for the particular gas by the ion gauge sensitivity relative to nitrogen.

(b) Hydrogen peak was off scale on the 10×10^{-10} amp scale.

An overpressure relay in the getter-ion pump circuit was originally designed to fire an explosive valve when the vacuum tank pressure rose to 4×10^{-6} torr. The argon tank connected to the explosive valve would then flood the vacuum chamber with argon gas. However, this safety circuit was not activated initially because of the pressure excursions of large magnitude but short duration cited above. The Cb-1Zr Sodium Pumped Loop experiment was shut down on two occasions[45] by the surges in the chamber pressure resulting from argon instabilities.

Initially, it was hoped that the argon instabilities would cease or diminish in amplitude so that the argon flooding system could be connected without fear of it being actuated by an argon instability in the getter-ion pump. After several hundred hours of loop operation, it became obvious that the instabilities were not diminishing in amplitude or frequency, and this safety circuit was redesigned. The relay built into the ionization gauge controller was put in series with the pressure sensitive relay in the getter-ion pump system. This second relay was designed to close when the chamber pressure exceeded 4×10^{-4} torr. Increasing the circuit activating pressure from 4×10^{-6} to 4×10^{-4} torr permitted operation of the argon flooding system with low probability of it being inadvertently triggered by an argon instability. No test shutdowns due to argon instabilities occurred during subsequent loop operation. Following completion of the 5000-hour test, consideration will be given to replacing the standard getter-ion pump elements with Varian's slotted "Super VacIon" getter-ion pump elements with slotted titanium cathode plates as pumps with this type of element have an argon pumping speed of 6 percent of the air speed compared to 1 percent for the standard elements.

---

(45) Hoffman. E. E. and Holowach, J., Cb-1Zr Pumped Sodium Loop, Potassium Corrosion Test Loop Development Topical Report No. 7, R67SD3015, General Electric Company, Cincinnati, Ohio, December 20, 1967, p. 141.

XI. DISTILLATION, DRAINING, AND DISASSEMBLY OF THE LOOP

The test chamber was opened on March 11, 1966, and the components examined visually by the NASA Technical Managers and program personnel. In general, the pretest and posttest appearance of the visible components were quite similar. Two views of the loop immediately following removal of the bell jar are given in Figures 99 and 100.

There have been numerous cases reported by various alkali metal corrosion investigators of deleterious effects on test components resulting from interactions between alkali metals, stripping agents, and the test components while removing residual alkali metal following completion of the corrosion experiment.[46, 47] Quite often it is difficult to determine unequivocally if the observed "corrosion" occurred during the test or while removing the alkali metal with the stripping agent. This was a particularly critical problem in the Cb-1Zr Corrosion Test Loop in areas such as the turbine simulator where alkali metal would not drain from the many narrow annuli and where interactions with stripping agents, such as alcohol or butyl cellosolve, might negate the effort to obtain very accurate weight change data on the turbine simulator components. For these reasons, it was concluded that vacuum distillation of the alkali metals from the loop circuits to the surge tanks prior to draining and sampling these systems would be desirable.

A. DISTILLATION OF SODIUM AND POTASSIUM FROM THE LOOP CIRCUITS

The first step in the preparation of the loop for distillation of the residual alkali metal following completion of the 5000-hour test was the removal of the thermal insulation shield assembly which surrounded and thermally insulated the boiler during test operation. The insulation was removed to expose the boiler coils directly to heat radiated from the distillation heaters

(46) Metals and Ceramics Division Annual Progress Report for Period Ending June 30, 1965, ORNL-3870, p. 130.

(47) Hoffman, E. E. and Holowach, J., Cb-1Zr Thermal Convection Loop, Potassium Corrosion Test Loop Development Topical Report No. 5, R67SD3014, General Electric Company, Cincinnati, Ohio, June 15, 1967, p. 72.

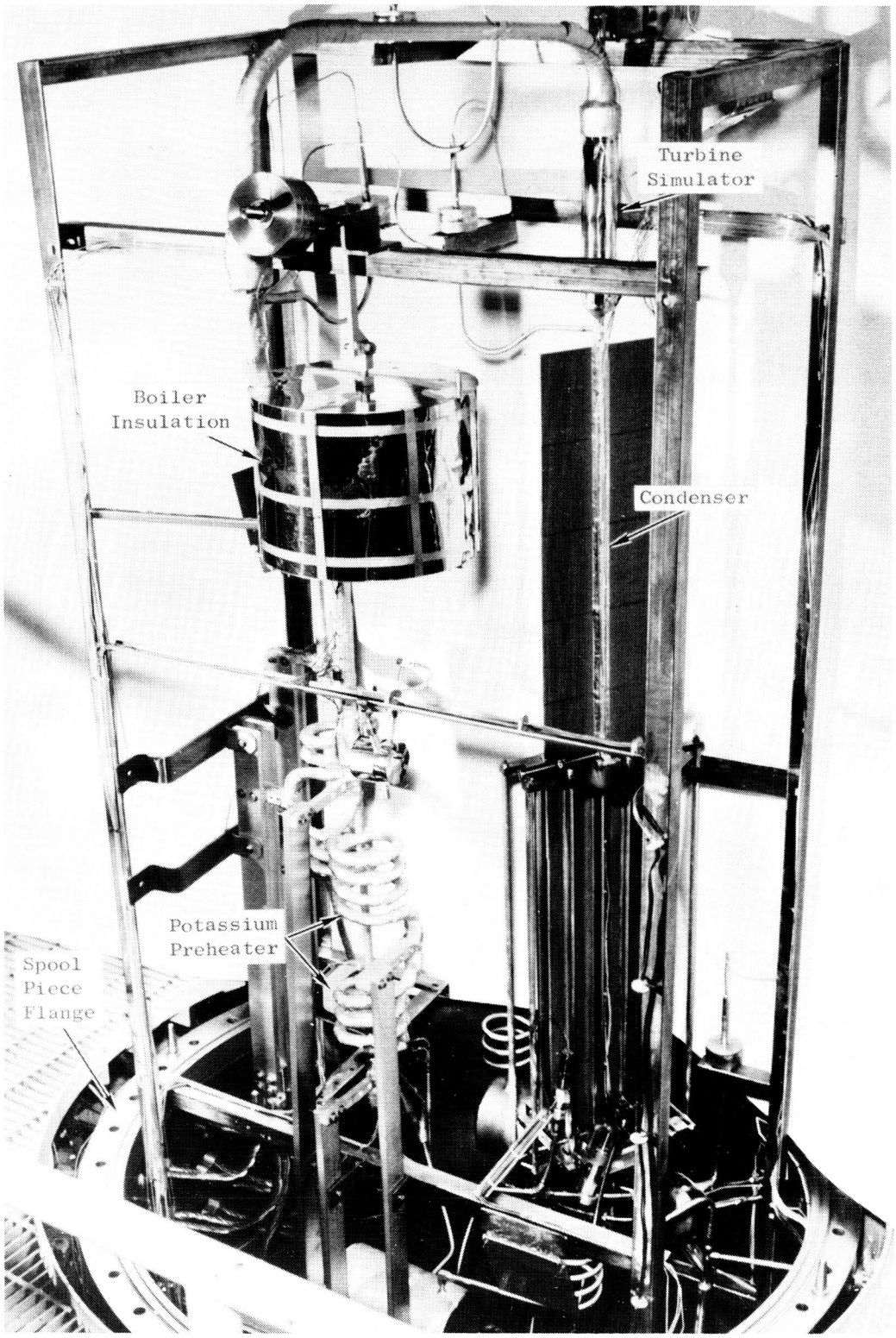

Figure 99. Cb-1Zr Corrosion Test Loop After Removal of the Vacuum Chamber Bell Jar Following Completion of the 5000-Hour Test. (Orig. C66031427)

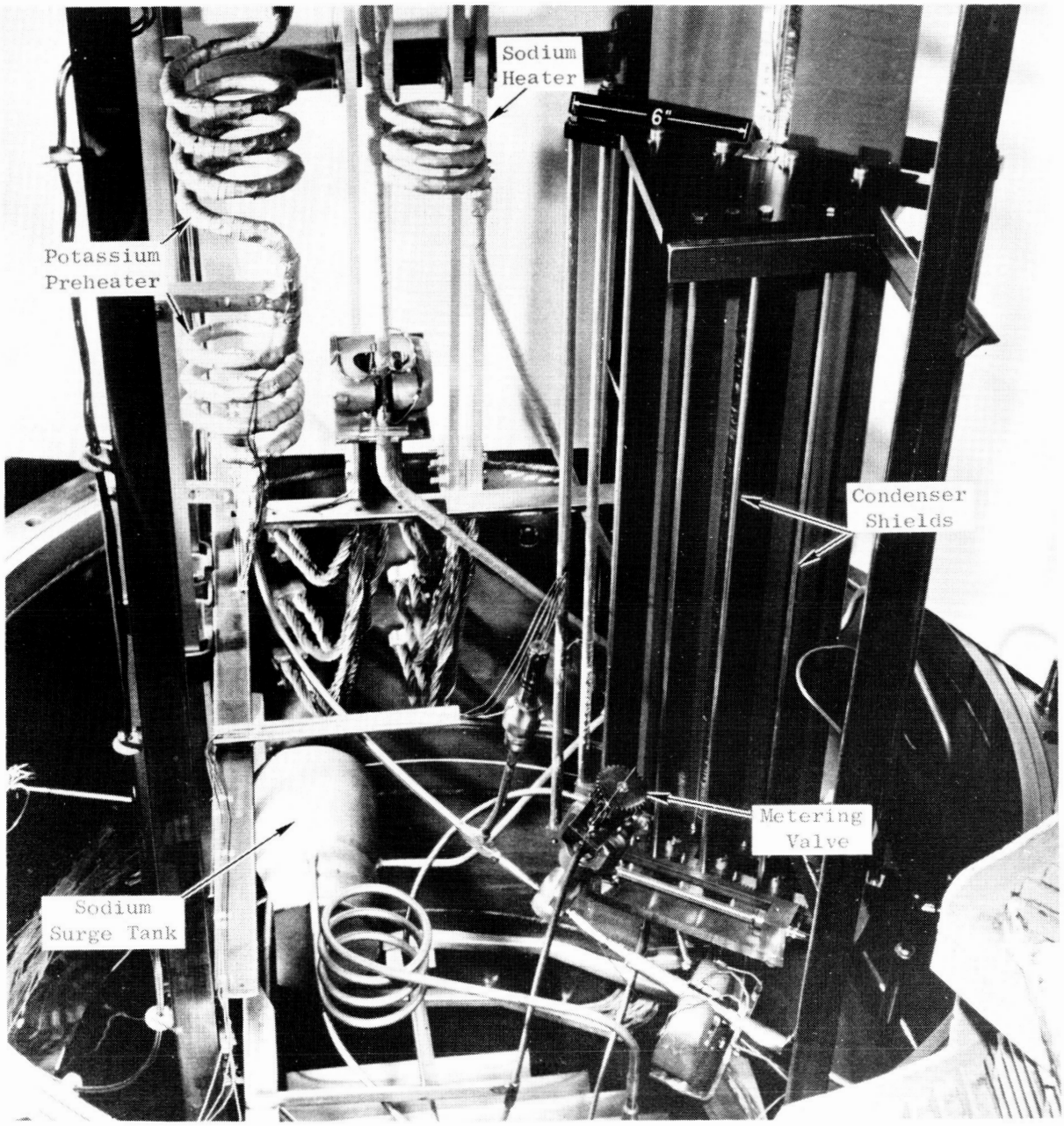

Figure 100. Lower Portion of the Loop Following Removal of the Vacuum Chamber Bell Jar. (Orig. C66031432)

and accelerate the distillation in the 244-inch-long tube-in-tube assembly.

Specimens of the 2-mil-thick Cb-1Zr alloy foil were also taken from the four regions of the loop listed below:

a) Nine-stage turbine simulator (single layer),

b) Sodium line, 3 inches from boiler inlet (12 layers),

c) Potassium vapor carryover line (12 layers), and

d) Top coil of sodium heater, 4 inches from top electrode (12 layers).

These specimens together with before-test specimens of foil were subjected to 90 degree reverse bending to failure to obtain a qualitative indication of the extent of possible contamination (and embrittlement) during the 5000-hour test. All specimens were very ductile, and no significant differences were detected. The results of several chemical analyses performed on the single layer of foil which surrounded the turbine simulator are reported in Section XII of this report.

The distillation heaters were six quartz infrared lamps[(a)] with tungsten filaments which were mounted on stainless steel brackets. These heater brackets were welded to the loop support structure as shown in Figure 101. The lamps were connected in parallel to the main heater power supply used in the loop operation. Two layers of stainless steel foil were wrapped around the loop support structure to thermally insulate the loop and quartz heaters from the test chamber bell jar as shown in Figure 102. Special precautions were taken in placing the quartz lamps so that the ends would protrude through the insulation out of the heated zone to reduce the possibility of failure of the end seals from overheating. The sodium and potassium surge tanks were also shielded from the quartz heaters to maintain a lower temperature than the loop so that the alkali metal distilled from the loop would condense in the cooler surge tanks located in the lower portion of the chamber.

After a low-power electrical checkout of the heating lamps, the bell jar was lowered to the spool section and the vacuum chamber sealed. The turbomolecular pump was used to rough pump the chamber to 5×10^{-4} torr. The ion

(a) General Electric Type 3800 Te/VB, 3800 watts, 570 volts, 1/2-inch OD x 43 1 2-inch long.

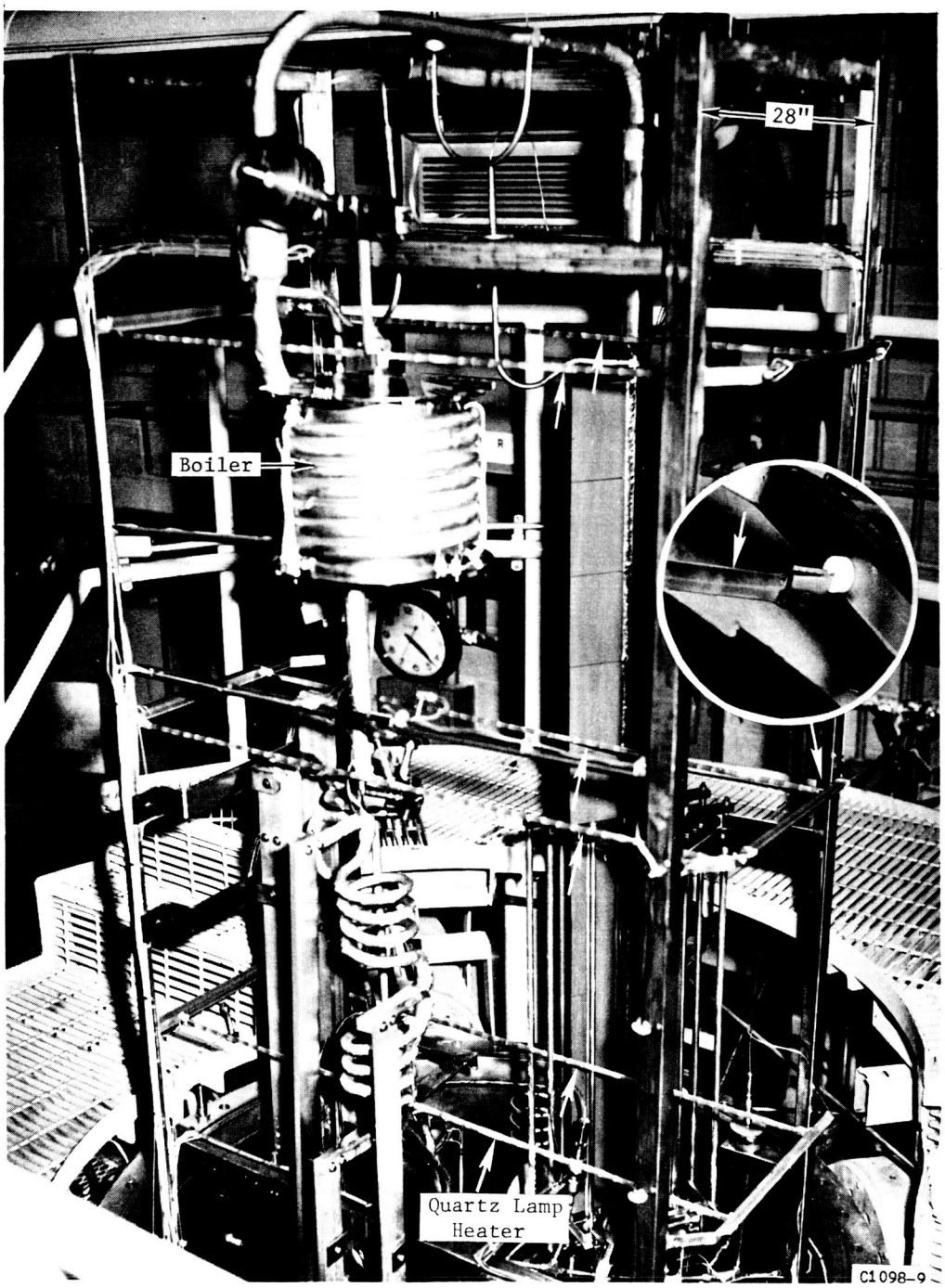

Figure 101. Cb-1Zr Corrosion Test Loop Following Installation of Quartz Lamp Heaters for Distillation. Typical Heater Mount Shown in Enlarged Insert. Six Quartz Heaters Indicated With Arrows. (Orig. C66031752, C66031753)

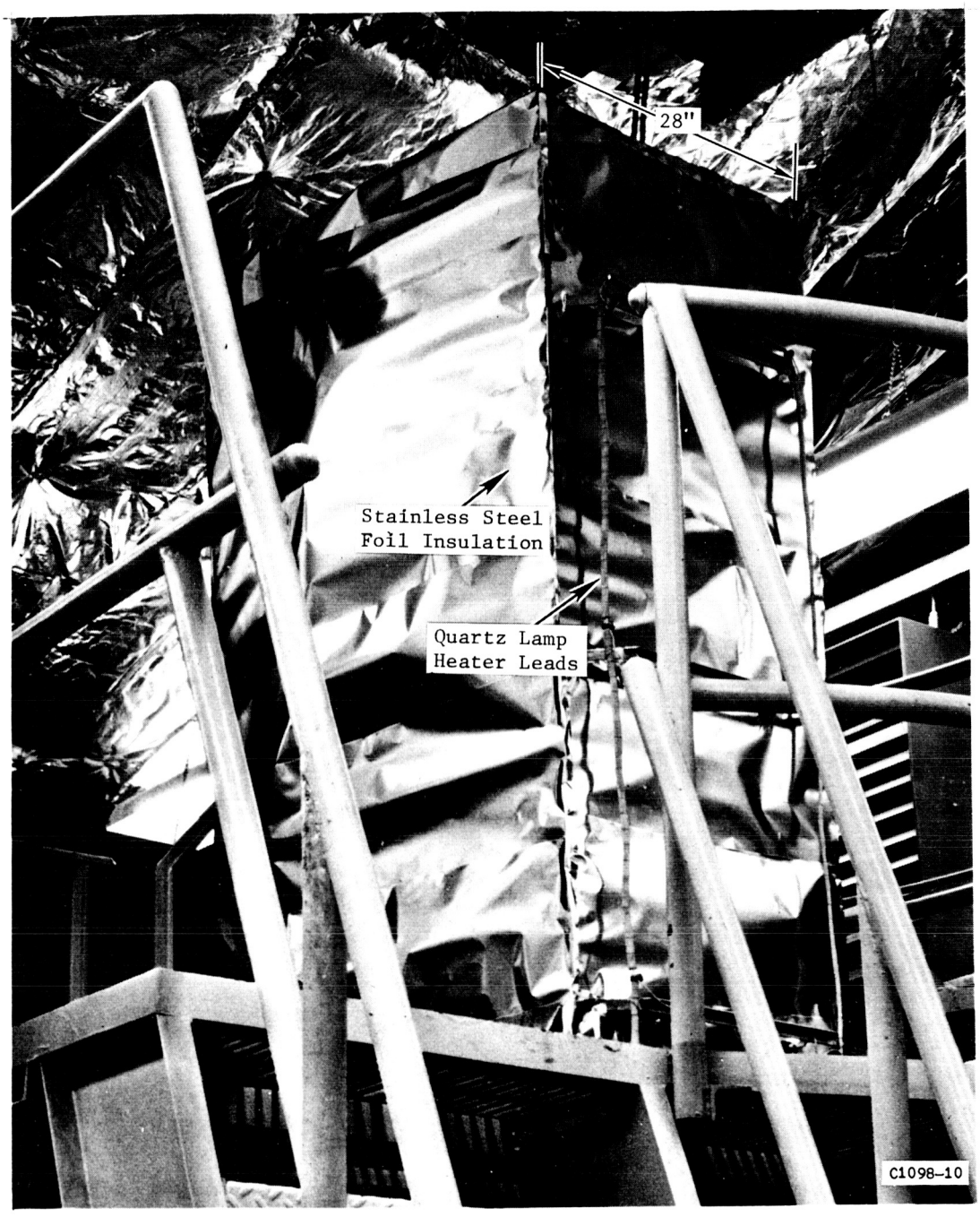

Figure 102. Loop Following Installation of Two Layers of Stainless Steel Foil Reflective Insulation in Preparation for Distillation of Alkali Metals From the Loop Circuts to the Surge Tanks. (Orig. C66041410)

pump was turned on and after approximately five hours the ion pump confined. The stainless steel foil thermal insulation which enclosed the loop not only contributed to the outgassing load but also reduced the conductance of the gases emanating from the surface of loop components. The chamber bakeout system was turned on after the chamber pressure was in the 10^{-7} torr range. The system was outgassed for approximately 50 hours with only the bakeout heaters on. The loop temperature during this period was approximately 500°F. The quartz heaters were then turned on at low power. The power to the EM pump was also turned on (approximately 10 percent of the rated power) to heat up the pump duct and to accelerate the outgassing of the metal foil insulation which surrounded the pump duct. During the next 30 hours, the quartz heaters were slowly increased in power to reach the desired distillation temperature of 1000°F. The power was increased in small increments to hold the chamber pressure in the 10^{-7} torr range. During this period the titanium sublimation pump was used to assist the ion pump in handling the outgassing load.

At 1200 on April 2, 1966, the distillation period began with the loop temperature at 960°F and the EM pump ducts at 1120°F. The vacuum chamber pressure at this time was 4×10^{-7} torr. The stated thermal conditions were maintained for 100 hours, and at the end of the distillation the chamber pressure had decreased to 8.7×10^{-8} torr.

B. DRAINING AND SAMPLING OF ALKALI METALS FROM THE LOOP

At the end of the 100-hour distillation period described above, the sodium and potassium were drained by gravity feed from the loop surge tanks to the charge tanks located in the transfer systems which were described in Section VI, Part C.

The sodium surge tank was gravity drained and subsequently pressurized to 10 psia with high-purity argon to assure complete transfer of sodium to the charge tank located in transfer system. Following the gravity drain of the potassium surge tank, the Cb-1Zr alloy isolation valve located between the surge tank and loop proper was closed and high-purity argon was used to pressurize the potassium surge tank to 10 psia to complete the transfer of residual potassium in the drain lines to the charge tank in the transfer

system. During a ten-minute period, no pressure rise was detected on the loop side of the isolation valve indicating that a gas tight seal had been achieved when the isolation valve was closed.

Samples of potassium and sodium were then taken from the charge tanks of the transfer system using the procedures described previously.[48] The remaining potassium and sodium in the charge tanks were pressurized through 5-micron stainless steel filters to the disposal tanks. The draining, sampling, and filtering operations described briefly above are covered in detail in Appendix K, Draining, Sampling, and Filtering of the Potassium and Sodium Circuits of the Loop, of this report.

C. ANALYSIS OF SODIUM AND POTASSIUM SAMPLES FROM THE LOOP

The sodium and potassium samples obtained from the loop surge tanks were analyzed for oxygen, nitrogen, total carbon, and metallic impurities. In addition, the residues extracted from the sodium and potassium by filtration during the transfer from the loop surge tanks to the disposal tanks were analyzed semiquantitatively to determine the concentrations of metallic elements.

The results obtained from these analyses are presented in Table XX. As shown in the table, the oxygen concentrations as determined by the amalgamation method for both sodium and potassium were at the 5 ppm level - the same level found before the start of the 5000-hour test. No nitrogen was detected in either sample. The carbon concentrations obtained were about 20 ppm which is considered a normal level for high-purity sodium and potassium. Both alkali metals contained metallic impurities at or near the limit of detection before the test, and the posttest results were essentially the same.

Spectrographic analysis of the minute amount of residue obtained by filtration of the sodium and potassium revealed no indication of columbium, zirconium, or molybdenum. Iron, chromium, and nickel were detected in the

(48) Dotson, L. E. and Hand, R. B., Purification, Analysis, and Handling of Sodium and Potassium - Potassium Corrosion Test Loop Development Topical Report No. 4., R66SD3012, General Electric Company, Cincinnati, Ohio, June 13, 1966, p. 35.

TABLE XX

RESULTS OF ANALYSES OF SODIUM, POTASSIUM, AND FILTER RESIDUES
AFTER THE 5000-HOUR ENDURANCE TEST OF THE PROTOTYPE LOOP

Sample Identity	Oxygen ppm	Nitrogen ppm	Carbon ppm	Metallic Elements, ppm in Alkali Metal																				
				Al	Ag	B	Be	Ca	Cb	Co	Cr	Cu	Fe	Mg	Mn	Mo	Ni	Pb	Si	Sn	Ti	V	Zr	Na
Sodium from Primary Loop Surge Tank after 5000-Hour Endurance Test, Sampled at 250°-300°F	5,6	<5 (ND)	18,26	<3	<3	<38	<3	<3	<13	<3	<3	<3	<3	<3	<3	<3	<3	<13	<3	<13	<3	<13	<13	--
Potassium from Secondary Loop Surge Tank after 5000-Hour Endurance Test, Sampled at 250°-300°F	4,6	<5 (ND)	20,21	<2	<2	<19	<2	2	<10	<2	<2	<2	<2	<2	<2	<2	<2	<10	10	<10	<2	<10	<10	24
Residues from Five-Micron, Type 316 SS, Sintered Filters																								
Sodium	--	--	--	-	-	-	-	-	ND	-	D	-	D	-	-	ND	D	-	-	-	-	-	ND	-
Potassium	--	--	--	-	-	-	-	-	ND	-	D	-	D	-	-	ND	D	-	-	-	-	-	ND	-

D = Detected
ND = Not Detected

residue, but this was not considered to be significant since these elements are attributed to contamination from the porous filter itself, which is made of stainless steel.

D. DISASSEMBLY AND EXAMINATION OF LOOP COMPONENTS

The disassembly of the loop was started immediately after the completion of the distillation and removal of the residual alkali metal from the loop. Following the opening of the vacuum chamber, the thermocouples, valve operating flexible cables, and electric power leads were disconnected to permit the transfer of the spool piece to the floor of the test area to facilitate the disassembly of the loop proper into its various components. It was also necessary to remove the EM pump electrical windings (stators) before moving the spool piece. This was accomplished by removing the stator flange bolts and rolling the stators back along the overhead trolleys. Prior to moving the spool piece, the potassium and sodium fill lines and the argon pressurization lines were cut with cold weld pinch-off devices which sealed the loop under a positive argon pressure. The pinch-off devices used are shown in Figure 103.

The procedure used to transfer the loop and spool section to the disassembly area was as follows. The bolts connecting the lower spool section flange to the sump flange were removed first. The bell jar was then lowered to the spool section and bolted to the upper spool section flange. The bell jar and spool section (with the loop) were hoisted vertically approximately 10 inches with the overhead hoist to allow a 2-ton fork lift truck to position a cushioned pallet under the spool section. The spool and bell jar were then lowered to the pallet. The hoisting bolts joining the spool to the bell jar were removed, and the bell jar alone was hoisted up to clear the top of the loop. The spool and loop were then moved from the test site to the floor of the disassembly area by the fork lift truck.

The first phase of loop disassembly was the removal of all thermocouples and thermal insulation. The thermocouples were removed intact and packaged with their identifying number. The components in the lower portion of the loop circuits are shown in Figure 104 following removal of insulation and thermocouples.

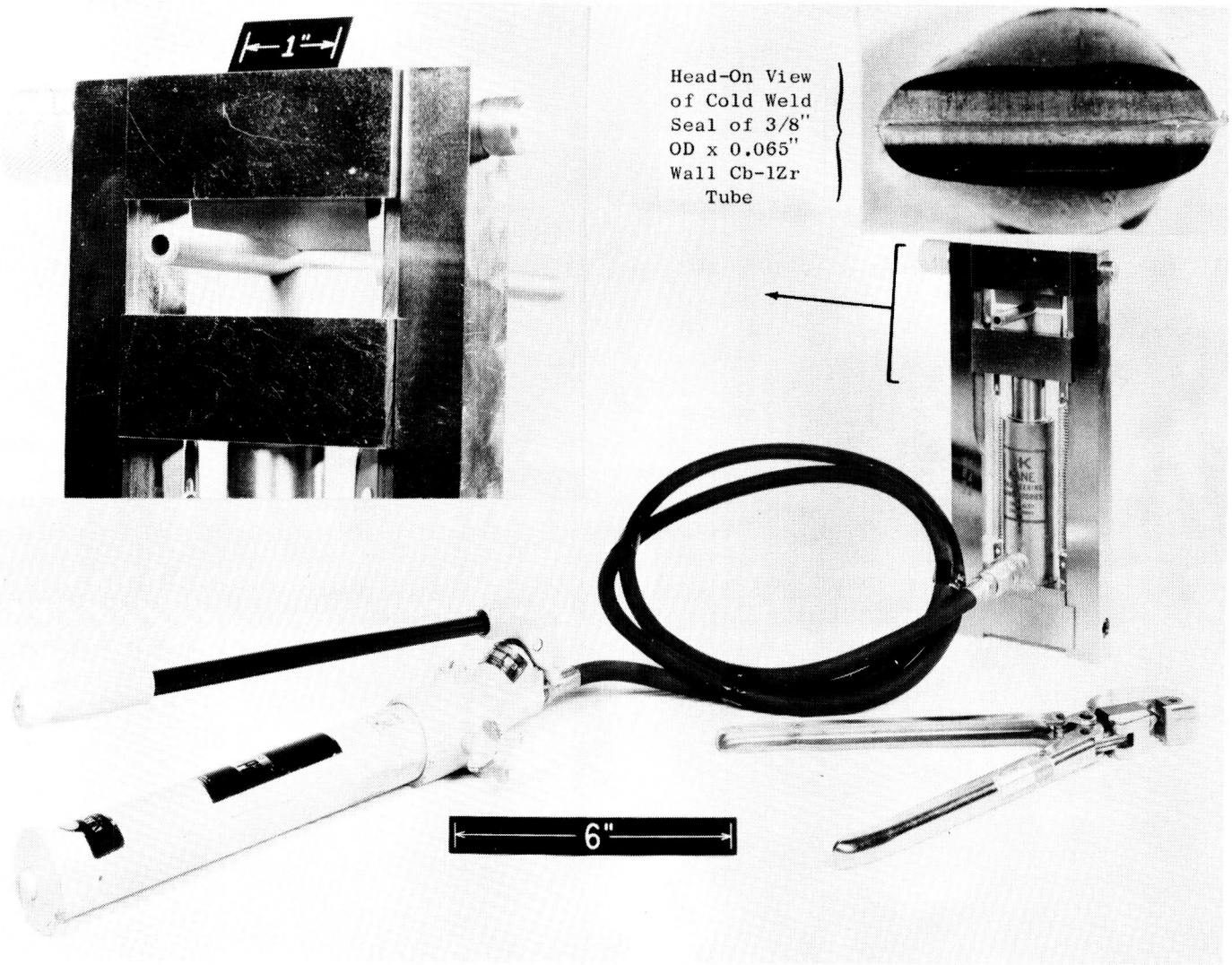

Figure 103. Manual and Hydraulic Cold Weld Pinch-Off Devices Used to Seal Cb-1Zr Alloy Tubing During Sectioning of Corrosion Test Loops. (Orig. C650621104)

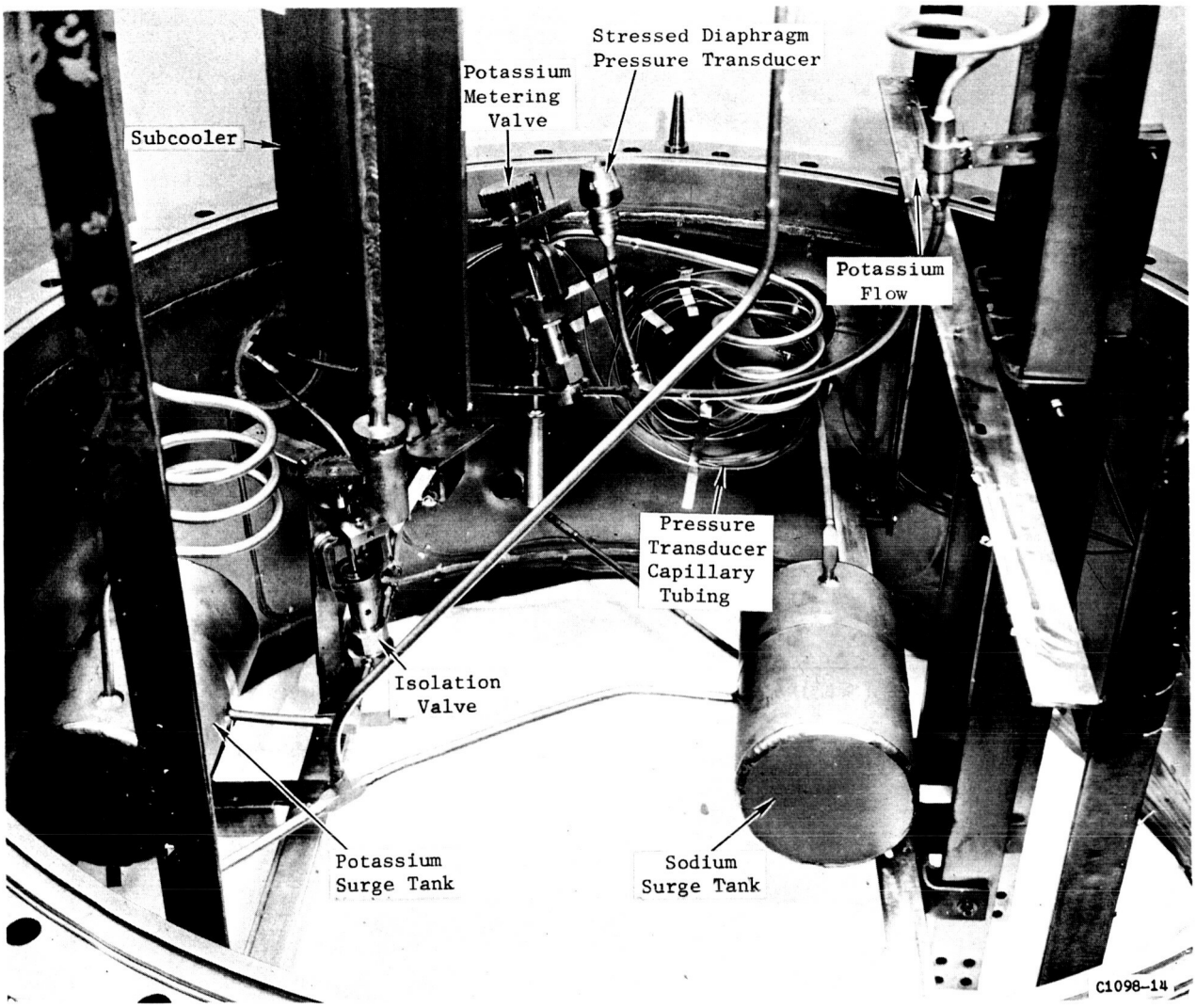

Figure 104. Lower Portion of the Loop Following Removal of Insulation and Condenser Shield Assembly. (Orig. C66050425)

The second phase of the disassembly was the division of the loop into its major components. The procedure used was to cut the connecting tube near each component with the cold weld pinch-off devices that sealed the tube as the cuts were made. This precaution was taken to allow a more careful examination of the components for residual alkali metal which might not have been removed during the posttest distillation.

The sodium and potassium pump ducts and the insulation assemblies which surrounded them were removed from the stainless steel cans which form the vacuum seal to the chamber wall. The two Cb-1Zr pump ducts are shown in Figure 105 following removal of the 20 layers of Cb-1Zr foil used to insulate the pump ducts from the stainless steel vacuum cans which surrounded them. In order to determine if any corrosion had occurred in the potassium pump, it was cut open to expose the helical portion for visual examination. This was accomplished by first removing the Cb-1Zr end caps. A small amount of residual potassium was detected after removal of these end caps, and this was removed by immersing the pump duct in butyl ethyl "Cellosolve."[(a)] One-half of the duct can was removed by milling two longitudinal slots to within a few mils of the helical duct and then forcing the slots apart. The pump duct's parts are shown in Figure 106 following disassembly. All parts of the pump appeared to be unaffected by the 5000-hour test.

A number of the loop components were radiographed prior to disassembly in order to determine if any notable changes had occurred during the test. Figure 107 shows prints of two radiographs of the boiler. Comparison of these radiographs with pretest radiographs revealed no obvious differences. During subsequent disassembly of the boiler, the coiled section was cut into a single loop and the potassium containment tube extracted from the sodium containment tube. The excellent appearance of these tubes following test is illustrated in Figure 108.

Examination of the iron titanate (Fe_2TiO_5) coating on the Cb-1Zr

(a) Trademark.

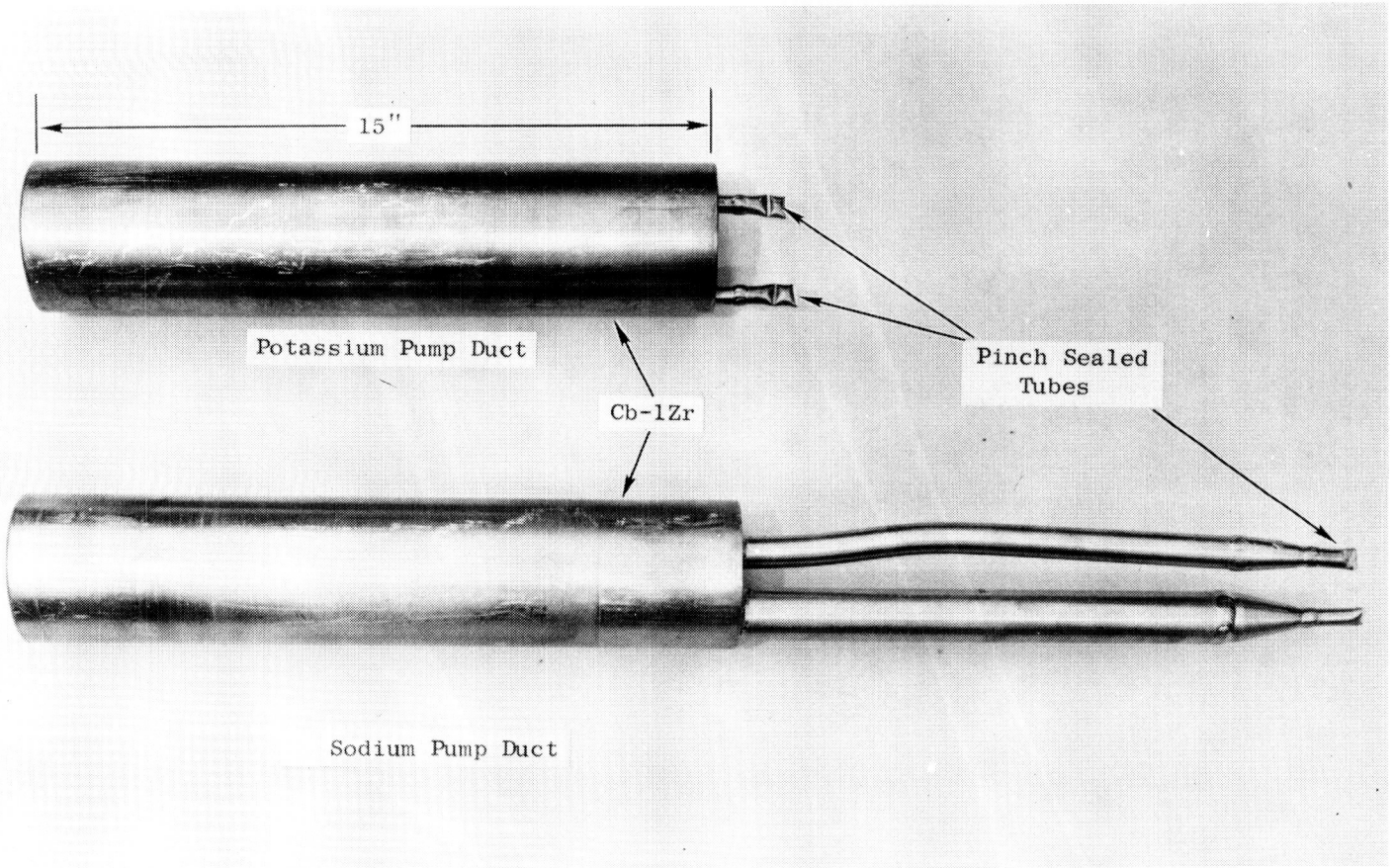

Figure 105. Potassium and Sodium Pump Ducts Following Separation From the Loop Circuits and Removal of the Vacuum Enclosure Cans and Cb-1Zr Insulating Foil. (Orig. C66042713)

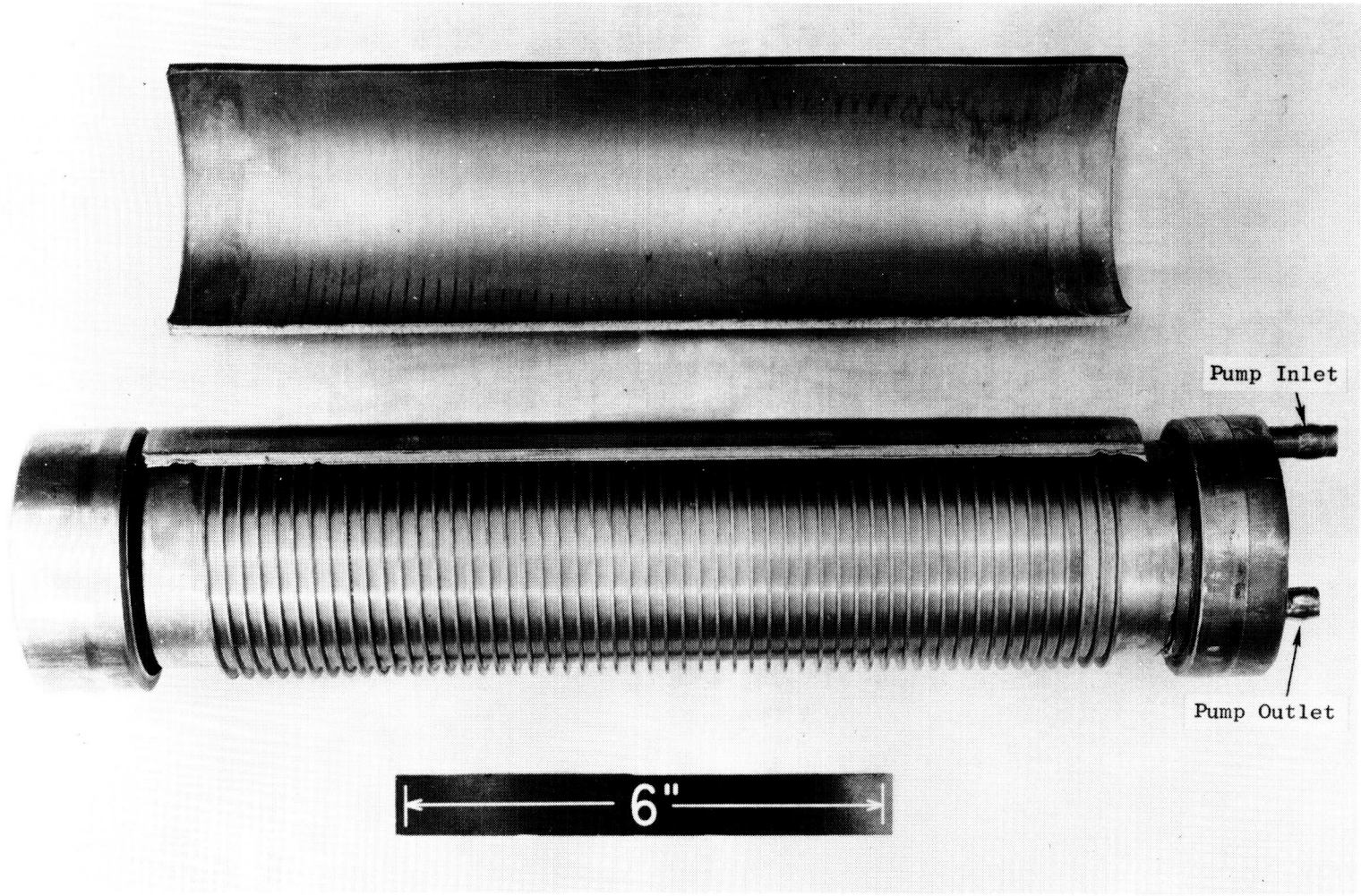

Figure 106. Potassium Pump Duct After Removal of Half of the Pump Duct Can Following Completion of the 5000-Hour Test. (Orig. C66052710)

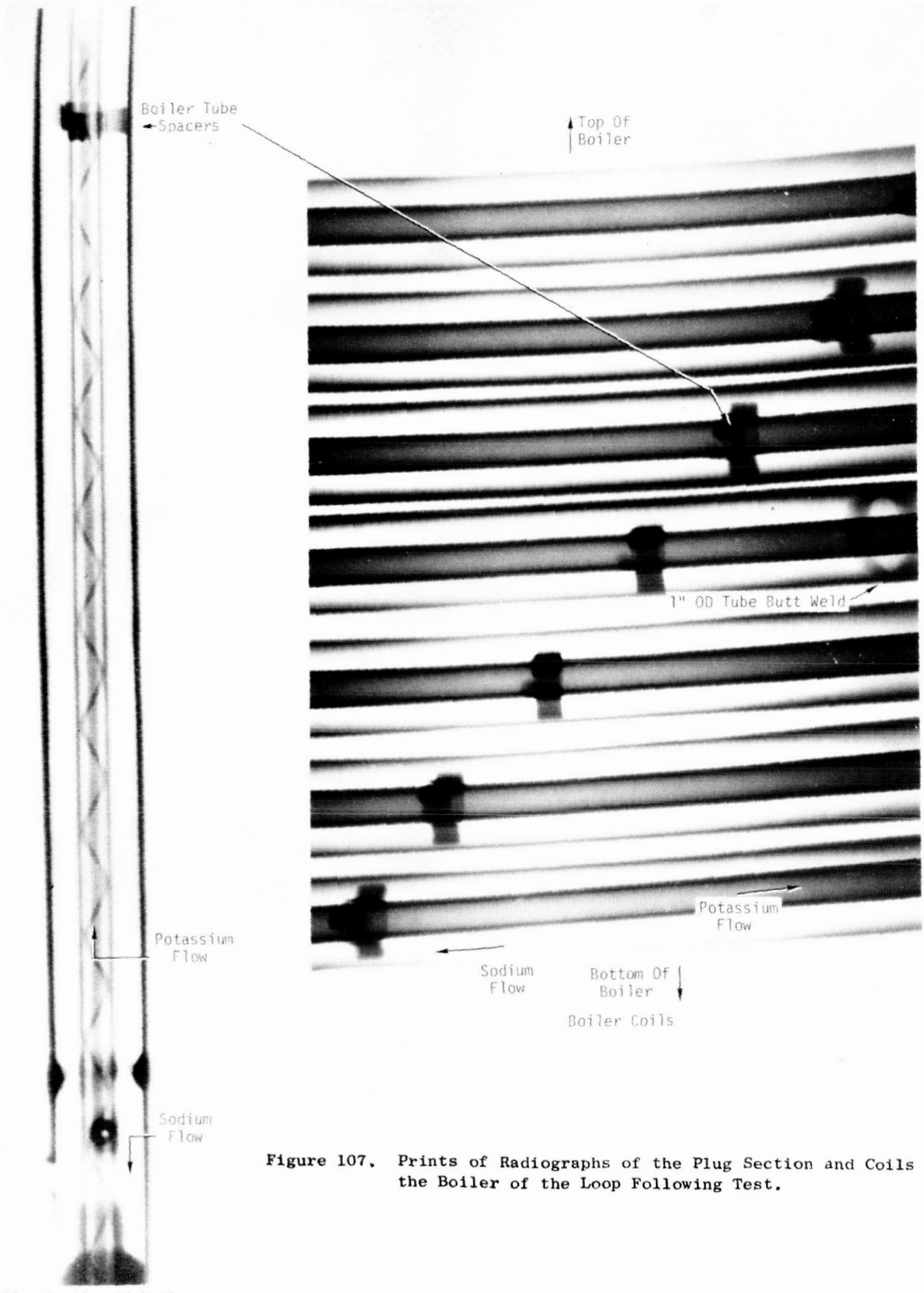

Figure 107. Prints of Radiographs of the Plug Section and Coils of the Boiler of the Loop Following Test.

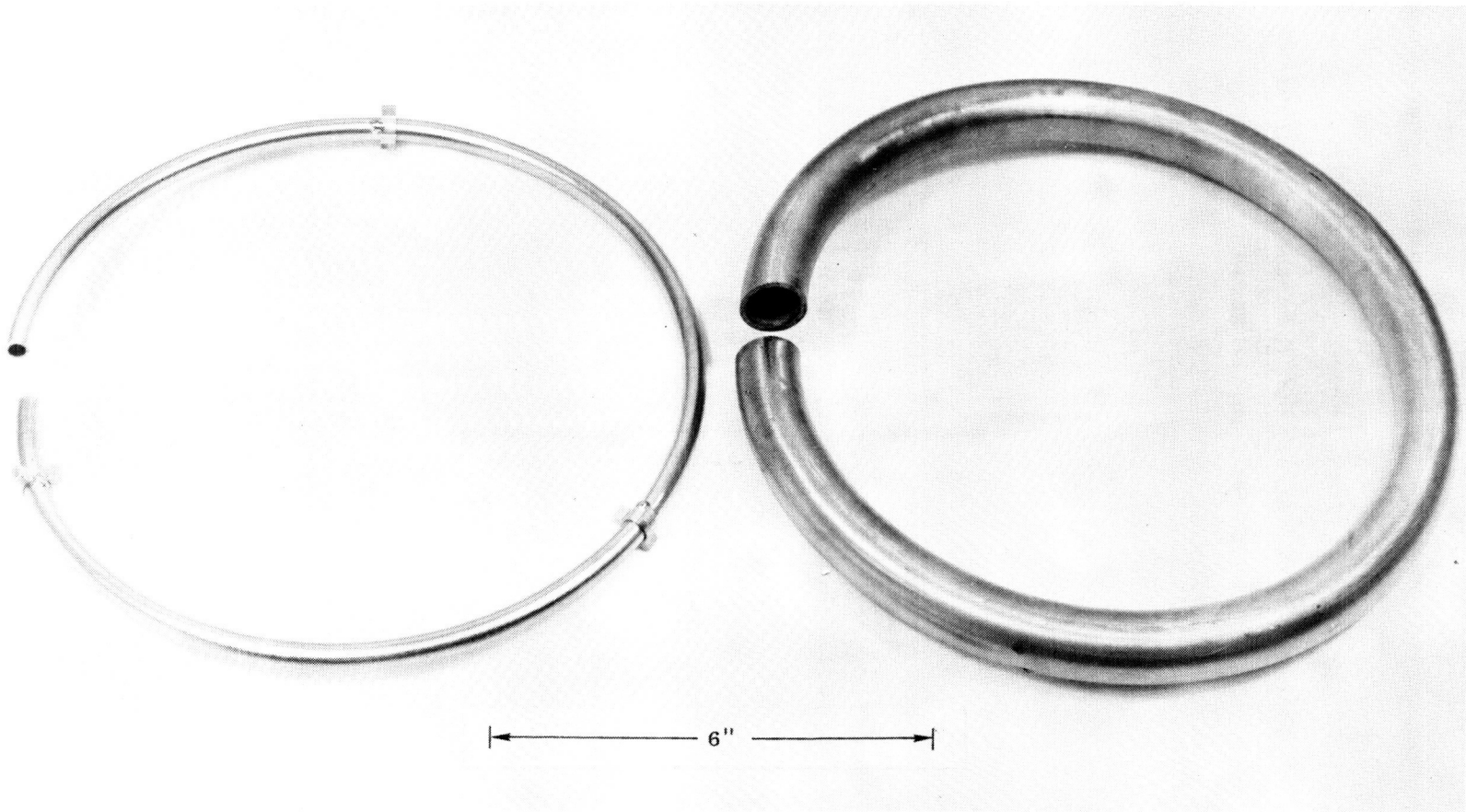

Figure 108. Potassium Containment Tube (3/8-Inch OD) and Sodium Containment Tube (1-Inch OD) from the Tube-in-Tube Helical Boiler. (Orig. C66051951)

condenser fins indicated that no deterioration or color change had occurred during the 5000 hours of loop operation. A portion of the condenser and an untested specimen are shown in Figure 109. The temperature of the 8-inch-wide by 60-inch-long fin varied from 1400°F in the hottest areas closest to the condenser tube to about 800°F in the cooler regions at the outer edges of the fins.

As discussed in the previous section of this report, the posttest evaluation of the operation characteristics of the metering and isolation valves indicated some binding in the valve gear drive system. During the disassembly, the valve drive system was carefully examined to determine the cause of this difficulty. The metering valve assembly is shown in Figure 110 following removal from the potassium circuit of the loop. Visual examination of the stainless steel drive gears of both the isolation and metering valve revealed that galling has occurred between the pinion gear and the spur gear. This galling was responsible for the difficult and erratic valve operation observed on several occasions when valve adjustments were attempted. The cause of the galling was a misalignment of the pinion gear due to an excessive tolerance in the fit of the pinion gear shaft in the tungsten carbide bushing. (A design change has been issued to correct this problem, and consideration is being given to the use of gear materials having good resistance to galling.) The bellows and plug assembly was then removed from the valve body. These components are shown in Figure 111. No evidence of wear or erosion was visible on either the Mo-TZM alloy plug or the Cb-1Zr seat after 5000 hours at 1100°F and a potassium liquid velocity of 17 ft/sec.

The most critical portion of the disassembly sequence was the removal of the Mo-TZM alloy nozzle and blade specimens from the Cb-1Zr casing of the turbine simulator. One requirement of the test was to obtain weight change data on the nozzles and blades. This requirement resulted in a design which incorporated a groove along the length of the nine-stage turbine simulator and the Cb-1Zr casing. A Cb-1Zr wire was inserted into this groove during assembly as illustrated in Figure 112. This wire served

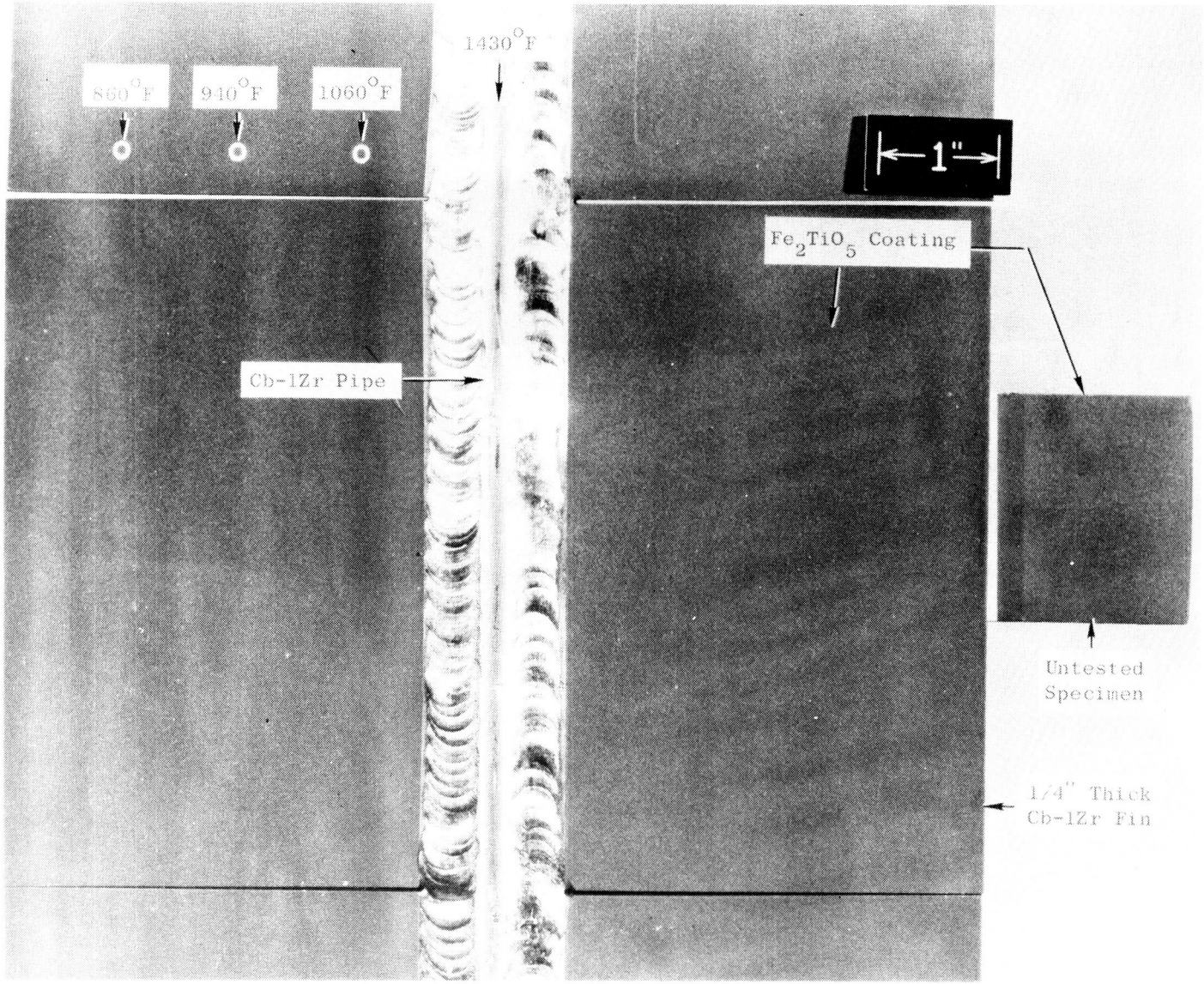

Figure 109. Condenser Pipe and Fin Following Completion of 5000-Hour Test. (C66050428)

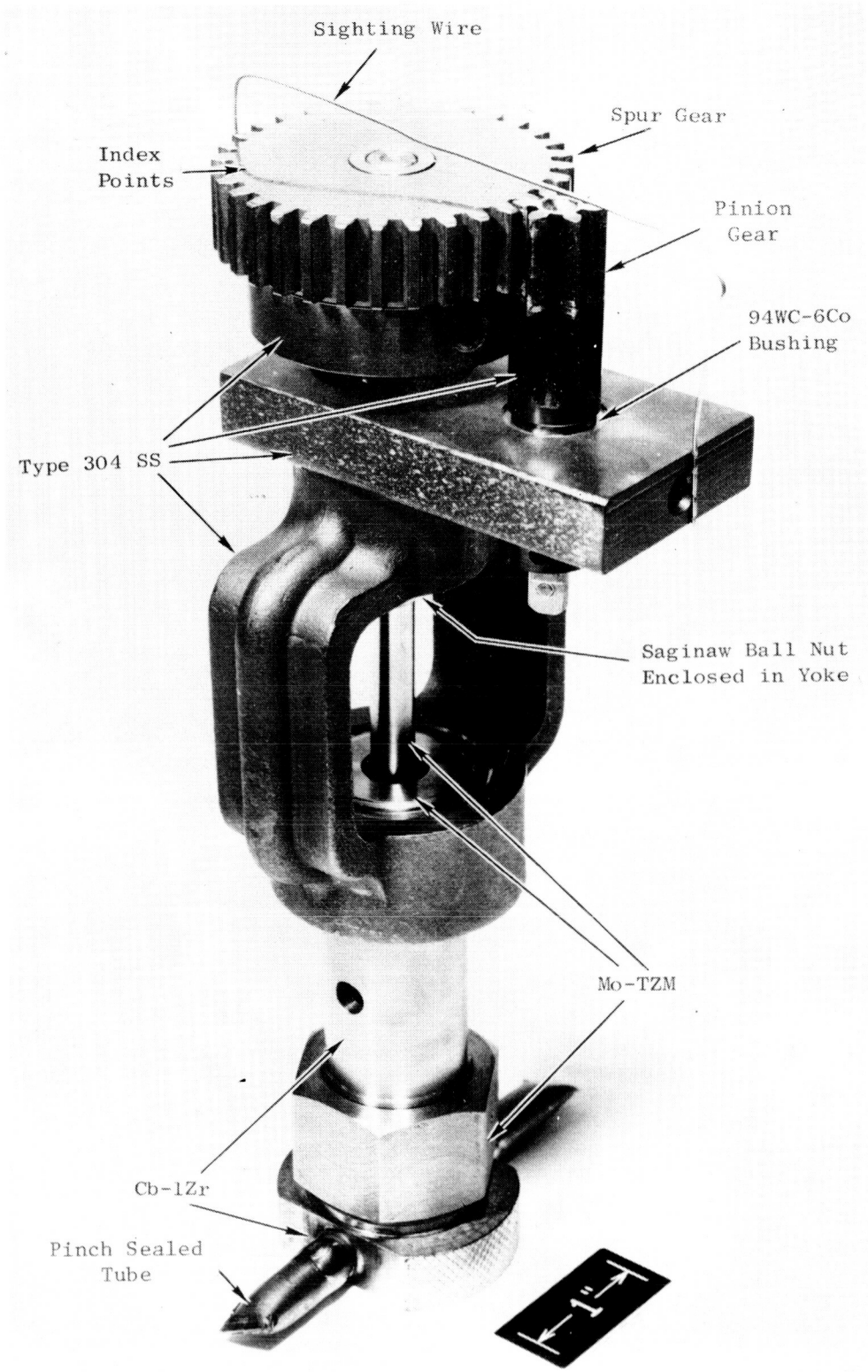

Figure 110. Metering Valve Following Completion of the 5000-Hour Test. (Orig. C66042917)

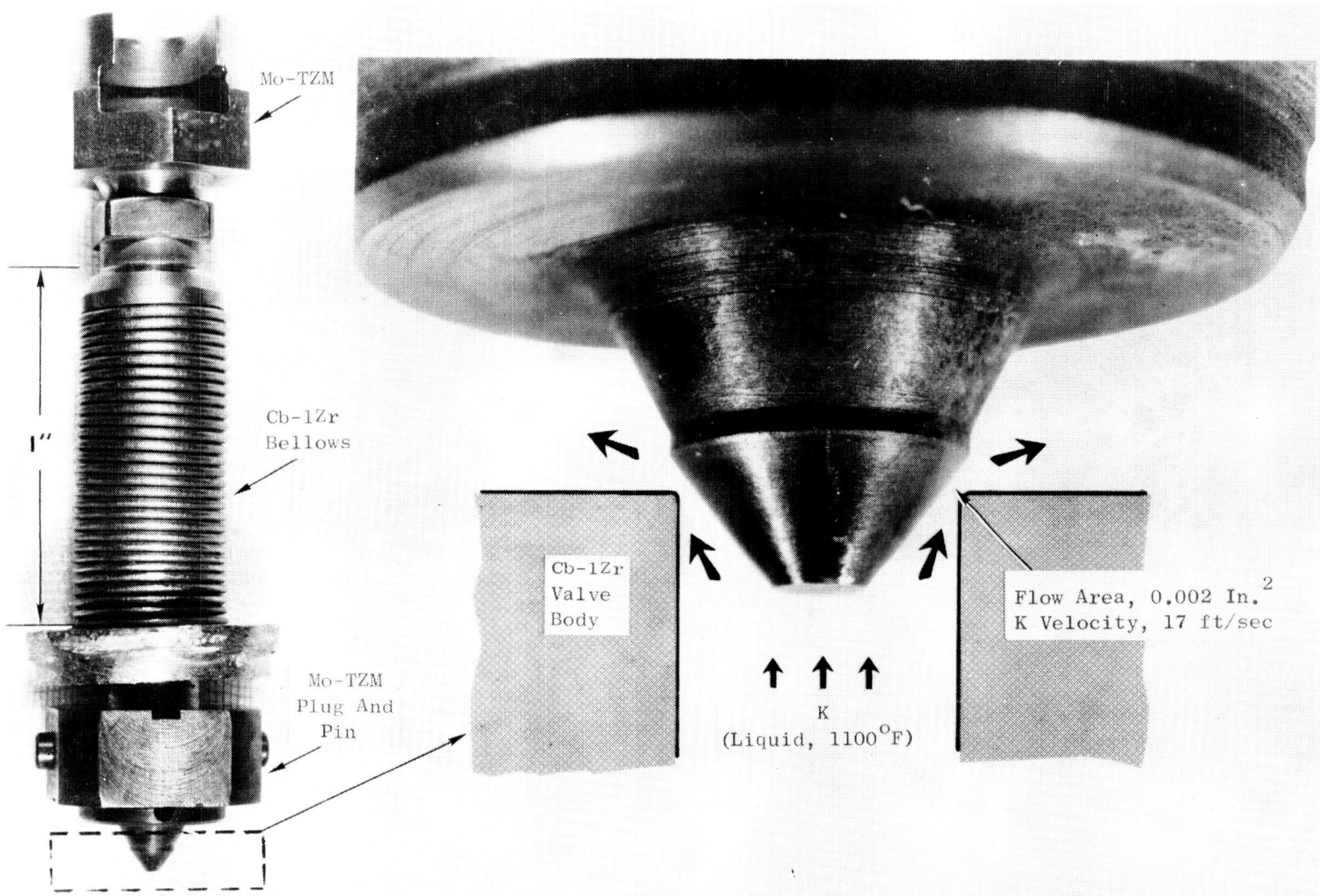

Figure 111. Bellows and Plug Assembly of the Metering Valve After Disassembly Following the 5000-Hour Test. (Orig. C66051948, C66051949)

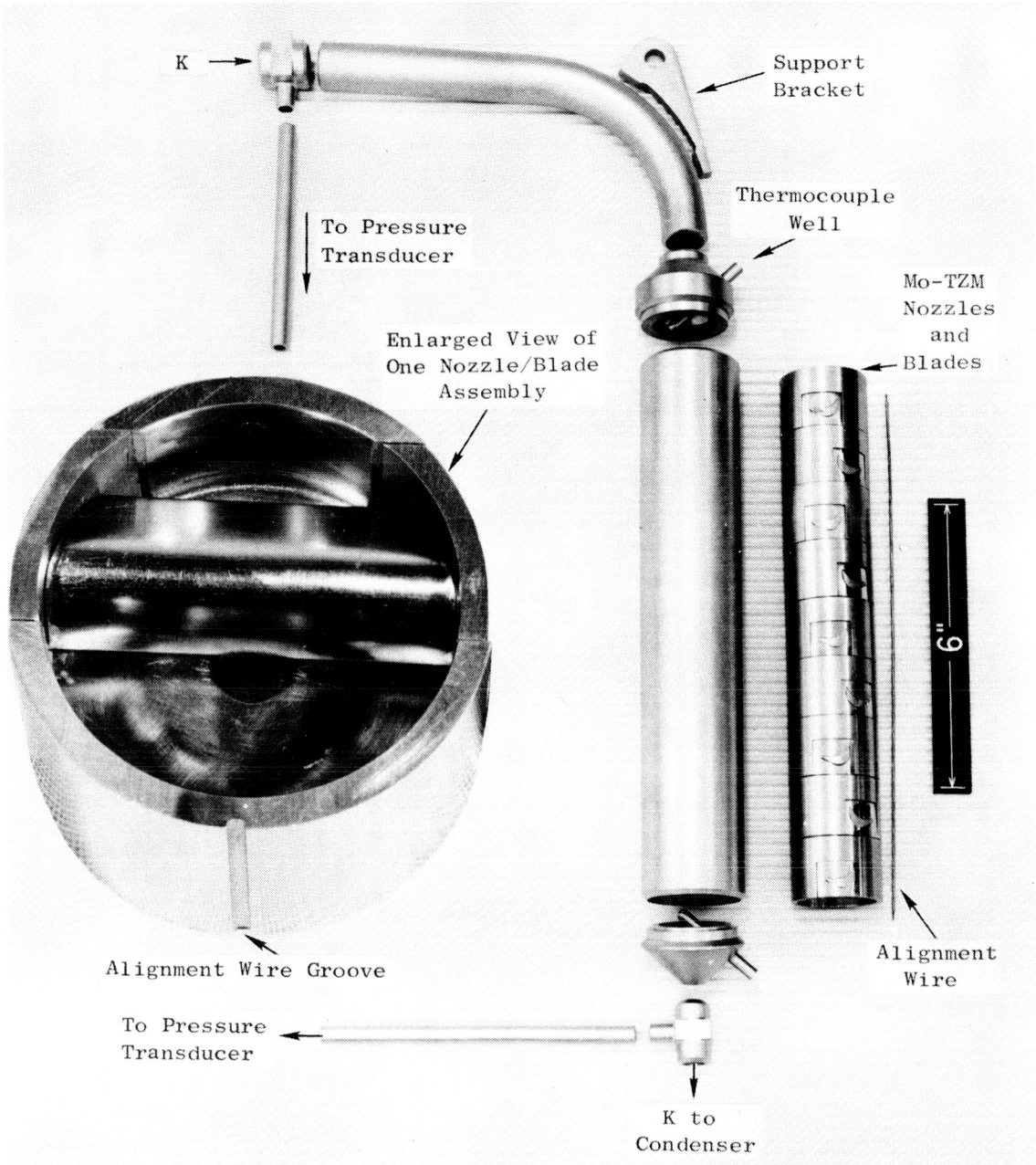

Figure 112. Nine-Stage Turbine Simulator Prior to Assembly Showing the Alignment Wire Which was Cut into During Component Disassembly to Permit Spreading of Specimen Casing and Removal of Nozzle and Blade Specimens. (Orig. C65062198, C65031228)

as a key in preventing rotation of the individual nozzles in the casing during test operation, but its primary purpose was to facilitate disassembly of the turbine simulator without damaging the nozzles and blades. By making a longitudinal cut through the Cb-1Zr casing over the wire, it was possible to spring open the casing and free the Mo-TZM specimens without cutting into them. The milled groove in the casing is shown in Figure 113. The enlarged view in this illustration shows the Cb-1Zr wire and the separation of the casing. Removal of the stack of nine nozzles and blades from the casing was done by spreading the slot approximately 1/16 inch and gently tapping the casing. The specimens slipped from the casing with no evidence of bonding between the casing and the specimens.

Following the removal of the Mo-TZM alloy turbine simulator nozzles and blade specimens from the Cb-1Zr containment casings, as described above, visual examinations at a magnification of 30 diameters were performed. The entrance side of the ten nozzles and the blade - blade pad assemblies are shown in Figure 114. The exit sides of the nozzles are shown in Figure 115. With the exception of a few small slightly darkened areas on the exit side of several of the blades, the specimens looked just as they did before the test. No evidence of impingement damage could be detected on any of the ten blade specimens. It may be noted in Figure 114 that the only blade specimen which gave a clear indication of the impingement area was the blade in Stage No. 1. The results of weight change measurements on the nozzles and blades are given in Table XXI and indicate that no significant weight changes occurred.

Flow patterns were evident as slight discolorations on both the concave and convex surfaces of some of the blade specimens as shown in Figure 116. No significant deposition or metal removal was associated with these "patterns" as indicated by the weight and dimensional change data discussed below in Table XXI or by subsequent metallographic evaluation reported in the next portion, Section XII, of this report.

Prior to the assembly of the turbine simulator, the throat diameters of the Mo-TZM alloy nozzle specimens were measured in order to determine

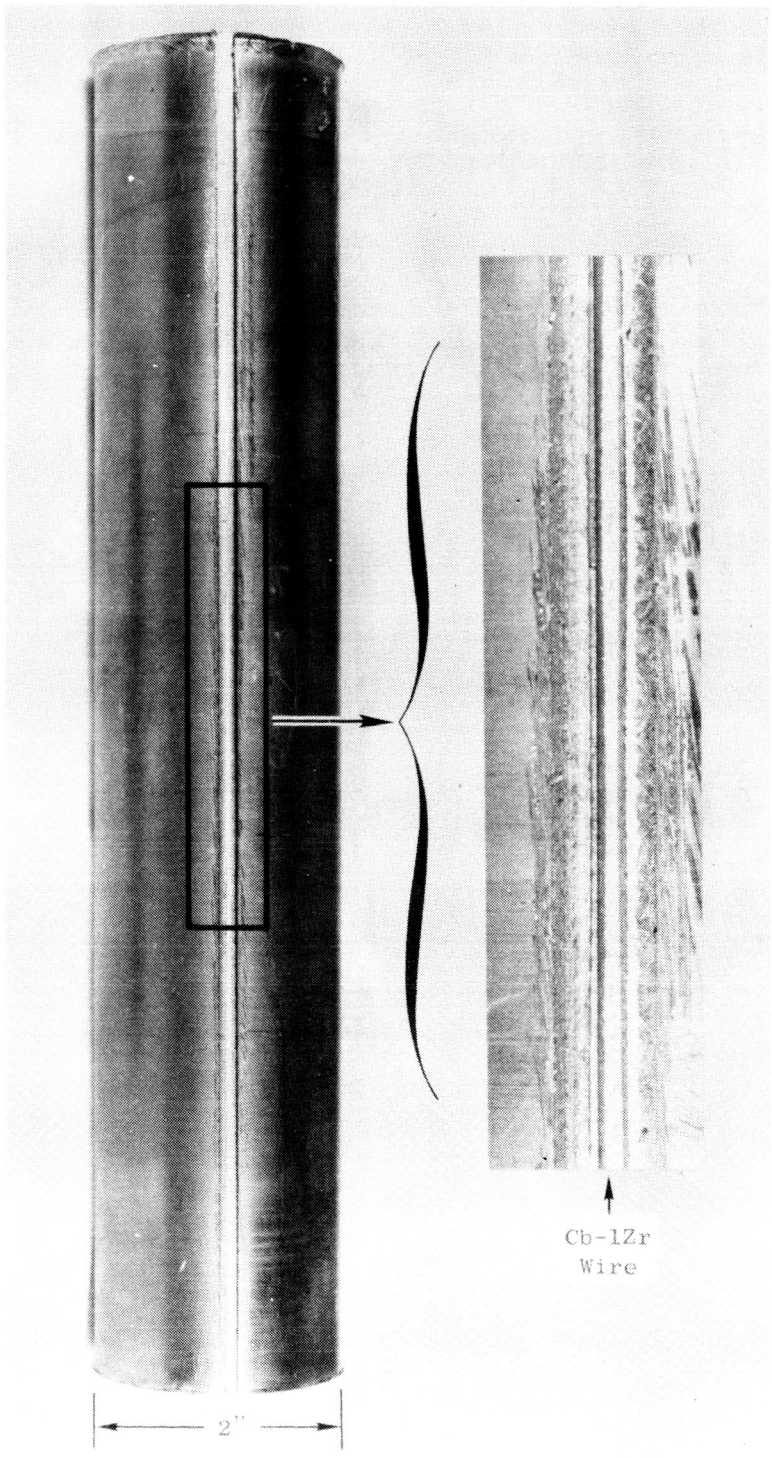

Figure 113. Cb-1Zr Casing of Nine-Stage Mo-TZM Alloy Turbine Simulator Showing Milled Groove and Cb-1Zr Alignment Wire Just Prior to Removal of Simulator Nozzles and Blades. (Orig. C66050517, C66050526)

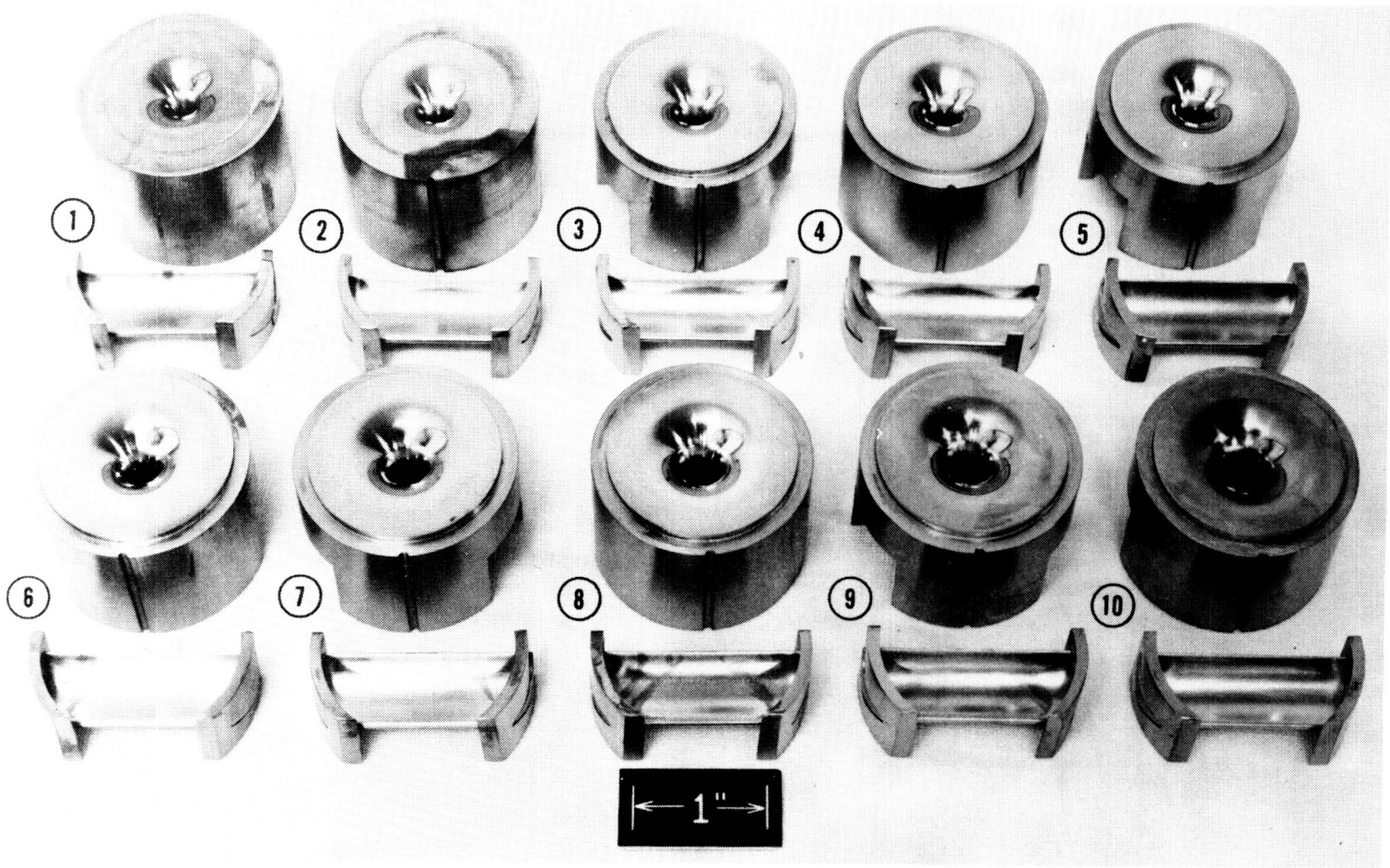

Figure 114. Mo-TZM Alloy Turbine Simulator Nozzles, Blade Specimens and Specimen Holding Pads Following 5000-Hour Exposure to Potassium. (Orig. C66050510)

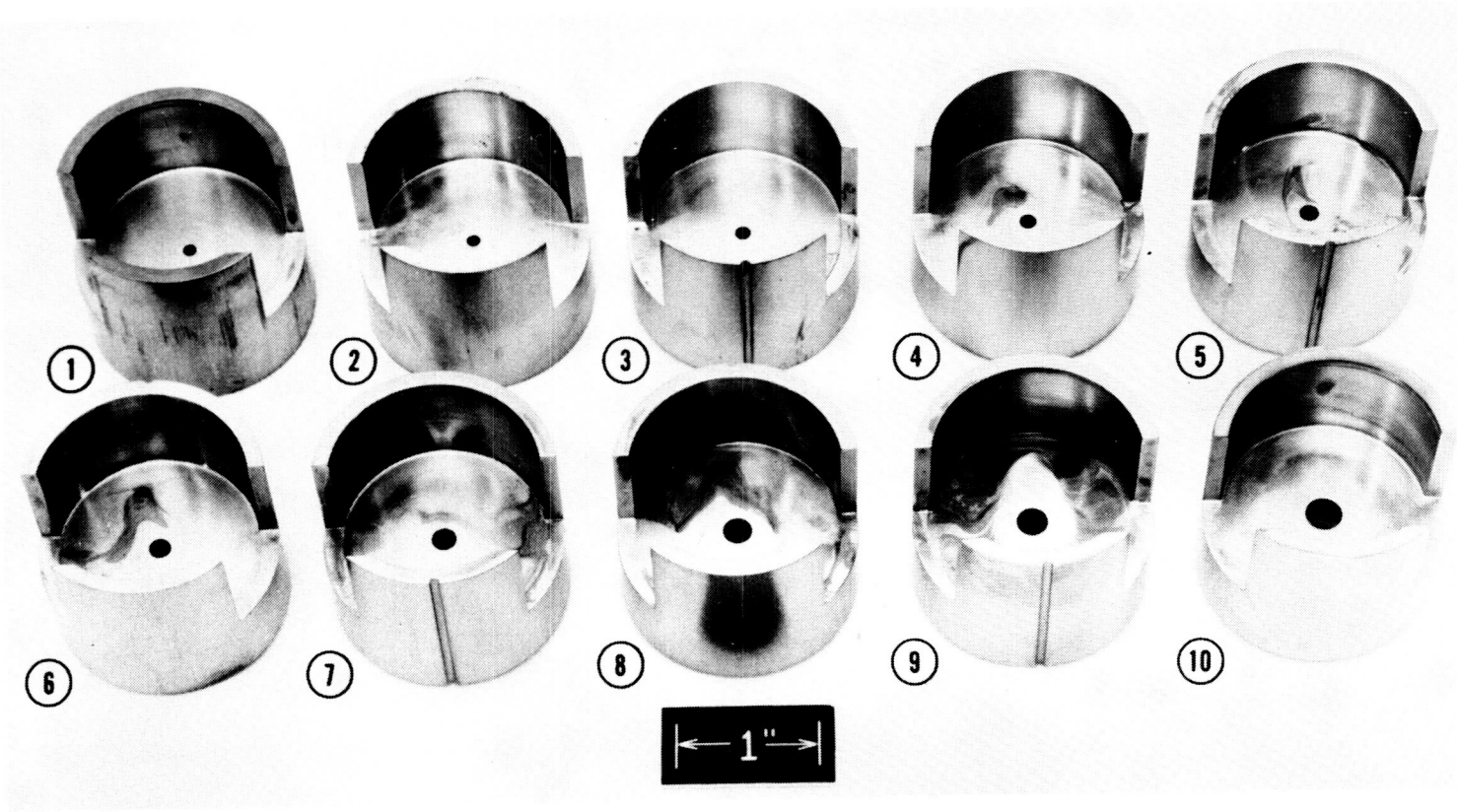

Figure 115. Outlet Side of Nozzles of Turbine Simulator Stages No. 1 Through No. 10. Nozzle Throat Diameters Increase From Nozzle No. 1 (Upper Left) to No. 10 (Lower Right). (Orig. C66050515)

TABLE XXI

SUMMARY OF DIMENSIONAL MEASUREMENT CHANGES ON THE Mo-TZM NOZZLES AND THE WEIGHT CHANGE DATA ON BOTH NOZZLE AND BLADE SPECIMENS

Stage No.	Nozzle Inlet Temperature, °F	Impingement Velocity, ft/sec	Quality	Nozzle Throat Diameters, Inch[a]			Weight Change,[b] g	
				Before Test	After Test	Change	Blade	Nozzle
1	2000	1125	138° superheat	0.099430	0.099445	+0.000015	-0.002	-0.001
2	1785	1350	88%	0.101090	0.101045	-0.000045	0	+0.008
3	1740	1200	↓	0.115280	0.115370	+0.000090	+0.001	+0.006
4	1700	1110		0.128995	0.129000	+0.000005	+0.001	+0.008
5	1660	1080		0.141187	0.141235	+0.000048	+0.001	+0.009
6	1620	1015		0.158037	0.158035	-0.000002	0	+0.006
7	1575	1045		0.175690	0.175707	+0.000017	0	+0.008
8	1535	845		0.205077	0.205085	+0.000008	-0.001	+0.007
9	1490	860		0.222787	0.222805	+0.000018	0	+0.008
10	1450	830		0.249220	0.249195	-0.000025	0	+0.007

(a) The accuracy of these measurements is ±0.00005 inch performed by the Sheffield Corporation, Dayton, Ohio.

(b) Nominal weight of blade specimens was 25 g; nominal weight of nozzles was 255 g. Weight change data obtained to four decimal places and reported to nearest mg.

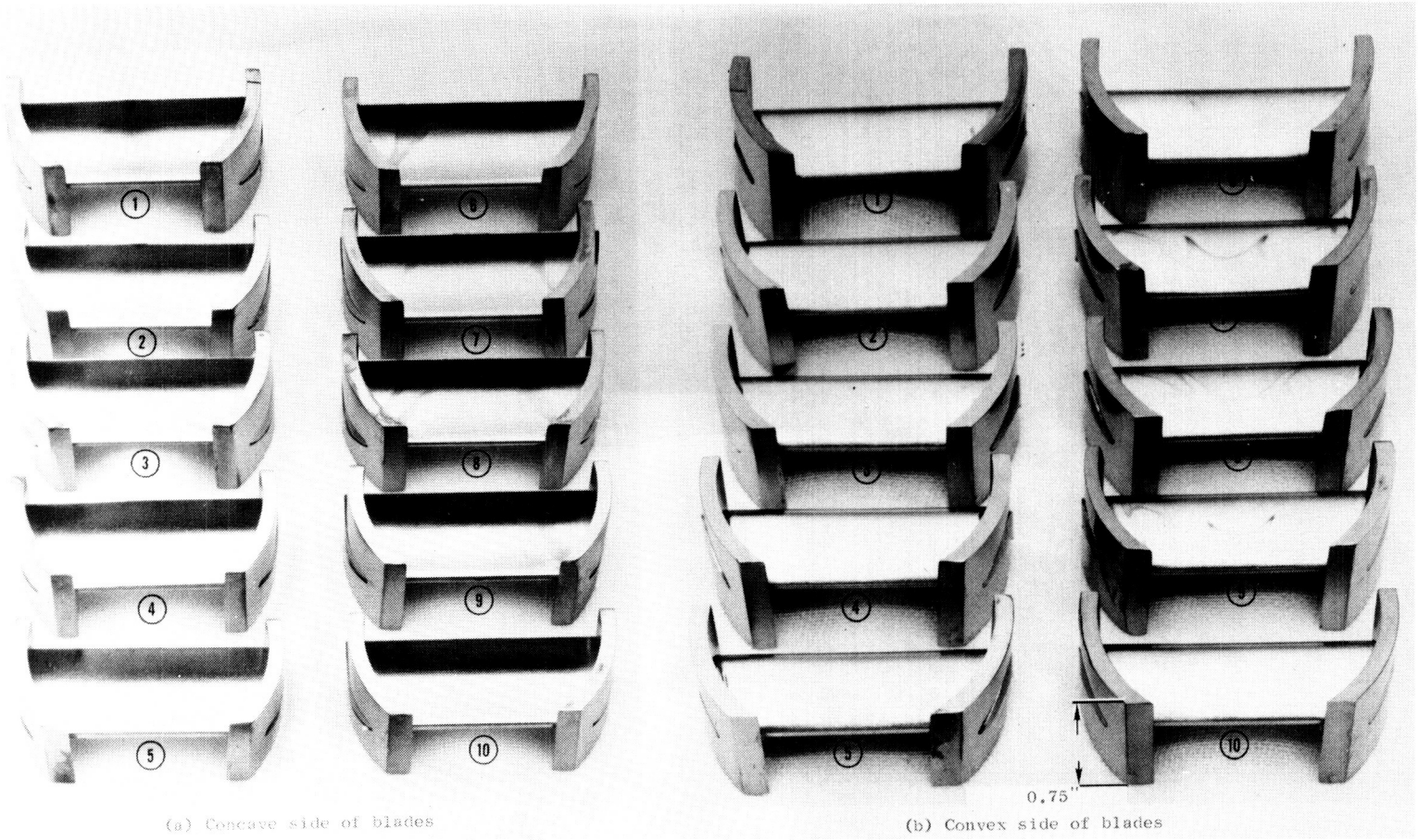

Figure 116. Photographs of Concave (a) and Convex (b) Sides of Mo-TZM Alloy Blade Specimens and Blade Pads Following Loop Disassembly. (Orig. C66050509, C66050516)

if minute enlargement or restriction of the nozzle throats occurred. The pretest and posttest measurements were performed by the Sheffield Corporation, Dayton, Ohio, by means of an electronic comparator using a frictionless electronic transducer directly compared to master gauge blocks. Results of these measurements are given in Table XXI and clearly indicate that no significant changes occurred during the 5000-hour test. The weight change results obtained both on the nozzle specimens (nominal weight, 255 g) and blade specimens (nominal weight, 25 g) are also given in Table XXI and indicate no significant changes. Minute amounts of metallic deposition are thought to be responsible for the very small weight gains observed on the nine blade specimens from the nine-stage, 88 percent quality turbine simulator region.

XII. CHEMICAL AND METALLURGICAL EVALUATION OF LOOP COMPONENTS

The extensive posttest evaluation performed on the Cb-1Zr and Mo-TZM components following draining and distillation of the alkali metals from the loop circuits included approximately 100 chemical analyses and the examination of 85 metallographic specimens, as well as weight change measurements, dimensional analysis, electron beam microprobe analysis, room temperature and elevated temperature tensile testing, bend testing, and hardness measurements. A discussion of the weight change data and the results of dimensional analysis performed on the Mo-TZM turbine simulator nozzle specimens was included in the previous section. As will be apparent in the discussion of results which follows, the greatest emphasis was placed on chemical analysis and metallographic examination in evaluating the compatibility of the various components with the test environments.

A. RESULTS OF CHEMICAL ANALYSIS OF LOOP COMPONENTS

The results of the various chemical analyses are presented in four parts below including:

1. Analysis of Cb-1Zr foil insulation samples,
2. Analysis of Mo-TZM alloy turbine simulator blade specimens,
3. Analysis of Cb-1Zr components from the potassium circuit, and
4. Analysis of Cb-1Zr components from the sodium circuit.

The vacuum fusion method was used to determine the oxygen, nitrogen, and hydrogen concentrations, and the combustion conductometric method was used to determine carbon concentrations for the Cb-1Zr and Mo-TZM alloy specimens discussed below.

1. Analysis of Cb-1Zr Foil Insulation Samples. Very thin refractory metal specimens exposed in high-temperature, high-vacuum environments are very sensitive indicators of the extent of contamination by elements such as oxygen, nitrogen, hydrogen, and carbon. The 0.002-inch-thick Cb-1Zr foil used to insulate the loop was ideal for this purpose. Samples of foil from the single layer of insulation that surrounded the nine-stage turbine simulator were submitted for analysis. The results obtained on these specimens are given in Table XXII. It may be noted that only the oxygen concentration of the

TABLE XXII

RESULTS OF CHEMICAL ANALYSIS OF Cb-1Zr FOIL TAKEN FROM THE SINGLE LAYER OF INSULATION THAT SURROUNDED THE NINE-STAGE TURBINE SIMULATOR DURING THE 5000-HOUR PROTOTYPE CORROSION LOOP TEST

Specimen	Chemical Analysis, ppm[(a)]			
	O	N	H	C
Before Test	244	50	3	85
Top Region (1400°F)	790	61	6	110
Bottom Region (1130°F)	750	45	12	120

(a) Results given are the average of duplicate analyses performed on the 0.002-inch thick foil.

foil changed significantly during the 5000-hour test. Although the increase of 546 ppm oxygen is significant, it should be noted that this amount of pickup per unit surface area would amount to less than 20 ppm in a 0.060-inch-thick tube wall, even if all the contamination is assumed to occur from one side and less than 10 ppm if two-side contamination of the foil is assumed.

2. Analysis of Mo-TZM Alloy Turbine Simulator Blade Specimens. The results of chemical analysis performed on specimens taken from the vapor impingement regions of four of the turbine simulator blade specimens are given in Table XXIII. A comparison of analytical results on tested and before-test specimens indicated no significant change in the oxygen, nitrogen, hydrogen, or carbon concentrations of these blade specimens.

3. Analysis of Cb-1Zr Components From the Potassium Circuit. The locations of the various samples of Cb-1Zr tubing (0.375-inch OD x 0.062-inch wall and 1.0-inch OD x 0.100-inch wall) taken from the potassium and the sodium circuit for chemical analysis are indicated in Figure 117. The operating conditions in the potassium and sodium circuits of the loop were indicated previously in Figure 84. Both total wall and gradient analyses of the tube walls were performed. The chemical analysis results obtained on specimens taken from the 3/8-inch-OD potassium containment tube from the tube-in-tube boiler are presented with the discussion of the results on the sodium circuit because the major changes in the chemistry of this tubing occurred on the sodium side.

Analytical results obtained on samples from various regions of the potassium circuit, as well as before test analyses of both the 3/8-inch-OD and 1-inch-OD tubing, are listed in Table XXIV. No significant changes were noted in the oxygen, nitrogen, hydrogen, or carbon concentrations of the various regions of the loop. The oxygen variations across the wall of the gradient samples were also minor. Oxygen transfer from the hotter to cooler regions of Cb-1Zr loops in which alkali metals are circulated has been observed in a number of tests,[49, 50] and it may be noted in Table XXIV that Specimen

(49) Hoffman, E. E. and Holowach, J., Cb-1Zr Thermal Convection Loop, Potassium Corrosion Test Loop Development Topical Report No. 5, R67SD3014, General Electric Company, Cincinnati, Ohio, June 15, 1967, p. 69.

(50) Hoffman, E. E. and Holowach, J., Cb-1Zr Pumped Sodium Loop, Potassium Corrosion Test Loop Development Topical Report No. 6, R67SD3015, General Electric Company, Cincinnati, Ohio, December 20, 1967, p. 161.

TABLE XXIII

RESULTS OF CHEMICAL ANALYSIS OF Mo-TZM ALLOY TURBINE SIMULATOR BLADE SPECIMENS* FOLLOWING THE 5000-HOUR TEST

Specimen Description	Nozzle Inlet Temperature, °F		Chemical Analysis, ppm O	N	H	C
Stage No. 1 Blade	2000		23	4	<1	120
			50	4	<1	130
		Avg.	36	4	<1	125
Stage No. 2 Blade	1785		8	2	<1	190
			25	3	<1	200
		Avg.	16	2	<1	195
Stage No. 3 Blade	1740		19	3	<1	160
			24	6	<1	160
		Avg.	21	4	<1	160
Stage No. 10 Blade	1450		26	3	<1	160
			20	3	<1	170
		Avg.	23	3	<1	165
Before Test	----		12	2	<1	150
			18	4	<1	190
		Avg.	15	3	<1	170

* Chemical analysis sample taken from the vapor impingement region of each blade.

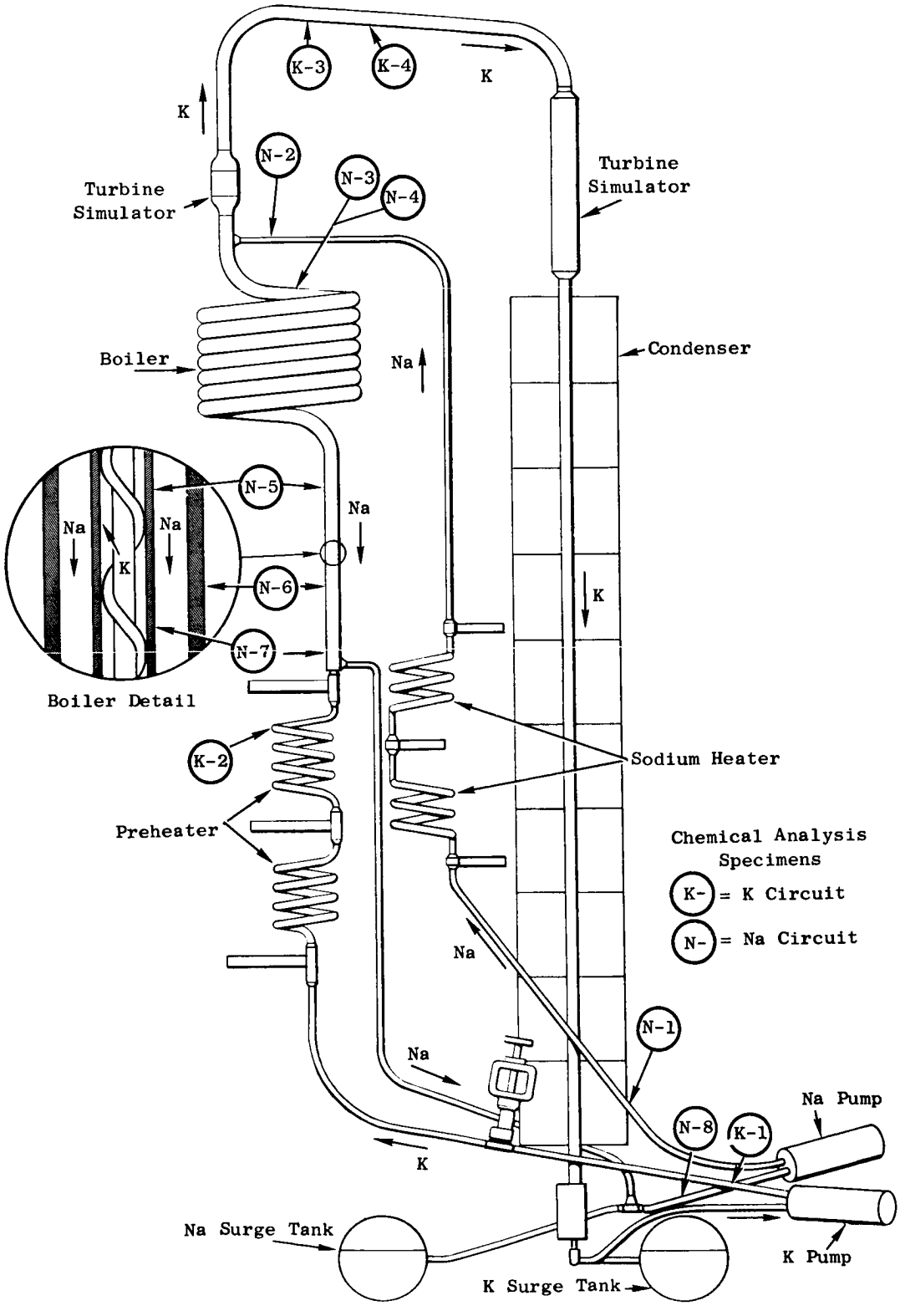

Figure 117. Location of Chemical Analysis Specimens Taken From the Potassium and Sodium Circuits of the Cb-1Zr Corrosion Test Loop.

TABLE XXIV. RESULTS OF CHEMICAL ANALYSIS OF Cb-1Zr SPECIMENS FROM THE POTASSIUM CIRCUIT OF THE Cb-1Zr CORROSION TEST LOOP FOLLOWING THE 5000-HOUR TEST

	Specimen Identification and Description	Tube Size OD	Temp., °F		Chemical Analysis, ppm O	N	H	C
(K-1)	EM pump outlet tube, total wall	3/8-Inch	1087		272	47	2	37
					283	50	4	44
				Avg.	277	48	3	40
(K-2)	Upper coil of preheater, total wall	3/8-Inch	1755		152	39	3	30
					173	48	3	35
				Avg.	162	43	3	32
	BOILER*							
(K-3)	Vapor carryover tube, insulated, total wall	1-Inch	1768		381	59	7	
					318	49	9	
					252	55	1	26
					265	60	2	35
				Avg.	304	56	5	30
	Vapor carryover tube, insulated, outer 0.033 inch of wall	1-Inch	1768		346	48	3	40
					363	73	3	40
				Avg.	354	60	3	40
	Vapor carryover tube, insulated, middle 0.033 of wall	1-Inch	1768		213	30	12	15
					241	58	15	24
				Avg.	227	44	13	19
	Vapor carryover tube, insulated, inner 0.033 inch of wall	1-Inch	1768		258	42	8	27
					260	56	9	36
				Avg.	259	49	8	32
(K-4)	Vapor carryover tube, uninsulated, total wall	1-Inch	1768		308	59	5	
					346	47	9	
					268	42	2	45
					275	58	3	47
				Avg.	300	51	5	46
	Vapor carryover tube, uninsulated, outer 0.033 inch of wall	1-Inch	1768		308	55	3	65
					328	62	4	68
				Avg.	318	59	3	66
	Vapor carryover tube, uninsulated, middle 0.033 inch of wall	1-Inch	1768		218	40	2	96
					242	41	4	107
					230	40	3	101
	Vapor carryover tube, uninsulated, inner 0.033 inch of wall	1-Inch	1768		272	57	1	57
					286	63	2	58
				Avg.	279	60	1	57
(K-5)	EM Pump inlet tube, total wall	3/8-Inch	583		272	57	1	57
					286	63	2	58
				Avg.	279	60	1	57
	EM Pump inlet tube, outer 0.020 inch of wall	3/8-Inch	583		291	49	2	82
					320	58	2	83
				Avg.	305	54	2	82
	EM Pump inlet tube, middle 0.020 inch of wall	3/8-Inch	583		388	37	2	48
					478	51	2	52
				Avg.	433	44	2	50
	EM Pump inlet tube, inner 0.020 inch of wall	3/8-Inch	583		286	49	1	68
					321	82	2	88
				Avg.	303	65	1	78
	Before test	3/8-Inch	----		236	38	1	32
					285	56	1	34
				Avg.	260	47	1	33
	Before test	1-Inch	----		245	50	7	40
					245	43	13	40
				Avg.	245	46	10	40

* Inner tube of boiler was exposed to sodium (OD) and potassium (ID). Significant changes in chemistry occurred only on the sodium side of the tube; therefore, the chemistry results are given in the sodium circuit table.

K-2, which was taken from one of the hotter regions of the loop (excluding the boiler itself), has an oxygen concentration approximately 100 ppm lower than the tubing before test.

A dramatic testimonial to the inertness of the test chamber environment is indicated by a comparison of the oxygen concentration of Specimens K-3 and K-4 in Table XXIV. These specimens, which were taken from the 1-inch-OD vapor carryover tube, were in close proximity and were at essentially the same temperature during test operation. However, Specimen K-3 was taken from a region which was wrapped with eight layers of Cb-1Zr foil insulation (see Figure 63), while Specimen K-4 was uninsulated to permit radiation heat loss in this region. Essentially no difference was noted in the total wall oxygen concentration of these specimens (304 ppm vs. 318 ppm), and these concentrations indicate an insignificant increase of 60-70 ppm during the 5000-hour test. The levels of oxygen contamination noted on these specimens are in general agreement with the changes noted in the foil specimens presented in Table XXII.

4. Analysis of Cb-1Zr Components From the Sodium Circuit. The location of the various chemical analysis samples of Cb-1Zr tubing taken from the sodium circuit are designated as the "N" specimens in Figure 117. Again, as for the potassium circuit described previously, both total wall and wall gradient specimens were analyzed to determine bulk compositional changes and local variations.

A review of the analytical results listed in Table XXV indicates that no significant changes in nitrogen, hydrogen, or carbon concentrations occurred in the various regions of the loop as a result of the 5000-hour test. The gradient analyses obtained on Specimen N-7 (3/8-inch-OD boiler tube near the sodium outlet - potassium inlet) suggest slight nitrogen and carbon depletions on the sodium side and increases of these elements on the potassium side, but unfortunately there was insufficient tubing in this region of the plug section of the boiler to permit additional confirming analyses.

The oxygen variations observed in the various regions of the sodium

TABLE XXV. RESULTS OF CHEMICAL ANALYSIS OF Cb-1Zr SPECIMENS FROM THE SODIUM CIRCUIT OF THE Cb-1Zr CORROSION TEST LOOP FOLLOWING THE 5000-HOUR TEST

	Specimen Identification and Description	Tube Size OD	Temp., °F		Chemical Analysis, ppm O	N	H	C
(N-1)	EM Pump outlet tube, total wall	3/8-Inch	1972		718	47	18	60
					727	61	19	70
				Avg.	723	54	18	65
(N-2)	Boiler inlet tube, total wall	3/8-Inch	2130		34	36	1	30
					38	47	2	60
				Avg.	36	41	1	45
	Boiler inlet tube, outer 0.020-inch of wall	3/8-Inch	2130		92	38	5	80
					100	40	6	80
				Avg.	96	39	5	80
	Boiler inlet tube, middle 0.020-inch of wall	3/8-Inch	2130		200	45	3	80
					239	53	5	90
				Avg.	220	49	4	85
	Boiler inlet tube, inner 0.020-inch of wall	3/8-Inch	2130		38	33	2	60
					42	41	3	60
				Avg.	40	37	2	60
(N-3)	Outer boiler tube, 6 inches from sodium inlet, total wall	1-Inch	2120		39	42	3	60
					41	48	4	70
				Avg.	40	45	3	65
(N-4)	Inner boiler tube, 6 inches from sodium inlet, total wall	3/8-Inch	1975		40	35	1	17
					73	46	2	26
				Avg.	56	40	1	22
(N-5)	Inner boiler tube, top of plug section 11 inches from sodium outlet, total wall	3/8-Inch	1900		160	41	6	19
					171	66	7	21
				Avg.	165	53	6	20
(N-6)	Outer boiler tube, 6 inches from sodium outlet, total wall	1-Inch	2050		148	52	4	30
					149	53	4	30
				Avg.	148	52	4	30
(N-7)	Inner boiler tube, bottom of plug section 1/2 inch from sodium outlet, total wall	3/8-Inch	1905		1210	50	15	66
					1270	56	19	73
				Avg.	1240	53	17	70
	Inner boiler tube, bottom of plug section 1 inch from sodium outlet, outer 0.020 inch of wall	3/8-Inch	1905		2415	12	6	50
					2475	19	7	58
				Avg.	2445	15	6	54
	Inner boiler tube, bottom of plug section 2 inches from sodium outlet, middle 0.020 inch of wall	3/8-Inch	1905		528	50	7	70
					548	69	8	74
				Avg.	538	60	7	72
	Inner boiler tube, bottom of plug section 3 inches from sodium outlet, inner 0.020 inch of wall	3/8-Inch	1905		104	84	5	153
					176	152	5	172
				Avg.	140	118	5	163
(N-8)	EM Pump inlet tube, total wall	3/8-Inch	1960		724	56	12	40
					737	60	13	70
				Avg.	730	58	12	55
	EM Pump inlet tube, outer 0.020-inch of wall	3/8-Inch	1960		325	67	5	70
					335	83	8	80
				Avg.	330	75	6	75
	EM Pump inlet tube, middle 0.020-inch of wall	3/8-Inch	1960		434	53	6	50
					456	67	7	60
				Avg.	445	60	6	55
	EM Pump inlet tube, inner 0.020-inch of wall	3/8-Inch	1960		1325	15	8	21
					1590	23	10	23
				Avg.	1457	19	9	22
	Before test	3/8-Inch	----		236	38	1	32
					285	56	1	34
				Avg.	260	47	1	33
	Before test	1-Inch	----		245	50	7	40
					245	43	13	40
				Avg.	245	46	10	40

circuit and the local oxygen gradients in the tube walls resulting from oxygen migration from the hotter regions of the loop to the cooler regions of the loop were the most striking that have been observed in any Cb-1Zr systems containing sodium and potassium which have been conducted by any laboratories to date. As indicated in the discussion of the chemical analysis results for the Cb-1Zr tubing in the potassium circuit, the oxygen migration has been noted in other systems of this type, but not to the extent observed in the sodium circuit of this loop. The discussion of the results given in Table XXV will be divided into two parts; a summary of the results obtained on specimens of tubing which were in contact with sodium only (N-1, N-2, N-3, N-6, and N-8), followed by a discussion of the more complex results obtained on specimens taken from the 3/8-inch-OD tubing in the boiler (N-4, N-5, and N-7) which had sodium in contact with the OD surface and potassium in contact with the ID surface.

Specimens taken from the cooler regions of the sodium circuit, N-1 (pump outlet, 1970°F) and N-2 (pump inlet, 1960°F), exhibited oxygen increases of approximately 570 ppm. The specimens taken from the hotter regions of the sodium loop, N-2 (boiler inlet tube, 2130°F), N-3 (outer boiler tube, 2120°F), and N-6 (outer boiler tube, 2075°F), showed oxygen depletions which varied from 110 ppm to 220 ppm. The hottest regions of the Cb-1Zr loop in contact with sodium had posttest oxygen concentrations of approximately 40 ppm.

The results obtained on specimens of the Cb-1Zr tubing from the boiler which were in contact with both sodium and potassium indicated large oxygen decreases in regions N-4 and N-5 where the sodium temperature was high (2100-2110°F) but very large increases (260 to 1240 ppm) in the last six inches of the sodium flow path near the boiler exit. As was indicated previously in Figure 84, approximately 70 degrees of the total sodium temperature drop of 130 degrees in the boiler occurred in this last six inches of the boiler. This sharp drop in sodium temperature resulted from the very high-heat flux across the tube wall to the potassium, which was converted from subcooled liquid to 50-60 percent quality vapor in the first six

inches of its flow path through the boiler. The sodium side of the 3/8-inch-OD tube in this region was covered with a very thin film of deposited crystals, and more information regarding the deposit will be presented in the following portions of this report describing metallographic evaluation and microprobe analysis.

The most significant oxygen analytical results on the boiler and adjacent regions are illustrated in Figure 118. Most amazing are the results of gradient analyses on the 3/8-inch-OD tube in the last six inches of the sodium circuit in the boiler, and these results are illustrated in the boiler plug detail enlargement in Figure 118. The outer 20 mils of this tube showed an increase of approximately 2200 ppm oxygen, while the inner 20 mils of this wall decreased about 100 ppm. This extreme oxygen gradient is surprising in view of the high operating temperatures in this region which should facilitate oxygen diffusion and flattening of the gradient.

The marked effect of temperature and heat flux on oxygen deposition and depletion is also emphasized by the analytical results obtained on the specimen of the 1-inch-OD tube (N-6, Table XXV) which was separated from the OD of the 3 8-inch tube (1270 ppm oxygen) discussed in the paragraph above by the 0.21-inch sodium annulus actually lost 100 ppm oxygen during the 5000-hour test.

Comparison of the oxygen concentrations of the sodium inlet and outlet tubes to the boiler (Figure 118) also illustrates the extent of oxygen migration from the hotter regions (2130°F, 36 ppm O) to the cooler regions (1985°F, 730 ppm O) with the inner 20 mils of sodium exit tube having an oxygen concentration of 1460 ppm.

B. METALLOGRAPHIC EVALUATION OF LOOP COMPONENTS

Metallographic examination of specimens taken from various regions of the loop circuits was a primary tool in evaluating the compatibility of loop components with the circulating fluids, sodium and potassium, and in determining the extent of contamination, if any, by the vacuum environment of the test chamber. A total of 85 metallographic specimens were prepared and examined, and the most significant observations are illustrated in the figures presented in the discussion which follows.

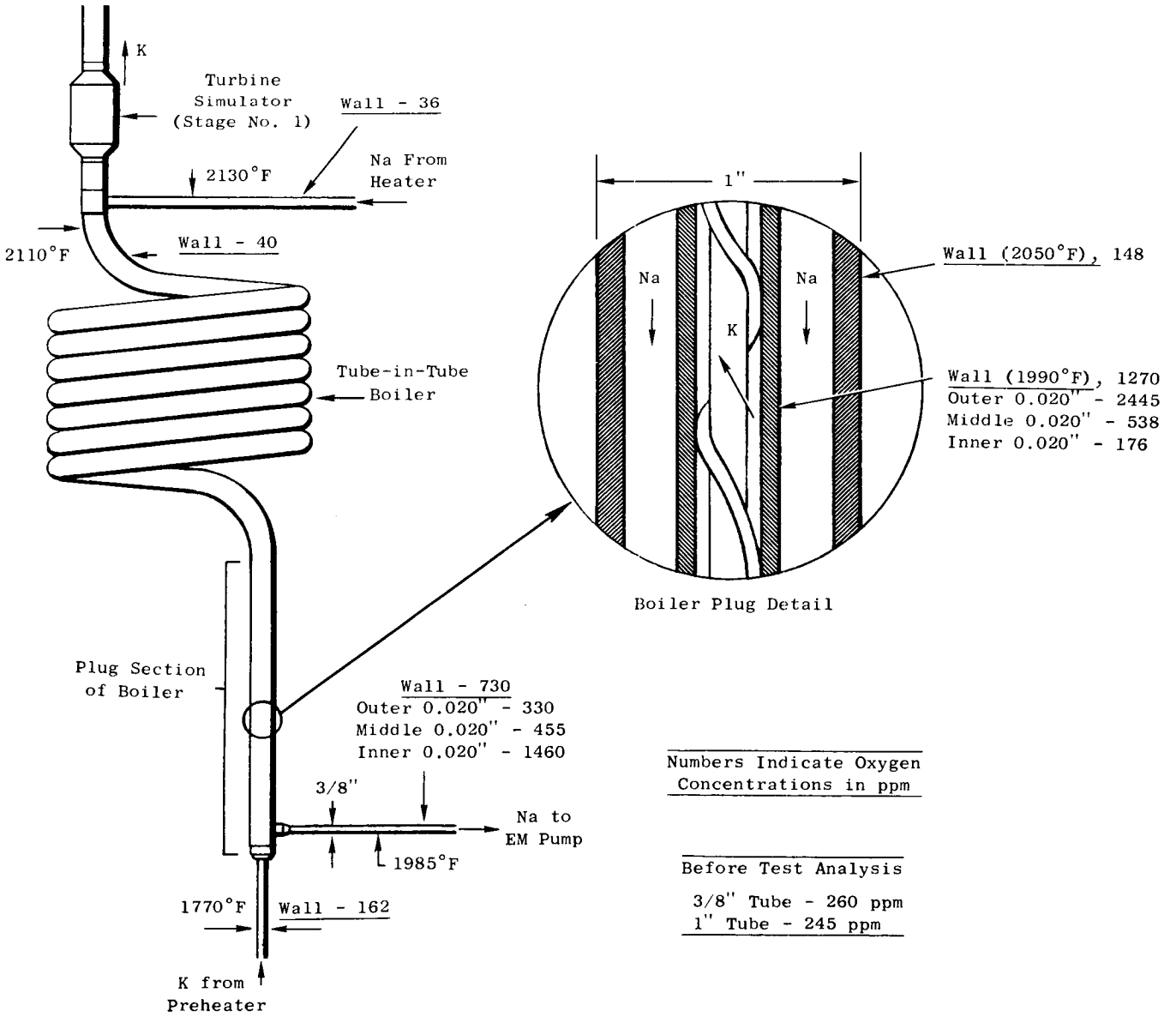

Figure 118. Oxygen Concentration of Various Regions of the Boiler of the Cb-1Zr Loop Following 5000-Hours Operation.

The results of the metallographic evaluations are divided into the six headings listed below:

1. Cb-1Zr metallographic specimens from the potassium circuit,
2. Cb-1Zr metallographic specimens from the sodium circuit,
3. Cb-1Zr metallographic specimens from the boiler,
4. Mo-TZM alloy metallographic specimens from the turbine simulators,
5. Metallographic evaluation of components of the potassium metering valve, and
6. Metallographic evaluation of the iron titanate coating on the Cb-1Zr condenser fin.

A brief description of the metallographic techniques used in preparing the specimens will be given. Since the greatest area of interest in evaluating the metallographic appearance of the specimens was the condition of the surface, great care was exercised, both in specimen preparation and in polishing, to achieve good edge preservation. This was normally achieved by nickel plating the individual specimens prior to mounting them in a cold setting epoxy resin (Araldite 502, Ciba Corporation). No effort was made to label the nickel plate regions which appear adjacent to the edges of the Cb-1Zr specimens in the photomicrographs which follow. Vibratory polishing was normally used as the final polishing procedure. The etchants used in the preparation of the two alloys are given below.

Cb-1Zr: 20%HNO_3-20%HF-60% Glycerin

Mo-TZM: Murakami's reagent; 10 g KOH-10 g $K_3Fe(CN)_6$-100 ml H_2O

The metallographic appearances of the total cross section and the ID surface of the two sizes of Cb-1Zr tubing which were used in fabricating most of the loop circuits are shown in Figure 119. Both the 3/8-inch-OD and 1-inch-OD tubing had a fine-grained recrystallized structure (ASTM Grain Size 7-8). The ID surface of the tubing was generally quite smooth as indicated in the 500X photomicrographs shown.

1. Cb-1Zr Metallographic Specimens From the Potassium Circuit. The location of the metallographic specimens taken from both the potassium and sodium circuits are indicated in Figure 120. Parts 1 and 2 of this discussion of metallographic results are confined to the non-boiler regions

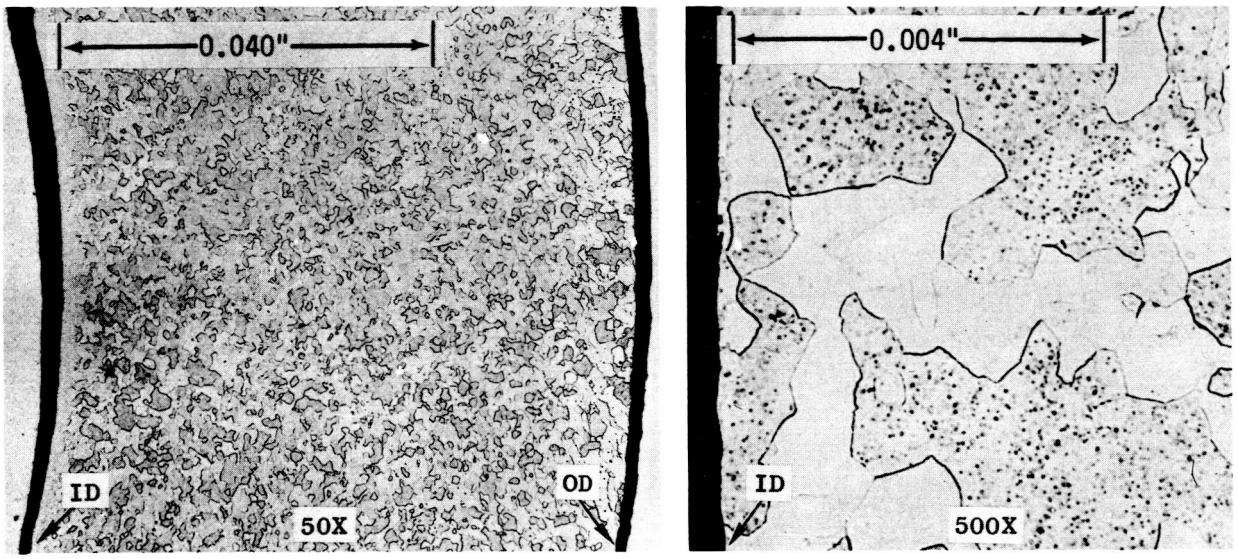

(a) Cb-1Zr Tube, 3/8-inch OD x 0.062-inch Wall (MCN-447)

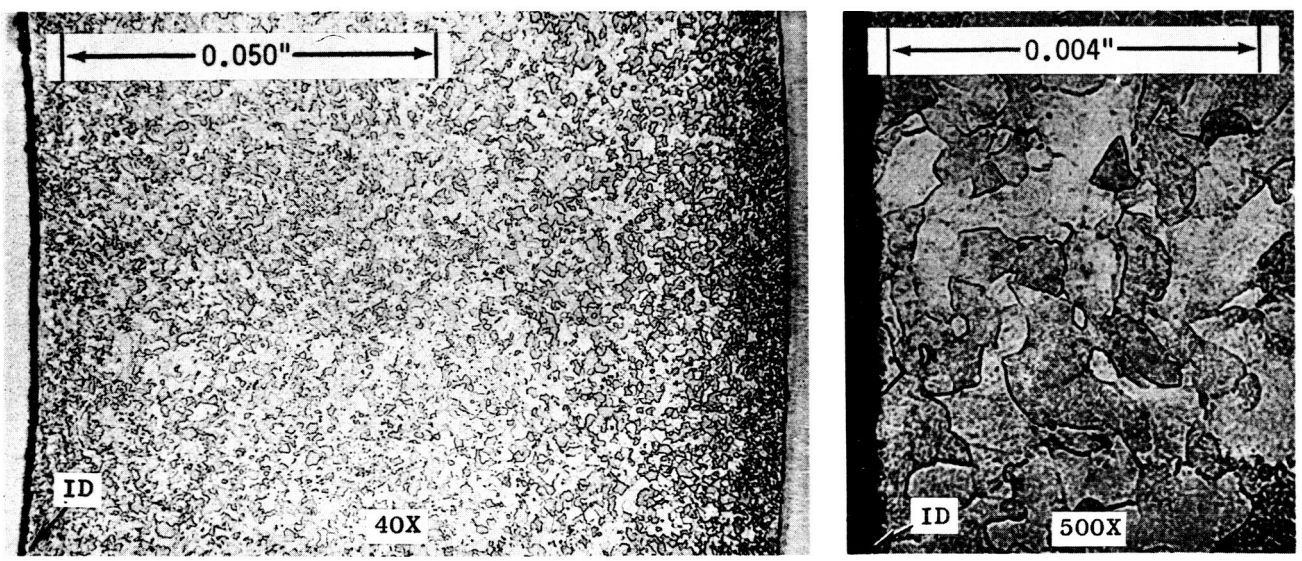

(b) Cb-1Zr Tube, 1.0-inch OD x 0.10" Wall (MCN 441)

Figure 119. Photomicrographs Illustrating Before Test Appearance of Cb-1Zr Tubing Used in Fabrication of the Cb-1Zr Corrosion Test Loop.

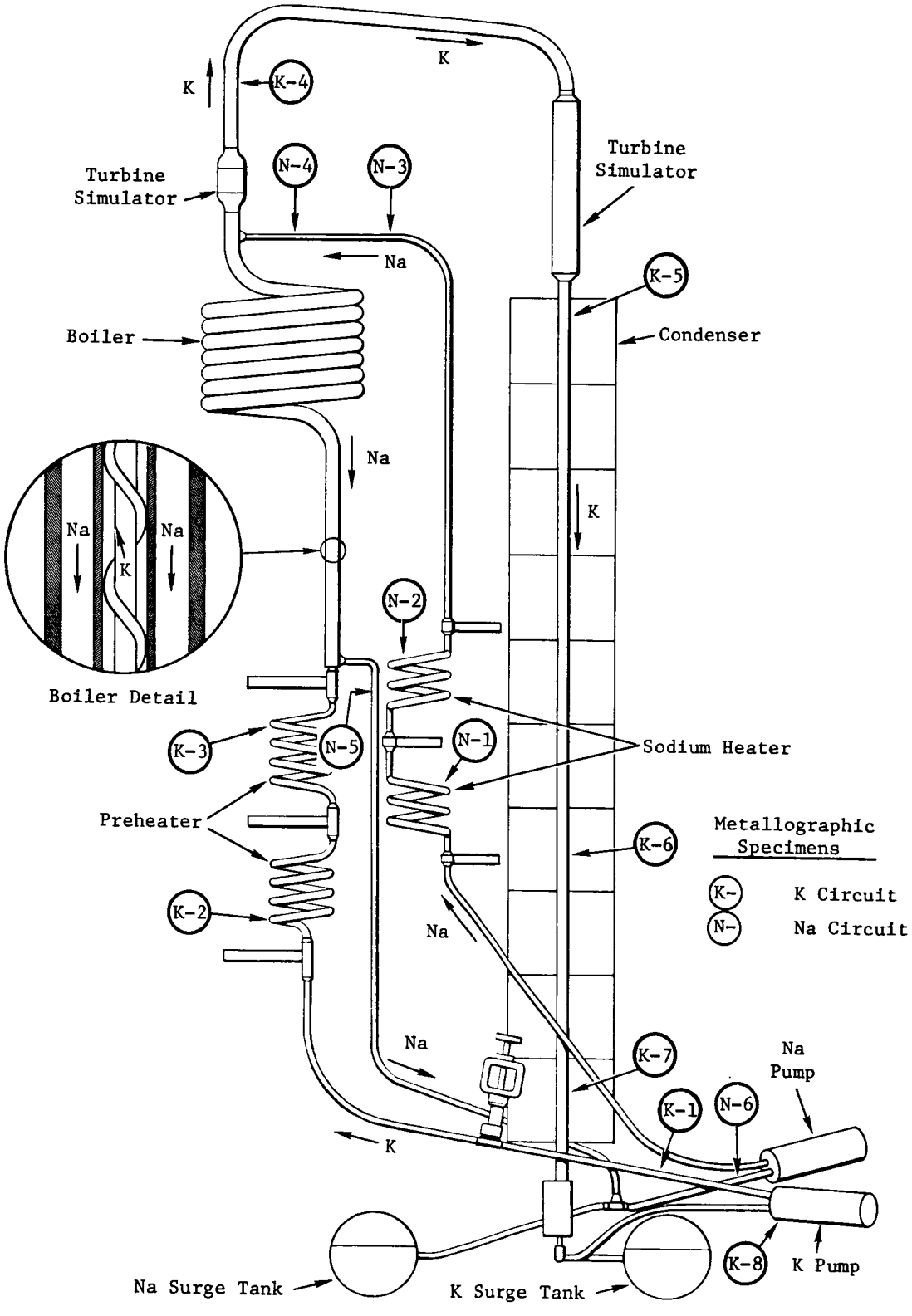

Figure 120. Location of Metallographic Specimens Taken From the Potassium and Sodium Circuits of the Cb-1Zr Corrosion Test Loop.

indicated in Figure 120. Part 3 will cover the more complex observations on the boiler materials, some of which are in contact with both potassium and sodium.

Specimens of the 3/8-inch-OD Cb-1Zr tube from the potassium pump outlet tube (K-1), the lower preheater coil (K-2), and the upper preheater coil (K-3), illustrated in Figures 121 and 122, show no indication of corrosion. Figure 122 (b) shows the metallographic appearance of a specimen of the 1-inch-OD tube taken from the vapor carryover line (K-4) and indicates no attack by potassium.

A series of 500X photomicrographs of the condenser and subcooler specimens (K-5, K-6, and K-7) are shown in Figure 123. Although these regions of the loop might at first appear to have suffered dissolutive attack due to the irregular surface appearance, this is not thought to be the case. The quality of the ID surface of this Cb-1Zr pipe (3/8-inch Schedule 80, 0.675-inch OD x 0.126-inch wall) was not as good as that of the tubing used in other regions of the loop. Pretest metallographic examination of the pipe revealed ID surface defects which had a maximum depth of 2-3 mils. The depth of these defects was less than the ultrasonic rejection level of the material specification for this size pipe (approx. 4 mils). Pretest pickling of the pipe, the standard treatment given all Cb-1Zr material prior to fabrication, rounded out the defects thereby eliminating sharp notches. Specimens of the pickled, before test Cb-1Zr pipe were nearly identical in metallographic appearance to the posttest specimens illustrated in Figure 123. Although it is not possible to conclude that dissolutive attack did not occur in the condenser/subcooler, the similarity of appearance of before and after test specimens and the fact that Specimen K-7, Figure 123 (c), from the 835°F region of the subcooler was quite similar in appearance to the "washed," 1425°F areas (K-5 and K-6) suggests that no significant attack occurred.

Metallographic evaluation was also performed on the Cb-1Zr wrapper which surrounded the potassium pump helix. A specimen was taken from near the potassium inlet to pump, as indicated in Figure 124, since this

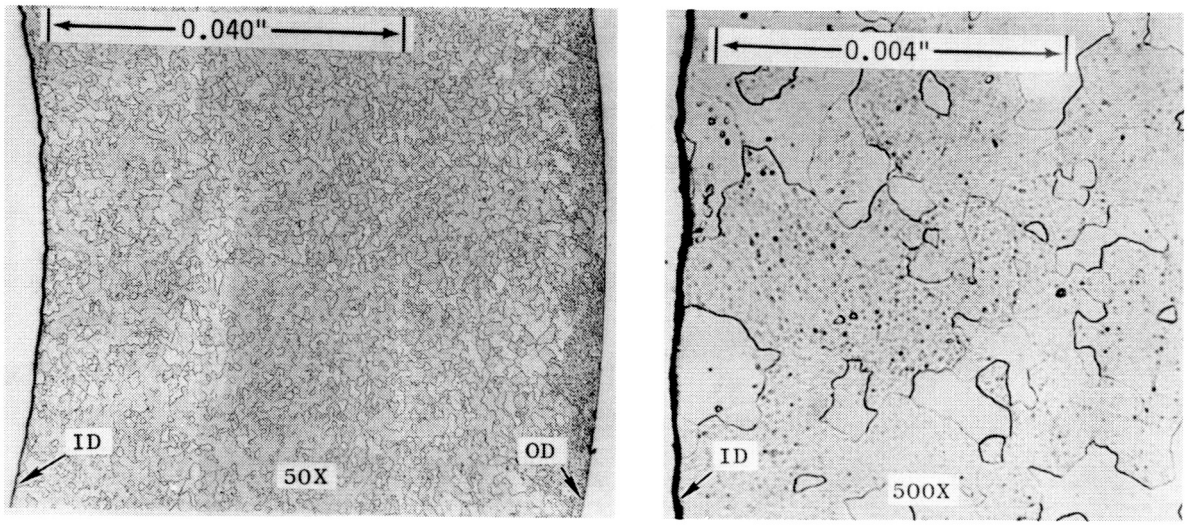

(a) Potassium Pump Outlet Tube (1087°F), Met. Spec. K-1

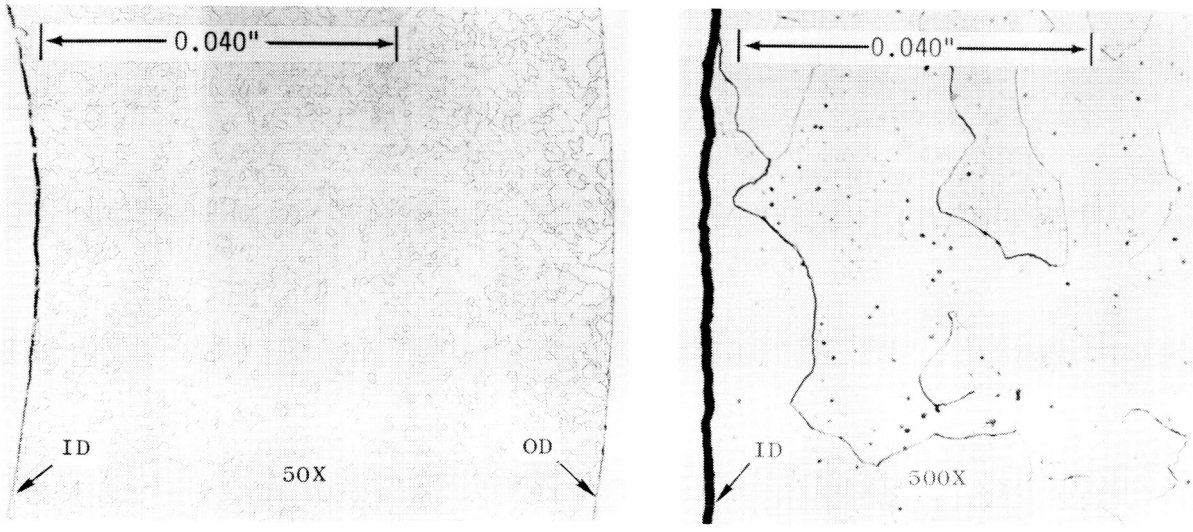

(b) Lower Coil of Potassium Preheater (1050°F), Met. Spec K-2

Figure 121. Cb-1Zr Tubing From Potassium Circuit. Specimen Locations Given in Figure 120.

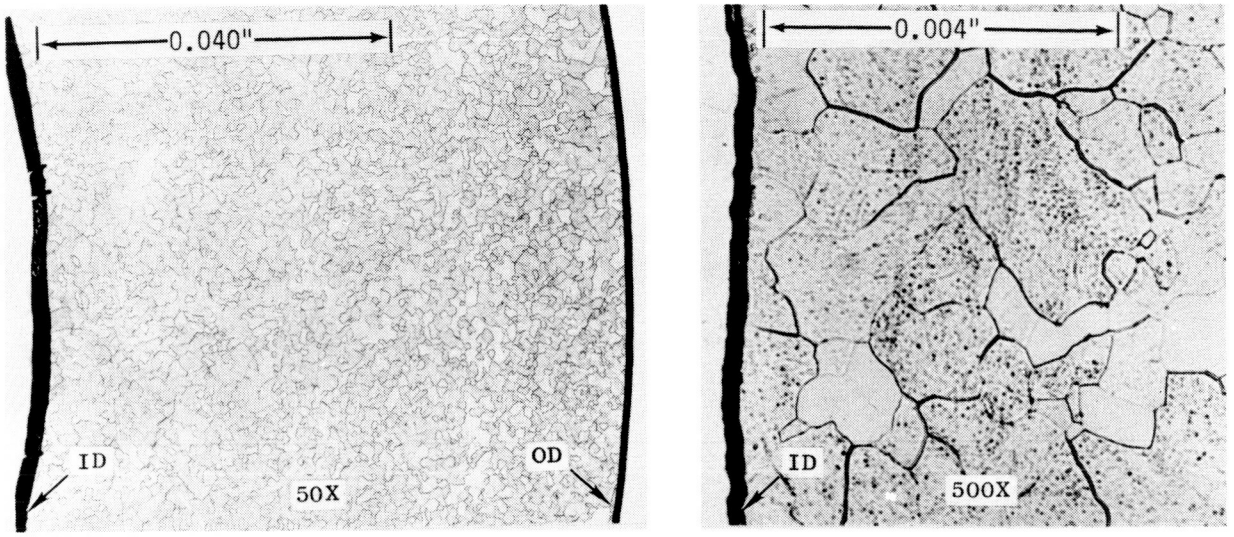

(a) Upper Coil of Potassium Preheater (1750°F), Met. Spec. K-3

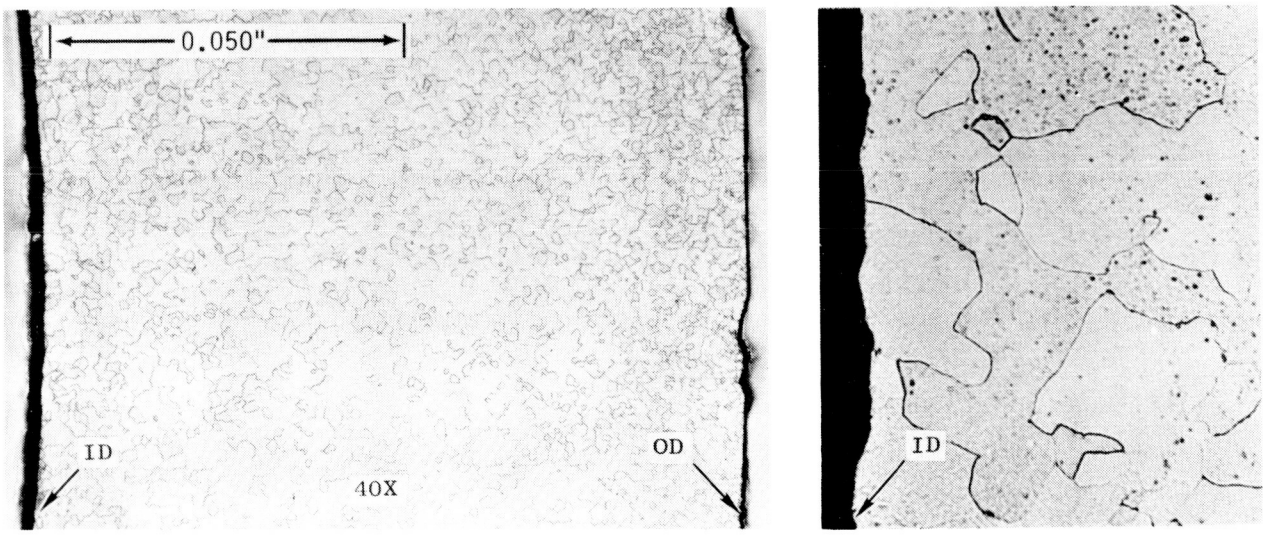

(b) Potassium Vapor Carryover Line (1850°F), Met. Spec. K-4

Figure 122. Cb-1Zr Tubing From Potassium Circuit. Specimen Locations Given in Figure 120.

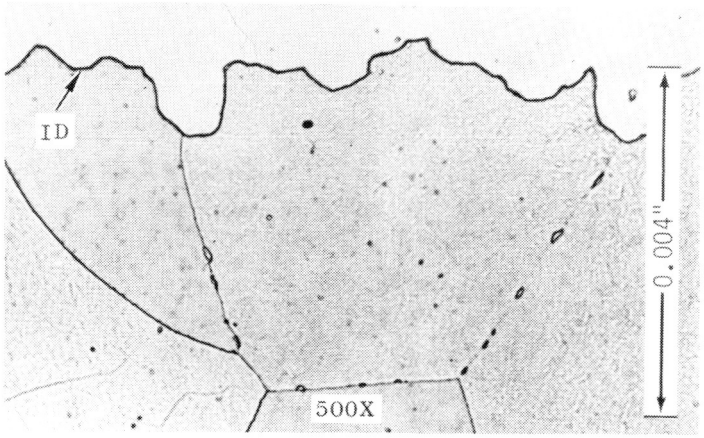

(a) Entrance Region of Condenser (1425°F), Met. Spec. K-5

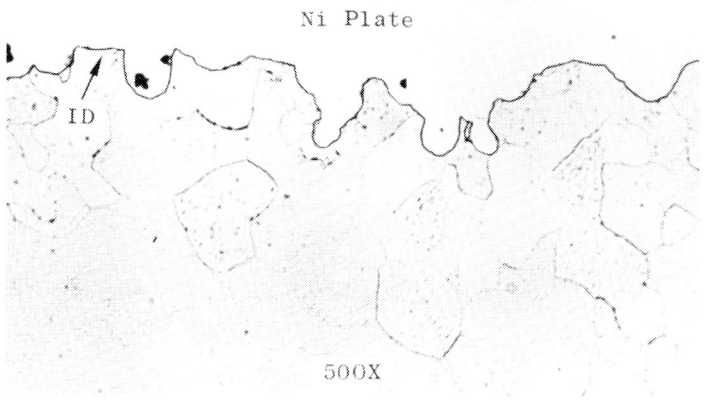

(b) Liquid/Vapor Interface Region of Condenser (1425°F), Met. Spec K-6

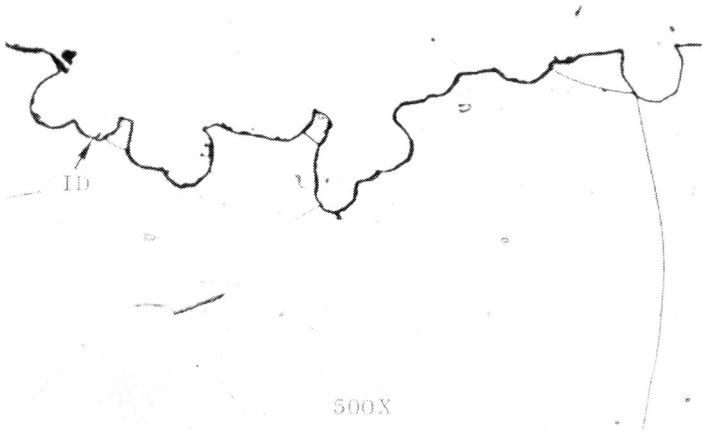

(c) Pipe Wall Near Subcooler Exit (835°F), Met. Spec. K-7

Figure 123. Photomicrographs of Condenser/Subcooler Cb-1Zr Pipe Following 5000-Hours Exposure to Potassium. Specimen Location Given in Figure 120.

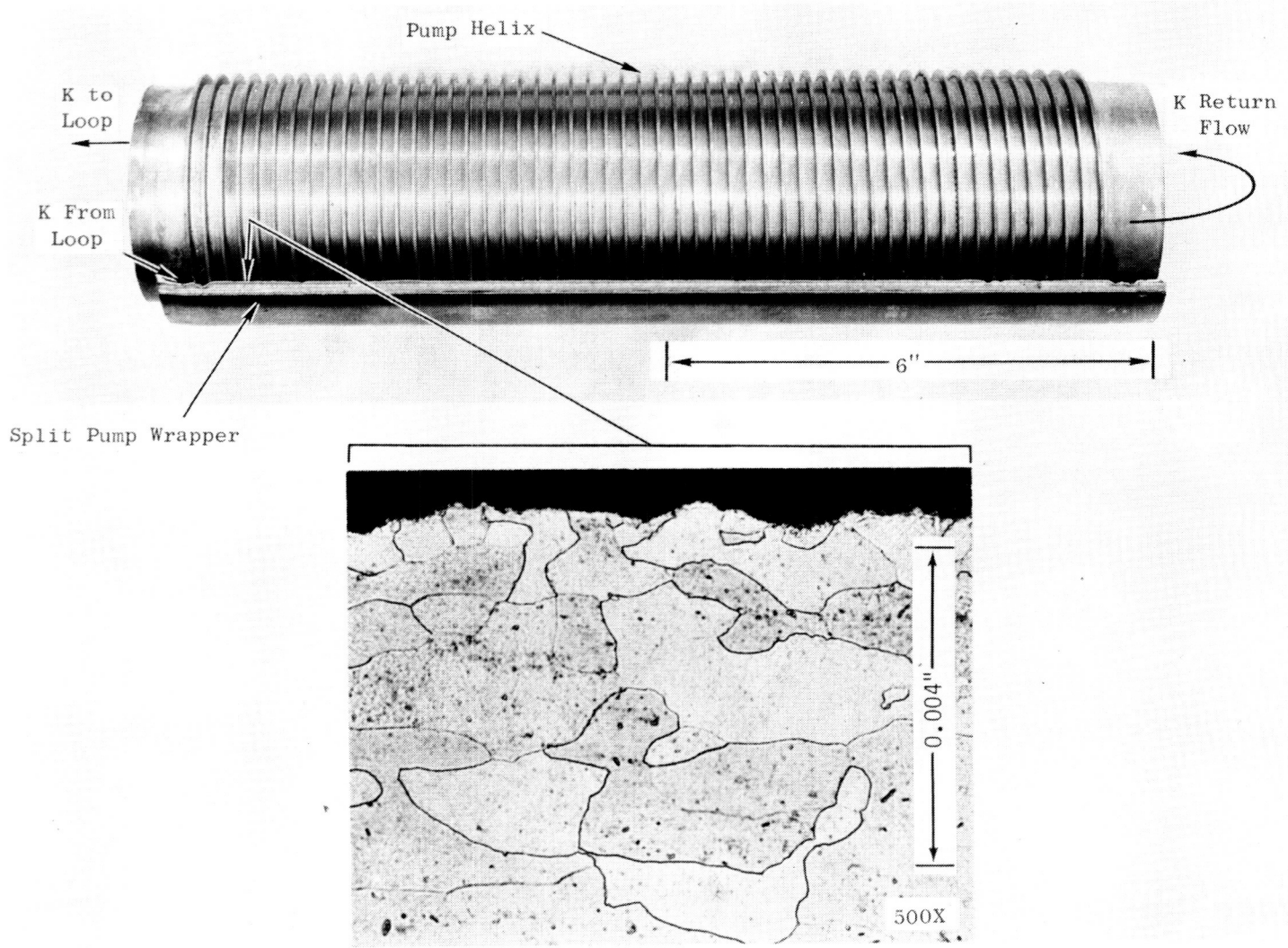

Figure 124. Photomicrograph of the Potassium Side of the Cb-1Zr Pump Wrapper Disassembly After the 5000-Hour Test. (Orig. C66052709, C041711)

area was considered to be a likely location of possible cavitation damage. No evidence of corrosion or cavitation damage was detected.

2. Cb-1Zr Metallographic Specimens From the Sodium Circuit. The location of the Cb-1Zr specimens from the sodium circuit discussed in this portion are indicated in Figure 120, shown earlier. Specimens of the 3 8-inch-OD tubing from the lower and upper sodium heater coils are shown in Figure 125. Although these specimens were taken from the hottest regions of the sodium circuit, no evidence of corrosion was detected. Phenomenal grain growth occurred in the portion of the tube wall that was deformed slightly by compression during the coil forming operation. The slight and variable amount of strain in these regions resulted in the abnormal grain growth which is quite apparent in Figure 125 (a) and (b). This phenomena, most usually referred to as "critical strain grain growth," was observed in the Cb-1Zr Thermal Convection Loop Test[51] conducted as a part of this contract, and a limited study of the effect of forming and subsequent heat treatment on grain growth in Cb-1Zr tubing was included in Appendix C of the referenced report.

The structure and surface condition of a specimen of the 3/8-inch-OD tubing from near the boiler inlet is illustrated in Figure 126 (a) and showed no attack. Only a limited amount of fine precipitate is apparent which is not surprising since the oxygen concentration of this region decreased from 260 to 36 ppm during the test. Cb-1Zr weldments in the loop exhibited excellent resistance to attack by the alkali metals as indicated by the posttest appearance of the longitudinal section of a butt weld near the boiler inlet shown in Figure 126 (b).

Proceeding around the sodium circuit, the Cb-1Zr specimens from the "low" temperature portion of the loop are presented in Figure 127. The specimen illustrated in Figure 127 (a) was from the boiler outlet region

(51) Hoffman, E. E. and Holowach, J., Cb-1Zr Thermal Convection Loop, Potassium Corrosion Test Loop Development Topical Report No. 5, R67SD3014, General Electric Company, Cincinnati, Ohio, June 15, 1967, p. 129.

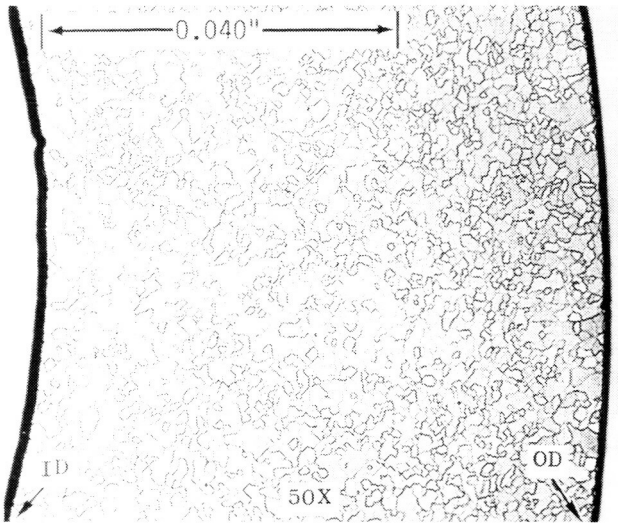

Neutral Axis of Bend

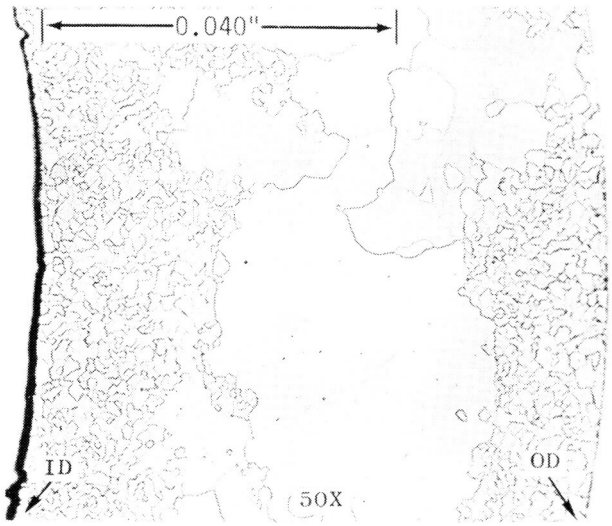

Compression Side of Bend

(a) Lower Sodium Heater Coil ($2100^{o}F$), Met. Spec. N-1

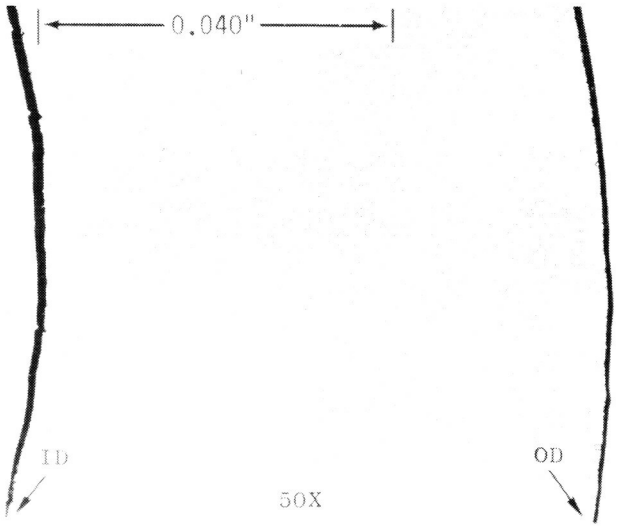

Neutral Axis of Bend

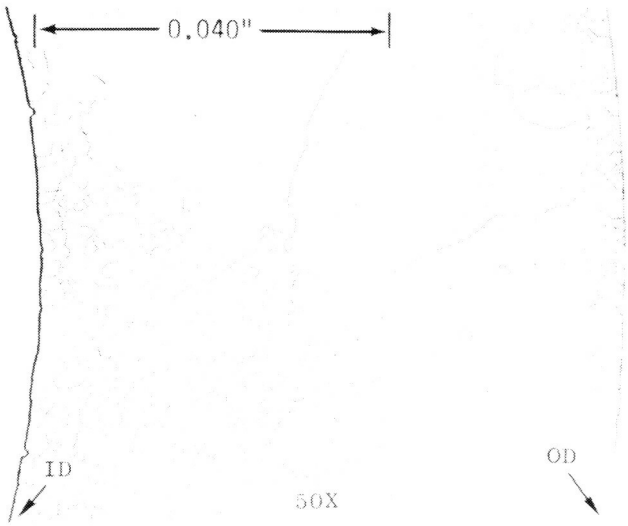

Compression Side of Bend

(b) Upper Sodium Heater Coil ($2150^{o}F$), Met. Spec. N-2

Figure 125. Cb-1Zr Tubing From Sodium Circuit Specimen Locations Given in Figure 120.

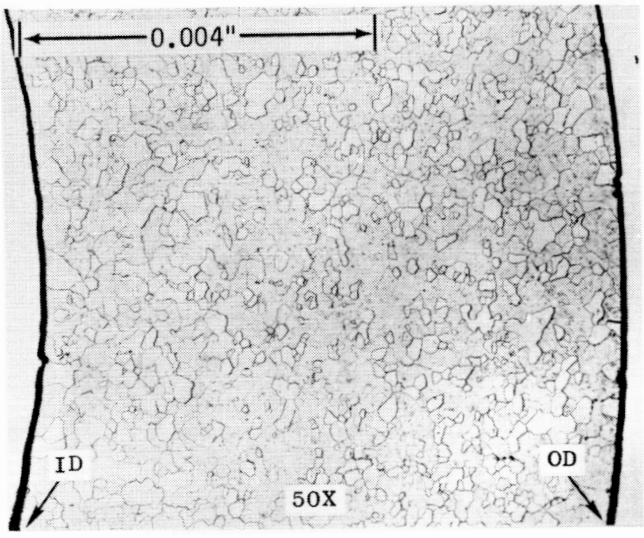

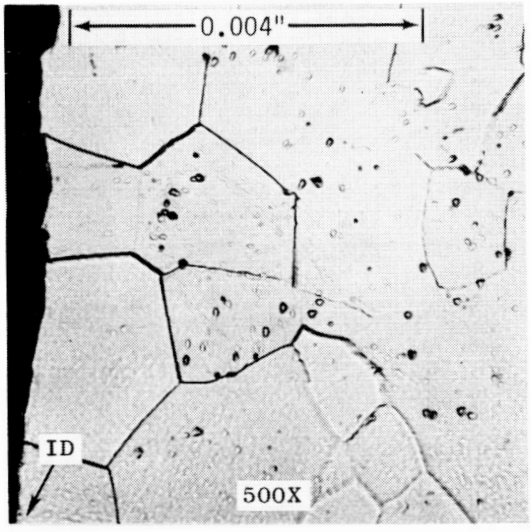

(a) Sodium Tube Near Boiler Inlet (2130°F), Met. Spec. N-3

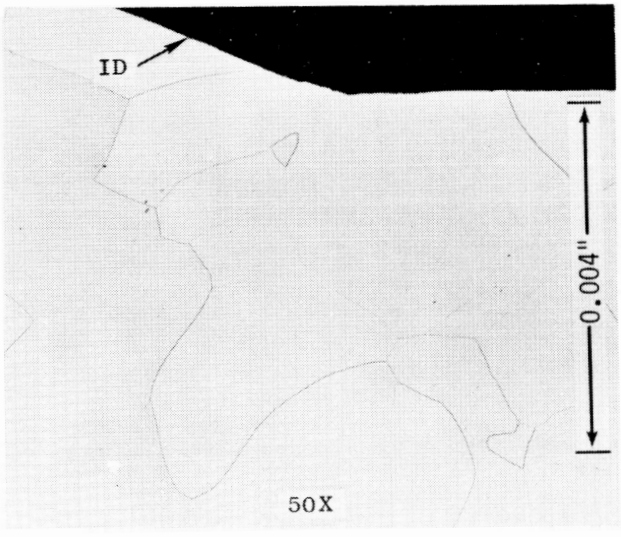

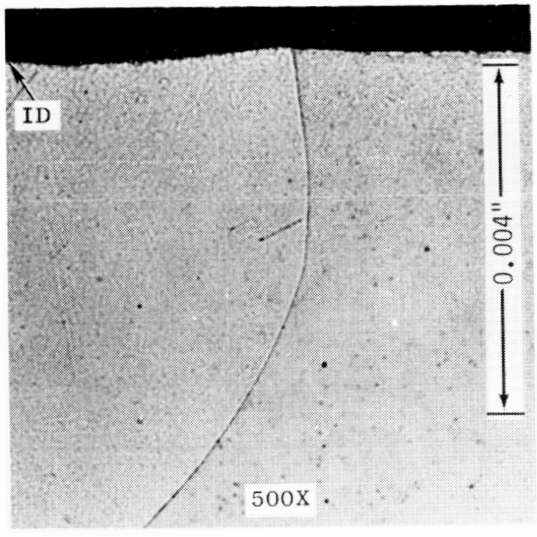

Weld Zone - Heat Affected Zone

Weld Zone

(b) Longitudinal Butt Weld in Sodium Tube Near Boiler Inlet (2130°F), Met. Spec. N-4

Figure 126. Cb-1Zr Tubing From Sodium Circuit Near Boiler Inlet. Specimen Locations Given in Figure 120.

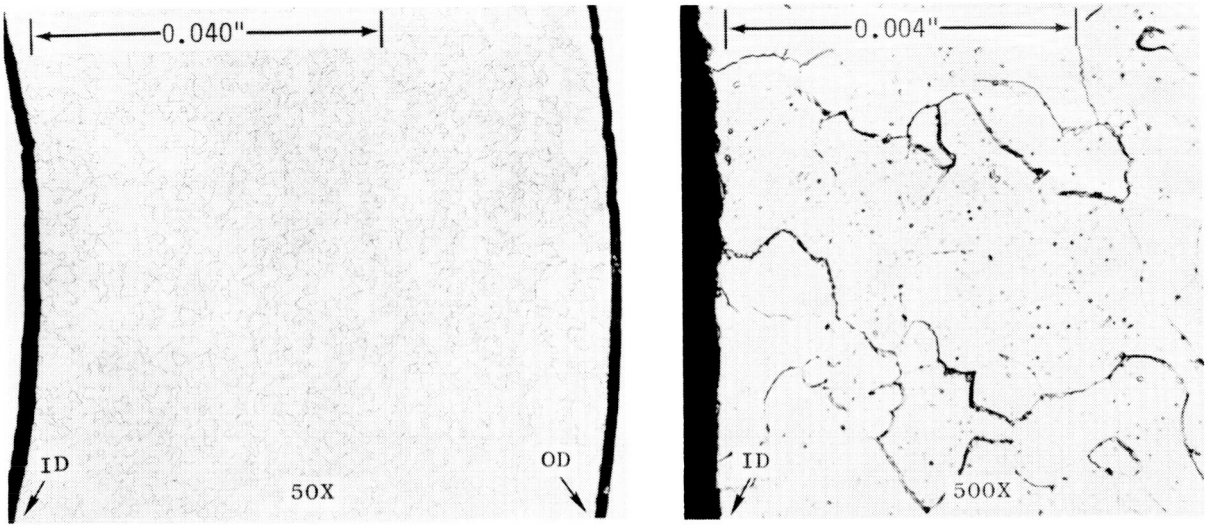

(a) Tube Wall Near Sodium Exit From Boiler (1985°F), Met. Spec. N-5

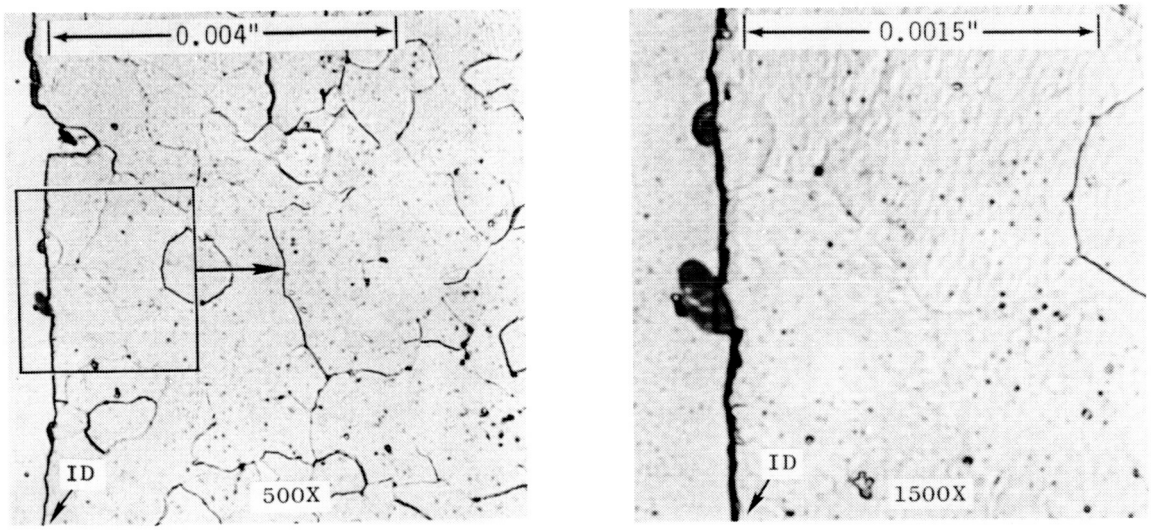

(b) Tube Wall Near Pump Inlet at High Magnification (1960°F), Met. Spec. N-6

Figure 127. Cb-1Zr Tubing Location in Sodium Return Line Between the Boiler and the EM Pump. Specimen Locations Given in Figure 120.

which experienced a substantial oxygen increase during the test (260 ppm to 730 ppm). A very steep oxygen gradient was measured across the wall, the inner 20 mils of the tube containing 1460 ppm oxygen following test. Although this gradient is real as confirmed by numerous chemical analyses, there is little metallographic evidence of this gradient in Figure 127 (a). Examination of this region at very high magnification did reveal very small ceramic-like particles similar in appearance to those found in significant quantity in the boiler regions discussed below. Figure 127 (b) shows several of these small grey particles found on the ID surface of the tube wall near the sodium pump inlet.

3. Cb-1Zr Metallographic Specimens From the Boiler. The most interesting metallographic observations were made on the specimens taken from the boiler. A diagram of the boiler showing the location of the first series of boiler specimens is given in Figure 128. In selecting the samples from the boiler for metallographic examination, the greatest emphasis was concentrated on the plug region of the boiler, since the very high test transfer rates and sharp temperature changes in this region would be expected to influence container material/fluid interactions.

Metallographic specimens of the 1-inch-OD sodium containment tube in the plug region of the boiler (Locations A, B and C) revealed no evidence of attack as shown in Figures 129 and 130 (a). The "sodium" and "potassium" surfaces of the 3/8-inch potassium containment tube from the top of the plug section, Location C in Figure 128, are shown in Figure 130 (b), and no evidence of attack is apparent. The metallographic appearance of specimens of both the sodium and potassium containment tubes from the mid-length region of the boiler, Location D, is given in Figure 131. No attack was detected, but some evidence of critical strain grain growth is apparent in both tubes at this location.

A butt weld in the 1-inch-OD sodium pipe located near the mid-length of the boiler is shown in Figure 132 and exhibited excellent corrosion resistance to the 2100°F sodium. The metallographic appearance of specimens of the 1-inch-OD and 3/8-inch-OD tubes from Location E (Figure 128), the highest temperature region of the boiler, is presented in Figures

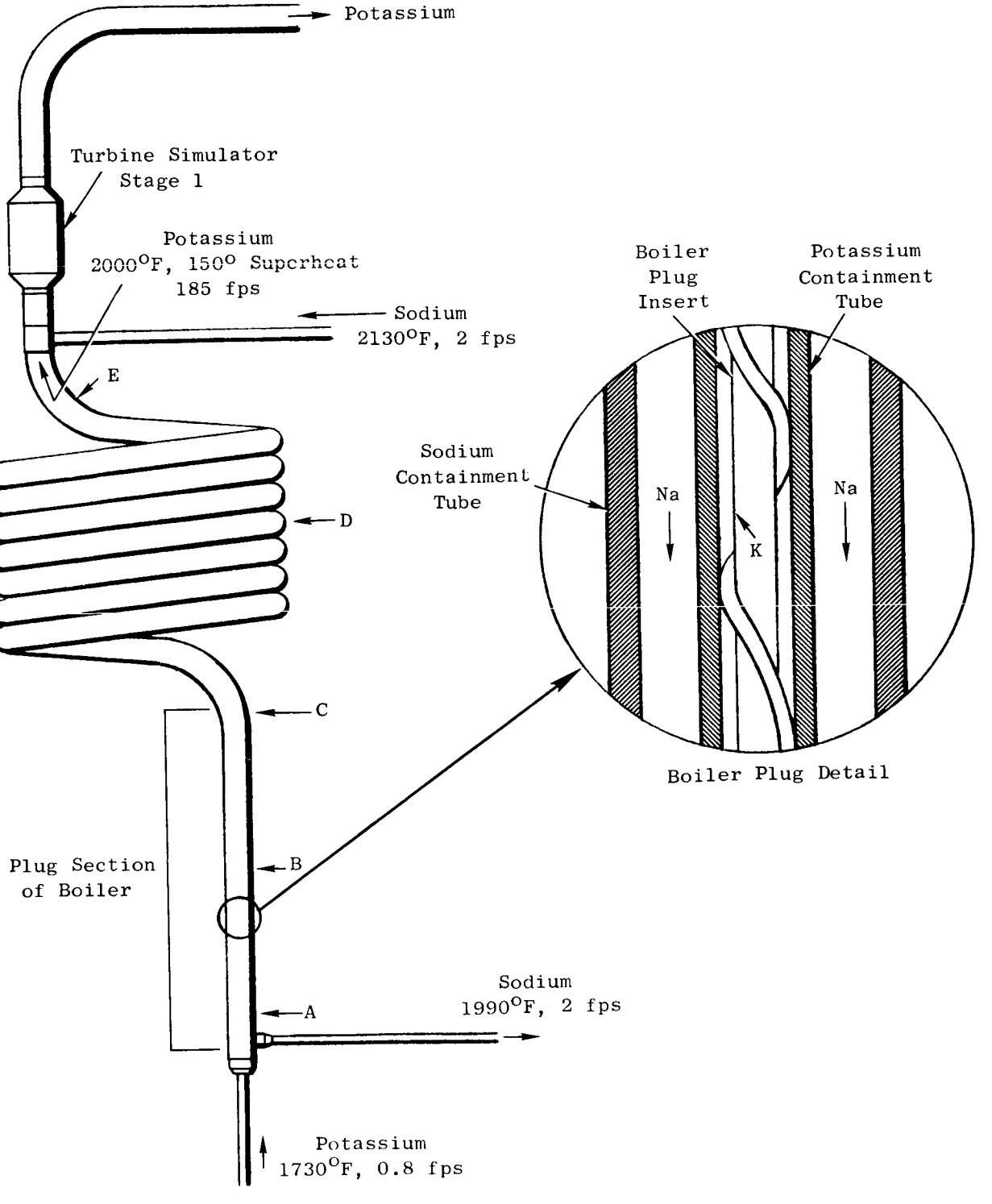

Figure 128. Boiler Diagram Showing the Location of Metallographic Specimens From Various Regions of the Boiler Shown in the Figures Which Follow.

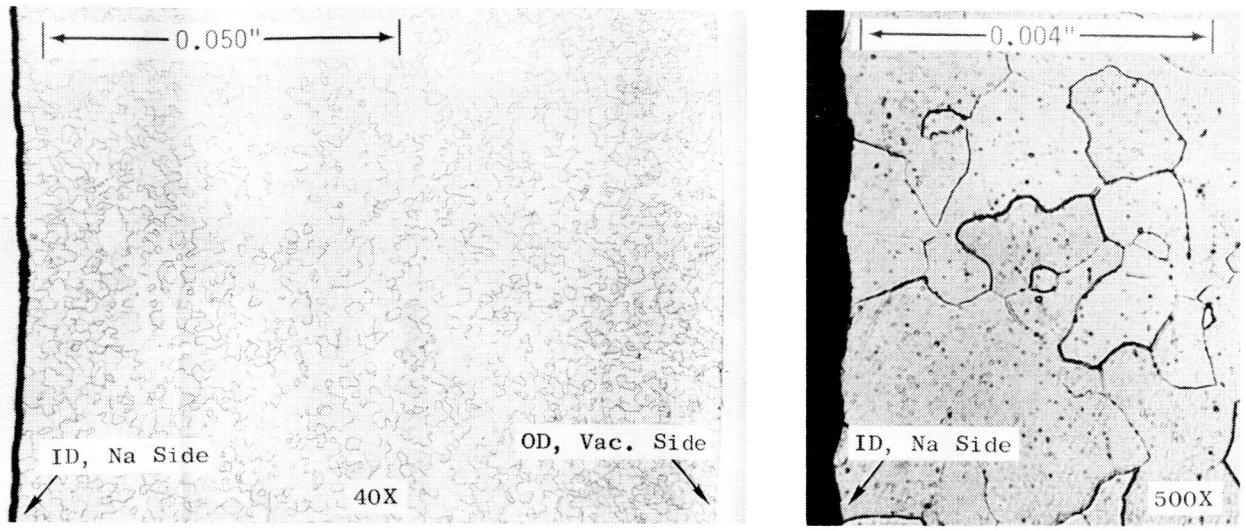

(a) Sodium Containment Tube (2000°F), Location A

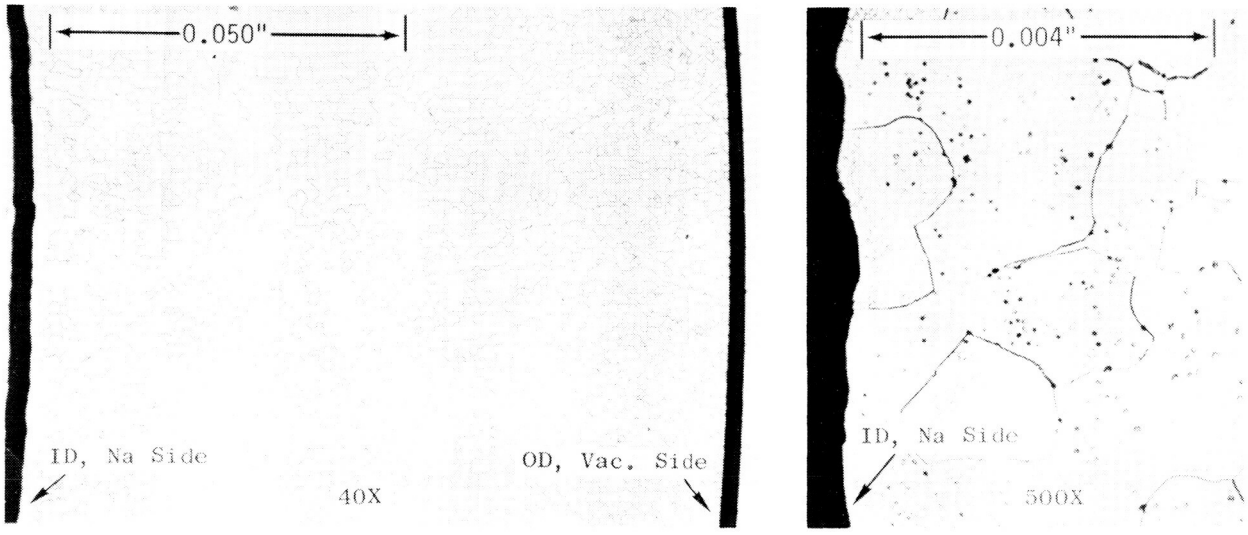

(b) Sodium Containment Tube (2080°F), Location B

Figure 129. Cb-1Zr Tubing From Boiler. Location of Metallographic Specimens Given in Figure 128. Vacuum Side and Sodium Side of 1-inch OD Tube Indicated.

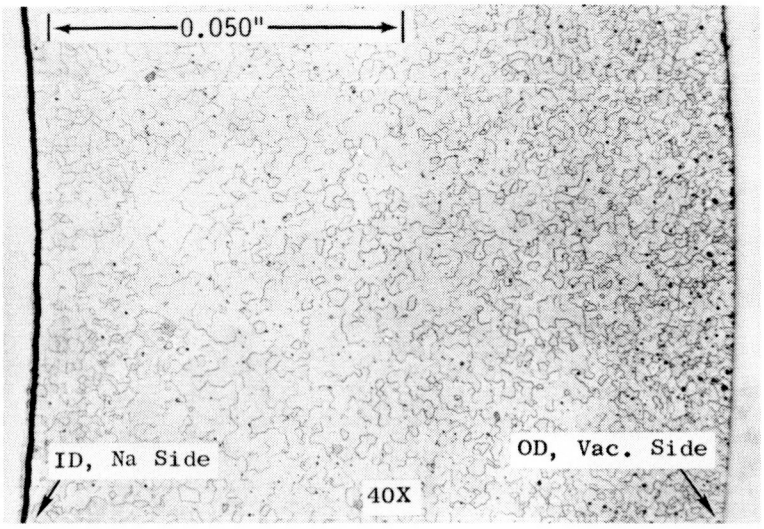

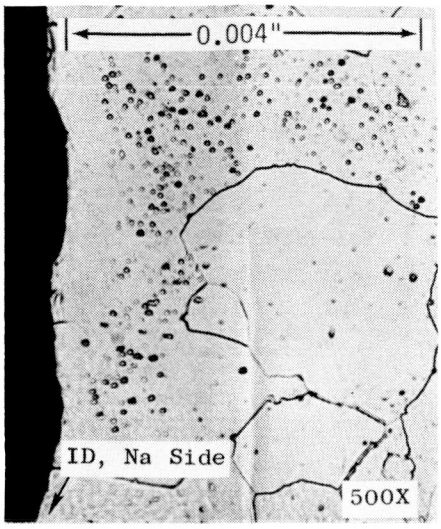

(a) Sodium Containment Tube (2100°F), Location C

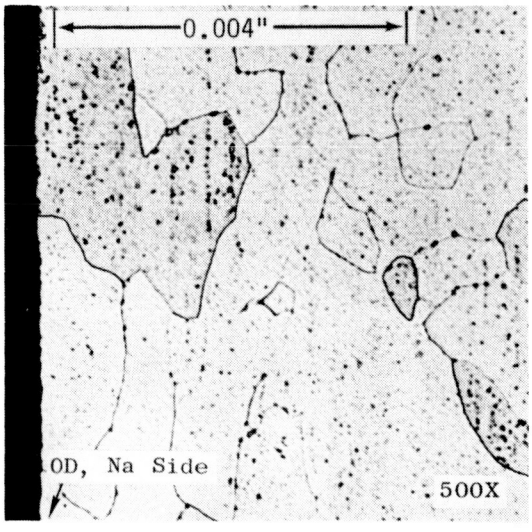

(b) Sodium Side of Potassium Containment Tube, Location C

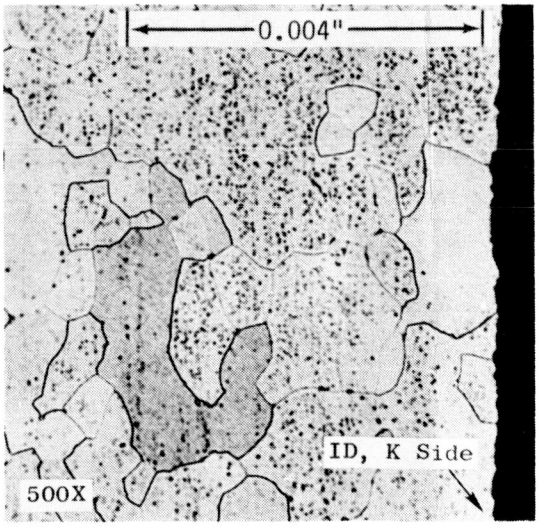

(c) Potassium Side of Potassium Containment Tube, Location C

Figure 130. Cb-1Zr Tubing From Boiler. Location of Metallographic Specimens Given in Figure 128.

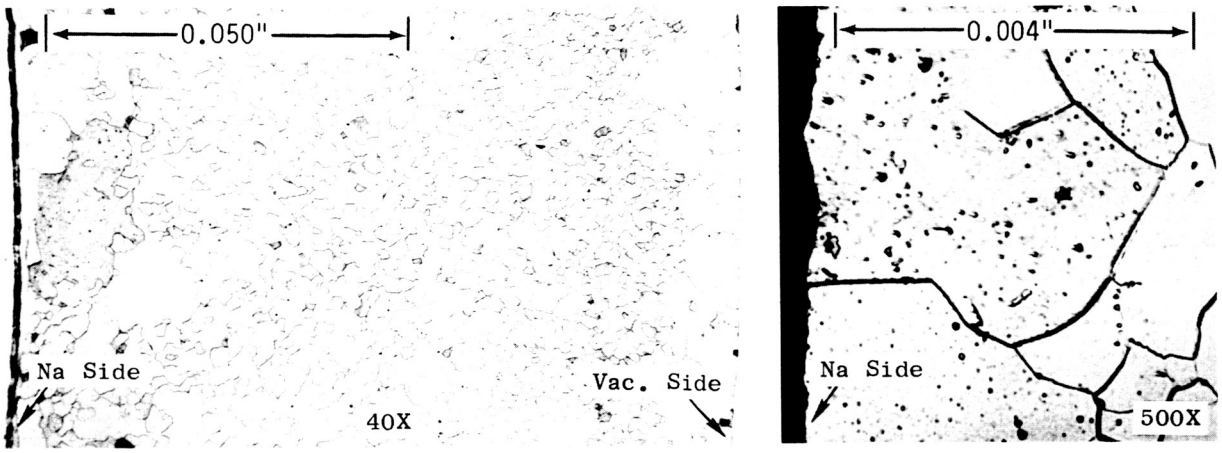

(a) Sodium Containment Tube (2120°F), Location D

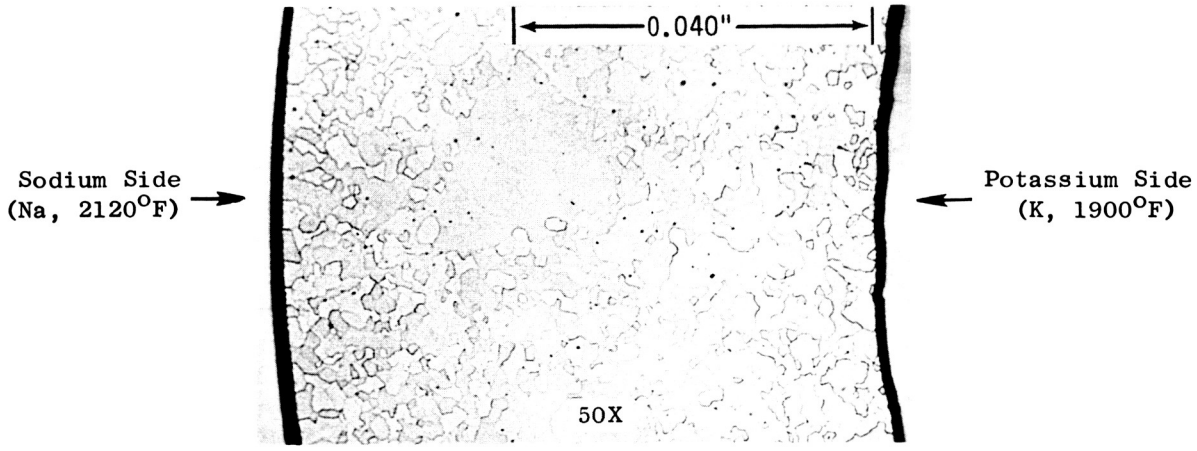

Potassium Containment Tube, Location D

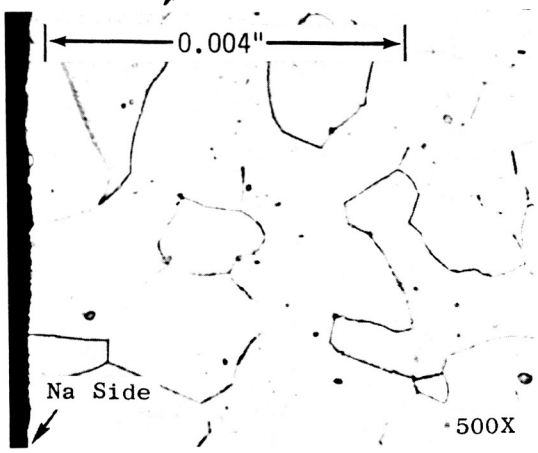

(b) Sodium Side of Potassium Containment Tube

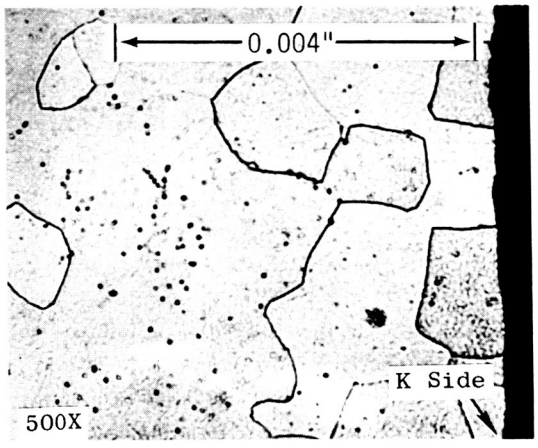

(c) Potassium Side of Potassium Containment Tube

Figure 131. Cb-1Zr Tubing From Boiler. Location of Metallographic Specimens Given in Figure 128.

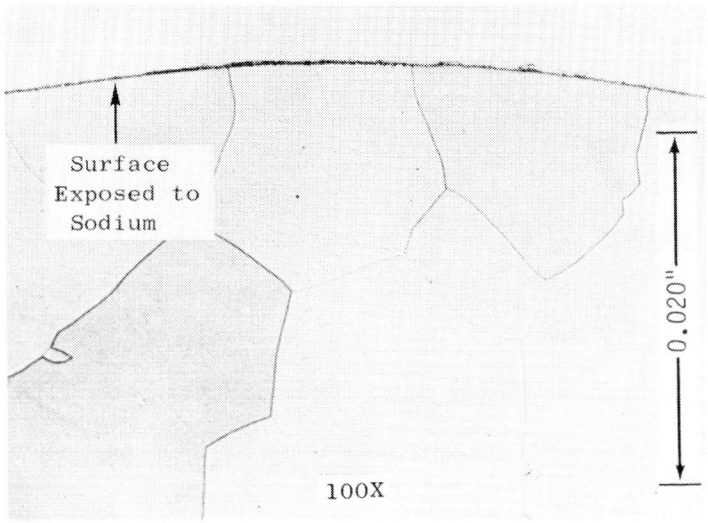

(a) Low Magnification View of Surface of Butt Weld

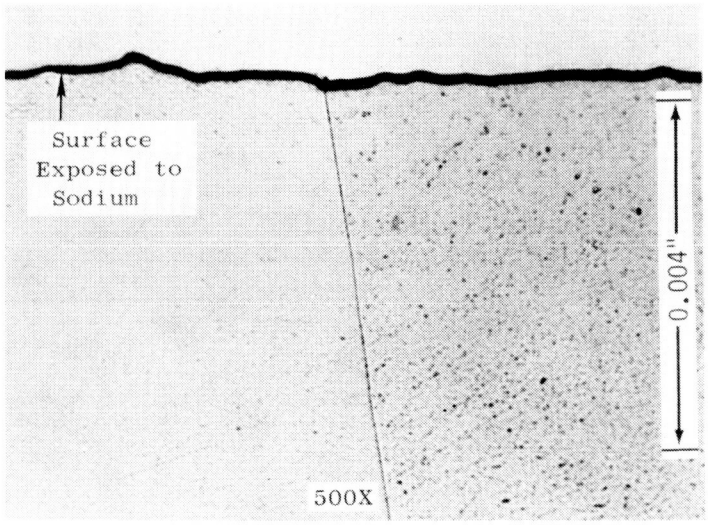

(b) High Magnification View of Surface of Butt Weld

Figure 132. Surface of Cb-1Zr Butt Weld in 1-inch OD Sodium Containment Tube From Boiler (Location D) Following Test. Location of Metallographic Specimens Given in Figure 128.

133 and 134. Both tubes show gross evidence of critical strain grain growth both in the neutral axis and compression regions of the bend. Areas are apparent in the 3/8-inch-OD tube, Figure 134 (b), where only two or three grains make up the entire tube wall. The small "notch" on the ID surface in this photomicrograph is thought to be a surface defect that was present before test.

A detailed presentation of the metallographic observations on the 3 8-inch-OD potassium tube in the plug region of the boiler will now be given. Figure 135 indicates the location from which the specimens were taken and shows the frosty deposit which covered the lower five inches of the 3/8-inch-OD tube. The sharp transition from no deposit to deposit which is readily apparent is attributed to the sharp drop in sodium temperature in this region. The appearance of the sodium side of the tube in the deposit region, Location A, is given at magnifications of 500 and 1500X in Figure 136 (a). The deposit is quite crystallographic in appearance, and the light areas in the particles result from reflected light shining through the translucent deposits. The sodium side of the tube illustrated in Figure 136 contained in excess of 2500 ppm oxygen, while the potassium side which showed no attack, contained less than 170 ppm. The evaluations performed to characterize this deposit are presented in Part C which follows. The appearance of both the sodium and potassium sides of the potassium containment tube in Location B (Figure 135) just before the deposition terminates, is quite similar to that observed in Location A with the exception that the deposit is thinner and less continuous as shown in Figure 137. Only one-half inch above the location illustrated in Figure 137, the appearance of both the sodium and potassium sides of the tube changed markedly as illustrated by Figure 138. No trace of deposit could be detected on the sodium side of the tube, and the surface of the potassium side was quite irregular. This roughness, although minor in terms of corrosion, is attributed to the violence and washing effect of vapor bubble nucleation in this region. The close proximity of the sharp transition from deposit to no deposit on the sodium side and from no attack to attack

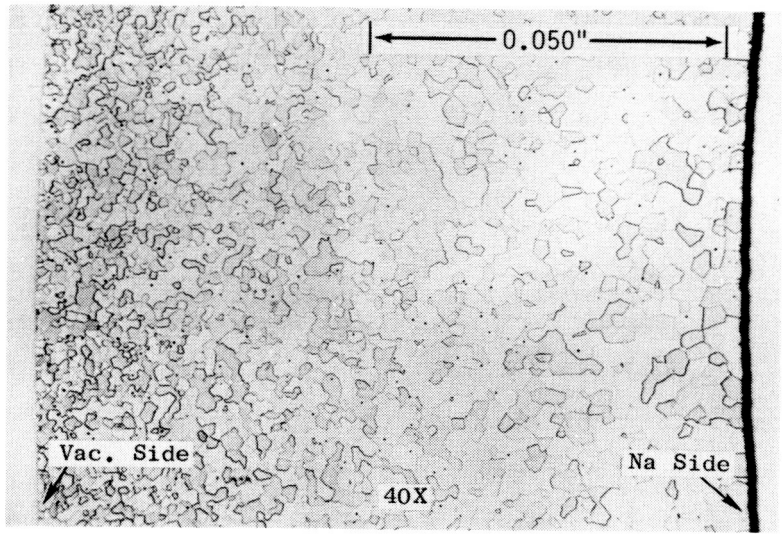

(a) Neutral Axis of Tube Bend

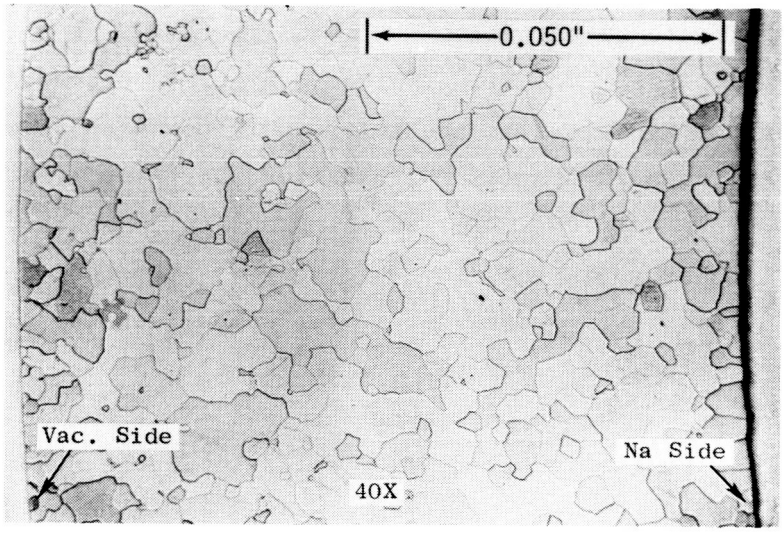

(b) Compression Side of Tube Bend

Figure 133. Sodium Containment Tube (1-inch OD) From Location E (2130°F) in Boiler Showing Effect of Boiler Forming on Critical Strain Grain Growth. Location of Metallographic Specimens Given in Figure 128.

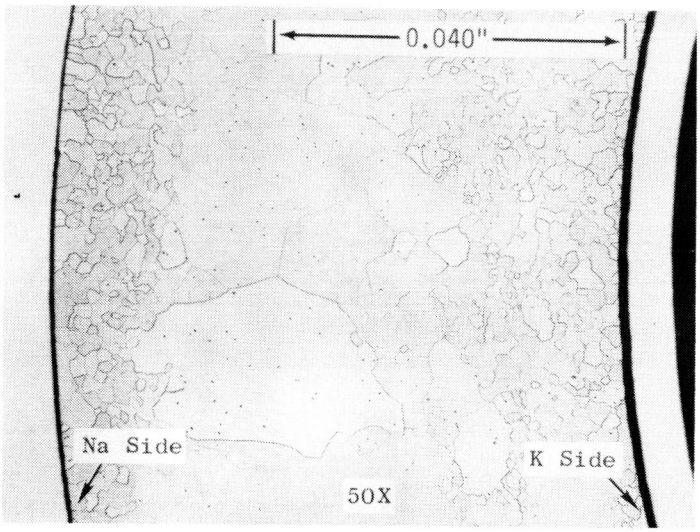

(a) Neutral Axis of Tube Bend

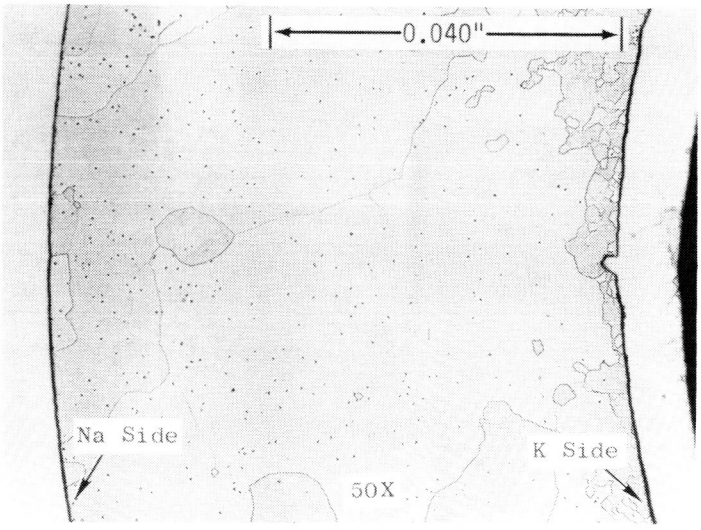

(b) Compression Side of Tube Bend

Figure 134. Potassium Containment Tube (3/8-inch OD) From Location E (Na, 2130°F; K, 2000°F) Showing Effect of Boiler Forming on Critical Strain Grain Growth. Location of Metallographic Specimens Given in Figure 128.

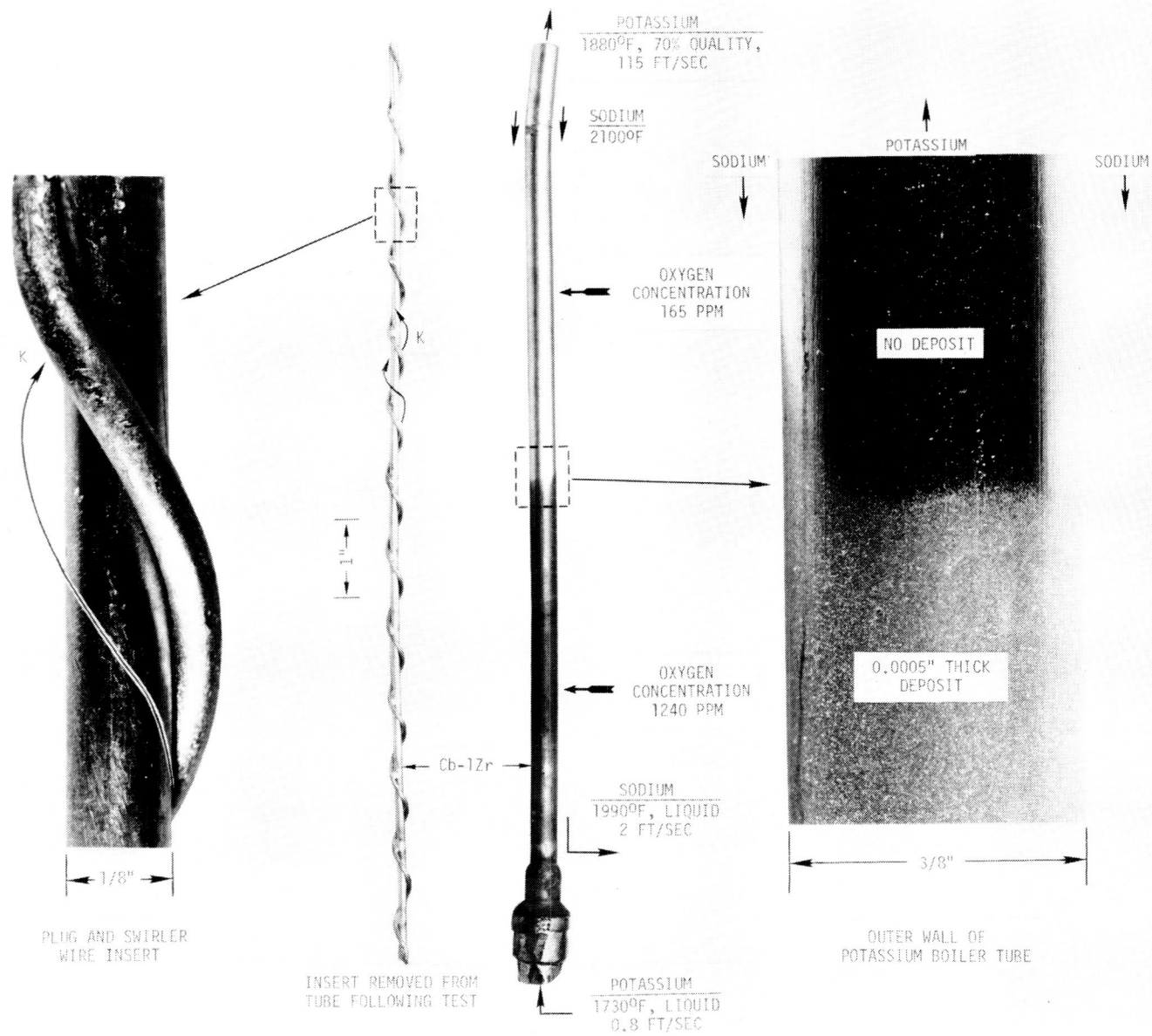

Figure 135. Cb-1Zr Components Taken From the Plug Region of the Boiler Showing the Location of Metallographic Specimens Shown in the Figures Which Follow.

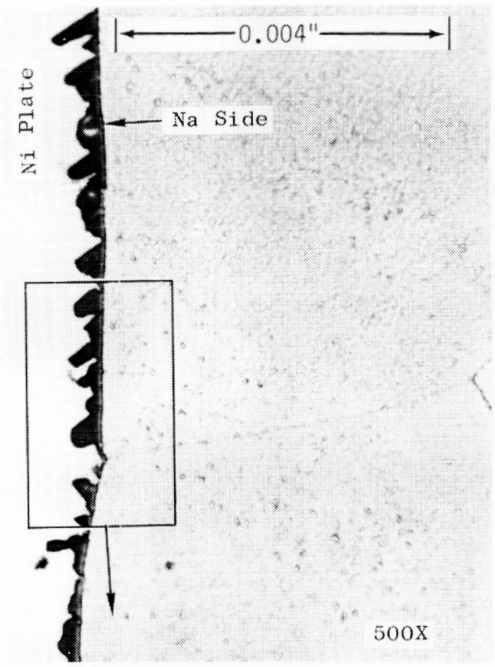

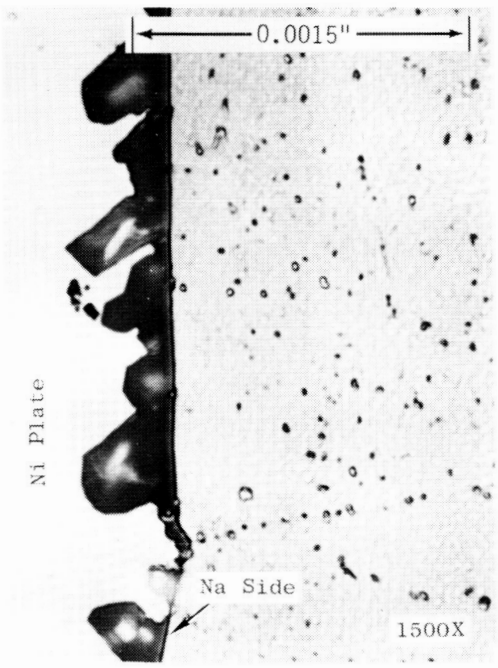

(a) Sodium Side of Potassium Containment Tube

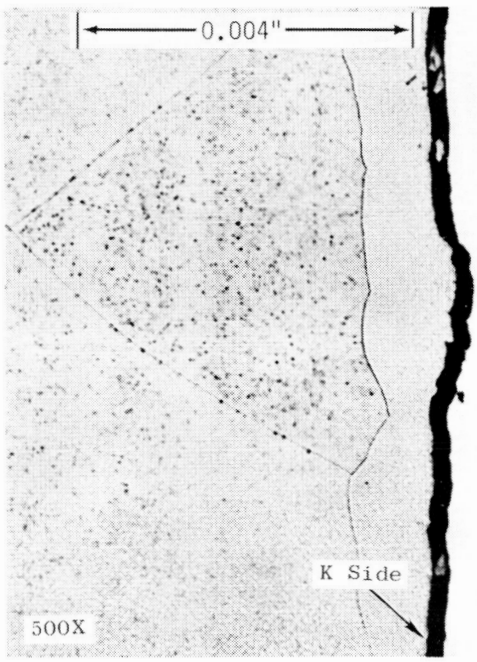

(b) Potassium Side of Potassium Containment Tube

Location A in Figure 135

Figure 136. Cb-1Zr Tube (3/8-inch OD) From Sodium Exit - Potassium Entrance Region of Boiler.

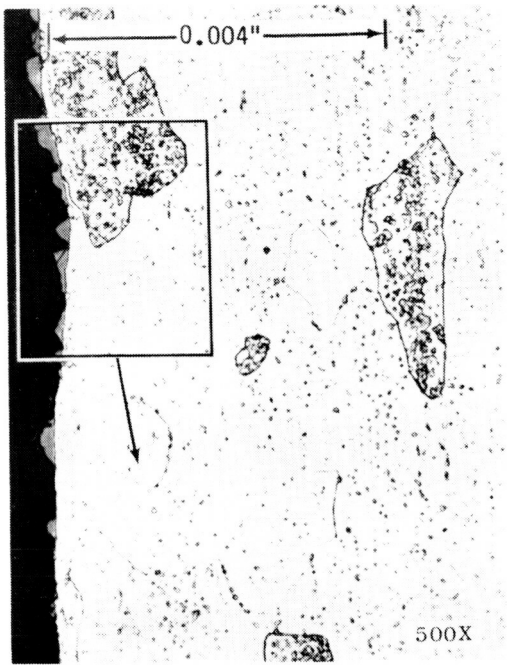

(a) Sodium Side of Potassium Containment Tube

(b) Potassium Side of Potassium Containment Tube

Location B in Figure 135

Figure 137. Cb-1Zr Tube (3/8-inch OD) From Boiler Plug Region, Five Inches From Potassium Boiler Entrance/Sodium Exit.

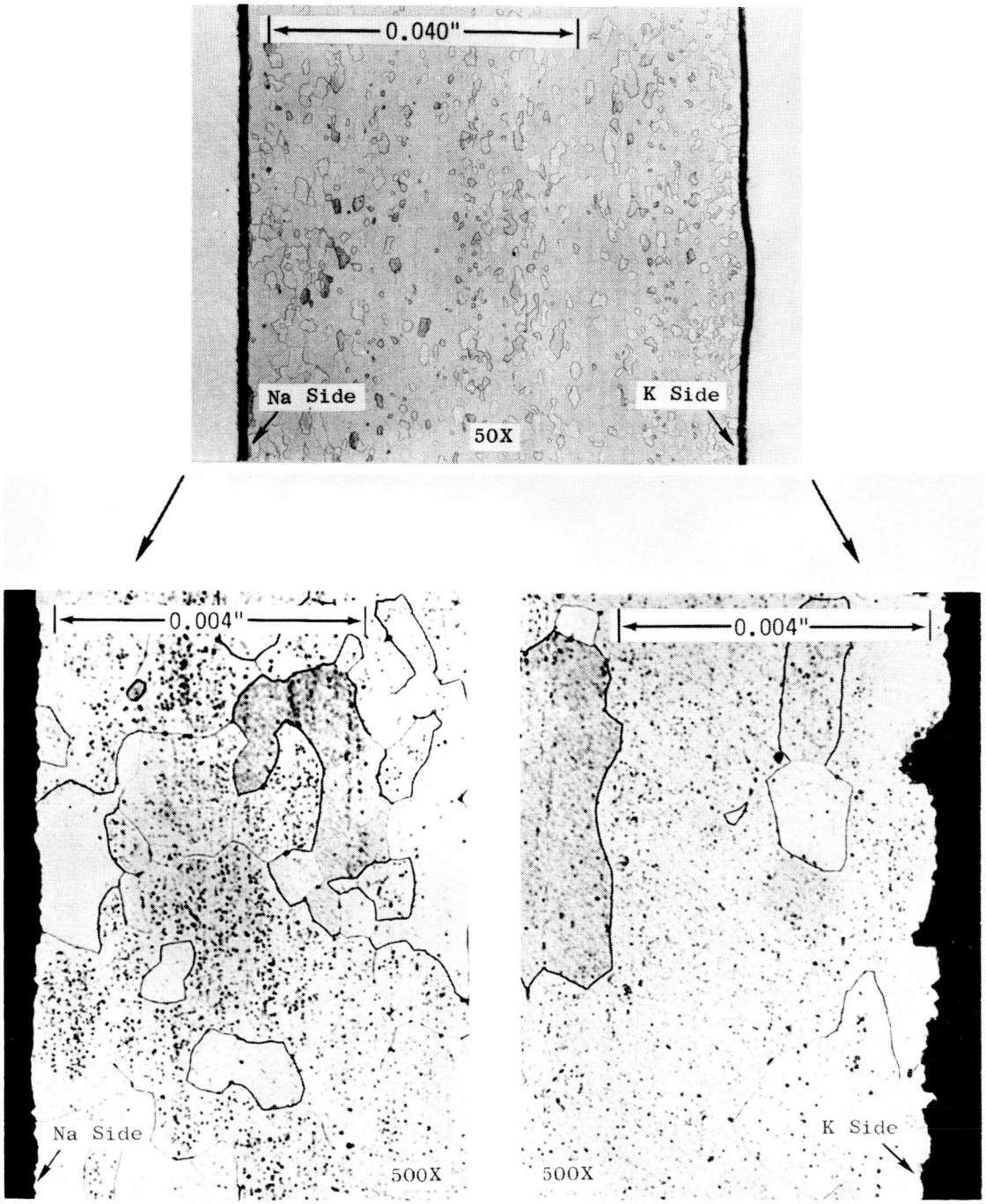

Figure 138. Cb-1Zr Potassium Containment Tube (3/8-inch OD) Six Inches From Potassium Boiler Entrance/Sodium Exit, Location C in Figure 135.

on the potassium side is reasonable evidence that potassium vapor bubble nucleation was occurring in this area 5-6 inches after the potassium entered the boiler.

4. Mo-TZM Alloy Metallographic Specimen From the Turbine Simulator. The excellent posttest appearance of the nozzle and blade specimens from the single- and nine-stage turbine simulators was shown previously in Figures 114, 115, and 116. The test conditions for each stage of the turbine simulator and the results of dimensional analysis and weight change measurements were presented in Table XXI in Section XI, Distillation Draining, and Disassembly, of this report. As was indicated in Table XXI, no significant change in nozzle throat dimension or in the weight of any of the nozzle or blade specimens was detected.

The excellent visual and metallographic appearance of the throat region of three of the nozzles is indicated in Figure 139. No evidence of throat damage was detected in any of the nozzles. Slight evidence of recrystallization of the surface regions of the throat of the hottest nozzle, No. 1, was detected. Twenty metallographic sections were prepared from the 10 Mo-TZM blades in the turbine simulator. Cross sections of the blades in the area of vapor impingement and near the outer portion of blade out of the path of vapor impingement were examined. No surface damage could be detected in any of the regions examined, and no differences in the appearance of the edge or face of any of the blades were observed. The typical appearance of the impingement edge of the blade specimens is given in Figure 140.

5. Metallographic Evaluation of Components of the Potassium Metering Valve. The components of the metering valve from the potassium circuit, which operated at approximately 1100°F during the 5000-hour test, were destructively evaluated. The excellent appearance of the very thin Cb-1Zr bellows and of the high-velocity region of the Mo-TZM alloy metering plug are indicated in the photomicrographs in Figure 141.

6. Metallographic Evaluation of the Iron Titanate Coating on the Cb-1Zr Condenser Fin. A number of specimens of the condenser fin were examined metallographically to determine if any changes in the structure

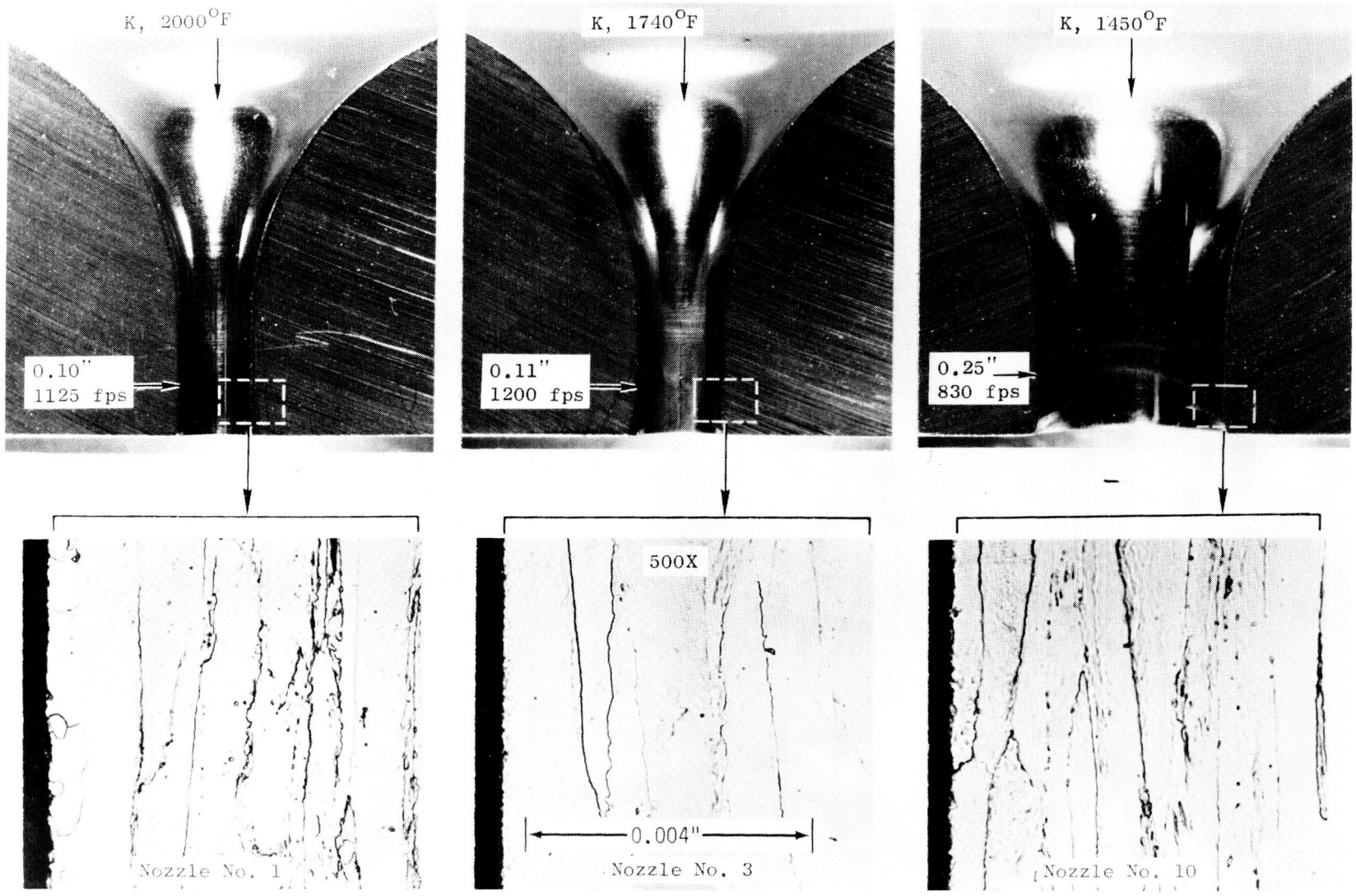

Figure 139. Cross Section Views and Photomicrographs of Turbine Simulator Nozzles Following Exposure to Potassium for 5000-Hours in the Cb-1Zr Corrosion Test Loop.

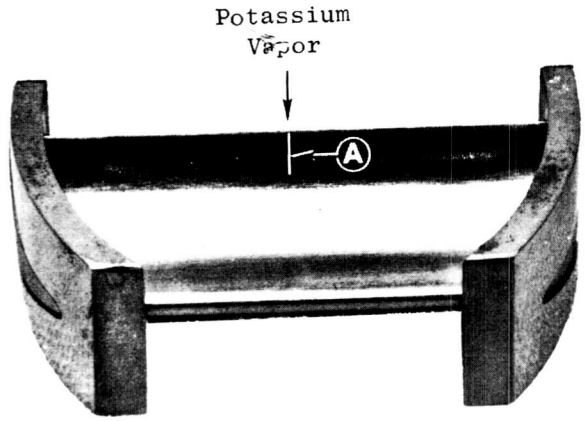

Blade Specimen and Holding Pads

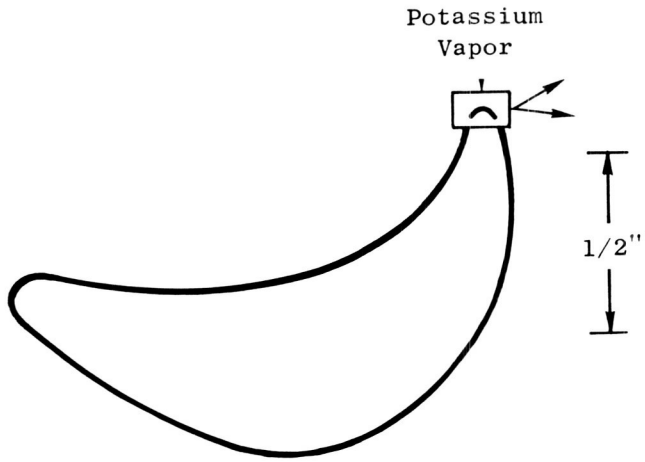

Cross Section of Blade Specimen

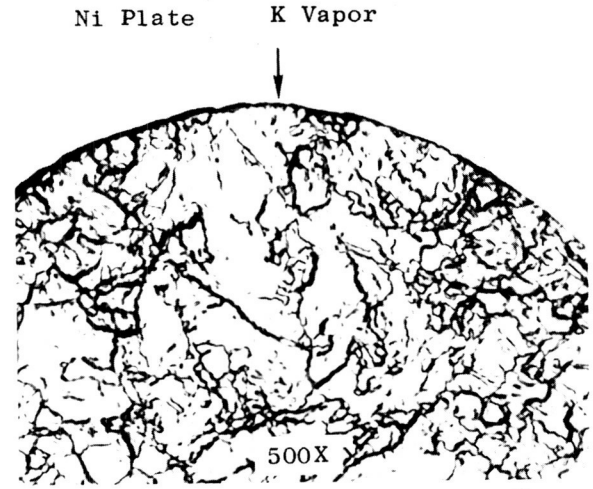

Blade Specimen No. 1, Region Ⓐ
Nozzle Inlet Temp., 2000°F
Impingement Velocity, 1125 ft/sec

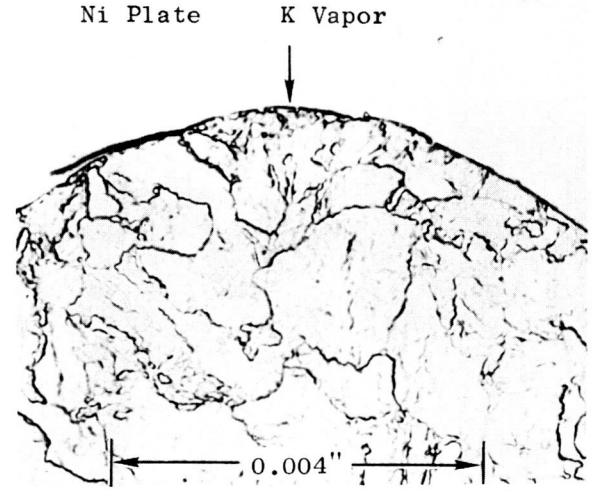

Blade Specimen No. 2, Region Ⓐ
Nozzle Inlet Temp., 1785°F
Impingement Velocity, 1350 ft/sec

Figure 140. Mo-TZM Turbine Simulator Blade Specimens Showing Microstructure of Impingement Area Following 5000-Hour Test.

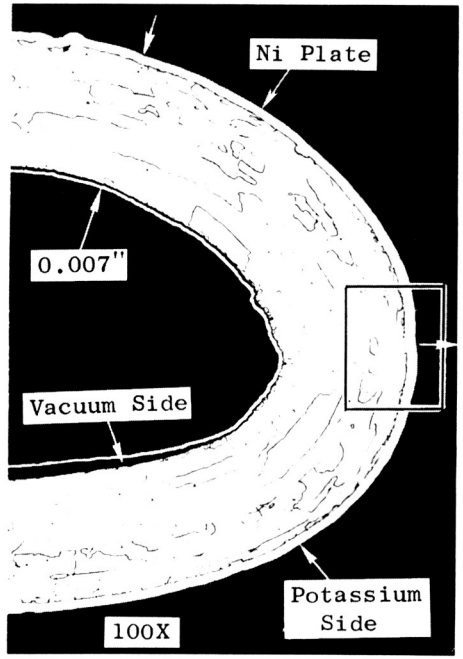

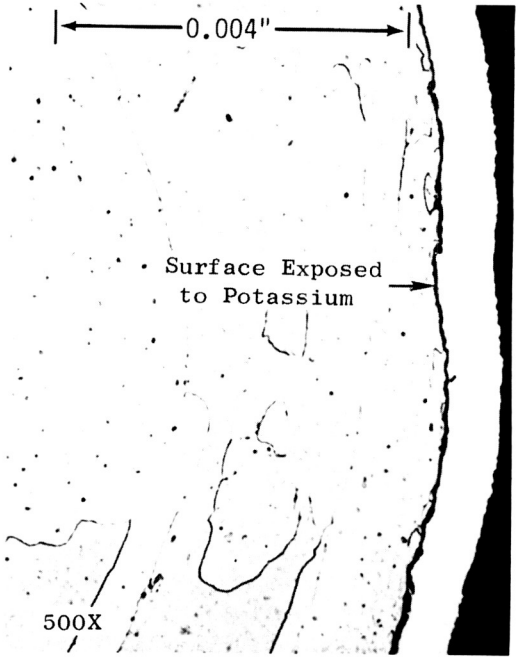

Cb-1Zr Bellows of Metering Valve (Inner Apex of Convolution)

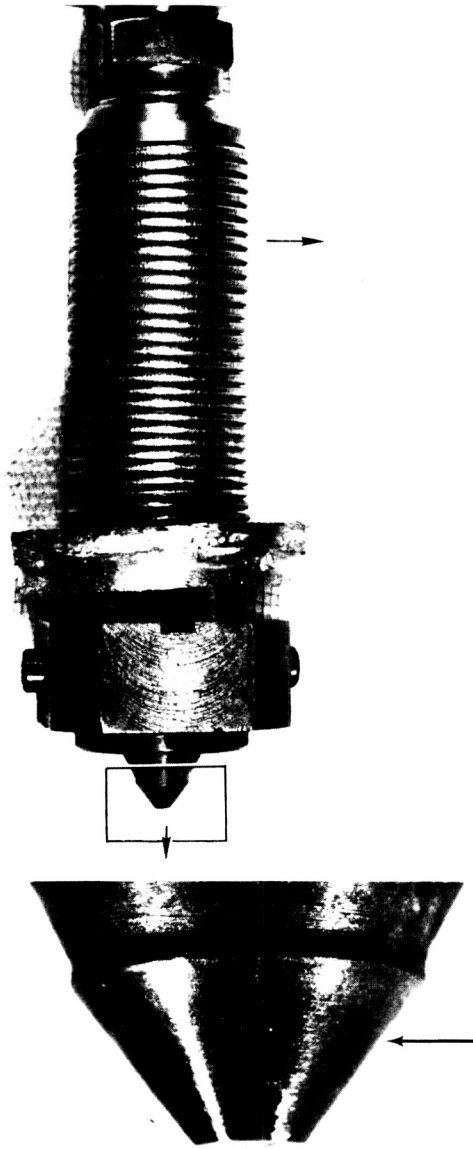

Mo-TZM Valve Plug

Surface of Valve Plug in High Velocity Region (17 fps)

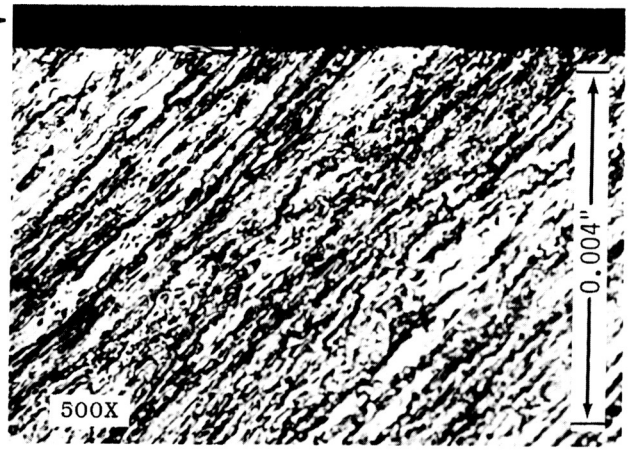

Figure 141. Metallographic Appearance of Metering Valve Components Following 5000-Hour Test.

or adherence had occurred during the 5000-hour test. The preliminary evaluations of the iron titanate conducted prior to its use on the condenser fins of the loop test are described in Appendix F, Test to Evaluate a High-Emittance Iron Titanate Coating for the Cb-1Zr Condenser Fin, of this report.

An overall view of the upper portion of the loop and an enlarged view of one of the condenser fins which indicates the area from which the metallographic specimens were taken are included in Figure 142. The coating thickness was quite uniform (3 to 4 mils) on the specimens examined. It may be noted in Figure 142 that a gap existed between the coating in the hottest region nearest the condenser pipe but was almost completely intact less than one-half inch from the pipe-to-fin weld. Other specimens further out along the fin, C, D, and E, were similar in appearance to before-test specimens.

C. ELECTRON BEAM MICROPROBE ANALYSES

Electron beam microprobe analyses were performed on a total of eight control and test loop specimens. These examinations were performed in the G. E. Material Development Laboratory of the Aircraft Engine Group using an EMX Electron Microprobe X-Ray Analyzer manufactured by the Applied Research Laboratory. Only three of the specimens yielded information of sufficient interest to warrant review, and these are presented below. A number of the specimens which will not be discussed were examined to determine if gross zirconium gradients were present in the walls of the Cb-1Zr tubes taken from various regions of the loop, other than the boiler, and none were found.

1. Non-metallic Deposit on the Sodium Side of the Potassium Containment Tube From the Plug Region of the Boiler. As was noted in the discussion of the metallographic results and indicated in Figures 135, 136, and 137, a thin layer of crystalline deposition was observed on the sodium side of the 3/8-inch-OD Cb-1Zr potassium containment tube in the lower half of the plug section of the boiler. The deposited material was extremely hard (D.P.H. above 800) and translucent, as is particularly apparent in Figure 136 (a) shown earlier. Unfortunately, there was not a sufficient amount of this deposit available to perform X-ray diffraction analysis,

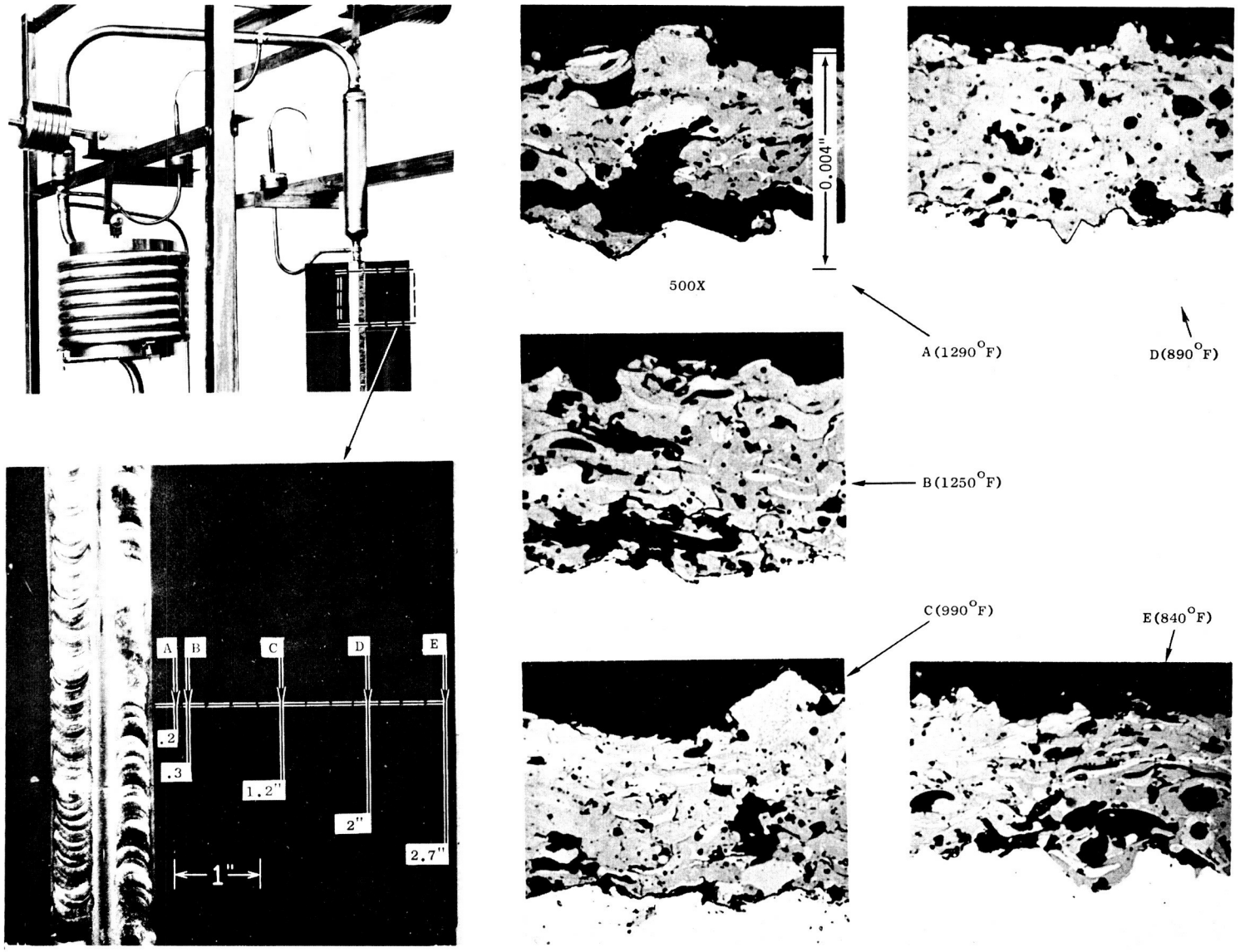

Figure 142. Metallographic Appearance of Iron Titanate Coating on Top Fin of Cb-1Zr Loop Condenser Following 5000 Hour Test.

and therefore microprobe analyses performed on metallographic specimens were the principal evaluation method used to characterize the deposit.

An X-ray wavelength scan of the deposit detected only zirconium. The zirconium X-ray image subsequently obtained is illustrated in Figure 143, together with an optical photomicrograph of the deposit, and clearly indicates the deposit is rich in zirconium. The graphical results obtained are given in Figure 144 and show that the deposit contains approximately 85 percent zirconium. A similar check for oxygen revealed an unmeasurable but detectable amount. It is estimated that the minimum detectable limit during this analysis for oxygen was approximately 10 percent, therefore, indicating that the oxygen present in the deposit was in excess of 10 percent.

Electron back-scatter images showing the Cb-1Zr alloy tube, the zirconium-rich deposit, and the nickel plate surrounding the deposit yielded very interesting results. Contrast in the back-scattered electron image can, for the most part, be related to differences in average atomic number throughout the specimen being examined. Therefore, materials with similar average atomic numbers within a specimen will not be resolved in the back-scatter electron image. Equipment limitations must also be considered and the microprobe unit used to study this specimen was capable of resolving atomic number differences as small as four atomic numbers. Also, the back-scattered electron intensity increases as the atomic number increases. The overall intensity of the back-scattered electrons from a specimen will be controlled by the electron beam current. Therefore, it is normal practice to observe the electron back-scatter (EBS) image as the beam current is increased and note the image contrast development. The material with the highest atomic number within the specimen will be observed first as the beam current is increased. This is illustrated in EBS Image No. 1 in Figure 145. The Cb-1Zr alloy tube (average atomic number of approximately 41) can be clearly seen while back-scattered electrons from the zirconium-rich deposit and nickel plate are below the detectable limit of the equipment. The location of the zirconium-rich deposit in the EBS

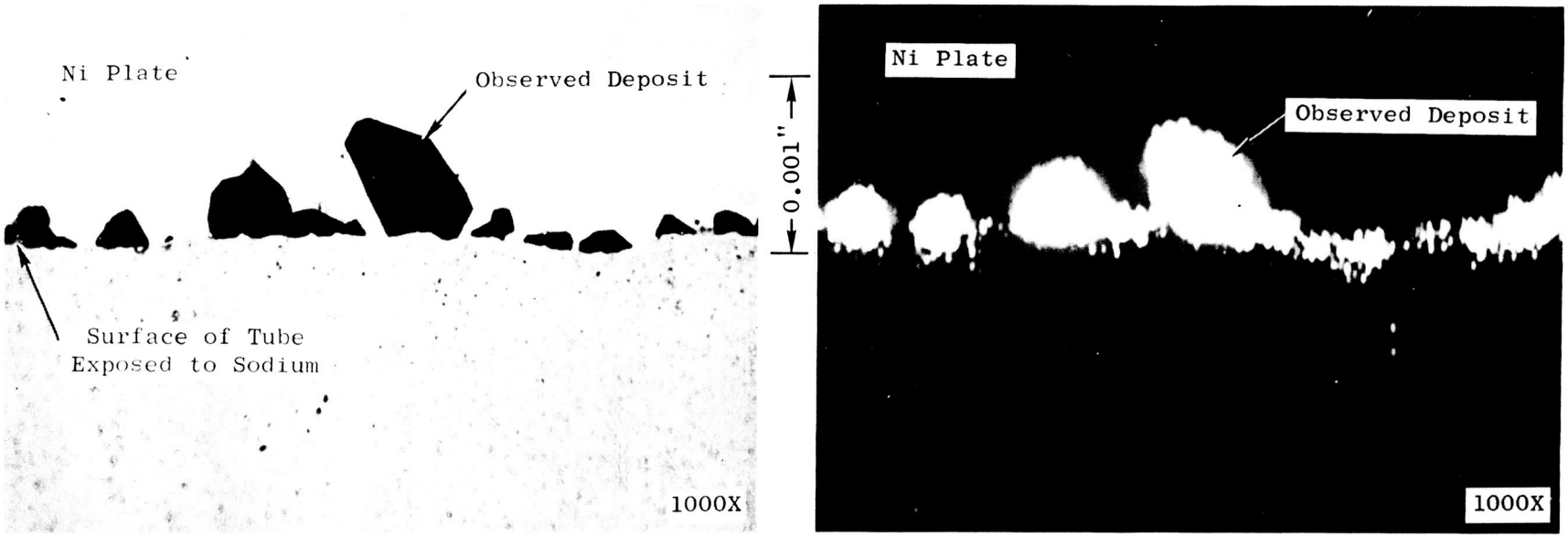

(a) Photomicrograph

(b) Zirconium X-ray Image Produced by Electron Beam Scan

Figure 143. Surface of Cb-1Zr Tube Specimen Taken from the Potassium Containment Tube in the Plug Section of the Boiler Showing Deposit.

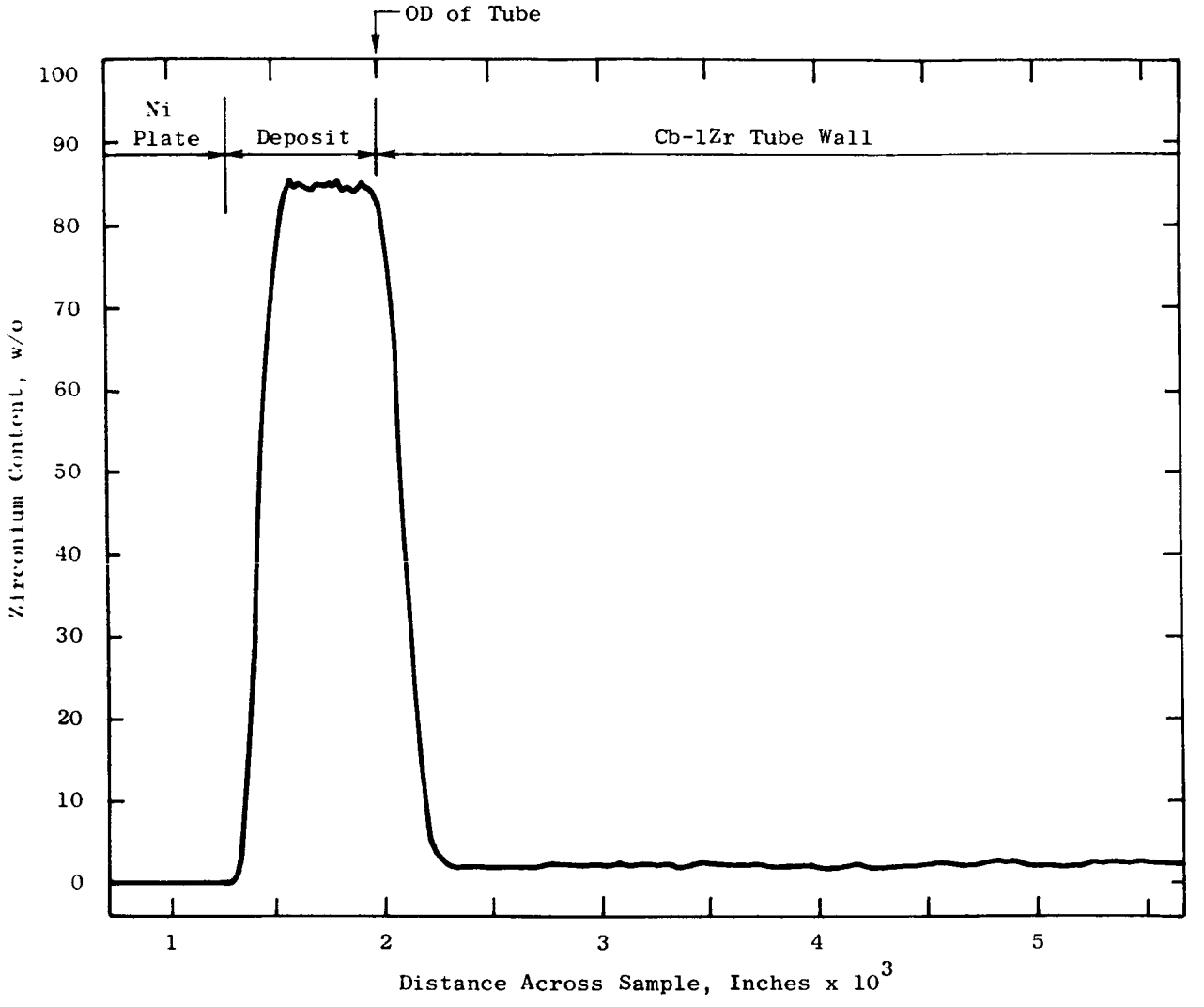

Figure 144. Electron Beam Microprobe X-ray Scan for Zirconium Across the Deposit Found on the Sodium Side of the Potassium Containment Tube in the Plug Region of the Boiler (see Figure 143).

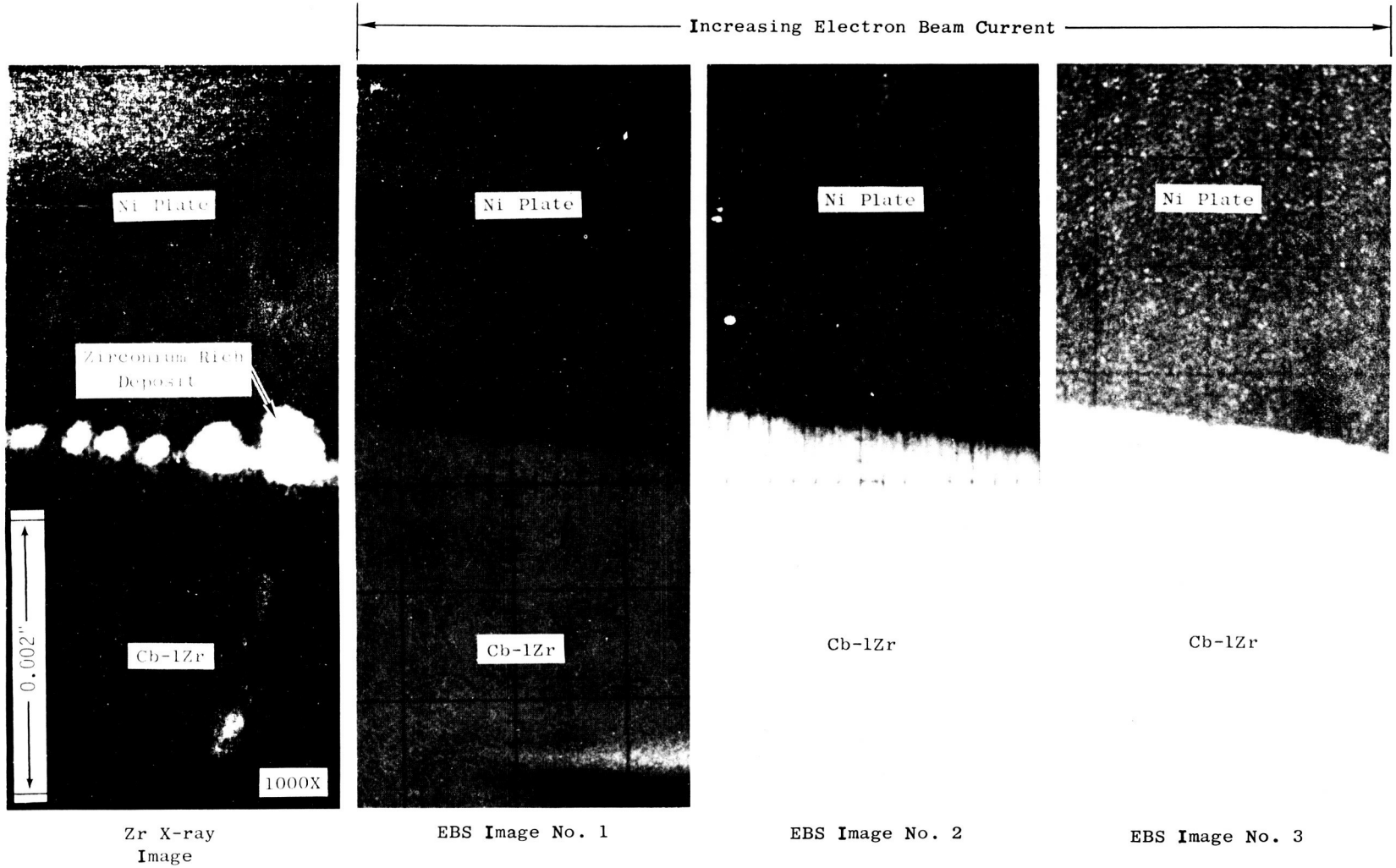

Figure 145. Zirconium X-ray Image and a Series of Electron Back Scatter (EBS) Images With Increasing Beam Current on the Deposit Region of the Cb-1Zr Specimen Illustrated in Figure 143. Lack of Contrast Between Scattering Intensity of Nickel Plate and Deposit Indicates that Average Atomic Number of Deposit Is Similar to that of Nickel (Ni-28, ZrO-24, Cb-1Zr-41, ZrO_2-19).

images is shown in Figure 145 by the zirconium X-ray image of the same area taken just prior to the EBS images. Note that the failure of the zirconium-rich deposit (approximately 85 percent Zr) to create a detectable electron intensity indicates that its average atomic number is significantly less than that for Cb-1Zr alloy. Since the atomic number for zirconium is 40 and normally could not be distinguished from Cb (atomic number 41) in an EBS image, the remaining constituents (approximately 15 percent) of the zirconium-rich deposit must have much lower atomic numbers to significantly reduce the average atomic number of the deposit.

Subsequent increasing of the electron beam current to a value which would make the electron intensity of another constituent detectable, revealed the back-scatter electron intensity of the nickel plate and zirconium-rich deposit to be nearly the same as shown by EBS Image No. 2 in Figure 145. This indicates that the average atomic number of the deposit is similar to that for nickel, which is 28. Further increasing of the beam current also developed no contrast between the nickel plate and the deposit as shown by EBS Image No. 3 in Figure 145.

Although an insufficient quantity of the deposit was available for a structure identification by X-ray diffraction, the foregoing microprobe results indicate that the deposit is ZrO. The stoichiometric composition of ZrO is 85 percent zirconium and 15 percent oxygen which agrees very closely with the analysis of the deposit. Also, the average atomic number of the deposit was found to be 28 ±4 and agrees well with the average atomic number for ZrO which was calculated to be 24. The possibility of the deposit being ZrO_2 has been discounted because the zirconium content of stoichiometric ZrO_2 is 74 percent, and the average atomic number for ZrO_2 is approximately 19. Both of these differences between ZrO and ZrO_2 are large enough that they would have been readily detected in the microprobe evaluation. Although the presence of ZrO is not shown on the Zr-O equilibrium diagram,[52] this does not exclude

[52] Elliot, R. P., Constitution of Binary Alloys, First Supplement, McGraw-Hill Book Company, 1965.

its existance, and in fact, ZrO has been reported by Schonberg.[53, 54] Schonberg reported the synthesis of a ZrO phase with a NaCl type structure and a lattice parameter varying between a_o = 4.584 Angstroms and a_o = 4.620 Angstroms.

An X-ray wavelength scan of the ID of the tube detected only columbium and zirconium to be present. A zirconium analysis scan across the entire wall of the tube revealed no significant zirconium gradient.

In summary, the observed deposit on the OD of the Cb-1Zr boiler tube appears to be ZrO. This deposit is quite similar in appearance to that observed by previous investigators in a 10,000-hour Cb-1Zr refluxing potassium capsule test[55] and a D-43 refluxing potassium capsule test.[56] However, the deposits observed in these earlier tests were reported as zirconium[55] and ZrO_2.[56] Similarity of appearance of these deposits with those observed on the wall of the boiler tube in this loop test suggests that the deposits, reported in the earlier capsule tests, may have been near ZrO in composition.

2. Cb-1Zr Sodium Tube Near Boiler Inlet. The high-temperature region (2130°F) of the Cb-1Zr sodium heater circuit near the boiler inlet was significantly depleted in oxygen concentration (260 ppm to 36 ppm) during the loop test and was also considered to be a likely region for zirconium depletion. Microprobe analysis of the specimen from this region revealed no zirconium gradient and a zirconium concentration near the nominal 1 percent level.

---

(53) Schonberg, N., "The Structure of the Metallic Quarternary Phase ZrTaNO," Acta Chemica Scandinavica, 8, No. 4, 1954, pp. 627-629.

(54) Schonberg, N., "On Metallic Phases in the Ti-P-O and Zr-P-O Systems," Acta Chemica Scandinavica, 8, No. 4, 1954, pp. 1460-1465.

(55) Engel, Jr., L. B. and Frank R. G., Evaluation of High-Strength Columbium Alloys for Alkali Metal Containment, NASA Contract NAS 3-2140, General Electric Company, Cincinnati, Ohio, R66SD3015, 1966, p. 35.

(56) Metals and Ceramics Division Annual Progress Report for Period Ending June 30, 1965, ORNL-3870, November 1965, p. 128.

3. Mo-TZM Turbine Simulator Nozzle. The metallographic specimen from the throat region of Nozzle No. 2 which operated at a nozzle inlet temperature of 1785°F was checked by microprobe analysis to determine if any depletion or deposition had occurred in this region. Only the normal concentrations of Mo, Zr, and Ti were observed in this region.

D. TENSILE TEST RESULTS ON Cb-1Zr TUBING

In order to determine the effect of the 5000 hours of exposure to flowing sodium on the mechanical properties of the 3/8-inch-OD Cb-1Zr tubing, twelve reduced gauge length tensile specimens were prepared from before-test tubing and tubing from two regions of the loop. The regions of the sodium circuit selected were the highest temperature region (boiler entrance) which experienced a gross oxygen decrease (260 ppm to 36 ppm) during the test and the coolest region of the loop (boiler exit) which exhibited an oxygen increase (260 ppm to 730 ppm) during the test. The results obtained are listed in Table XXVI. The before-test specimens and the specimens taken from the high and low oxygen regions of the loop were very similar in mechanical properties at both room temperature and 2000°F, which is somewhat surprising in view of the differences in thermal exposure and oxygen concentration. The extremely ductile nature of the fractures in all these specimens as well as the similarity of all fractures in appearance is quite apparent in Figure 146, which shows one of each of the pairs of specimens tested.

E. BEND TEST RESULTS ON Cb-1Zr TUBING

The posttest ductility of 1/2-inch-long tube sections taken from eleven regions of the loop was checked by flattening the tubes in a hydraulic press. A strip of 0.060-inch-thick sheet was used as an internal support for the 3/8-inch-OD x 0.062-inch wall tubing and a 0.10-inch-thick sheet was used as an internal support for the 1.0-inch-OD x 0.10-inch wall tubing. Measurements of the specimens during metallographic examination indicated bend radii equal to one-half the tube wall thicknesses for both sizes of tubing.

TABLE XXVI

RESULTS OF TENSILE TESTS PERFORMED ON REDUCED GAUGE LENGTH Cb-1Zr TUBE TENSILE SPECIMENS TAKEN FROM THE SODIUM CIRCUIT OF THE CORROSION TEST LOOP

Specimen	Oxygen Conc, ppm	Room Temperature			2000°F[a]		
		Yield Strength psi	Ultimate Tensile Strength psi	Elong. %	Yield Strength psi	Ultimate Tensile Strength psi	Elong. %
Before Test	260	18,300	34,000	40	11,000	14,600	50.0
	260	19,100	37,400	34	11,700	16,800	42.0
Boiler Inlet Tube 2130°F	36	18,400	31,100	38	10,800	15,700	47.0
	36	18,600	31,600	36	9,500	13,800	52.0
Boiler Outlet Tube, 1985°F	730	15,600	33,900	33	10,000	14,300	38.5
	730	16,900	32,800	36	10,300	15,000	51.5

(a) Tested in a vacuum environment; pressure less than 1×10^{-6} torr.

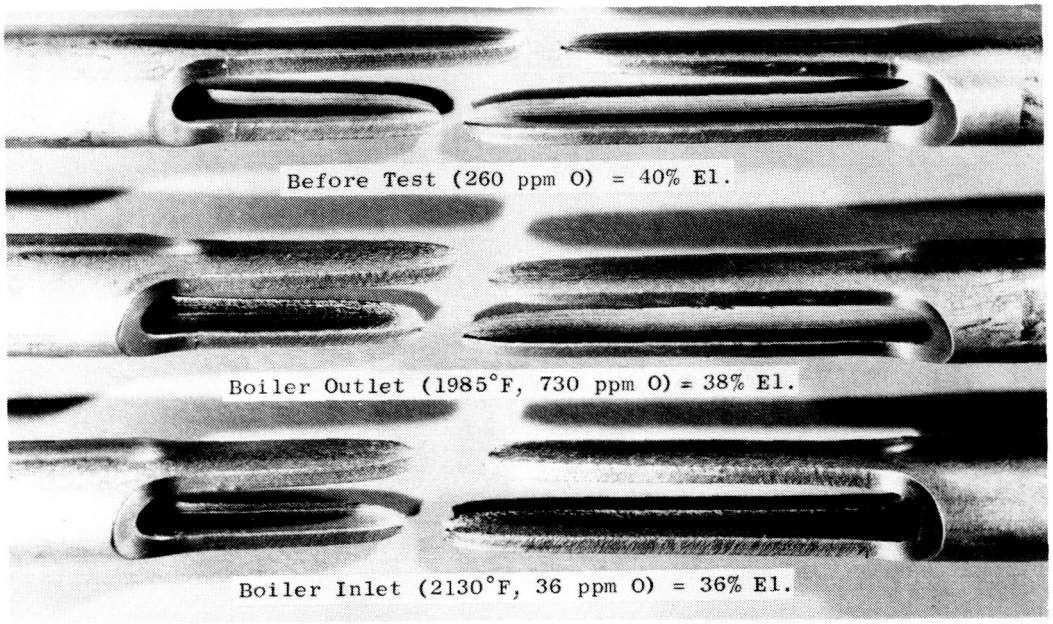

(a) Tested at Room Temperature

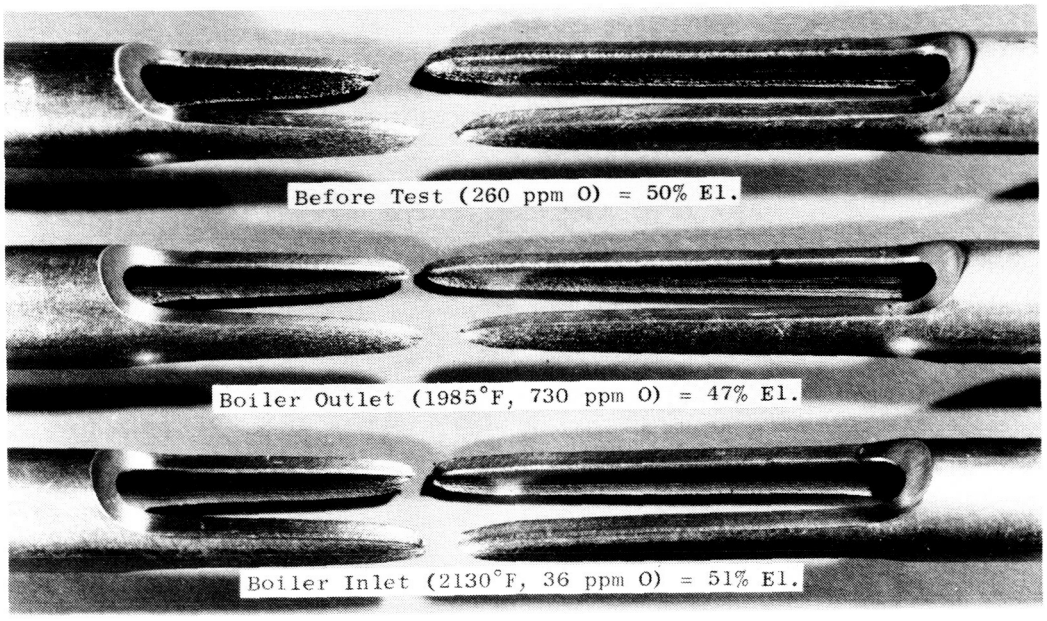

(b) Tested at 2000°F, 1 x 10^{-6} Torr

Figure 146. Appearance of Fractures of Reduced Gauge Length Tube Tensile Specimens Prepared From 3/8-inch OD Cb-1Zr Tubing Taken From the Sodium Circuit of the Cb-1Zr Corrosion Test Loop. (C66100343, C66100345)

The samples selected were taken from both the potassium and sodium circuit and were representative of the environmental exposures of all regions of the loop. All specimens were examined with a stereomicroscope at 30X following bending as well as metallographically to determine if any cracking could be detected. In no case was even shallow surface cracking observed as a result of this qualitative, but very severe bend operation. The excellent ductility of these specimens is typified by the results illustrated in Figure 147 which shows the metallographic appearance of the apex of the bend of the specimen selected from the potassium containment tube in the plug region of the boiler. The OD of the 3 8-inch Cb-1Zr tube was covered with a very thin layer of ZrO crystals as may be seen in the high magnification view. The region shown in the enlarged view (500X) contained considerably more than 2500 ppm oxygen since the outer 20 mils of this tube analyzed 2450 ppm oxygen.

As was indicated in Figure 133 and 134 of this section, a considerable amount of grain growth was observed in the hottest regions of the coiled portions of the boiler. The macro-appearance of the surfaces of bend specimens of the 1-inch-OD Cb-1Zr tubing taken from two regions of the boiler are shown in Figure 148. The specimen shown in Figure 148(a) was taken from the high temperature region (2100°F) and displays a very irregular surface typical of deformation of a ductile large-grained structure while the bend specimen from the fine-grained 2000°F region was quite smooth. No cracking was observed in either specimen.

F. MICROHARDNESS EVALUATION OF Cb-1Zr AND Mo-TZM COMPONENTS

Microhardness surveys were performed on a number of Cb-1Zr tube specimens from both the sodium and the potassium circuits to determine if any gross changes in hardness had occurred which might contribute information regarding the effect of the alkali metals and test chamber environment on the contaminment alloy. Selected specimens of the Mo-TZM alloy turbine simulator blade specimens were also evaluated.

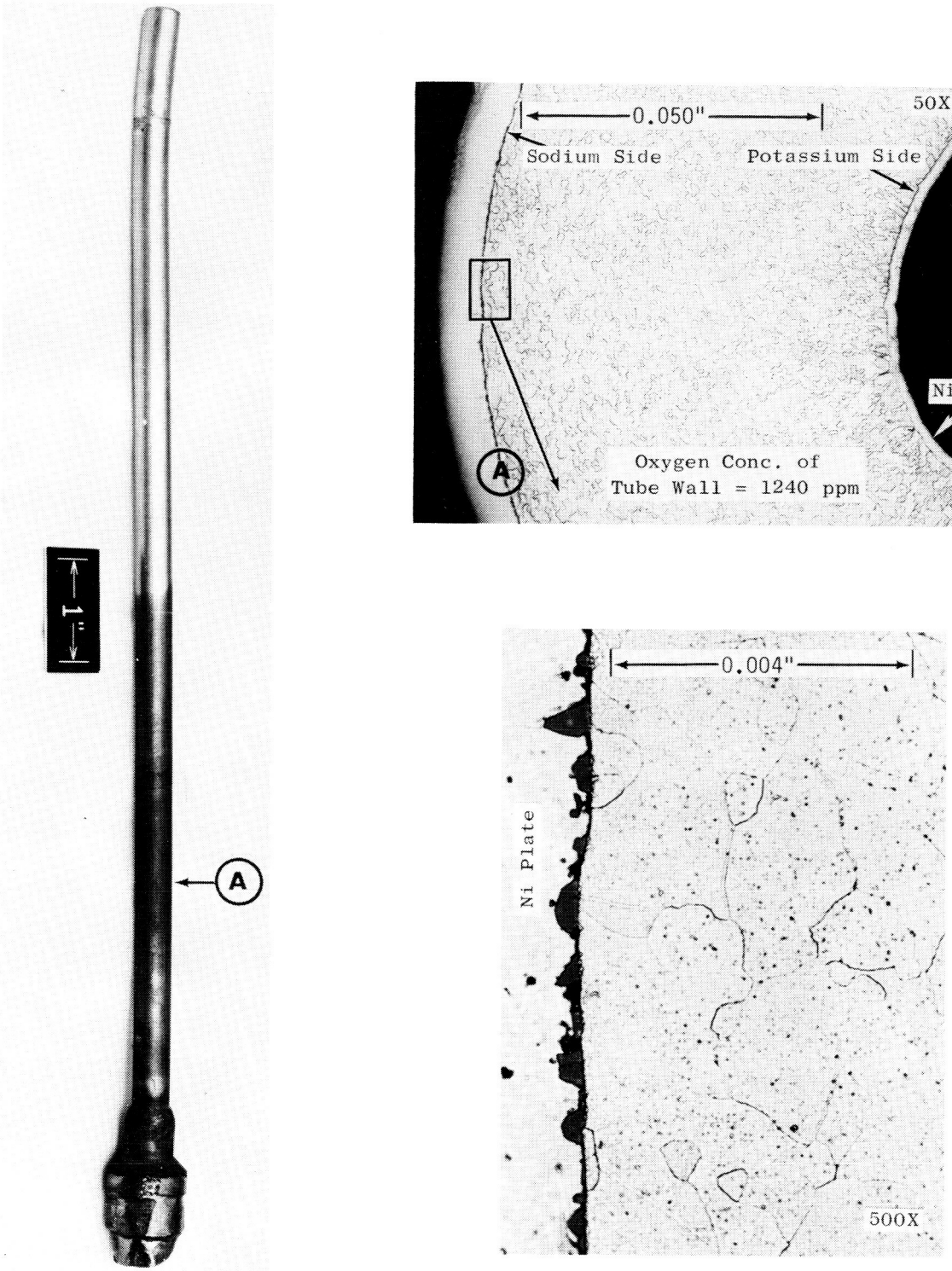

Figure 147. Cb-1Zr Tube Specimen Which Was Taken From the High-Oxygen Concentration (1240 ppm) Region of the Plug Section of the Boiler and Flattened to a Bend Radius of 0.030-Inch to Illustrate the Ductility of the Tubing.

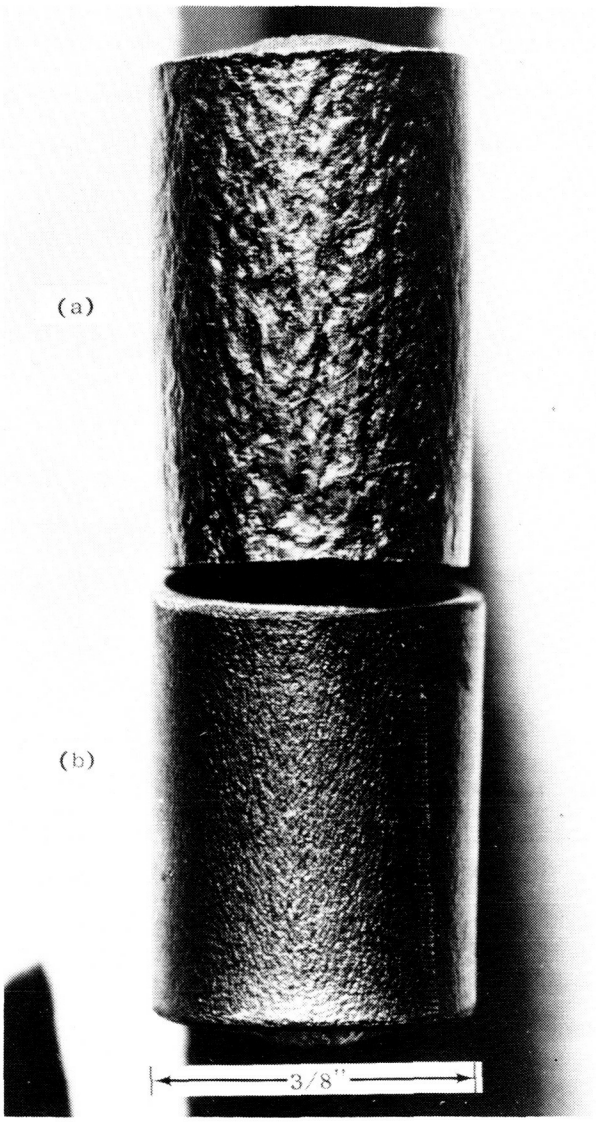

(a) Outer Surface of the 1-inch OD Tube From the 2100°F, Large Grain Size Region of the Boiler

(b) Outer Surface of the 1-inch OD Tube From the 2000°F, Small Grain Size Region of the Boiler

Figure 148. Surfaces of Flattened Specimens of the 1-inch OD Cb-1Zr Sodium Containment Tube Illustrating the Ductility of the Tubing Following Test and the Effect of Grain Size on Surface Appearance.

The results obtained on Cb-1Zr tube specimens from representative regions throughout the loop are listed in Table XXVII. It is suprising to note that the differences between the various specimens and differences across the wall on specimens known to have substantial oxygen gradients are extremely small. The specimen of 3/8-inch-OD tubing from the boiler plug region which contained 1240 ppm oxygen, with a very steep decreasing oxygen gradient going from the sodium side to the potassium side, had a Knoop Hardness which varied between 90 and 96. Comparison of the hardness values obtained on the 1-inch-OD Cb-1Zr tube from insulated and uninsulated regions of the vapor carryover line showed no hardness differences. In summary, no significant hardness changes or differences were observed in the Cb-1Zr tube specimens evaluated. These results are consistent with the results of the tensile test evaluations discussed previously in Part D of this section.

The microhardness of metallographic specimens of the Mo-TZM alloy turbine simulator blades from Stages 1, 2, 3 and 10 were determined along the concave surface and impingement region of the blades approximately 4 mils from the surface of the blades. The Knoop Hardness Numbers (100 g load) obtained varied between 311 and 363 in the four blade specimens as compared to a variation of 342 to 356 observed in the before test blade specimen. These results indicate no significant change in microhardness of the Mo-TZM as a result of the 5000-hour test.

TABLE XXVII

RESULTS OF MICROHARDNESS SURVEYS OF THE Cb-1Zr TUBING FROM VARIOUS REGIONS OF THE Cb-1Zr CORROSION LOOP FOLLOWING THE 5000-HOUR TEST

Specimen Location	Oxygen Conc.[a]	Tube Size, OD	Temp. °F	Foil Insulation[b]	Knoop Hardness Number, 100 g Load[c]		
					3 mils from ID	Center	3 mils from OD
Na, Pump Outlet	723	3/8"	1972	Yes	91	100	108
Na, Boiler Inlet	36	3/8"	2130	Yes	107	107	117
Na, Boiler	40	1.0"	2120	Yes	87	86	94
Na, Boiler	148	1.0"	2050	Yes	83	93	90
Na, Pump Inlet	730	3/8"	1960	Yes	88	87	96
Na/K Boiler Plug	165	3/8	~2000	(d)	101	99	106
Na/K Boiler Plug	1240	3/8"	~1900	(d)	96	93	90
K, Vapor Tube	304	1.0"	1775	Yes	95	95	92
K, Vapor Tube	300	1.0"	1770	No	95	83	92
Before Test	260	3/8"	-	-	97	96	99
Before Test	245	1.0"	-	-	116	103	130

(a) Oxygen concentration of total wall.

(b) Designates whether or not tube was covered with multiple layers of Cb-1Zr foil insulation.

(c) Each hardness number is the average reading on at least three hardness impressions.

(d) OD of potassium containment tube was surrounded by a sodium filled annulus.

XIII. EVALUATION OF LOOP PERFORMANCE

The main objective of the Cb-1Zr Corrosion Test Loop was to evaluate the refractory alloys in boiling and condensing potassium environments which simulate projected space electric power systems. The loop components were, therefore, primarily designed to achieve boiling and condensing in the loop to meet the desired test condition for the materials corrosion test and not as high-performance components for specific space applications. However an evaluation of the various loop components is included in this section since similar components will be required in future test loops capable of reliable operation for extended periods.

A. METERING AND ISOLATION VALVES

The metering valve operated satisfactorily during the entire 5000-hour test. The valve was extremely useful in contributing to the stability of the loop illustrated in Figure 87 in the operation portion (Section X) of this report. The flow characteristics of the valve as previously described made the valve extremely sensitive to small adjustments in the plug position; however, the pressure drop across the valve could be controlled as needed by careful adjustments.

The isolation valve, which was used to isolate the surge tank from the loop, was operated during the test startup. However, a zero-leakage seal could not be made with the 5 ft-lbs of torque applied with the rotary feedthrough. The limited torque available was insufficient to deform the metal-to-metal contact between the Mo-TZM plug and the Cb-1Zr valve seat to form a leak-tight seal. This deficiency, however, did not limit the usefulness of the isolation valve, since in the closed position the high flow resistance of the valve effectively reduced the communication between the surge tank and loop during unstable periods of operation.

The actuation of the valves with flexible cables and magnetic-coupled rotary feedthroughs presented no operating problems during the test. The inherent springiness in the flexible cable required careful adjustment to prevent overshooting of a position but was easily controlled.

After the completion of the 5000-hour test, the valves were repeatedly opened and closed. The operation of the valve was very smooth for the first 0.030 inch of travel and became progressively rougher as the valve was opened to its full travel. Visual examination of the stainless steel drive gears on both the isolation and metering valves revealed that some galling had occurred between the pinion gear and the spur gear. The galling was due in large measure to a misalignment of the pinion gear resulting from excessive clearance between the pinion gear shaft in the tungsten carbide bushing. The clearance was made greater than the standard recommended practice to accommodate the maximum thermal expansion possible between the stainless steel pinion gear and the tungsten carbide bushing. Future gear drives will have less clearance between the shaft and bushing and the gears will be fabricated from a material having good resistance to galling.

B. VAPOR BUBBLE NUCLEATOR

The vapor bubble nucleator was not used during the 5000-hour test to stabilize the loop. The loop was operated in a stable condition by adjusting the pressure drop across the metering valve as described in Section X of this report. The nucleator heater was operated at 200 watts to prevent a cold spot from developing at the inlet to boiler where the nucleator was located.

C. HELICAL INDUCTION ELECTROMAGNETIC PUMP

The sodium EM pump again proved to be a reliable, trouble-free component as previously demonstrated in the Cb-1Zr Pumped Sodium Loop. No degradation in the performance was observed during the 5000 hours of operation at inlet and outlet temperatures of 1960°F and 1972°F, respectively.

The potassium EM pump also proved to be reliable but had a tendency to vapor lock at low-flow, high-head conditions as reported in the operating section. After reducing the discharge pressure from 160 psia to 125 psia by decreasing the pressure drop across the metering valve, no further operational problems were encountered. In all future EM pump designs for low-flow, high-head operation, the outlet tube will be thermally isolated from the inlet side of the pump to eliminate the vapor lock problem.

D. PERMANENT MAGNET FLOWMETER

Both the sodium and potassium flowmeters operated during the entire 5000-hour test without any detectable change in the performance. During steady state operations, the sodium flowmeter magnet temperature was 690°F (sodium temperature - 1985°F), and the potassium flowmeter magnet was 510°F (potassium temperature - 955°F). The magnets were calibrated before and after the 5000-hour test with no measurable change in the magnetic flux density as shown in Figure 149. In future tests at higher operating temperatures, additional reflective thermal insulation can be added to the pole face of the magnet to shield it from the uninsulated section of the flowmeter tube to maintain the magnet temperature below the 900°F stabilization temperature.

E. SODIUM HEATER AND POTASSIUM PREHEATER

The sodium heater and potassium preheater performed during the 5000-hour test in the same trouble-free manner as reported for a similar heater design evaluated in the 2650-hour Cb-1Zr Pumped Sodium Loop Test.[57] The sodium heater operated at a maximum temperature of 2150°F; the potassium preheater operated at a maximum temperature of 1750°F.

The temperature gradient in the sodium heater electrodes from the heater coil to the copper bus bar are shown in Figure 150. A slight rise in electrode temperature was noted in both the center and top electrode temperature during the test. This slight increase may have resulted from a small decrease in the emittance of grit blasted electrodes or a small decrease in thermal conductivity across the Cb-1Zr electrode - copper bus bar interface. The 0.25-inch-diameter thermal dams and the high-emittance surface of the electrodes were effective in reducing temperature of the copper - Cb-1Zr interface region to a safe operating temperature. However, in future tests at higher operation temperatures, the electrode length will be increased.

---

(57) Hoffman, E. E. and Holowach, J., Cb-1Zr Pumped Sodium Loop Potassium Corrosion Test Loop Development Topical Report No. 6, R67SD3015, General Electric Company, Cincinnati, Ohio, December 20, 1967.

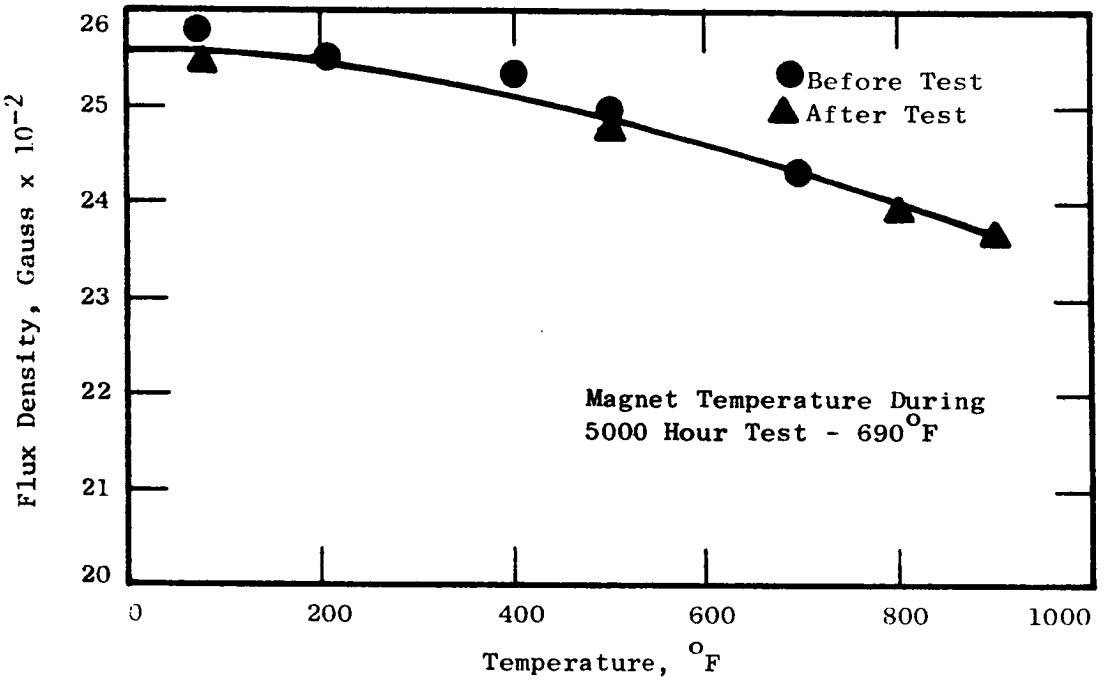

Figure 149. Flux Density vs Temperature of Sodium Flowmeter Magnet Before and After 5000 Hour Loop Test.

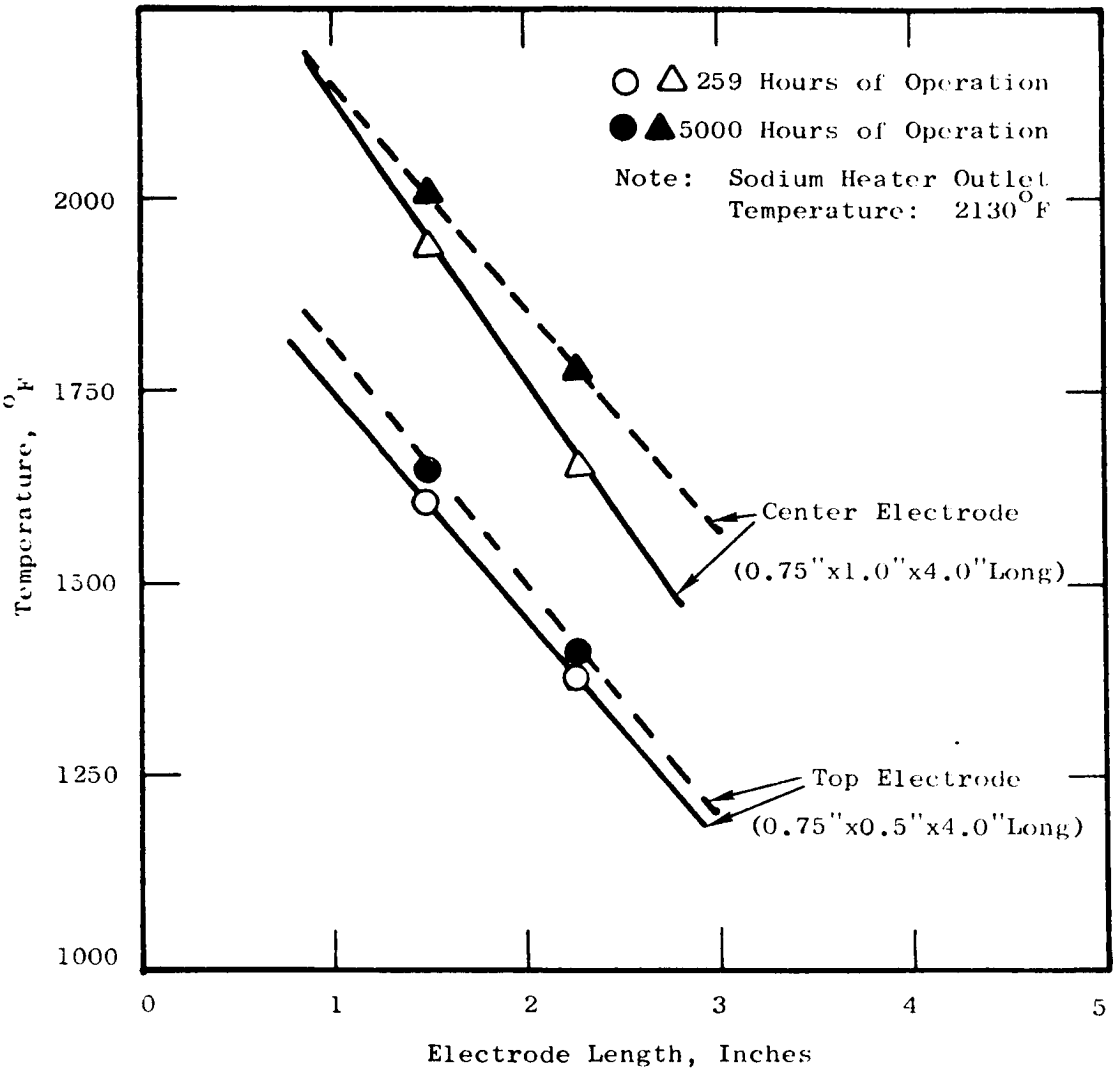

Figure 150. Temperature Distribution in Sodium Heater Electrodes After 259 Hours and 5000 Hours of Test Operation.

The effectiveness of the Cb-1Zr dimpled reflective foil thermal insulation was again demonstrated in the 5000-hour test. Although no heat balance measurements were made to determine its effectiveness, the heat losses were acceptable, and no apparent change was observed during the test.

F. BOILER

The tube-in-tube, counterflow potassium boiler operated at the design test conditions for the entire 5000 hours without any significant change in the performance. The boiling temperature and location of the nucleate boiling zone could be easily controlled by adjusting the potassium flow rate and/or the power input. The boiler was operated at the design conditions except during the startup and during the incidents which are detailed in the operation section.

The boiler proved to be approximately twice the length required for 100 percent quality potassium vapor; however, as described in the design section (Section II, E), the boiler was purposely lengthened to insure that 100 percent quality potassium vapor was obtained even during off-design operation since erosion damage from entrained liquid entering the turbine simulator could overshadow the erosion due solely to vapor impingement on the test nozzle and blade specimens.

Two off-design test cases were obtained on the boiler during the initial startup and are summarized in Table XXVIII. The sodium temperature distribution in the boiler for both cases is compared in Figure 151. In the run on 7-31-65, the large temperature gradient which indicates a high-heat transfer and boiling rate is located near the potassium exit; in the run on 8-2-65, the large temperature gradient has moved to the potassium entrance region of the boiler. In each case, for approximately the same potassium flow rate, the potassium was completely vaporized and superheater 115° above the saturation temperature as determined by the measured vapor pressure at the exit of the boiler. The ability of the boiler to produce superheated potassium vapor at the boiler exit even when the nucleate boiling region was located substantial distances beyond the plug (entrance) region reflects the

TABLE XXVIII

SUMMARY OF THE LOOP BOILER PERFORMANCE FOR TWO RUNS DURING LOOP STARTUP

Time	7-31-65, 1215	8-2-65, 1015
Sodium Flow Rate	451 lb/hr	818 lb/hr
Sodium Temperature, In	2092°F	2040°F
Sodium Temperature, Out	1872°F	1916°F
Sodium Temperature Drop Across Boiler	220°F	124°F
Boiler Heat Input Including Losses	32,200 Btu/hr	33,200 Btu/hr
Potassium Flow Rate	36.1 lb/hr	37.8 lb/hr
Saturation Temperature at Boiler Exit	1754°F	1788°F
Superheat Temperature	1869°F	1903°F
Degrees Superheat	115°F	115°F
Heat Input		
Heat of Vaporization	28,100 Btu/hr	29,200 Btu/hr
Superheat	800 Btu/hr	860 Btu/hr
Preheat	1,370 Btu/hr	1,460 Btu/hr
Total Heat Input to Potassium	30,270 Btu/hr	31,420 Btu/hr
Boiler Heat Loss	2,600 Btu/hr	3,330 Btu/hr
Total Heat Transfer	32,870 Btu/hr	34,700 Btu/hr

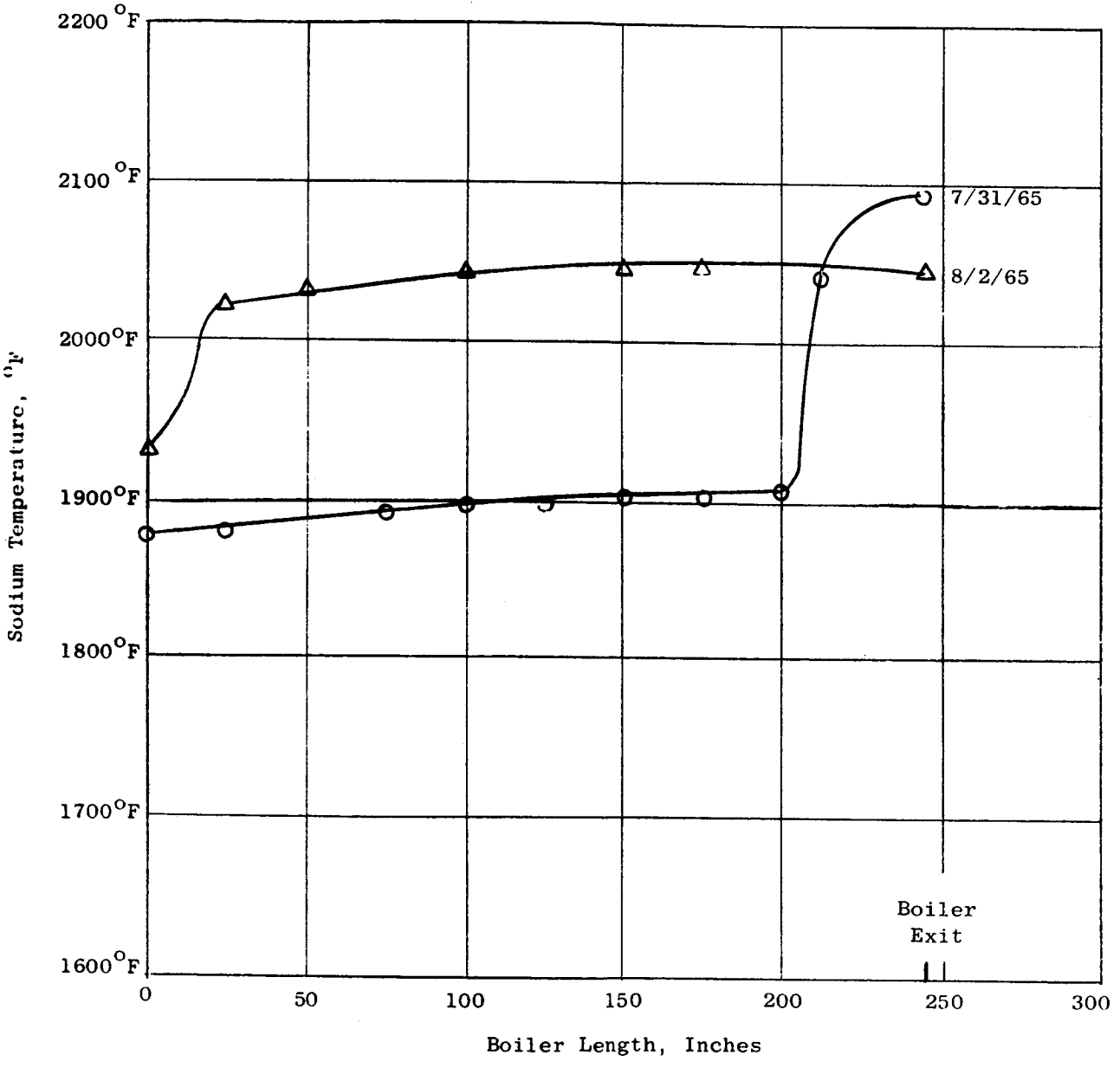

Figure 151. Sodium Temperature Distribution in the Boiler for Two Off-Design Conditions During Test Startup.

conservative design which was utilized to assure that the vapor entering the first stage of the turbine simulator was superheated.

Another significant difference in the two test runs is the ratio of the sodium flow rate to the potassium flow rate. Although the potassium flow rate was essentially constant for the two runs, the sodium flow rate was increased from 451 to 818 lbs/hour for the run on 8-2-65. The sodium flow rate was increased to limit the maximum heater exit temperature to 2150°F at the design test conditions.

Test data obtained on the loop after 259 hours of operation which is representative of the test conditions during the first 1785 hours of loop operation are shown in Figure 152. The pressures at several locations in the potassium circuit and the corresponding saturation temperatures in the vapor and two-phase regions are listed. The sodium temperature profile in the boiler and the calculated potassium quality and temperature as a function of boiler length are given in Figure 153. The calculated qualities indicated are based on calculations involving potassium flow, potassium boiler inlet temperature, sodium flow, and the drop in the measured sodium temperatures as a function of boiler length. The calculated boiling temperature varied from 1910°F at the boiler inlet to 1880°F at approximately 122 inches from the inlet where 100 percent quality vapor is reached. The remaining 118 inches of boiler was used to superheat the vapor to 1995°F. The 133°F of superheat reported is the difference between the measured temperature of the potassium vapor at the boiler exit, 1995°F, and the saturation temperature, 1862°F, as determined by the measured boiler exit pressure, 100 psia. The located heat flux in the boiler calculated from the slope of the sodium temperature gradient varies from over 400,000 Btu/hr/ft^2 in the 12-inch-long plug to less than 2000 Btu/hr/ft^2 in the superheat region near the exit of the boiler.

The test data obtained from the loop at 5000 hours are shown in Figure 154. No significant change in the operating conditions were detected during the entire test. A comparison of the Cb-1Zr Rankine System Corrosion Loop

8-13-65 10:00 Hours Test Time: 259 Hours

Heater: 46.4A/378V
Preheater: 32A/92V/2.02KW
Nucleater: 3A/60V
Primary Flow: 2.43 GPM/3.72 MV
Secondary Flow: 0.110 GPM/0.185 MV
Boiling Temperature*: 1910°F
Superheat: 133°F (1995°-1862°F)

* Saturation Temperature at Boiler Entrance Pressure, 116 psia

NOTE: Temperature Shown in °F.

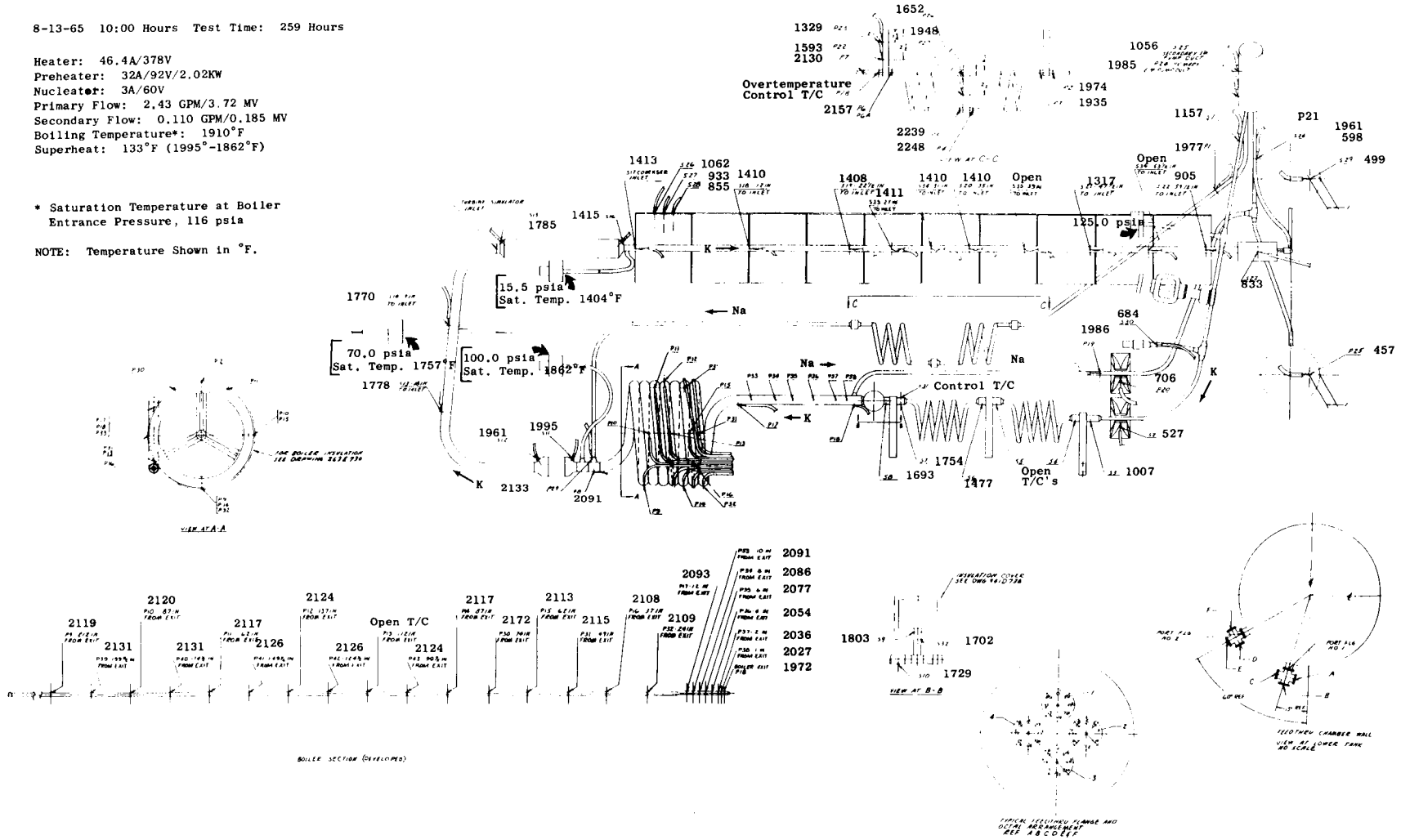

Figure 152. Cb-1Zr Corrosion Test Loop Thermocouple Instrumentation Layout.

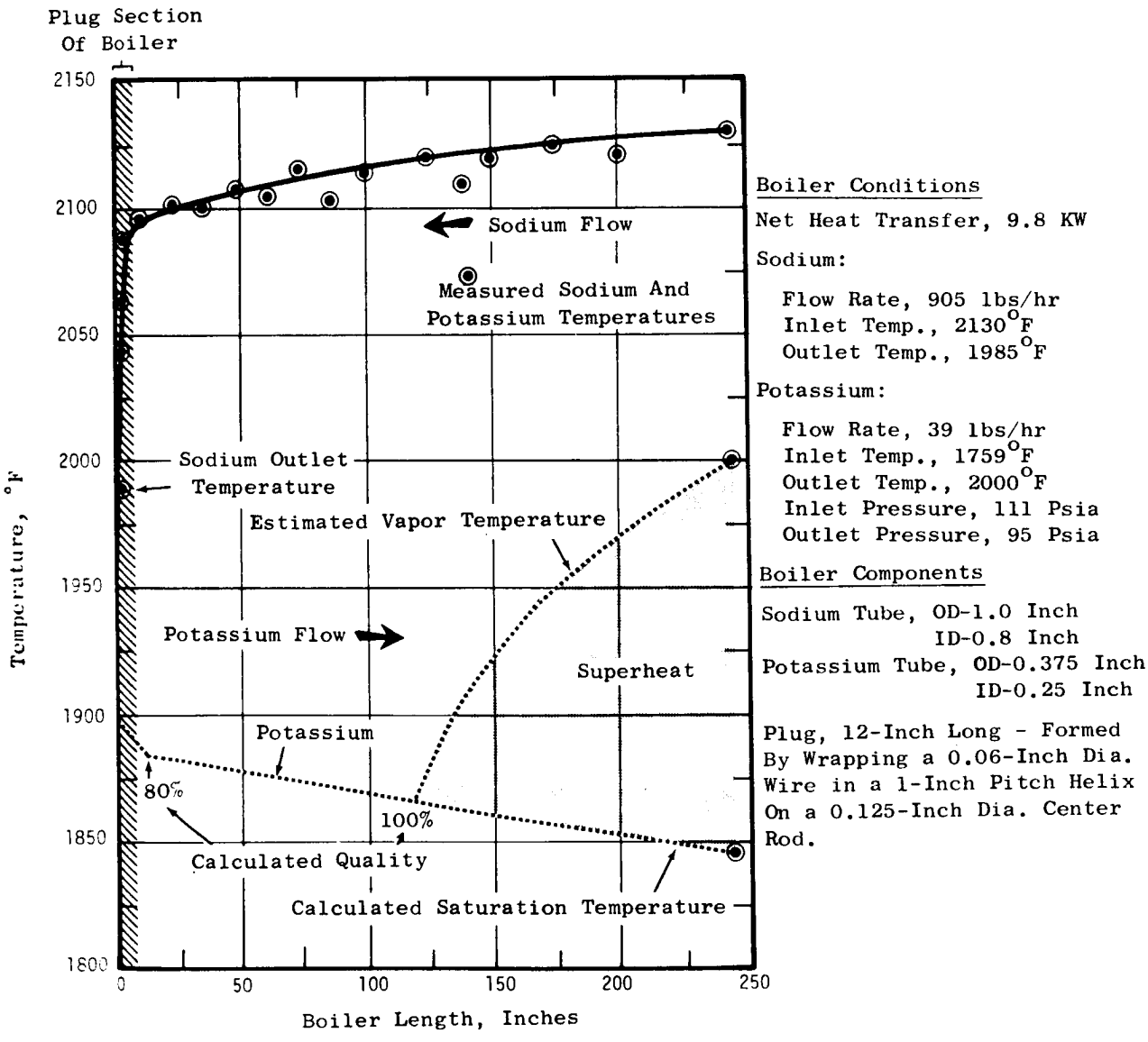

Figure 153. Cb-1Zr Corrosion Test Loop Boiler Operating Conditions After 5000-Hours Operation.(C67032479)

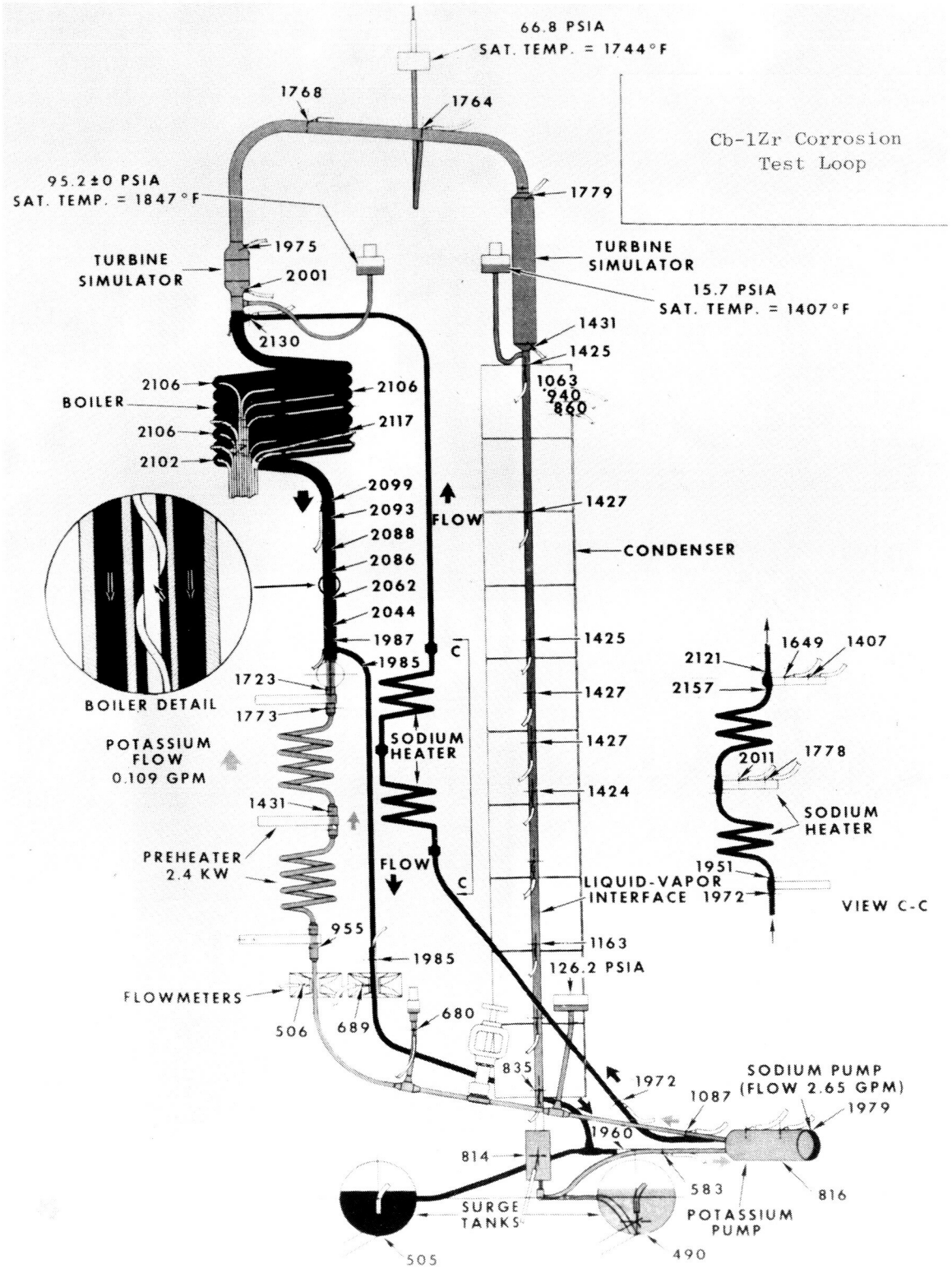

Figure 154. Test Conditions at 5000 Hours Just Prior to Test Shutdown. (CDC5458)

test operating conditions and published test data[58] obtained from the 300 KW Heat Transfer Loop is shown in Table XXIX. Although the Cb-1Zr Corrosion Loop was not designed or fully instrumented for heat transfer data, the test results are in general agreement.

G. TURBINE SIMULATOR

The thermodynamic performance of the 10-stage turbine simulator was given previously in Table XXI in Section X of this report. The calculated vapor velocity at the throat of the turbine simulator nozzles varied from 1125 ft sec in the first nozzle to 830 ft/sec in the tenth nozzle. The variance from design throat velocity of 1000 ft/sec was due in part to differences in the actual operating conditions and the reference design. In the reference design, 112.7 psia, which is equivalent to the saturation pressure at 1900°F, was assumed as the turbine simulator inlet pressure. In actual operation, the 1900°F boiling region was concentrated in the plug, rather than being uniformally distributed along the length of the boiler, resulting in a larger pressure drop between the boiler inlet and the entrance of the turbine simulator. The actual measured pressure at the inlet to the turbine simulator was 100 psia or 13 psi less than the design pressure. The lower pressure resulted in a decrease in the vapor density from 0.230 lb/ft^3 to 0.183 $lb\ ft^3$ or approximately 10 percent. Since the throat velocity of a nozzle for a given flow rate is inversely proportional to the density, a higher-than-design velocity was reached in nozzles No. 1 to 7. On the other hand, the throat velocities in nozzles No. 7 to 10 were less than the design velocity because the condenser was operating at 1413° or 63°F above the reference design condensing temperature of 1350°F. The higher vapor density, therefore resulted in a lower throat velocity since the density of vapor at 1413°F (16.2 psia) is 40 percent higher than at the design pressure of 11.6 psia. The condenser was operated at the higher-than-design pressure to increase the inlet pump pressure as added safety to prevent the pump from vapor locking.

An added complication in the determination of the performance of the turbine simulator was that the nozzles were originally designed using the

---

(58) Peterson, J.R., High-Performance "Once-through" Boiling of Potassium in Single Tubes at Vapor Temperatures From 1500°F to 1750°F, NASA Contract NAS 3-2528. General Electric Company, Cincinnati, Ohio, November 7, 1966, p. 141.

TABLE XXIX

PERFORMANCE OF Cb-1Zr RANKINE SYSTEM CORROSION TEST LOOP BOILER COMPARED TO 300 KW HEAT TRANSFER TEST DATA

	300 KW* Data Point	Cb-1Zr Corrosion Loop Test
Sodium Boiler Tube, OD	2.37 inch	1.0 inch
Sodium Boiler Tube, ID	2.07 inch	0.8 inch
Potassium Boiler Tube, OD	0.75 inch	0.375 inch
Insert Center Body, OD	0.67 inch	0.25 inch
Pitch-to-Diameter Ratio	6	4
Boiler Length	91 inches	240 inches
Potassium Inlet Temperature	1340°F	1760°F
Potassium Outlet Temperature	1633°F	2000°F
Potassium Outlet Saturation Temperature	1422°F	1840°F
Potassium Vapor Superheat	211°F	160°F
Thermal Power Input	82 kw	9.8 kw
Boiler Pressure Drop	34 psi	16 psi
Sodium Inlet Temperature	1870°F	2130°F
Sodium Outlet Temperature	1804°F	1985°F
Average Heat Flux	219,000 $\frac{Btu}{hr.\ ft^2}$	30,000 $\frac{Btu}{hr.\ ft^2}$
Critical Potassium Vapor Quality	70%	70 - 80%
Critical Heat Flux	446,000 $\frac{Btu}{hr.\ ft^2}$	560,000 $\frac{Btu}{hr.\ ft^2}$
Radial Acceleration Developed by Insert	82.4 g's	392 g's
Sodium Heat Transfer Coefficient	4000 $\frac{Btu}{hr.\ ft^2\ °F}$	5400 $\frac{Btu}{hr.\ ft^2\ °F}$
Average Nucleate Boiling Heat Flux	385,000 $\frac{Btu}{hr.\ ft^2}$	500,000 $\frac{Btu}{hr.\ ft^2}$

* Peterson, J. R., High-Performance "Once-Through" Boiling of Potassium in Single Tubes at Vapor Temperatures from 1500°F to 1750°F, NASA Contract NAS 3-2528, General Electric Company, Cincinnati, Ohio, November 7, 1966, p. 141.

potassium vapor properties reported by Walling and Lemmon[59] and the performance data were computed using the data of Stone, et al.[60] which became available after the Cb-1Zr Corrosion Loop was partially fabricated. The variations between the actual test conditions and the reference design test conditions are considered minor and did not significantly compromise the compatibility evaluation performed on test components following completion of the experiment.

The measured throat diameters of the nozzles before and after test are also given in Table XXI in Section X. No significant change in dimensions was observed in any of the nozzles.

H. CONDENSER SUBCOOLER

The finned tube, radiant condenser/subcooler proved to be extremely stable and operated for the 5000 hours without any detectable change in performance. The liquid-vapor interface could be easily detected and its movement followed during the operation by observing the temperature gradient in the condenser tube thermocouples as shown in Figure 155. The temperature gradient in the condenser fins is shown in Figure 156. The temperature profile of the condenser fin is plotted for the 427-hour and 5000-hour points of test operation and indicate no change in the heat rejection characteristics of the iron titanate coated fin during the test. Since the loop operated at essentially one test condition, the shutter assembly did not require any adjustments after the initial test conditions were reached. The shutter assembly was, however, operated during the shutdown operation after 5000 hours of test. The shutter could be fully opened and fully closed with only a few inch-pounds of torque which was comparable to the pretest value.

---

(59) Walling, J.F. and Lemmon, A.W., Jr., The Experimental P-V-T Properties of Potassium to 1150°C. Battelle Memorial Institute, BATT-1673-T4, April 1963.

(60) Stone, J.P., et al., High Temperature Properties of Sodium, Potassium and Cesium. NRL Report 6128, August 1964.

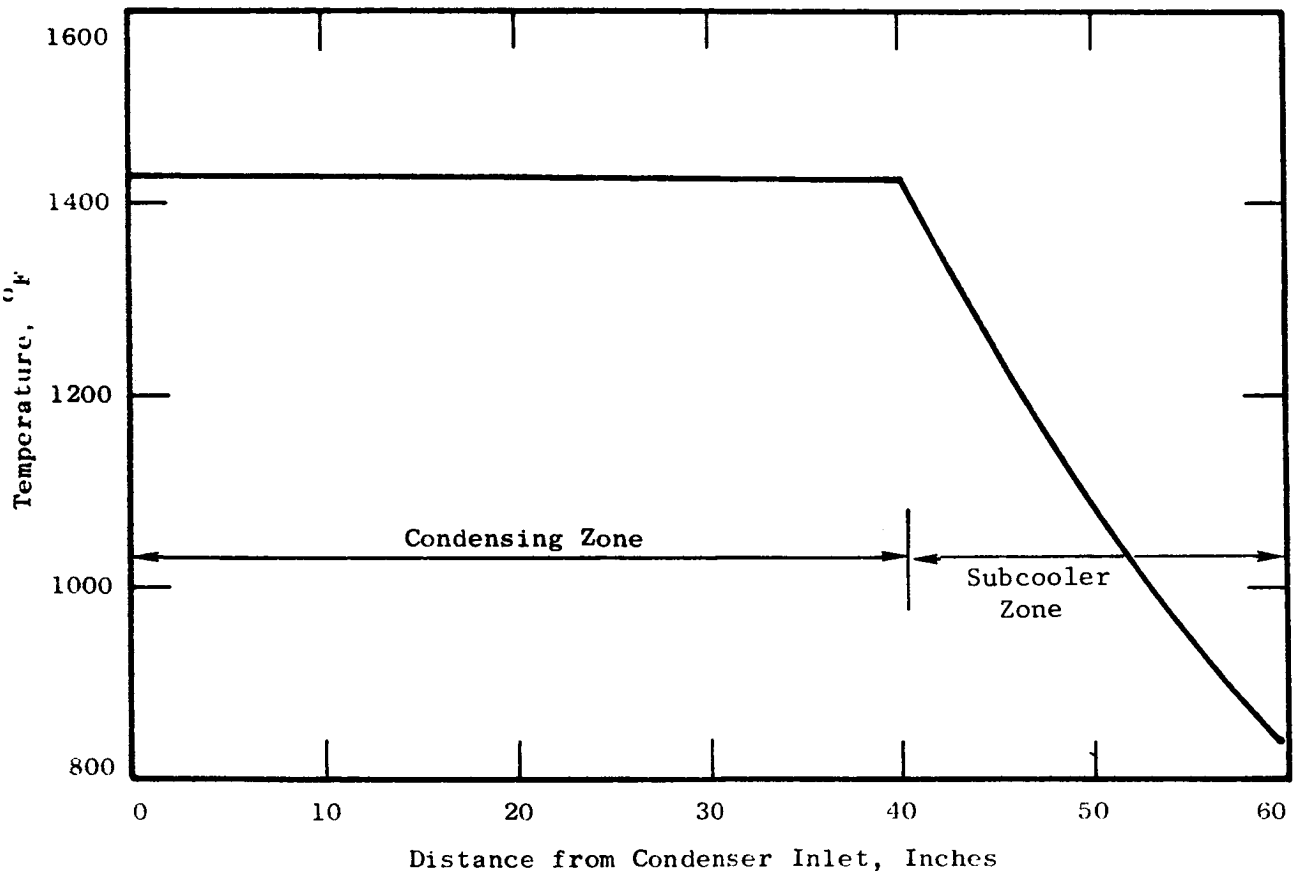

Figure 155. Temperature Distribution in the Condenser/Subcooler of the Loop.

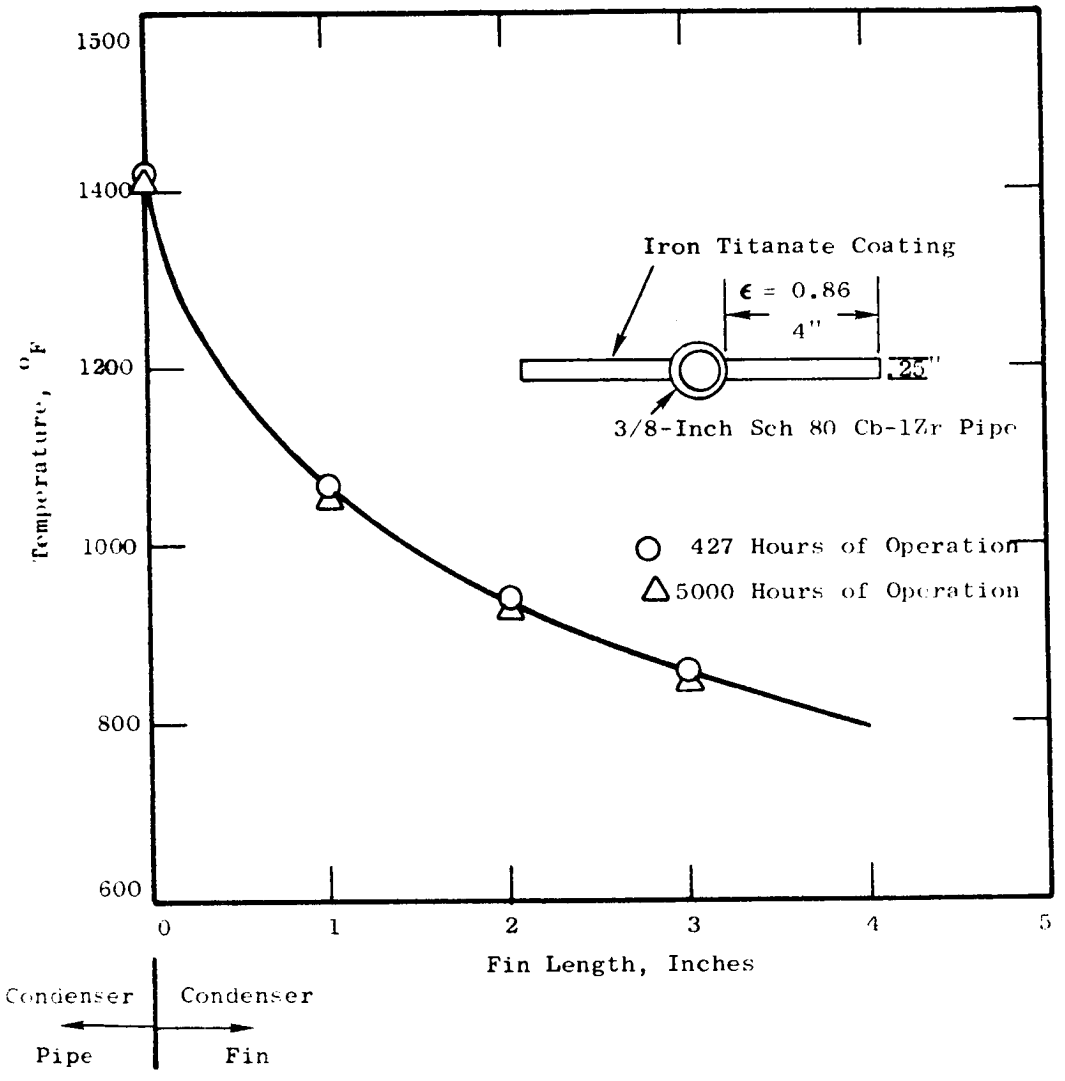

Figure 156. Temperature Distribution in the Condenser Fin at Steady State Conditions.

I. SLACK DIAPHRAGM PRESSURE TRANSDUCER

The four slack diaphragm pressure transducers used in measuring the operating pressure of the potassium circuit of the Cb-1Zr Corrosion Loop were calibrated before and after the 5000-hour test. The calibrations were made with the pressure transducers in the test position with the readout equipment used in the test operation. The pressure transducers were calibrated between 0-150 psia against a Wallace and Tiernan gauge calibrated to ± 0.1% of full scale. The millivolt output was measured by a recording potentiometer with an accuracy of ± 1/4 percent of full scale (50 millivolts).

The accuracy of the slack diaphragm pressure transducer as rated by the Taylor Instrument Company is ± 1/2 percent of the full range at 14.7 psia barometric pressure and room temperature. The effect of temperature on the output of the pressure transducer was estimated by the vendor to be 0.008 psi/°F at the sensing element and 0.002 psi/ft/°F around the capillary tube.

The pretest calibration was made with the potassium circuit filled and the vacuum chamber at 500°F which was the estimated operating temperature of the sensing element and capillary tube. The calibration after 3000 hours of operation was made following the distillation treatment and draining operations described above. The transducers were calibrated at 950°F and 600°F during the cooldown period following the draining of the loop surge tanks. The higher temperature calibration tests after loop operation were possible because of the addition of infrared quartz heating lamps which were installed for distilling of the residual potassium from the loop before disassembly as illustrated in Figure 101.

The results of the calibration before and after the 5000-hour test are shown in Figure 157. No significant change in the accuracy of the pressure transducers was detected; the test data were within the ± 1/2 percent accuracy of the calibration system. Results obtained on all the transducers were similar.

The effect of temperature as estimated by the vendor was far too

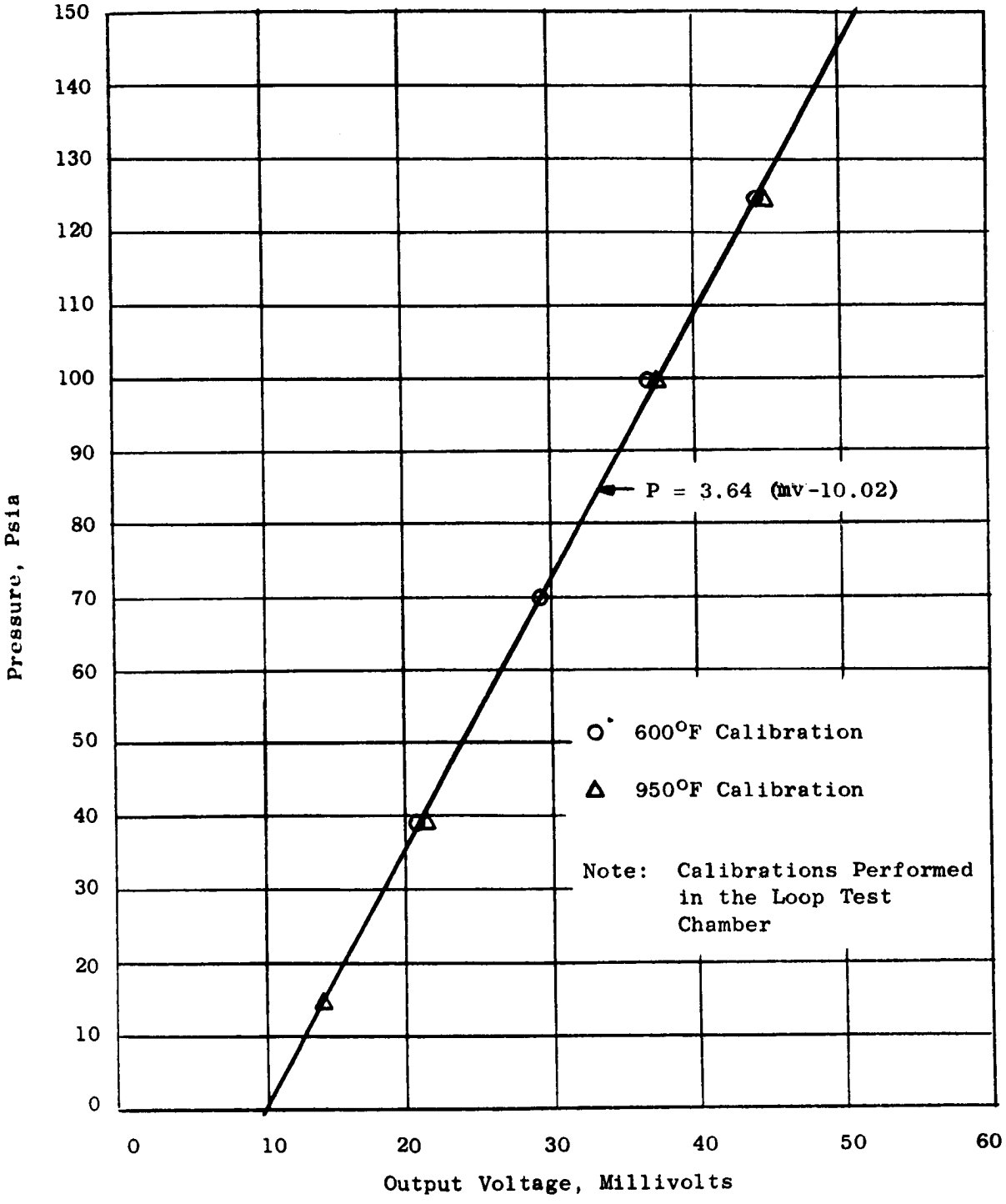

Figure 157. Calibration of the Slack Diaphragm Pressure Transducer That was Used to Measure the Potassium Boiler Outlet Pressure. Calibration was Performed Following Completion of the 5000-Hour Test.

pessimistic. In fact, the difference in the calibration between the 600° and 950°F calibration could not be detected by the calibration equipment used. If the estimated temperature effect was correct, the 350°F change around the 15-ft long capillary tube would have resulted in an indicated pressure change of 10.5 psi which could easily have been detected with the calibrating equipment used.

The results of the calibration given in Figure 158, showed that no significant change in the performance of the pressure transducer was observed and that the ± 1/2 percent accuracy specified by the vendor can be attained. Although no significant effect of the temperature on the sensing element or capillary tube was observed, it is recommended that future calibration tests of this type be performed at or near the anticipated operating temperatures.

J. STRESSED DIAPHRAGM PRESSURE TRANSDUCER

The stressed diaphragm pressure transducer which has a response of up to 100 cps was used to supplement the low frequency response (1 cps) of the slack diaphragm pressure transducer in measuring the pressure fluctuations during periods of unstable boiling as described in the operation section. The stressed diaphragm pressure transducer consists of a pressure housing and a thin diaphragm which serves as a stressed member. The deflection of the diaphragm, which is a function of the pressure on it, is the measured quantity. Any creep or relaxation of the stressed diaphragm results in a change in the output of the pressure transducer, thus, the stressed diaphragm is far more sensitive to drift and temperature changes than the slack diaphragm pressure transducer. Frequent recalibration of this type of pressure transducer is required if the pressure transducer is to be used in measuring the absolute magnitude of the pressure.

In the 5000-hour test, the stressed diaphragm pressure transducer could not be used to measure the absolute pressure in the loop because of erratic drift in the output even during steady state conditions. It was, however, extremely useful in measuring the frequency and amplitude

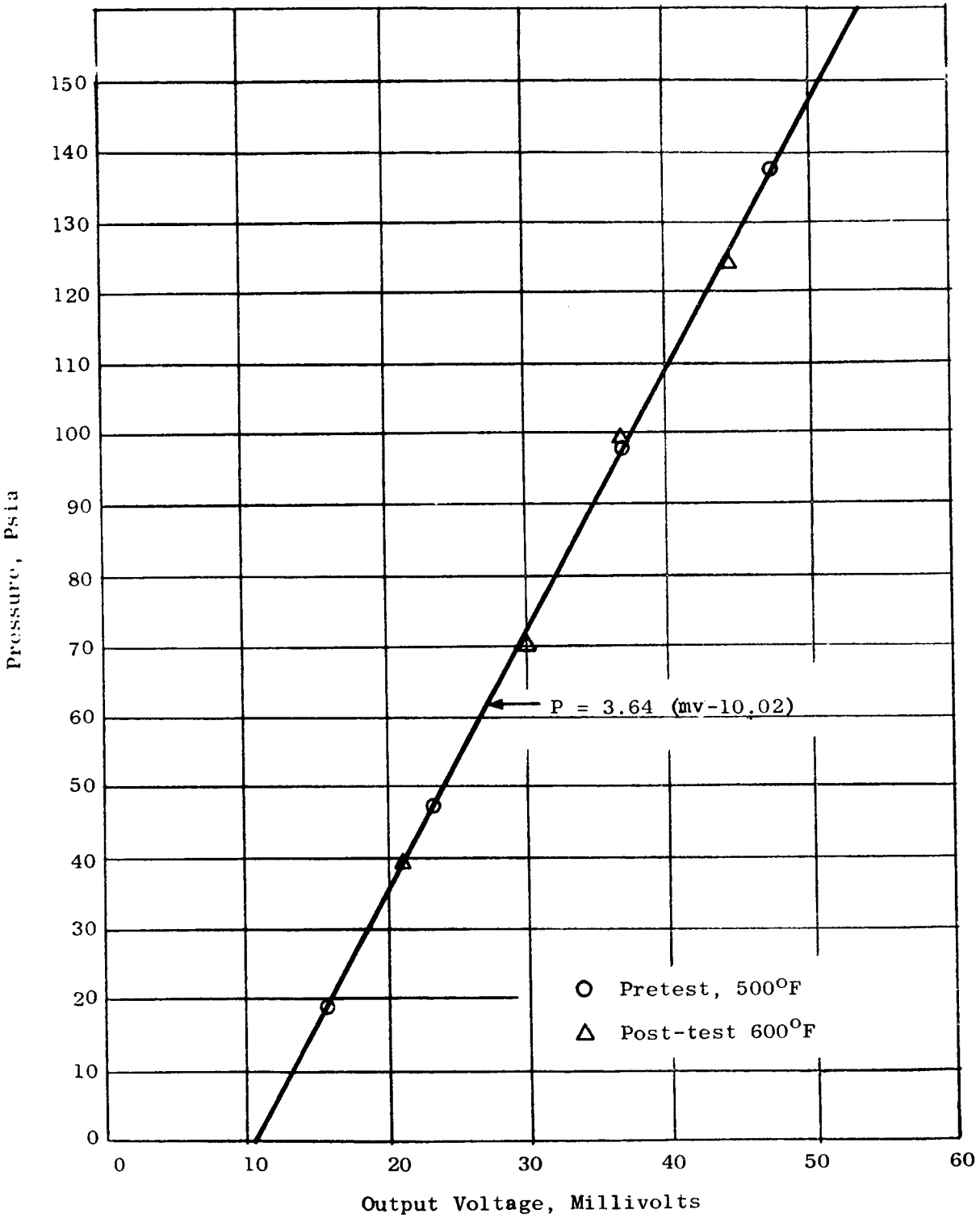

Figure 158. Comparison of the Pretest and Posttest Calibration of the Slack Diaphragm Pressure Transducer Used to Measure Boiler Outlet Pressure.

of high-frequency pressure fluctuations as described in Section X of this report.

K. TEMPERATURE MEASUREMENT

The experience and techniques developed in instrumenting the Cb-1Zr Pumped Sodium Loop described in Topical Report No. 6 in this series were reflected in the excellent reliability of the Cb-1Zr Corrosion Test Loop thermocouples. Only six of the seventy-nine thermocouples failed during the 5000-hour test. Four of the failed thermocouples were of the split spot-welded type; the other two thermocouples which failed were of the beaded type used in thermocouple wells. Two well-type and two split spot-welded thermocouples were open at the junction due to a weld failure; the other two thermocouples had secondary junctions in the lead wires which resulted in erratic emf outputs. No detectable change or drift in the emf output of the loop thermocouples were observed during the test due to temperature or the vacuum environment.

XIV. SUMMARY AND CONCLUSIONS

The primary purpose of the Cb-1Zr Corrosion Test Loop experiment was to determine the compatibility of the working fluid, potassium, with the containment alloy, Cb-1Zr, and the turbine simulator alloy, Mo-TZM, under two-phase flow conditions. An additional purpose of this program was the development of a prototype design for subsequent use in the fabrication of an advanced alloy corrosion test loop. An evaluation of the corrosion resistance of the Cb-1Zr alloy to the heater fluid, sodium, was also an important aspect of the test. Earlier refractory metal - alkali metal corrosion experiments in the form of refluxing capsules, single-phase thermal convection loops, and single-phase pumped loops had indicated that the Cb-1Zr and Mo-TZM alloys were quite resistant to attack by the alkali metals. The Cb-1Zr Thermal Convection Loop, which was operated at temperatures to 2380°F for 1000 hours, and the Cb-1Zr Pumped Sodium Loop, which was operated at a maximum temperature of 2065°F for 2650 hours, preceded the Cb-1Zr Rankine System Corrosion Test Loop in this two-year test program, and the lessons learned and the techniques developed in these earlier tests contributed immeasurably to the success of the later experiment. In these preliminary tests, however, it was not possible to match many of the important Rankine System conditions. The principal design guidelines for the Corrosion Test Loop were to match projected system conditions as closely as practical.

The Cb-1Zr alloy was used to construct the loop with the following exceptions: turbine simulator nozzles and blade specimens - Mo-TZM alloy, pressure transducer diaphragm - T-222 tantalum alloy, and valve seats - Mo-TZM alloy. In many cases, fabrication of the loop components from these refractory alloys required the development or utilization of advanced joining techniques. The loop was contained in a 4-foot-diameter by 11-foot-high vacuum chamber, equipped with a 2400-liter/sec getter-ion pump. During the 5000-hour test, the pressure was maintained at approximately 2×10^{-8} torr, and the partial pressures of contaminating species were maintained at significantly lower pressure

All of the loop components performed satisfactorily during the 5000-hour test. Potassium boiling took place predominately in the first 12 inches of the boiler. The 150° of superheat put into the potassium vapor was

achieved in the remaining 230 inches. With the exception of the instabilities noted while changing loop operating conditions, the system was extremely stable with no temperature fluctuations in excess of 5°F or pressure fluctuations in excess of 0.5 lb/in.^{2}.

Evaluation of the Cb-1Zr components in the potassium loop revealed no significant corrosion or chemical changes. Even portions of the potassium loop tubing which were directly exposed to the test chamber environment (not covered with insulating Cb-1Zr foil) showed less than 50 ppm oxygen increase which is positive proof of the low oxygen concentration of the test chamber environment.

The most striking metallurgical phenomenon observed in the sodium heater loop was the decreased oxygen concentration in the Cb-1Zr tubing in the hottest regions and the increased oxygen concentration in the region of sharpest temperature drop in the loop, i.e., the last six inches of the plug section of the boiler. The oxygen concentration of the Cb-1Zr tube in the hottest regions (2130°F) of the sodium loop decreased from 260 ppm to 36 ppm during the test, and the tube wall from the plug region increased from 260 to 1240 ppm. A very thin deposit (maximum thickness, 0.0005 inch) of grey crystals was found in the region of decreasing sodium temperatures near the sodium exit from the boiler. Electron beam microprobe analysis of these crystals indicated a zirconium concentration of approximately 85 percent. Additional investigations of these crystals indicate that they are probably the compound, ZrO. Severe bend testing and both room temperature and 2000°F tensile tests on tube sections high in oxygen concentration revealed no changes in ductility, tensile strength, or yield strength as a result of the oxygen migration. The dramatic transition from oxygen depletion to enrichment in the plug region of the Cb-1Zr boiler resulted from the sharp drop in sodium temperature in this region.

In summary, evaluation of the corrosion test loop after 5000 hours of operation under two-phase potassium flow conditions revealed only insignificant amounts of corrosion with respect to the proposed application. This conclusion is also supported by many other corrosion tests that are pertinent even though they did not match projected Rankine cycle power plant operating conditions as closely as was possible in the Cb-1Zr Corrosion Test Loop.

XV. PUBLISHED REPORTS

Quarterly Progress Reports	For Quarter Ending
Report No. 1 (No NASA No.)	October 15, 1963
Report No. 2 (NASA-CR-54008)	January 15, 1963
Report No. 3 (NASA-CR-54081)	April 15, 1964
Report No. 4 (NASA-CR-54167)	July 15, 1964
Report No. 5 (NASA-CR-54269)	October 15, 1964
Report No. 6 (NASA-CR-54344)	January 15, 1965
Report No. 7 (NASA-CR-54735)	April 15, 1965
Report No. 8 (NASA-CR-54843)	July 15, 1965
Report No. 9 (NASA-CR-54912)	October 15, 1965
Report No. 10 (NASA-CR-54990)	January 15, 1966

Topical Reports

Report No. 1 - "Purification and Analysis of Helium for the Welding Chamber" by T. F. Lyon, NASA-CR-54158, July 1, 1965.

Report No. 2 - "Materials and Process Specifications for Refractory Alloy and Alkali Metals" by R. G. Frank, D. N. Miketta, W. H. Kearns, W. R. Young, and R. B. Hand, R66SD3007, December 13, 1965.

Report No. 3 - "Materials Specifications for Advanced Refractory Alloys" by D. N. Miketta and R. G. Frank, NASA-CR-54761, October 1, 1965.

Report No. 4 - "Purification, Analysis, and Handling of Sodium and Potassium" by L. E. Dotson and R. B. Hand, R66SD3012, June 13, 1966.

Report No. 5 - "Sodium Thermal Convection Loop" by E. E. Hoffman and J. Holowach, R67SD3014, June 15, 1967.

Report No. 6 - "Cb-1Zr Pumped Sodium Loop" by E. E. Hoffman and J. Holowach, R67SD3015, December 20, 1967.

XVI. APPENDICES

A. List of Drawings of the Cb-1Zr Rankine System Corrosion Test Loop.

B. Major Drawings of the Cb-1Zr Rankine System Corrosion Test Loop.

C. Nomenclature Used in Design Calculations.

D. Boiler Plug Design.

E. Refluxing Potassium Tests to Evaluate to Mo-TZM Inserts in Cb-1Zr Capsules.

F. Test to Evaluate a High Emittance Iron Titanate Coating for the Cb-1Zr Condenser Fin.

G. Calibration of the Partial Pressure Analyzer.

H. Calibration of W-3Re/W-25Re Thermocouple Wire.

I. Test Startup Procedure.

J. Stress-Corrosion Cracking of the Vacuum Chamber Cooling Channel.

K. Drawing, Sampling, and Filtering of the Potassium and Sodium Circuits of the Loop.

APPENDIX A

LIST OF DRAWINGS OF THE Cb-1Zr RANKINE SYSTEM CORROSION TEST LOOP

ASSEMBLY TITLE Cb-1Zr RANKINE SYSTEM CORROSION TEST LOOP ASSEMBLY NO. 246R925

PROGRAM TITLE POTASSIUM CORROSION TEST LOOP DEV. CONTRACT NO. NAS 3-2547

ITEM NO.	DRAWING NUMBER	DWG LEVEL 1	2	3	4	DESCRIPTION/TITLE	REV.	ISSUE DATE
	246R925 G1 x					Loop Assembly	E	6/21/65
	246R900	1				Support Structure Assembly	G	6/21/65
	246R903	2				Sodium Heater Coil Assembly	E	6/21/65
	263E706	3				Turbine Simulator Assembly	F	6/21/65
	119C2857 G10	3	1			Nozzle Assembly	A	9/28/64
	119C2853 P10	3	2			Nozzle	A	10/2/64
	119C2858 G1	3	3			Blade Assembly		7/21/64
	119C2857 G9	3	1			Nozzle Assembly	A	9/28/64
	119C2853 P9	3	2			Nozzle	A	10/2/64
	119C2858 G1	3	3			Blade Assembly		7/21/64
	119C2857 G8	3	1			Nozzle Assembly	A	9/28/64
	119C2853 P8	3	2			Nozzle	A	10/2/64
	119C2858 G1	3	3			Blade Assembly		7/21/64
	119C2857 G7	3	1			Nozzle Assembly	A	9/28/64
	119C2857 G7	3	2			Nozzle	A	10/2/64
	119C2858 G1	3	3			Blade Assembly		7/21/64
	119C2857 G6	3	1			Nozzle Assembly	A	9/28/64
	119C2853 P6	3	2			Nozzle	A	10/2/64
	119C2858 G1	3	3			Blade Assembly		7/21/64
	119C2857 G5	3	1			Nozzle Assembly	A	9/28/64
	119C2853 P5	3	2			Nozzle	A	10/2/64
	119C2858 G1	3	3			Blade Assembly		7/21/64
	119C2857 G4	3	1			Nozzle Assembly	A	9/28/64
	119C2853 P4	3	2			Nozzle	A	10/2/64
	119C2858 G1	3	3			Blade Assembly		7/21/64
	119C2857 G3	3	1			Nozzle Assembly	A	9/28/64
	119C2853 P3	3	2			Nozzle	A	10/2/64
	119C2858 G1	3	2			Blade Assembly		7/21/64
	119C2857 G2	3	1			Nozzle Assembly	A	9/28/64
	119C2853 P2	3	2			Nozzle	A	10/2/64

Final Issue Date: 6/21/65

LIST OF DRAWINGS

ASSEMBLY TITLE Cb-1Zr RANKINE SYSTEM CORROSION TEST LOOP **ASSEMBLY NO.** 246R925

PROGRAM TITLE POTASSIUM CORROSION TEST LOOP DEV. **CONTRACT NO.** NAS 3-2547

ITEM NO.	DRAWING NUMBER	DWG LEVEL 1	2	3	4	DESCRIPTION/TITLE	REV.	ISSUE DATE
	119C2858 G1	3	3			Blade Assembly		7/21/64
	119C2857 G1	3	1			Nozzle Assembly	A	9/28/64
	119C2853 P1	3	2			Nozzle	A	10/2/64
	119C2858 G1	3	3			Blade Assembly		7/21/64
	263E715 G1	4				Boiler Assembly	F	6/21/65
	263E726 G1	5				Ass'y-Tube K, Gas Press. Tube Ass'y	B	6/21/65
	SK-56131-456 P1	5	1			Bimetallic Joint Assembly	A	8/17/64
	263E727	6				Na Gas Press. Tube Ass'y (Sod)	B	6/21/65
	941D753 P2	6	1			Fitting	A	2/3/65
	SK-56131-456 P1	5	1			Bimetallic Joint Assembly	A	8/17/64
	263E729	7				K Pump Outlet Assembly	A	12/22/64
	941D753 P1	6	1			Fitting	A	2/3/65
	119C2835 G2	7	1			Transducer & Mounting Tube Assembly	C	2/2/65
	119C2836	7	1	1		Retainer Cap	B	2/2/65
	119C2837 G2	7	1	2		Transducer Body Assembly	C	2/2/65
	142B1804 P1	7	1	2	1	Tube		10/5/64
	142B1737 P1	7	1	2	2	Retainer Body	C	2/3/65
	142B1863 G1	7	1	2	3	Diaphragm Assembly		2/2/65
	165A5734 P1	7	1	2	3	1 Diaphragm		2/2/65
	142B1739 P2	7	1	2	4	Housing	C	2/2/65
	142B1740 P2	7	1	2	5	Housing Cap	B	2/2/65
	142B1839	7	1	3		LVDT Coil Assembly	A	1/13/65
	119C2838 P1	7	1	4		Reducer	B	2/2/65
	119C2875	7	2			Press. Transducer & Tube Assembly		7/21/64
	SK56131-356 G5	7	2	1		Press. Transducer Assembly	D	2/3/65
	263E732 G2	7	3			High Tem. (Metering) Valve Assembly	A	12/8/64
	142B1815 P1	7	3	1		Modified Bushing	A	12/8/64
	142B1816 P1	7	3	2		Pinion Gear Drive		11/18/64
	119C2893 G1	7	3	4		Ball Bearing Stem Assembly	A	2/21/65
	119C2891 G1	7	3	5		Modified Yoke	B	2/3/65

Final Issue Date: 6/21/65

LIST OF DRAWINGS

Cb-1Zr RANKINE SYSTEM CORROSION
ASSEMBLY TITLE TEST LOOP ASSEMBLY NO. 246R925

PROGRAM TITLE POTASSIUM CORROSION TEST LOOP DEV. CONTRACT NO. NAS 3-2547

ITEM NO.	DRAWING NUMBER	DWG LEVEL 1	2	3	4	DESCRIPTION/TITLE	REV.	ISSUE DATE
	142B1814 P1	7	3	5	1	Gear Mount		11/18/64
	142B1807	7	3	6		Adapter Bonnet		11/18/64
	142B1806 P1	7	3	7		Swivel Guide		11/18/64
	142B1813 P1	7	3	8		Swivel Screw		11/18/64
	142B1812 P1	7	3	9		Gasket		11/18/64
	142B1811 P1	7	3	10		Bonnet Nut		11/18/64
	119C2904 P1	7	3	11		Bonnet		11/18/64
	165A5671 P1	7	3	12		Bellows Ring and Stem		11/16/64
	165A5670 P1	7	3	13		Pin		11/16/64
	165A5669 P1	7	3	14		Plug		11/16/64
	165A5667 P1	7	3	15		Body and Nipples		11/16/64
	165A5668 P1	7	3	16		Metering Plug		11/16/64
	142B1859	7	3	17		Retainer Collar		12/11/64
	941D728 G1	8				K, Preheat Coil Assembly	B	6/21/64
	941D730 G1	9				Tube Fill & Dump Tube Ass'y	A	9/28/64
	SK-56131-456 P1	5	1			Bimetallic Joint Assembly	A	8/17/64
	941D753 P3	6	1			Fitting	A	2/3/65
	941D732 G1	10				Na Fill & Dump Tube Ass'y	A	9/28/64
	SK-56131-456 P1	5	1			Bimetallic Joint Assembly	A	8/17/64
	941D753 P1	6	1			Fitting	A	2/3/65
	941D738 G1	11				Vapor Bubble Nucleator Ass'y	C	1/28/65
	119C2863 G1	11	1			Nucleator Assembly	B	1/28/65
	142B1769 P1	11	2			Nucleator Pin		7/21/64
	941D747 G1	11	3			Housing Nucleator Assembly	B	12/28/64
	142B1767 P1	11	4			Nucleator R.H. Coil		7/21/64
	142B1767 P2	11	4			Nucleator L.H. Coil		7/21/64
	142B1771 P1	11	5			Nucleator Electrode Ass'y	A	12/23/64
	142B1770 P1	11	6			Nucleator Nut		7/21/64
	142B1770 P2	11	6			Nucleator Nut		7/21/64
	142B1768 G1	11	7			Nucleator Bus Bar Ass'y	B	12/23/64

Final Issue Date: 6/21/65

LIST OF DRAWINGS

Cb-1Zr RANKINE SYSTEM CORROSION
ASSEMBLY TITLE TEST LOOP ASSEMBLY NO. 246R925

PROGRAM TITLE POTASSIUM CORROSION TEST LOOP DEV. CONTRACT NO. NAS 3-2547

ITEM NO.	DRAWING NUMBER	DWG LEVEL 1	2	3	4	DESCRIPTION/TITLE	REV.	ISSUE DATE
	165A5718 P1	11	8			Nucleator Insulator	A	8/28/61
	165A5620 P1	11	9			Nucleator Insulator	A	8/28/61
	165A5721 P1	11	10			Nucleator Pin	A	8/28/61
	941D739 G1	12				Condenser	F	1/28/65
	119C2909 G1	12	1			Sub-Cooler Reservoir		11/18/61
	941D715 P1	13				Boiler Outlet Tube		7/21/64
	941D746 P1	14				K Pump Inlet Tube		7/21/64
	941D748 G1	15				K Tank Outlet Assembly		7/21/64
	941D753 P3	6	1			Fitting	A	2/3/65
	263E752 G1	7	3			High Temp (on-Off) Valve Ass'y	A	12/8/61
	142B1815 P1	7	3	1		Modified Bushing	A	12/8/64
	142B1816 P1	7	3	2		Pinion Gear Drive		11/18/64
	142B1817 P1	7	3	3		Gear Bushing		11/18/61
	119C2893 G1	7	3	4		Ball Bearing Stem Ass'y	D	5/22/66
	119C2891 G1	7	3	5		Modified Yoke	B	2/3/65
	142B1811 P1	7	3	5		Gear Mount		11/18/61
	142B1807 P1	7	3	6		Adapter Bonnet		11/18/61
	142B1806 P1	7	3	7		Swivel Guide		11/18/61
	142B1813 P1	7	3	8		Swivel Screw		11/18/61
	142B1812 P1	7	3	9		Gasket		11/18/61
	142B1811 P1	7	3	10		Bonnet Nut		11/18/61
	119C2904 P1	7	3	11		Bonnet		11/28/61
	165A5671 P1	7	3	12		Bellows, Ring and Stem		11/16/61
	165A5670 P1	7	3	13		Pin		11/16/6
	165A5669 P1	7	3	14		Plug		11/16/61
	165A5667 P1	7	3	15		Body and Nipples		11/16/61
	119C2828 G1	16				Mounting Tube & Pressure Transducer Assembly	B	6/21/65
	SK-56121-556 G5	7	2	1		Pressure Transducer Assembly	C	8/28/61
	119 C2868 P1	17				Bus Bar		7/21/61

Final Issue Date: 6/21/65

LIST OF DRAWINGS

ASSEMBLY TITLE: Cb-1Zr RANKINE SYSTEM CORROSION TEST LOOP — ASSEMBLY NO. 246R925

PROGRAM TITLE: POTASSIUM CORROSION TEST LOOP DEV. — CONTRACT NO. NAS 3-2547

ITEM NO.	DRAWING NUMBER	DWG LEVEL 1	2	3	4	DESCRIPTION/TITLE	REV.	ISSUE DATE
	119C2868 P2	17				Bus Bar		7/21/64
	119C2870 G1	18				Sodium Heater Cable Ass'y		7/21/64
	142B1649 P1	18	1			Cable Connector		4/21/64
	142B1650 P1	18	2			Cable Connector		4/21/64
	119C2832 G1	19				Surge Tank Ass'y		7/21/64
	119C2872 P1	20				Bus Bar		7/21/64
	119C2872 P2	20				Bus Bar		7/21/64
	119C2872 P3	20				Bus Bar		7/21/64
	119C2873 G1	21				K Pre-Heater Cable Ass'y		7/21/64
	142B1649 P1	18	1			Connector		4/21/64
	142B1650 P1	18	2			Connector		4/21/64
	142B1754 P1	22				Spacer		7/21/64
	142B1754 P2	22				Spacer		7/21/64
	142B1761 P1	23				Insulator	A	8/28/64
	142B1764 P1	24				Transducer Connector	B	10/2/64
	142B1782 G1	25				Electrical Feedthrough Assembly	A	12/17/64
	SK-56131-326	26				Electrical Feedthrough Assembly		12/18/63
	SK-56131-372 G1	27				Argon/Liquid Metal Feedthrough Ass'y	A	8/28/64
	263E730 G1	28				Sodium Pump Inlet Tube	B	6/12/65
	941D753 P1	6	1			Fitting	A	2/3/65
	119C2878 G1	29				Tube & Press. Transducer Ass'y	C	6/21/65
	SK-56131-356 G5	7	2	1		Pressure Transducer Ass'y		8/28/64
	119C2877 G1	30				Tube & Press. Transducer Ass'y	C	6/21/65
	SK-56131-356 G5	7	2	1		Pressure Transducer Ass'y		8/28/64
	SK-56131-366 G1	31				Pump Inlet Reducer Ass'y	D	8/28/64
	DK-56131-367	32				Pump Outlet Reducer Ass'y	C	8/28/64
	246R935 G1	33				Spool Section Ass'y	B	6/21/65
	165A5625 P1	33	1			Tube Bracket Pad		8/28/64
	165A5624 P1	33	2			Bracket Tube	A	9/28/64
	263E754 G1	34				Shield Drive Assembly	A	12/14/64

Final Issue Date: 6/21/65

LIST OF DRAWINGS

ASSEMBLY TITLE: Cb-1Zr RANKINE SYSTEM CORROSION TEST LOOP — ASSEMBLY NO. 246R925

PROGRAM TITLE: POTASSIUM CORROSION TEST LOOP DEV. — CONTRACT NO. NAS 3-2547

ITEM NO.	DRAWING NUMBER	DWG LEVEL 1	2	3	4	DESCRIPTION/TITLE	REV.	ISSUE DATE
	142B1834 P1	34	1			Race Mount		11/18/64
	142B1833 P1	34	2			Outer Race		11/18/64
	142B1832 P1	34	3			Inner Race		11/18/64
	142B1797 P1	34	5			Washer	A	11/18/64
	119C2760 G1	34	6			Rotating Condenser Shield	B	1/4/65
	142B1831 G1	34	7			Rack Drive Assembly	A	2/4/65
	142B1826 P1	34	7	1		Drive Screw		11/18/64
	142B1827 G1	34	7	2		Bracket	B	2/4/65
	142B1825 P1	34	8			Thrust Bearing		11/18/64
	911D787 G1	34	9			Base	C	6/21/65
	142B1830 P1	34	10			Rack Support		11/18/64
	119C2913 P1	34	11			Rack		11/18/64
	119C2921 P1	34	12			Spacer Rod		12/17/64
	142B1829 P1	34	13			Rack Support		11/18/64
	142B1828 P1	34	14			Clamp		11/18/64
	911D794 P1	34	15			Upper Support Plate	B	6/21/65
	263E760 G1	35				Boiler Radiation Shield Ass'y		2/10/65
	911D801 G1	35	1			Boiler Shield Inner Cover Ass'y		2/10/65
	911D798 G1	35	2			Boiler Shield Cover Ass'y	A	2/10/65
	911D797 G1	35	3			Support Spider	A	2/10/65
	911D800	35	4			Boiler Shield Outer Cover Ass'y	A	6/21/65
	119C2926	35	5			Bottom Plate		2/10/65
	119C2927	35	6			Heat Radiation Shield		2/10/65
	142B1861	35	7			Boiler Shield Support Rod	B	6/21/65
	142B1862	35	8			Clevis	A	2/10/65
	142B1860	35	9			Support		2/10/65
	246R945	36				Insulation and Instrumentation	A	2/10/65
	142B1817 P1	7	3	3		Gear Bushing		11/18/64

Final Issue Date: 6/21/65

APPENDIX B

MAJOR DRAWINGS OF THE Cb-1Zr RANKINE SYSTEM CORROSION TEST LOOP

Figure No.	Title	GE-SPPS Drawing No.
159	Cb-1Zr Rankine System Corrosion Test Loop Assembly	246R925 (Rev. E)
160	Loop Support Structure Assembly	246R900 (Rev. G)
161	Sodium Heater Coil Assembly	246R903 (Rev. E)
162	Turbine Simulator Assembly	263E706 (Rev. F)
163	Turbine Simulator Nozzle Assembly	119C2857 (Rev. A)
164	Turbine Simulator Nozzle	119C2853 (Rev. A)
165	Turbine Simulator Blade Assembly	119C2858
166	Boiler Assembly	263E715 (Rev. F)
167	Gas Pressure Tube Assembly for Potassium Circuit	263E726 (Rev. B)
168	Bimetallic Joint Assembly	SK56131-456 (Rev. A)
169	Gas Pressure Tube Assembly for Sodium Circuit	263E727 (Rev. B)
170	Potassium Pump Outlet Assembly	263E729 (Rev. A)
171	Stressed Diaphragm Pressure Transducer and Mounting Tube Assembly[a]	119C2835 (Rev. C)
172	High Temperature Valve Assembly	263E752 (Rev. A)
173	Ball Bearing Stem Assembly of the High-Temperature Valve	119C2893 (Rev. A)
174	Potassium Preheater Coil Assembly	941D728 (Rev. B)

[a] Complete set of drawings of this component included in Topical Report No. 6, Cb-1Zr Pumped Sodium Loop.

APPENDIX B (Continued)

MAJOR DRAWINGS OF THE Cb-1Zr RANKINE SYSTEM CORROSION TEST LOOP

Figure No.	Title	GE-SPPS Drawing No.
175	Vapor Bubble Nucleator	941D738 (Rev. C)
176	Potassium Condenser and Subcooler	941D739 (Rev. F)
177	Condenser Shield Drive Assembly	263E754 (Rev. A)

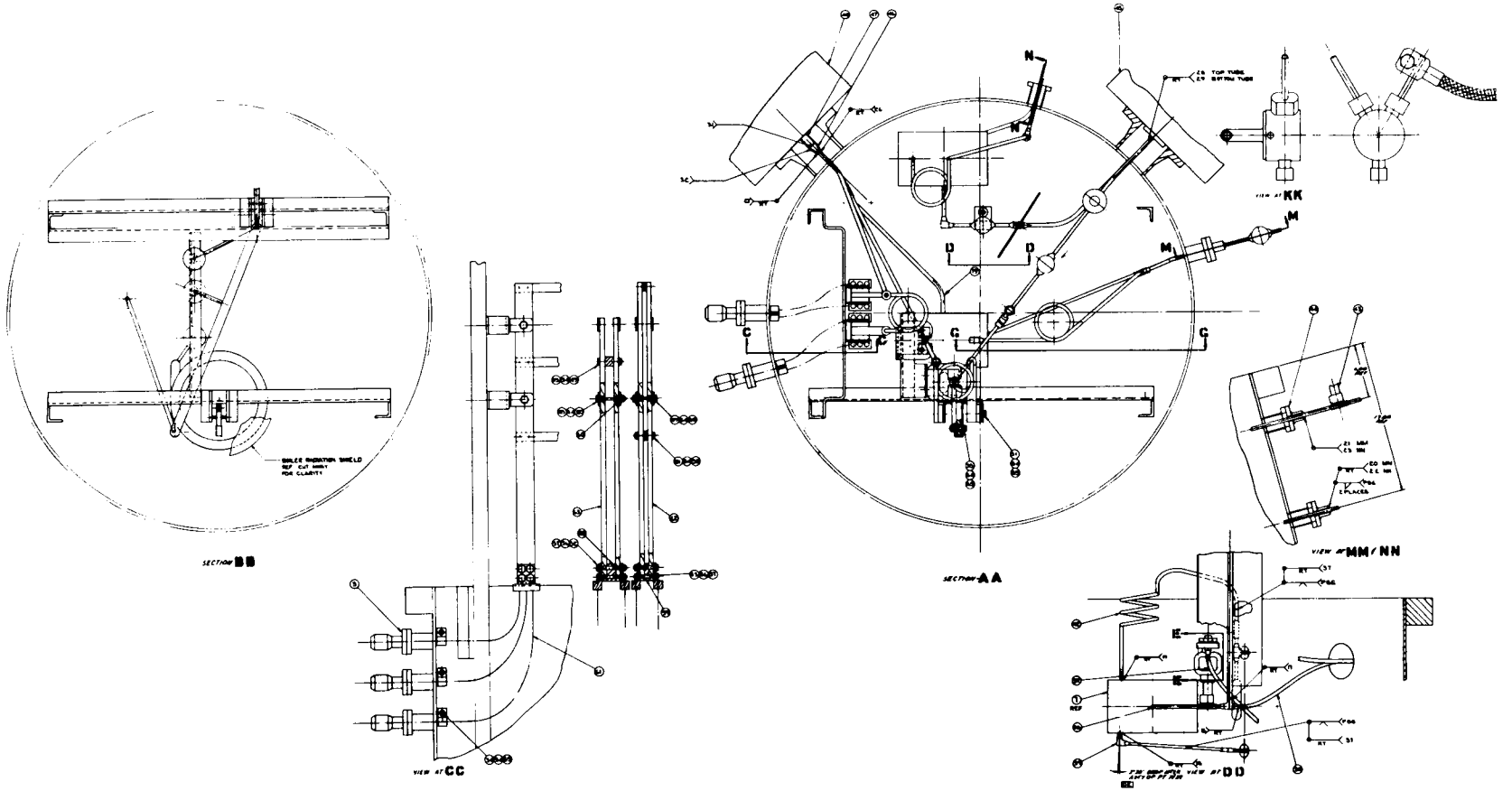

Figure 159. Cb-1Zr Rankine System Corrosion Test Loop Assembly.

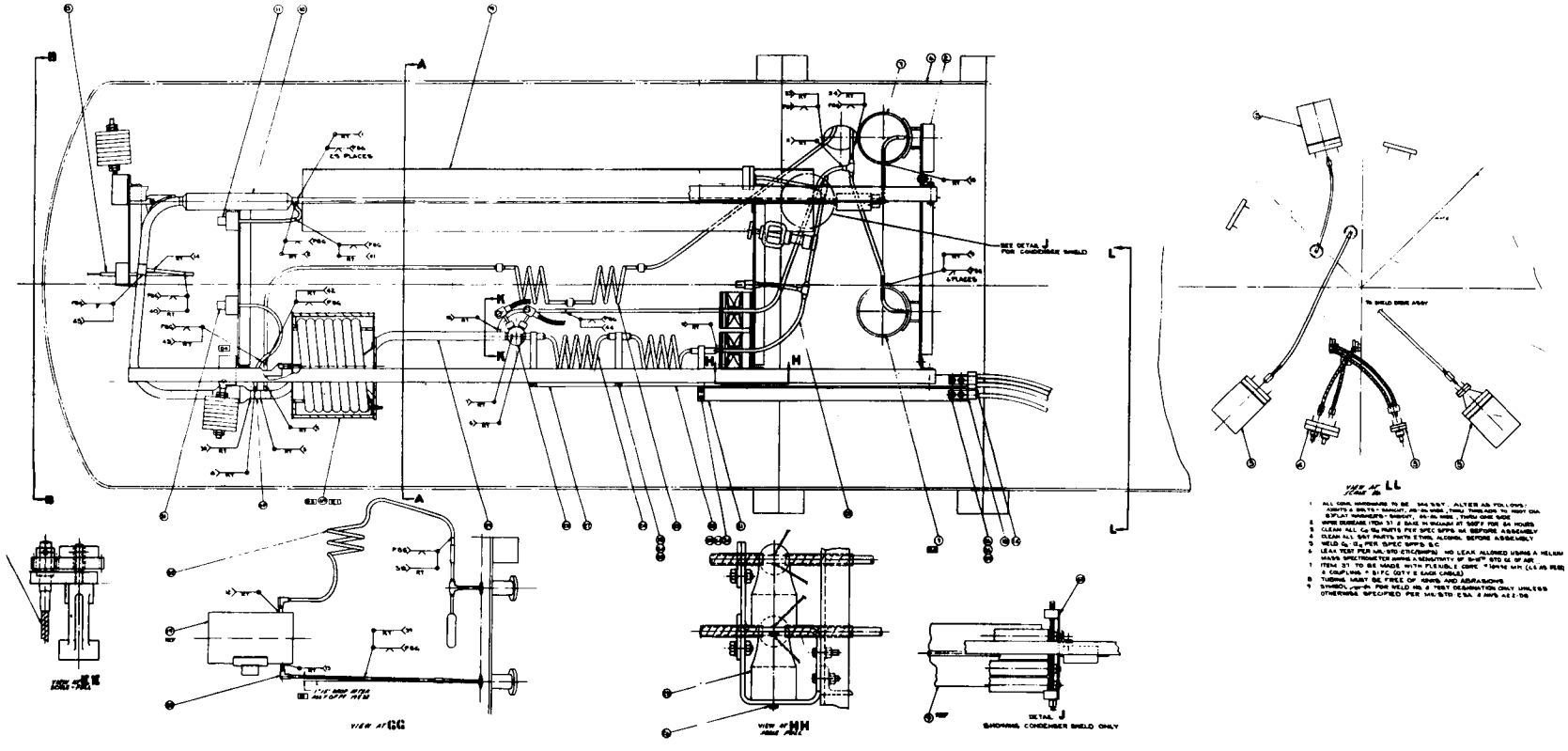

Figure 159 Cont'd. Cb-1Zr Rankine System Corrosion Test Loop Assembly.

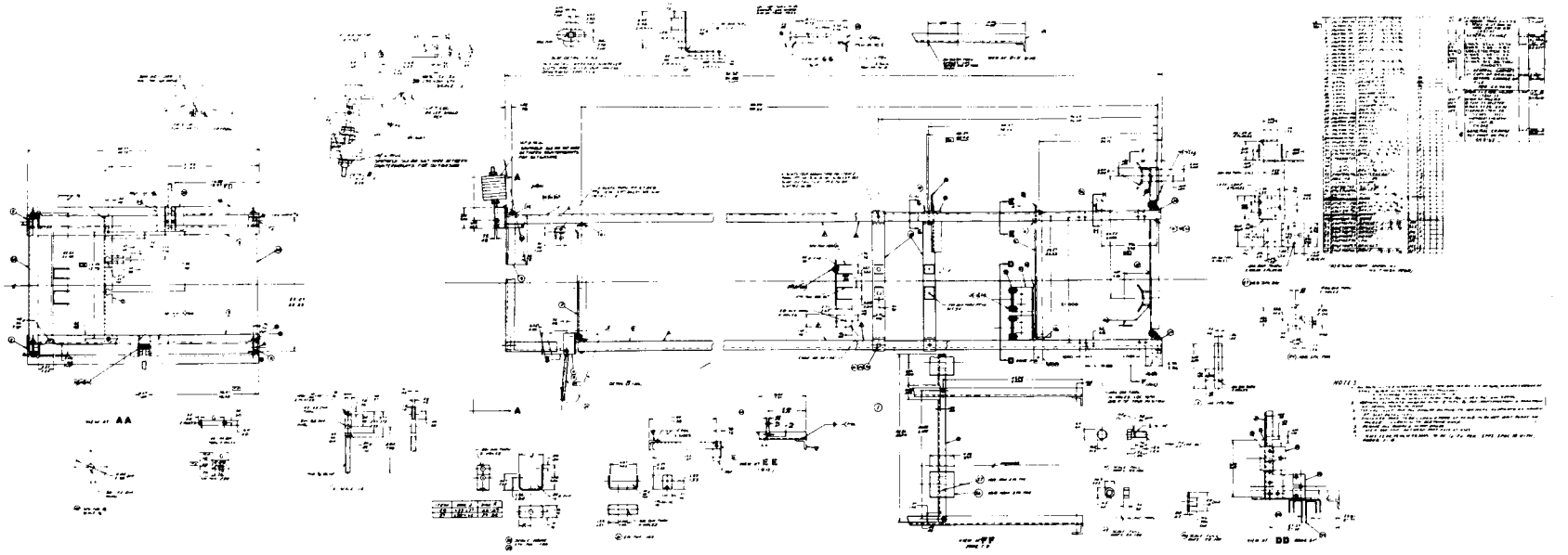

Figure 160. Loop Support Structure Assembly.

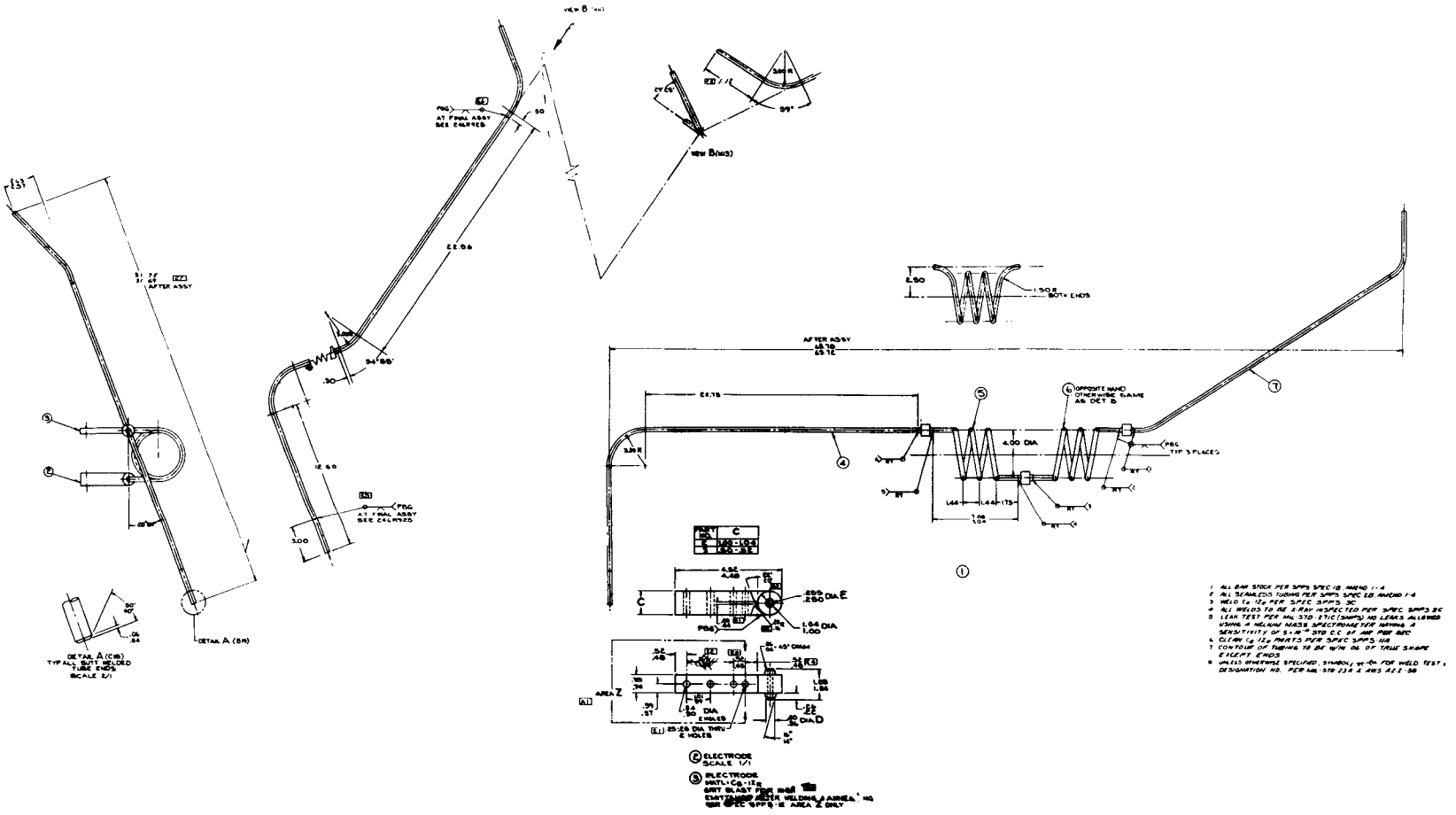

Figure 161. Sodium Heater Coil Assembly.

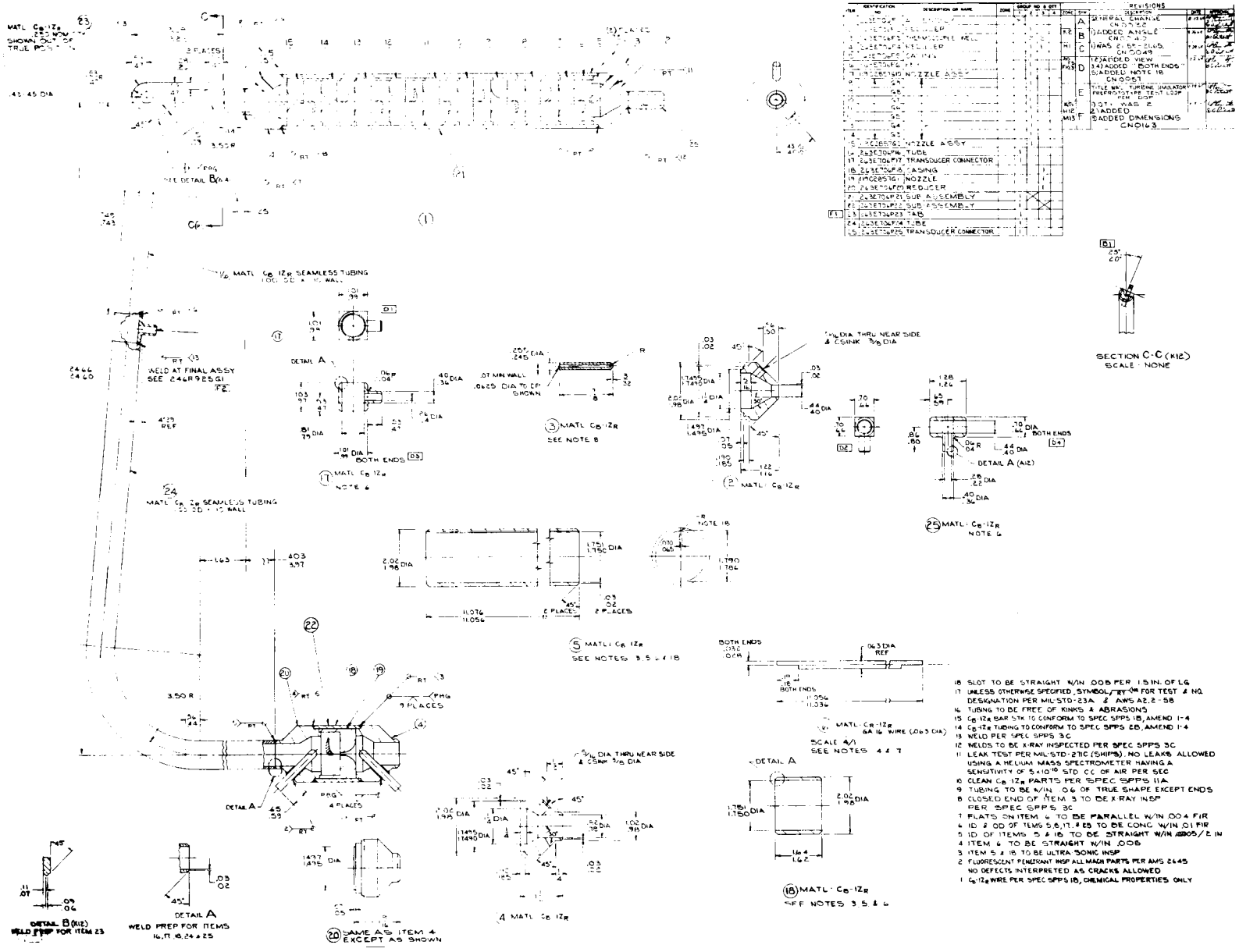

Figure 162. Turbine Simulator Assembly.

ITEM	IDENTIFICATION NO.	DESCRIPTION OR NAME	ZONE	GROUP NO. & QTY 1	2	3	4	5	6	7	8	9	10
1	1190285761	ASSEMBLY		X									
2	G2				X								
3	G3					X							
4	G4						X						
5	G5							X					
6	G6								X				
7	G7									X			
8	G8										X		
9	G9											X	
10	G10												X
11	1190285881	BLADE ASSY		1	1	1	1	1	1	1	1	1	1
12	1190285381	NOZZLE		1									
13	P2				1								
14	P3					1							
15	P4						1						
16	P5							1					
17	P6								1				
18	P7									1			
19	P8										1		
20	P9											1	
21	P10												1

REVISIONS			SIZE	1190285 7	REV A
			CONT ON SHEET	SH NO.	
ZONE	SYM	DESCRIPTION	DATE	APPROVAL	
B5 A6	A	1) WAS SURF A 2) DELETED DIA A 3) NOTE 1 WAS "...TO DIA A" CN00 49	9-28-64		

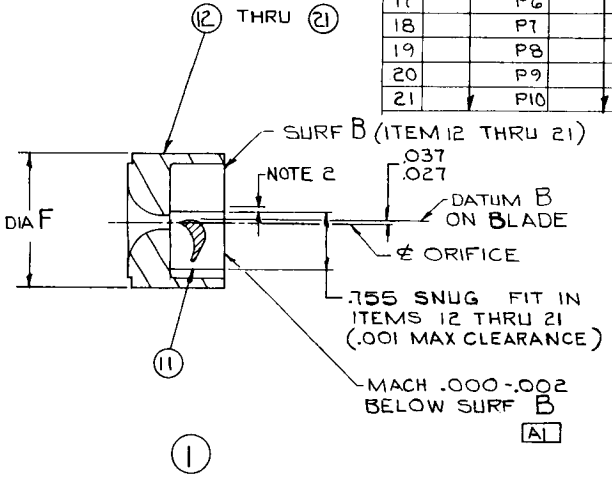

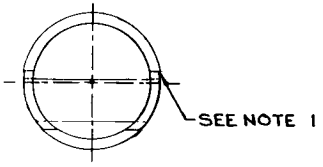

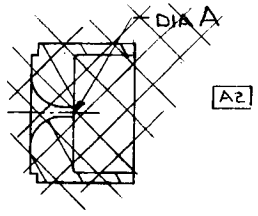

A3
1. ITEM 11 TO BE CENTERED IN RELATION TO DIA F W/IN .010 FIR
2. .06 OVER LAP ONTO ITEM 12 THRU 21 WHEN MACHINING ITEM 11 FLUSH WITH SURF B
3. BAG & TAG WITH IDENT NO. & SERIAL NO.
4. CLEAN PARTS WITH ETHOL ALCOHOL BEFORE ASSY
5. NO DISTORTION OF DIA F ALLOWABLE AFTER ASSY

Figure 163. Turbine Simulator Nozzle Assembly.

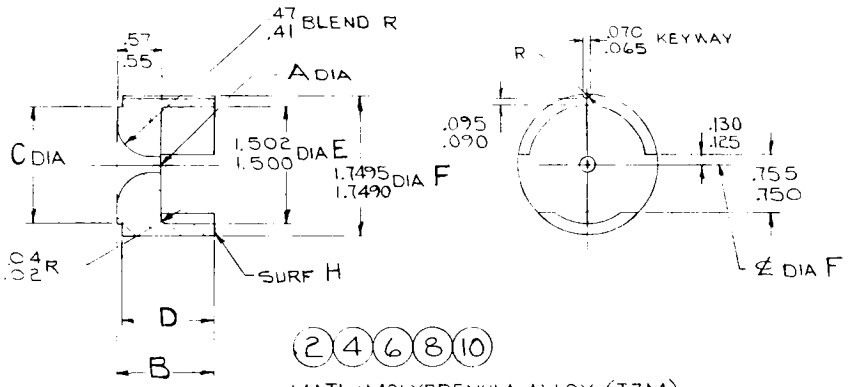

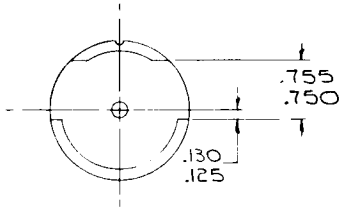

ITEM	A DIA	B DIM	C DIA	D DIM
1	.099 - .100	1.249 1.250		
2	.100 - .101	1.249 - 1.250		
3	.115 - .116	1.24 - 1.26	1.495 - 1.497	1.180 - 1.181
4	.128 - .129			
5	.141 - .142			
6	.158 - .159			
7	.175 - .176			
8	.205 - .206			
9	.221 - .222			
10	.249 - .250	1.24 - 1.26	1.495 - 1.497	1.180 - 1.181

1 DYE-PENETRANT INSP PER AMS 2646. NO DEFECTS INTERPRETED AS CRACKS ALLOWED
2 ROUGH POLISHING TO BE DONE WITH ALUMINA GRIT CLOTH
3 MOLYBDENUM ALLOY (TZM) PER SPEC SPPS 15
4 DIA C & E TO BE CONC WITH DIA F W/IN .002 FIR
5 DIA A TO BE CONC WITH DIA F W/IN .005 FIR
6 ALL SURF TO BE ELECTRO-POLISHED WITH .0005 MAX MATL REMOVAL
7 SURF H TO BE SQ WITH DIA F W/IN .001 FIR
8 KEYWAY TO BE PARALLEL WITH DIA F W/IN .005 FIR
9 BAG & TAG WITH PART NO. & SERIAL

Figure 164. Turbine Simulator Nozzle.

ITEM	IDENTIFICATION NO.	DESCRIPTION OR NAME	ZONE	GROUP NO. & QTY 1	2	3	4
1	1190285 8 P1	ASSEMBLY		X			
2	P2	BLADE		1			
3	P3	BLOCK		1			
4	P4	BLOCK		1			

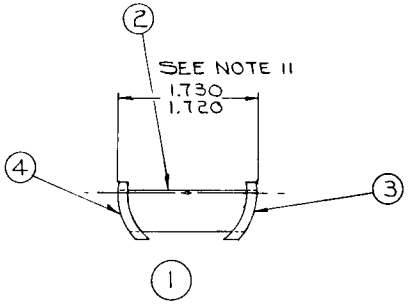

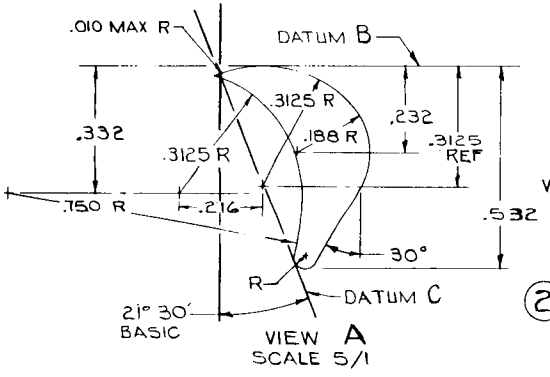

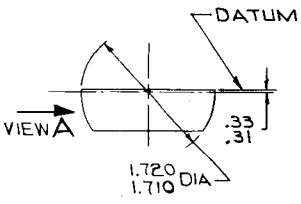

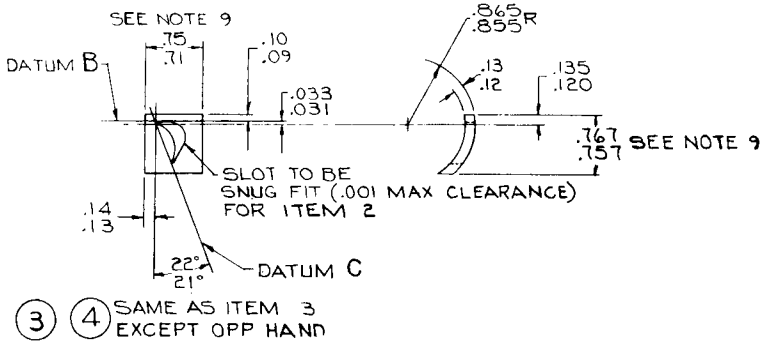

1. CLEAN ALL PARTS WITH ETHOL ALCOHOL
2. ALL POLISHING TO BE DONE WITH ALUMINA GRIT CLOTH
3. ITEM 2 TO HAVE .005 MAX TWIST BETWEEN ENDS
4. CONTOUR DIMENSIONS APPLY TO ITEM 2
5. CONTOUR TO BE W/IN .005 OF TRUE SHAPE EXCEPT AREA 1/4 FROM ENDS MAY HAVE ADDITIONAL .005 STOCK REMOVAL AT ASSY.
6. CONTOURED SURFACES TO BE 16/ OR BETTER
7. SLOT IN ITEM 3 & 4 TO BE SNUG FIT FOR ITEM 2
8. MAX .010 LOCALIZED GAP BETWEEN SNUG FIT CONTOURS
9. PROCESS DIM, SEE NEXT ASSY FOR FINISH MACH DIM
10. MOLYBDENUM ALLOY, TZM, PER SPEC SPPS 15
11. ITEM 2 NOT TO EXTEND OUTSIDE OF ITEMS 3 & 4
12. CONTOUR OF ITEM 2 TO BE ELECTRO-POLISHED WITH A MAX MATL REMOVAL OF .0005
13. ITEM 2 TO BE DYE-PENETRANT INSP PER AMS 2646 NO DEFECTS INTERPRETED AS CRACKS ALLOWED
14. BAG & TAG PARTS WITH IDENT NO. & SERIAL NO.

Figure 165. Turbine Simulator Blade Assembly.

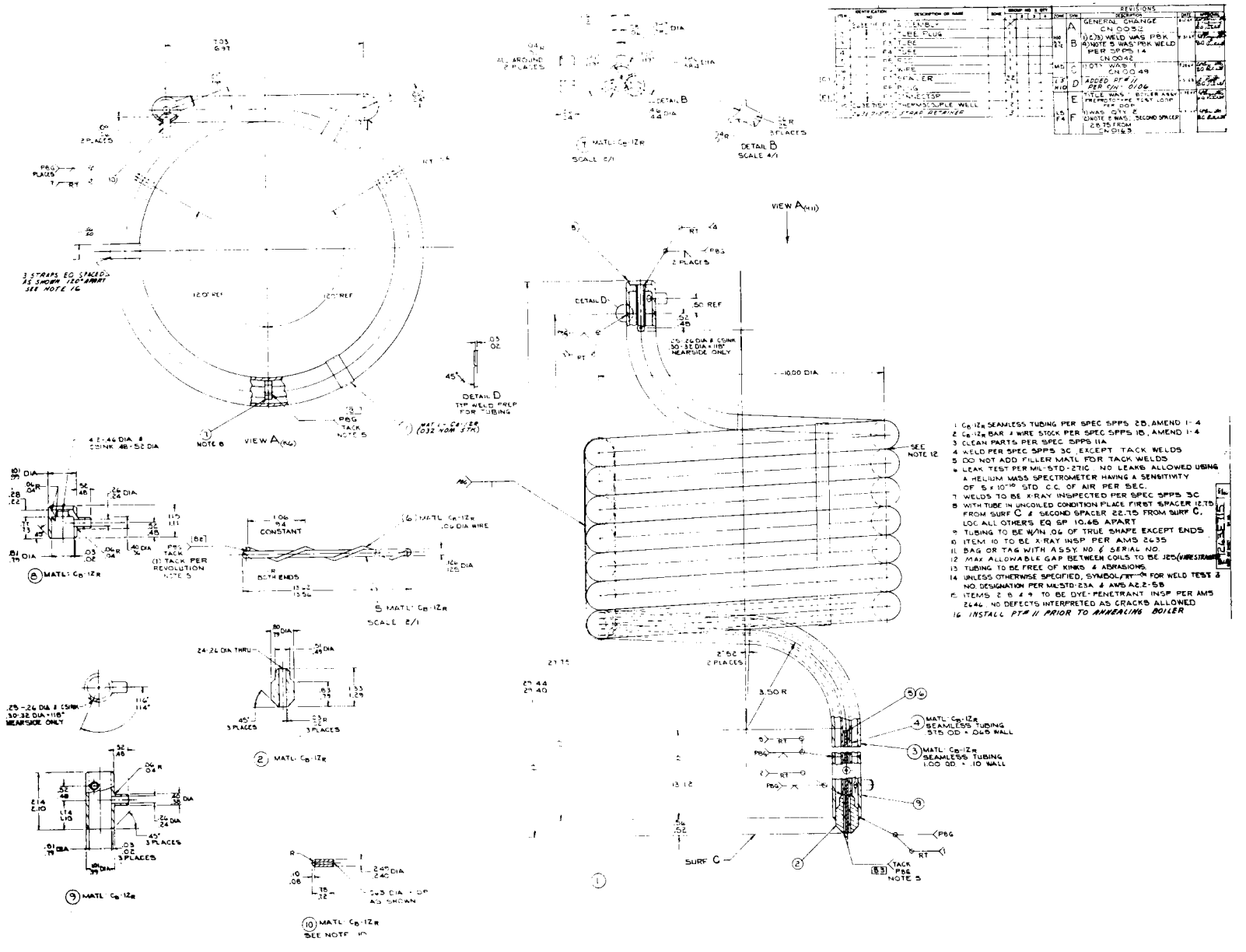

Figure 166. Boiler Assembly.

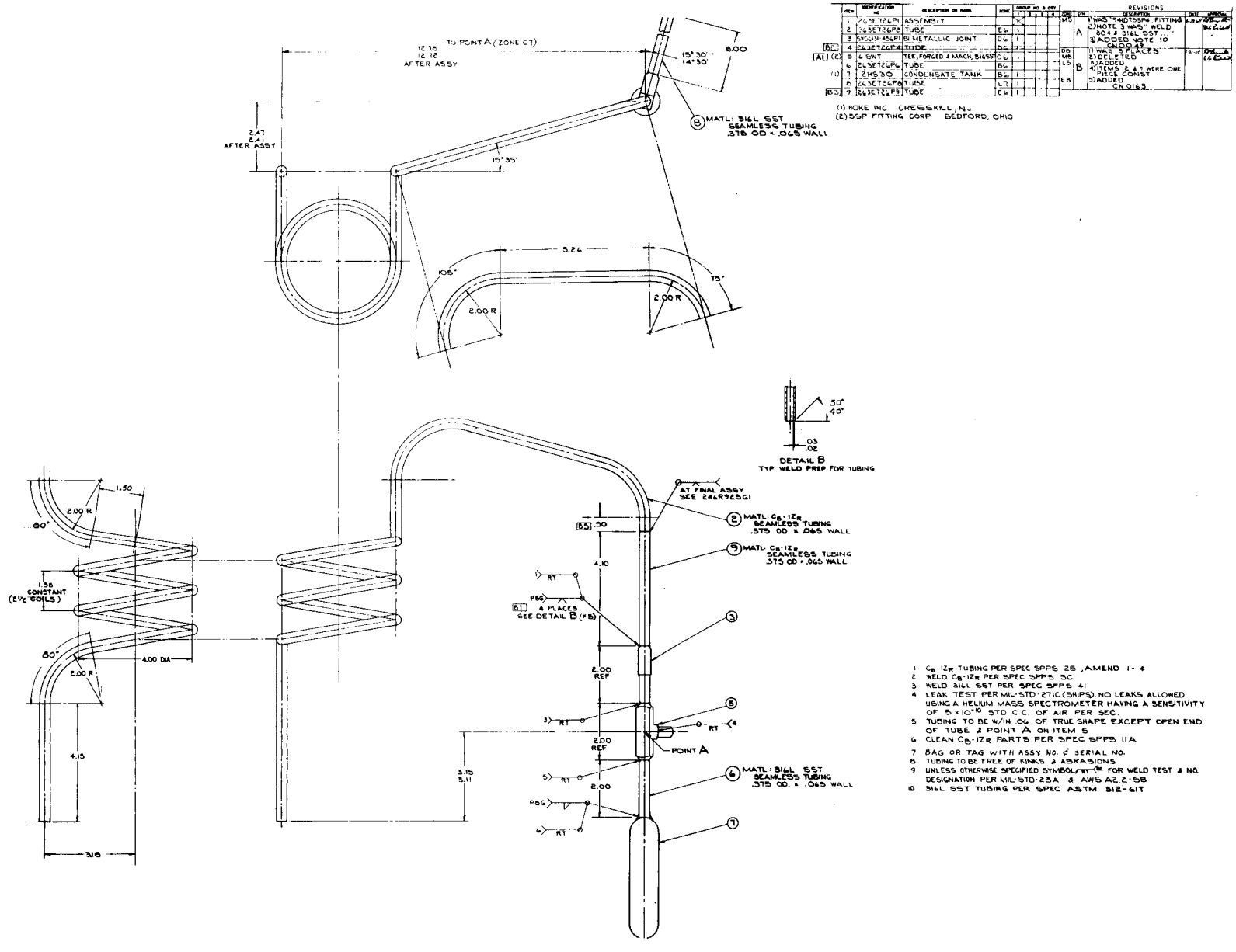

1. C_8 12R TUBING PER SPEC SPPS 28, AMEND 1-4
2. WELD C_8-12R PER SPEC SPPS 3C
3. WELD 316L SST PER SPEC SPPS 4I
4. LEAK TEST PER MIL-STD-271C (SHIPS). NO LEAKS ALLOWED USING A HELIUM MASS SPECTROMETER HAVING A SENSITIVITY OF 5×10^{-10} STD C.C. OF AIR PER SEC.
5. TUBING TO BE W/IN .04 OF TRUE SHAPE EXCEPT OPEN END OF TUBE @ POINT A ON ITEM 5
6. CLEAN C_8-12R PARTS PER SPEC SPPS 11A
7. BAG OR TAG WITH ASSY No. & SERIAL NO.
8. TUBING TO BE FREE OF KINKS & ABRASIONS
9. UNLESS OTHERWISE SPECIFIED SYMBOL/RT-C_8 FOR WELD TEST & NO. DESIGNATION PER MIL-STD-23A & AWS A2.2-58
10. 316L SST TUBING PER SPEC ASTM 312-61T

Figure 167. Gas Pressure Tube **Assembly for Potassium Circuit.**

ITEM	IDENTIFICATION NO.	DESCRIPTION OR NAME	ZONE	GROUP NO. & QTY 1	2	3	4
1	SK56131-456	ASSY		X	X		
2	P2	NIPPLE 316 SST		1	1		
3	P3	NIPPLE CB-1ZR		1	1		

REVISIONS			
SYM	DESCRIPTION	DATE	APPROVED
A	1) GROUP 2 ADDED CN 0033	9.17.64	[illegible]

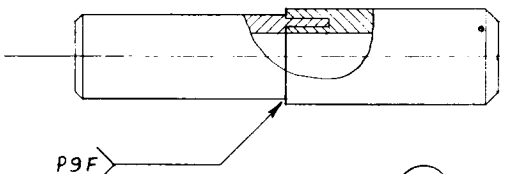

(1) ASSEMBLY

GROUP NO.	A	B
1	1.04 1.00	1.04 1.00
2	2.04 2.00	4.04 4.00

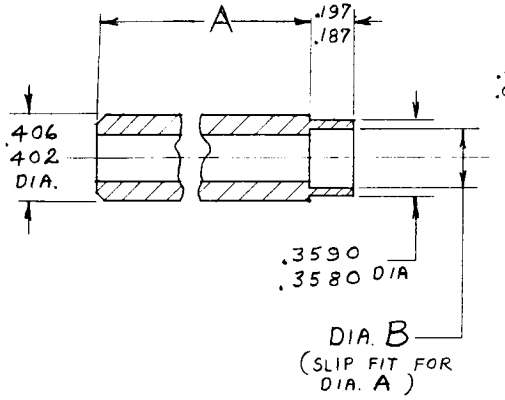

(2) NIPPLE
MATL: TYPE 316 SST

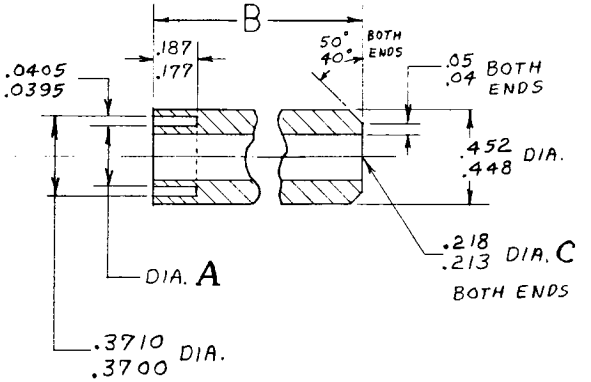

(3) NIPPLE
MATL. Cb-1Zr

NOTES:

1- REMOVE ALL BURRS & SHARP EDGES
2- DIA'S. A & B TO HAVE .0005" MAX. OUT OF ROUNDNESS.
3- DIA'S. A & B TO BE CONCENTRIC WITH DIA. C WITHIN .002 F.I.R.
4- BRAZING TO BE IN ACCORDANCE WITH SPPS SPEC. 9A
5- Cb-1Zr PER SPEC SPPS 2B WITH AMENDMENTS 1-4
6- 316 SST TUBING PER SPEC. ASTM-A-213-61T
7. BAG OR TAG WITH ASSY. NO & SER. NO.

MF

Figure 168. Bimetallic Joint Assembly.

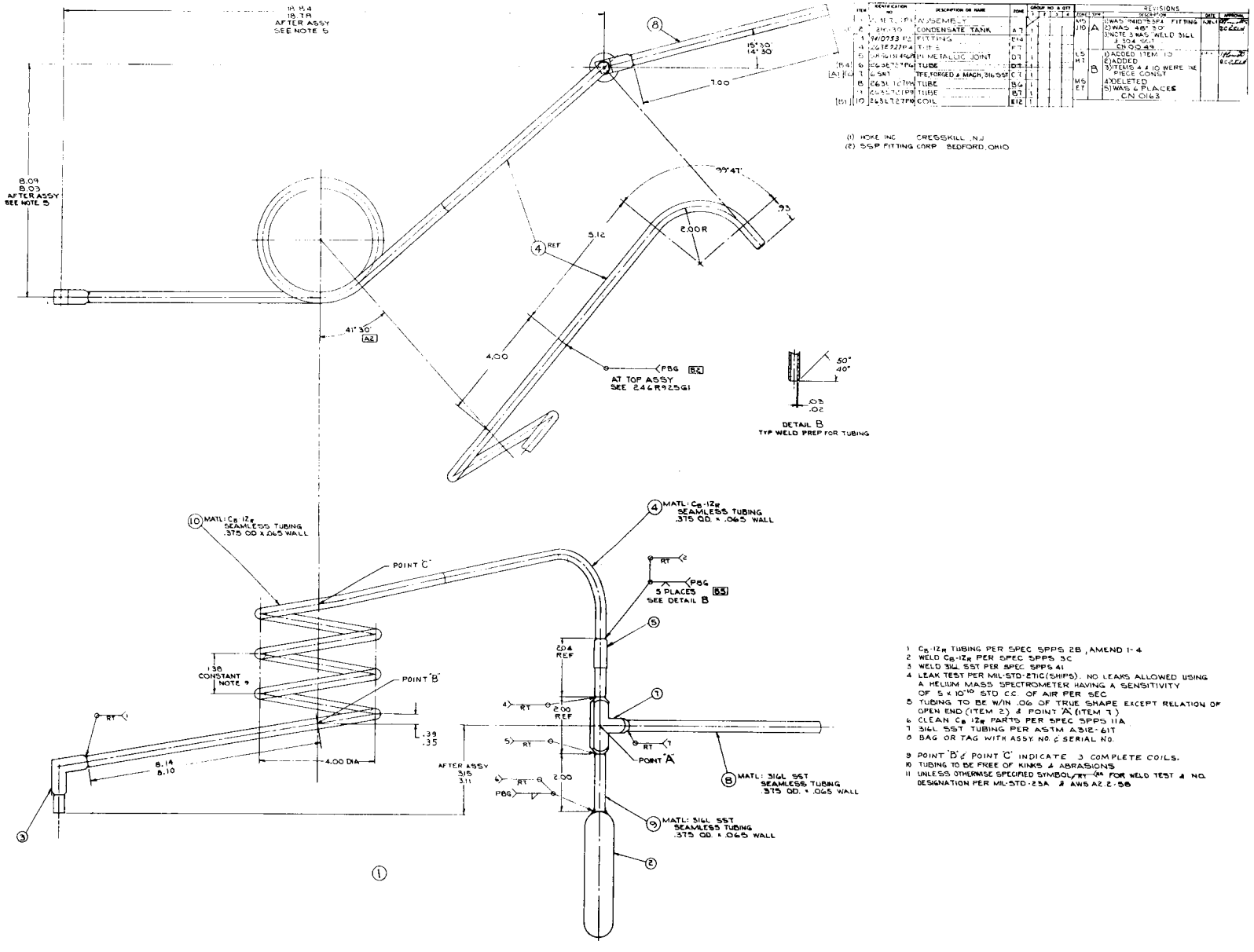

ITEM	IDENTIFICATION NO	DESCRIPTION OR NAME	ZONE	GROUP NO. & QTY 1	2	3	4
1	1" NPT - PIPE	ASSEMBLY		1			
2	2M-30	CONDENSATE TANK	A7	1			
3	94107S3 #2	FITTING	E14	1			
4	246E922P4 A	TEE	E7	1			
5	246J151 #6	METALLIC JOINT	D7	1			
6	246E922P4	TUBE	D5	1			
7	6 SST	TFE FORGED & MACH. 316 SST	E7	1			
8	2631 1C1P4	TUBE	B6	1			
9	2631 1C1P3	TUBE	B7	1			
10	2631 T27P8	COIL	E12	1			

ZONE	SYM	DESCRIPTION	DATE	APPROVAL
M5 J10	A	1) WAS "NIDISPA" FITTING 2) WAS 48° 30' 3) NOTE 3 WAS "WELD 316L & 304 PER CN 0049		
L5 M7 M5 E7	B	1) ADDED ITEM 10 2) ADDED 3) ITEMS 4 & 10 WERE ONE PIECE CONST 4) DELETED 5) WAS 6 PLACES CN 0163		

(1) HOKE INC CRESSKILL, N.J.
(2) SSP FITTING CORP BEDFORD, OHIO

1 $Cb\text{-}1Zr$ TUBING PER SPEC SPPS 2B, AMEND 1-4
2 WELD $Cb\text{-}1Zr$ PER SPEC SPPS 3C
3 WELD 316L SST PER SPEC SPPS 4I
4 LEAK TEST PER MIL-STD-271C(SHIPS). NO LEAKS ALLOWED USING A HELIUM MASS SPECTROMETER HAVING A SENSITIVITY OF 5×10^{-10} STD CC OF AIR PER SEC.
5 TUBING TO BE W/IN .06 OF TRUE SHAPE EXCEPT RELATION OF OPEN END (ITEM 2) & POINT 'A' (ITEM 7)
6 CLEAN $Cb\text{-}1Zr$ PARTS PER SPEC SPPS 11A
7 316L SST TUBING PER ASTM A312-61T
8 BAG OR TAG WITH ASSY. NO. & SERIAL NO.
9 POINT 'B' & POINT 'C' INDICATE 3 COMPLETE COILS.
10 TUBING TO BE FREE OF KINKS & ABRASIONS
11 UNLESS OTHERWISE SPECIFIED SYMBOL RT-AA FOR WELD TEST & NO. DESIGNATION PER MIL-STD-25A & AWS A2.2-58

Figure 169. Gas Pressure Tube Assembly for Sodium Circuit.

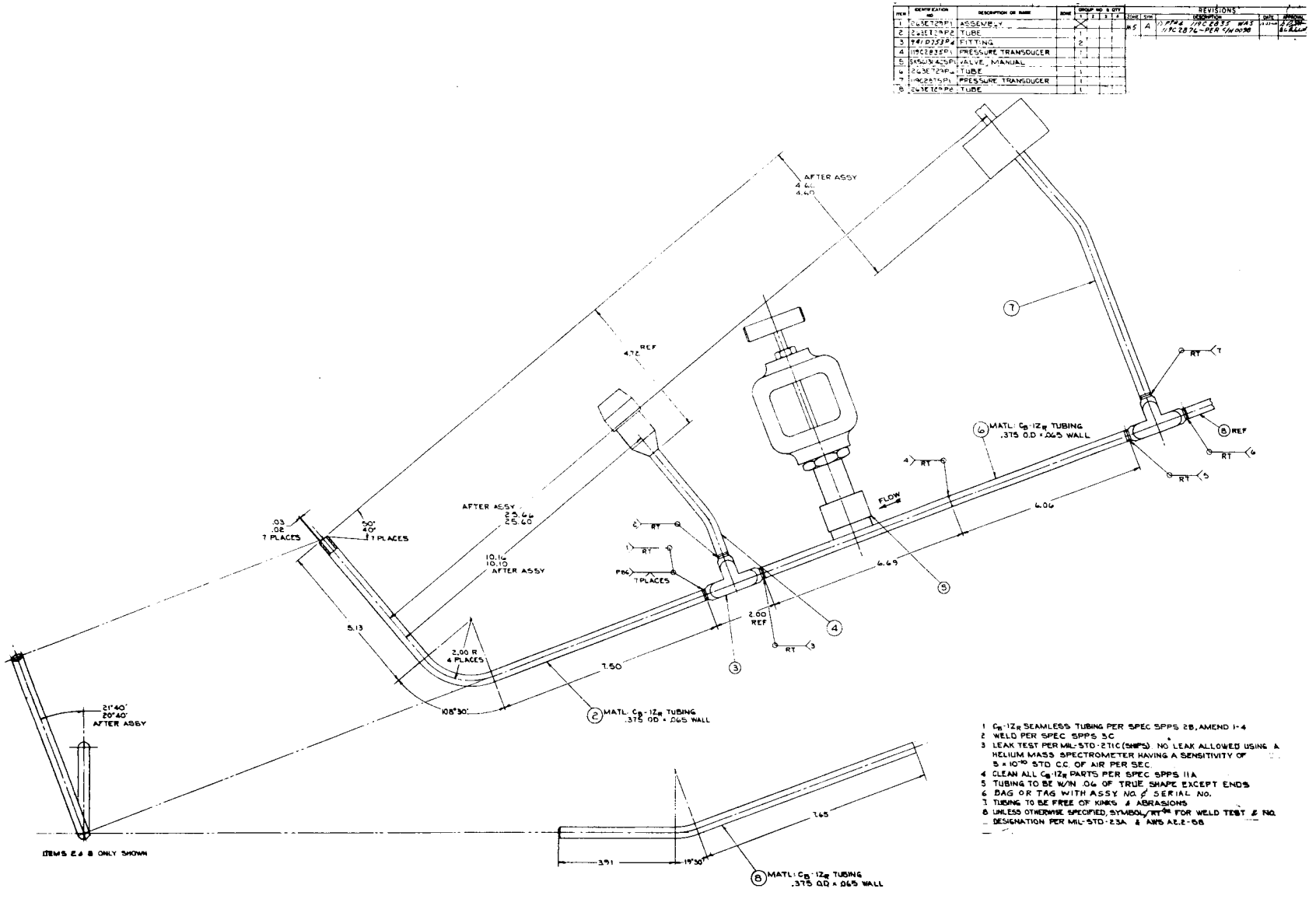

Figure 170. Potassium Pump Outlet Assembly.

ITEM	IDENTIFICATION NO.	DESCRIPTION OR NAME	ZONE	GROUP NO. & QTY 1	2	3	4
1	119C3835 G1	ASSY		X			
2	119C2836 P1	CAP- RETAINER		1	1		
3	119C2837G1	BODY- ASSY		1			
~~4~~ A1	~~119C2838 P1~~	~~REDUCER~~		~~1~~			
5 B1 A2	1428/1839P1	LVDT COIL		1	1		
6	119C2835 G2	ASSY			1		
7	119C2837 G2	ASSY- BODY			1		

ZONE	SYM	REVISIONS DESCRIPTION	DATE	APPROVAL
	A	1) DELETED ITEM 4 2) ADDED ITEM 5 3) ADDED NOTE 4 CN 0058	10-5-64	
	B	1) WAS: "SEE NOTE 4, LVDT ASSY" 2) DELETED NOTE 4 CN 0093	12-18-64	
	C	ADDED GROUP 2 PER C/N 0113	2-2-65	

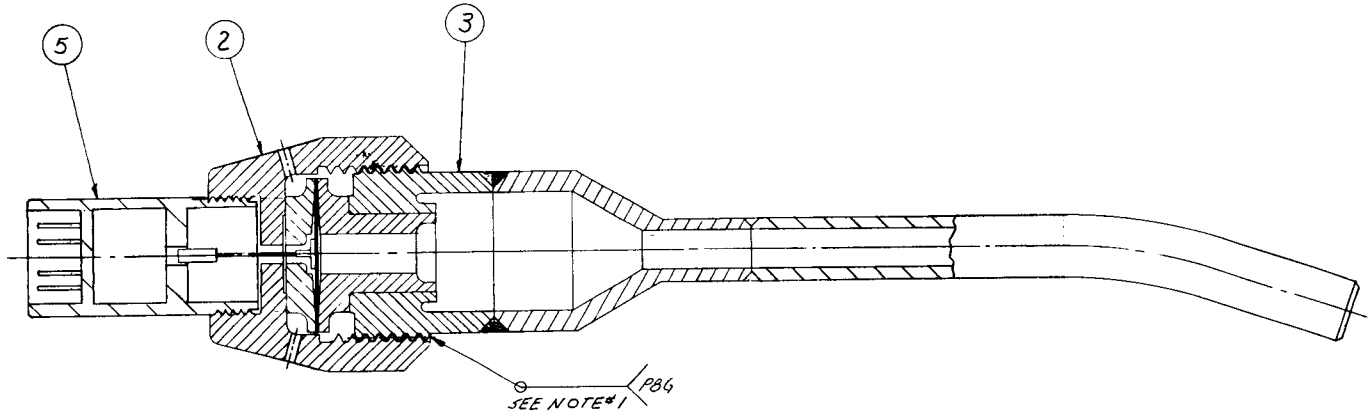

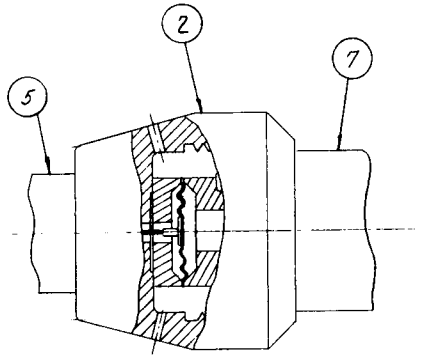

(1) G1

(6) G2
OTHERWISE SAME AS GROUP 1

B2 ~~4 FROM MODEL NO. 411M14-300 PRESS. TRANSDUCER CONSOLIDATED CONTROLS CORP.~~
3 MASS SPECTROMETER LEAK TEST PER MIL STD 271B
2 WELDING OF C81200 MAT'L PER SPPS SPEC 3C
1. AFTER ASSEMBLY OF PT 2 WITH PT 3 TACK WELD AS SHOWN

Figure 171. Stressed Diaphragm Pressure Transducer and Mounting Tube Assembly(a).

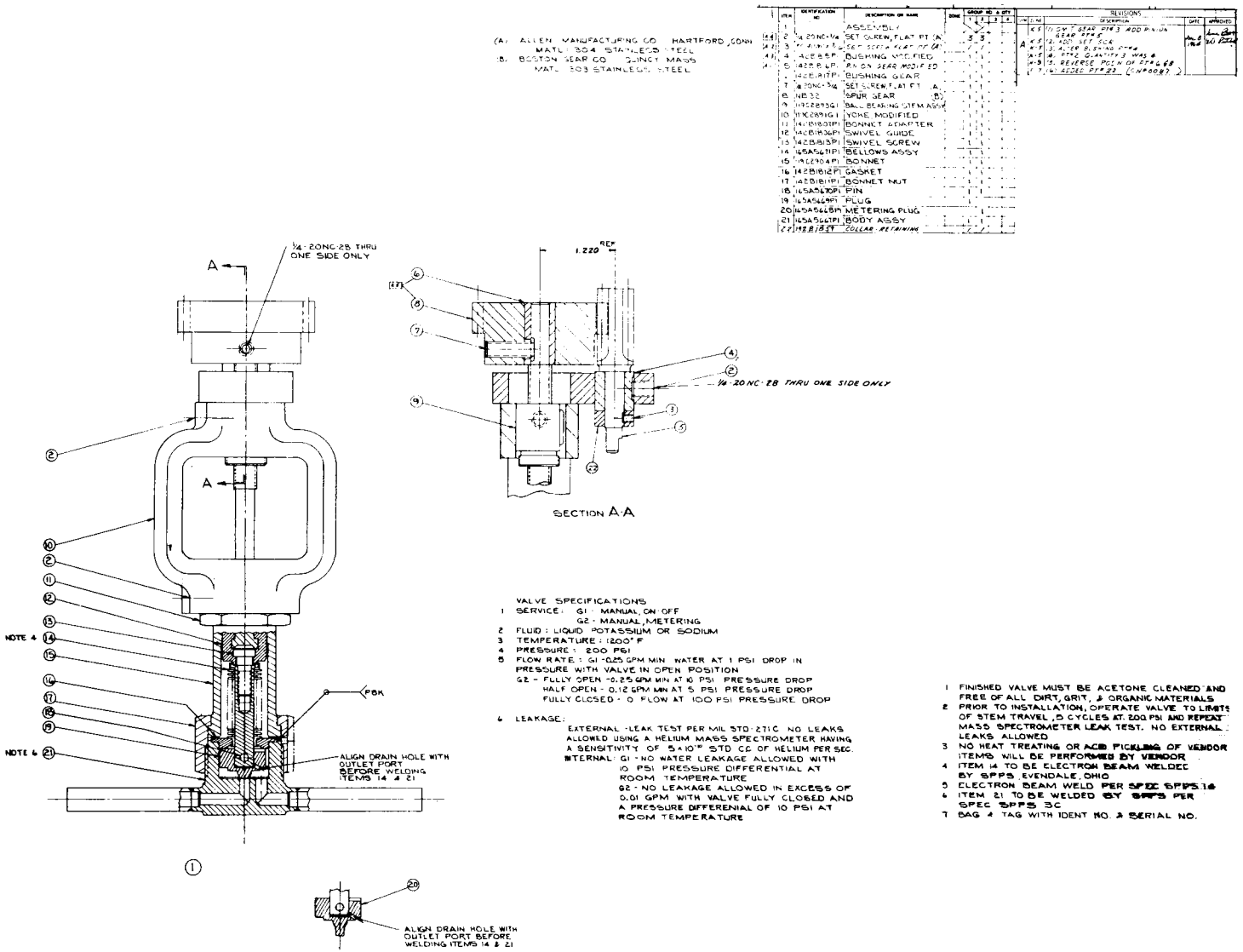

Figure 172. High-Temperature Valve Assembly.

ITEM	IDENTIFICATION NO.	DESCRIPTION OR NAME	ZONE	GROUP NO. & QTY 1	2	3	4
1	1190289 3 P1	BALL SCREW		1			
2	1190289 3 P2	BALL NUT		1			
3	1190289 3 P3	BALL RETURN GUIDE		2			
4	1190289 3 P4	CLAMP		1			
A1 NOTE 2 5	1/16 DIA	TUNGSTEN CARBIDE BALL		62			
NOTE 1 6	5667029	SCREW		2			

SYM	ZONE	DESCRIPTION	DATE	APPROVED
A	E6 C3	1) WAS SYNTHETIC SAPPHIRE BALL 2) WAS 99.99 % AL_2O_3, SINGLE CRYSTAL CN 0163	4-27-66	
B		NOTE 3 WAS SPEC SPPS-15 CN 0311		
C		ISSUED FOR RECORD ONLY PER DOP	5-13-66	
D		REMOVED FOR RECORD ONLY NO CHANGE PER DOP	5-27-66	

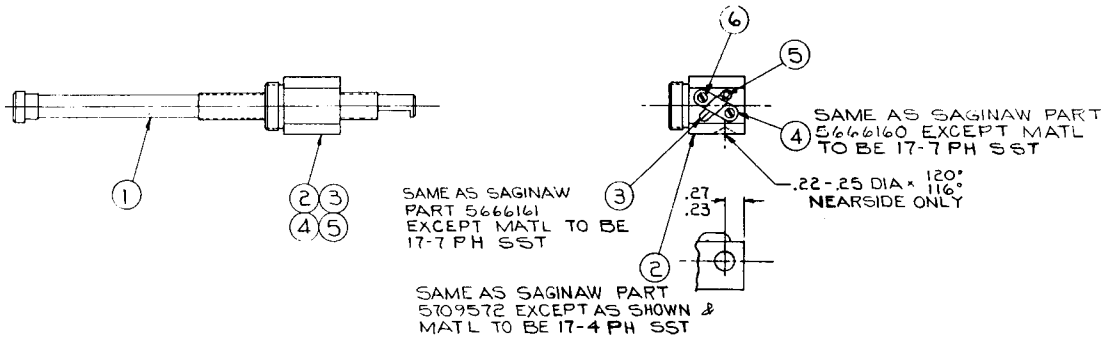

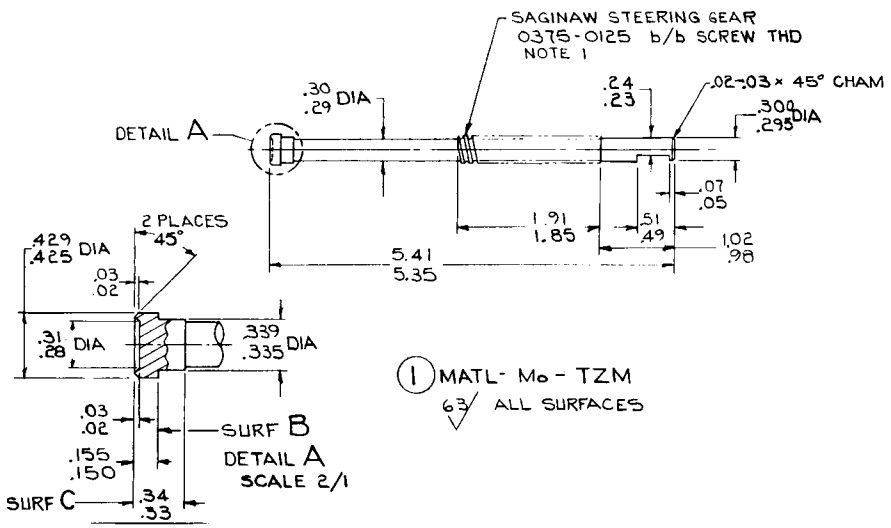

1 SAGINAW STEERING GEAR DIV., SAGINAW, MICH.

A2 2 BALLS TO BE 94 % Wc, 6 % Co AND MEET FOLLOWING REQUIREMENTS:
SIZE TOL- ± .0001
SPHERICITY- .000025

3 TZM ROD PER SPEC 01-0009-00-B

4 SURF B & C TO BE PARALLEL TO EACH OTHER & PERPENDICULAR TO ℄ OF b/b SCREW THD W/IN .005 FIR

5 BAG & TAG WITH IDENT NO. & SERIAL NO.

Figure 173. Ball Bearing Stem Assembly of the High-Temperature Valve.

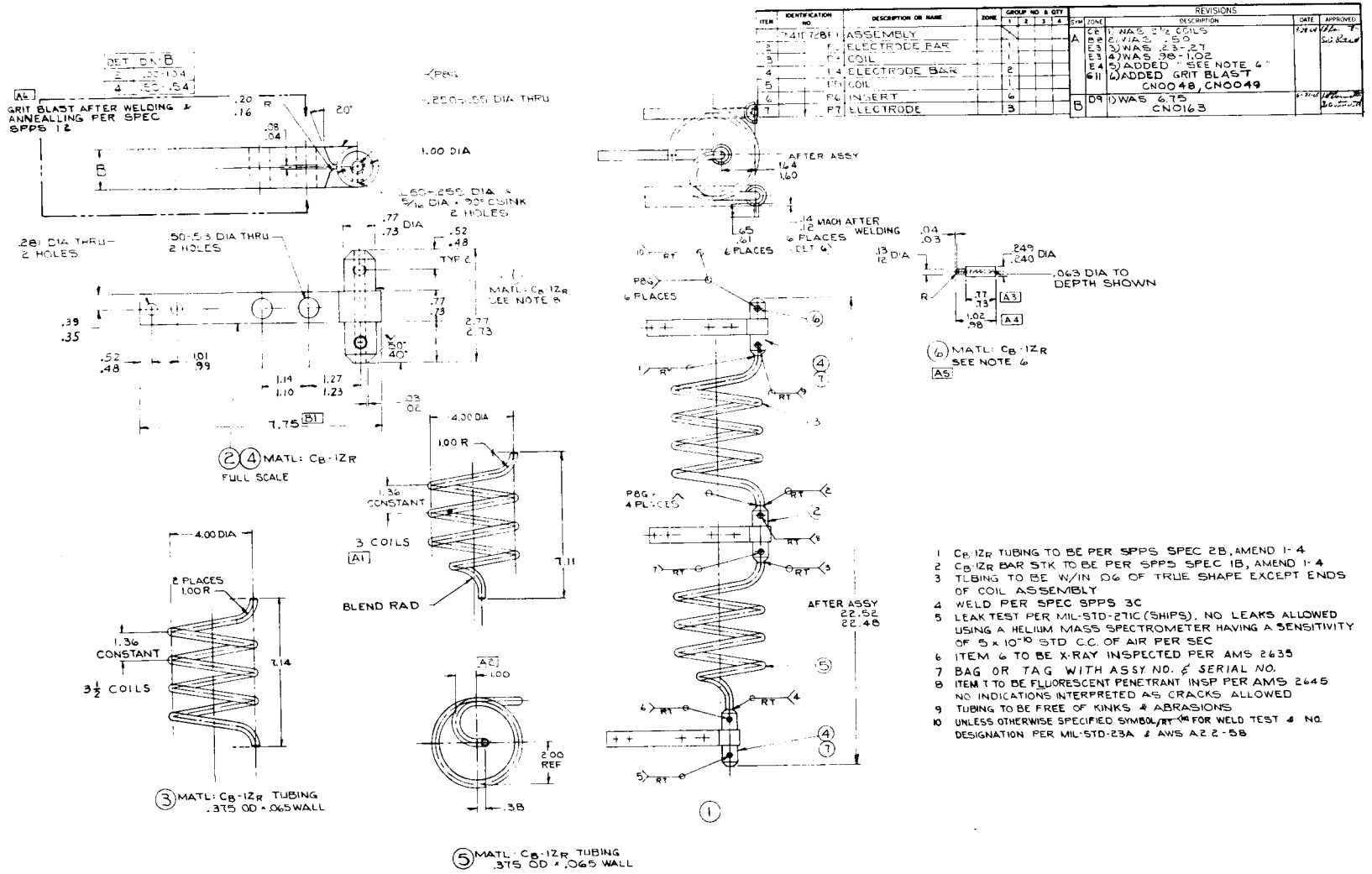

Figure 174. Potassium Preheater Coil Assembly.

ITEM	IDENTIFICATION NO.	DESCRIPTION OR NAME	ZONE	GROUP NO. & QTY 1	2	3	4
1	941D738	ASSY		X			
2	119C286361	NUCLEATOR	C-11	1			
3	COMM.	THERMOCOUPLE	C-10	AR			
4	142B1769	SCR	C-9	4			
5	941D747	HOUSING ASSY.	D-7	1			
6	142B1767-P2	COIL - L.H	D-6	1			
7	142B1771	ELECTRODE	E-6	2			
8	142B1770-P1	NUT	E-5	2			
9	142B1767-P1	COIL - R.H.	D-4	1			
10	142B1768	BUS BAR	D-4	1			
11	142B1770-P2	NUT	C-5	1			
12	165A5718	INSULATOR		2			
13	165A5720	INSULATOR		1			
14	165A5721	PIN		3			

REVISIONS

SYM	ZONE	DESCRIPTION	DATE	APPROVED
A		1) DELINEATION ITEM 10 CLARIFIED CN0036	[illegible]	[illegible]
B	E 4	1) WAS ITEM 13 CN0049	[illegible]	[illegible]
C		TITLE WAS: BUBBLE COMPONENT CORROSION PREPROTOTYPE TEST LOOP PER DOP	[illegible]	[illegible]

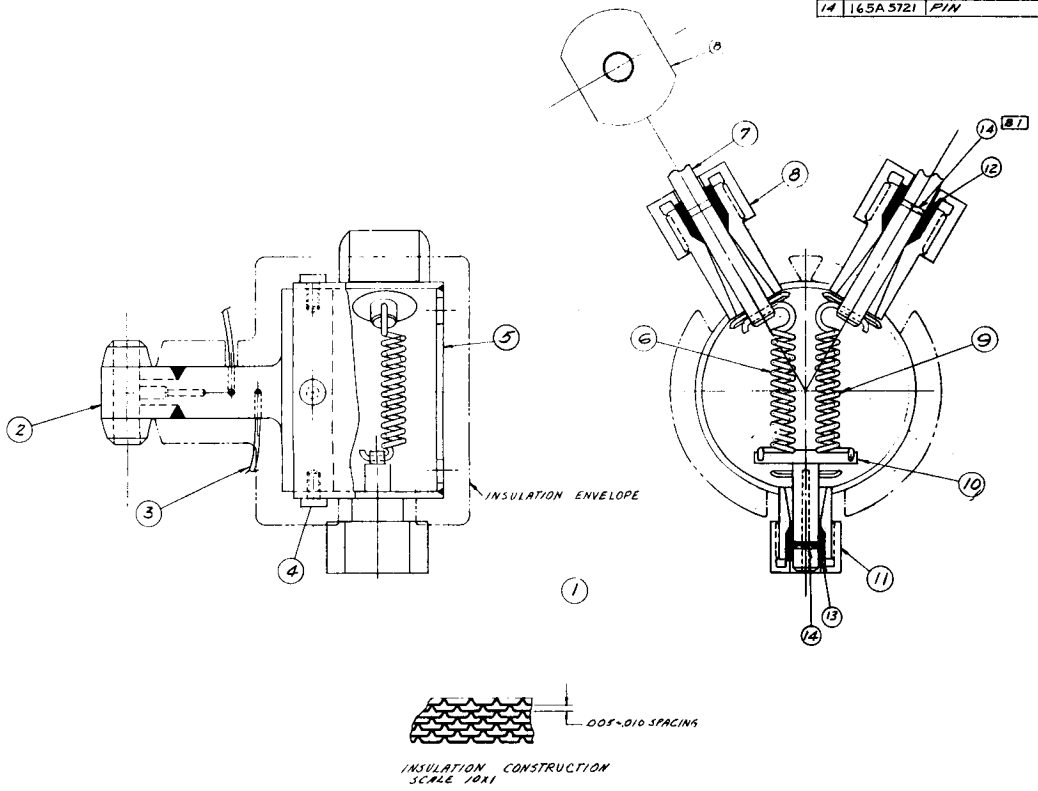

Figure 175. Vapor Bubble Nucleator.

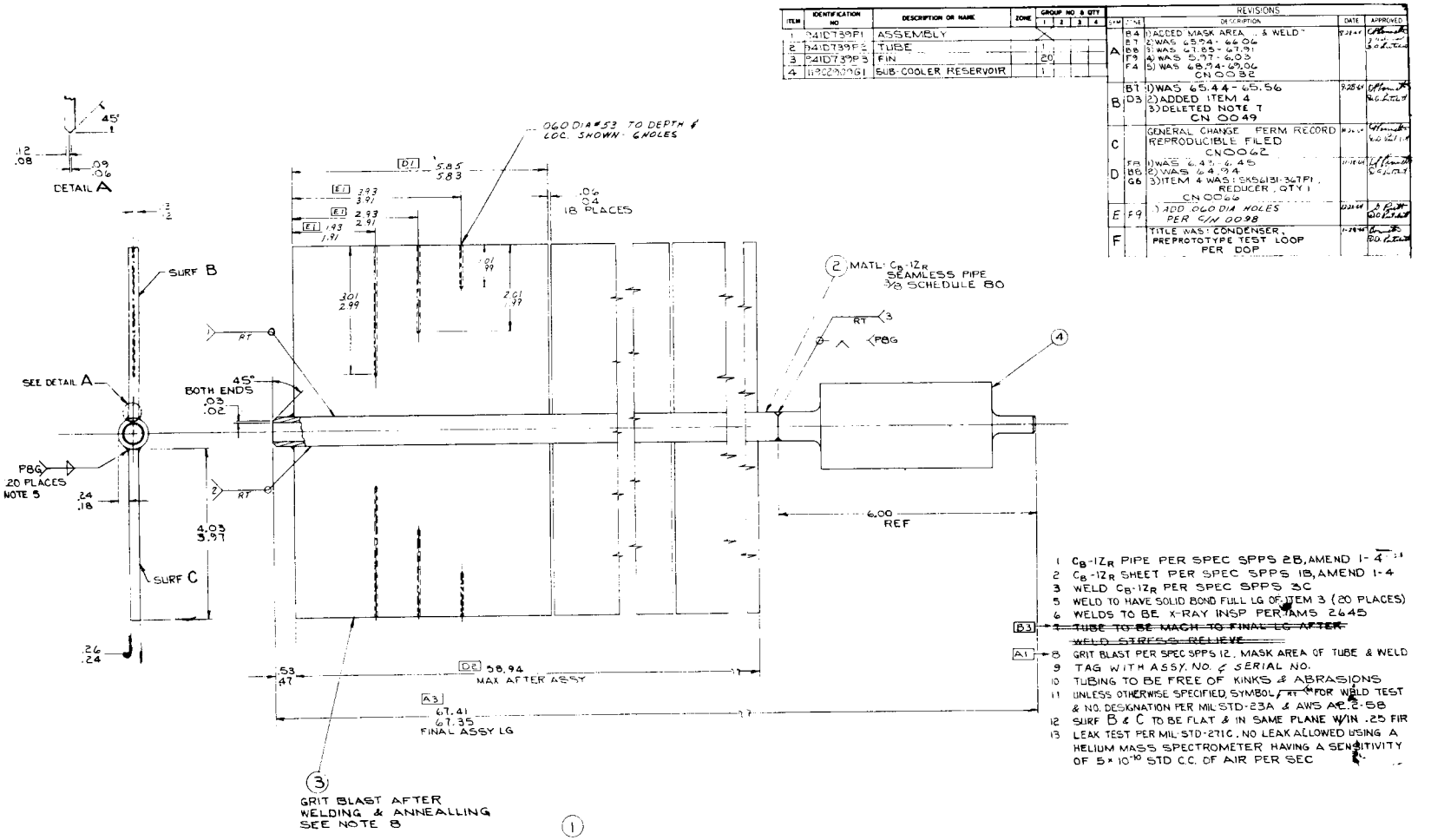

Figure 176. Potassium Condenser and Subcooler.

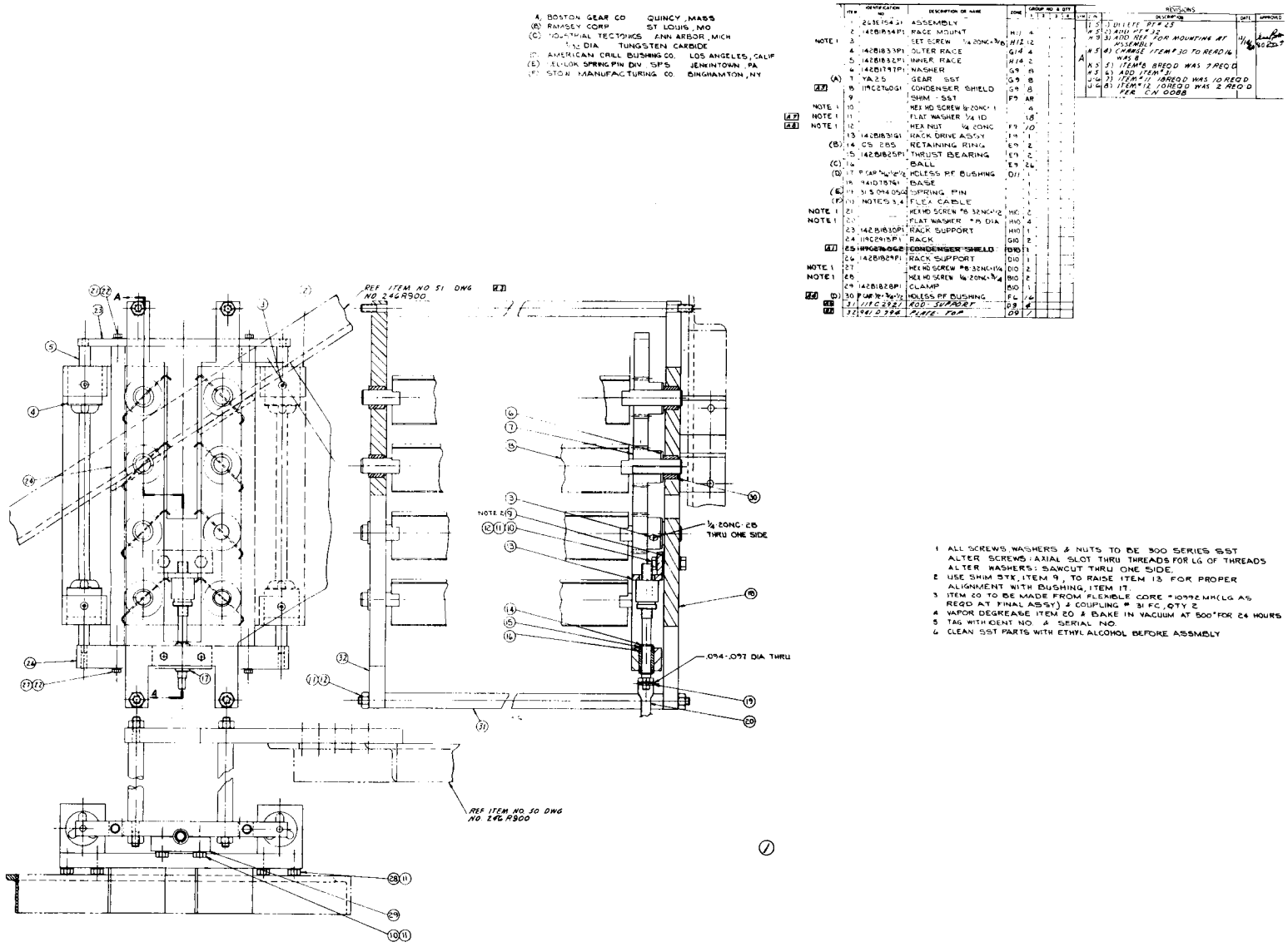

Figure 177. Condenser Shield Drive Assembly.

APPENDIX C

NOMENCLATURE

Latin Letter Symbols

A	Area	ft^2
C	Constant pressure heat capacity	$Btu/(lb_m-°F)$
D	Tube diameter	inches
E	Electric potential	volts
f	Fanning friction factor	dimensionless
G	Mass velocity	$lb_m/(ft^2-sec)$
g	Acceleration due to gravity	$ft/(sec^2)$
g_c	Conversion factor	$32.2\ (ft-lb_m)/(sec^2-lb_f)$
H	Enthalpy	Btu/lb_m
h	Heat transfer coefficient	$Btu/(hr-ft^2-°F)$
h_{fg}	Latent heat of vaporization	$Btu/(lb_m)$
K	Slip ratio; ratio of average vapor velocity to average liquid velocity	dimensionless
k	Thermal conductivity	$Btu/(hr-ft-°F)$
L	Boiler tube length	inches
P	Static pressure	psia
P/D	Insert twist ratio, tube diameters per 360° revolution of helix	dimensionless
Q	Rate of heat transfer	Btu/sec
q''	Heat flux	$Btu/(hr-ft^2)$
R	Thermal resistance	$(hr-ft^2-°F)/Btu$
T	Temperature	°F
t	Time	seconds
U	Overall heat transfer coefficients	$Btu/(hr-ft^2-°F)$
V	Velocity, volume	ft/sec
W	Mass flow rate	lb_m/sec
w	Angular velocity	radians/sec
x	Flowing quality	dimensionless
z	Distance along boiler tube from potassium inlet	inches

Greek Letter Symbols

Δ	Difference	dimensionless
μ	Viscosity	$lb_m/(ft\text{-}hr)$
ρ	Density	lb_m/ft^3
Φ	Two-phase frictional pressure loss multiplier integrated with respect to quality from 0 to x	dimensionless
ϕ	Local two-phase frictional pressure loss multiplier	dimensionless

Subscripts

a	Axial or axial component
B	Boiling
c	Refers to point of critical heat flux
f	Refers to the liquid phase
G	Refers to pressure gages
g	Refers to the vapor phase
i	Inside, inlet
K	Potassium
L	Losses
Na	Sodium
NB	Nucleate boiling
O	Overall
o	Outlet, outside
p	Primary fluid
R	Radial
s	Shell, static
sat	Refers to the saturation curve
si	Refers to the inside of the boiler shell
sc	Refers to the subcooled heating region
SH	Refers to the vapor superheating region
t	Tube, throat
TB	Refers to the transition boiling region

Subscripts (continued)

TP	Two-phase
TPF	Two-phase friction
v	Refers to vapor phase
w	Wall

Dimensionless Groups

N_{Nu}	Nusselt number,	$\frac{hD}{k}$
N_{Pe}	Peclet number,	$\frac{DGC}{k}$
N_{Pr}	Prandtl number,	$\frac{C\mu}{k}$
N_{Re}	Reynolds number,	$\frac{DG}{\mu}$

APPENDIX D

BOILER PLUG DESIGN

A series of air flow tests were completed to determine the flow characteristics of a flow swirling device or insert proposed for the Cb-1Zr Corrosion Test Loop boiler to promote heat transfer in the low-quality (0-15%) entrance region. The flow swirler or insert consists of a 0.060-inch-diameter wire helically wound around a 0.125-inch-diameter center rod which is 12 inches long. The flow tests were made primarily to determine the effect of pitch on the pressure drop. The pitch is defined as the linear axial travel of the insert per revolution.

The 1 2-inch, 1-inch and 2-inch pitch inserts tested are shown in Figure 178; tests were also made for the tube without an insert for comparison with published friction factor data. A summary of the test conditions for the preprototype boiler and the pressure drop test is given in Table XXX. Typical test data for the air flow tests are presented in Table XXXI. The test results are summarized in Table XXXII for a tube Reynolds number of 40,000. The pressure drop for the 1/2-inch pitch was considered excessive, and the 1-inch pitch insert was selected for the preprototype boiler.

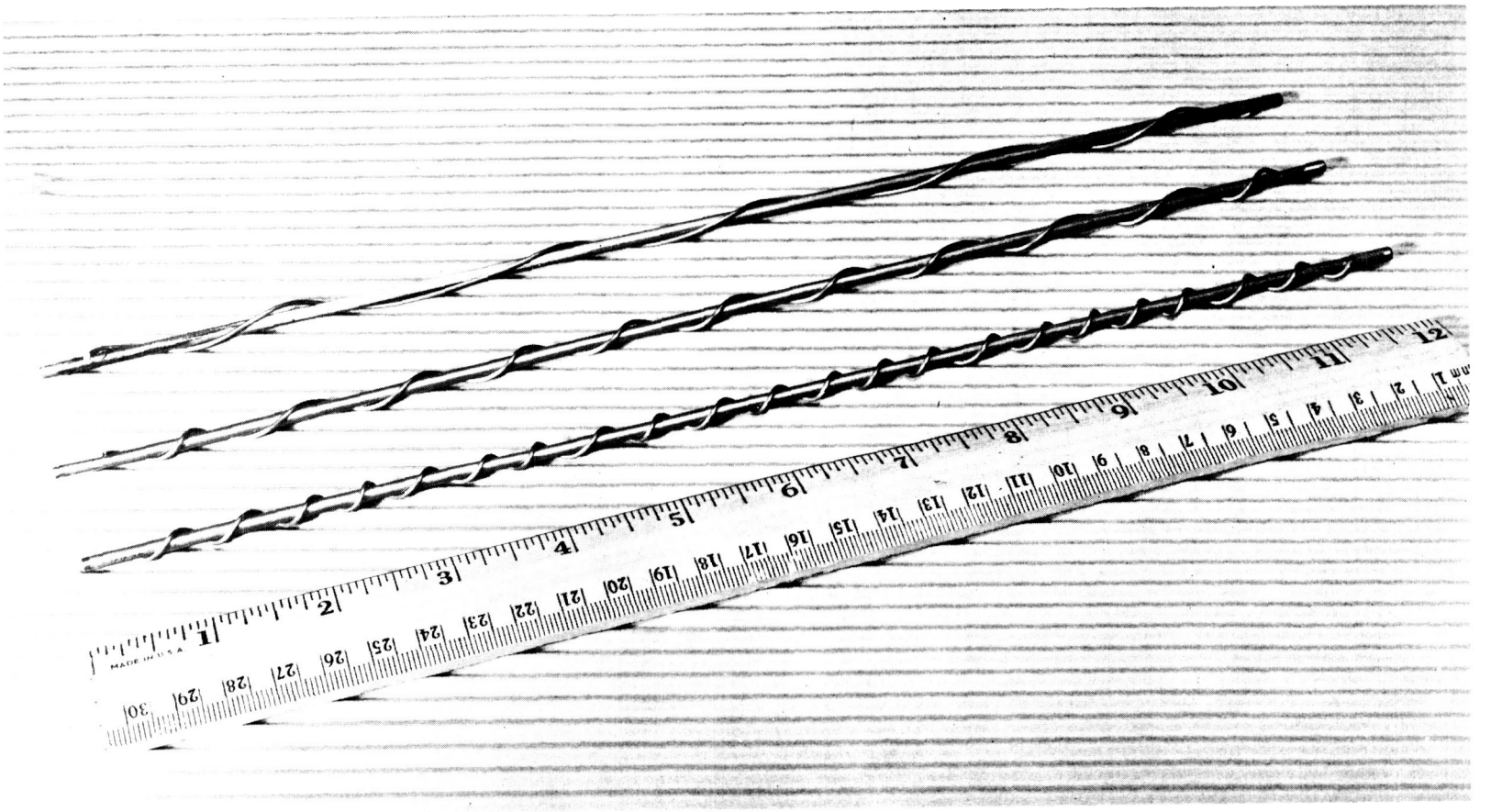

Figure 178. Boiler Tube Inserts Used in Pressure Drop Tests. (C64022107)

TABLE XXX

SUMMARY OF Cb-1ZR CORROSION TEST LOOP DESIGN CONDITIONS AND PRESSURE DROP TEST OF A BOILER INSERT

	Cb-1Zr Corrosion Test Loop	Pressure Drop Test
Gas	Potassium Vapor	Air
Temperature	1900°F	R.T.
Pressure at Exit	110 psia	14.7 psia
Viscosity	0.0535 lb/hr ft	0.045 lb/hr ft
Density	0.2 lb/ft^3	0.076 lb/ft^3
Tube ID	0.25 inch	0.25 inch
Maximum Flow Rate	40 lb/hr	33.5 lb/hr
Reynolds Number	46,700	46,700

TABLE XXXI

TEST RESULTS OF 1/2", 1", AND 2" PITCH INSERT IN A 0.25" ID TUBE

Run No.	Flow Rate lb/Sec	Inlet Temp., °F	No Insert psi	2" Pitch psi	1" Pitch psi	1/2" Pitch psi
1	0.00104	69	0.034	0.265	0.435	1.33
2	0.00269	69	0.114	0.810	1.34	3.83
3	0.00311	69	0.226	1.60	2.55	7.15
4	0.00414	69	0.372	2.47	4.17	16.69
5	0.00706	69	0.916	6.22	9.57	23.3

TABLE XXXII

FRICTIONAL PRESSURE DROP CHARACTERISTICS OF THE Cb-1Zr CORROSION TEST LOOP BOILER INSERT IN AIR AT Re = 40,000

	Friction Factor	Friction Factor Multiplier
Bare Tube - No Insert	0.0067	1
2-Inch Pitch Insert	0.048	7
1-Inch Pitch Insert	0.075	11
1 2-Inch Pitch Insert	0.255	38

APPENDIX E

REFLUXING POTASSIUM TESTS TO EVALUATE Mo-TZM INSERTS IN Cb-1Zr CAPSULES

Prior to initiation of testing of the Cb-1Zr Corrosion Loop described in this report, two potassium reflux capsule tests were conducted in a getter-ion pumped vacuum chamber to evaluate possible mass transfer reactions between the alloy selected for evaluation in the turbine simular of the loop, Mo-TZM, and the loop containment material, Cb-1Zr. These tests were deemed advisable prior to the loop test itself as a result of conflicting data which had been obtained in earlier testing[61] which indicated that under certain conditions Mo-TZM was severely attacked by potassium in two-phase systems. Test durations of 2500 and 5000 hours were selected for the capsule tests. The capsules were made from 1-inch-OD x 0.080-inch-thick wall Cb-1Zr alloy seamless tubing and were approximately 10 inches long. The capsule design is illustrated in Figure 179. The ID of the capsules was gun drilled and honed to a 32 rms finish. Five, 1-inch-long Mo-TZM alloy inserts having a 0.080-inch-thick wall are located in the condensing zone of the capsules. The inserts were accurately machined to fit the ID of the capsule and also have a 32 rms finish. Thermocouple wells were located in the top and bottom of the capsules such that temperature measurements could be made in the center of both the boiling zone and the condensing zone. Prior to testing, the Mo-TZM alloy inserts were accurately weighed and measured.

The test facility was designed in a manner to permit an accurate measure of the condensing rate of the potassium vapor on the surface of the Mo-TZM specimens located in the condensing region of the capsule. Information regarding the condensing rate is needed in experiments of this type since the total amount of dissolution of alloy on which the very pure potassium is condensing should increase with increasing

(61) Private communication from J. H. DeVan, Oak Ridge National Laboratory.

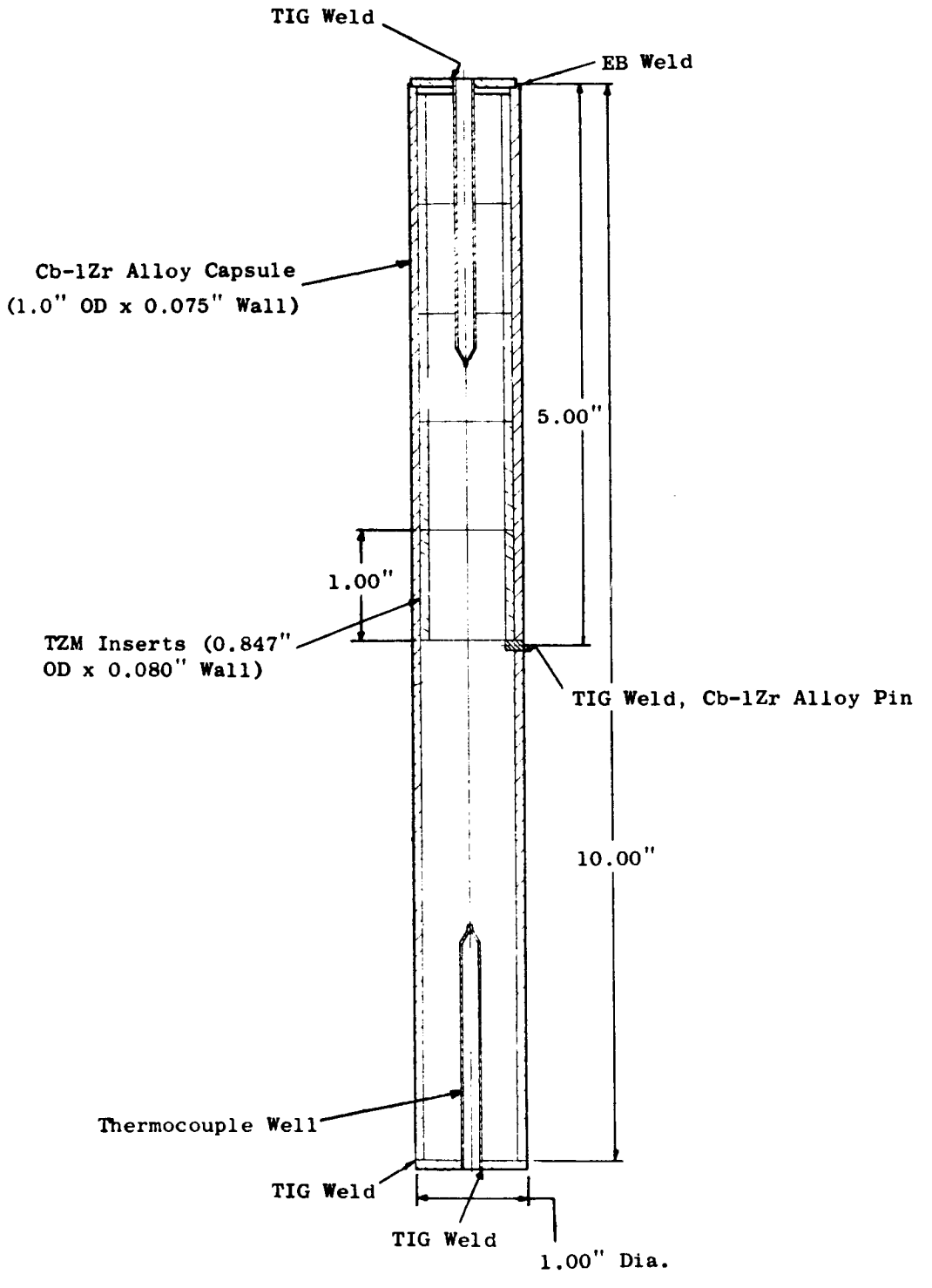

Figure 179. Cb-1Zr Refluxing Potassium Corrosion Capsule Containing TZM Alloy Inserts in Condensing Region.

condensing rate.

The test components of one of the capsules, which were located in an 18-inch-diameter getter-ion pumped vacuum chamber, are illustrated schematically in Figure 180. The condensing rate will be determined by two means. The heat rejected to the Dowtherm "A" filled, water-cooled heat sink will be measured and the condensing rate determined by dividing this value by the heat of condensation for potassium at the condensing temperature. Temperature of the water entering and leaving the Dowtherm jacket will be measured with thermistors inserted in the inlet and exit water lines. The temperature of the potassium will be measured by thermocouples located in the thermocouple wells. The rate will also be determined by means of a radiation calculation. The radiating surface temperature will be measured by using an optical brightness pyrometer and a W-3Re/W-25Re thermocouple. The exterior of the condensing zone of each of the Cb-1Zr capsules was machined to generate a fine thread (184 threads/inch) on the surface to increase the effective emittance of this region and thereby increase the condensing rate. This technique was used in preference to a previously used procedure of grit blasting the surface with Al_2O_3. It was found in earlier studies that residual Al_2O_3 particles embedded in the surface of the Cb-1Zr resulted in high oxygen concentrations in these regions which made it impossible to determine the extent of oxygen contamination which might occur during the refluxing test.

The potassium transfer and capsule sealing were accomplished in an electron beam welding chamber. This unit incorporated facilities for transferring potassium directly from the hot trap to the capsules in a vacuum environment of 5×10^{-5} torr. The potassium was transferred to the capsule by pressurizing the hot trap, filling the calibrated stainless steel ladle with the proper amount of potassium and then pouring the potassium through the stainless steel funnel into the capsule using a vacuum rotary feedthrough. After the capsule lid was manually placed on the capsule with the manipulator, the capsule

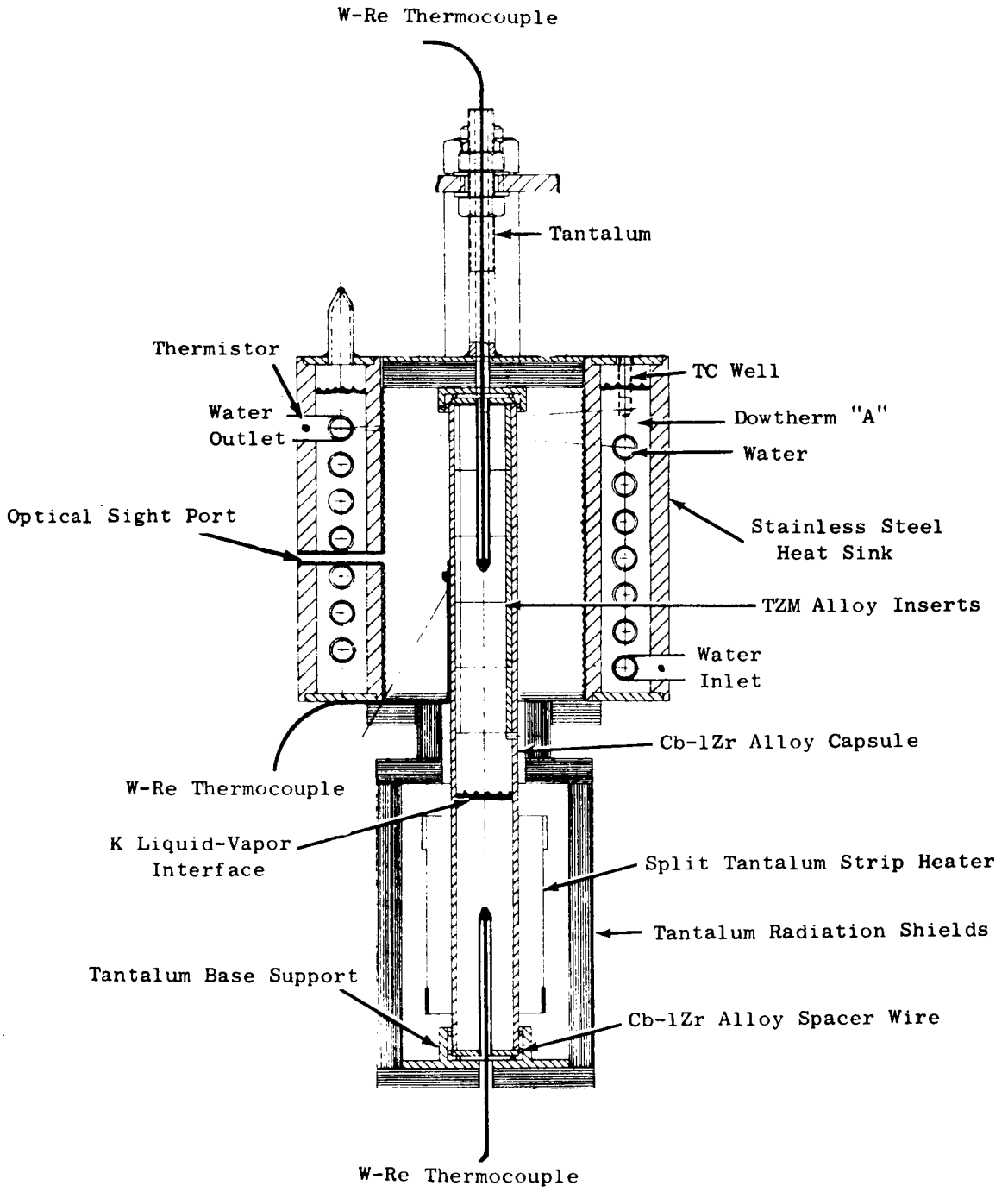

Figure 180. Components of the Refluxing Potassium Capsule Test Systems, Cb-1Zr Capsules With Mo-TZM Alloy Inserts.

was positioned under the electron beam welding gun at the opposite end of the chamber by means of the motor driven capsule carriage. The lid was then seal welded to the top of the capsule as the capsule was rotated about its own axis. The potassium used to fill these capsules was obtained from Mine Safety and Appliance Research Corporation as their high-purity grade. The potassium was vacuum distilled and then hot trapped at 1300°F for 25 hours. An analysis of this potassium at the time of capsule filling showed 8.7 and 11.7 ppm oxygen, and the concentrations of metallic elements were all less than 5 ppm.

The refluxing tests were conducted in the vacuum chamber shown in Figure 181. This system consists of an 18-inch-diameter x 30-inch-high bakeable chamber connected to a 400-liter/second getter-ion pump. The chamber is capable of reaching the 10^{-10} torr range when empty at room temperature. Three cryogenic molecular sieve roughing pumps are used to pump the system down initially. Figure 182 shows the two test capsule furnaces, heat exchangers, and associated equipment installed in the vacuum chamber prior to starting the test. The thermistor read-out and control shown is used to monitor the inlet and outlet temperature of the water which extracts heat from the Dowtherm "A"[(a)] which fills the heat exchangers. Dowtherm "A" was chosen as the fluid to fill the heat exchanger cavity because of its low vapor pressure in the temperature range of interest, 200° to 300°F. One of the heat exchangers which surrounds the condenser region of the refluxing capsule is shown in Figure 183 prior to installation in the test facility. The internal surface of the heat exchanger was threaded to increase its absorptivity. Following welding of the water lines to the vacuum feedthrough tubes, thermistors were positioned inside the water lines at the inlet and outlet positions of each heat exchanger in order to permit accurate measurement of the temperature rise of the water. The total heat radiated was determined by measuring only the flow rate of the cooling

(a) Dow Chemical Company, Midland, Michigan

Figure 181. High Vacuum Test Chamber (10^{-10} Torr Range) in Which Cb-1Zr/Mo-TZM Refluxing Potassium Chamber Tests Were Performed. (C64051216)

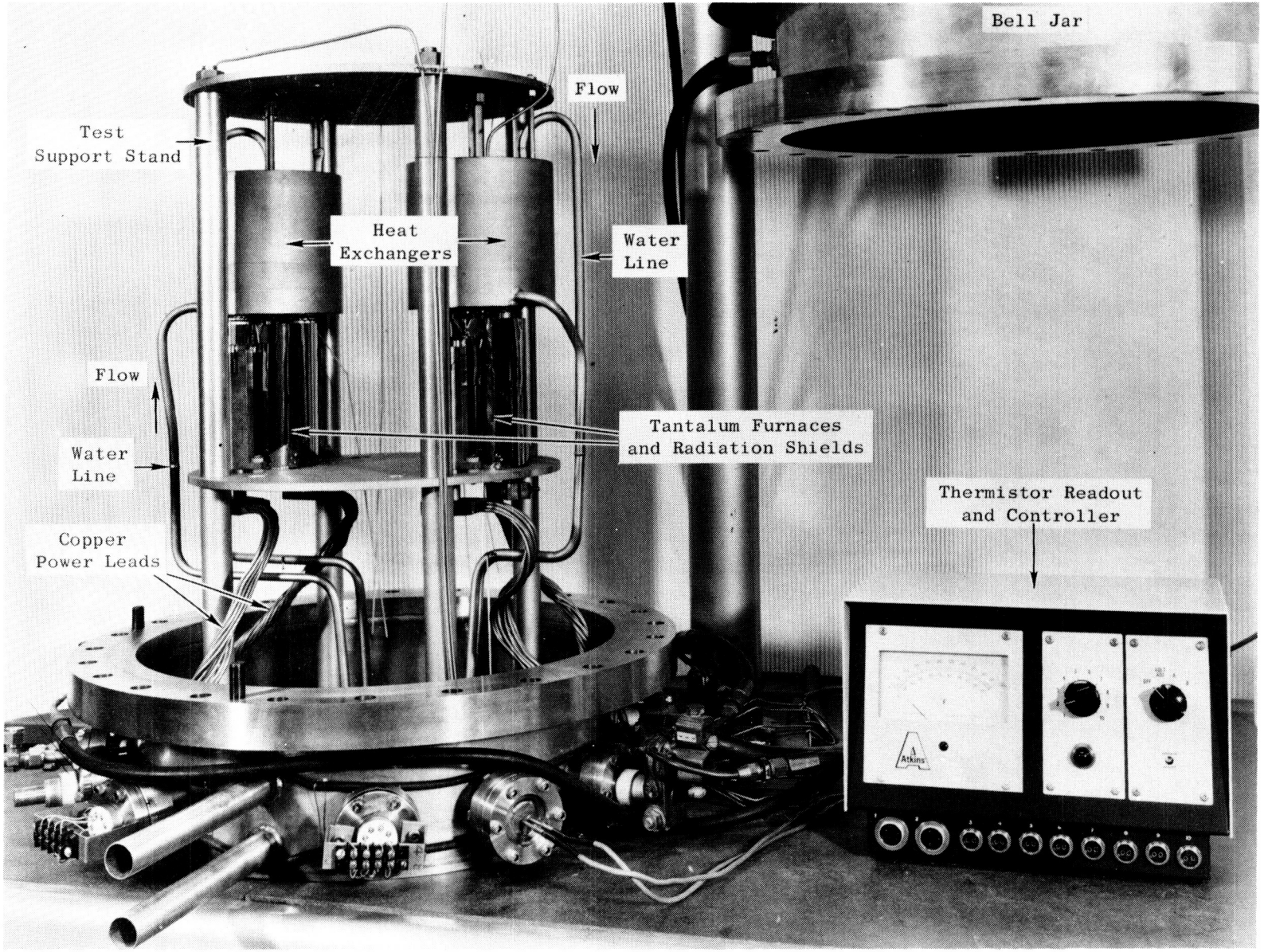

Figure 182. Reflux Corrosion Capsule Test Facility with Bell Jar Removed. (C64110419)

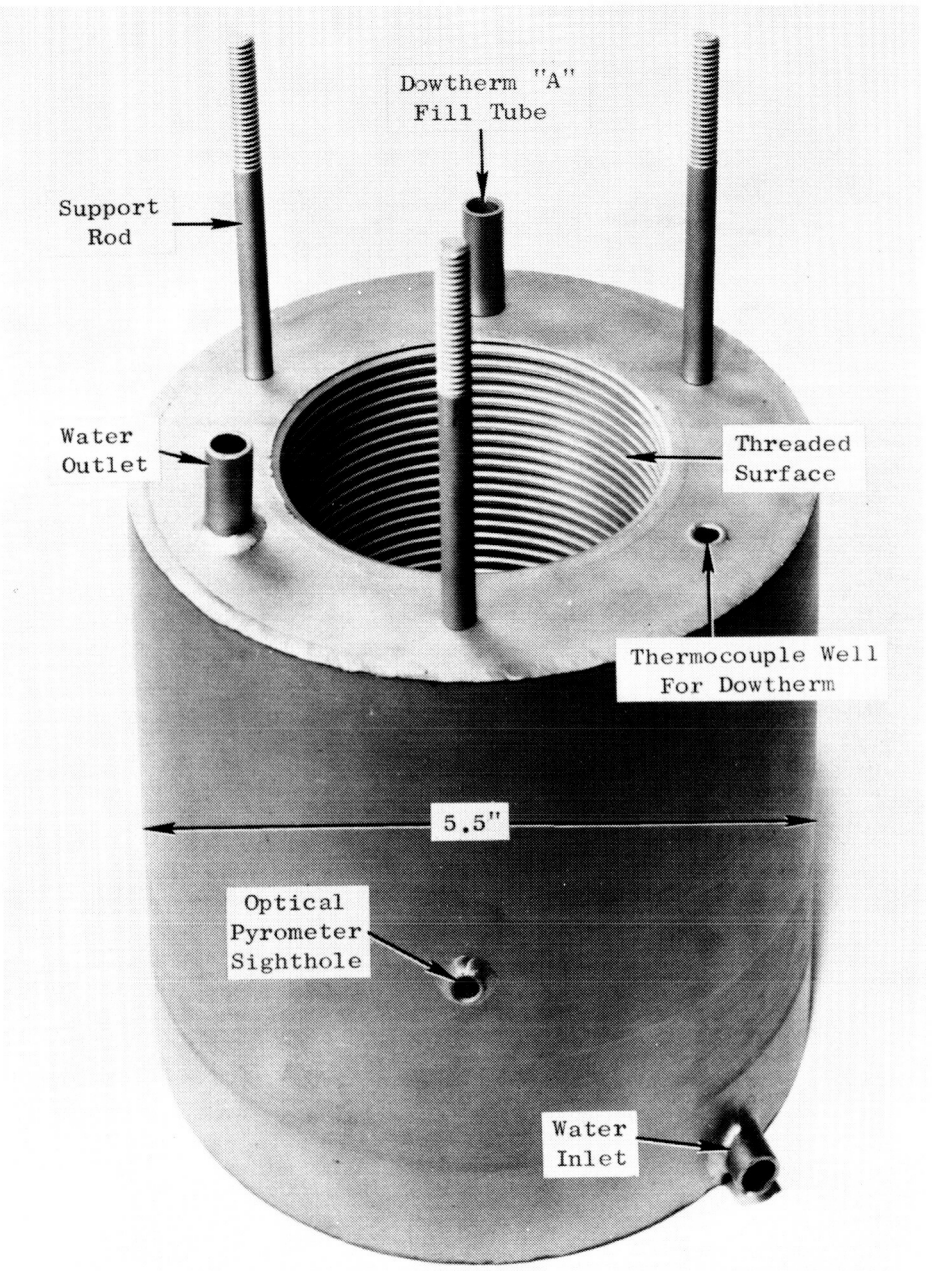

Figure 183. Water-Cooled, Dowtherm-Filled Heat Exchanger for the Cb-1Zr-Mo-TZM Refluxing Potassium Test Facility. (C64101924)

water and the inlet and outlet water temperatures at the heat exchanger. Water flow-measurements were determined by weighing volumes collected in a ten-minute period. Because of the relatively low temperatures of the water, its temperature rise may be accurately measured with the thermistors positioned at the inlet and outlet locations in the water lines of the heat exchanger.

After placing the capsules in the test facility and instrumenting them with W-3Re/W-25Re thermocouples, the ultrahigh vacuum chamber was sealed and evacuated to a pressure of 50 microns of Hg using a molecular sieve trapped mechanical pump. Using cryogenic sorption pumps, the pressure was reduced to 1.5 microns of Hg at which time the getter-ion pump was started. The pressure prior to bakeout was 2.0×10^{-8} torr. After a 14-hour bakeout at 400°F, the pressure decreased to 2.2×10^{-9} torr. The pressure in the test chamber during test startup and the 5000-hour test period is indicated in Table XXXIII.

Power was applied to both heaters and the test temperature of 2000°F was reached in 45 hours while the pressure was maintained at less than 1×10^{-6} torr. Unstable boiling was encountered in the temperature range 1300° to 1700°F in both capsules. The liquid potassium temperature was recorded as high as 148°F above the vapor temperature during this unstable condition, and as low as 18°F above the vapor temperature during moments of violent boiling. At capsule temperatures above 1800°F, the capsules operated in a very stable manner with a temperature differential of less than six degrees between the vapor well and liquid well thermocouple readings.

The condensing rate during the first 3300 hours of the test varied from a minimum of 28 lbs/ft^2 hr to a maximum of 30.9 lbs/ft^2 hr. Calculations of the emittance of the threaded Cb-1Zr alloy condenser wall based on the measured heat rejection and system temperatures yielded a value of 0.23. This value was considerably less than was anticipated for this type of surface.

Following completion of the tests, the capsules were removed from the test chamber, and a preliminary evaluation was performed on the test components. The capsules were opened in the vacuum/purge welding

TABLE XXXIII. TEST CHAMBER PRESSURE DURING 2500-HR AND 5000-HR, 2000°F REFLUXING POTASSIUM CAPSULE TESTS

Test Period	Pressure, Torr
Initial pumpdown	2.0×10^{-8}
Chamber at 60°F after 14 hr of bakeout at 400°F	2.2×10^{-9}
Capsules heated to 2000°F over a 45 hr period	1×10^{-6} (max.)
0-20 hr	9×10^{-7} to 2×10^{-7}
20-100 hr	2×10^{-7} to 1×10^{-7}
100-500 hr	1×10^{-7} to 2×10^{-8}
500-2500 hr	2×10^{-8} to 6×10^{-9}
2500 hr	2500-hour capsule removed from test chamber
Chamber at 60°F after 14 hr of bakeout at 400°F	2.3×10^{-9}
5000-hr capsule heated to 2000°F over a 2-1/2 hr period	2.0×10^{-7} (max.)
2500-2540 hr	2×10^{-7} to 7.8×10^{-9}
2540-5000 hr	7.8×10^{-9} to 5×10^{-9}
Chamber at 60°F following completion of test	9×10^{-10}

chamber, and the boiler and condenser portions of the capsule were placed in a vacuum distillation unit which has been described in an earlier report.[62] The distillation unit was evacuated to 1×10^{-5} torr and heated to 875°F. Pumping was continued on the system for 4 hours at which time the evacuation line was valved shut. Distillation continued for 38 hours. The distillation unit was then allowed to cool to room temperature and subsequently was opened in the vacuum/purge welding chamber. All the potassium from the two ends of the capsule (21.8 gm total) had collected on the air-cooled condenser, and none was detected on the top portion of the capsule which contained the Mo-TZM alloy inserts or in the boiler region where most of the potassium was located prior to distillation. Following distillation, the five Mo-TZM alloy tubular inserts were removed from the condenser region of each of the capsules.

The appearance of the various components of the 2500-hour capsule test is illustrated in Figure 184. As may be noted in this photograph, the areas of the Cb-1Zr alloy which were in contact with liquid during the test were dark in appearance while the areas in contact with vapor retained a bright appearance. The reverse was true for the Mo-TZM alloy specimens. The insert specimens were darkened in the areas in contact with liquid (annulus between capsule and specimens) and bright in appearance on the ID surfaces which were in contact with condensing vapor.

Weight change data obtained on the five Mo-TZM alloy insert specimens located in the condenser region and the Cb-1Zr alloy sheet specimen from the boiler (liquid) region are given in Table XXXIV. As may be noted in this table, the Mo-TZM alloy specimens experienced only minor weight changes during the 2500-hour test. Mo-TZM specimen #1 showed a very slight weight gain and all or a portion of this gain is attributed to pickup of very small particles of Cb-1Zr from the test

(62) Potassium Corrosion Test Loop Development, Quarterly Progress Report No. 5 for Period Ending October 15, 1964, NASA Contract NAS 3-2547, NASA-CR-54269, p. 17.

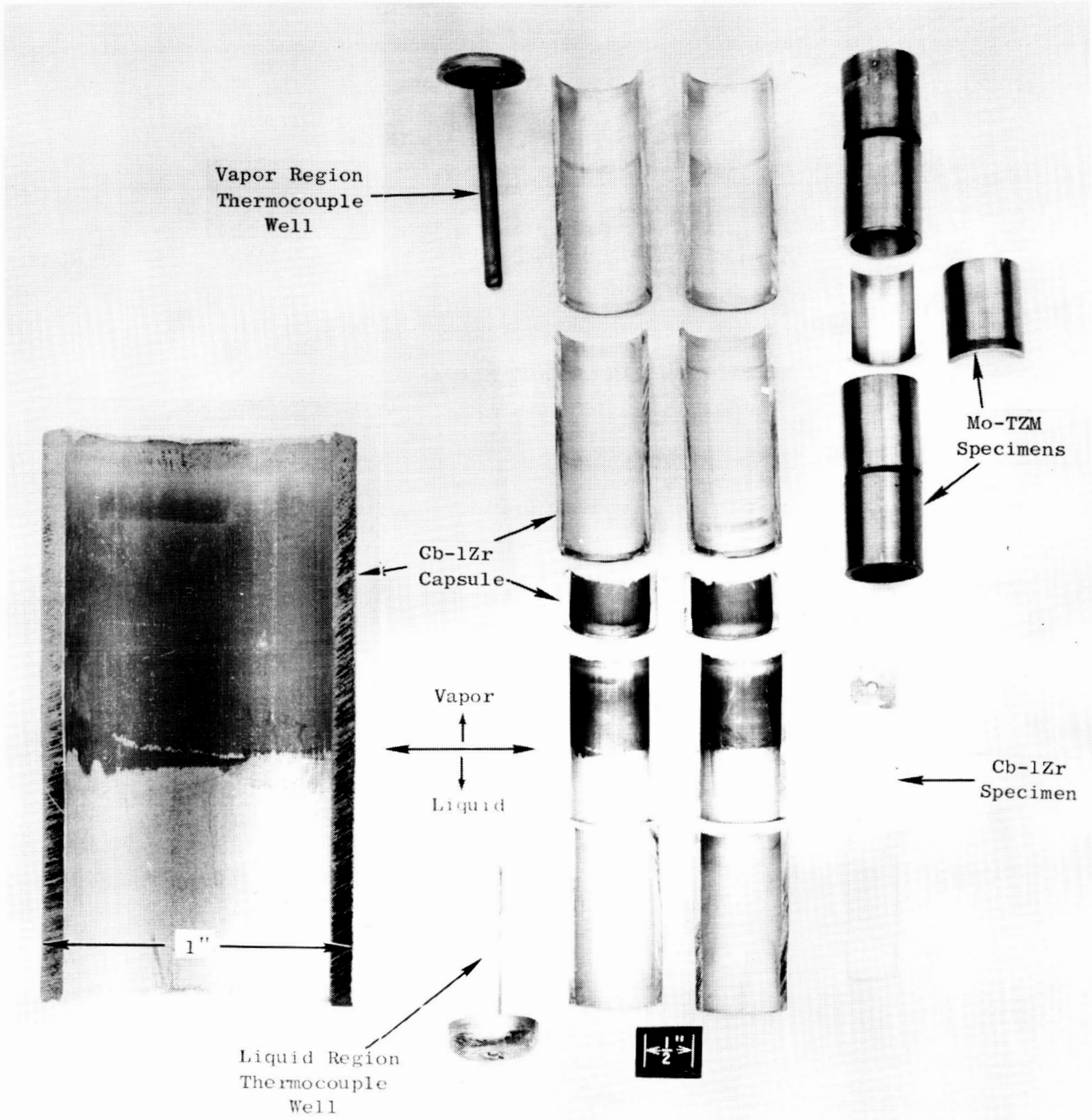

Figure 184. Potassium Reflux Capsule Components Following 2,500-Hour Test at 2000°F. Enlarged View of Cb-1Zr Capsule Wall at Liquid-Vapor Interface Shown on the Left.

TABLE XXXIV. WEIGHT CHANGE DATA OBTAINED ON SPECIMENS FOLLOWING Cb-1Zr/Mo-TZM REFLUXING POTASSIUM CAPSULE TEST

Test Conditions:

Test Duration: 2,500 Hours

Capsule Temperature: 2000°F

Condensing Rate: 30.4 lbs/ft^2/hr (0.248 gm/cm^2/min)

Specimen	Weight, gm		Weight Change	
	Before	After	mg	mg/cm^2[1]
Mo-TZM[2] #1 (Top of Condenser)	27.2833	27.2843	+1.0	+0.07
Mo-TZM #2	31.5581	31.5575	-0.6	-0.04
Mo-TZM #3	31.6653	31.6650	-0.3	-0.02
Mo-TZM #4	31.6128	31.6134	+0.6	+0.04
Mo-TZM #5 (Bottom of Condenser)	31.6507	31.6552	+4.5	+0.32
Cb-1Zr[2] (Boiler Region)	19.0209	19.0221	+1.2	+0.04

[1] Loss of 25.7 mg/cm^2 for Mo-TZM alloy is equivalent to 1 mil of uniform surface removal.

[2] Nominal dimension of Mo-TZM insert specimens (inches):

	Length	OD	Wall Thickness
Specimen #1	0.87	0.85	0.078
Specimens #2, #3, #4, #5	1.0	0.85	0.078

[3] Nominal dimensions of Cb-1Zr sheet specimen:

0.5-inch wide x 3-1/2 inches long x 0.0792-inch thick.

capsule in several areas where detectable bonding occurred between the insert and the capsule.

Weight change data on the five Mo-TZM alloy insert specimens from the 5000-hour capsule test and the results of chemical analysis on the inner 10 mils of the insert specimens from this capsule are given in Table XXXV. The largest weight loss observed was approximately thirty times that of the largest weight loss observed in the 2500-hour test but was still small enough to be considered insignificant, being equivalent to 0.00005 inch of uniform surface removal. The results of chemical analyses indicate no significant change in the oxygen, nitrogen, or hydrogen concentrations of the specimens. A slight decrease in the carbon concentration was noted and will be discussed later in this section.

The appearance of the various capsule components is illustrated in Figure 185 (a) and is quite similar to the appearance of the components from the 2500-hour test. The areas of the Cb-1Zr capsule in contact with liquid potassium (boiler region and the region containing the Mo-TZM alloy inserts) were bright, while the vapor region above the liquid-vapor interface had a darkened appearance. As may be noted in Figure 185 (a), the portions of the Cb-1Zr sheet specimen which extended above the liquid-vapor interface were also darkened during the test. Spectrographic analysis was performed on scrapings taken from the dark regions and the bright regions of the Cb-1Zr sheet specimens to determine if the discoloration might be due to transfer of Mo or Ti from the Mo-TZM alloy specimens located in the condenser region. No differences were detected. In addition, no variation in the zirconium concentration in the two regions could be detected.

The results of chemical analysis performed on various samples of the Cb-1Zr capsule and the sheet specimen are given in Table XXXVI. No significant changes in the nitrogen, hydrogen, and carbon concentrations were observed. The results indicate a buildup of the oxygen level in the boiler (liquid) region and the darkened regions of the capsule and in the sheet specimen above the liquid-vapor interface. The results

TABLE XXXV. WEIGHT CHANGE AND CHEMISTRY DATA OBTAINED ON Mo-TZM ALLOY INSERT SPECIMENS FROM THE CONDENSER REGION OF A Cb-1Zr CAPSULE FOLLOWING EXPOSURE TO POTASSIUM FOR 5000 HOURS AT 2000°F[1]

Specimen	Weight, gm		Weight Change		Chemical Analysis, ppm[3]			
	Before	After	mg	mg/cm²[2]	O	N	H	C
Mo-TZM[4] #6 (Top of Condenser)	26.6525	26.6358	-16.7	-1.2				
Mo-TZM #7	31.6158	31.5974	-18.4	-1.3	22	4	2	120
Mo-TZM #8	31.6250	31.6250	0	0				
Mo-TZM #9	31.5949	31.6155	+20.6	+1.4	61	7	5	100
Mo-TZM #10 (Bottom of Condenser)	31.6504	31.6519	+1.5	+0.1				
Mo-TZM Before Test Specimen (MCN 103)	--	--	--	--	39	7	5	190

[1] Average potassium condensing rate: 29.0 lbs/ft²/hr (0.24 gm/cm²/min).

[2] Loss of 25.7 mg/cm² for Mo-TZM alloy is equivalent to 1 mil of uniform surface removal.

[3] Analyses performed on inner 0.010-inch of wall of tubular inserts. Values given are the average of duplicate analyses.

[4] Nominal dimensions of Mo-TZM alloy insert specimens (inches):

	Length	OD	Wall Thickness
Specimen #6	0.85	0.85	0.078
Specimen #7, #8, #9 and #10	1.0	0.85	0.078

TABLE XXXVI. RESULTS OF CHEMICAL ANALYSIS OF Cb-1Zr CAPSULE FOLLOWING COMPLETION OF 5000-HOUR, 2000°F REFLUXING POTASSIUM TEST[1,2]

	Chemical Analysis, ppm[3]			
	O	N	H	C
Capsule Wall[4,5]				
Condenser Region Wall	268	93	5	100
Inner 0.010-Inch of Condenser Wall	240	104	6	90
Vapor Region 1-Inch Above Liquid-Vapor Interface, Inner 0.010-Inch of Wall	291	106	8	50
Boiler Region Wall	272	96	7	60
Inner 0.010-Inch of Boiler Wall	427	114	9	80
Before Test	184	95	1	40
Sheet Specimen from Boiler Region[6]				
Dark Region Above Liquid-Vapor Interface	533	24	5	70
Bright Region Below Liquid-Vapor Interface	472	25	7	90
Following Removal of 0.010-Inch From Each Surface	289	36	5	-
Before Test	210	33	2	40

[1] Mo-TZM alloy tubular inserts located in the condenser region.

[2] Average potassium condensing rate: 29.0 lbs/ft^2/hr (0.24 gm/cm^2/min).

[3] Values given are the average of duplicate analyses.

[4] Nominal dimensions of Cb-1Zr capsule: 1-inch OD x 0.075-inch wall x 10 inches long.

[5] Analyses are for total wall unless otherwise specified.

[6] Nominal dimensions of Cb-1Zr sheet specimen: 0.5-inch wide x 0.079-inch thick x 3.5-inch long. Specimen weighed 18.9019 gm before test and gained 6.9 mg (0.26 mg/cm^2).

obtained on the inner 10 mils of the boiler wall and the total cross section and core (inner 60 mils) of the sheet specimen indicate that the bulk of oxygen pickup via the potassium is concentrated near the surface of the Cb-1Zr components. The apparent oxygen migration from the condenser region to the boiler region is consistent with results obtained in refluxing potassium Cb-1Zr capsule tests at General Electric[63] and Oak Ridge National Laboratory.[64]

Calculations of the oxygen increase in the Cb-1Zr specimen in the boiler region plus the increase noted in the inner 10 mils of the boiler region wall indicate an oxygen addition of approximately 25 mg during the 5000-hour test. Based on the low oxygen content of the potassium (0.18 mg) and the insignificant change noted in the Mo-TZM alloy specimens, it is tentatively concluded that the principal source of oxygen was from the Cb-1Zr wall in the condenser region, possibly enhanced by the diffusion of oxygen from the external environment through the capsule wall. However, the amount of oxygen contamination from the external environment is very low.

The microstructure of the various capsule components is illustrated in Figure 185. A view of the total cross section of one of the Mo-TZM alloy inserts and enlarged views of the inner and outer surfaces of this insert are shown in Figure 185 (b). No corrosion or surface layers were detected. Varying amounts of recrystallization were detected in the Mo-TZM alloy specimen. The structure of the inner wall of the capsule was approximately 75 percent recrystallized to a depth of 10 mils, and the remainder of the wall was approximately 40 percent recrystallized. The predominance of the recrystallized structure near the surface, the slight carbon reduction noted in the inner 10 mils of the Mo-TZM specimen (Table XXV), and the slight increase in carbon

(63) Engel, Jr., L. B. and Frank, R. G., Evaluation of High-Strength Columbium Alloys for Alkali Metal Containment, NASA-CR-54226, 1964.

(64) Metals and Ceramics Division Annual Progress Report for Period Ending June 30, 1965, Oak Ridge National Laboratory, ORNL-3870, p. 128.

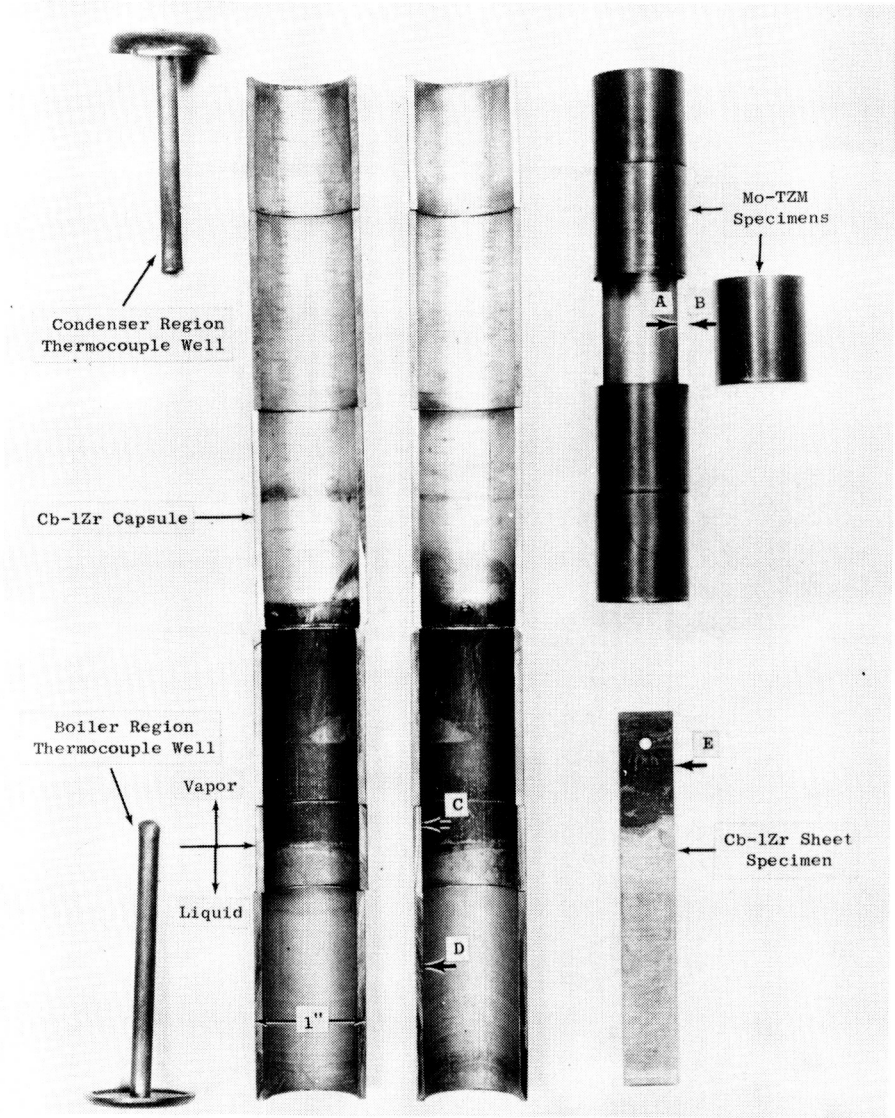

a) Capsule Components (Orig. C65083169)

Figure 185. Potassium Reflux Capsule Components Following 5000-Hour Test at 2000°F.

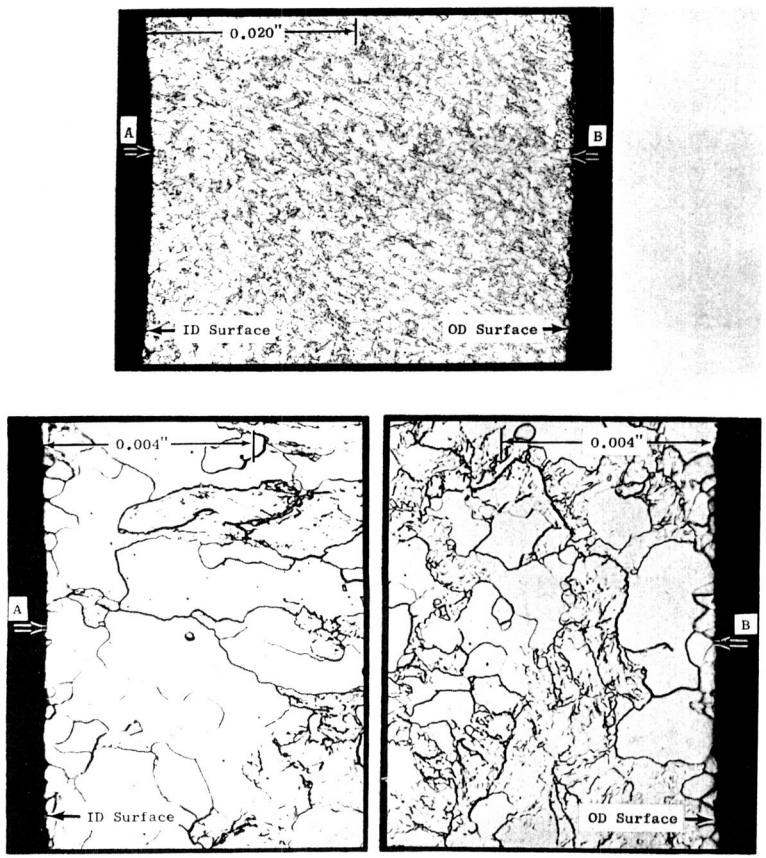

b) Microstructure of Mo-TZM Specimen

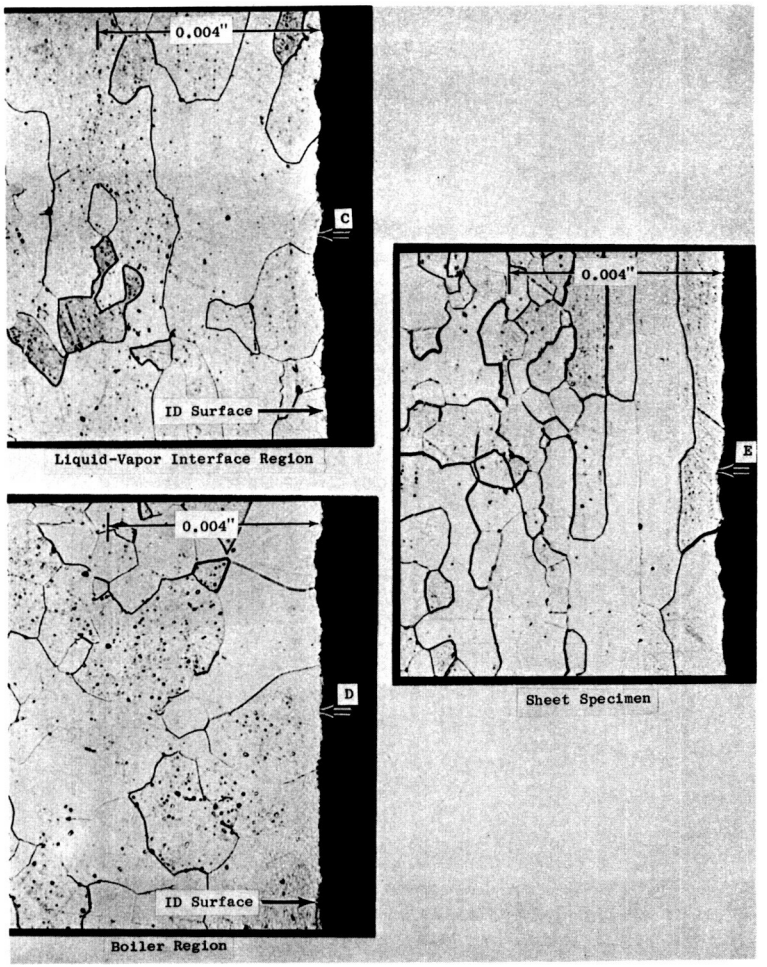

c) Microstructure of Cb-1Zr Test Components

Figure 185. Continued

concentration noted in the Cb-1Zr specimens suggests that decarburization of the Mo-TZM alloy may have contributed to the recrystallization gradient noted.

The metallographic appearance of the surface of the Cb-1Zr capsule in the liquid region and the vapor region above the liquid-vapor interface is shown in Figure 185 (c). No corrosion was observed in either these specimens or the sheet specimen which is also shown. A special effort was made to retain any possible surface layers which might be responsible for the dark appearance of the vapor region of the Cb-1Zr alloy capsule. The specimens from this region were nickel plated prior to metallographic preparation to aid in edge preservation. A discontinuous layer with a maximum thickness of 0.1 mil was detected. This layer, which was very fragile, is thought to contain a high concentration of oxygen and may be a complex compound(s) of oxygen, potassium, columbium, and zirconium of the type suggested by the studies of Litman.[65]

It is concluded from the results of this 5000-hour test and the 2500-hour test which preceded it that Mo-TZM alloy is compatible with condensing potassium under these test conditions, and the results further substantiated the selection of the Mo-TZM alloy as the turbine alloy for evaluation in the Cb-1Zr Rankine System Corrosion Test Loop.

(65) Litman, A. P., "The Effect of Oxygen on the Corrosion of Niobium by Liquid Potassium," ORNL-3751, July 1965.

APPENDIX F

TEST TO EVALUATE A HIGH-EMITTANCE IRON TITANATE COATING FOR THE Cb-1Zr CONDENSER FIN

In order to increase the heat rejection capability of the 0.25-inch-thick x 4-inch-wide x 60-inch-long fin of the Cb-1Zr Corrosion Test Loop, the use of a high-emittance coating of iron titanate (Fe_2TiO_5) on the Cb-1Zr alloy fin was considered. A test program to evaluate this coating and others for Cb-1Zr was in progress at Pratt & Whitney Aircraft under NASA sponsorship. A total hemispherical emittance of 0.85-0.87 had been measured[66] for an iron titanate coating on Cb-1Zr tubing which operated for 1950 hours at 1700°F in a vacuum of 10^{-8} torr. Pratt & Whitney also determined that the 4-mil-thick iron titanate coating would withstand rapid thermal cycling with no detectable deterioration in coating integrity.

The test which will be described below was conducted by General Electric in order to determine the thermal cycling characteristics of the iron titanate coating under test conditions quite similar to those which would exist in the Cb-1Zr Corrosion Test Loop. Test specimens for this study were coated by R. Emanuelson of Pratt & Whitney. One specimen was grit blasted with alumina and the other with silicon carbide prior to the applications of the 3.5-mil layer of iron titanate by plasma-arc spraying using a nonoxidizing gas to form the plasma.

The test equipment consisted of an electrical resistance, radiation-type furnace with a thermal capacity of 1.5 kw. All thermal insulation consisted of multiple layers of tantalum foil separated by a 0.020-inch-diameter wire. The heater element was a single helical coil fabricated from 0.050-inch-diameter tungsten wire. Two Cb-1Zr specimens, 0.25-inch thick x 2-inch wide x 2.5-inch long, were inserted into the furnace opposite the tungsten heating element as shown in Figure 186. Approximately

(66) Semiannual Progress Report, Determination of the Emissivity of Materials, Report Period: May 14-Nov. 15, 1964, R. C. Emanuelson, Pratt & Whitney Aircraft, NASA Contract NAS 3-4174, NASA-CR-54268.

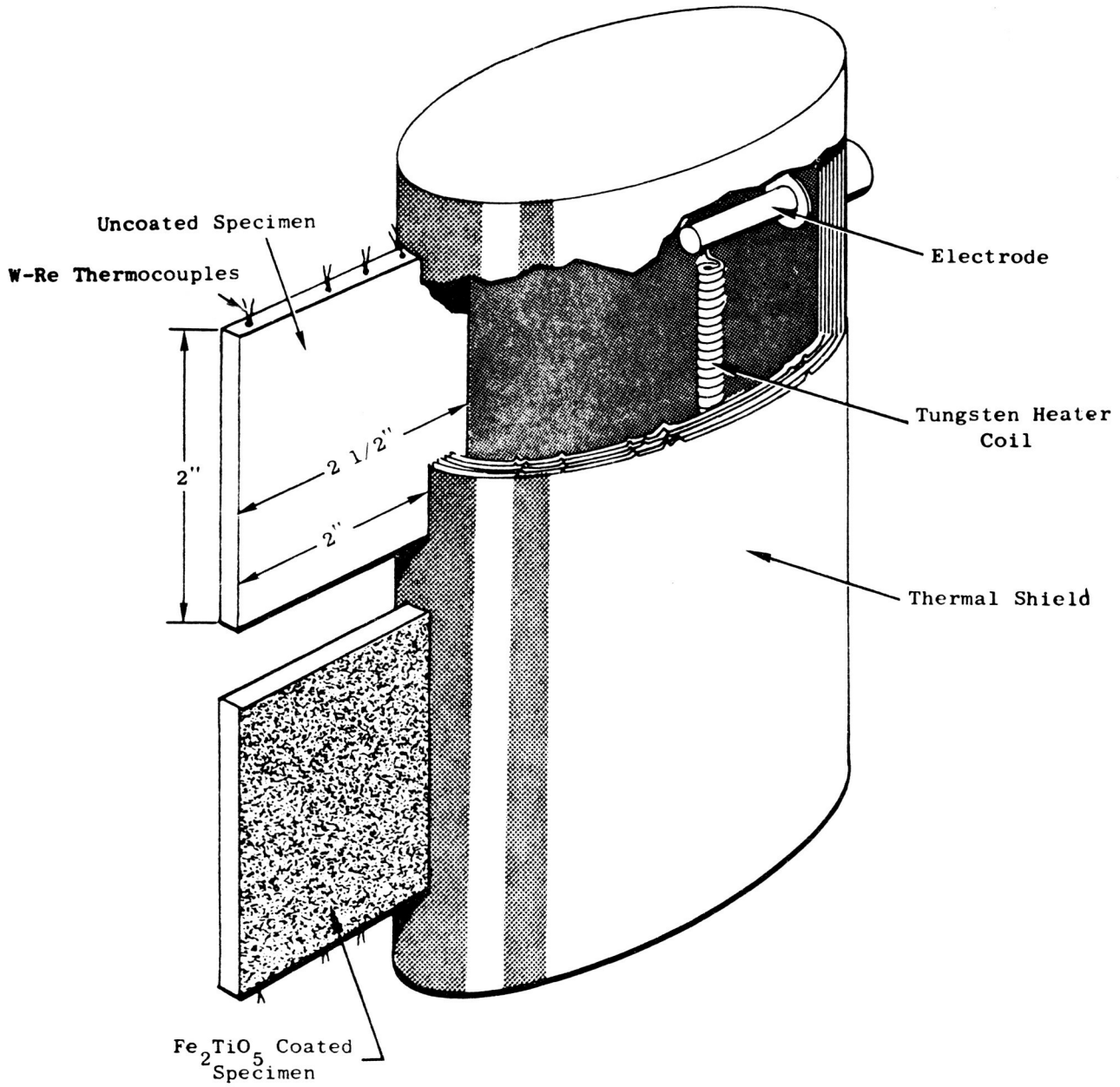

Figure 186. Test Configuration Used in the Evaluation of the High-Emittance, Fe_2TiO_5 Coating on Cb-1Zr Alloy Specimens. Uncoated, Grit-Blasted Specimen Included for the Purpose of Comparison. Specimens Radiated Heat to the Water Cooled Walls of a 10^{-8} Torr Vacuum Chamber.

0.5 inch of the fin was left uncoated, and this portion of the specimen was inserted into the furnace. The remaining 2-inch x 2-inch section of the fin projected out from the furnace and was held in position by small tantalum tabs which were spot welded to the furnace. The entire furnace with specimens was mounted in a 24-inch-diameter ultrahigh vacuum system capable of 1×10^{-9} torr operation. The chamber walls were water cooled to remove radiation heat loads from the specimens and furnace.

The test configuration illustrated in Figure 186 shows an uncoated and a coated specimen. For the first 236 hours of the test, the top specimen was an iron-titanate-coated specimen which was grit blasted with silicon carbide prior to application of the coating. The two coated samples differed only in the precoating surface roughening process. The bottom specimen was prepared by grit blasting with alumina grit, and the top specimen was grit blasted with SiC grit. After 236 hours of testing, this specimen was replaced with the uncoated grit-blasted specimen as shown in Figure 186.

Longitudinal temperature gradients in the specimen were measured by five W-3Re/W-25Re thermocouples attached to the edge of each specimen. These thermocouples were also used to obtain cooling rages during the thermal transient portion of the cycle. Following the initial heating of the specimens to a maximum coated region temperature of 1500°F, the specimens were held at temperature for 77 hours. At this time the daily thermal cycling of the specimens was initiated. A test cycle consisted of the following: turning off the electrical power to the furnace in approximately one minute, allowing the specimens to cool by radiation to the chamber walls to a temperature of 150°F and then reheating the specimens to a temperature of 1500°F (temperature of hottest coated region) over a one-hour period. Seven thermal cycles of this type were completed in a total of 236 hours of test operation. The test was interrupted after 236 hours of test operation and seven thermal cycles to replace the silicon carbide grit-blasted, iron-titanate-coated specimen with an uncoated, grit-blasted specimen.

During the 236 hours of test operation, essentially no differences were detected in the temperature profiles of the two coated specimens as illustrated in Figure 187. No changes occurred with time or following cycling. This would suggest that there were no changes in coating integrity or emittance. Visual examination of the two specimens following opening of the test chamber revealed no evidence of spalling or coating deterioration.

As was mentioned above, an uncoated, alumina grit-blasted specimen was then substituted for the silicon carbide grit-blasted and coated specimen in order to obtain a comparison of the heat rejection properties of these two surface treatments.

The test was continued until a total of 1000 hours of test time had been completed. During the 1000-hour test, the alumina grit-blasted, coated fin specimen was subjected to 25 thermal cycles at approximately 24-hour intervals during the first 750 hours of the test. Following the 25th cycle, the specimen was held at temperature for an additional 250 hours and then subjected to one final cycle. A summary of the thermal history of the coated specimen is given below:

At temperature:	922 hours
Cooling to 150°F:	52 hours
Heating to 1500°F:	26 hours
TOTAL	1000 hours

During the experiment, the pressure in the system (with the specimens at temperature) decreased from 9.0×10^{-9} torr at the start of the test to 9.5×10^{-10} torr at the completion of the test.

The temperature distributions along the coated and the grit-blasted fin specimens are shown in Figure 188. The effectiveness of the coating treatment is quite evident, yielding a fin end temperature of 1070°F compared to a temperature of 1245°F for the grit-blasted, uncoated specimen.

The end temperature of a Cb-1Zr fin specimen having the dimensions of the specimens used in this experiment, as a function of surface emittance was calculated using the relationships developed by S. Leiblein.[67] The

(67) Leiblein, S., Analysis of Temperature Distribution and Radiant Heat Transfer Along a Rectangular Fin of Constant Thickness, NASA Technical Note D-196, November 1959.

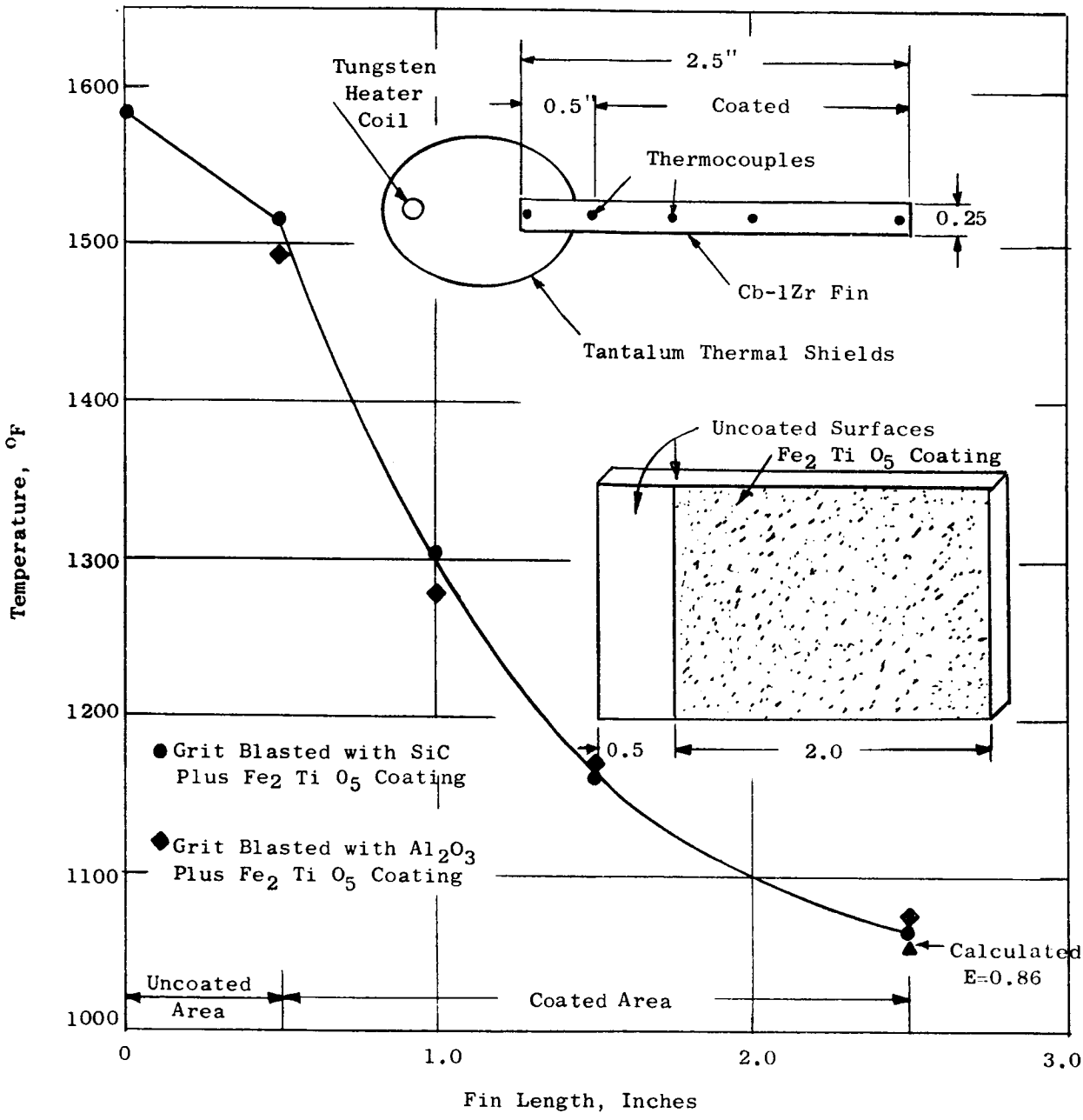

Figure 187. Steady State Temperature Profile of Fe_2 Ti O_5 Coated Cb-1Zr Alloy Specimens During Coating Evaluation Test. One Specimen Grit Blasted with SiC Prior to Coating with Fe_2 Ti O_5 and the other was Grit Blasted with Al_2O_3 Prior to Coating.

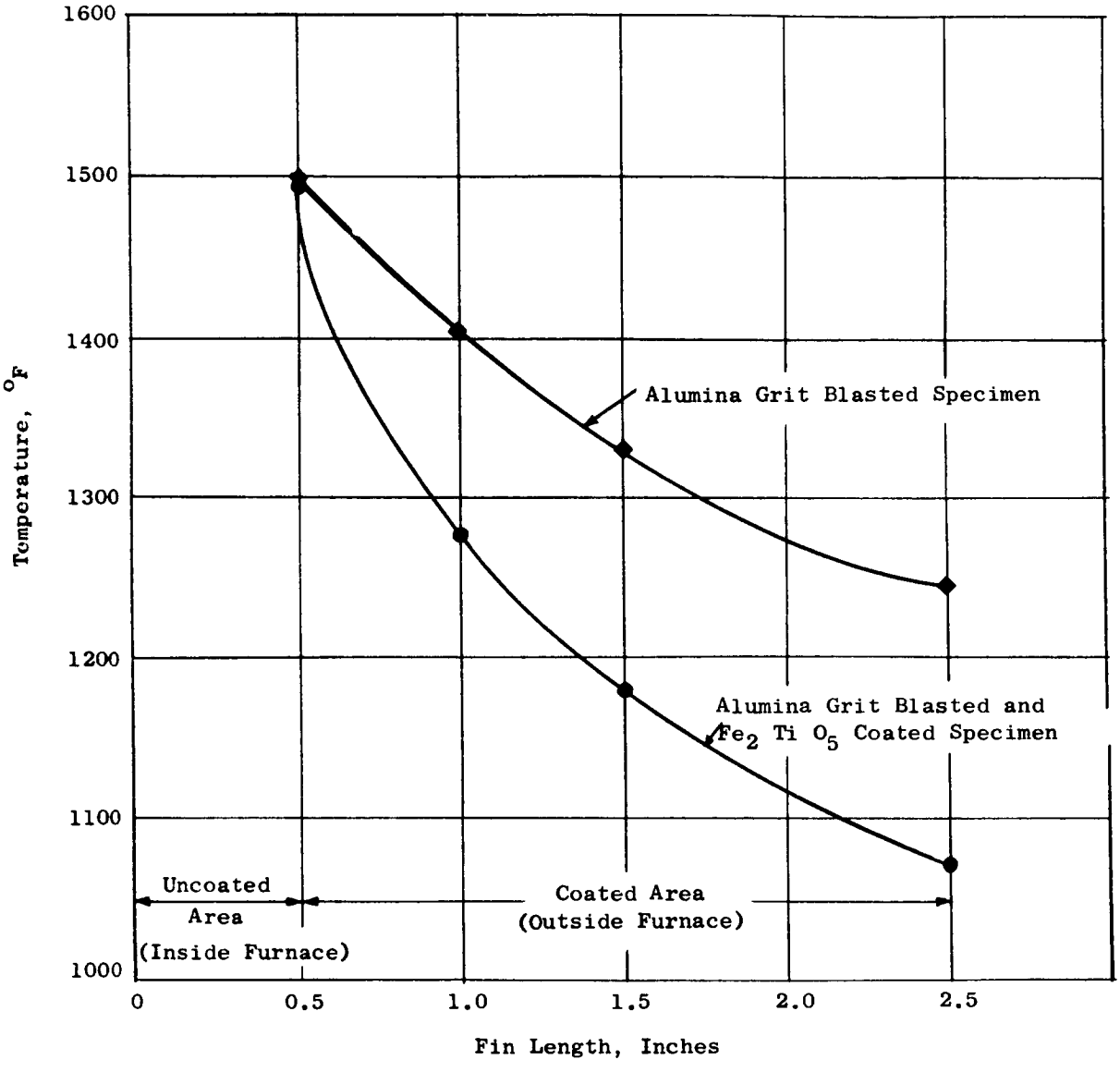

Figure 188. Steady State Temperature Profile of Coated and Uncoated Cb-1Zr Alloy Fin Specimens During Coating Evaluation Test.

curve developed is shown in Figure 189. The actual end temperature of the coated fin, 1070°F, and the actual emittance valve measured by Pratt & Whitney[68] for this coating at 1800°F on tubular specimens are also shown on this figure. It may be noted that the actual end temperature is within 10°F of the calculated value based on the measured emittance (0.85-0.87). The discrepancy, though small, would be even less if the outer edge (1/4-inch x 2-inch) of the specimen had been coated.

It may also be noted in Figure 189 that the effective emittance of the uncoated, grit-blasted specimen was approximately 0.3, which is considerably less than the value of 0.42 previously measured[69] on sheet specimens. Differences in the grit blasting treatment could be responsible for the different emittance values.

The surface appearance of the coated specimen following the evaluation test is shown in Figure 190 (a) and (b). No significant alteration in the before- and after-test appearance was detected by examination with a steromicroscope at 30 diameters. Cross sections of the coating and Cb-1Zr substrate before and after test are shown in Figure 190 (c) and (d). Some evidence of cracking and interface separation is apparent in the tested fin in the high-temperature (1500°F) region. Areas of the fin which were at lower temperatures (1070-1280°F) had the same metallographic appearance as the before-test specimen. Since no changes were detected in the temperature profile as a function of test time, the deterioration observed had a negligible effect on the heat rejection characteristics of the coating, and the coating was determined to be satisfactory for the application. The description of the actual method used to apply the iron titanate coating to a stainless steel condenser mockup and the actual Cb-1Zr condenser is included in Section IV, Loop Fabrication, of this report.

---

(68) Semiannual Progress Report, Determination of the Emissivity of Materials, Report Period: May 14-Nov. 15, 1964, R. C. Emanuelson, Pratt & Whitney Aircraft, NASA Contract NAS 3-4174, NASA-CR-54268.

(69) Potassium Corrosion Test Loop Development, Quarterly Progress Report No. 4 for Period Ending July 15, 1964, NASA Contract NAS 3-2547, NASA-CR-54167, p. 49.

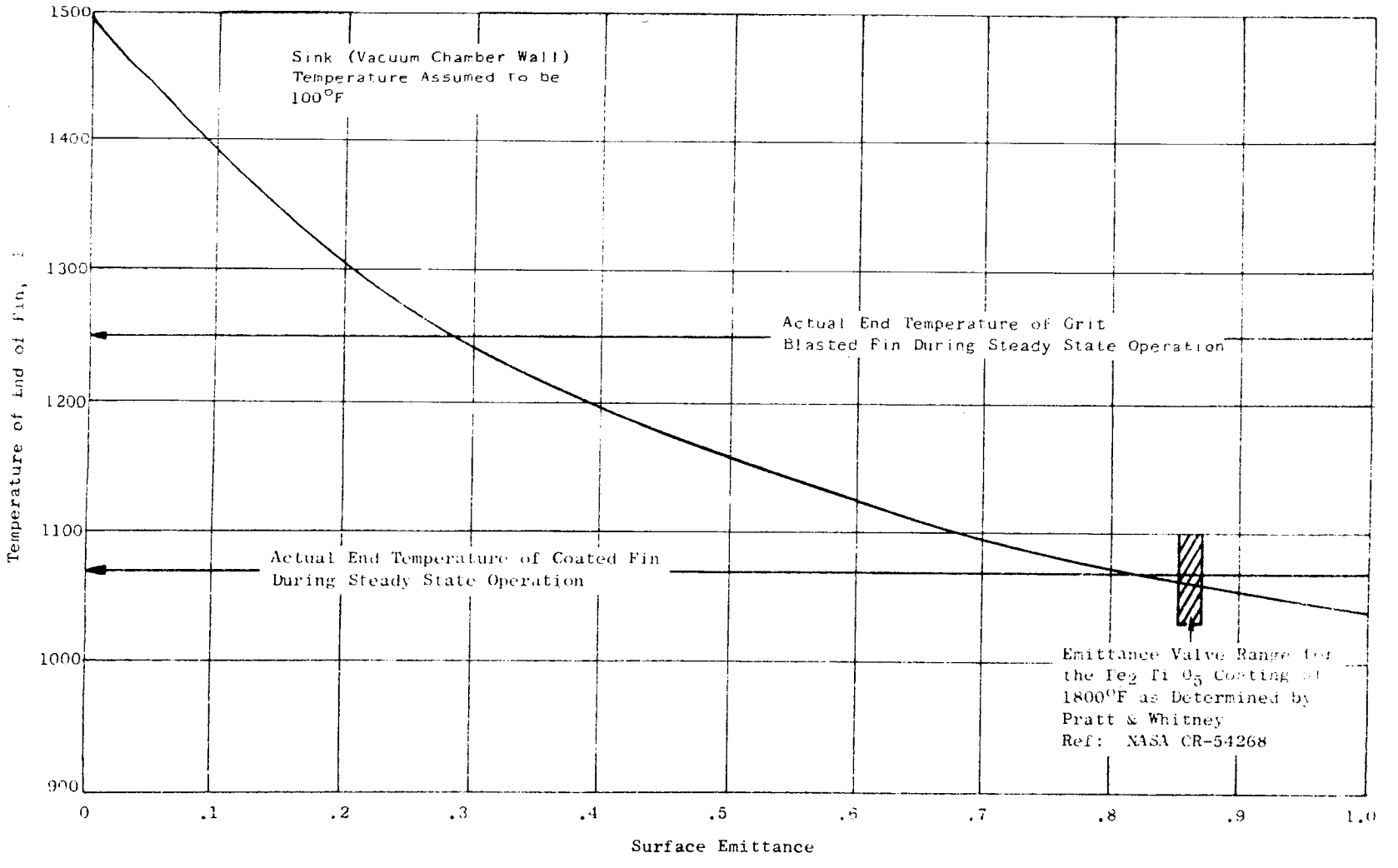

Figure 189. End Temperature of a 2-Inch x 2-Inch x 0.25-Inch Thick Cb-1Zr Fin with a Base Temperature of 1500°F as a Function of Surface Emittance.

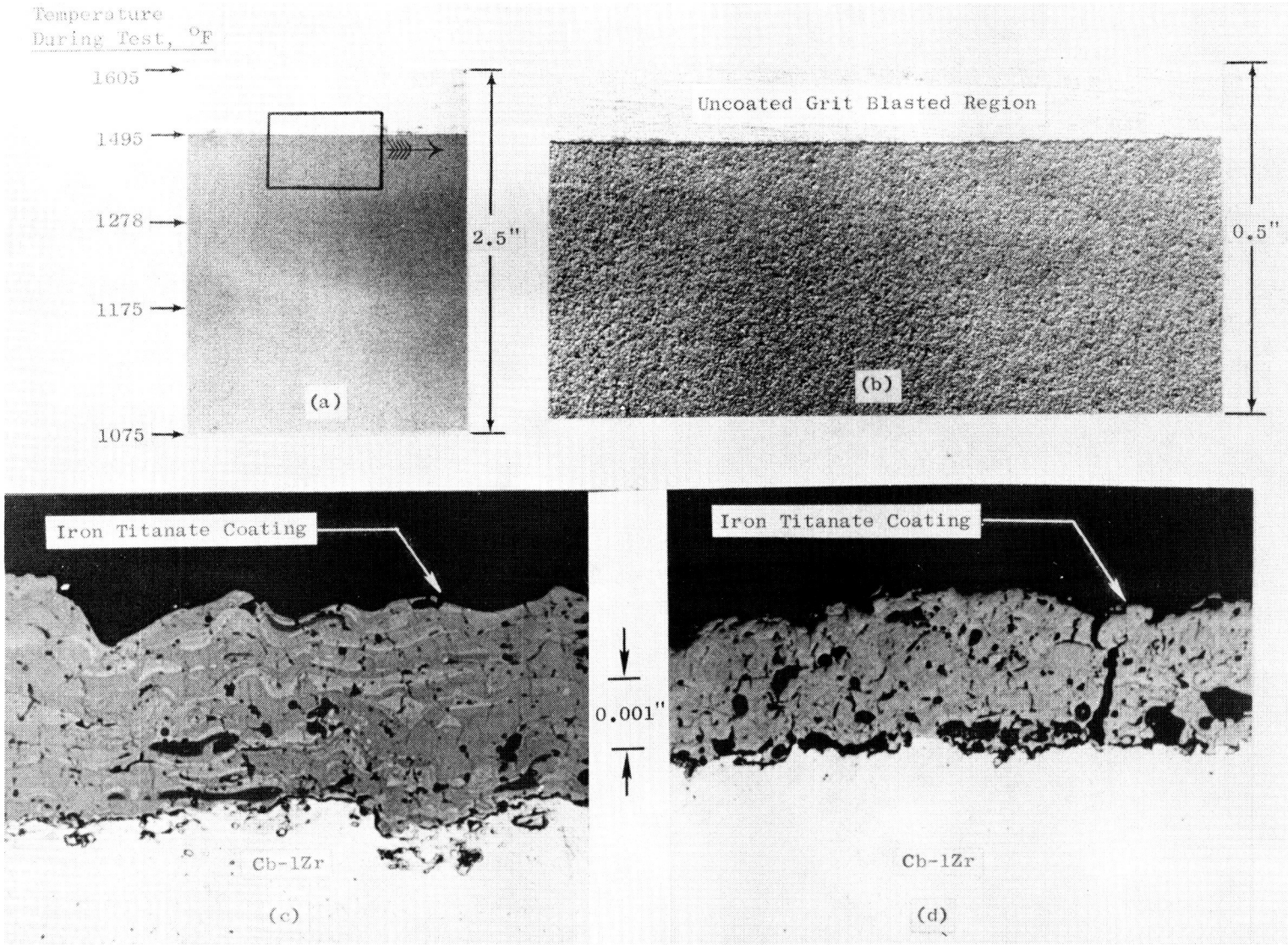

Figure 190. Cb-1Zr Alloy Fin Specimen Coated with Iron Titanate. The Appearance of the Surface of the Coating at Low Magnification After the 1,000-Hour Evaluation Test is Shown in (a) and (b). Metallographic Cross Sections of the Coating Before Test (c) and After Test (d) are also Included.

APPENDIX G

CALIBRATION OF THE PARTIAL PRESSURE GAS ANALYZER

During the operation of the Cb-1Zr Rankine System Corrosion Test Loop, a General Electric Company partial pressure analyzer[(a)] was used to monitor the composition of the residual gases in the vacuum chamber. The analyzer tube, control unit, and scan recorder are described and illustrated in Section V, Test Equipment, in the body of this report. A more detailed description of the system and the calibration procedures used will now be described.

The partial pressure gas analyzer for the vacuum chamber was adjusted for optimum performance and calibrated for hydrogen, helium, nitrogen, and argon. The analyzer tube used had an exposed ion source in order to obtain pressure data corresponding closely to the actual pressures within the chamber due to the very high conductance between the chamber and mass spectrometer ion source. The analyzer tube was mounted on the chamber sump as illustrated earlier in Figure 54. The electronic control used to operate the analyzer tube had both logarithmic and linear read-out, provisions for single-peak monitoring, and improved stability in the accelerating voltage circuitry.

In order to reduce the inventory of inert gases in the getter-ion pump elements and to facilitate the calibration operation, a baffle was located in the 16-inch-diameter duct between the getter-ion pump and the chamber sump. This baffle was a circular piece of stainless steel sheet which, in the closed position reduced the conduction cross section area by a factor of 75 to 1. The baffle could be rotated around its diameter by a magnetically operated rotary feedthrough[(a)] so that, in the open position, the total duct conductance was obtained. This baffle could be partially or completely closed whenever it was desired to decrease the gas load to the getter-ion pump. The baffle was used on initial startup of the pump and during chamber bakeout when the gas

(a) Model 22PC110

load was normally high. The baffle was also closed during admission of gases used to calibrate the partial pressure analyzer to prevent excessive gas flow to the pump while maintaining relatively high chamber pressures. This was particularly useful for the helium and argon calibration since these inert gases are not effectively removed by the getter-ion pump.

The partial pressure analyzer calibration procedure used was similar to that used in an earlier loop test.[70] With the baffle closed, a pure gas was admitted to the chamber, a reading of the ion gauge was made, and a mass spectrum was obtained. This process was repeated at various pressures for each of the four calibrating gases. Appropriate corrections were applied when appreciable partial pressures of gases other than the calibrating gas were present. The average sensitivity of the partial pressure analyzer for each of the calibrating gases was then calculated. **The sensitivity is here defined as the analyzer ion current divided by the pressure indicated by the ion gauge. The sensitivity for each of the four calibrating gases is plotted in Figure 191. Although a smooth curve is usually obtained with such a plot, in this particular case the helium sensitivity appears to be low. The sensitivity of gases for which no calibration has been made is obtained by extrapolating a smooth curve** through the two points at higher masses (N_2 and Ar) as shown by the dashed line in Figure 191. This particular partial pressure analyzer has been found to be extremely sensitive, due principally to cesiation of the electron multiplier by high-temperature bakeout. The sensitivity to hydrogen is about a factor of 700 greater than that obtained for the analyzer used for the Cb-1Zr Pumped Sodium Loop[70] tests. Experience with partial pressure analyzers on the present program demonstrates the wide variation of sensitivity from one analyzer to another and also from one gas to another for a particular analyzer.

The partial pressure analyzer was initially calibrated before the loop was installed in the vacuum chamber. However, after the loop was

(a) Varian Associates Model No. 954-5026.

(70) Hoffman, E. E. and Holowach, J., Cb-1Zr Pumped Sodium Loop, NASA CR-1135, November 1968, p. 240.

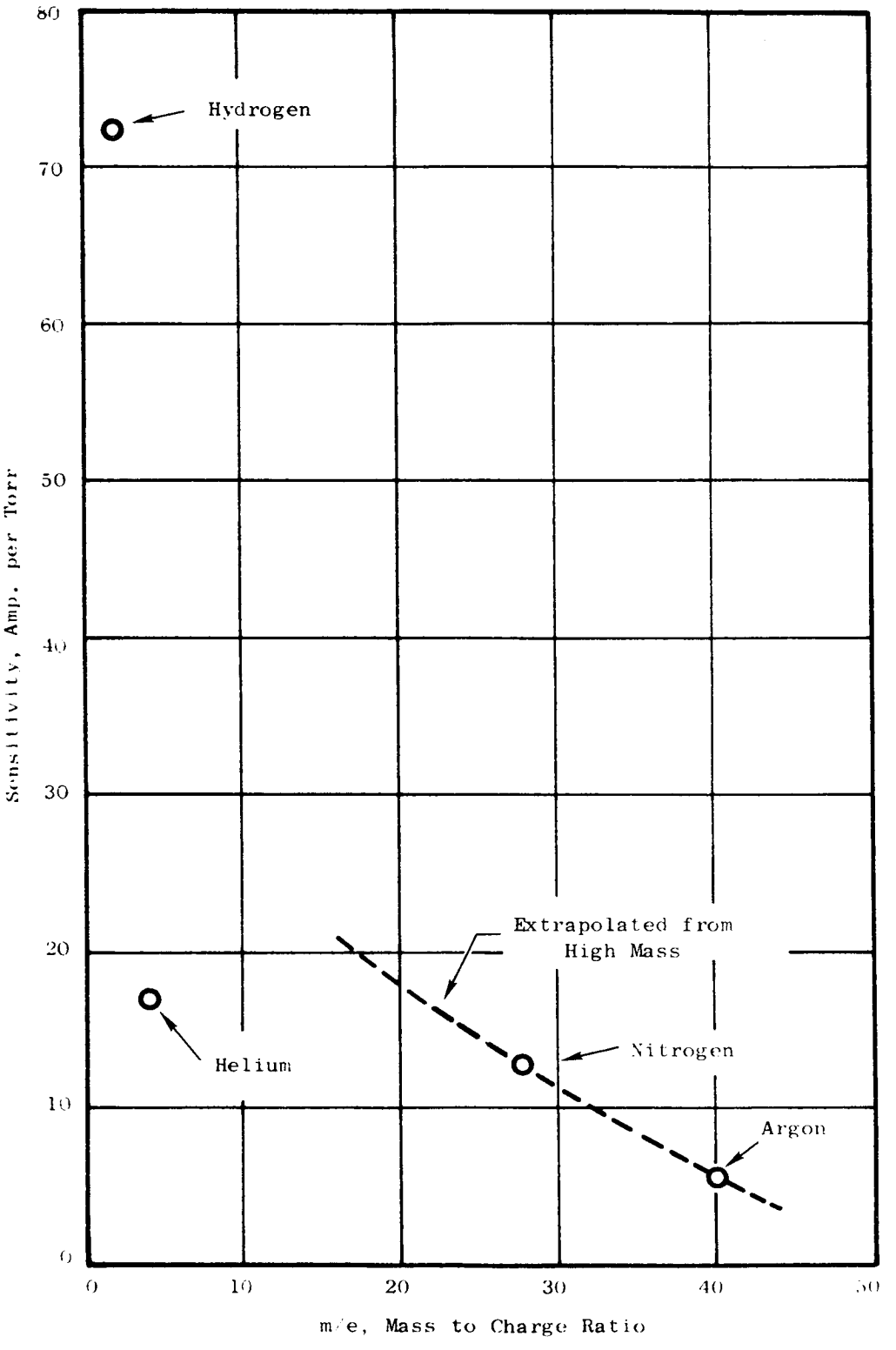

Figure 191. Sensitivity of Partial Pressure Analyzer, Initial Calibration (3-3-65).

installed in the chamber and the chamber once again evacuated and baked out, the sensitivity was quite low compared to that obtained in the initial calibration. This loss of sensitivity has been generally observed when the electron multiplier is exposed to the atmosphere. The electron multiplier was then baked out at about 600°F for 20 hours with a resulting increase in sensitivity to about 5 percent of its previous level.

After the loop was installed in the chamber, there was no opportunity to perform an accurate calibration of the analyzer because of the relatively high pressure (10^{-7} torr range) within the chamber. For the calculation of the various partial pressures during loop operation, it was thus necessary to indirectly obtain the required calibration factors. The calibration factor is here defined as that number by which the ion current is multiplied to give the indicated ion gauge partial pressure of a particular gas. The general procedure used in obtaining these factors was to assume that the relative sensitivity from one gas to another was the same as for the initial calibration, and that the sum of the calculated partial ion gauge pressures is equal to the ion gauge reading. A summary of the calibration factors used throughout the Cb-1Zr Loop test is given in Table XXXVII. The third column of Table XXXVII shows the results of the initial calibration of the analyzer. Three separate sets of calibration factors were used throughout the duration of the test. The first set of factors, shown in column 4 of Table XXXVII, was used for spectra obtained between -77 and +187 test hours. At 187 test hours, the deflection electrode voltages were readjusted, and new calibration factors were calculated. These factors, shown in column 5 of Table XXXVII, were used for spectra obtained between 187 and 3809 test hours. During the test shutdown at 3809 test hours, a new analyzer tube was installed and used until the conclusion of the test. This change in analyzer tubes necessitated another evaluation of the calibration factors for the different species, as given in the sixth column of Table XXXVII. At the conclusion of the 5000-hour test, an attempt was made to calibrate the analyzer tube. Difficulties were encountered in this calibration due to the relatively high pressure (10^{-8} torr range) in the chamber and inability to hold constant pressure when a pure gas was admitted to the chamber. Furthermore, addition of

one gas to the chamber resulted in considerable increase in the pressures of the other gases. In spite of these problems, calibration factors within about 20 percent of the values shown in column 6 of Table XXXVII were obtained for H_2, He, N_2, and Ar.

In the last column of Table XXXVII, the relative ion gauge sensitivities for the various species are listed. True partial pressure of a particular gas may be obtained by dividing the indicated ion gauge partial pressure by the relative ion gauge sensitivity.

TABLE XXXVII

RESIDUAL GAS ANALYSIS CALIBRATION FACTORS FOR THE Cb-1Zr RANKINE SYSTEM CORROSION TEST LOOP

Parent Specie	m/e*	Calibration Factor, Ki, torr/amp				Relative Ion Gauge Sensitivity
		Initial Calibration 3-3-65	-77 to +187 Test Hours	+187 to 3,809 Test Hours	3,809 to 5,000 Test Hours	
H_2	2	0.0138	0.25	0.28	14	0.42
He	4	0.059	0.54	1.2	23	0.19
CH_4	16	0.048	1.4	0.97	19	1.07
H_2O	18	0.053	2.4	1.1	21	0.89
N_2 or CO	28	0.079	3.7	1.6	31	1.00
O_2	32	0.10	5.7	2.0	39	0.84
Ar	40	0.17	8.2	3.5	68	1.56
CO_2	44	0.27	16.4	5.5	105	1.37

* m/e = mass/charge.

APPENDIX H

CALIBRATION OF W-3Re/W-25Re THERMOCOUPLE WIRE

Calibration of the thermocouple wire to be used in the Cb-1Zr Rankine System Corrosion Test Loop was conducted in a high-vacuum environment with sample thermocouples made from the same spools of wire which was to be used to instrument the loop. The following is a detailed description of the apparatus used, the configuration of the calibration thermocouples, and a discussion of the test results, including data required to define a characteristic curve for the thermocouple wire.

The calibration was conducted in a vacuum furnace chamber constructed especially for the purpose. A sketch of this unit is shown in Figure 192. It consists of a 6-inch-OD tube approximately 2 feet in length with appropriate high-vacuum flanges to provide access to either end. A total of seven 1.5-inch ports were provided for power and thermocouple lead feedthroughs. An isothermal block, 2.6-inch OD and 15 inches long and made of Mo-TZM alloy, was mounted vertically in the center of the chamber. Various components of the calibration system are shown in Figure 193. Thermocouples to be calibrated were installed in a 0.5-inch hole drilled along the axis of the block approximately 7 inches deep from the lower end. A similar hole was provided from the top end of the block with a 0.25-inch web between the bottoms of the two holes. The upper hole was used for optical pyrometer readings of block temperature. Standard reference Pt/Pt-10Rh thermocouples were installed in the bottom hole together with the W-3Re/W-25Re thermocouples to be calibrated. The optical pyrometer and the Pt/Pt-10Rh thermocouples were used as independent means of measuring isothermal block temperatures.

The isothermal block was heated by means of a split cylindrical resistance element made from 0.005-inch-thick tantalum foil. The element was supported on the 450-amp feedthroughs so that it was concentric with the isothermal block. Cylindrical radiation shields were provided to minimize the heat losses from the element to the walls of the chamber. A total of 12 shields were constructed of 0.005-inch-thick foil separated

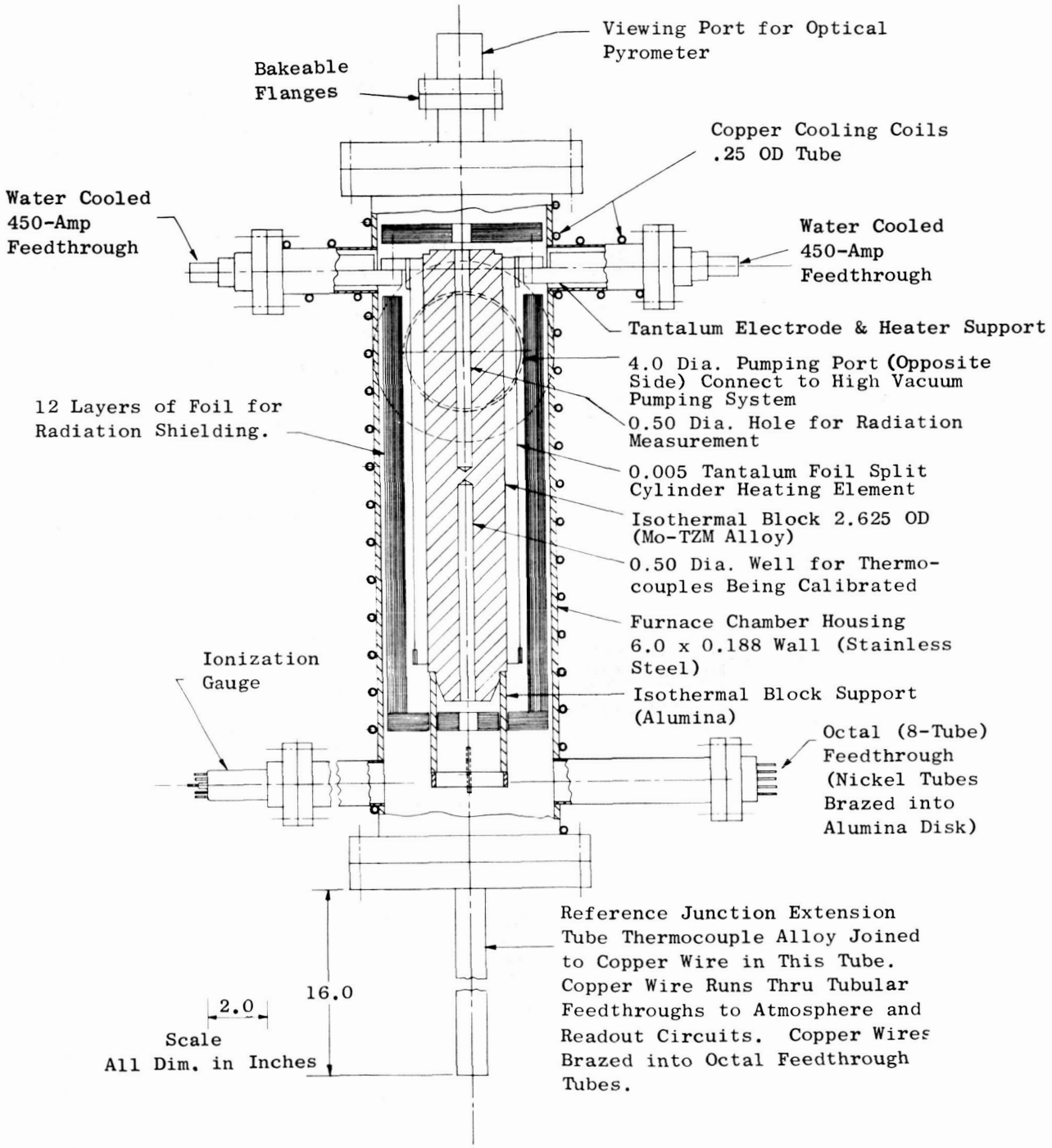

Figure 192. Vacuum Furnace for Calibrating W-3Re/W-25Re Thermocouple Wire.

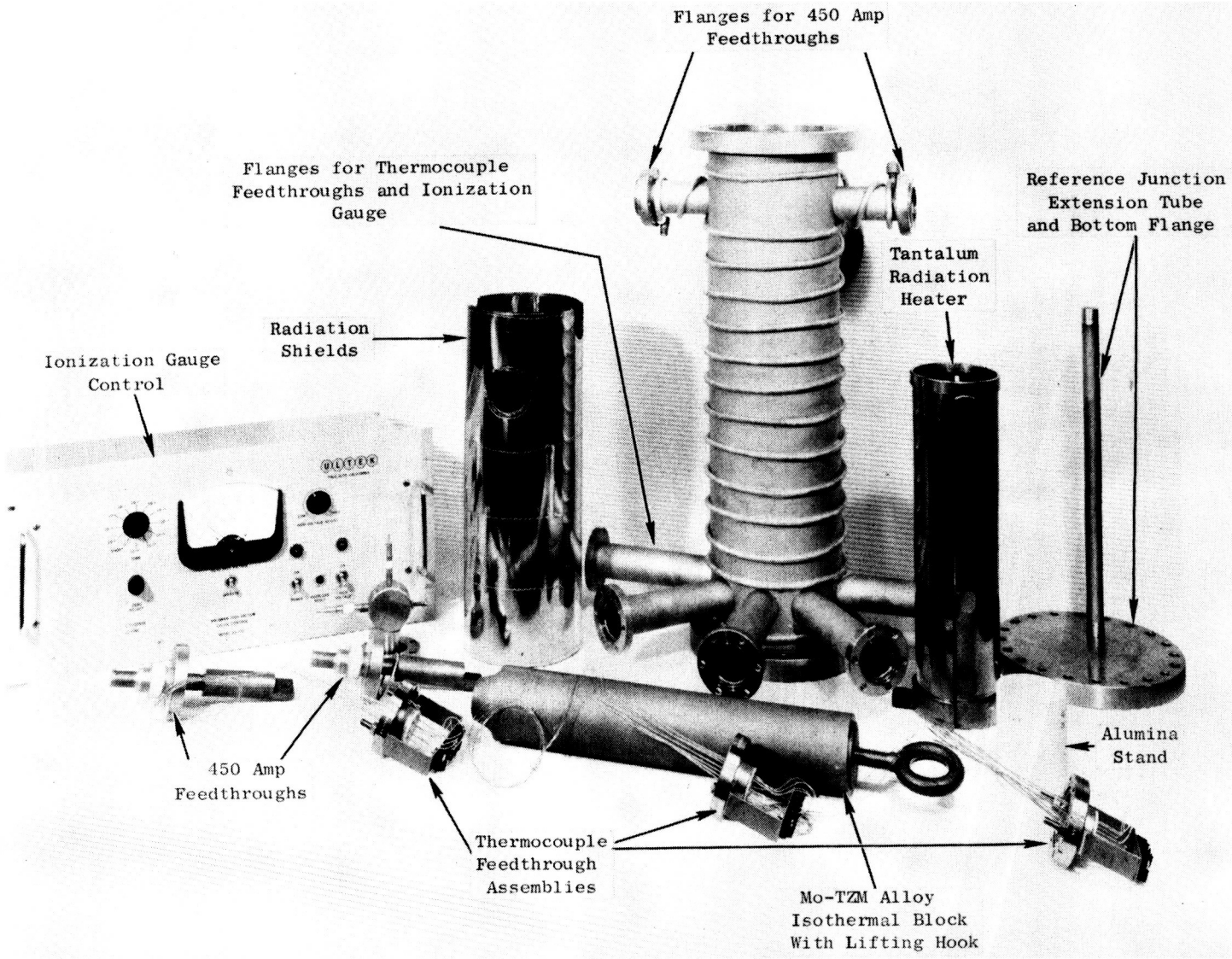

Figure 193. Components of Thermocouple Calibration Vacuum Furnace Before Assembly. (C65012206)

by 0.020-inch tantalum wire. A view into the furnace chamber prior to installation of the isothermal block is shown in Figure 194.

The copper wire thermocouple leads were brought out through Varian nickel tube feedthroughs which consisted of eight 0.040-inch-ID tubes brazed into an alumina disc which was brazed to a 2 3/4-inch-OD high-vacuum flange. The copper wires were brazed into the nickel tubes and connected to the thermocouple leads within the vacuum chamber in an extension tube welded to the bottom flange of the vacuum chamber. During calibration tests, the extension tube (1-inch OD x 16 inches long) containing the wire junctions was immersed in an ice bath to establish the cold junction reference.

A Varian Model UHV-14 nude ionization gauge was installed in one of the 1.5-inch-OD tube extensions on the furnace chamber by means of a 2 3 4-inch-OD flange. The furnace chamber was attached to the bell jar of a Varian vacuum system containing a 1000-liter/second ion pump as shown in Figure 195. Also shown in this picture are the switches and readout instrument used during the calibration. The readout instrument was a Honeywell Precision Indicator with an accuracy of ± 0.02 percent of any individual millivolt span from 1 to 70 with a 3-microvolt dead band.

An optical pyrometer was used to check the absolute block temperature. The 1.5-inch-diameter viewport window mounted on the upper chamber flange and the specific instrument lens had been calibrated, and correction factors provided by calibration were used to compensate individual readings. Thermocouples to be calibrated were arranged as shown in Figure 196. Two Pt Pt-10Rh reference thermocouples made of 0.020-inch-diameter wire were strung through a 4-hole 99 percent purity alumina insulator (0.187-inch OD). A piece of Cb-1Zr tubing (0.250-inch OD) was drilled out to make a tight fit and was slipped over the 4-hole insulator containing the Pt Pt-10Rh reference thermocouples. Samples of the W-3Re and W-25Re wire to be calibrated were strung through 2-hole 99 percent alumina insulators (0.062-inch OD) 30 inches long, and a 1-inch length of 2-hole 0.032-inch 99.5 percent BeO was added to eliminate contact and possible

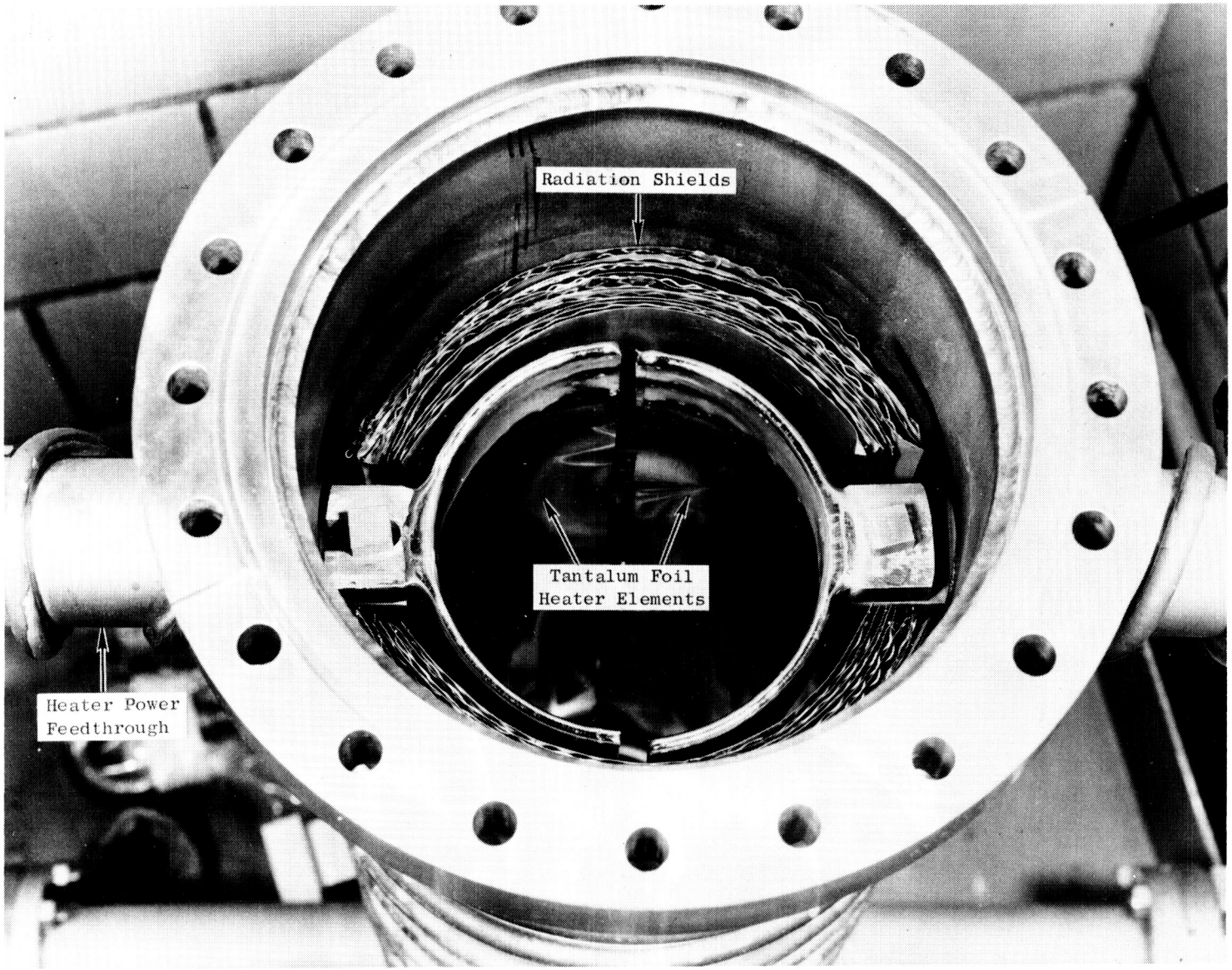

Figure 194. Inside of Thermocouple Calibration Furnace Prior to Insertion of Mo-TZM Alloy Isothermal Block. (Orig. C6502230)

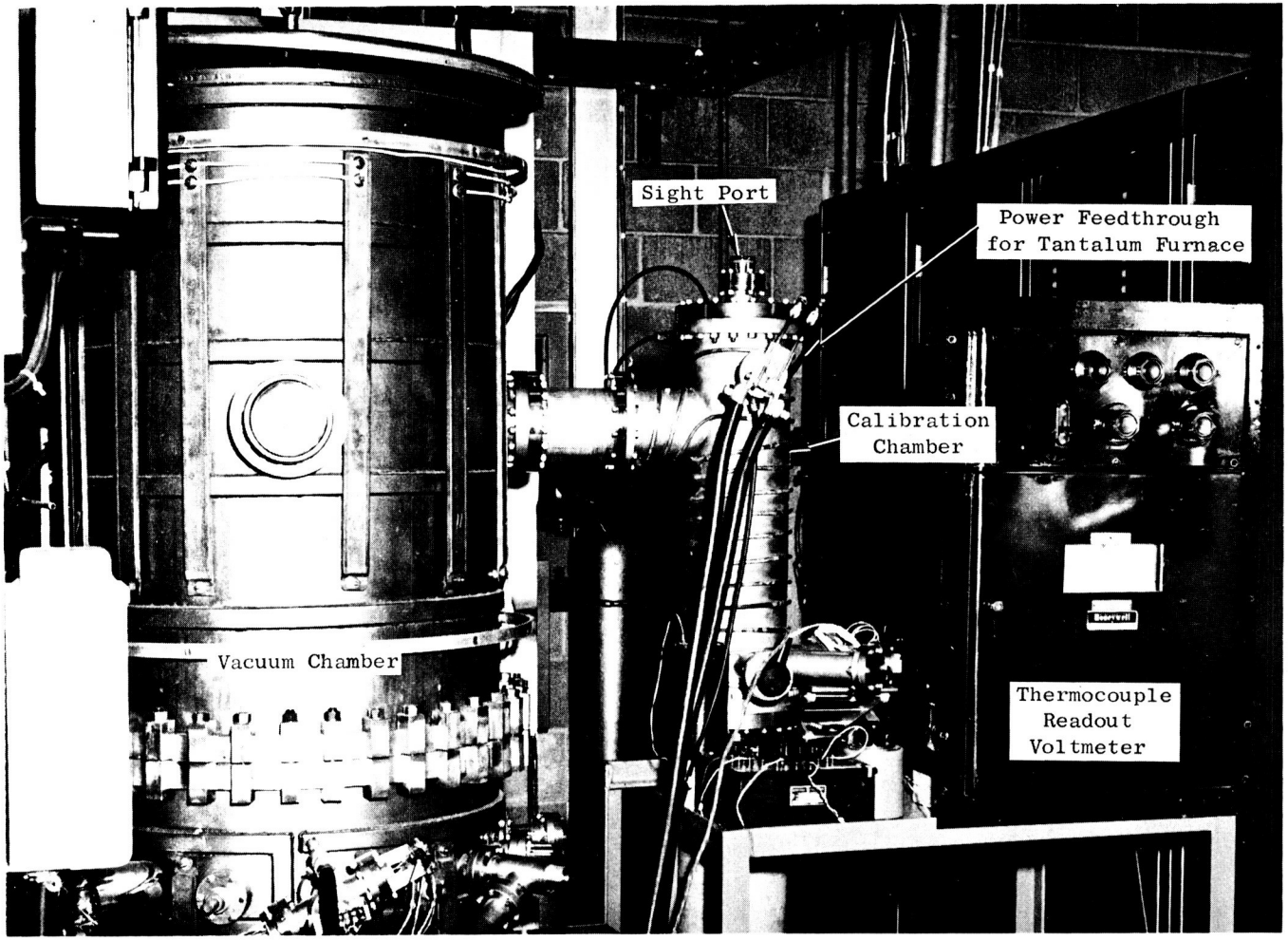

Figure 195. Thermocouple Calibration Furnace Attached to the 24-Inch Diameter Getter-Ion Pumped Vacuum Chamber. (Orig. C65040528)

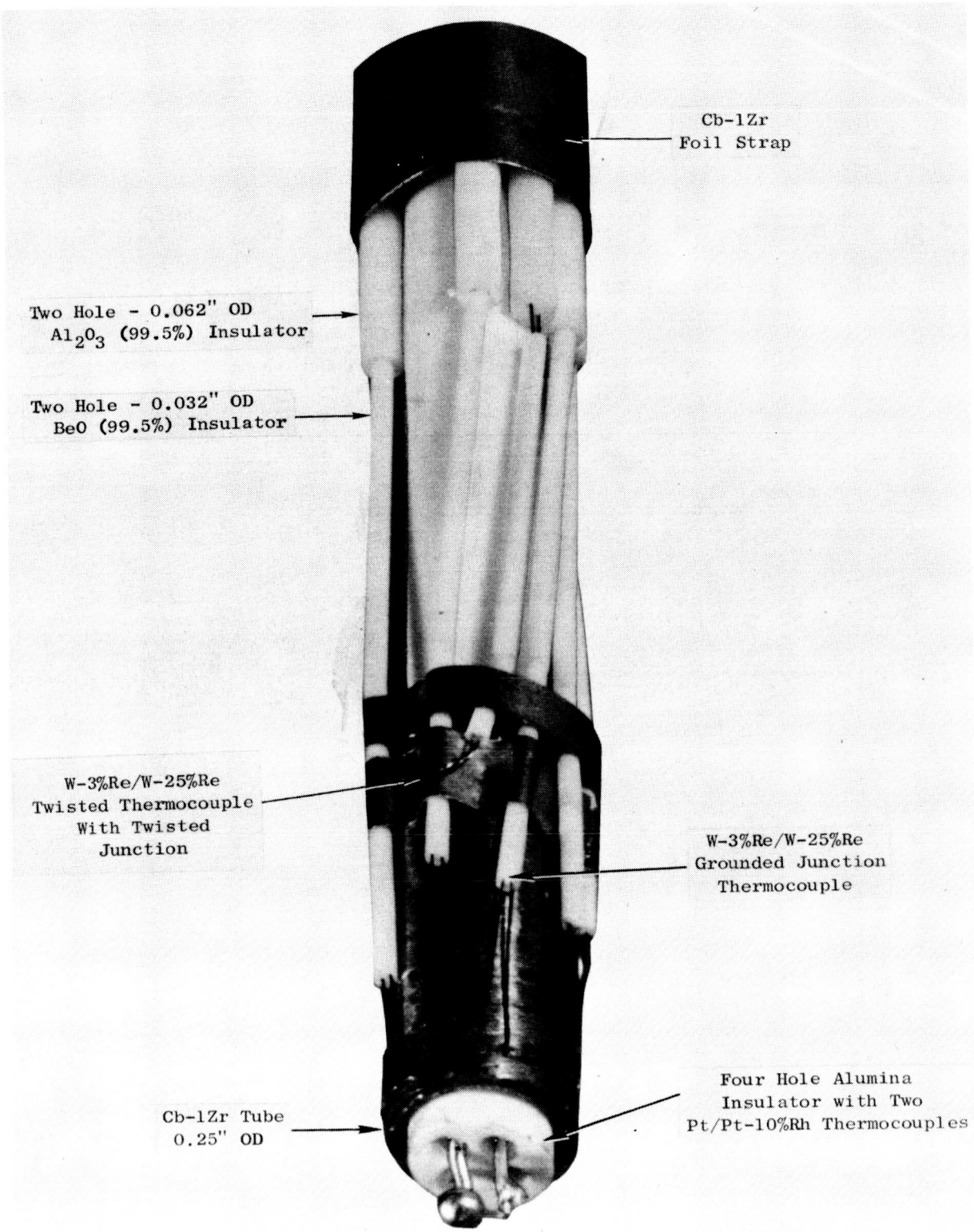

Figure 196. Thermocouple Bundle Used in Calibration of W-3%Re/W-25%Re Thermocouple Wire for the Prototype Corrosion Loop. (Orig. C65031521).

reaction between Cb-1Zr and alumina. Four such thermocouples were made from consecutive lengths of wire to be used for instrumenting the loop. These individual thermocouple assemblies with four other samples of different wire were attached to the insulator containing the reference thermocouples by means of Cb-1Zr foil straps. The entire assembly was made rigid to eliminate the possibility of slippage between various parts. Three of the hot junctions were formed by resistance welding the individual alloy wires to the Cb-1Zr tube in a manner similar to that to be used in the actual loop application. A copper alloy tip was used with the spot welder, and the weld area was flooded with argon during the welding procedure. One hot junction was formed by twisting the alloy wires together with no spot weld. Both types of junctions are evident in Figure 196.

The assembly described above was inserted in the calibration furnace as a single unit and strapped down to the chamber structure so that none of the thermocouple wires was in contact with the isothermal block. Copper leads from the vacuum feedthroughs were joined to the alloy wires by twisting both wires together. A copper-constantan thermocouple junction was located in the extension tube to measure the actual cold junction temperature. Calibration data were taken during three temperature cycles. During these runs, the pressure in the calibration furnace varied between a low of 2×10^{-8} torr at 400°F and a high of 6×10^{-6} torr at 2400°F.

Data were reduced by the following procedure.

Step 1. Cold junction temperature was converted from millivolts (copper-constantan thermocouple) to degrees Fahrenheit.

Step 2. Block temperature was determined by adding an emf equivalent to the cold junction temperature to the reference thermocouple output and converting the sum to degrees Fahrenheit by means of National Bureau of Standards Bulletin 561. An average of the two Pt/Pt-10Rh thermocouple readings (never more than 2.8°F of difference) was used as the actual block temperature.

Step 3. A table of output values for each thermocouple being calibrated was prepared from test data in the range 32° - 140°F.

Step 4. The millivolt signal equivalent to the reference junction temperature as defined in Step 1 above was calculated for each thermocouple being calibrated by linear interpolation of the table defined as Step 3.

Step 5. A corrected output signal was calculated by adding the millivolt signal determined in Step 4 above to the measured value. This information was used to generate a characteristic curve of corrected output millivolts vs the actual block temperature determined in Step 2 above.

Step 6. In order to facilitate curve plotting and permit use of an expanded scale, a straight line defined by co-ordinates (0, 0) and (24, 2400) where the first number is corrected millivolt output signal, and the second is temperature in °F was used as a base line, and the difference between this line and the corrected output millivolts was calculated. The difference is plotted vs temperature as Figure 197.

The curve shown in Figure 197 is an average of all data points taken during three temperature cycles over the range from 80° to 2400°F for two thermocouples with different hot junction configurations but from the same spools of alloy wire. All but 8 of 35 stable points fall within 4°F of this line. Maximum deviation of any stable point from the line (up to 2200°F) is 9°F. The actual values used to define the curve are listed in Table XXXVIII. These are not actual test points but were picked off of the best line through the test data so that linear interpolation between any two points would cause a maximum error of 0.5°F.

A comparison between the two reference thermocouples and the optical pyrometer readings is shown in Table XXXIX. Optical readings were taken from 17 inches looking through a 1.5-inch-high vacuum viewport at the bottom of the 0.5-inch-diameter, 7-inch-deep hole in the isothermal block. Correction factors based on calibration procedures were applied to the raw optical readings for the vacuum viewport window and the pyrometer lens. The generally good agreement is an indication that the block temperature was reasonably uniform and that all factors used to make the temperature measurements were consistent.

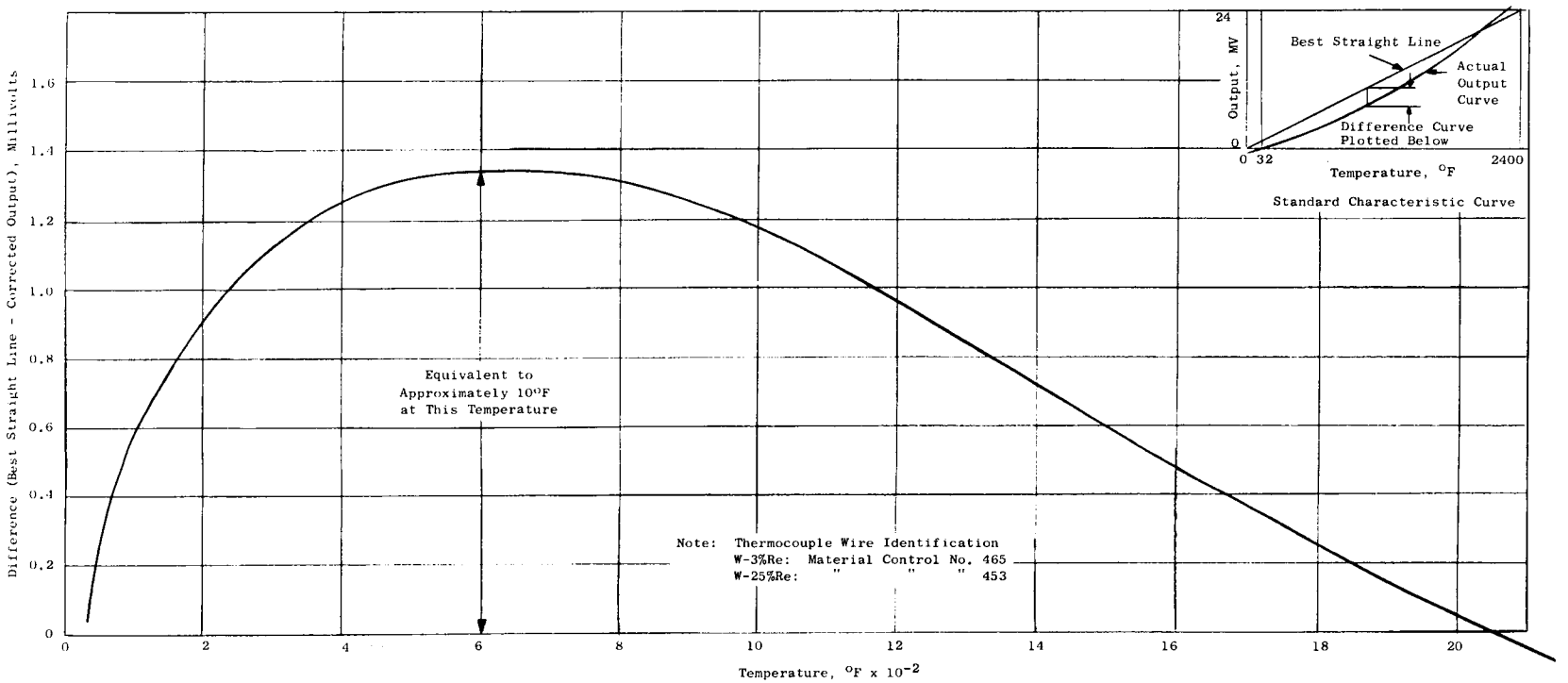

Figure 197. Difference Curve Versus Temperature Obtained in Calibration of Two W-3Re/W-25Re Thermocouples Made from Wire Used to Instrument the Cb-1Zr Rankine System Corrosion Test Loop.

TABLE XXXVIII. CHARACTERISTIC CURVE FOR W-3%Re/W-25%Re BASED ON VACUUM CALIBRATION DATA

Temp, °F	Millivolts Below Best[1] Straight Line	Millivolts Above Best[1] Straight Line	Total Output in Millivolts with 32°F Reference Junction
32.0	0.320		0
100.0	0.587		0.413
160.0	0.790		0.810
200	0.908		1.092
250	1.028		1.472
300	1.126		1.874
350	1.196		2.304
400	1.253		2.747
450	1.298		3.202
480	1.315		3.485
510	1.324		3.776
610	1.338		4.762
670	1.339		5.361
730	1.330		5.970
790	1.313		6.587
830	1.296		7.004
900	1.251		7.749
950	1.215		8.285
1000	1.173		8.827
1100	1.073		9.927
1200	0.961		11.039
1300	0.840		12.160
1450	0.662		13.838
1650	0.416		16.084
1750	0.300		17.200
1850	0.193		18.307
1950	0.092		19.408
2050	0		20.500
2150	--	0.086	21.586
2250	--	0.167	22.667
2350	--	0.240	23.740

[1] Defined by coordinates (millivolts, temperature), (0, 0) (24, 2400).

TABLE XXXIX. COMPARISON OF REFERENCE THERMOCOUPLES AND OPTICAL PYROMETER READINGS DURING THERMOCOUPLE WIRE CALIBRATION IN VACUUM

Reading No.	Thermocouples			Optical Pyrometer[2]			
	A[1] °F	B[1] °F	Average Thermocouple Indication °F	Corrected Temp. °F	Sight Glass Correction °F	Lens Corrected °F	Raw Optical Reading °F
26	1542.3	1544	1543.15	1549	+ 8.5	-10[3]	1550
27	1734.3	1731.6	1732.95	1726	+ 9.4	- 3	1720
29	1935.8	1933.3	1934.55	1915	+10.4	+ 5	1900
30	2031.9	2029.1	2030.5	2030	+10.8	+ 9	2010
31	2180.1	2177.9	2179.0	2182	+13.0	+14	2155
32	2338.2	2336.4	2337.3	2340	+15.3	+15	2310
33	2217.8	2215.2	2216.5	2209	+13.6	+15	2190
40	1622.1	1620.2	1621.15	1612	+ 9	- 7	1610
41	1794.8	1792.9	1793.85	1795	+ 9.8	0	1785
42	1997	1995	1996	1999	+10.7	+ 8	1980
43	2319	---	2319	2316	+15	+16	2285

[1] Pt/Pt-10%Rh thermocouples, 0.20-inch diameter, in 99.0% Al_2O_3

[2] Pyro Micro Optical Pyrometer, Serial No. M5344, Pyro Instrument

[3] Extrapolated from available data.

APPENDIX I

TEST STARTUP PROCEDURE

The test operation portion of the Cb-1Zr Rankine System Corrosion Loop Test Plan is included below with a schematic diagram of the loop, Figure 198, and the instrumentation drawing, Figure 199, showing the location of thermocouples on various loop components.

TEST OPERATION

A. Recording of Test Data

The test operator will maintain an official log book of all pertinent test data, observations and test progress to present a complete but concise history of the loop operation. In addition to the log book, he will record daily all test data on a standard test data sheet maintained in chronological order in a loose leaf notebook. A partial pressure gas analysis of the residual gases in the vacuum chamber will be recorded daily.

B. Operating Instructions

The project engineer will instruct and qualify all loop operators in the control and operation of the loop and auxiliary test equipment. In addition to these instructions, a complete file of loop drawings and equipment manuals will be available to the operator at the test site. A thorough review of the safety and protection circuits of the loop will be made during the operation of the test. No safety circuit will be bypassed without written permission in the log book by the project engineer or project manager.

C. Test Startup

The loop and vacuum chamber have previously completed an initial bakeout and are currently at room temperature at a total pressure less than 1×10^{-8} torr. During the following operation the rate of increasing the loop temperature will be controlled by the outgassing rate of the loop components as they exceed the bakeout temperature. The permissible vacuum chamber pressures as a function of temperature are listed at the end of this section (C.22).

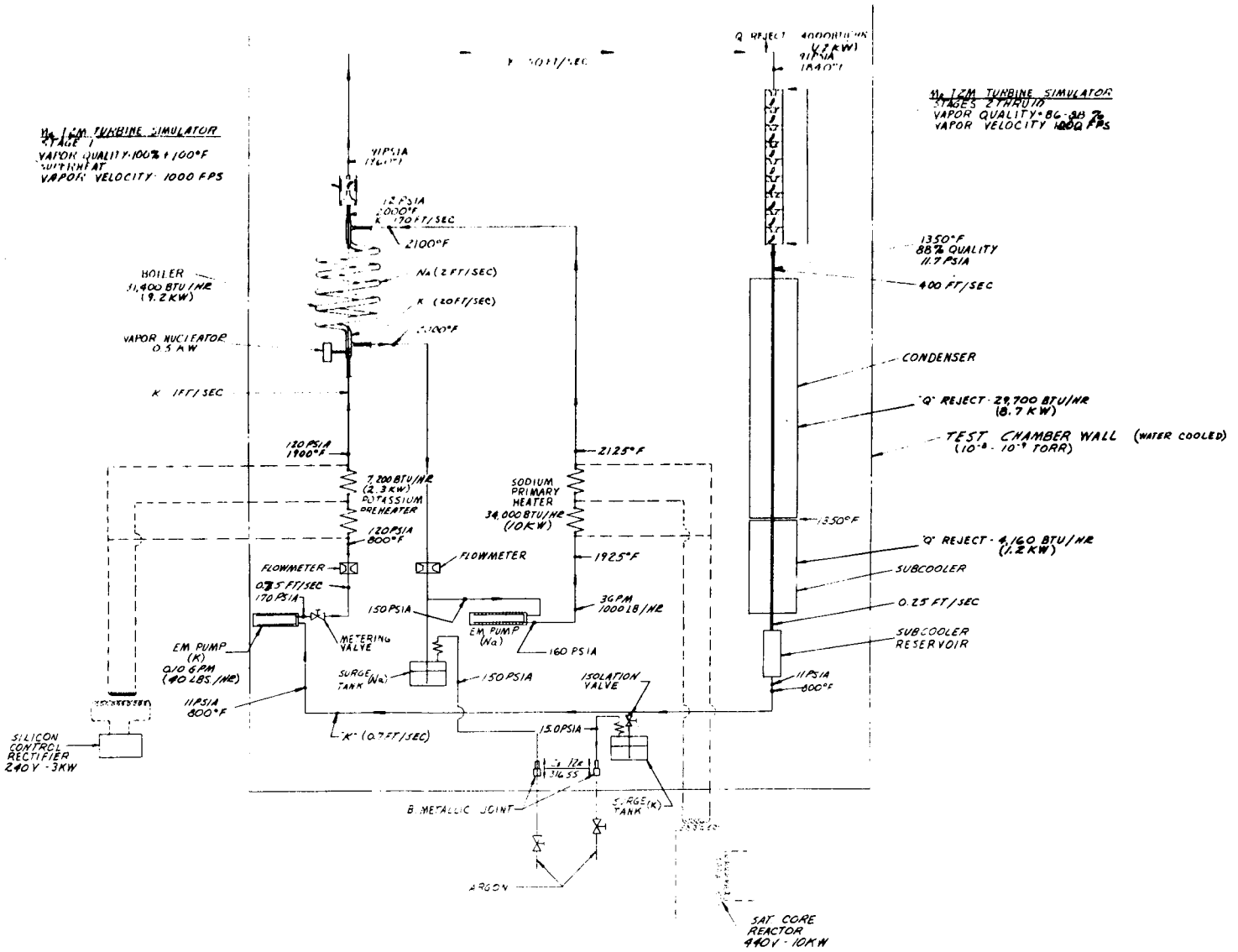

Figure 198. Schematic Diagram of the Cb-1Zr Rankine System Corrosion Test Loop.

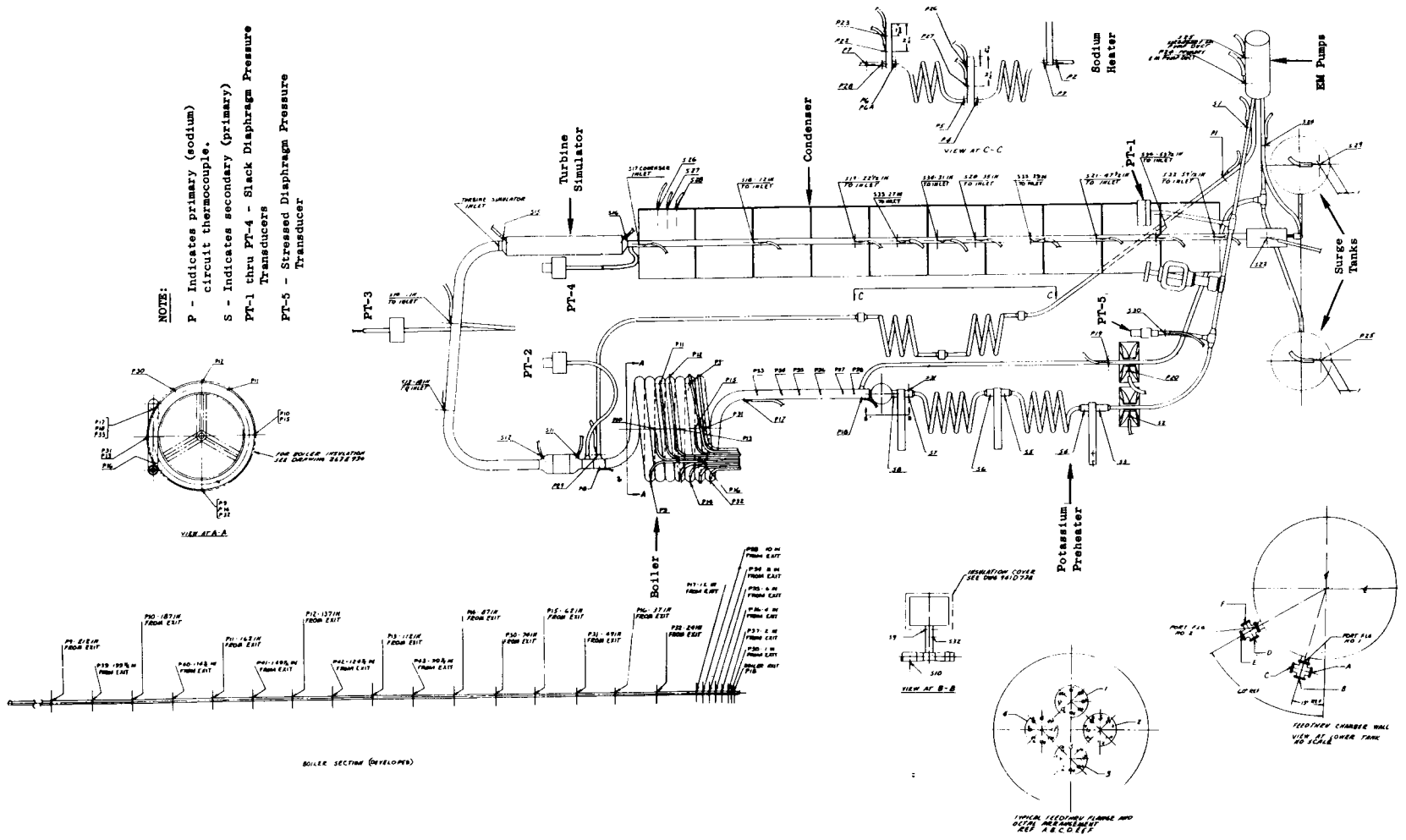

Figure 199. Cb-1Zr Rankine System Corrosion Test Loop Thermocouple Instrumentation Layout.

The potassium and sodium inventory are solidified in their respective surge tanks under vacuum. The following procedures will be used to fill the primary (sodium) and secondary (potassium) loops and to bring the loop to the design operating conditions.

1. Turn on the vacuum chamber electrical heaters for 500°F bakeout of bell jar, sump, and spool section.
2. Turn primary and secondary EM pump power to 10 percent of full power and allow the pump temperature to increase to 500°F and then adjust the power to maintain 500°F.
3. To fill the primary loop, check the surge tank temperature and if the temperature is greater than 250°F, increase the argon pressure to 150 psia.
4. The primary loop will fill automatically as the sodium is forced out of the surge tank into the loop.
5. The fill will be detected by the indicated flow on the flowmeter recorder and temperature changes in the primary circuit.
6. Before filling the secondary loop, open the isolation valve.
7. Close the metering valve with 1 ft-lb of torque.
8. Slowly increase the argon pressure of the primary loop to 2.0 psia which is equivalent to a 70-inch column of potassium above the surge tank (0.0283 lbs/sq in/in of potassium at 480°F).
9. Verify the height of the rising potassium in the condenser by the change in temperature of thermocouples on condenser/subcooler pipe. Temperature change at T/C S-17 (condenser inlet) indicates K at proper height. No change in temperature should be detected in the preheater side of the loop.
10. Close the isolation valve with 2 ft-lbs of torque.
11. Increase the secondary gas pressure to 100 psia in the surge tank and check for internal leak across the isolation valve seat by a pressure change on the pressure transducer PT-1.
12. If no leak is detected after one hour reduce the argon pressure to 15 psia.
13. Boiling operation can now be started.
14. Slowly increase the temperature of the primary circuit to 1350°F on manual control with flow rate at 2 gpm.
15. Check the power setting of the secondary EM pump and adjust to 10 percent.
16. Slowly open the metering valve to 40-45° rotation which will be equivalent to a 20 to 40 psi drop at design.
17. Boiling and condensing in the secondary loop will begin with this operation. Maintain flow and power input conditions until thermal equilibrium is achieved in secondary circuit.

18. Check the potassium vapor quality at the boiler exit.

    a. If quality is 100 percent or less, decrease the potassium flow rate to obtain 25° to 75°F of superheat in potassium vapor.

    b. If vapor is superheated, slowly increase the potassium flow rate while maintaining 25° to 75°F of superheat.

19. Slowly increase the temperature of the primary loop in 25°F increments.

20. Turn power on potassium preheater and adjust power to obtain a boiler inlet temperature 25°F below the potassium saturation temperature.

21. Continue to increase the primary loop temperature, the secondary flow rate, and the preheater temperature until the following test conditions are reached:

Boiling Temperature	-	1900° ± 25°F
Superheat Temperature	-	2000° ± 10°F
Condensing Temperature	-	1350° ± 25°F
Potassium Flow Rate	-	35 lb/hr ± 5 lb/hr

    Nominal values of pressures, temperature, flow velocities, and power inputs to various loop components are given in Figure 198.

22. The maximum test chamber pressures which shall not be exceeded during test startup and operation are given below:

Test Period	Maximum Loop Temp., °F	Maximum Ionization Gauge Pressure Torr
Bakeout	500	5×10^{-5}
Test Startup	1000	1×10^{-5}
Test Startup	1500	5×10^{-7}
At Test Conditions		
0-100 Hrs.	2125	1×10^{-7}
100-500 Hrs.	2125	5×10^{-8}
500-5000 Hrs.	2125	1×10^{-8}

    In the event that the ionization gauge pressure limitations given for the loop operation are exceeded, a partial pressure scan will be obtained to determine the concentration of reactive gases. These results will be reported to the project engineer immediately to obtain approval to continue the test.

23. Continue test at above conditions for 5000 hours.

24. The effect of a change in the potassium flow, temperature, or inventory are summarized in Table XXXX.

D. Loop Shutdown Procedures

1. Normal - The following procedure will be used when a scheduled loop shutdown has been requested by either the project engineer or project manager for either loop or facilities maintenances which will prevent the normal operation of the loop. The shutdown procedure will normally require one hour, and all adjustments will be made in small, carefully controlled increments to avoid liquid carryover to the turbine simulator.

a. In sequence, decrease:

i. Secondary pump power

ii. Preheater power

iii. Heater power

iv. Primary pump power

b. When the temperature of the loop is less than 1000°F, turn off all loop power.

c. Evacuate primary and secondary surge tank to 0 psia.

d. Primary circuit will dump automatically; do not dump secondary circuit unless it is requested by either the project manager or project engineer.

2. Emergency - The following procedure will be used only in event of:

Severe leak in the loop.

Loss of electrical power or water supply, which will prevent normal loop operation.

Abnormal behavior of the loop including loop pressure or temperature excursions following establishment of steady state operation.

a. In sequence, without delay:

i. Heater power off

ii. Preheater power off

iii. Primary and secondary pump power off

iv. Evacuate primary and secondary surge tanks to 0 psia. Primary loop will be dumped automatically when primary surge tank is evacuated.

TABLE XXXX

Cb-1Zr RANKINE SYSTEM CORROSION TEST LOOP OPERATION

Operation	Results of Operation	
	Pressure Changes	Temperature Changes
1. Increase potassium flow rate Quality 100%	Pressure drop increases across turbine simulator	Condenser temperature decreases; boiling temperature increases
2. Decrease potassium flow rate Quality 100%	Pressure drop decreases across turbine simulator	Condenser temperature increases; boiling temperature decreases
3. Increase sodium temperature Flow rate constant Quality 100%	Pressure drop increases across turbine simulator	Boiler temperature increases; condenser temperature decreases
4. Decrease sodium temperature Flow rate constant Quality 100%	Pressure drop decreases across turbine simulator	Boiler temperature decreases; condenser temperature increases
5. Increase potassium inventory Flow rate constant Quality 100%	Loop pressure increases and pressure drop across turbine simulator decreases	Boiler temperature increases; condenser temperature increases
6. Decrease potassium inventory Flow rate constant Quality 100%	Loop pressure decreases and pressure drop across turbine simulator increases	Boiler temperature decreases; condenser temperature decreases

b. If the leak is observed in the secondary system, open the isolation valve. Secondary system will then dump.

c. After secondary loop has been dumped, close the isolation valve with 2 ft-lbs of torque.

APPENDIX J

STRESS-CORROSION CRACKING OF VACUUM CHAMBER COOLING CHANNEL

1. Description of Vacuum Chamber

The failure which will be described in this appendix occurred in a water cooling channel of the 4' x 11' vacuum chamber, which was used in the 5000-hour loop test. The vacuum chamber which is constructed of Type 304L SS is shown in Figure 200. Heat radiated from the Cb-1Zr Corrosion Loop to the chamber wall is removed by water flowing through water channels located on the chamber walls.

2. Test Shutdown Caused by Failure of Chamber Wall and Resultant Pressure Rise

At approximately 0800 on January 8, 1966, the test was shut down after 3809 hours of continuous operation because of a pressure rise in the vacuum chamber. As shown in Figure 201, the pressure rose rapidly from the normal level of 2.1×10^{-8} torr to approximately 1×10^{-6} torr in 17 minutes. Since the pressure trace gave no indication of being an argon instability, as first suspected, the test engineer gave instructions to shut down the test.

Partial pressure scans taken after the test loop had been shut down indicated high concentrations of water vapor, and subsequent leak checking established that leaks were present between the water channel in the spool piece and the vacuum side in addition to numerous leaks from the water side of the cooling channel to the air side.

3. Description of Spool Piece, Examinations and Evaluation of the Cooling Channel Failure

A sketch of the spool piece is shown in Figure 202. The water channels on this component and the direction of the water flow are indicated. A cross section of a typical channel is also illustrated. During the leak checking operations, it became apparent that a large water-to-vacuum leak was present in a region where the top cooling channel of the spool crossed a vertical weld in the chamber wall. The channel in this region was cut away as shown in Figure 203, and an attempt was made to repair

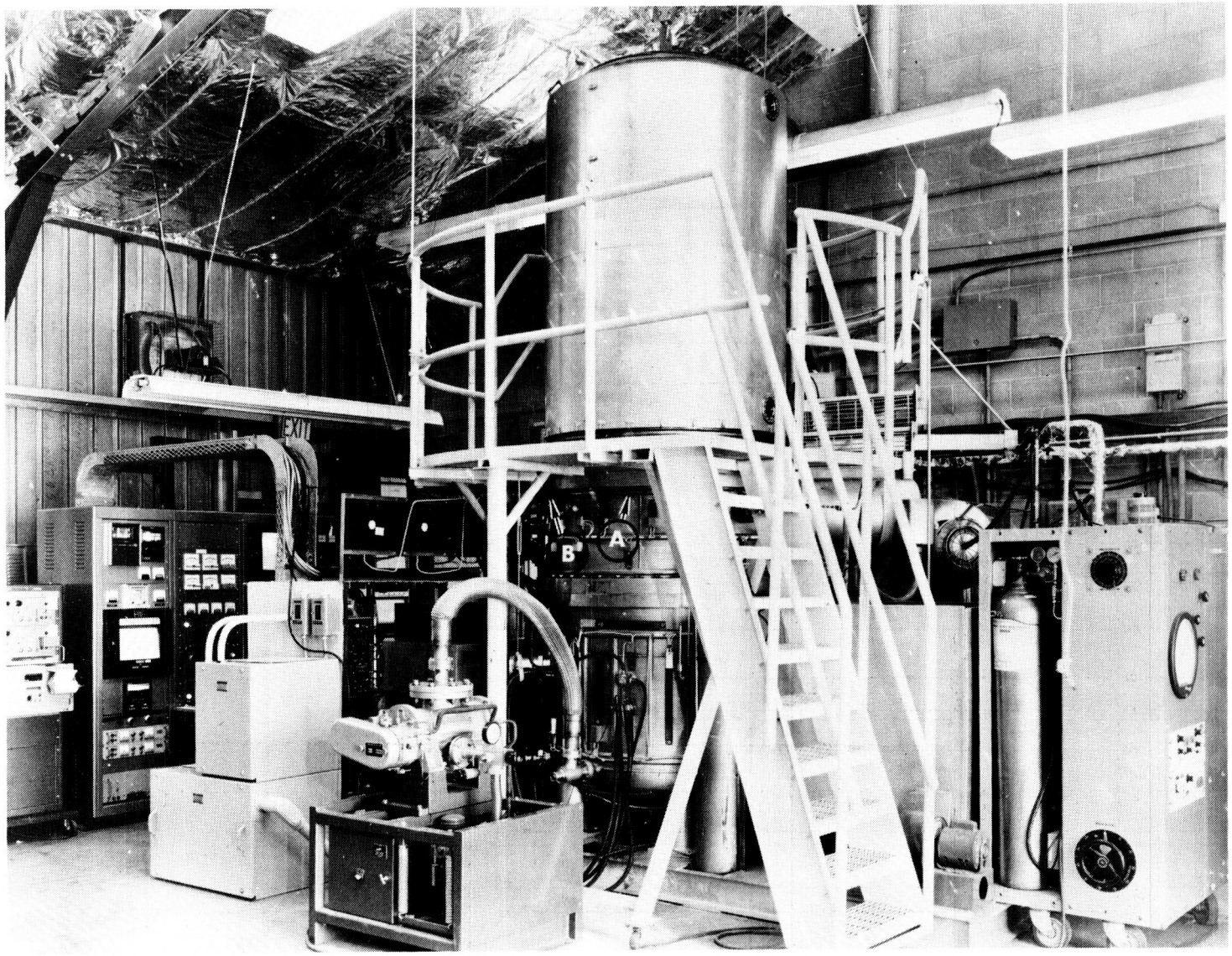

Figure 200. Cb-1Zr Corrosion Loop Test Chamber and Associated Equipment. Water Channel in Which Stress-Corrosion Cracking Occurred is Indicated by Arrows. (C65080602)

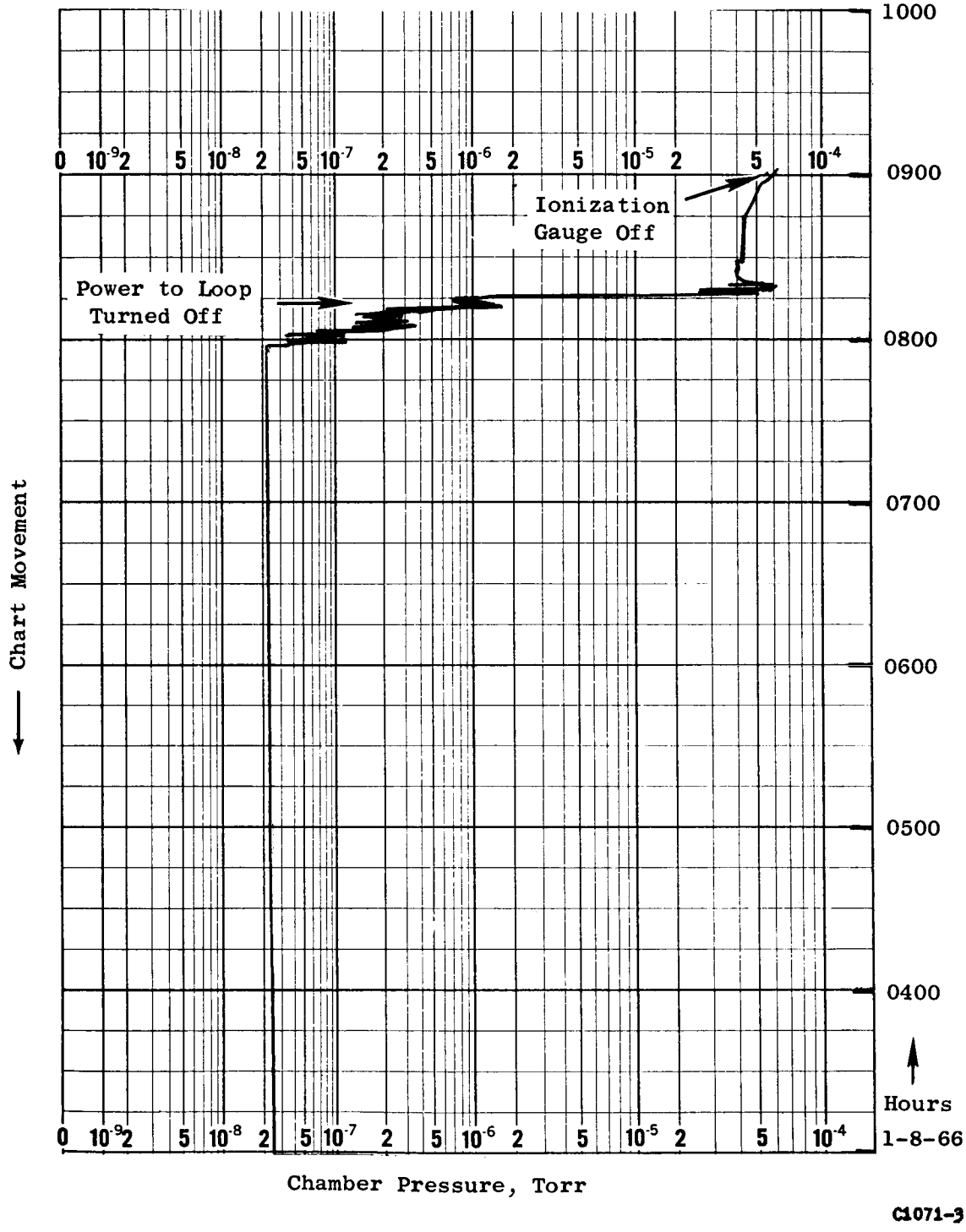

Figure 201. Cb-1Zr Corrosion Loop Vacuum Chamber Pressure During Period When the Test was Shutdown Because of a Water-to-Vacuum Leak in the Top Cooling Channel of the Spool Piece.

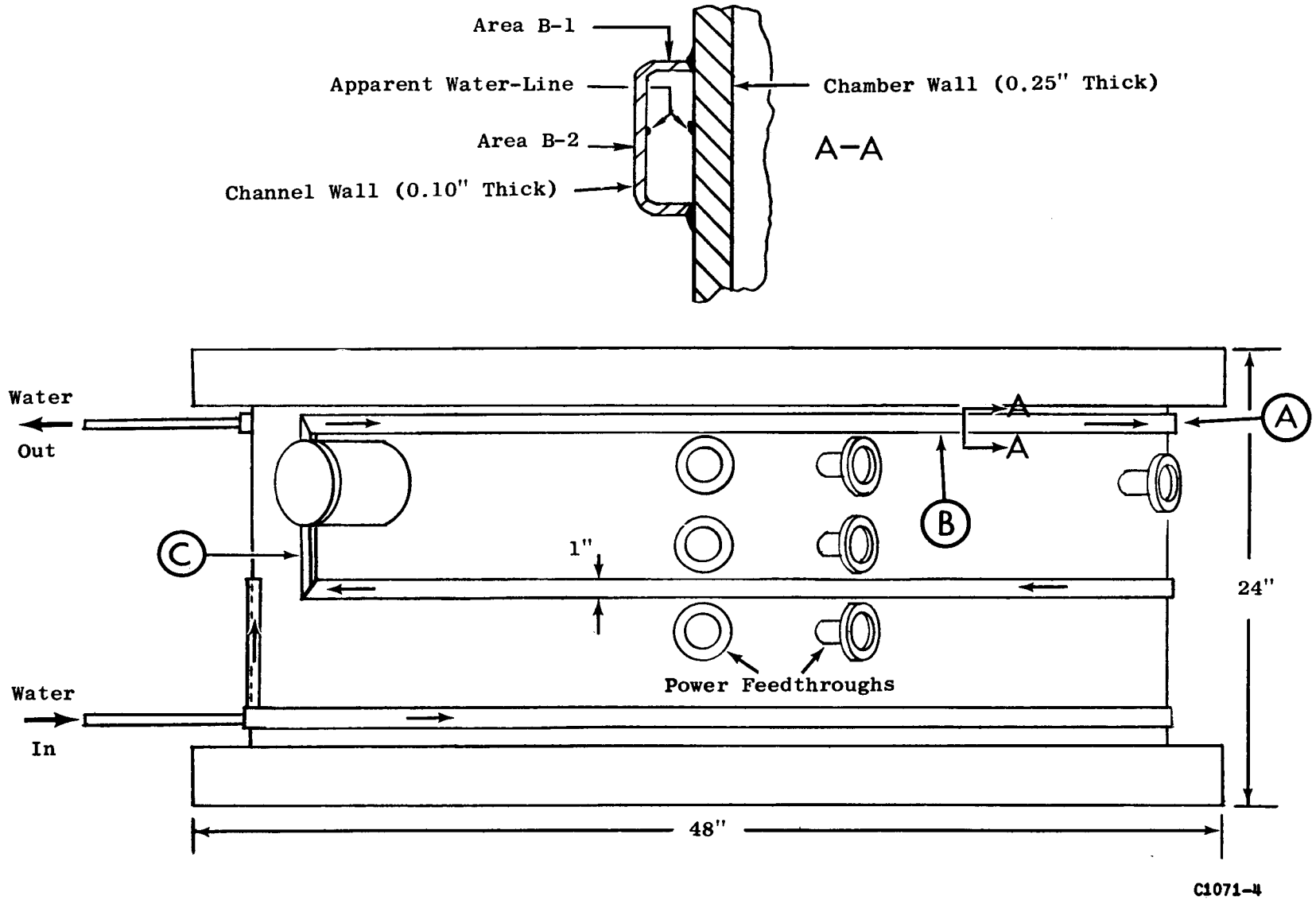

Figure 202. Spool Section of Vacuum Chamber Showing Locations, A, B, and C, Where Portions of the Cooling Channel Were Removed. Cross Section of Top Channel Shows Location of Metallographic Samples, B-1 and B-2, and Location of the Water-Line Deposits.

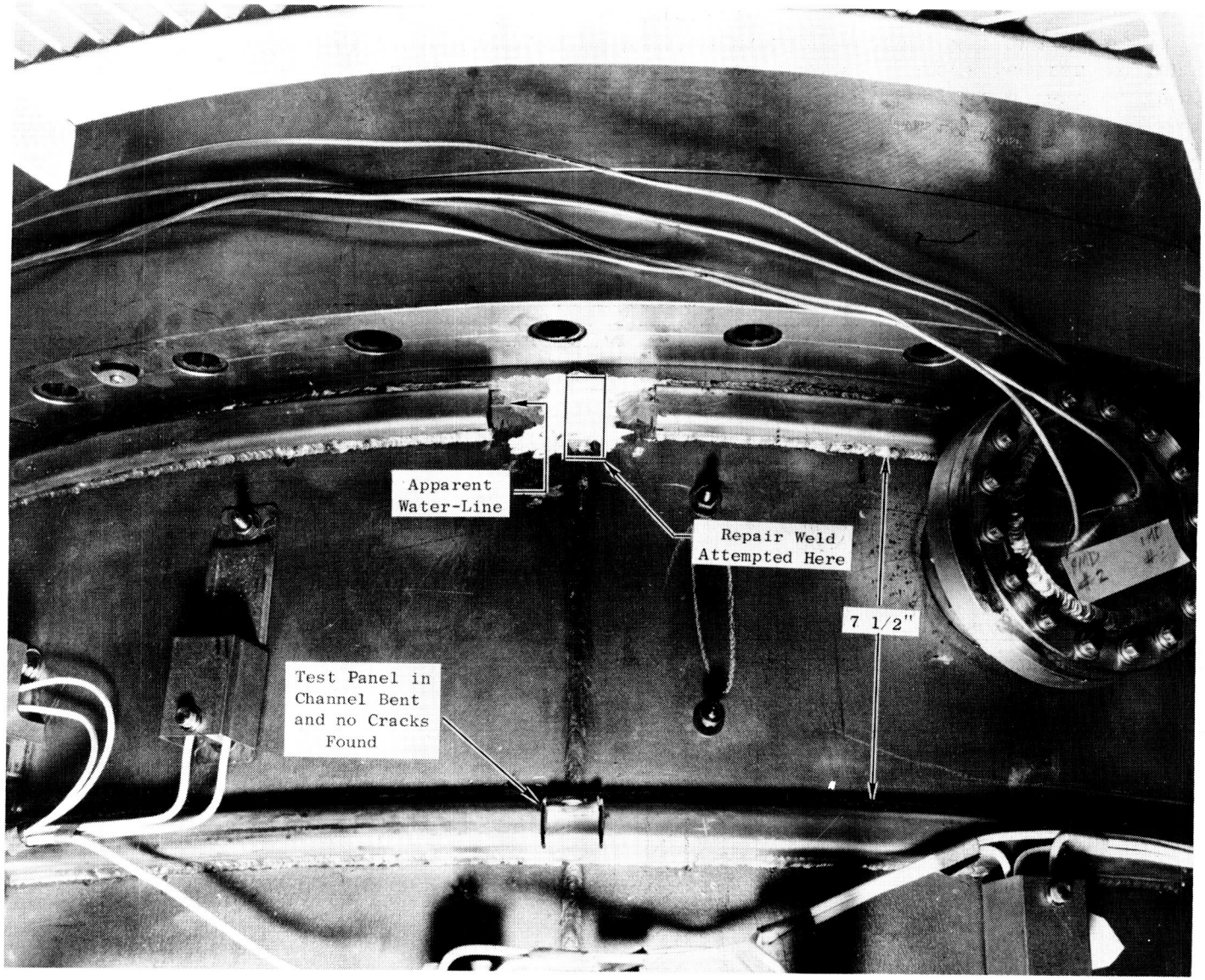

Figure 203. Upper Portion of the Spool Piece of the Chamber Corresponding to Area (A) in Figure 2 Showing Where First Section of Cracked Water Channel was Removed. Lower Channel was Found to be Ductile and Free of Cracks. (C66011401)

a visible crack in the chamber wall by welding. This resulted in the opening up of a multitude of cracks in adjacent portions of the chamber wall. At this point, corrosion of some type was suspected, and another section of top channel approximately 10 inches long was removed for additional inspection. This area is shown in Figure 204. Examination of the section of removed channel indicated gross cracking of the 0.1-inch-thick channel as shown in Figure 205. Figure 205(a) shows the inside surface of the top portion of the channel. Numerous marks made by the grinder used to remove the channel are evident. The complete destruction of the channel wall is apparent in Figure 205(b) which is an enlarged view of a segment of the channel following slight bending. Visual inspection of the chamber wall proper also indicated a multitude of cracks in the upper portion of the channel. Close examination of the cutaway regions of the chamber wall shown in Figures 203 and 204 revealed a thin line of white deposit near the mid-height of the channel. A corresponding line was found on the segment of channel which had been removed. A portion of this channel was bent so that equal amounts of deformation were given to regions above and below the deposit line. This specimen is shown in Figure 206. The line of white deposits and cracking observed in the region above this line are shown in this photograph. No cracks were detected in the deformed segment of channel located below the deposit line.

Metallographic examination of cross sections of the channel from the lower, uncracked region and the upper, cracked region are shown in Figure 207. (The hardness impressions shown are discussed later in this report.) Additional photomicrographs of the cracked regions are shown in Figure 208 at higher magnifications. The transgranular nature of the cracks is typical of stress-corrosion cracking in austenitic stainless steels.[71]

4. Additional Test Results

In an effort to shed as much light as possible on the conditions

---

(71) Phelps, E. H. and Mears, R. B., "The Effect of Composition and Structure of Stainless Steel Upon Resistance to Stress-Corrosion Cracking," First International Congress on Metallic Corrosion, London, April 1961, Butterworths (1962), p. 325.

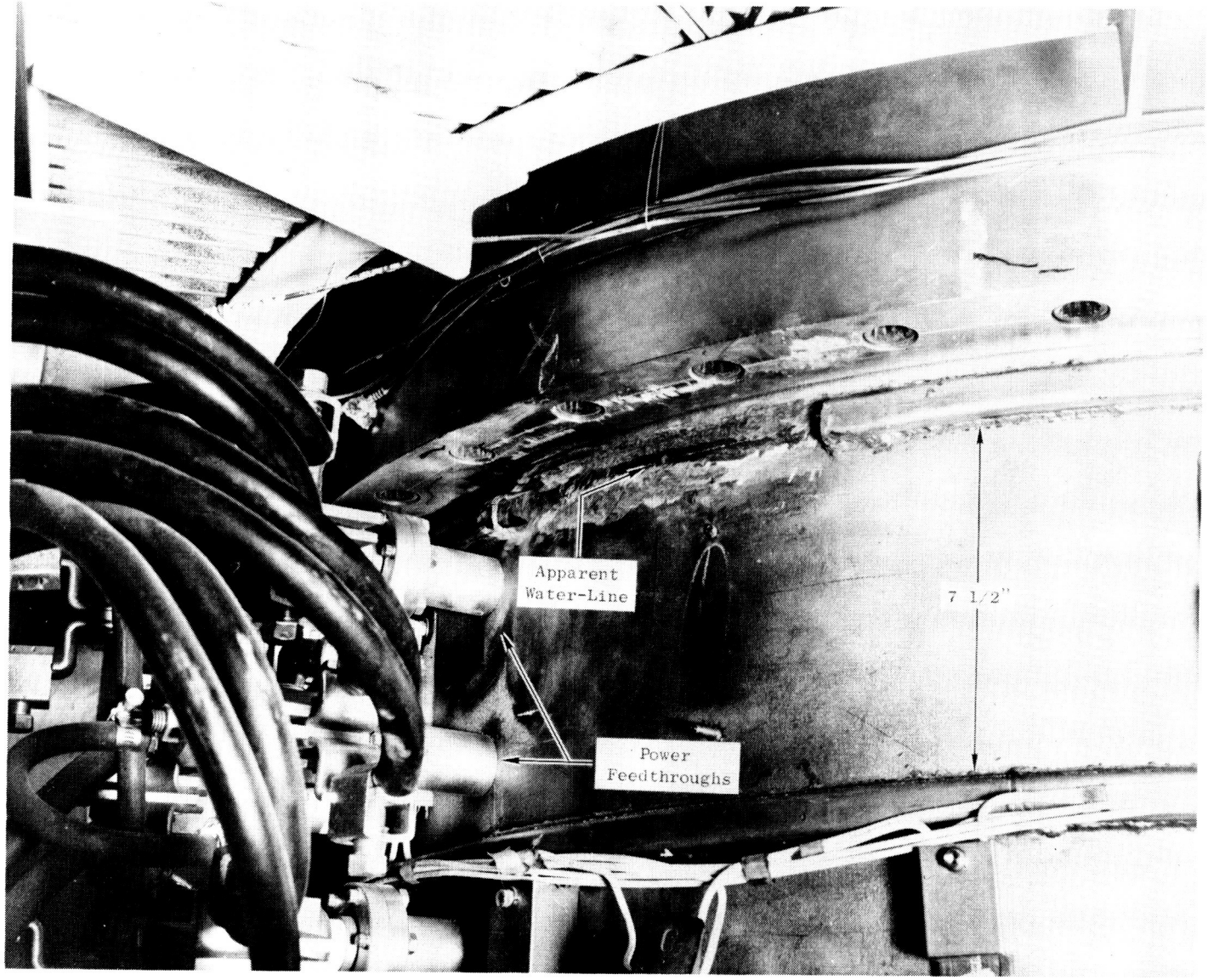

Figure 204. Upper Portion of the Spool Piece of the Chamber Corresponding to Area (B) in Figure 2 Showing Where Section of Cracked Water Channel was Removed. (C66011403)

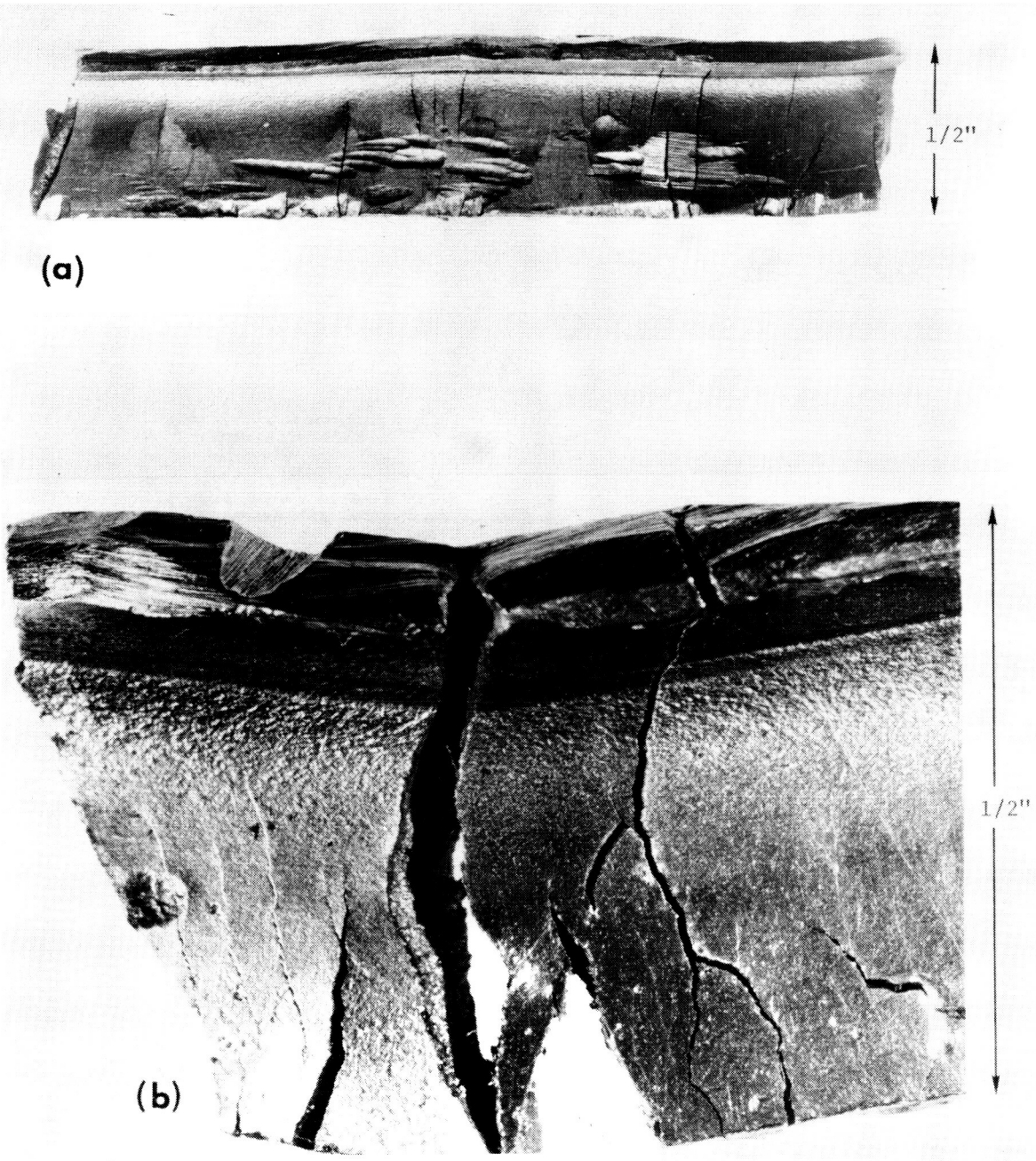

Figure 205. Water Side of the Top Portion of the Upper Cooling Channel of the Chamber Spool Piece. Section Shown was Taken from Area B-1 Indicated in Figure 4. Sample Shown in (b) is Typical of the Region Shown in (a) After Slight Bending. Grinding Marks on the Surface Shown in (a) Occurred During Removal of the Channel.

a) C66012125; b) C66011802

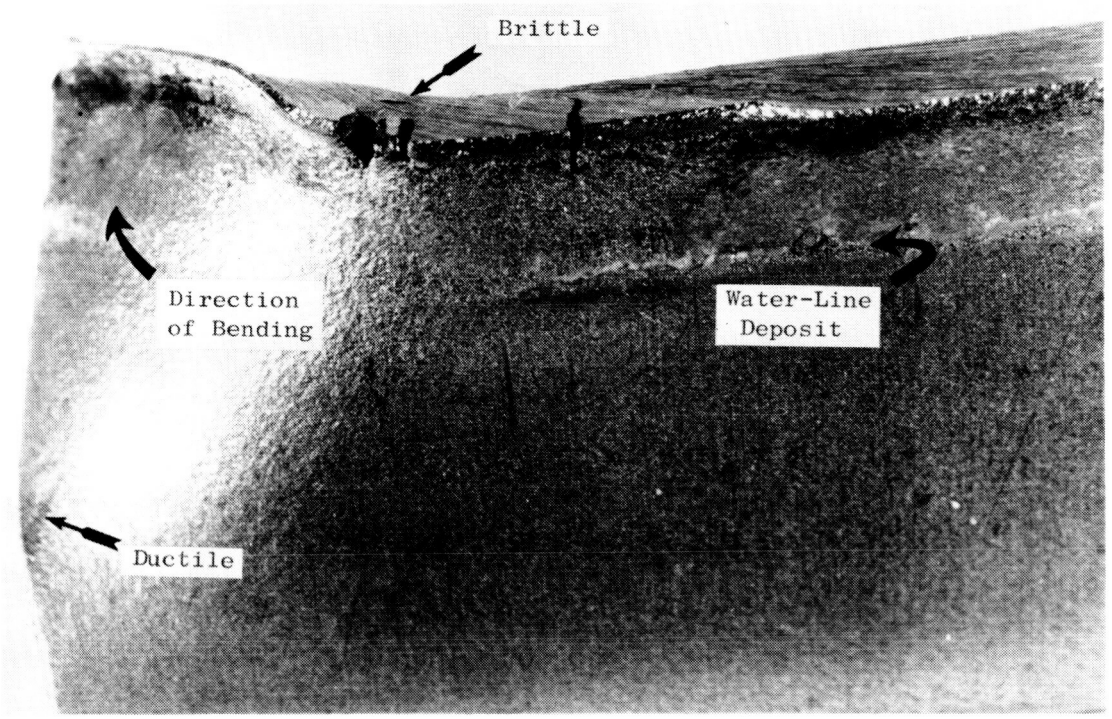

Figure 206. Appearance of Water Side of a Specimen Cut From the Region of the Top Cooling Channel Nea · the Water-Line Deposit. Corner of the Specimen was Bent to Illustrate Brittleness of the 0.10-Inch Thick Channel Above the Deposit Line. (C66011803)

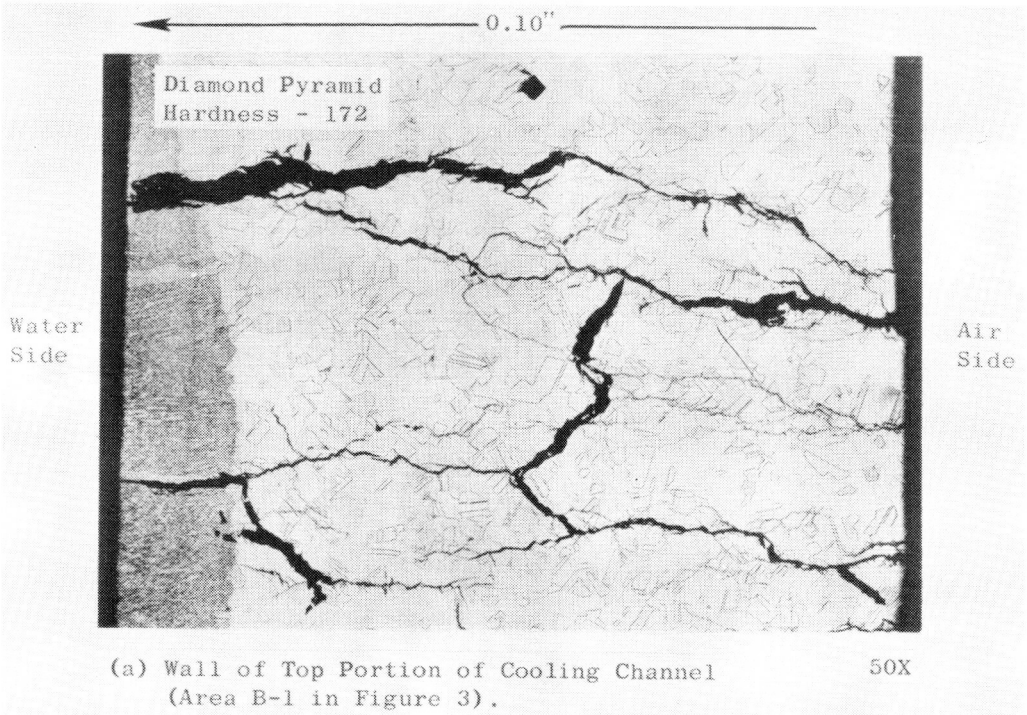

(a) Wall of Top Portion of Cooling Channel (Area B-1 in Figure 3). 50X

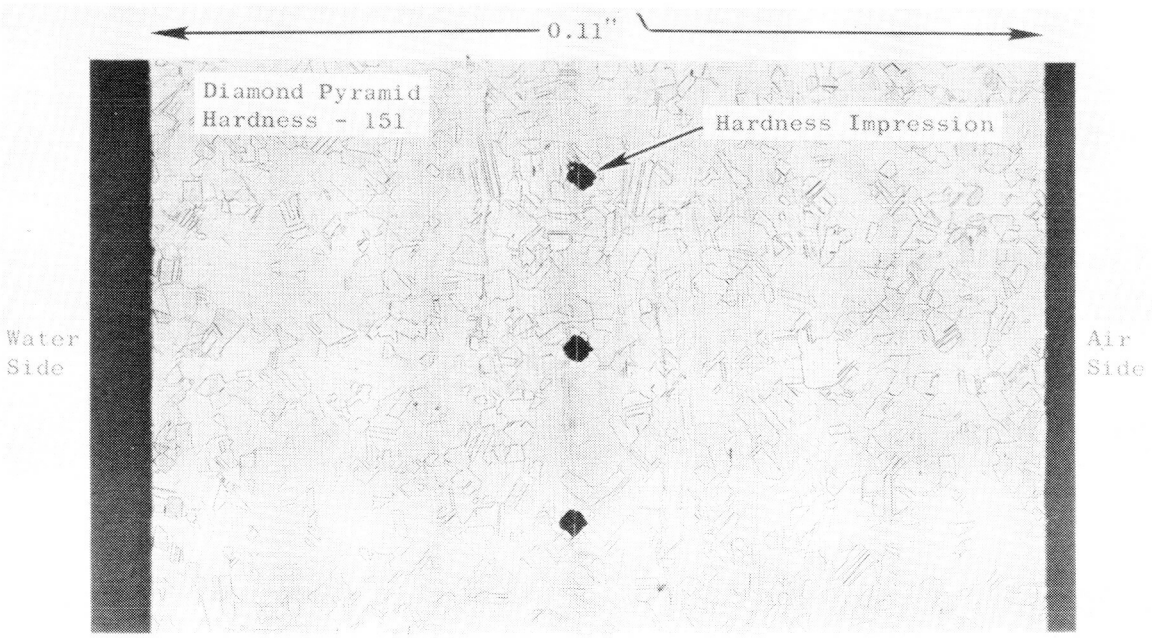

(b) Wall of Lower Portion of Cooling Channel (Area B-2 in Figure 3). 50X

Figure 207. Metallographic Sections of the Top Portion (a) and Lower Portion (b) of the Upper Water Cooling Channel of the Chamber Spool Piece.

Etchant: 10g Oxalic Acid, 100cc Water, Electrolytic

a) B290118
b) B290217, B290218

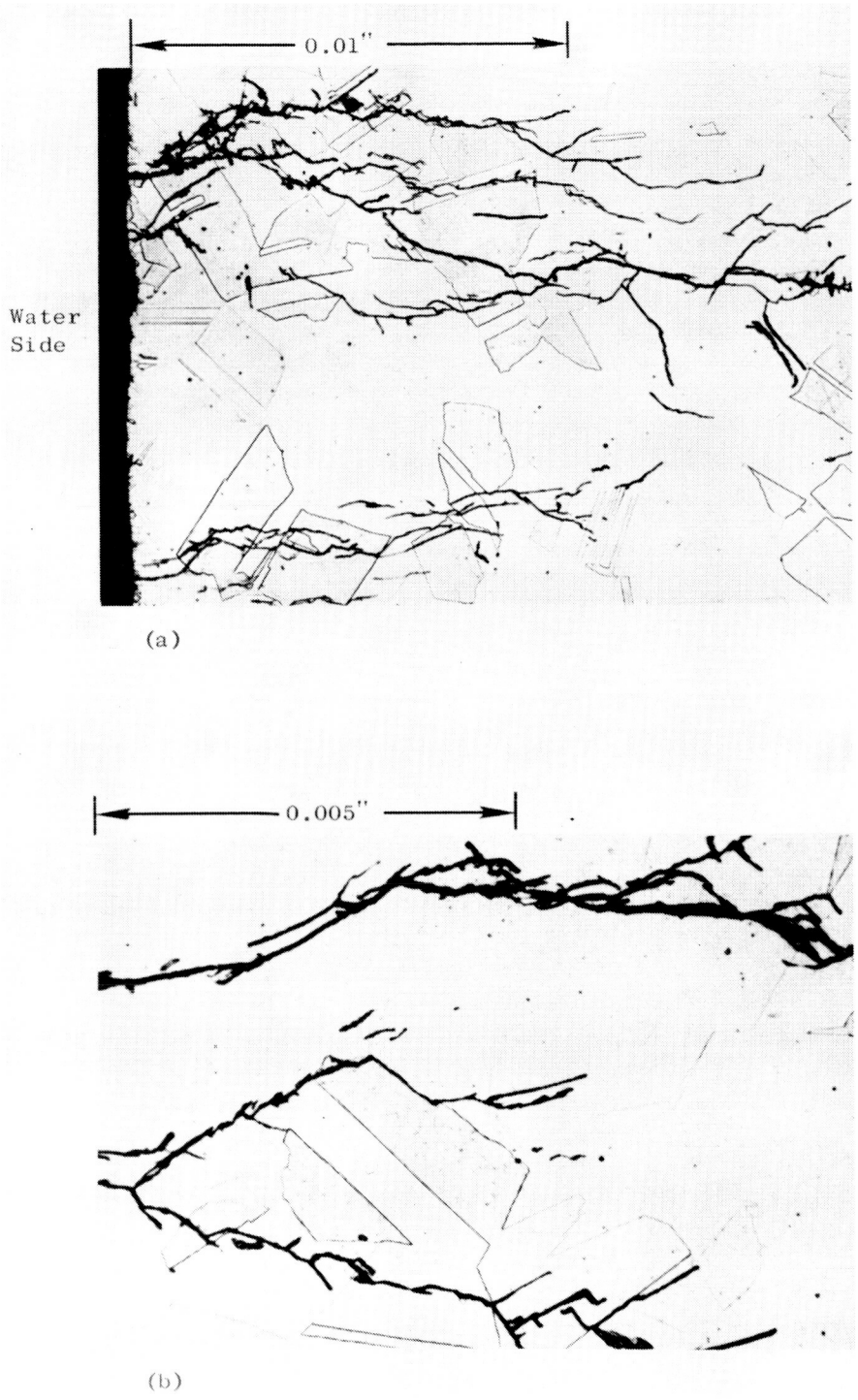

Figure 208. Photomicrographs of the Water Cooling Channel Wall at Two Magnifications. Note the Transgranular Nature of the Cracks Typical of Stress-Corrosion Cracking.

Etchant: 10g Oxalic Acid, 100cc Water, Electrolytic

a) B290115, 250X
b) B330112, 500X

responsible for the water channel failure described above, a number of tests were conducted, and these results are described below.

The results of analyses performed on a sample of the vacuum chamber cooling water are given in Table XXXXI. The chloride concentration is thought to be the most significant aspect of the analytical results since the presence of chlorides and stress are normally the essential elements required to produce stress-corrosion cracking in stainless steel.(72) (The referenced ASTM report is one of the most condensed and useful sources of information on the problem of stress-corrosion cracking and will be cited a number of times in this section.) Although the chloride concentration is no doubt an important factor in most cases of stress-corrosion cracking, it should be pointed out that for some failures, "chlorides and stress were concluded to be the most likely cause of failure although sensitive chemical determinations did not disclose their presence."(72)

Several additional quotes from the ASTM report are felt to be relevant to the cracking of the cooling channel. "It is abundantly clear from this survey that no water of whatever degree of purity can be trusted as long as there is a mechanism whereby dissolved solids (chlorides) can be concentrated. There are numerous cases (of stress-corrosion cracking) involving only several ppm of chlorides. In the majority of these cases concentration has occurred by thermal means."(73) Regarding the pH of the water, the ASTM reference reported incidents of stress-corrosion cracking for cases where the pH's varied from values of 2 to 14.

Samples of the upper cooling channel of the spool piece were analyzed to determine the carbon, hydrogen, nitrogen, and oxygen concentrations of both the cracked and the adjacent uncracked areas, and these results

---

(72) Report on Stress-Corrosion Cracking of Austenitic Chromium-Nickel Stainless Steel, ASTM Special Technical Publication No. 264, Published by American Society for Testing Materials, March 1960, p. 6.

(73) Ibid, p. 9.

TABLE XXXXI

ANALYSIS* OF WATER SAMPLE TAKEN FROM COOLING CHANNEL EXIT LINE

	Chemical Analysis, ppm
Total hardness as $CaCO_3$	130
Calcium as $CaCO_3$	54
Magnesium as $CaCO_3$	76
Carbonate as $CaCO_3$	0
Bicarbonates as $CaCO_3$	42
Chlorides as Cl	26
Chlorine as Cl_2	0

*pH: 8.15

Conductance: 350×10^{-6} mhos

TABLE XXXXII

CHEMICAL ANALYSES OF SAMPLES OF TYPE 304L STAINLESS STEEL* FROM THE TOP COOLING CHANNEL OF THE VACUUM CHAMBER SPOOL PIECE

	Chemical Analysis, ppm				
	C	H	N	O	S
Cracked Sample	260, 290	10	459	313**	-
Uncracked Sample	210, 270	5	444	100	90

*Type 304L SS was the specified material of construction, and spectrographic analysis of samples of the cracked channel indicated that the material was this type of stainless steel.

**Cracked surfaces slightly oxidized when heated during leak checking operations. This was probably responsible for the high oxygen concentration.

are given in Table XXXXII. The carbon and sulfur concentrations were found to be below the specified maximum value[74] of 300 ppm. Spectrographic analysis confirmed that the channel material was of the 18-8 non-stabilized stainless steel-type which includes Type 304L SS.

Hardness surveys were conducted on the metallographic specimens taken from the cracked region, B-1 in Figure 202, and the uncracked region, B-2 in Figure 202. The average of ten hardness impressions in the cracked region yielded a DPH* value of 172. The average hardness value obtained in the uncracked specimen was DPH-151. These hardness values may be compared with handbook[75] values for Type 304 SS which indicated the following hardnesses in the various conditions: annealed-DPH-125, 10 percent cold work-DPH-160, and 20 percent cold work-DPH-205. This comparison suggests that both the upper portion (B-1) and the vertical portion (B-2) of the channel had the equivalent of approximately 10 percent cold work, which would be sufficient to contribute to stress-corrosion cracking if the other conditions, such as chloride and dissolved oxygen in the water, were also present. Although there was metallographic evidence of cold work in the structure of the channel in the bends (DPH-200), the structure of the specimens in the flat regions of the channel (DPH-151-172) showed little evidence of cold work (see Figures 207 and 208).

In an effort to determine if stress-corrosion cracking had occurred in the other cooling channels of the spool piece or in the channels of the other sections of the vacuum chamber shown in Figure 200, a number of cuts were made in selected locations. One of these test panels is shown in Figure 203. Three sides of the test panel were cut, and the "flap" was then bent out approximately 75°. The inner surface was then

---

(74) ASTM Designation A240-63.

* Diamond Pyramid Hardness, Load: 500 g.

(75) Metals Handbook, Vol. 1, 8th Edition, 1961, p. 544.

examined visually for cracks. No cracks, pits, or significant amounts of corrosion products were found. Additional test panels were cut and bent at location C in Figure 202 and in the top cooling channels of both the sump and the bell jar sections of the vacuum chamber. In all cases the channels were free of cracks and very similar in appearance to the middle channel of the spool piece described above.

5. Discussion

Review of the findings of this investigation indicates that stress-corrosion cracking of the stainless steel cooling channel was responsible for the chamber failure.

The critical factors associated with most of the stress-corrosion failures discussed in the ASTM report,[72] i.e., fabrication and welding stresses, chlorides, and dissolved oxygen, were present in the chamber cooling channels. It seems most probable that the localized natures of the failure in the top half of the upper channel of the spool piece was caused by concentration of chlorides on the walls in this region. The water-line deposit shown in Figures 203, 204, and 206 indicates that this channel was only partially filled by the cooling water. The partially filled condition in this channel is attributed to: (a) extensive blockage of the inlet and outlet water flow in the spool piece by the accumulation of corrosion products in the water-line fittings as illustrated in Figure 209 and (b) the location of the water outlet fitting at the midpoint of the top channel. The location of the fitting at this point permitted the channel to drain to the approximate location of the water-line deposit with the low-flow condition which resulted from the partial blockage of the restrictions in the inlet and outlet fittings.

The outlet temperature of the cooling water from the cracked channel did not exceed 120°F during the 3809 hours of continuous test loop operation which preceded the failure. Although this would appear to be quite low for evaporation and concentration of chlorides, approximately 34 percent of the reported stress-corrosion failures[76] occurred with systems operating between 100°F and 200°F. It was also reported that

---

(76) Reference 72, p. 11.

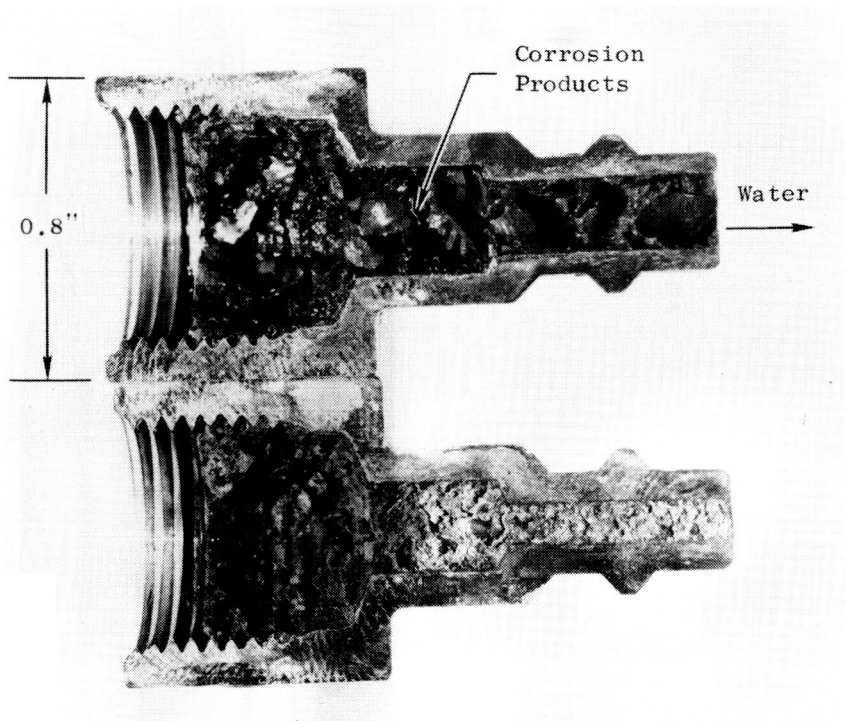

Figure 209. Cadmium-Plated Steel Fitting Used to Connect Water Inlet and Outlet Lines to Spool Piece Cooling Channel. Both Inlet and Outlet Fittings Partially Plugged with Corrosion Products. (C66012124)

a significant number of cases of stress-corrosion cracking have occurred at or near room temperature.

It is of interest to note that in the reported incidents of stress-corrosion cracking[77] 65 percent of the cases involved components containing stresses introduced by fabrication and welding. Stresses of both types were present in the region of most extensive cracking of the cooling channel. The hardness data obtained on the cooling channel specimens indicated that stress induced by cold work was certainly present.

The phenomena responsible for the failure seems to be quite obvious at this time. The cracked channel has been isolated from the other channels* and will be pumped by a vacuum system independent of the main chamber pumping system. The repaired channel and the turbomolecular pumping system which will be used to maintain the pressure in the "cracked" channel in the 10-7 - 10-8 torr range are shown in Figure 210.

Modifications of the chamber cooling system are planned following completion of the 5000-hour test which will minimize the possibility of a recurrence of this problem. The modifications planned are listed below:

a. The spool piece of the chamber in which the cracking of the cooling channels was observed will be rebuilt by the vendor using only the flanges from the cracked spool piece.
b. The inlet and outlet fittings of the water cooling system on the spool piece will be located so as to assure that the channels are completely filled with water during test operation.
c. Valves will be placed on the outlet side of each of the water cooling circuits.
d. Stainless steel fittings will be used to replace the cadmium plated steel quick disconnect fittings in the water cooling circuits.
e. Full flow filters will be placed in each of the cooling circuits to prevent particulate material from entering the cooling circuits.

---

(77) Reference 72, p. 8.

* The removed segments of the channel were replaced with new stainless sheet, and the remaining cracks were sealed with epoxy resin recommended for vacuum applications.

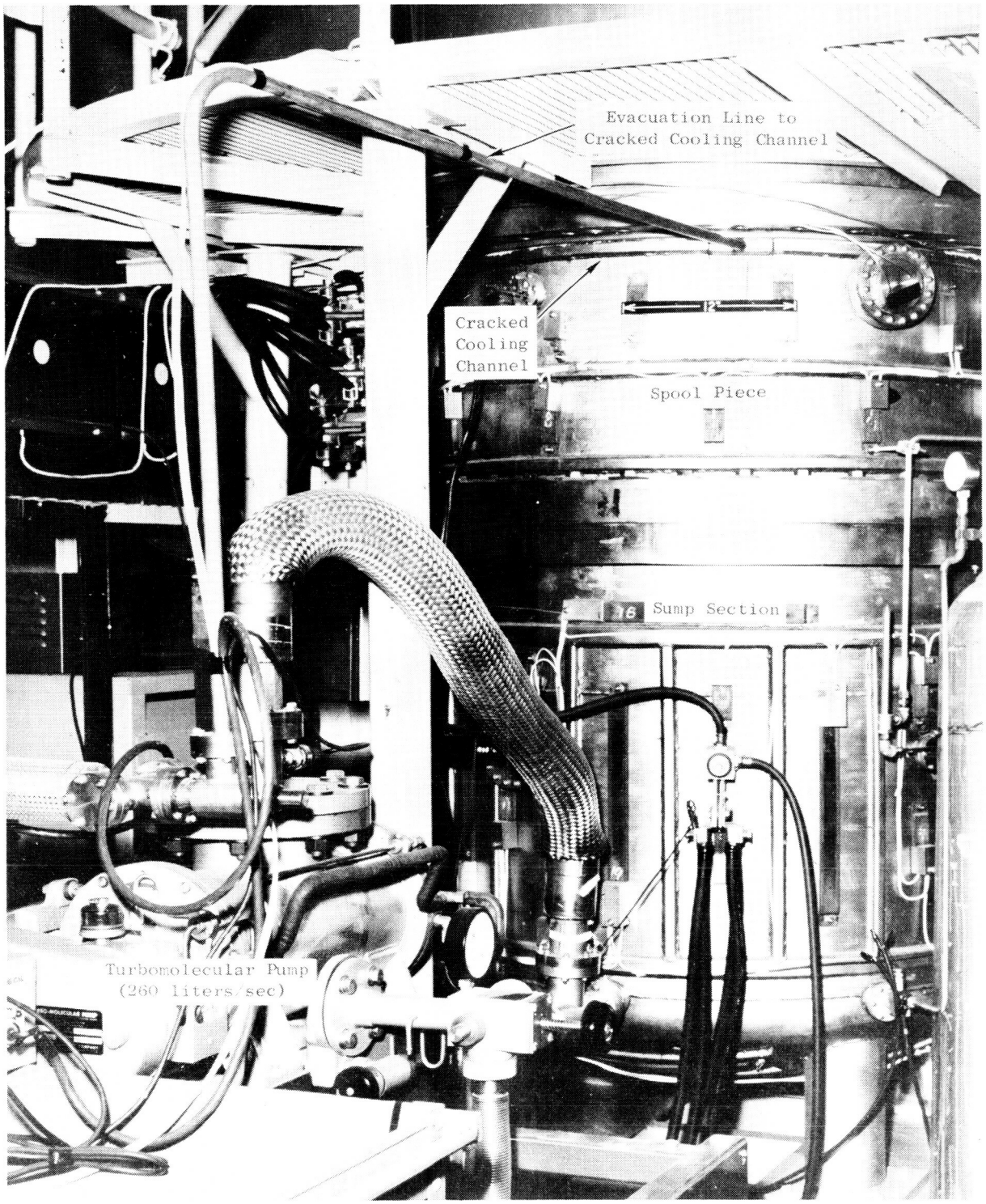

Figure 210. Spool Piece and Sump Section of the Prototype Corrosion Loop Test Chamber Showing the Evacuation Line and the Turbomolecular Pumping System Used to Pump Cracked Cooling Channel to a Pressure of 10^{-8} Torr.

(C66031015)

f. Low-flow switches will be placed in each of the three parallel circuits in the chamber cooling system. Low flow in any one of the circuits will activate an alarm on the control panel.

g. The flow in each circuit will be measured every 100 hours to assure that low-flow switches are operating properly and to detect any reduction in flow.

In summary, the cracking observed in the stainless steel water cooling channel described above is attributed to operation with a partially filled water cooling channel, and the modifications and procedures described will prevent a recurrence of this in the future.

APPENDIX K

DRAINING, SAMPLING, AND FILTERING OF THE POTASSIUM AND SODIUM CIRCUITS OF THE LOOP

Following completion of the 100-hour distillation period during which sodium and potassium were collected in the respective surge tanks located in the lower portions of the test chamber, the draining, sampling, and filtering of the loop circuits were initiated.

The posttest procedures used to prepare the transfer and sampling systems prior to the transfer of the alkali metals from the loop surge tanks and the subsequent sampling and filtering of the alkali metals are described in detail in the following section.

POTASSIUM LOOP SAMPLING PROCEDURE

Operation and Purpose

Prior to draining the potassium into the transfer system charge pot, the following operations were carried out.

1. Attached high-vacuum sampler and filtration system to the transfer system to obtain samples and filter most of the alkali metal into the disposal tank.

2. Blew residual alkali metal from transfer lines into the disposal tank to minimize contamination of the test metal with the fill metal.

Procedure

1. (a) Cleaned, assembled, and attached high-vacuum sampler. See schematic diagram (Figure 211).
   (b) Assembled a 5-micron filter by TIG welding with backup gas.
   (c) Installed the filter and transfer line between valves U and W with swagelok and conoseal connections where possible--otherwise welded with backup gas.
   (d) Helium leak checked all connections of the assembly. Maximum allowable leakage = 5×10^{-10} std cc/sec.
2. (a) Evacuated the transfer system lines through valve Z with valves FF, W, S, DD, and the bottom sample tube valve closed (sampler and transfer line were already under vacuum from leak checking operation).
   (b) Heated all transfer system lines to 250 ± 30°F and outgassed the sampler until the pressure rise rate was less than one micron-liter per minute.
   (c) Closed valves X and GG and pressurized the sampler and charge pot to 15 psia. See Figure 211.
   (d) Opened valve GG and blew argon through valves GG, T, and V into the disposal tank until pressures equalized.
   (e) Opened valve X, closed Valve T, and again evacuated the disposal tank.
   (f) Closed valve X, pressurized the sampler to 15 psia, and blew argon through the valve on the bottom of the sample tube through valves U and V into the disposal tank until the pressures equalized.

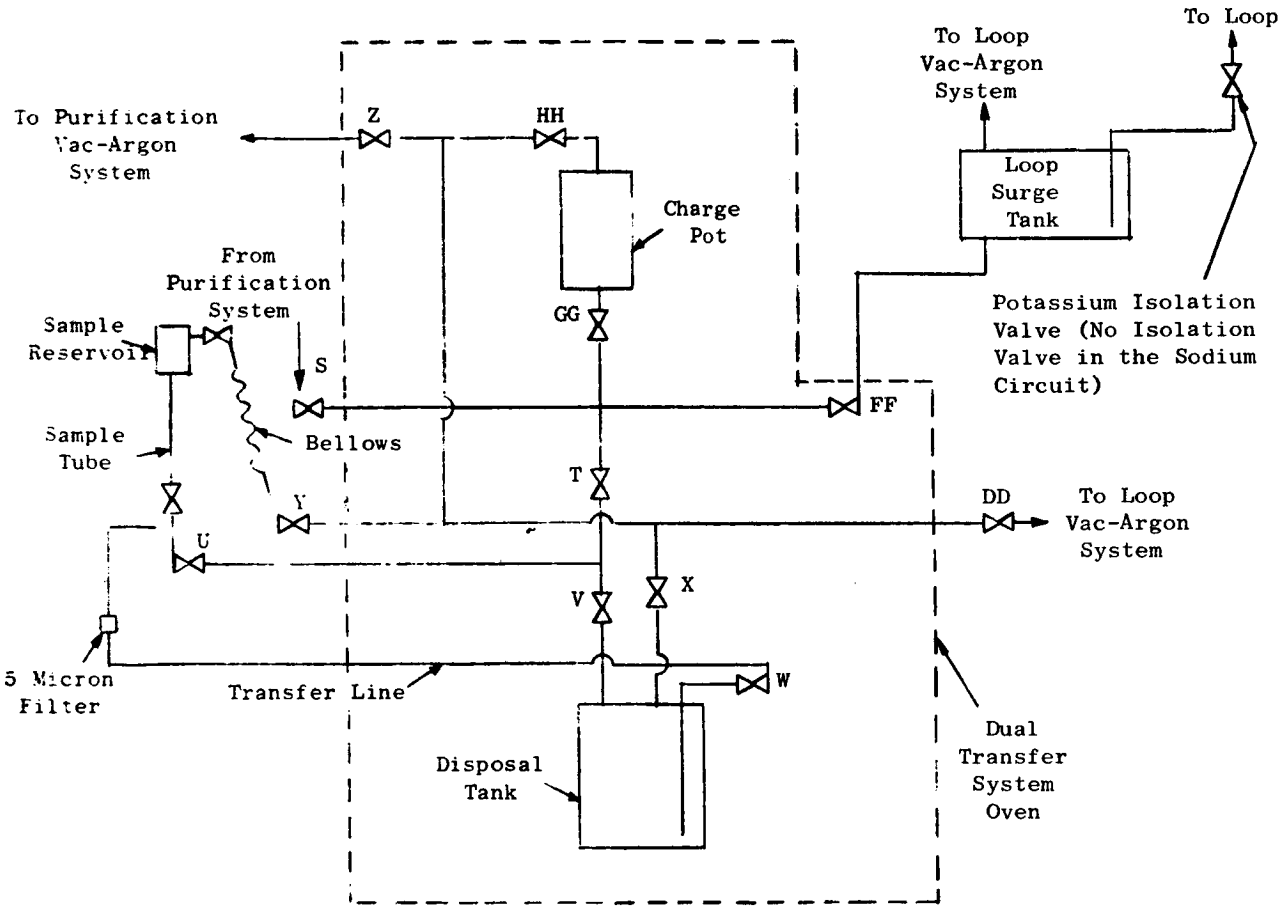

Figure 211. Schematic Diagram of the Cb-1Zr Corrosion Test Loop Draining, Sampling and Filtering System.

POTASSIUM LOOP SAMPLING PROCEDURES (Cont'd)

Operation and Purpose	Procedure
	(g) Opened valve X, closed sample tube bottom valve, and evacuated transfer system lines through valve Z.
3. Drained potassium into the transfer system charge pot as previously indicated.	
4. Obtain potassium sample from charge tank.	4. (a) Closed valves FF, DD, GG, V, W, S, and the valve on the bottom of the sample tube. See Figure 211. Double checked that valves V and W were closed.
	(b) Closed valves Y and X with the sampler and disposal tank evacuated.
	(c) Opened valve GG, opened the valve on the bottom of the sample tube, and flushed about 100 cc of potassium into the sampler reservoir.
	(d) Closed the valve on the bottom of the sampler tube, opened valve Y to pressurize the sampler, and cooled the sample to room temperature.
5. Filtered the remaining potassium into the disposal tank.	5. (a) Pressurized the charge pot to 15-17 psia.
	(b) Opened valve W and filtered the potassium in the charge pot into the disposal tank. Filtration was complete when a rapid pressure drop occurred, followed by a constant pressure reading.
	(c) Closed valve W, opened valve X, and cooled transfer system to room temperature at 15-17 psia after sampling and filtering potassium charge.

SODIUM LOOP SAMPLING PROCEDURE

Operation and Purpose	Procedure
Prior to draining the sodium into the transfer system charge pot, the following operations were carried out.	
1. Attached high-vacuum sampler and filtration system to the transfer system to obtain samples and filtered most of the alkali metal into the disposal tank.	1. (a) Cleaned, assembled, and attached high-vacuum sampler. See Figure 211. (b) Assembled 5-micron filter by TIG welding with backup gas. (c) Installed the filter and transfer line between valves U and W with swagelok and conoseal connections where possible - otherwise welded with backup gas. (d) Helium leak checked all connections of the assembly. Maximum allowable leakage = 5×10^{-10} std cc/sec.
2. Flow residual alkali metal in transfer lines into the disposal tank to minimize contamination of the hot metal with the fill metal.	2. (a) Evacuated the transfer system lines through valve Z with valves FF, W, S, DC, and the bottom sample tube valve closed (sampler and transfer line were already under vacuum from leak checking operation). (b) Heated all transfer system lines to 250 ± 30°F and outgassed the sampler until the pressure rise rate was less than one micron-liter per minute. (c) Closed valves X and GG and pressurized the sampler and charge pot to 15 psia. (d) Opened valve GG and blew argon through valves GG, T, and V into the disposal tank until pressures equalized. (e) Opened valve X, closed valve T, and again evacuated the disposal tank. (f) Closed valve X, pressurized the sampler to 15 psia, and blew argon through the valve on the bottom of the sample tube through valves U and V into the disposal tank until pressures equalized.

SODIUM LOOP SAMPLING PROCEDURE (Cont'd)

Operation and Purpose	Procedure
	(g) Opened valve X, closed sample tube bottom valve, and evacuated transfer system lines through valve Z.
3. Drained sodium into the transfer system charge pot as previously indicated.	
4. Obtained sodium sample from charge tank.	4. (a) Closed valves FF, DD, GG, V, W, S, and the valve on the bottom of the sample tube. See Figure 211. Double checked that valves V and W were closed.
	(b) Closed valves Y and X with the sampler and disposal tank evacuated.
	(c) Opened valve GG, opened the valve on the bottom of the sample tube, and flushed about 100 cc of sodium into the sampler reservoir.
	(d) Closed the valve on the bottom of the sample tube, opened valve Y to pressurize the sample, and cooled the sample to room temperature.
5. Filtered the remaining sodium into the disposal tank.	5. (a) Pressurized the charge pot to 15-17 psia.
	(b) Opened valve W and filtered the sodium in the charge pot into the disposal tank. Filtration was complete when a rapid pressure drop occurred, followed by a constant pressure reading.
	(c) Closed valve W, opened valve X, and cooled transfer system to room temperature at 15-17 psia after sampling and filtering potassium charge.

XVII. REFERENCES

(1) Hoffman, E. E. and Holowach, J., Cb-1Zr Thermal Convection Loop, Potassium Corrosion Test Loop Development Topical Report No. 5, R67SD3014, General Electric Company, Cincinnati, Ohio, June 15, 1967.

(2) Hoffman, E. E. and Holowach, J., Cb-1Zr Pumped Sodium Loop, Potassium Corrosion Test Loop Development Topical Report No. 6, R67SD3015, General Electric Company, Cincinnati, Ohio.

(3) Hoffman, E. E. and Holowach, J., Cb-1Zr Pumped Sodium Loop, Potassium Corrosion Test Loop Development Topical Report No. 6, R67SD3015, General Electric Company, Cincinnati, Ohio.

(4) Hoffman, E. E. and Holowach, J., Cb-1Zr Pumped Sodium Loop, Potassium Corrosion Test Loop Development Topical Report No. 6, R67SD3015, General Electric Company, Cincinnati, Ohio.

(5) Hoffman, E. E., "Boiling Potassium Stability Studies," Metal and Ceramic Division Annual Progress Report for Period Ending May 31, 1963, ORNL-3470, November 11, 1963, p. 114-118.

(6) Private Communication, R. E. MacPherson, Oak Ridge National Laboratory.

(7) Private Communication, C. J. Klamut, Brookhaven National Laboratory.

(8) Tippets, F. E., Alkali Metal Boiling and Condensing Investigations, Report No. 5, NASA Contract NAS 3-2528, General Electric Company, Cincinnati, Ohio, April 20, 1964, p. 12.

(9) Alkali Metals Boiling and Condensing Investigation, Quarterly Progress Report No. 4, NASA Contract NAS 3-2583, SPPS, MSD, General Electric Company, July 1963.

(10) Alkali Metals Boiling and Condensing Investigations, Quarterly Progress Report No. 6, NASA Contract NAS 3-2583, SPPS, MSD, General Electric Company, May 1964.

(11) AEC-NASA Liquid Metals Information Meeting, CONF-650411, 1965, p. 237.

(12) Rossbach, R. J., Space-Vehicle Rankine Cycle Power Plant Potassium - Turbine Development, ASME 63-WA-326, November 1963.

(13) Faires, V., Applied Thermodynamics, The MacMillan Company, New York, 1947, p. 351.

(14) Ewing, C. T., Stone, J. P., Spann, J. R., Steinkuller, E. W., Williams, D. D., and Miller, R. R., High-Temperature Properties of Potassium, NRL Report 6233, September 24, 1965.

XVII. REFERENCES (Cont'd)

(15) Dotson, L. E., Emittance Coating Studies on Cb-1Zr Alloy, General Electric Company Report, R61FPD571, March 15, 1962.

(16) Emanuelson, R. C., Determination of the Emissivity of Materials, Semiannual Progress Report for Period May 14, 1964 to November 15, 1964, Pratt and Whitney Aircraft, NASA CR-54268.

(17) Affel, R. G., Burger, G. H., and Pearce, C. L., Calibration and Testing of 2- and 3 1/2-in. Magnetic Flowmeters for High-Temperature NaK Service, ORNL-2793.

(18) Frank R. G., et al., Material and Process Specifications for Refractory Alloy and Alkali Metals - Potassium Corrosion Test Loop Development Topical Report No. 2, R66SD3007, December 13, 1965, General Electric Company, Cincinnati, Ohio.

(19) Lyon, T. F., Purification and Analysis of Helium for the Welding Chamber, Potassium Corrosion Test Loop Development Topical Report No. 1, NASA CR-54168, General Electric Company, Cincinnati, Ohio, July 1, 1965, p. 35.

(20) Hoffman, E. E. and Holowach, J., Cb-1Zr Pumped Sodium Loop, Potassium Corrosion Test Loop Development Topical Report No. 6, R67SD3015, General Electric Company, Cincinnati, Ohio, December 20, 1967, p. 35.

(21) Hoffman, E. E. and Holowach, J., Cb-1Zr Pumped Sodium Loop, Potassium Corrosion Test Loop Development Topical Report No. 6, R67SD3015, General Electric Company, Cincinnati, Ohio, December 20, 1967, p. 42.

(22) Ibid, p. 37.

(23) Hoffman, E. E. and Holowach, J., Cb-1Zr Pumped Sodium Loop Potassium Corrosion Test Loop Development Topical Report No. 6, R67SD3015, General Electric Company, Cincinnati, Ohio, December 20, 1967, p. 51.

(24) Frank, R. G., et al., Material and Process Specifications for Refractory Alloy and Alkali Metals - Potassium Corrosion Test Loop Development Topical Report No. 2, R66SD3007, December 13, 1965, General Electric Company, Cincinnati, Ohio, p. 269.

(25) Cheronis, N. D., Techniques of Organic Chemistry, Interscience Publishers, Inc., New York, N. Y., 1954, p. 466-467.

(26) Barrington, Alfred A., High Vacuum Engineering, Prentice-Hall, Inc. Englewood Cliffs, N. J., 1963, p. 91.

(27) Hayward, W. H. and Jepsen, R. L., "A Simple High Vacuum Gauge Calibration System," Transactions of the American Vacuum Society, 1962.

XVII. REFERENCES (Cont'd)

(28) Hoffman, E. E. and Holowach, J., Cb-1Zr Thermal Convection Loop, Potassium Corrosion Test Loop Development Topical Report No. 5, R67SD3014, June 15, 1967, General Electric Company, Cincinnati, Ohio, p. 63.

(29) Hoffman, E. E. and Holowach, J., Cb-1Zr Pumped Sodium Loop, Potassium Corrosion Test Loop Development Topical Report No. 6, R67SD3015, December 20, 1967, General Electric Company, Cincinnati, Ohio, p.83.

(30) Dotson, L. E. and Hand, R. B., Purification, Analysis, and Handling of Sodium and Potassium - Potassium Corrosion Test Loop Development Topical Report No. 4, R66SD3012, General Electric Company, Cincinnati, Ohio, June 13, 1966, p. 15.

(31) Frank, R. G., et al., Material and Process Specifications for Refractory Alloy and Alkali Metals - Potassium Corrosion Test Loop Development Topical Report No. 2, R66SD3007, December 13, 1965, General Electric Company, Cincinnati, Ohio.

(32) Hendricks, J. W. and McElroy, D. L., High Temperature, High Vacuum Thermocouple Drift Tests, ORNL-TM-833, August 1964.

(33) Hoffman, E. E. and Holowach, J., Cb-1Zr Sodium Thermal Convection Loop, Potassium Corrosion Test Loop Development Topical Report No. 5, R67SD3014, General Electric Company, Cincinnati, Ohio, June 15, 1967, p. 31.

(34) Hoffman, E. E. and Holowach, J., Cb-1Zr Pumped Sodium Loop, Potassium Corrosion Test Loop Development Topical Report No. 6, R67SD3014, General Electric Company, Cincinnati, Ohio, December 20, 1967, p. 90.

(35) Affel, R. G., Burger, G. H., and Pearce, C. L., Calibration and Testing of 2- and 3 1/2-Inch Magnetic Flowmeters for High Tempera- NaK Service, Oak Ridge National Laboratory, ORNL-2793, p. 16.

(36) Alkali Metals Boiling and Condensing Investigations, Quarterly Progress Report No. 11, NASA Contract NAS 3-2528, NASA-CR-54405, April 23, 1965, p. 41.

(37) Bond, J. A. and Converse, G. L., Vaporization of High Temperature Potassium in Forced Convection at Temperatures from 1800°F to 2100°F, NASA CR-843, July 1967, p. 113.

(38) Harrison, R. W., The Compatibility of Biaxially Stressed D-43 Alloy with Refluxing Potassium, NASA CR-807, June 1967, P. 7.

(39) Generation of Long-Time Creep Data on Refractory Alloys at Elevated Temperatures, Twelfth Quarterly Report, NASA Contract NAS 3-2545, NASA-CR-72044.

(40) Rutherford, S. L., et al., "On Pumping Mechanisms in Getter-Ion Pumps Employing Cold-Cathode Gas Discharges," American Vacuum Society Symposium Transaction, 1960, Pergamon Press, New York, 1961, p. 380.

(41) Roberts, R. W. and Vanderslice, T. A., Ultra-High Vacuum and Its Applications, Prentice-Hall, Inc., Englewood Cliffs, N. J. (1963), p. 19.

(42) Jepsen, R. L., et al., "Stabilized Air Pumping with Diode-Type Getter-Ion Pumps," American Vacuum Society Vacuum Symposium Transactions, 1960, Pergamon Press, Inc., New York, 1961, pp.45-50.

(43) Hoffman, E. E. and Holowach, J., Cb-1Zr Pumped Sodium Loop, Potassium Corrosion Test Loop Development Topical Report No. 6, R67SD3015, General Electric Company, Cincinnati, Ohio, December 20, 1967, p. 150.

(44) Brubaker, W. M., "A Method of Greatly Enhancing the Pumping Action of a Penning Discharge," American Vacuum Society Vacuum Symposium Transactions, 1960, Pergamon Press, Inc., New York, 1961, p. 302.

(45) Hoffman, E. E. and Holowach, J., Cb-1Zr Pumped Sodium Loop, Potassium Corrosion Test Loop Development Topical Report No. 7, R67SD3015, General Electric Company, Cincinnati, Ohio, December 20, 1967, p. 141.

(46) Metals and Ceramics Division Annual Progress Report for Period Ending June 30, 1965, ORNL-3870, p. 130.

(47) Hoffman, E. E. and Holowach, J., Cb-1Zr Thermal Convection Loop, Potassium Corrosion Test Loop Development Topical Report No. 5, R67SD3014, General Electric Company, Cincinnati, Ohio, June 15, 1967, p. 72.

(48) Dotson, L. E. and Hand, R. B., Purification, Analysis, and Handling of Sodium and Potassium - Potassium Corrosion Test Loop Development Topical Report No. 4., R66SD3012, General Electric Company, Cincinnati, Ohio, June 13, 1966, p. 35.

(49) Hoffman, E. E. and Holowach, J., Cb-1Zr Thermal Convection Loop, Potassium Corrosion Test Loop Development Topical Report No. 5, R67SD3014, General Electric Company, Cincinnati, Ohio, June 15, 1967, p. 69.

(50) Hoffman, E. E. and Holowach, J., Cb-1Zr Pumped Sodium Loop, Potassium Corrosion Test Loop Development Topical Report No. 6, R67SD3015, General Electric Company, Cincinnati, Ohio, December 20, 1967, p. 161.

XVII. REFERENCES (Cont'd)

(51) Hoffman, E. E. and Holowach, J., Cb-1Zr Thermal Convection Loop, Potassium Corrosion Test Loop Development Topical Report No. 5, R67SD3014, General Electric Company, Cincinnati, Ohio, June 15, 1967, p. 129.

(52) Elliot, R. P., Constitution of Binary Alloys, First Supplement, McGraw-Hill Book Company, 1965.

(53) Schonberg, N., "The Structure of the Metallic Quarternary Phase ZrTaNO," Acta Chemica Scandinavica, 8, No. 4, 1954, pp. 627-629.

(54) Schonberg, N., "On Metallic Phases in the Ti-P-O and Zr-P-O Systems," Acta Chemica Scandinavica, 8, No. 4, 1954, pp. 1460-1465.

(55) Engel, Jr., L. B. and Frank, R. G., Evaluation of High-Strength Columbium Alloys for Alkali Metal Containment, NASA Contract NAS 3-2140, General Electric Company, Cincinnati, Ohio, R66SD3015, 1966, p. 35.

(56) Metals and Ceramics Division Annual Progress Report for Period Ending June 30, 1965, ORNL-3870, November 1965, p. 128.

(57) Hoffman, E. E. and Holowach, J., Cb-1Zr Pumped Sodium Loop Potassium Corrosion Test Loop Development Topical Report No. 6, R67SD3015, General Electric Company, Cincinnati, Ohio, December 20, 1967.

(58) Peterson, J. R., High Performance "Once-through" Boiling of Potassium in Single Tubes at Vapor Temperatures From 1500°F to 1750°F, NASA Contract NAS 3-2528, General Electric Company, Cincinnati, Ohio, November 7, 1966, p. 141.

(59) Walling, J. F. and Lemmon, A. W., Jr., The Experimental P-V-T Properties of Potassium to 1150°C, Battelle Memorial Institute, BATT-4673-T4, April 1963.

(60) Stone, J. P., et al., High Temperature Properties of Sodium, Potassium and Cesium, NRL Report 6128, August 1964.

(61) Private Communication from J. H. DeVan, Oak Ridge National Laboratory.

(62) Potassium Corrosion Test Loop Development, Quarterly Progress Report No. 5 for Period Ending October 15, 1964, NASA Contract NAS 3-2547, NASA-CR-54269, p. 17.

(63) Engel, Jr., L. B. and Frank, R. G., Evaluation of High-Strength Columbium Alloys for Alkali Metal Containment, NASA-CR-54226, 1964.

XVII. REFERENCES (Cont'd)

(64) Metals and Ceramics Division Annual Progress Report for Period Ending June 30, 1965, Oak Ridge National Laboratory, ORNL-3870, p. 128.

(65) Litman, A. P., "The Effect of Oxygen on the Corrosion of Niobium by Liquid Potassium," ORNL-3751, July 1965.

(66) Semiannual Progress Report, Determination of the Emissivity of Materials, Report Period: May 14-Nov. 15, 1964, R. C. Emanuelson, Pratt & Whitney Aircraft, NASA Contract NAS 3-4174, NASA-CR-54268.

(67) Leiblein, S., Analysis of Temperature Distribution and Radiant Heat Transfer Along a Rectangular Fin of Constant Thickness, NASA Technical Note D-196, November 1959.

(68) Semiannual Progress Report, Determination of the Emissivity of Materials, Report Period: May 14-Nov. 15, 1964, R. C. Emanuelson, Pratt & Whitney Aircraft, NASA Contract NAS 3-4174, NASA-CR-54268.

(69) Potassium Corrosion Test Loop Development, Quarterly Progress Report No. 4 for Period Ending July 15, 1964, NASA Contract NAS 3-2547, NASA-CR-54167, p. 49.

(70) Hoffman, E. E. and Holowach, J., Cb-1Zr Pumped Sodium Loop, NASA CR-1135, November 1968, p. 240.

(71) Phelps, E. H. and Mears, R. B., "The Effect of Composition and Structure of Stainless Steel Upon Resistance to Stress-Corrosion Cracking," First International Congress on Metallic Corrosion, London, April 1961, Butterworths (1962), 325.

(72) Report on Stress-Corrosion Cracking of Austenitic Chromium-Nickel Stainless Steel, ASTM Special Technical Publication No. 264, Published by American Society for Testing Materials, March 1960, p. 6.

(73) Ibid, p. 9.

(74) ASTM Designation A240-63.

(75) Metals Handbook, Vol. 1, 8th Edition, 1961, p. 544.

(76) Reference 72, p. 11.

(77) Reference 72, p. 8.

NASA-Langley, 1970 —— 17 E-5303